# SYNTHESIS AND BIOLOGICAL ACTIVITY STUDIES OF SOME NEW BENZOFURAN DERIVATIVES

**Sam Ali Mohammed Mohammed DAWBAA**

**Eskişehir 2021**

# SYNTHESIS AND BIOLOGICAL ACTIVITY STUDIES OF SOME NEW BENZOFURAN DERIVATIVES

**Sam Ali Mohammed Mohammed DAWBAA**

**PhD Thesis**

**Department of Pharmaceutical Chemistry**

**Supervisor: Prof. Dr. Ahmet Çağrı KARABURUN**

**Eskişehir**

**Anadolu University**

**Graduate School of Health Sciences**

**December 2021**

# ÖZET

BAZI YENI SÜBSTİTÜE BENZOFURAN TÜREVLERİNİN SENTEZLERİ VE BİYOLOJİK AKTİVİTE ÇALIŞMALARI

Sam Ali Mohammed Mohammed DAWBAA
Farmasötik Kimya Anabilim Dalı
Anadolu Üniversitesi, Sağlık Bilimleri Enstitüsü, Aralık 2021
Danışman: Prof. Dr. Ahmet Çağrı KARABURUN

Benzofuran, endüstride ve ilaç sektöründe yaygın olarak işlev gören kaynaşmış bisiklik bir yapıdır. Benzofuranın ekonomik faydaları ve sentezleme kolaylığı, onu daha sonraki araştırma çalışmaları için bir kullanışlı bir hedef haline getirmektedir. Bu tezde, yeni terapötik ajanlar tasarlamak için temel bir yapı olarak benzofuran seçilmiştir. Literatür incelemelerimizde, Alzheimer hastalığının (AH) palyatif tedavisinde kullanılabilecek yeni asetilkolin esteraz (AChE) inhibitörlerinin tasarımı için, benzofuran iskeletinin uygun bir ana yapı olacağı değerlendirilmiş, toplam 42 hibrit benzofuran ve piperazin türevi tasarlanmıştır. Tasarlanan moleküller, referans AChE inhibitörü donepezil'e benzer şekilde enzimin aktif bölgesine bağlanma uyumuna sahip olacak şekilde planlanmışlardır. Hedef ürünlerin tümü başarıyla sentezlenmiş ve yapıları NMR, IR ve kütle spektrometrisi ile aydınlatılmıştır. Biyolojik aktivite çalışmaları, AChE, butirilkolin esteraz (BChE) ve β-amiloid (Aβ) üzerinde *in vitro* testler kullanılarak gerçekleştirilmiştir. Sonuçlar, **D25**, **D30**, **D40** ve **D41** adlı dört bileşiğin aktif olduğunu ve AChE'ı inhibe ettiğini gösterirken, BChE'a karşı herhangi bir aktivite gözlemlenmemiştir. Öte yandan, bileşik **D25** ve **D41**, referans inhibitör ile karşılaştırılabilir seviyede iyi Aβ agregasyonu inhibitör aktivitesi gösterirken, **D30** ve **D40** daha zayıf bir Aβ agregasyonu inhibitör aktivitesi göstermiştir. Sitotoksisite araştırması, bu bileşiklerin makul güvenliğe sahip olduğunu göstermiştir. Aktif bileşiklerin bağlanma modlarını analiz etmek için moleküler yerleştirme analizi yapılmıştır. Bu tezdeki aktif bileşiklerin, AH'nın tedavi stratejilerinde yararlı ajanlar oldukları ve daha ileri çalışmalar için değerlendirilmeleri düşünülmektedir.

**Anahtar Sözcükler:** Benzofuran, Alzheimer hastalığı, Asetilkolin esteraz ihibitörü, β-amiloid, Moleküler modelleme.

## ABSTRACT

SYNTHESIS AND BIOLOGICAL ACTIVITY STUDIES OF SOME NEW BENZOFURAN DERIVATIVES

Sam Ali Mohammed Mohammed DAWBAA

Department of Pharmaceutical Chemistry

Anadolu University, Graduate School of Health Sciences, December 2021

Supervisor: Prof. Dr. Ahmet Çağrı KARABURUN

Benzofuran is a fused bicyclic scaffold that is functionalized widely in the industrial and pharmaceutical sectors. The economic benefits and ease of synthesizing benzofuran make it a target for further research studies. In this thesis, benzofuran was selected as a scaffold to design new therapeutic agents. After reviewing the literature, benzofuran scaffold was found suitable for the design of new acetylcholine esterase (AChE) inhibitors that can be employed in the palliative treatment of Alzheimer's disease (AD). A total of 42 hybrid benzofuran and piperazine derivatives were designed. The designed molecules were planned to have binding fit in the active site of the enzyme similar to that of the reference AChE inhibitor donepezil. All of the target products were synthesized and analyzed by $^{1}$H NMR, $^{13}$C NMR, IR and mass spectrometry. The biological activity studies were achieved using *in vitro* assay on AChE, butyrylcholine esterase (BChE) and β-amyloid. The results showed that four compounds namely **D25**, **D30**, **D40**, and **D41** were active and inhibited AChE while no activity was observed against BChE. On the other hand, compounds **D25** and **D41** showed good Aβ aggregation inhibitory activity comparable to the reference inhibitor, while compounds **D30** and **D40** displayed a weaker Aβ aggregation inhibitory activity. The cytotoxicity investigation of the active compounds showed that these compounds have plausible safety. Molecular docking study was achieved to analyze the binding modes of the active compounds. The four compounds **D25**, **D30**, **D40**, and **D41** are thought to be useful agent in the treatment strategies of AD and accordingly are recommended for further studies.



**Keywords:** Benzofuran, Alzheimer's disease, Acetylcholine esterase inhibitor, β-amyloid, Molecular docking.

## ACKNOWLEDGEMENT

Here I'm so grateful for this achievement. During the thesis, I went through a lot of obstacles, and I owe a lot of thanks to those who helped me complete my Ph.D. First of all, I thank Allah for helping me with my educational journey.

I then owe a lot of gratitude to my supervisor Prof. Dr. Ahmet Çağrı KARABURUN for leading me through the hard tasks of the thesis and for his valuable directions without which I could have been unable to achieve a lot.

I thank my colleague Mr. Asaf Evrim EVREN for being so much helpful in the laboratory's works and communication with other laboratories in which we carried out some of the required experiments and studies.

Dr. Serkan LEVENT and Mrs. Betül AYDIN helped in the chemical analysis of the synthesized products, thus I thank them for their efforts.

I cannot forget the help of Associ. Prof. Dr. Begüm Nurpelin SAĞLIK in carrying out the biological studies investigations and analysis of the therapeutic activity results and I owe her a lot of thanks.

Mr. Abdullah Burak KARADUMAN helped in performing the cytotoxicity study and thus I present my thanks to him.

I also thank Thamar University and Ministry of Higher Education and Scientific Research for their support through the scholarship program abroad. I present my thanks to Anadolu University too for facilitating my research and providing the required materials and instruments. Also, I owe a lot of gratitude for the DOPNA laboratory where the chemical analysis and biological activity were achieved.

Last but not least, I owe my family a debt of gratitude for being so supportive and encouraging.

## STATEMENT OF COMPLIANCE WITH ETHICAL PRINCIPLES AND RULES

**01/11/2021**

I hereby truthfully declare that this thesis is an original work prepared by me; that I have behaved in accordance with the scientific ethical principles and rules throughout the stages of preparation, data collection, analysis and presentation of my work; that I have cited the sources of all the data and information that could be obtained within the scope of this study, and included these sources in the references section; and that this study has been scanned for plagiarism with "scientific plagiarism detection program" used by Anadolu University, and that "it does not have any plagiarism" whatsoever. I also declare that, if a case contrary to my declaration is detected in my work at any time, I hereby express my consent to all the ethical and legal consequences that are involved.

## TABLE OF CONTENTS

**Page**

**Page**

## LIST OF TABLES

**Page**

## LIST OF FIGURES

**Page**

**Page**

**Page**

**Page**

**Page**

**Page**

**Page**

**Page**

**Page**

**Page**

## LIST OF ABBREVIATIONS

| | |
|---|---|
| $^{1}$H NMR | : Proton nuclear magnetic resonance |
| 2D | : Two-dimensional |
| 3D | : Three-dimensional |
| $^{13}$C NMR | : Carbon-13 nuclear magnetic resonance |
| Aβ | : Beta amyloid |
| AChE | : Acetylcholinesterase |
| AD | : Alzheimer's disease |
| α-syn | : Alpha synuclein |
| APCI | : Atmospheric pressure chemical ionization |
| ApoE | : Apolipoprotein E |
| APP | : Amyloid precursor protein |
| ASAP | : Atmospheric solid analysis probe |
| ATC | : Acetylcholine iodide |
| ATCC | : American Type Culture Collection |
| ATR | : Attenuated total reflection |
| BACE-1 | : β-secretase |
| BBB | : Blood-brain barrier |
| BChE | : Butyrylcholine esterase |
| BTC | : Butyrylcholine iodide |
| *c* | : Concentration of the sample in Beer's law |
| CAS | : Catalytic anionic site in Acetylcholinesterase |
| CMS | : Compact mass spectrometer |
| d | : Doublet |
| dd | : Doublet of doublet |
| DMF | : Dimethyl formamide |
| DMSO | : Dimethyl sulfoxide |
| DMSO-$d_6$ | : Deuterated dimethyl sulfoxide |
| EDTA | : Ethylenediamine tetraacetic acid |
| EOAD | : Early-onset Alzheimer's disease |
| ε | : Molar absorptivity in Beer's law |
| ESI | : Electrospray ionization |

| | |
|---|---|
| γ | : Chemical shift in NMR spectrum |
| GIT | : Gastrointestinal tract |
| GSK-3 | : Glycogen synthase kinase-3 |
| HMBC | : Heteronuclear multiple bond correlation |
| HRMS | : High-resolution mass spectroscopy |
| HSQC | : Heteronuclear single quantum correlation |
| $IC_{50}$ | : 50% Inhibitory concentration |
| IR | : Infrared |
| IT | : Ion trap |
| *J* | : coupling constant |
| *l* | : Path length of light in Beer's law |
| LCMS | : Liquid chromatography mass spectrometry |
| LOAD | : Late-onset Alzheimer's disease |
| m/z | : mass/charge |
| MAO | : Monoamine oxidase |
| MCI | : Mild cognitive impairment |
| MMBO | : 2-methyl-5-(3-{4-[(S)-methylsulfinyl]phenyl}-1-benzofuran-5-yl)-1,3,4-oxadiazole |
| M.P. | : Melting point |
| MTT | : 3-(4,5-Dimethylthiazol-2-yl)-2,5-diphenyltetrazolium bromide |
| NFT | : Neurofibrillary tangles |
| NMDA | : N-methyl-D-aspartate |
| NSAIDs | : Non-steroidal anti-inflammatory drugs |
| PAS | : Peripheral anionic site in Acetylcholinesterase |
| PBS | : Phosphate buffer |
| PDB | : Protein data bank |
| PEG-400 | : Polyethylene glycol 400 |
| ppm | : Part per million |
| PSEN1 | : Presenilin-1 |
| PSEN2 | : Presenilin-2 |
| rpm | : Rotation per minute |
| RT | : Room temperature |
| sAPP | : Secreted amyloid precursor protein |

| | |
|---|---|
| SSRIs | : Selective serotonin reuptake inhibitors |
| t | : Triplet |
| TLC | : Thin-layer chromatography |
| TMS | : Tetramethylsylane |
| TOF | : Time of flight |
| TPSA | : Topological polar surface area |
| UV | : Ultraviolet |

## 1. INTRODUCTION

The design of new molecules is a reliable method to introduce new drug candidates to the clinical system. A wide range of chemically synthesized drugs provided solutions for a variety of crucial diseases [1–7]. Thus, it is worthy to design novel drug candidates benefiting from the appropriate characteristics of small molecules. The design process, in this case, depends mainly on targeting a druggable biological entity and validation of the whole procedure [8]. The targeting process is achieved by applying the idea of privileged structures which are molecular scaffolds with certain binding abilities that can be benefited from in synthesizing selective ligands through changing their functional groups and these ligands eventually be suitable to a range of respective biological targets [9].

Benzofuran is an interesting privileged structure that can be employed in the synthesis of promising drug agents. The ability of benzofuran to interact desirably with certain biological targets offered it various therapeutic applications *i.e.* antiarrhythmic drugs *e.g.* amiodarone and dronedarone [10, 11], antifungal agents *e.g.* griseofulvin [12], uricosuric agents *e.g.* benzobromaron [13], and antidepressants *e.g.* vilazodone [14]. The geometry of the benzofuran scaffold can be exploited in targeting druggable biomolecules which require for their activity a fused five membered-six membered rings. One of the likely targets is the acetylcholine esterase (AChE) enzyme which interacts with a variety of ligands with different ring systems including ligands containing an indene ring as a basic core *e.g.* donepezil [15, 16]. One of the main therapeutic applications of inhibiting AChE in the central nervous system is the symptomatic treatment of Alzheimer's disease (AD) [15]. Donepezil is an AChE inhibitor that proved efficient in reducing the emergence of apathy in patients with mild to moderate AD [17]. It is thought that benzofuran can be useful in synthesizing analogs of donepezil by replacing the indene ring with benzofuran and certain changes in the remaining functional groups.

The purpose of this study is to synthesize novel benzofuran derivatives. The design of the new molecules is based on donepezil, hence AChE is the targeted biomolecule for the designed molecules to display their activity as inhibitors. The molecules are expected to have the ability to penetrate the blood-brain barrier and act centrally. They might be effective in treating certain symptoms of AD. Benzofuran was chosen as the core scaffold of the molecules. Three main positions on the benzofuran were determined as substitution

sites and 42 derivatives were planned by changing the functional groups on these sites. The substitution sites on benzofuran were C-2, C-3, and C-5. C-2 is bonded to a carbonyl group to which various piperazine derivatives were bonded *via* amidation reactions. C-3 was bonded to a methyl group in some molecules and remained unsubstituted in others. C-5 was designed to have different substituent groups including H, $OCH_3$, Cl, and $NO_2$. After the synthesis stage and the confirmation analysis of the synthesized compounds, biological evaluation was done *via in vitro* enzyme studies using AChE and Butyrylcholine esterase (BChE) as targets for the inhibitory activity of the compounds. The most active compounds were further studied *via* molecular docking to explain the ligand-receptor interactions.

## 2. LITERATURE REVIEW

### 2.1. Drug Design and Research

Medicinal chemistry is a science resulting from the intersection of multiple disciplines including organic chemistry, pharmacology, pharmacognosy, biochemistry, molecular biology, computational chemistry, and physical chemistry [18]. Accordingly, medicinal chemists should have an appreciated knowledge of those sciences to be able to design new therapeutic agents.

Drug design is a general descriptive term indicating all of the procedures involved in the planning and synthesis of the respective compound(s) which finally might result in a promising lead compound. It includes invention and discovery acts with an emphasis on a targeted approach based on the available knowledge and technology [19]. A *hit* in medicinal chemistry is a compound that could exceed a critical threshold in binding a target biomolecule or modification of a functional signal related to it [20]. The hit becomes a *validated hit* if its identity and purity are confirmed altogether with multiple therapeutic activity confirmations [20]. A *lead* in its turn is a result of validated hits researches with proven biological activity and selectivity and is considered the starting point of new drug development [20, 21]. The design process although ends its job by reaching the lead molecule, it still has a major role in the optimization of the lead compound during the following stages. The optimization of the lead molecule is achieved to minimize the toxicity and enhance the potency, specificity, and pharmacokinetic profile (absorption, distribution, metabolism, and elimination) [21, 22]. The optimization process involves changes in the functional groups of the lead compound to achieve the desired properties. These changes should be designed through plenty of planning and using the required tools such as *in silico* (computer-based) studies [23, 24].

Modern drug research has powerful tools that make the duration of design and experimentation much shorter than ever before. Drug research includes a sequence of phases. To begin with, a structure of a target biomolecule is discovered, verified, and validated as a candidate site for drug therapy. Following this phase, structure-based and computer-aided drug designs are achieved. The designing phase is followed by the synthesis of the designed hits or extraction and chemical modification of active substances of natural origin. The obtained molecules are then investigated for the activity by initial *in vitro* tests. If approved successfully in the initial activity studies, the compounds are further investigated in animal models after being approved of having an

appreciated toxicity profile. Finally, clinical trials can confirm a test compound's suitability as a medicine for patients [25]. The processes involved in drug design and research are illustrated in Figure 2.1.

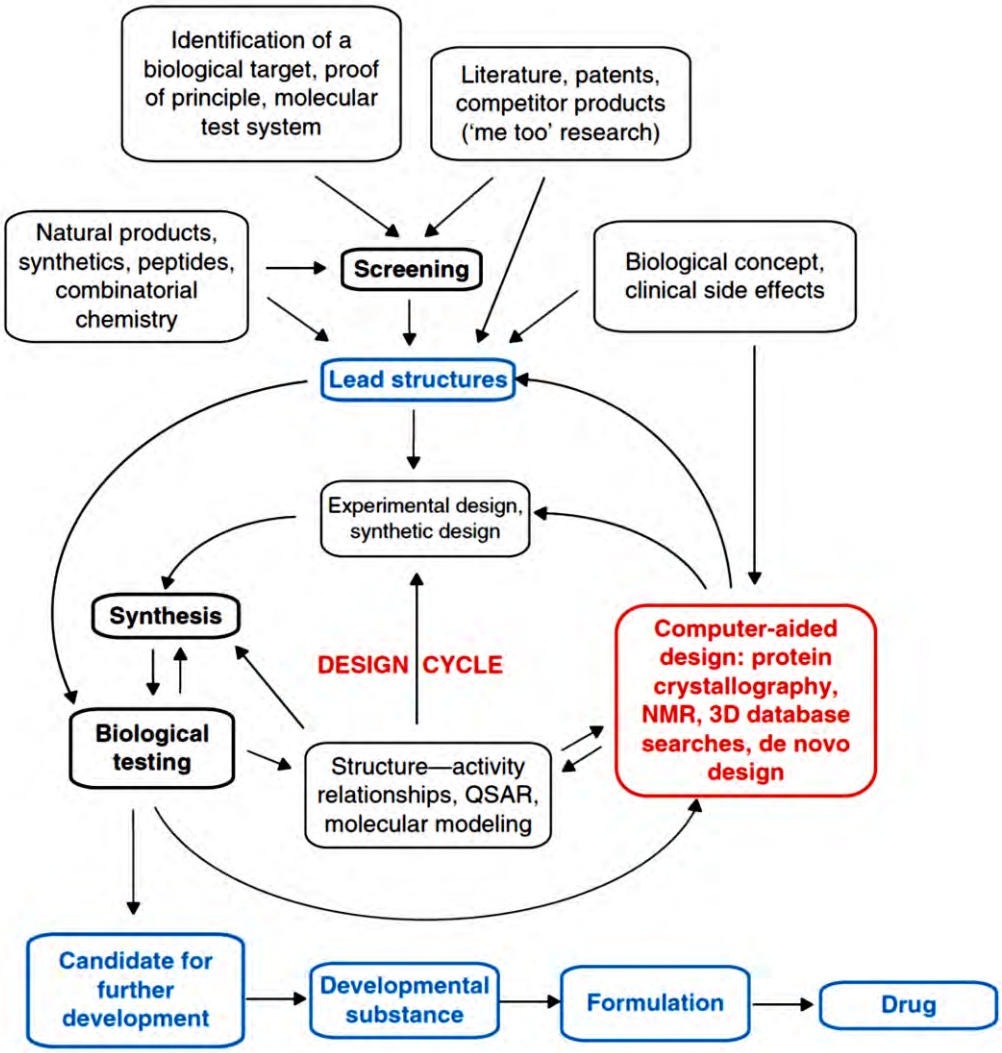


**Figure 2.1.** *Detailed illustration of interrelated processes of drug design and research [25]*

In this thesis, the design of the targeted molecules was based on donepezil (ligand-based drug design). Donepezil is a parasympathomimetic agent which acts by inhibiting acetylcholine esterase (AChE) centrally [15, 16]. It is a drug used to improve mental function in Alzheimer's disease patients [26, 27]. As the data of donepezil [28] and AChE [29] is available, their combination as a ligand-receptor complex was used to contemplate and design an agent which has a similar spatial size and physicochemical characteristics, hence, likely similar therapeutic activity. Benzofuran was thought of as a candidate that might mimic the indene ring found in donepezil and for this reason, was chosen as the

basic scaffold from which druggable derivatives of anti-choline esterase activity were designed.

## 2.2. Chemistry of Benzofuran

Benzofuran is a colorless, oily, water-insoluble liquid with a boiling point of 173°C. It is probably formed during coal mining by cyclodehydration of 2-ethylphenol [30]. Benzofurans is a fused scaffold of two rings benzene and furan. The system can be found either as benzo[*b*]furan or benzo[*c*]furan as illustrated in Figure 2.2. For descriptive purposes, benzo[*b*]furan is called benzofuran and benzo[*c*]furan is named isobenzofuran through various texts and in the literature [31]. The subject of this thesis is only benzo[*b*]furan for which benzofuran term will be used through all of the following sections.

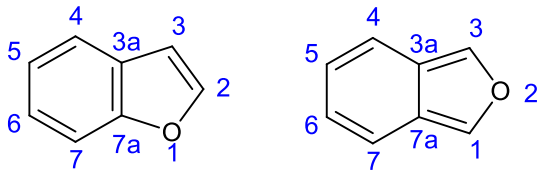


**Figure 2.2.** *Chemical structures of benzofuran scaffolds*

The benzofuran and isobenzofuran scaffolds can also be found in reduced forms known as coumaran and phthalan, respectively [32]. Their structures are illustrated in Figure 2.3.

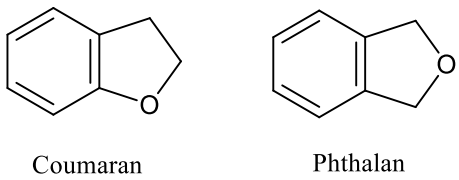


**Figure 2.3.** *Chemical structures of reduced benzofuran forms*

Benzofuran has higher aromaticity than isobenzofuran. It also has comparable aromaticity with that of benzothiophene but is slightly higher [32]. However, the aromaticity of benzofuran is less than that of indole [33]. On the other hand, benzofuran

is a more stable ring than isobenzofuran. This is explained by the topological charge stabilization rule which states that the best stabilization of a ring is achieved by the introduction of an electronegative heteroatom into the position of the greatest charge in the isoconjugate isoelectronic hydrocarbon. The indenyl anion from which benzofuran and isobenzofuran are depicted structurally has the greatest charge density at positions 1 and 3 of the five-membered ring, hence, the introduction of oxygen in one of these positions produces maximum stabilization of the electron density [32]. The distribution of charge on the indenyl ion is illustrated in Figure 2.4.

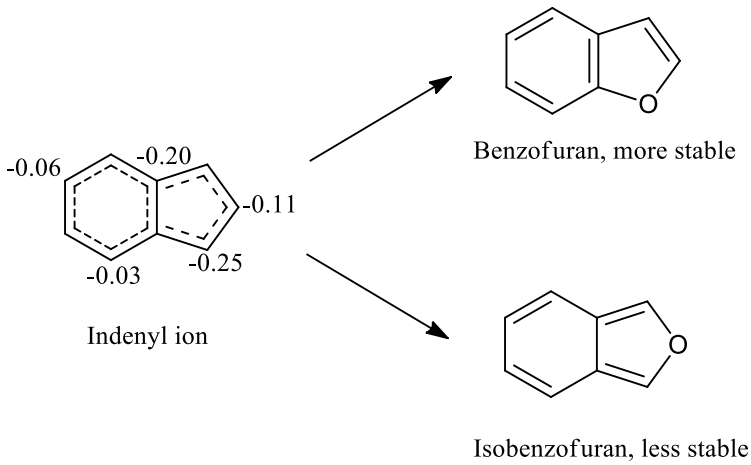


**Figure 2.4.** *Application of topological charge stabilization rule in the formation of benzofuran and isobenzofuran*

### 2.2.1. Nuclear magnetic resonance (NMR) analysis of benzofuran

Various works reported the NMR analysis of benzofuran. Black and Heffernan [34] reported the proton NMR spectrum of pure benzofuran in carbon tetrachloride and deuterated acetone. Considering the numbering of benzofuran as shown in Figure 2.2, the chemical shifts (γ) obtained in carbon tetrachloride and acetone (inside parentheses) were 6.66 (6.76), 7.13 (7.23), 7.19 (7.30), 7.42 (7.51), 7.49 (7.63), and 7.52 (7.78) for H3, H5, H6, H7, H4, and H2, respectively. The proton near the oxygen atom of benzofuran is the most deshielded by the strong electronegative oxygen, hence, its chemical shift is the highest. Meta coupling between H-4 and H-6 takes place occasionally where the coupling constant ($J_{4,6}$) can reach up to 1.28 Hertz (Hz). In addition, other second-order couplings have less chance to happen. Such couplings include $J_{3,7}$, $J_{4,7}$, $J_{5,7}$ where their values are 0.87, 0.80, and 0.92 Hz, respectively [32].

On the other hand, $^{13}C$ NMR spectrum of benzofuran was obtained by Okuyama and Fueno [35] where they used carbon disulfide ($CS_2$) as a solvent. The chemical shifts of the carbons numbered as in Figure 2.2 were reported as 106.9, 111.8, 121.6, 123.2, 124.6, 127.9, 145.1, and 155.5 for C3, C7, C4, C5, C6, C3a, C2, and C7a, respectively [32]. In comparison to the $^{1}H$ NMR, the carbons bonded to the electronegative oxygen are the most deshielded and their chemical shifts are the highest.

Introducing substituent groups into benzofuran might change the chemical shifts of the protons and carbons of the ring. The type of functional group bonded in any position of the ring should be considered. The ability of the substituents to contribute to the shielding or deshielding of the nuclei of the near atoms depends mainly on four factors: local diamagnetic field, local paramagnetic field, shielding due to remote currents, others. The local diamagnetic and paramagnetic fields are contributed by electrons near the respective nucleus. The remote currents can arise from electrons circulating around nearby nuclei (other than the immediate ones). Other contributors might include hydrogen bonding, solvent shifts, unpaired electrons, etc [36].

### 2.2.2. Ultraviolet (UV) analysis of benzofuran

Benzofuran was reported to have absorbance in three UV regions. The UV regions in which the absorbances were observed were 244, 274, and 281 nm, while the molar absorptivity was reported to be 4.03, 3.39, and 3.42, respectively [30]. The molar absorptivity (ε) is the proportionality constant in Beer's law: $A=\varepsilon lc$, where $l$ is the path length of the light and $c$ is the concentration of the substance [37].

### 2.2.3. Infrared (IR) analytical spectrum of benzofuran

The IR spectrum of benzofuran was reported by Colentz Society [38] in 1960 and the hard and digital copies of the spectrum are available on the webpage of the National Institute of Standards and Technology of the United States of America [39].

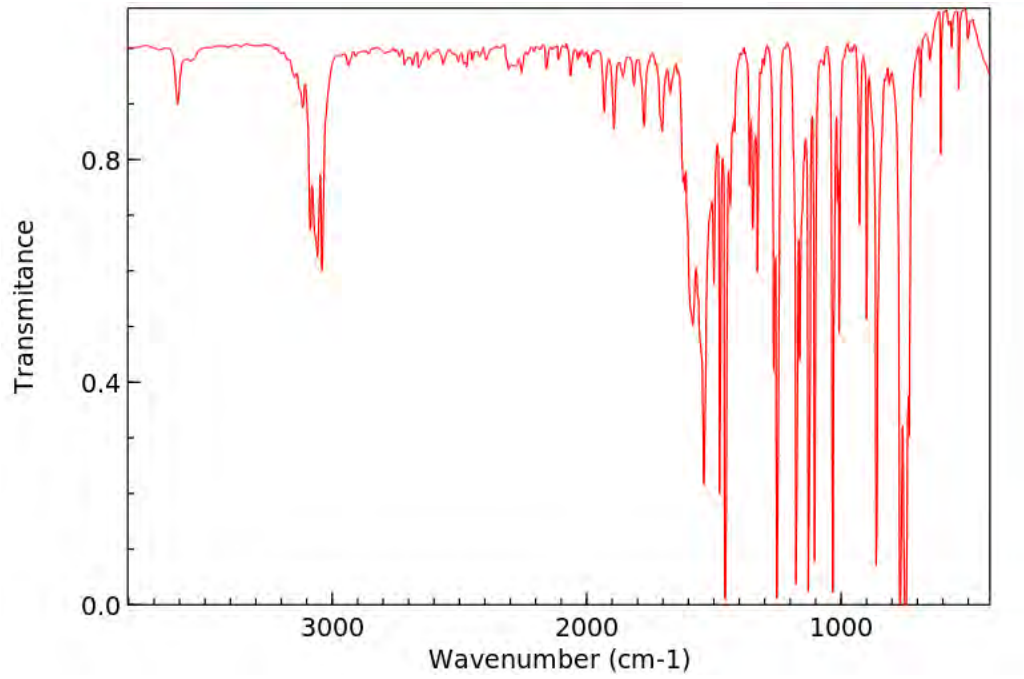


**Figure 2.5.** *Digitized copy of the IR spectrum of benzofuran [39]*

## 2.3. Synthesis of Substituted Benzofuran

### 2.3.1. Rap-Stoermer benzofuran synthesis

Rap-Stoermer synthesis involves the reaction of 2-hydroxy derivatives of benzaldehyde or acetophenone with α-haloketones to produce 2-carbonyl substituted benzofurans. The reaction is carried out in polar aprotic solvents like N,N-dimethylformamide (DMF), acetone, or acetonitrile. It also requires a temperature between 80 and 120°C with the use of a basic catalyst such as potassium carbonate [40].

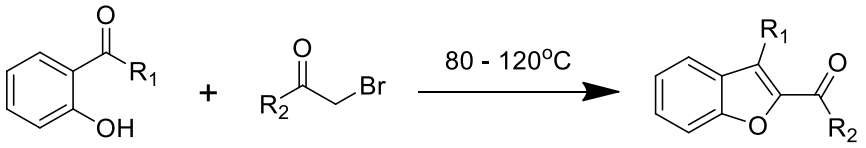


**Figure 2.6.** *Rap-Stoermer synthesis of benzofuran*

Demirayak *et al.* (2002) [41] reported the synthesis of aryl(benzofuran-2-yl)ketoximes while Gündoğdu-Karaburun *et al.* (2006) [42] reported the synthesis of [3-(imidazol-1-yl/triazol-1-ylmethyl) benzofuran-2-yl] ketoximes using Rap-Stoermer reaction for the synthesis of benzofuran. They achieved the reaction using acetonitrile as a solvent and potassium carbonate as a catalyst under reflux. Their benzofuran derivatives

were obtained in yields between 64-70%. Similarly, Alperen (2019) synthesized some benzofuran derivatives for antimicrobial activity [43]. Many other researchers have carried out Rap-Stoermer reaction using different solvents like polyethylene glycol (PEG-400) [44], acetone [45, 46], and DMF [46, 47]. On the other hand, other basic catalysts could be used in Rap-Stoermer reaction such as potassium hydroxide or cesium carbonate [48].

### 2.3.2. Metal-catalyzed benzofuran synthesis

Different transition metal catalysts were reported to be useful in the synthesis of certain derivatives of benzofuran [49]. Palladium (Pd), copper (Cu), platinum (Pt), ruthenium (Ru), and rhodium (Rh), and many other metals were used by different researchers in the cyclization of benzofuran [49]. A few examples are discussed below.

#### 2.3.2.1. *Palladium-catalyzed benzofuran synthesis*

Palladium salts were used as catalysts in the synthesis of benzofuran derivatives from o-halophenols and alkynes under mild conditions. Among the used salts were Bis(triphenylphosphine)palladium(II) diacetate ($Pd(OAc)_2(PPh_3)_2$) [50], and Bis(triphenylphosphine)palladium(II) dichloride ($PdCl_2(PPh)_3$) [51] in DMF in the presence of CuI and under basic conditions provided by piperidine or triethylamine [52].

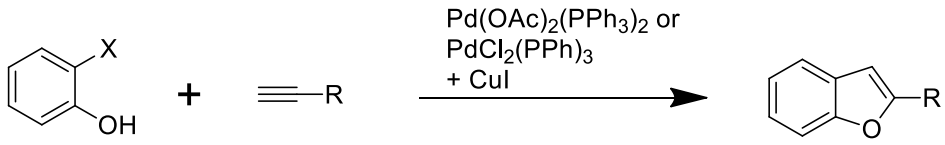


**Figure 2.7.** *Production of benzofuran using palladium salts*

Tris(dibenzylideneacetone)dipalladium(0) ($Pd_2(dba)_3$) was used by Willis *et al*. (2004) in the synthesis of benzofuran from enolate and halo-arene. The reaction involved intramolecular C-O bond formation in the presence of palladium derivative as a catalyst, Bis[phenyl] ether (DPEphos), and a base in toluene and a temperature of 110°C [53].

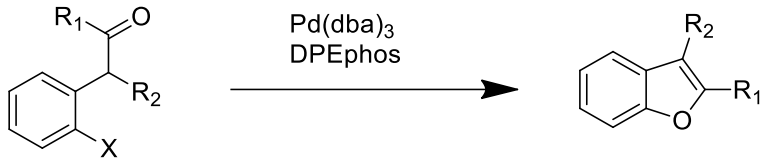


**Figure 2.8.** *Synthesis of benzofuran by intramolecular C-O bond formation using Pd(dba)$_3$ catalyst*

Another catalyst is palladium(II) trifluoroacetate Pd(TFA)$_2$ used by Jiang *et al*. (2016) to synthesize 3-sulfenylbenzofuran derivatives. They used 2-alkynylphenols with arylboronic acid and sulfur. A complex reaction medium of copper iodide (CuI), 1,10-phenanthroline (Phen), silver carbonate ($Ag_2CO_3$), and potassium phosphate ($K_3PO_4$) in the ionic liquid butylmethylimidazolium chloride ([Bmim]Cl) was used [54].

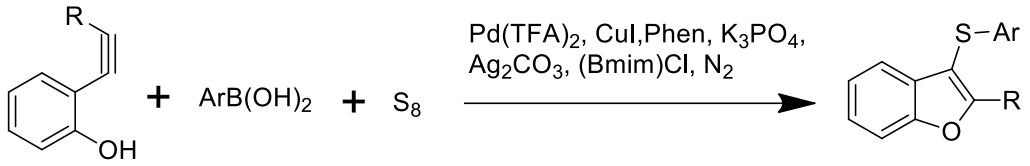


**Figure 2.9.** *Synthesis of 3-sulfenylbenzofuran derivatives using Pd(TFA)$_2$ catalyst*

Liu and coworkers (2016) used Pd/C for the catalysis of the cyclization of o-alkenylphenols to produce benzofuran derivatives. A simple reaction medium was used and composed of DMF and $N_2$ at a temperature of 140°C [55].

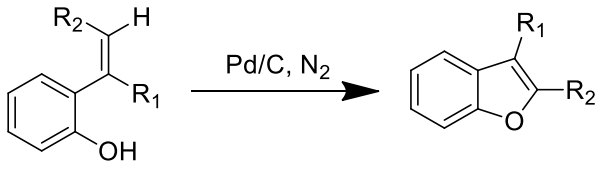


**Figure 2.10.** *Intramolecular cyclization of 2-alkenylphenol using Pd/C*

### 2.3.2.2. *Copper-catalyzed benzofuran synthesis*

Copper halides, particularly copper iodide and bromide are the most used form of the catalyst. The catalyst could be used in combination with other catalysts and reagents [56]. It frequently involves one-step intramolecular cyclization to produce the respective benzofuran. For example, Chen *et al*. (2005) synthesized substituted-benzofuran derivatives by cyclization of o-halobenzyl alkyl ketone using CuI as a metal catalyst and

$K_3PO_4$ [57]. The reaction was achieved in DMF at 105°C. The reaction is represented in Figure 2.11. This method showed tolerability to various substituted groups ($R_1$ and $R_2$) which indicates its usability for the synthesis of benzofuran derivatives of many organic classes.

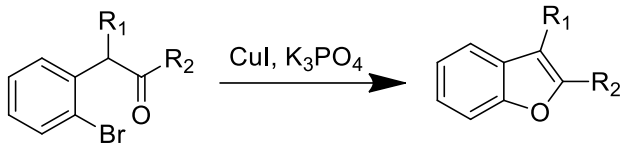


**Figure 2.11.** *Cyclization of o-halobenzyl alkyl ketone to produce benzofuran using a copper catalyst*

A mixture of two metal catalysts can also be used for the synthesis of benzofurans. Nagamochi *et al*. (2007) showed that a cross-coupling Cu- and Pd-catalysis can produce benzofuran from terminal alkynes and gem-dibromovinyl [58]. They used Pd/C and CuI in toluene, tri(o-tolyl)phosphine, and diisopropylamine and heated the mixture to 100°C as seen in Figure 2.12.

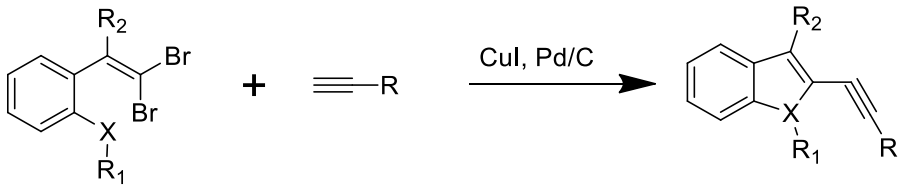


**Figure 2.12.** *Using a mixture of Cu and Pd catalysts in the synthesis of certain benzofurans*

### 2.3.2.3. *Other transition metal catalysts for benzofuran synthesis*

Wu and Li (2017) collected the available methods of metal-catalyzed synthesis of benzofuran in their book [49]. In addition to Pd and Cu, many other metals were reported in the synthesis of various benzofuran derivatives in the literature. For example, a Grubbs catalyst (ruthenium-based) was reported in the synthesis of benzofurans *via* a ring-closing metathesis mechanism [59]. Hashmi and Wolfle (2009) [60] reported the use of phosphine gold(I) bis-(trifluoromethanesulfonyl)imidate complex ($Ph_3PAuNTf_2$) or known as Gagosz's catalyst [61] which is a gold-based catalyst in the synthesis of furan-yn-ols and benzofurans. Many other metal-based catalysts were also used in the synthesis of benzofurans e.g. silver including $AgNO_3$, $Ag_3PO_4$, and AgOTf, zinc including $Zn(OTf)_2$, and iridium-based like $(IrCpCl_2)_2$, and ruthenium like $CpRuCl(PPh_3)_2$ [62–67].

## 2.4. Therapeutic Roles of Benzofuran Derivatives

### 2.4.1. Natural sources of benzofuran containing bioactive compounds

Benzofuran has been attracting interest due to its wide range of applications and contributions in drugs and the diagnosis of diseases [68–71]. The emergence of benzofuran derivatives in natural sources invoked the researches about their biological activities. Such derivatives are distributed in plant families including Rutaceae, Liliaceae, Cyperaceae, Krameriaceae, Lauraceae, and Asteraceae with the latter being a major source of natural benzofuran derivatives [72]. For specific determination of particular sources, various benzofuran derivatives were isolated from *Machilus glaucescens*, *Ophryosporus charua*, *Ophryosporus lorentzii*, *Krameria ramosissima*, and *Zanthoxylum ailanthoidol* [73].

### 2.4.2. A general outline of the therapeutic activities of benzofuran containing agents

Investigations showed that benzofuran derivatives might be useful therapeutic agents. In other words, this class of compounds showed anti-inflammatory [74–76], anticancer [77–82], antiparasitic [83–85], antimicrobial [41, 42, 86–88], anti-Alzheimer's disease [89–92], anti-diabetic [93–96], and monoamine oxidase (MAO) inhibitory [97–100] activities. Benzofuran moiety forms a part of the chemical skeleton of some opioid antagonists and analgesics such as morphine, codeine, oxycodone, naltrexone, ethylmorphine, and nalbuphine [68, 99, 101]. Some clinically used drugs in the treatment of class-III arrhythmias such as amiodarone and dronedarone also bear a benzofuran scaffold [10]. Benzbromarone is a uricosuric agent used in the treatment of gout and has a benzofuran ring as part of its chemical structure [13, 102]. Moreover, benzofuran containing vilazodone is a serotonin partial agonist and serotonin reuptake inhibitor used as an antidepressant agent [14, 103–105]. Griseofulvin and cicerfuran also include a benzofuran nucleus in their structure which contributes to their activity as natural antifungal agents [12, 106, 107]

### 2.4.3. Literature review of benzofuran derivatives with Anti-Alzheimer's disease activity

Various works reported the synthesis and therapeutic activity investigations of compounds containing benzofuran scaffold as promising agents in the treatment of AD [90]. Byun *et al*. (2008) synthesized a series of novel aminostyrylbenzofuran derivatives and investigated their inhibitory activity against β-amyloid (Aβ) formation. They found that two compounds illustrated in Figure 2.12 were active compared to a reference compound [108]. The $IC_{50}$ activities of compounds A and B were 0.07 and 0.08 μM, respectively, whereas that of the standard drug was 8 μM.

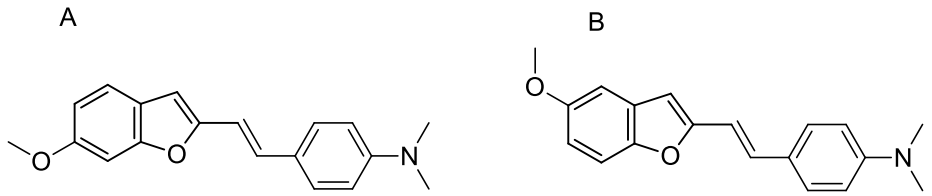


**Figure 2.13.** *Benzofuran derivatives which have Aβ inhibitory activity*

Nadri *et al*. (2010) synthesized a group of benzofuranone-benzylpyridinium compounds and tested their inhibitory activity against AChE. Among the synthesized compounds, two compounds as shown in Figure 2.14 were more potent inhibitors than the reference compounds donepezil. Compounds A, B, and donepezil were reported to have $IC_{50}$ values of 10 ± 6.87, 22 ± 6.25, and 28 ± 6.62 nmol/L [109].

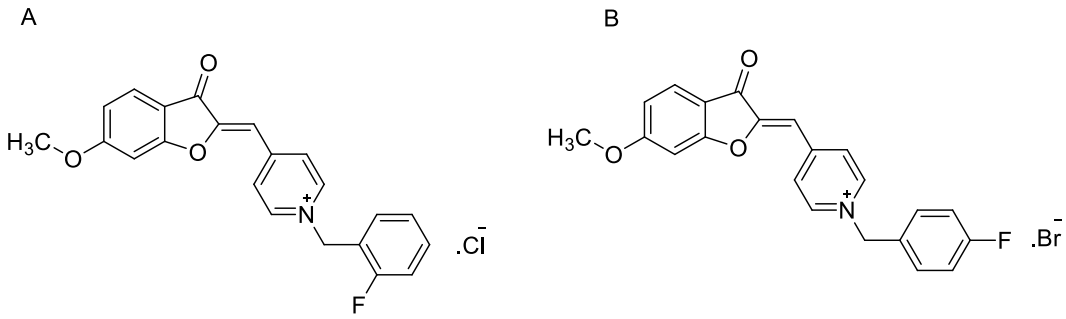


**Figure 2.14.** *Benzofuranone derivatives as potent AChE inhibitors [109]*

Rivière *et al*. (2010) extracted various stilbene derivatives from natural products and tested their inhibitory activity against β-Amyloidaggregation. They showed that scirpusin A and ε-viniferin glucoside have a strong inhibition of Aβ aggregation. ε-

viniferin glucoside showed $IC_{50}$ of 0.2 ± 0.3 μM more potent than the standard compound curcumin which displayed $IC_{50}$ of 10 ± 2 μM [110].

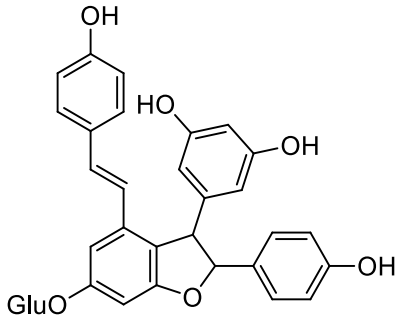


**Figure 2.15.** *ε-viniferin glucoside [110]*

A study by Zhou *et al*. (2010) showed that a benzofuran bonded piperazine derivative (Figure 2.16) displayed AChE inhibitory activity comparable to that of the reference compound donepezil. They reported the synthesis of benzofuran derivatives through an unusual rearrangement from coumarins [111].

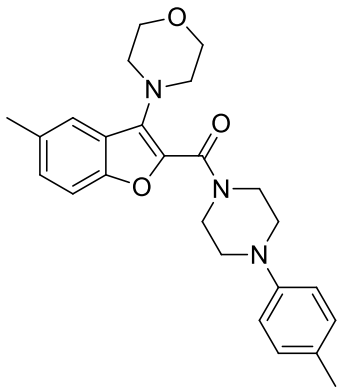


**Figure 2.16.** *Benzofuran derivative with AChE inhibitory activity [111]*

Mitterreiter *et al*. (2010) proposed a new technique to inhibit *β*-secretase by alkalinization of the acidic endosome environment in which the enzyme works optimally, thus, preventing the enzyme from cleaving the precursor proteins into *β*-amyloid. The reported method involved the use of two weak basic drugs namely bepridil and amiodarone as seen in Figure 2.17 which are used clinically in the treatment of certain cardiovascular disorders. Amiodarone is a benzofuran derivative that is used as a class-III antiarrhythmic agent. Both drugs increased the endosomal pH mildly in therapeutic

doses and inhibited the cleaving ability of *β*-secretase. Additionally, both drugs modulated *γ*-secretase independently of the alkalinization technique [112].

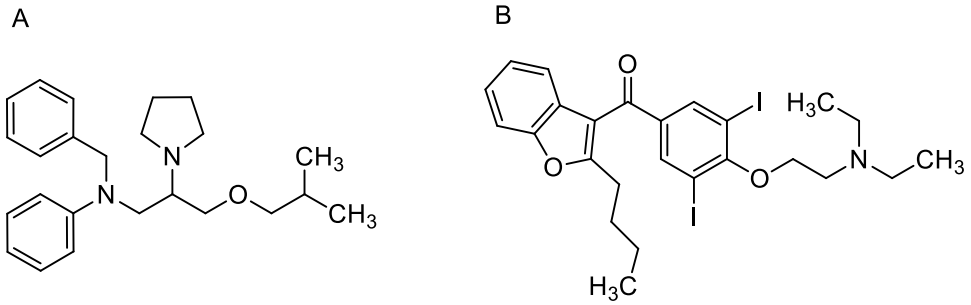


***Figure 2.17.*** Bepridil (A) and amiodarone (B) which showed β- and γ-secretase inhibition

A study by Onishi *et al*. (2011) showed that 2-methyl-5-(3-{4-[(S)-methylsulfinyl]
phenyl}-1-benzofuran-5-yl)-1,3,4-oxadiazole (MMBO) inhibited *tau* phosphorylation through the inhibition of glycogen synthase kinase-3 (GSK-3). *Tau* is a major component of the neurofibrillary tangles, a characteristic of AD. MMBO displayed activity *in vitro* and *in vivo*. It could decrease hippocampal tau phosphorylation and its chronic administration suppressed tau pathogenesis [113]. Moreover, a patent belonging to Davidowitz *et al*. (2021) included benzofuran analogs that inhibit the formation of tau oligomers [114]. However, a high-throughput screening by Crowe *et al*. (2007) to identify inhibitors of tau fibrillization resulted in false-positive compounds (false inhibitors of tau) including the class of benzofuran derivatives. The screening was achieved using a total of about 51000 compounds and led to identifying two 2,3-di(furan-2-yl)-quinoxalines as positive inhibitors of tau fibrillization [115]. The structure of the false-positive benzofuran derivative is shown in Figure 2.18 **- B**.

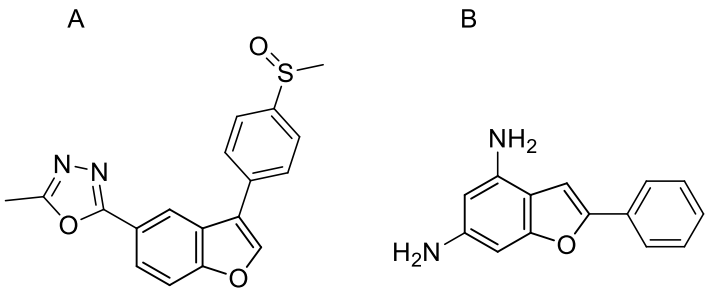


***Figure 2.18.*** Chemical structure of (A) MMBO, an inhibitor of GSK-3, (B) false tau fibrillization inhibitor [113, 115]

Another work by Baharlo *et al*. (2015) reported the synthesis of benzofuran-based N-benzylpyridinium derivatives and tested their AChE inhibitory activity. All of the synthesized compounds showed impressive activities with some reaching 7-folds more potency than that of donepezil [116]. The skeleton of the compounds is shown in Figure 2.19.

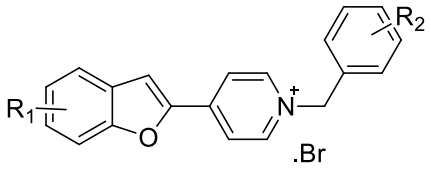


***Figure 2.19.*** The basic core skeleton of potent AChE inhibitor benzofuran derivatives [116]

Mostofi *et al*. (2015) designed and synthesized benzofuran derivatives with admirable AChE inhibitory activities. The compound shown in Figure 2.20 displayed equipotent AChE inhibition to that of the standard agent donepezil hydrochloride [117].

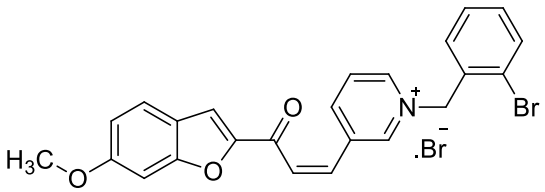


**Figure 2.20.** *Donepezil's equipotent inhibitor of AChE [117]*

Xiaoming *et al* (2015) synthesized 26 tacrine-benzofuran hybrid compounds and investigated their abilities to inhibit AChE, *β*-amyloid, and *β*-secretase which are thought to be key bio-targets in AD. The hybrid compound shown below Figure 2.21. displayed subnanomolar human AChE inhibition. Moreover, it showed good inhibitory activity of *β*-amyloid aggregation and *h*BACE-1 activity [89].

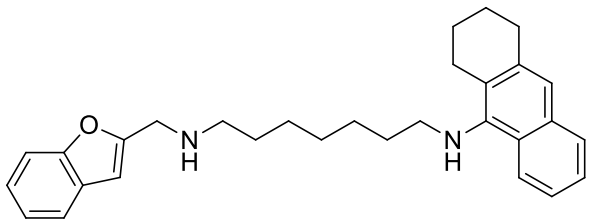


***Figure 2.21.*** AChE, BACE-1, and β-amyloid aggregation inhibitor reported by Xiaoming *et al*. [89]

Delogu *et al*. (2016) studied AChE and BChE inhibitory activities of synthesized 2-phenylbenzofuran derivatives. Most of the synthesized compounds showed selectivity toward BChE inhibition. Only one compound showed comparable BChE inhibitory activity to the standard drug galantamine ($IC_{50}$= 30.3 ± 1.9 and 28.3 ± 2.1 μM, respectively). The structure of the compound is shown in Figure 2.22 [118].

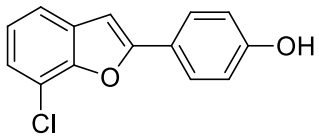


**Figure 2.22.** *2-phenylbenzofuran derivative as a BChE inhibitor [118]*

Another research by Pouramiri *et al*. (2016) also reported the synthesis of 2-phenylbenzofuran derivative as active AChE inhibitors. The most active compounds are illustrated in Figure 2.23. Compounds A and B showed 74.31 and 73.02 %inhibition in comparison to the reference donepezil at 23 μM concentration [119].

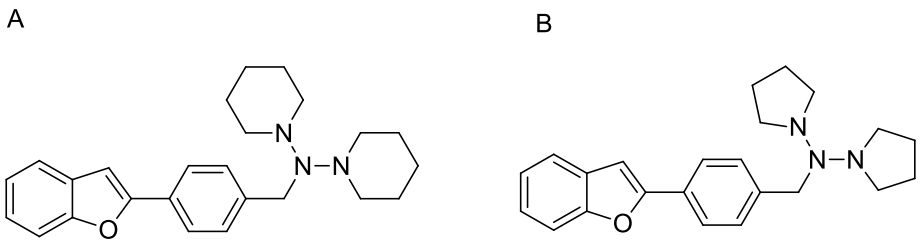


**Figure 2.23.** *2-arylbenzofuran derivatives as AChE inhibitors [119]*

Blain *et al*. (2016) reported that a benzofuran derivative named FRM-36143 and as shown in Figure 2.24 has γ-secretase modulating and β-amyloid reducing activities. They concluded that the compound was able to reverse the effect of presenilin mutations which are thought to be a cause of familial AD [120].

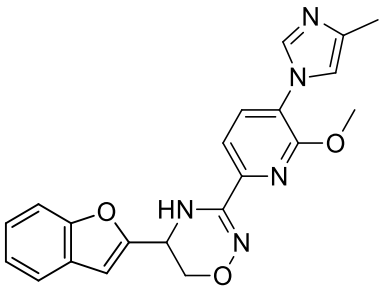

**Figure 2.24.** *Compound FRM-36143 [120]*

## 2.5. Alzheimer's Disease: An Overview

### 2.5.1. Definition and epidemiology

Alzheimer's disease (AD) is a neurodegenerative disorder that is characterized by a progressive deficit in memory and impaired cognitive and behavioral functions which ultimately results in dementia [121]. Clinically, it involves impairment of anterograde memory (memory responsible for learning new information), language visuospatial ability, praxis, and/or executive functioning. [122]. Following the onset of memory disturbances and one of the aforementioned impairments, behavioral features like depression, sleep disturbance, agitation, and psychosis may arise throughout the disease. Mild cognitive impairment (MCI) is a prodromal state that may precede the development of AD and affects people with memory difficulties only and those individuals are at greater risk to develop AD in the subsequent years [123]. AD is considered the leading cause of dementia with a worldwide prevalence of 3.9% in people aged 60 years and above [124]. It is thought to begin 20 years or more before symptoms arise [125]. The survival rate from the disease is low in young ages but it probably has not much importance if the disease is diagnosed in the elderly [123].

### 2.5.2. Mechanism of the disease

Accumulation of Aβ is the prevailing hypothesis for the pathogenesis of AD [126]. Amyloid precursor protein (APP) is a transmembrane protein produced in many cells including those of the central nervous system. APP undergoes cleavage through amyloidogenic and nonamyloidogenic pathways [127]. The second step in both pathways involves cleavage by γ-secretase. In the nonamyloidogenic pathway, the first step of APP cleavage is achieved by α-secretase to produce secreted APP (sAPP) which is an extracellular product in addition to a membrane-bound C-terminal 83 amino acid

fragment (C83). The amyloidogenic pathway's first step is carried out by β-secretase (or called BACE-1, β-site APP cleavage enzyme 1) which produces sAPPβ and C99. γ-secretase further cleaves C99 to produce extracellular Aβ and membrane-bound APP intracellular domain (AICD). Aβ is normally a soluble entity but it is thought that the overproduction or the reduced clearance of Aβ stimulates it to form oligomers leading to the formation of amyloid fibrils that ultimately forms the known Aβ plaques [126, 127].

Aβ is thought to be toxic in both soluble and insoluble forms [126, 128]. It affects cellular functions by inducing sequential events including hyperphosphorylation of the protein tau which leads to the production of neurofibrillary tangles (NFT), inflammation, oxidative stress, and excitotoxicity. These events cause cell death and impairment of the cholinergic neurotransmission [126]. Other studies suggest the independence of these events of the effects of Aβ initiation [129]. The whole mechanism is illustrated in Figure 2.25.

α-synuclein (α-syn) is a protein that accumulates in the Lewy bodies in the substantia nigra in Parkinson's patients. Aβ, tau, and α-syn were demonstrated to act like prions which means that they undergo refolding into infectious misfolded forms and might induce misfolding of other endogenous proteins. This mechanism attracted interest and is thought to be possible in causing neurodegenerative diseases including AD [130].

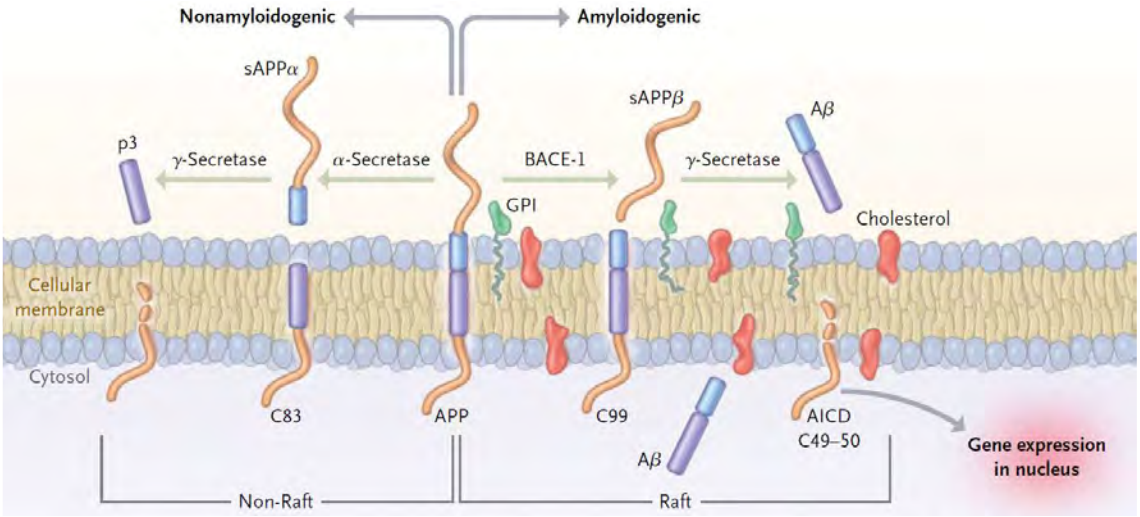


**Figure 2.25.** *Mechanism of AD [127]*

### 2.5.3. Risk and protective factors

Various factors that may contribute to AD include aging, family history, female gender, head injury and traumas, atherosclerosis, diabetes mellitus, hyperchromocysteinemia, metabolic syndrome, genetics, and Down's syndrome [122, 131–136]. Atherosclerotic conditions might also include hypercholesterolemia, hypertension, smoking, systemic inflammation, increased fat intake, and obesity [122, 136]. Genetic factors are classified according to the onset of the disease into those causing early-onset AD (EOAD) and those leading to late-onset AD (LOAD). EOAD causing mutated genes include amyloid precursor protein (APP), presenilin-1, and -2 (PSEN1, PSEN2) [137–139]. Apolipoprotein E (ApoE) functions as a carrier of cholesterol and has three forms ApoE2, ApoE3, and ApoE4. It was reported that ApoE4 is one of the non-negligible risk factors of AD [122].

As protective measures, different acts and factors can contribute to the putative inhibition of AD. Education, physical activity, and mind activating habits are among the preferable acts that could help protect against AD. The use of nonsteroidal anti-inflammatory drugs (NSAIDs) was reported to decrease the risk of AD in those individuals who suffer from certain inflammatory conditions and are at risk to develop AD [140, 141]. Other substances which have a positive protective effect include statins due to their role in lowering the cholesterol level which is thought to be one of AD risk factors [142]. A study showed that the use of niacin on a dietary basis may protect against AD and age-related cognitive impairments [143]. Although some researches indicated the possible role of oxidative stress in the pathogenesis of AD, other studies concluded insignificant relation of antioxidants to reduced risk of the disease [144, 145].

### 2.5.4. Treatment

Today, there is no proven method to slow, stop, or prevent AD. The current pharmacological treatments involve the use of agents that alleviate the symptoms of the disease. Cholinesterase inhibitors are the first-line treatments for mild to moderate cases of AD. Donepezil, galantamine, rivastigmine, and tacrine are approved cholinesterase inhibitors for use in AD. Memantine is an N-methyl-D-aspartate (NMDA) receptor antagonist. It is used to reduce the risk of excitotoxicity resulting from the over-stimulation by NMDA. Memantine can be used alone or as adjuvant to cholinesterase

inhibitors as needed particularly in severe cases. It might be helpful in the treatment of behavior disturbances [126, 146].

Certain medications are used for the management of mood changes, behavior, and sleep. Selective serotonin reuptake inhibitors (SSRIs) and some tricyclic antidepressants are the main groups used for such conditions. Escitalopram has superior benefits over other SSRIs and can be used as a first-line agent. Trazodone and mirtazapine have sedating properties making them preferable in mood and sleep disturbances simultaneously [126].

Various studies indicated the beneficial use of active or passive immunizations with Aβ. Schenk *et al*. (1999) showed that active immunization attenuated levels of Aβ in the brain of mice. Aβ plaques were prevented in young mice while the progression of AD-like neuronal deterioration was reduced in older mice [147]. Regarding passive immunization, the use of anti-Aβ antibodies reversed the deficits in memory of APP mouse model. It was suggested that a soluble pool of Aβ which is removable from the brain is responsible for the cognitive deficit and its removal by the immunization techniques led to increasing plasm levels of Aβ [121, 148].

# 3. MATERIALS

## 3.1. Chemicals

| | |
|---|---|
| 2′-Hydroxyacetophenone | Sigma-Aldrich, Germany |
| 2′-Hydroxy-5′-methoxyacetophenone | Aldrich, Germany |
| 2′-Hydroxy-5′-chloroacetophenone | Aldrich, Germany |
| 2′-Hydroxy-5′-nitroacetophenone | Aldrich, Germany |
| 2-Hydroxybenzaldehyde | Sigma-Aldrich, Germany |
| 2-Hydroxy-5-methoxybenzaldehyde | Sigma-Aldrich, Germany |
| 2-Hydroxy-5-chlorobenzaldehyde | Sigma-Aldrich, Germany |
| 2-Hydroxy-5-nitrobenzaldehyde | Sigma-Aldrich, Germany |
| N,N-dimethylformamide (DMF) | Sigma-Aldrich, Germany |
| Potassium carbonate | Sigma-Aldrich, Germany |
| Sodium hydroxide | Sigma-Aldrich, Germany |
| Thionyl chloride | Merck, Germany |
| Acetone | Merck, Germany |
| 1-Phenylpiperazine | Acros Organics, USA |
| 1-(2-Furoyl)piperazine | Aldrich, Germany |
| 1-Benzylpiperazine | Sigma-Aldrich, Germany |
| 1-Methylpiperazine | Aldrich, Germany |
| 1-Ethylpiperazine | Aldrich, Germany |
| 1-[2-(Dimethylamino)ethyl]piperazine | Acros Organics, USA |
| Ethyl acetate | Honeywell, Riedel-de-Haen, Germany |
| Petroleum ether | Riedel-de-Haen, Germany |
| n-Hexane | Honeywell, Riedel-de-Haen, Germany |
| Diethyl ether | Sigma-Aldrich, Germany |
| Ethanol | Merck, Germany |
| DMSO-d6 | Merck, Germany |
| Hydrochloric acid | Sigma-Aldrich, Germany |
| Chloroform | Sigma-Aldrich, Germany |
| Diethylether | Sigma-Aldrich, Germany |

| | |
|---|---|
| TLC plates silica gel 60 F254 | Merck, Germany |
| AChE-E.C.3.1.1.7, electric eel | Sigma, Germany |
| BChE-E.C. 3.1.1.8, equine serum | Sigma, Germany |
| Acetylcholine iodide (ATC) | Fluka, Germany |
| Butyrylcholine iodide (BTC) | Fluka, Germany |
| Donepezil | Sigma, Germany |
| Horseradish peroxidase | Sigma, Germany |
| Ampiflu$^{TM}$ red | Sigma, Germany |
| Beta Amyloid 1-42 (Aβ42) Ligand Screening Assay kit | Biovision, USA |
| NIH/3T3 cell line | ATCC, USA |
| PBS | Gibco, UK |
| Trypsin | Sigma, Germany |
| EDTA | Sigma, Germany |
| MTT dye | Sigma, Germany |

### 3.2. Instruments and Tools

| | |
|---|---|
| Electronic balance | Mettler Toledo, USA |
| Melting-point apparatus | Barnstead Electrothermal, UK |
| Incubator | Heraeus, Germany |
| Infrared spectrophotometer | Shimadzu-IR Affinity-1S, Japan |
| Mass spectrophotometer | Shimadzu, LCMS-IT-TOF, Japan |
| Magnetic stirrer and heater | Heidolph, MR 3003, Germany |
| Nuclear magnetic resonance spectrometer | Bruker, Ultrashield 300 MHz, USA |
| Sterile cabinet | Class II Type A2 (CHC-222A2-60), South Korea |
| Ultraviolet lamp | Camag, Switzerland |
| Vortex | Wisemix, South Korea |

# 4. METHODS

## 4.1. Chemical Synthesis Methods

### 4.1.1. A general method for the synthesis of 3, 5-substituted ethyl benzofuran-2-carboxylate (A)

Eight different substituents were used in the synthesis of ethyl benzofuran-2-carboxylate as illustrated in Figure 4.1. The substituents in position 5 included H, $OCH_3$, Cl, and $NO_2$ whereas the substituents in position 3 were H and $CH_3$. 5-substituted-2-hydroxyacetophenone (15 mmol) was weighed into a flask, and then 50 mL of N, N-dimethylformamide (DMF) as a solvent and 2 equivalents of potassium carbonate ($K_2CO_3$) as a catalyst were added, successively. Ethyl 2-bromoacetate (1 equivalent) was added lastly at once (no need for gradual addition) using a pipette at room temperature (RT) while the mixture is being stirred. The mixture was stirred for five minutes at RT then heated at 120°C for 2 hours. The reaction's endpoint was monitored *via* thin-layer chromatography (TLC) and compact mass spectrometry (CMS). The mixture was then cooled to RT and poured gradually into ice water with vigorous stirring. The formed precipitate was obtained *via* filtration. The dry product was recrystallized from ethanol.

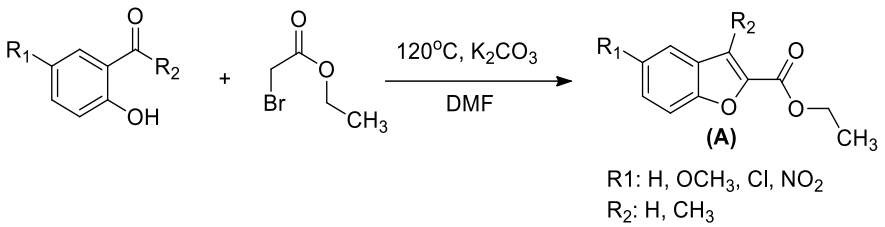


**Figure 4.1.** *Synthesis of 5,3-substituted ethyl benzofuran-2-yl carboxylate*

### 4.1.2. Synthesis of 3, 5-substituted benzofuran-2-carboxylic acid (B)

Products obtained from method **A** were hydrolyzed using a strong base as illustrated in Figure 4.2. 11 mmol of **A** was weighed into a flask and 50 mL of 2 M aqueous NaOH solution was added. The starting materials **A** are not soluble normally in aqueous solutions and could be observed floating on the top of the solvent. The mixture was stirred vigorously under reflux for 8 hours. The dissolution of the starting substance is an indication of hydrolysis. The reaction was monitored *via* TLC and CMS. After the reaction's ending, the mixture was cooled down to RT and acidified using 10% HCl

solution. The formed precipitate after acidification was obtained *via* filtration. The well-dried product was used in the next reaction without further processing.

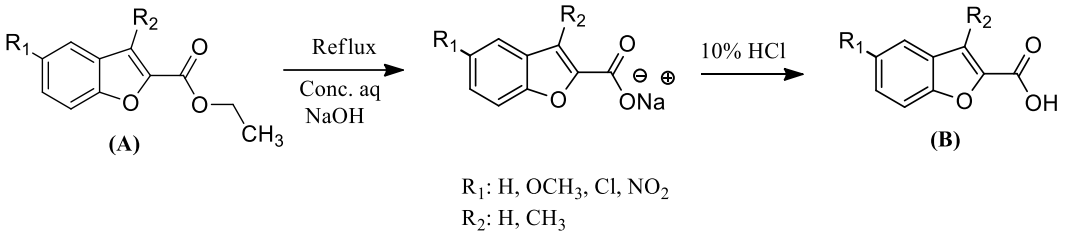


**Figure 4.2.** *Synthesis of 5,3-substituted ethyl benzofuran-2-carboxylic acid*

### 4.1.3. Synthesis of 3, 5-substituted benzofuran-2-carbonyl chloride (C)

To activate the carbonyl group for the reaction with a nucleophile, product **B** was first chlorinated using thionyl chloride ($SOCl_2$) as seen in Figure 4.3. About 10 mmol of **B** was weighed into a flask followed by gradual addition of $SOCl_2$ (10 mL $SOCl_2$ for every 1 g of **B**) while stirring. $SOCl_2$ served both as a reactant and a solvent, hence no other solvent was used. The mixture was stirred for 10 minutes at RT then refluxed for 4 hours. The reaction's ending was monitored *via* TLC and CMS. The mixture was cooled down to RT after the reaction was finished. The content of the flask was emptied into a beaker which was left in the hood to allow $SOCl_2$ to evaporate. Without further processing, the obtained solid product was stored in air-tight vials between 2-8°C in the refrigerator till the next usage.

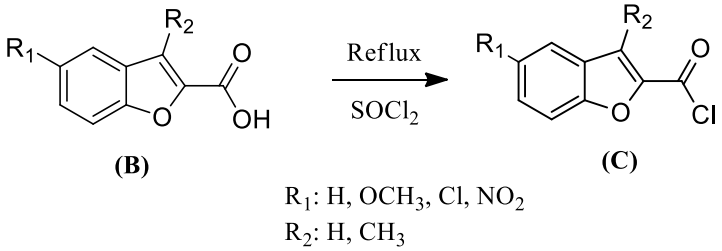


**Figure 4.3.** *Synthesis of 5,3-substituted ethyl benzofuran-2- carbonyl chloride*

### 4.1.4. Synthesis of (3, 5-substituted benzofuran-2-yl)(piperazin-1-yl)methanone derivatives (D1-D42)

The targeted products were synthesized by reacting **C** products with piperazine derivatives as shown in Figure 4.4. The obtained target products are shown in Table 4.1.

It should be mentioned that all of the derivatives synthesized in the context of this thesis are new except compounds **D11**, **D18**, and **D37** which are previously synthesized in the literature, and the details are given in **section 5.1**. Piperazine derivative (1.5 mmol) was weighed into a flask and solved with 30 mL of acetone. Potassium carbonate (3 mmol) was then added, and the mixture was stirred at RT for 5 minutes. Compound **C** (1.5 mmol) was added lastly into the mixture at once (no need for gradual addition). The reaction proceeded for 1 hour at RT. The endpoint of the reaction was monitored using TLC and CMS. The mixture was transferred into a beaker and placed in the hood to evaporate the solvent. The products were worked-up according to their state of matter as follows:

- The liquid products were separated from the remaining $K_2CO_3$ by extraction using chloroform, as a solvent, and filtration. The filtrate containing the target products was left in the hood to allow chloroform to evaporate and the remaining liquids were stored in an air-tight vial without further treatment.
- The solid products were obtained by solving the residue in water and filtration. The solid residues on the filter paper were washed several times using water then dried. The products were recrystallized from ethanol.

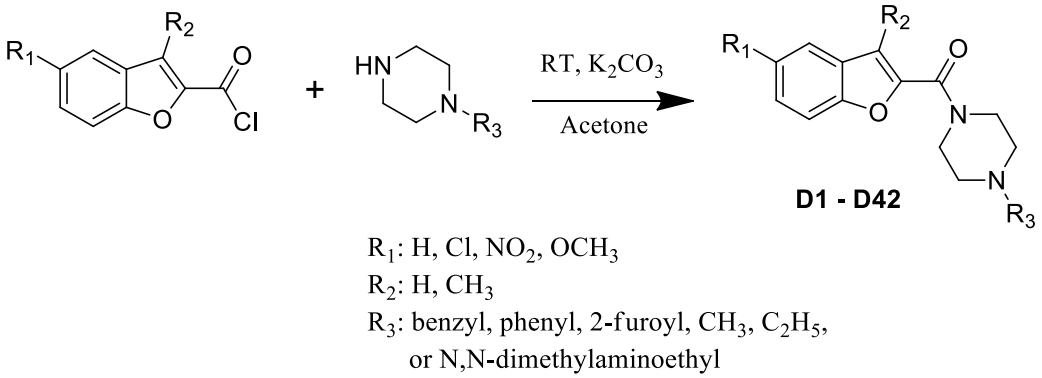


**Figure 4.4.** *Synthesis of (benzofuran-2-yl)(piperazin-1-yl) methanone derivatives*

**Table 4.1.** *Targeted (benzofuran-2-yl)(piperazin-1-yl) methanone products*

| Compound code | $R_1$ | $R_2$ | $R_3$ |
|---|---|---|---|
| **D1** | H | $CH_3$ | Phenyl |
| **D2** | H | $CH_3$ | 2-Furoyl |
| **D3** | H | $CH_3$ | $CH_3$ |
| **D4** | H | $CH_3$ | $C_2H_5$ |
| **D5** | H | $CH_3$ | N,N-dimethylaminoethyl |
| **D6** | H | H | Phenyl |
| **D7** | H | H | 2-Furoyl |
| **D8** | H | H | $CH_3$ |
| **D9** | H | H | $C_2H_5$ |
| **D10** | H | H | N,N-dimethylaminoethyl |
| **D11** | Cl | $CH_3$ | Phenyl |
| **D12** | Cl | $CH_3$ | 2-Furoyl |
| **D13** | Cl | $CH_3$ | $CH_3$ |
| **D14** | Cl | $CH_3$ | $C_2H_5$ |
| **D15** | Cl | $CH_3$ | N,N-dimethylaminoethyl |
| **D16** | Cl | H | Phenyl |
| **D17** | Cl | H | 2-Furoyl |
| **D18** | Cl | H | $CH_3$ |
| **D19** | Cl | H | $C_2H_5$ |
| **D20** | Cl | H | N,N-dimethylaminoethyl |
| **D21** | $NO_2$ | $CH_3$ | Phenyl |
| **D22** | $NO_2$ | $CH_3$ | 2-Furoyl |
| **D23** | $NO_2$ | $CH_3$ | $CH_3$ |
| **D24** | $NO_2$ | $CH_3$ | $C_2H_5$ |
| **D25** | $NO_2$ | $CH_3$ | N,N-dimethylaminoethyl |
| **D26** | $NO_2$ | H | Phenyl |
| **D27** | $NO_2$ | H | 2-Furoyl |
| **D28** | $NO_2$ | H | $CH_3$ |
| **D29** | $NO_2$ | H | $C_2H_5$ |
| **D30** | $NO_2$ | H | N,N-dimethylaminoethyl |
| **D31** | $OCH_3$ | $CH_3$ | Phenyl |
| **D32** | $OCH_3$ | $CH_3$ | 2-Furoyl |
| **D33** | $OCH_3$ | $CH_3$ | $CH_3$ |
| **D34** | $OCH_3$ | $CH_3$ | $C_2H_5$ |
| **D35** | $OCH_3$ | $CH_3$ | N,N-dimethylaminoethyl |
| **D36** | $OCH_3$ | $CH_3$ | Benzyl |
| **D37** | $OCH_3$ | H | Phenyl |
| **D38** | $OCH_3$ | H | 2-Furoyl |
| **D39** | $OCH_3$ | H | $CH_3$ |
| **D40** | $OCH_3$ | H | $C_2H_5$ |
| **D41** | $OCH_3$ | H | N,N-dimethylaminoethyl |
| **D42** | $OCH_3$ | H | Benzyl |

## 4.2. Chemical Analysis

### 4.2.1. High-resolution mass spectrometry (HRMS)

A liquid chromatography-mass spectrometer instrument with a combined ion trap and time-of-flight technology (LCMS-IT-TOF) (Shimadzu, Kyoto, Japan) was used. The samples were prepared in acetonitrile and filtered through 22 μm pore size filters into flacon vials where 1 mL of the sample solution was required. The samples were analyzed in positive and negative mode by an electrospray ionization (ESI) technique. Acetonitrile containing 0.1% formic acid and water was used as a gradient mobile phase system. Shim-Pack FC-ODS (150 x 2 mm, 2 μm) C18 HPLC column was used for the analysis in which reversed-phase chromatographic separation was carried out. A sample volume of 20 μL was injected by the autosampler into the LC. Following the chromatographic separation, the eluted product was sent to the MS and ionized *via* the ESI method and the mass spectrum was recorded.

### 4.2.2. Proton nuclear magnetic resonance ($^{1}$H NMR) spectrometry

Bruker UltraShield 300 MHz (United States) was used for $^{1}$H NMR analysis. The samples (10 μg) were prepared in 0.5 mL deuterated dimethylsulphoxide (DMSO-$d_6$) each, and tetramethylsilane (TMS) was used as a reference standard.

### 4.2.3. Carbon-13 nuclear magnetic resonance ($^{13}$C NMR) spectrometry

The same Bruker UltraShield instrument was used to obtain the $^{13}$C NMR of the prepared substances. DMSO-$d_6$ was used as a solvent in the preparation of the samples (10 μg sample/ 0.5 mL). TMS was also used as the internal standard. The magnetic field was set to 75 MHz.

### 4.2.4. Infra-red (IR) spectrometry

The IR spectra of the synthesized compounds were obtained *via* Shimadzu-IR Affinity-IS instrument. The sample application was achieved by placing 10 mg of substance (either solid or liquid) into the attenuated total reflection (ATR) chamber. The spectrum was then obtained, and the detection of the peaks was achieved automatically.

### 4.3. Monitoring of the Chemical Reactions

#### 4.3.1. Thin-layer chromatography (TLC)

All the reactions were followed up and monitored *via* TLC. Merck silica gel 60 $F_{254}$ (silica gel coated with fluorescent indicator $F_{254}$) aluminum TLC plates and Ultraviolet (UV) Cabinet with 254 and 365 nm UV modes were used. Each sample from the reaction medium was dissolved by heating in ethanol for compounds **A** and **D1**-**D42**, and in DMF for compounds **B** and **C**. The reaction samples were applied on the baseline of TLC plates together with reference substances of the reactants. The mobile phase used was petroleum ether: ethyl acetate in 9:1 and 1:1 proportion for the TLC of compounds **A** and **D1**-**D42**, respectively. The separation process in the TLC of compounds **B** and **C** needed a more polar mobile phase, and for this reason, the polarity was increased by the addition of ethanol to the previous mobile phase to be in 1:1:2 proportion petroleum ether: ethyl acetate: 96% ethanol. All of the reactants and products were detectable under 254 nm wavelength except ethyl bromoacetate, and methyl, ethyl, and N,N-dimethylaminoethyl derivatives of piperazine which were undetectable under any wavelength.

#### 4.3.2. Compact mass spectrometry

Advion's Expression-S Compact Mass Spectrometer (CMS) was used for the follow-up of the reactions altogether with TLC. The sampling was achieved using an Atmospheric Solids Analysis Probe (ASAP) method where a minimum amount of the sample is provided to the mass spectrometer after it is spiked using a specialized sampling probe. The mass/charge (m/z) range was set between 80-500 where the substances' molecular weights can be detected. Atmospheric Pressure Chemical Ionization (APCI) is the fragmentation technique used by the instrument. The results were provided as a spectrum of relative intensity against m/z.

### 4.4. Melting Point Determination

Mettler Toledo-MP90 Melting Point System was used for the determination of the melting point of the solid compounds. Capillary tubes were closed on one side and the solid samples were inserted through the opened side. The capillary tube was filled up to 0.5 cm from the bottom. Six samples could be inserted at the same time into the heating chamber of the instrument. The temperature was set between 50°C at the start and 300°C

at the end. A video was recorded for each melting point determination of each six-sample batch. The melting point was detected appropriately by investigating the recorded videos.

### 4.5. Anti-Acetylcholinesterase (AChE) Activity Investigation

The inhibition potentials of the synthesized compounds against acetylcholinesterase were investigated. All the solutions for the biologic activity studies were prepared fresh and used during 7 days from their preparation. During the biological activity studies, ultrapure water was used for the preparation of the solutions. Ultrapure water was obtained by Millipore, Milli-Q Synthesis A10 distillation unit. BioTek-Precision Power (USA) robotic pipetting system was used for the required volume measurements of the solvents and solutions. The spectrophotometric absorbance measurements of the prepared samples in 96-will plates were achieved using BioTek-Synergy H1 Microplate Reader (USA).

The biological activity investigations were achieved in two stages. First, the test compounds were prepared in $10^{-3}$ and $10^{-4}$ M concentrations in 2% DMSO and evaluated for their inhibition activity percentage (0-100%) against acetylcholinesterase enzyme. Secondly, compounds that have more than 50% inhibition rate in their $10^{-4}$ M concentrations were then prepared in smaller concentrations down to $10^{-9}$ and evaluated accordingly. In this study, the inhibition activity of the synthesized compounds against AChE and BChE enzymes was evaluated using a modified Ellman method [149].

#### 4.5.1. Preparation of AChE and BChE enzymes solutions

To prepare the enzymes solutions, a 1% gelatin solution in water was prepared to dissolve the AChE and BChE enzymes. The enzymes were prepared in 500 U/mL concentration using the gelatin solution as a solvent. To prepare a stock solution of 5 U/mL concentration, 1 mL of the prepared enzyme solution was diluted to 100 mL in water using a volumetric flask. The stock solution was then divided into 0.7 mL portions and stored at -20°C. Before using the enzyme solution portions for the activity tests, they were melted, and their temperature was increased to room temperature. The concentration of each portion was then diluted to 2.5 U/mL using water by completing their 0.7 mL volumes to 1.4 mL.

### 4.5.2. Preparation of acetylthiocholine iodide (ATC) solution (0.075 M)

0.217 g of ATC was dissolved in water and the volume was made to 10 mL. The solution was divided into 0.4 mL portions and stored at -20°C till the next usage.

### 4.5.3. Preparation of butyrylthiocholine iodide (BTC) solution (0.075 M)

0.237 g of BTC was dissolved in water and its volume was completed into 10 mL. This solution was divided into 0.4 mL portions and stored at -20°C till the next usage.

### 4.5.4. Preparation of 5,5-dithiobis(2-nitrobenzoic acid) (DTNB) solution (0.01 M)

0.396 g of DTNB was dissolved in water. 0.15 g of sodium bicarbonate was added to the solution and the volume of the mixture was completed to 100 mL. The solution was divided into 3 mL portions and stored at -20°C till the next usage.

### 4.5.5. Preparation of phosphate buffer solution (pH= 8.0)

Amount of 13.61 g potassium dihydrogen phosphate was dissolved in 1 L of water. The pH of the prepared solution was set into 8±0.1 using a 0.1 N potassium hydroxide solution and controlled *via* a pH meter. The solution was then filtered through a 0.22 µm pore filter and stored at 4°C till its next use.

### 4.5.6. AChE and BChE inhibition tests

A modified Ellman method was used to study the ability of the synthesized compounds to inhibit the targeted enzymes. The temperature of the stored test solutions was brought to 20-25°C before starting the tests. 96-well plates were used for the tests and a total of 210 µL of the test mixture was placed in each well. The 210 µL test solution per well contained 140 µL phosphate buffer, 20 µL enzyme, 20 µL inhibitor, 20 µL DTNB, and 10 µL ATC/BTC solution. Before mixing these solutions, they were grouped into two main solutions. The first solution mixture included 70 µL buffer, 20 µL enzyme, and 20 µL DTNB while the second solution mixture was composed of 70 µL buffer and 10 µL ATC/BTC.

To start the test, the first solution mixture and the test compound solution as an inhibitor were placed in each well (110 µL first mixture, 20 µL inhibitor/well) using Biotek Precision pipetting system. Four replicates for each concentration of the inhibitor

were achieved. Then, the plate was placed in Biotek-Synergy H (USA) microplate reader to mix the content of the plate for 5 minutes. The plate was then incubated at 25°C for 15 minutes. After the incubation, the second test mixture (80 μL) was added to each well of the plate using the dispenser of the microplate reader. The contents of the plate were mixed for 30 seconds then the first absorbance reading at 412 nm was obtained. The plate's contents were mixed for further 5 minutes to finish their reaction and a second absorbance reading was obtained after that.

The %inhibition was obtained by the following formula after calculating the difference between the first and second absorbance readings: 4.1)

B: Blank (solution mixture with no test compound and substrate (ATC/BTC))

C: Control (solution mixture with no test compound)

A(B): absorbance readings difference of the blank

A(C): absorbance readings difference of the control

A(I): absorbance readings difference of the respective test compound

The $IC_{50}$ value was calculated for each compound from the inhibition curve obtained using Microsoft Office Excel-360. The inhibition curve was drawn using non-linear regression analysis of the sigmoid dose-response curve.

### 4.6. β-Amyloid Aggregation Inhibition Activity

A fluorometric method was used in testing the ability of the compounds to inhibit the aggregation of Aβ [149]. Amyloid-Beta 1-42 (Aβ42) Ligand Screening Assay kit (BioVision, Milpitas, CA, USA) was used.

### 4.7. Prediction of the Pharmacokinetic Profile

The pharmacokinetic profile of the most active compounds was predicted *via* in silico means using the SwissADME database [150, 151]. The required properties like lipophilicity, water-solubility, absorption from gastrointestinal tract (GIT), blood-brain barrier permeability, permeation through the skin, number of violations to Lipinski's rule-of-five (drug-likeness) [152, 153], and number of hydrogen-bond (H-bond) acceptors and donors were calculated. The calculated predictions of the target compounds were compared to those of the reference drug donepezil.

### 4.8. Cytotoxicity Investigation

To study the safety of the most active molecules on normal cells, Maurine embryonic fibroblast NIH/3T3 (American Type Culture Collection ATCC CRL-1658$^{TM}$) cell line was used. Dulbecco's Minimum Essential Medium supplemented with 10% fetal bovine serum and 1% penicillin-streptomycin (100 IU/mL – 100 mg/mL) was used.

#### 4.8.1. Cell culture

Under sterile conditions, cell culture was carried out using NIH/3T3 cell line and Dulbecco's medium. The cells were produced by incubation at 37ºC in a 5% $CO_2$ atmospheric environment. The cells were subcultured and proliferated by trypsinization once or twice a week.

#### 4.8.2. The proliferation of the cells

Following the incubation period, the medium was removed and trypsin-EDTA (Ethylene diamine tetraacetate) solution was added to the flasks (1X) (3-5 mL for 75 mL volumes and 1-3 mL for 25 mL volumes). The flasks then were kept in the incubator for 3 – 5 minutes. The cells were checked whether they separated or not from the surface using a microscope. At least twice the volume of trypsin-EDTA solution was added to the cells, which were separated from the surface by gentle tapping when necessary. A cell suspension was then separated by pipetting. The cell suspension was centrifuged at 1200 rotation per minute (rpm) for 5 minutes at +4ºC followed by the removal of the supernatant. A suitable volume of medium was added by pipetting to the formed cell pellet to form a suspension. The cell count was performed after mixing 10 µL of cell suspension and 10 µL of trypan blue solution.

NIH/3T3 cells were seeded into 96-well plates by adding 1 x $10^4$ cells/100 µL in each well and incubated for 24 h. At the end of the incubation period, the upper part of the cell culture plates was removed by inversion. The cells then were washed with phosphate buffer and the washing solution was removed from the medium. After incubation, 8 different concentrations in the range 1 – 0.000316 mM of the test compounds **D25**, **D30**, **D40**, and **D41** were prepared using solvent and medium. The prepared concentrations were added to each well of the plate where 8 repetitions were achieved for each concentration. Growth solvent (medium only) and control solution

(solvent and medium used to dissolve the test compounds) were added to the wells and the plates were incubated for 24 h. After the incubation, the solvents in the wells were removed.

MTT solution was prepared in 5 mg/mL concentration using phosphate buffer (PBS). This solution was diluted in 1: 10 proportion using medium and 10 µL (0.5 mg/mL) was added to each well and incubated for 3 h. The MTT solution was then removed by inverting the plates. Next, 100 µL of dimethylsulfoxide (DMSO) was added to each well dissolving the previously formed formazan salts. The plates were shaken gently to mix the contents and the absorbance was read at 540 nm in a microplate reader. % inhibition values were calculated for each concentration of the thesis substances (**D25**, **D30**, **D35**, and **D41**). The $IC_{50}$ values of the substances were determined by non-linear regression analysis and their cytotoxic properties were interpreted. MTT cytotoxicity test was repeated 3 times.

### 4.9. Molecular Docking

The most active compounds which showed good AChE inhibitory activity were evaluated for their binding patterns to the active site of the enzyme. For this reason, molecular docking was achieved using Schrodinger's Maestro interface 2020. The required protein crystal of AChE (PDB: 4EY7) was downloaded from the protein data bank (PDB) and processed using the Protein Preparation Wizard tool of Maestro. AChE crystal was preprocessed followed by the deletion of chain B-D. Optimization was eventually performed. The test molecules were optimized using LigPrep tool of Maestro. The bond lengths and most stable conformers of these ligands were optimized using OPLS3e force field. The same force field protocol was also applied in the preparation of the protein crystal. Finally, the required grid was prepared using Glide and molecular docking was achieved using the same tool.

# 5. RESULTS AND DISCUSSION

## 5.1. Synthesis of the Targeted Products

The targeted products were synthesized through four steps. The general plan started by Rap-Stoermer benzofuran synthesis as the major nucleus in the targeted products. Rap-Stoermer synthesis involves the reaction of 2-hydroxyacetophenone derivatives with α-brominated carbonyl compounds *e.g.* ethyl 2-bromoacetate. The presence of a base as a catalyst is mandatory as illustrated in the mechanism in **Figure 5.2**. All the compounds were derivatives of ethyl benzofuran-2-carboxylate from which the next synthesis proceeded. Different yields were obtained possibly due to the activation and deactivation of the respective ring systems used by the action of the groups at positions 5 and 3 of benzofuran. Those yields were enough to proceed to the next reaction.

The next reaction involved the hydrolysis of the ester at position 2 of benzofuran. Basic hydrolysis was achieved using a 2 M aqueous solution of NaOH and reflux. It is noteworthy to mention that all of the benzofuran reactants were poorly soluble in aqueous solvents, but the suspended reactants were gradually dissolved in the basic solution under reflux which was an indication of successful hydrolysis as the resulting carboxylic acid salts with sodium are soluble in aqueous solutions. To get the carboxylic acid derivatives out of their solutions, they were expelled out of their salts by acidifying the solutions and they were precipitated in pure forms.

The carboxylic acids were then chlorinated to their respective acyl chlorides. The carboxylic acids are weak toward the reaction with amines in contrast to very reactive acyl chlorides. Hence, the carboxylic acids were converted into their very reactive acyl chloride forms. The chlorination was achieved by refluxing the acids in $SOCl_2$. $SOCl_2$ was chosen over other chlorinating reagents for its volatility which facilitates the reaction's work-up by just evaporating the reagent at RT in the hood. The chlorination yields are admirably high and only little loss was observed.

The final reaction in the synthesis plan involved reacting the acyl chlorides with various piperazine derivatives to attain the targeted products. Schotten-Baumann reaction conditions were used in the synthesis of the final products. Schotten-Baumann reaction involves the acylation of amines with acyl chlorides under basic conditions. $K_2CO_3$ was enough to neutralize the acid resulting from the acylation reaction and thus prevent the acid from reacting with the unreacted amines which would have diminished the yields.

This reaction proceeded by $SN_2$ mechanism as piperazines are secondary amine derivatives [154, 155].

As stated before in **section 4.1.4**, the synthesized compounds are new derivatives of benzofuran except compounds **D11**, **D18**, and **D37** which are previously synthesized by other researchers who used them for different therapeutic targets. Compound **D11** was synthesized by Youssif *et al*. [156] and investigated for its antitumor activity which was reported to be low in comparison to the reference doxorubicin. On the other hand, compound **D18** was synthesized by Engelhardt *et al*. [157] and was tested for its histamine-4 receptor inhibitory activity. The compound showed pKi of 6.6±0.1 as binding affinity to the histamine-4 receptor. Finally, compound **D37** was also previously synthesized by Zour *et al*. [158] and was investigated for its neuropharmacological action. As a result, the three compounds **D11**, **D18**, and **D37** are not original in this thesis and were synthesized to protect the integrity of the planned design in the thesis.

### 5.1.1. Rap-Stoermer synthesis of ethyl 3, 5-substituted benzofuran-2-carboxylate

Eight different products were synthesized according to method A described in **section 4.1.1**. The yield differed according to each product but, in general, the range was between 27-87%. Derivatives having methyl group at position 3 of benzofuran had yields of 42%, 79%, 55%, 27% when the 5-substituent was H, $OCH_3$, Cl, and $NO_2$, respectively. The yields of the unsubstituted derivatives at position 3 were 65%, 87%, 63%, and 50% for 5-substitution with H, $OCH_3$, Cl, and $NO_2$, respectively. The general structure is illustrated in Figure 5.1 and the mechanism of Rap-Stoermer synthesis is shown in Figure 5.2.

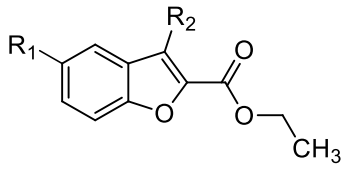


$R_1$: H, $OCH_3$, Cl, NO2

$R_2$: H, $CH_3$

**Figure 5.1.** *Ethyl benzofuran-2-carboxylate derivatives*

The colors of 3-methylated H, $OCH_3$, Cl, and $NO_2$ derivatives are white, light-brown, light-brown, and orange, respectively; while those of the 3-unsubstituted

derivatives are white for all of them except the 5-$NO_2$ substituted derivative, which has a pale-yellow color.

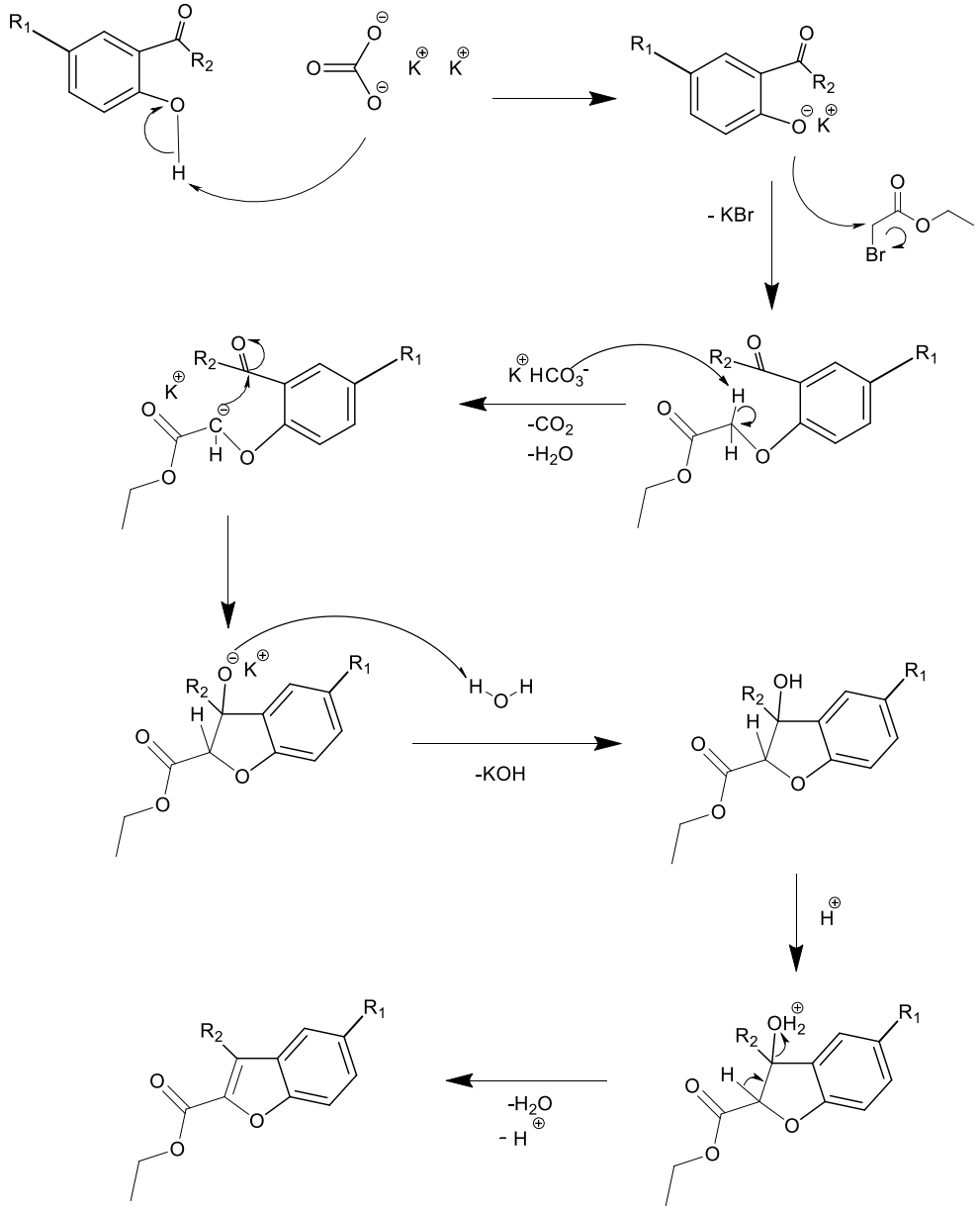


**Figure 5.2.** *Reaction mechanism of Rap-Stoermer synthesis of benzofuran*

### 5.1.2. Synthesis of 3, 5-substituted benzofuran-2-carboxylic acid (B)

The compounds obtained from method **A** were hydrolyzed using a concentrated aqueous solution of sodium hydroxide as described in **section 4.1.2**. Derivatives having methyl group at position 3 of benzofuran had yields of 93%, 84%, 82%%, 76% when the 5-substituent was H, $OCH_3$, Cl, and $NO_2$, respectively. The yields of the derivatives

lacking the methyl group at position 3 were 74%, 78%, 91%, and 82% for 5-substitution with H, $OCH_3$, Cl, and $NO_2$, respectively.

The colors of the 3-methyl substituted derivatives were light-brown, brown, white, and dark brown for H, $OCH_3$, Cl, and $NO_2$ substitutions at position 5, respectively. Whereas the color of the 3-unmethylated derivatives was white for all of them except the 5- $NO_2$ derivative which was brown. The mechanism of the base-catalyzed hydrolysis of these esters is illustrated in Figure 5.3 [155].

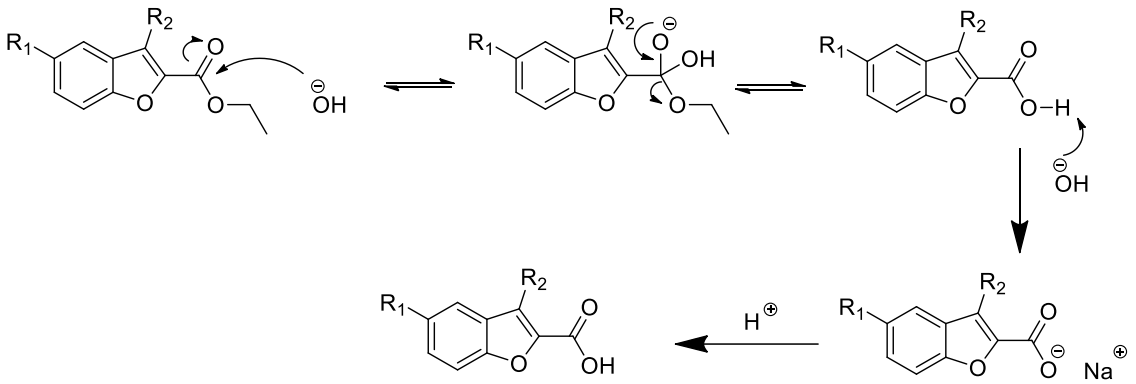


**Figure 5.3.** *Mechanism of base-catalyzed hydrolysis of the benzofuran esters [155]*

### 5.1.3. Synthesis of 3, 5-substituted benzofuran-2-carbonyl chloride (C)

Benzofuran-2-carboxylic acid derivatives gained by method **B** were chlorinated using thionyl chloride as described in **section 4.1.3**. Yields were 95, 88, 90, and 70% for the 3-methyl derivatives of 5- H, $OCH_3$, Cl, and $NO_2$-benzofuran, respectively. Those of the 3-unmethylated derivatives were 96, 94, 95, and 83%, respectively.

The colors of the obtained products as respective to 5- H, $OCH_3$, Cl, and $NO_2$ were brown, dark brown, yellowish-white, and reddish-brown for the 3-methylated derivatives. While the color of the 3-unmethylated ones was white for all of them except the 5- $NO_2$-benzofuran derivative which was brown. The mechanism of chlorinating carboxylic acids to produce acid chlorides using $SOCl_2$ is illustrated in Figure 5.4 as described by Clayden *et al*. [155].

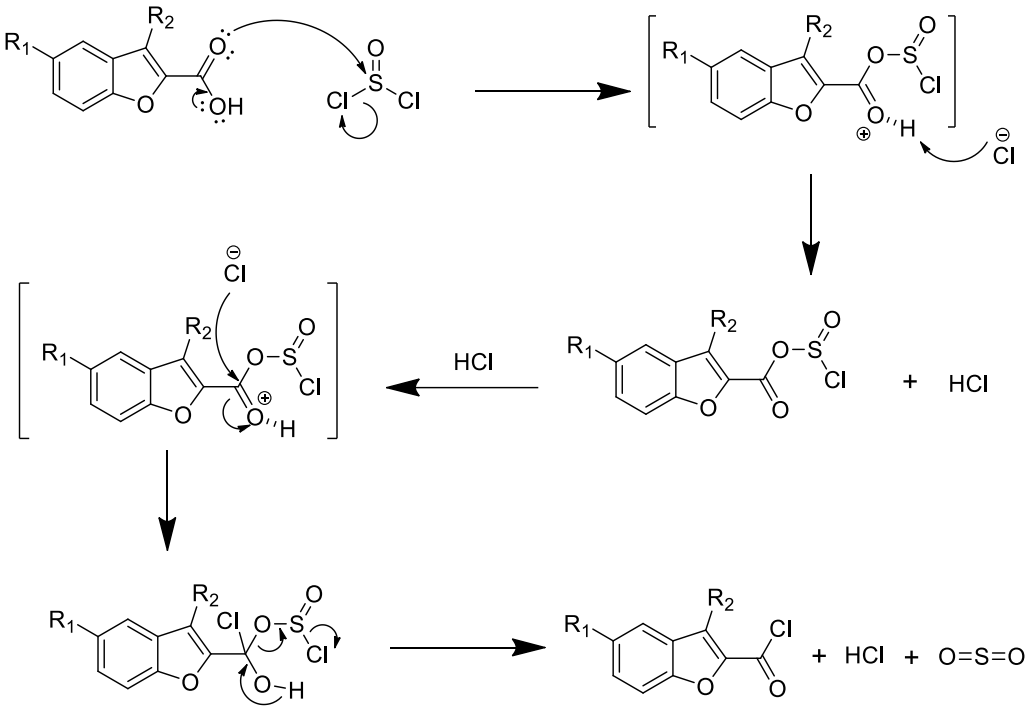


**Figure 5.4.** *Mechanism of chlorination of benzofuran-2-carboxylic acid [155]*

### 5.1.4. Schotten-Baumann synthesis of (3, 5-substituted benzofuran-2-yl)(piperazin-1-yl)methanone derivatives (D1-D42)

The targeted products were obtained using a nucleophilic substitution reaction as described in **section 4.1.4** and by the mechanism of Schotten-Baumann in Figure 5.5. The products were approved relying on the analytical monographs which are detailed in the following subsections.

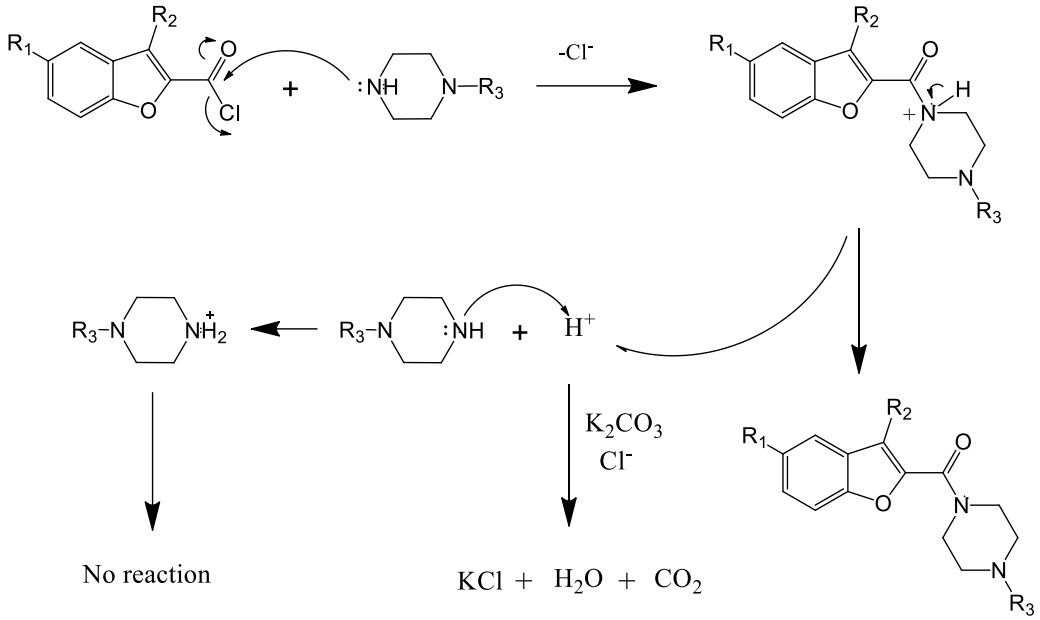


**Figure 5.5.** *Mechanism of Schotten-Baumann describing the synthesis of amide products* ***D1-D42***

### 5.1.4.1. *(3-methylbenzofuran-2-yl)(4-phenylpiperazin-1-yl)methanone (D1)*

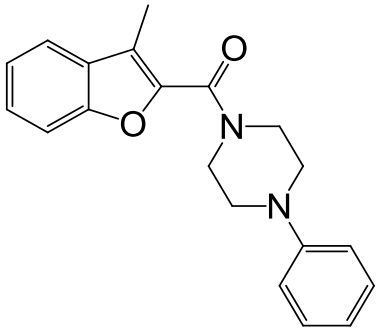


**Figure 5.6.** *Molecular structure of compound **D1***

**Physical Properties: Texture:** solid crystals, **Melting Point (M.P.):** 109-111ºC**, Color:** light brown, **Yield:** 75%.

**IR (ATR) $\upsilon_{max}$ ($cm^{-1}$):** 3060 ($SP^2$ C-H stretching, aromatic), 2927-2798 ($SP^3$ C-H stretching, methylenes of piperazine), 1614 (C=O stretching, amide), 1435 (C=C stretching, aromatic), 1290-1209 (C-O stretching, ether), 1147, 1004 (C-N stretching, tertiary amine and/or ether), 930-695 (C-H aromatic out-of-plane bending).

**$^1$H NMR (300 MHz) (DMSO-$d_6$) $\delta$ (ppm):** 2.37 (s, 3H, **3-methyl**benzofuran), 3.21 (brs, 4H, piperazine-3, 5), 3.77 (t, *J*= 4.76 Hz, 4H, piperazine-2, 6), 6.82 (t, *J*= 7.25 Hz, 1H, phenyl-4), 6.97 (d, *J*= 7.91, 2H, phenyl-2, 6), 7.23 (t, *J*= 7.41, 2H, phenyl-3,5), 7.34 (t, *J*= 7.03 Hz, 1H, benzofuran-5), 7.45 (t, *J*= 7.74 Hz, 1H, benzofuran-6), 7.62 (d, *J*= 8.24 Hz, 1H, benzofuran-7), 7.72 (d, *J*= 7.61Hz, 1H, benzofuran-4).

**$^{13}$C NMR (300 MHz) (DMSO-$d_6$) $\delta$ (ppm):** 9.04 (**3-methyl**benzofuran), 42.25 (piperazine), 46.12 (piperazine), 49.22 (piperazine), 112.06, 116.43, 119.06, 119.80, 119.93, 121.22, 123.69, 126.99, 128.95, 129.48, 144.18, 151.17, 153.39, 160.27 (benzofuran-**CO**-piperazine).

**HRMS (m/z):** $[M + 1]^+$ calculated: 321.1598; found: 321.1598.

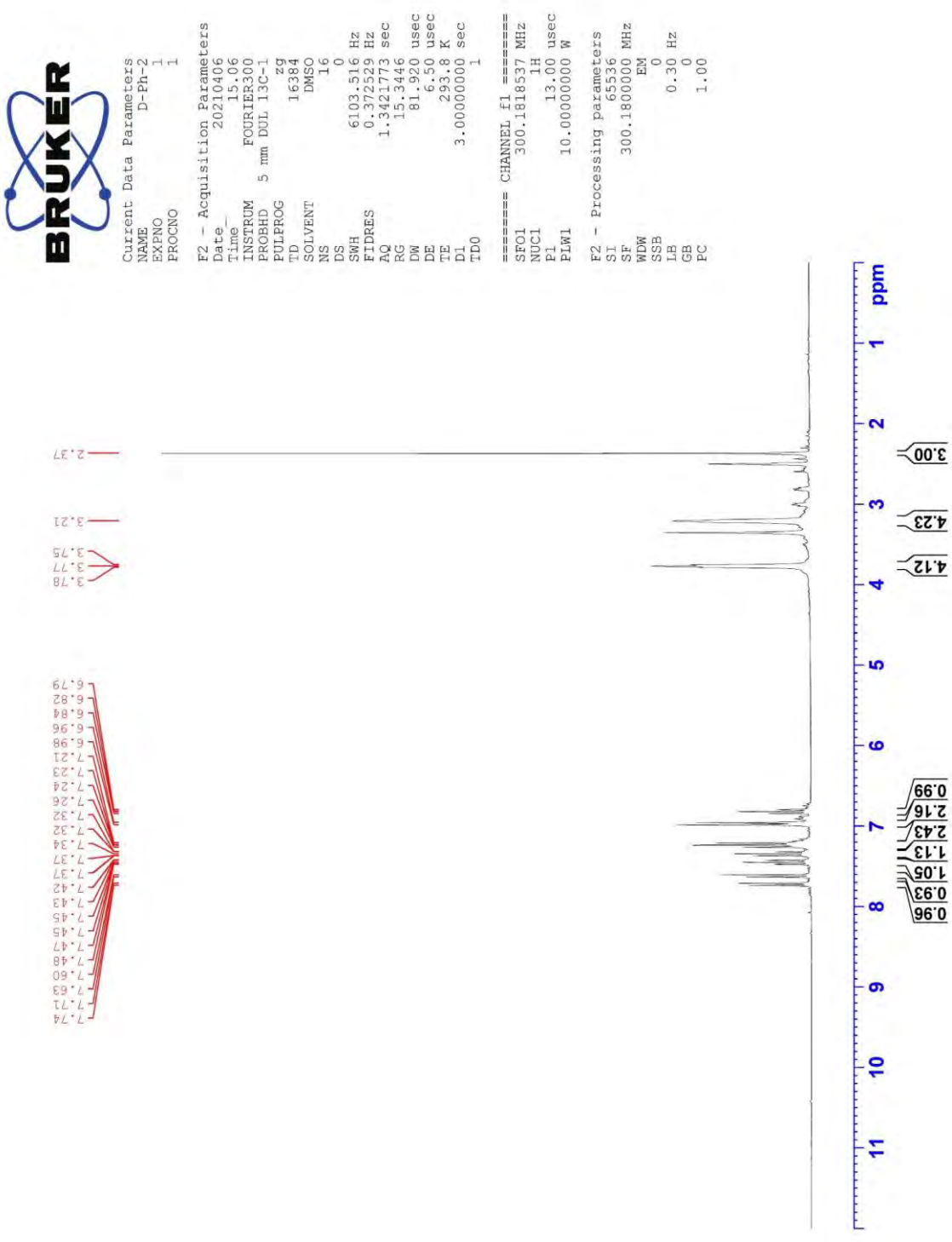


**Figure 5.7.** *$^{1}$H NMR spectrum of compound **D1***

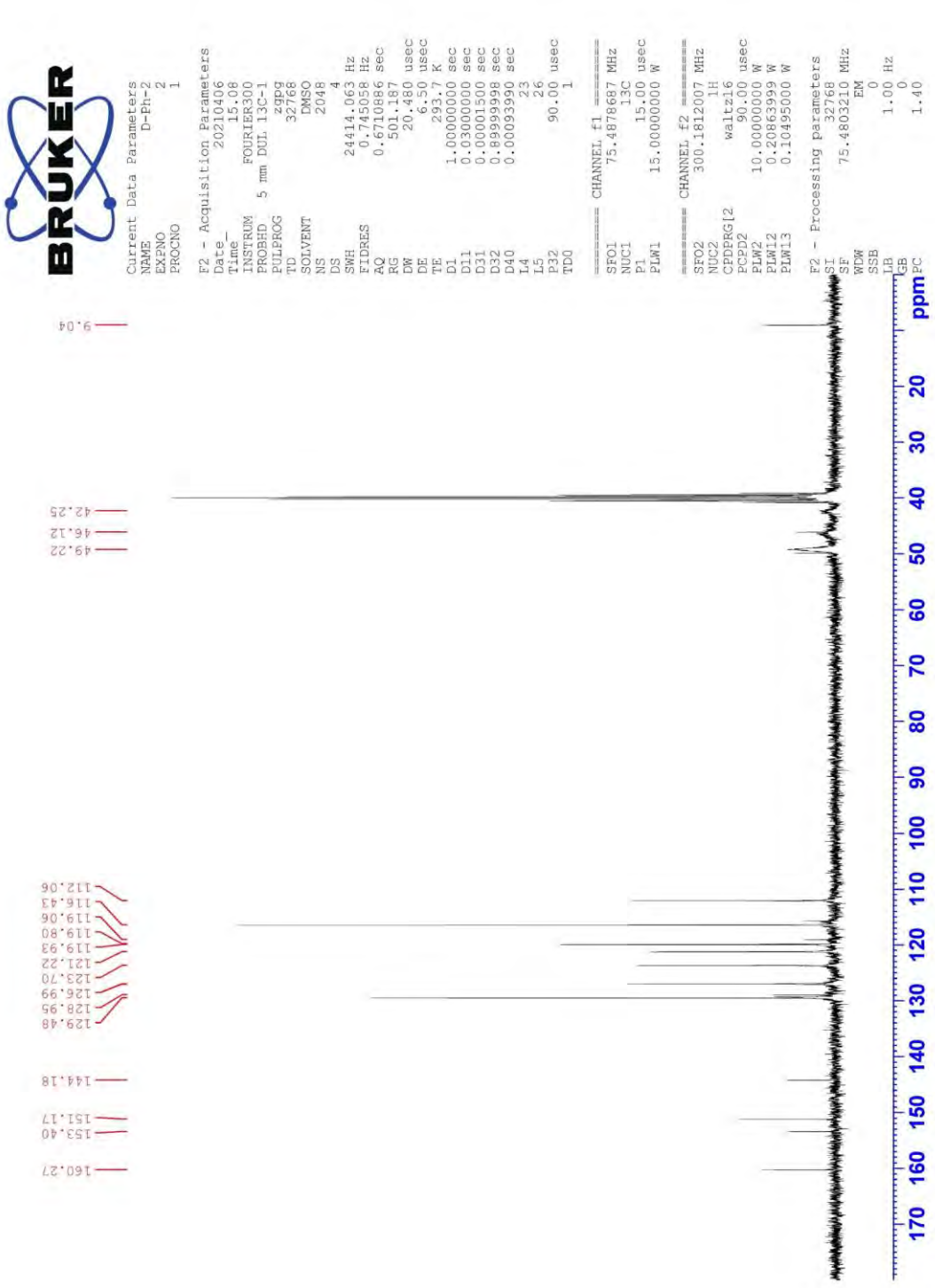


**Figure 5.8.** *$^{13}$C NMR spectrum of compound **D1***

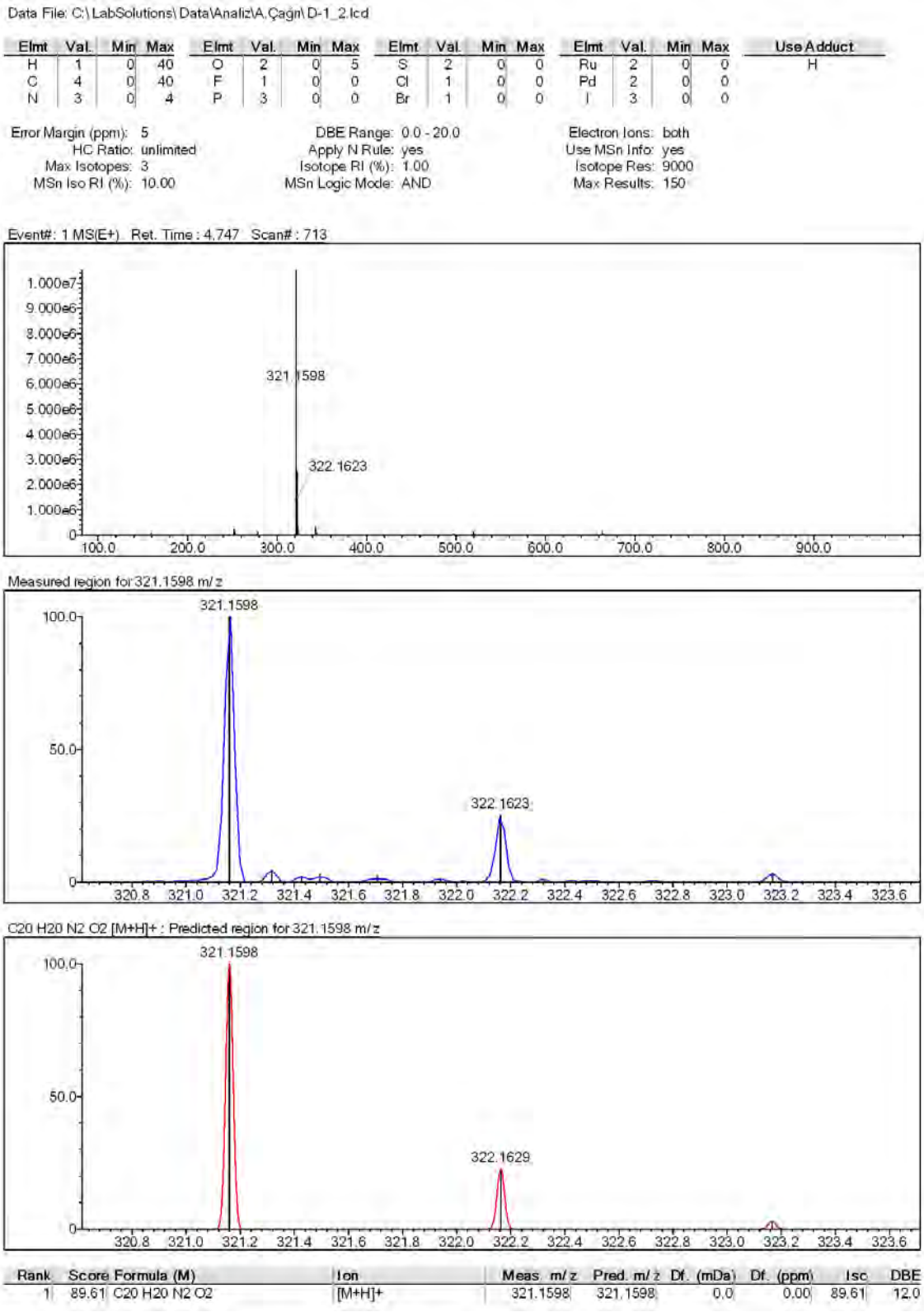


**Figure 5.9.** *High-resolution mass spectrum of compound **D1***

DOPNALAB

| | Item | Value |
|---|---|---|
| | Acquired Date&Time | 27.05.2021 14:52:02 |
| | Acquired by | System Administrator |
| | Filename | C:\Users\dopnalab\Desktop\sa\11.ispd |
| | Spectrum name | 11 |
| | Sample name | 1 |
| | Sample ID | |
| | Option | |
| | Comment | |
| | No. of Scans | 15 |
| | Resolution | 4 [cm-1] |
| | Apodization | Happ-Genzel |

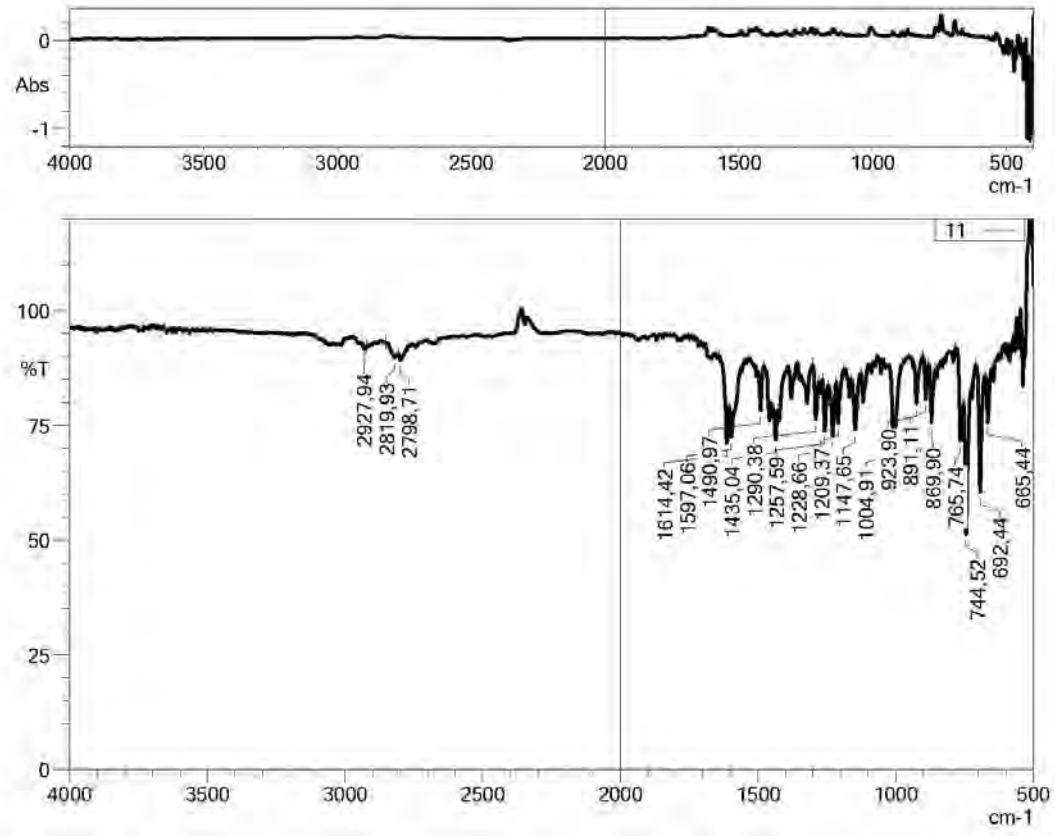


**Figure 5.10.** *IR spectrum of compound **D1***

### 5.1.4.2. *(4-(furan-2-carbonyl)piperazin-1-yl)(3-methylbenzofuran-2-yl)methanone (D2)*

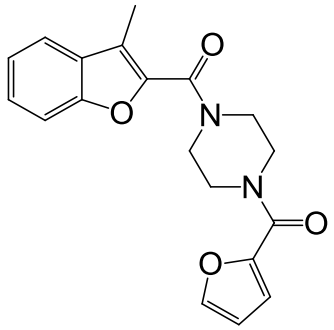

**Figure 5.11.** *Molecular structure of compound **D2***

**Physical Properties: Texture:** solid crystals, **Color:** white, **M.P.:** 90-92ºC**, Yield:** 95%.

IR (ATR) $\upsilon_{max}$ ($cm^{-1}$): 3100-3003 ($SP^2$ C-H stretching, aromatic), 2916-2860 ($SP^3$ C-H stretching, methylenes of piperazine), 1620 (C=O stretching, amide), 1485-1423 (C=C stretching, aromatic), 1255 (C-O stretching, ether), 1163, 1001 (C-N stretching, tertiary amine and/or ether), 933-665 (C-H aromatic out-of-plane bending).

$^1$H NMR (300 MHz) (DMSO-$d_6$) $\delta$ (ppm): 2.38 (s, 3H, **3-methyl**benzofuran), 3.72-3.74 (m, 8H, piperazine-2, 3, 5, 6), 6.65 (dd, *J*= 3.45, 1.73 Hz, 1H, furan-4), 7.05 (d, *J*= 3.44 Hz, 1H, furan-3), 7.34 (t, *J*= 7.01 Hz, 1H, benzofuran-5), 7.45 (t, *J*= 7.74 Hz, 1H, benzofuran-6), 7.62 (d, *J*= 8.24 Hz, 1H, benzofuran-7), 7.73 (d, *J*= 7.58 Hz, 1H, benzofuran-4), 7.87 (d, *J*= 0.97 Hz, 1H, furan-5).

$^{13}$C NMR (300 MHz) (DMSO-$d_6$) $\delta$ (ppm): 9.08 (**3-methyl**benzofuran), 42.41 (piperazine), 46.77 (piperazine), 111.87, 112.10, 116.46, 120.15, 121.25, 123.71, 127.06, 128.93, 143.95, 145.43, 147.16, 153.41, 158.91(piperazine-**CO**-furan), 160.48 (benzofuran-**CO**-piperazine).

**HRMS (ESI) (m/z) $[M+1]^+$:** for $C_{19}H_{18}N_2O_4$ calculated: 339.1339; found: 339.1340.

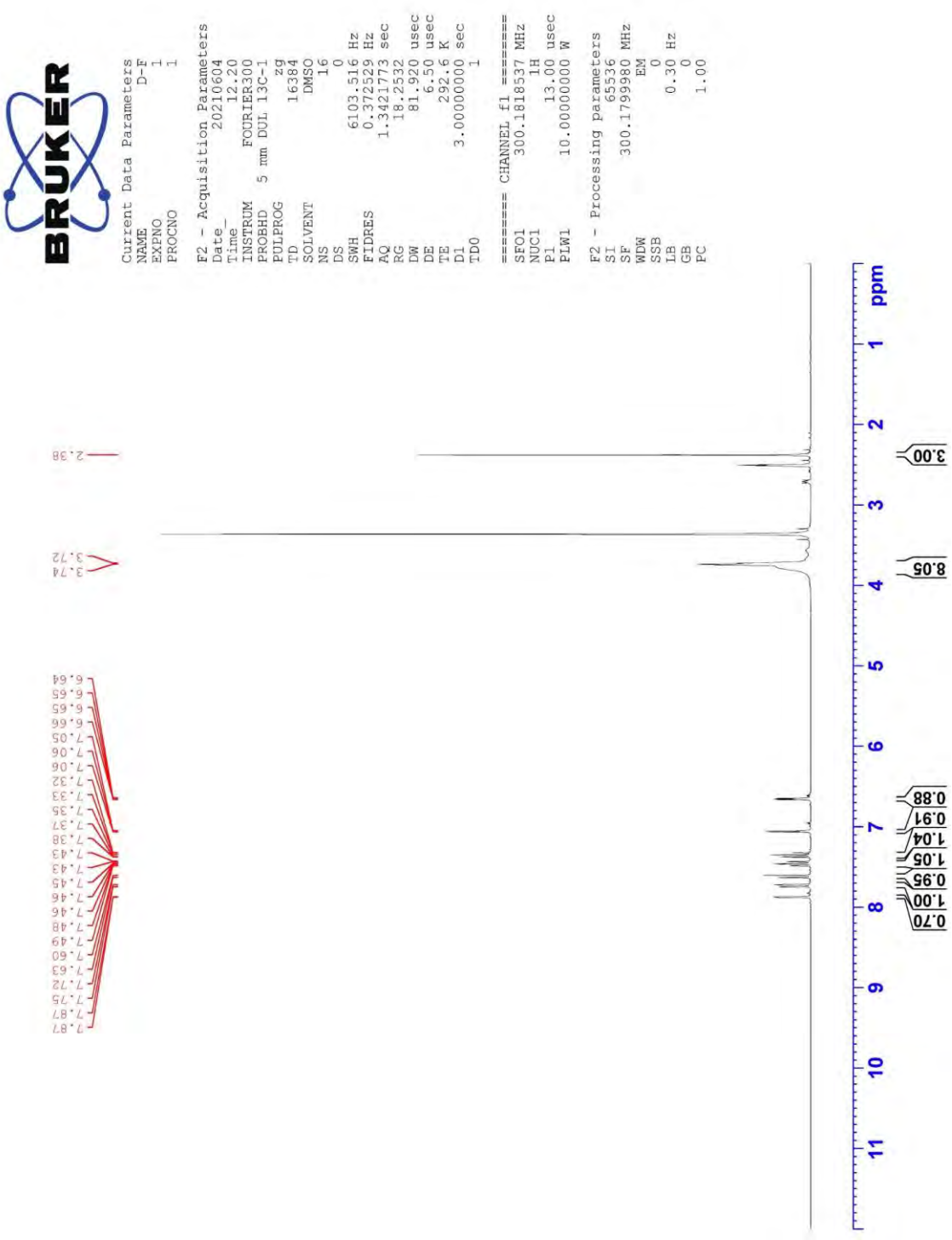


**Figure 5.12.** *$^{1}H$ NMR spectrum of compound **D2***

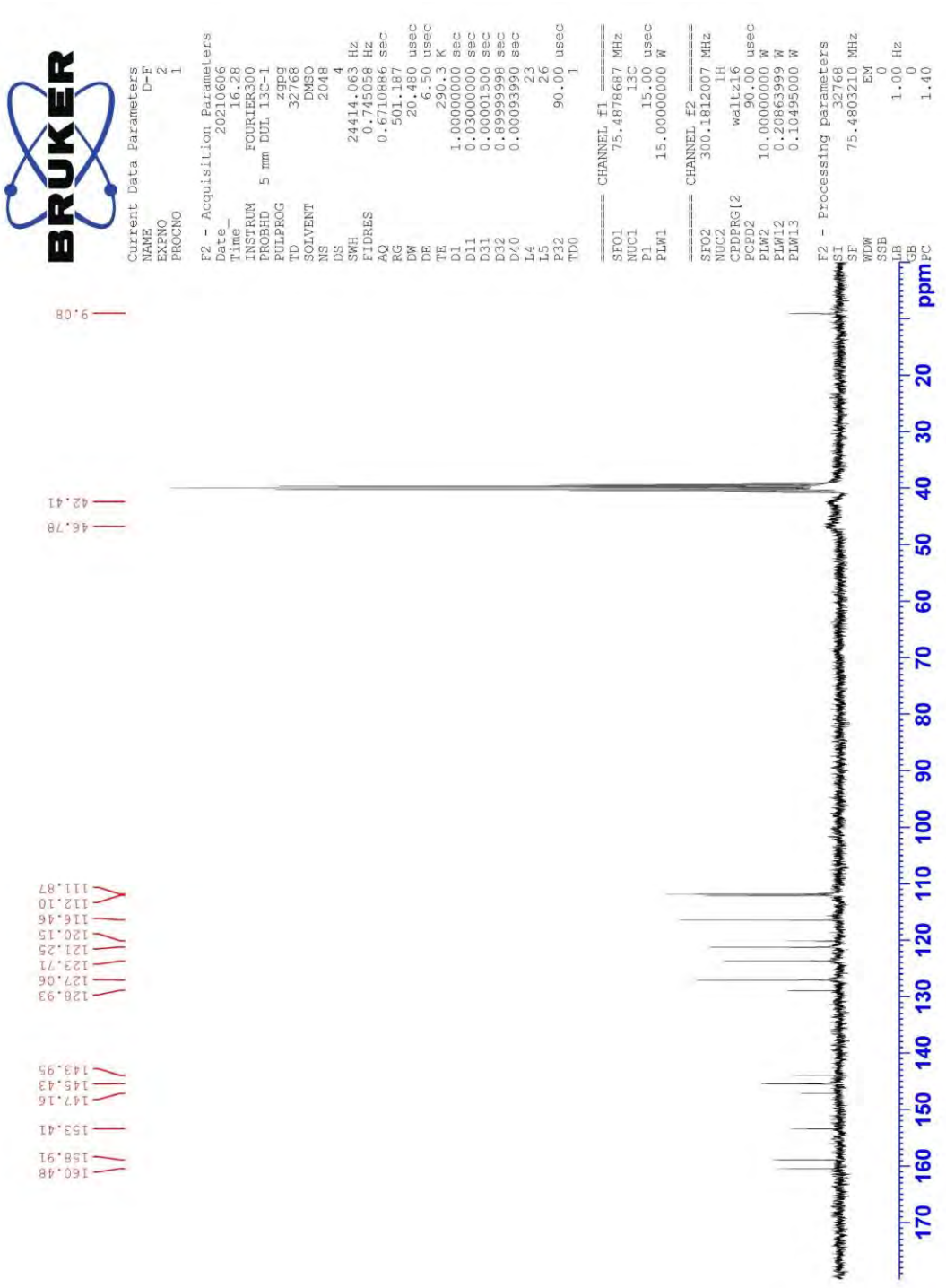


**Figure 5.13.** *[13]C NMR spectrum of compound **D2***

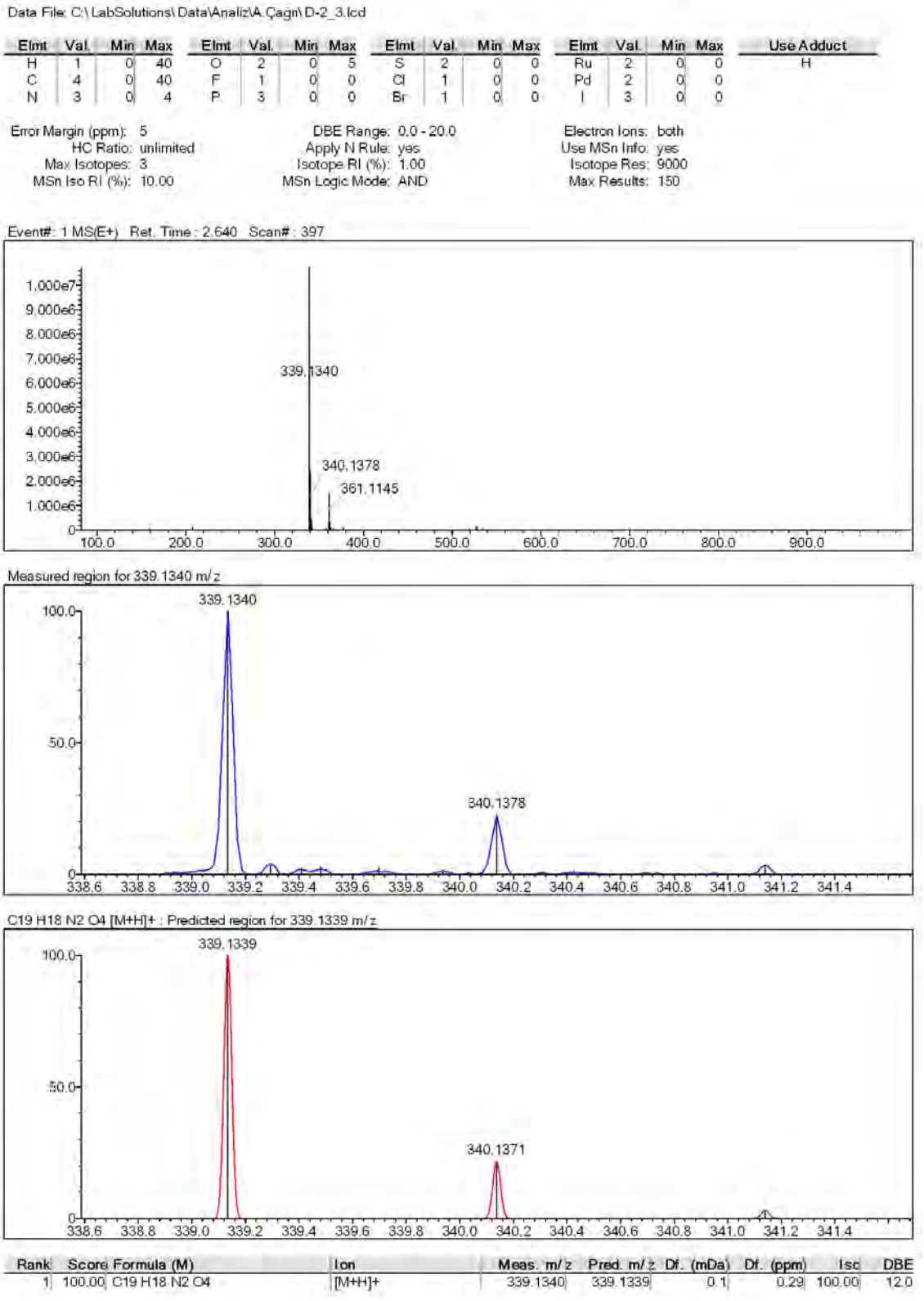


**Figure 5.14.** *High-resolution mass spectrum of compound* ***D2***

DOPNALAB

| | Item | Value |
|---|---|---|
| | Acquired Date&Time | 27.05.2021 14:58:19 |
| | Acquired by | System Administrator |
| | Filename | C:\Users\dopnalab\Desktop\sa\21.ispd |
| | Spectrum name | 21 |
| | Sample name | 2 |
| | Sample ID | |
| | Option | |
| | Comment | |
| | No. of Scans | 15 |
| | Resolution | 4 [cm-1] |
| | Apodization | Happ-Genzel |

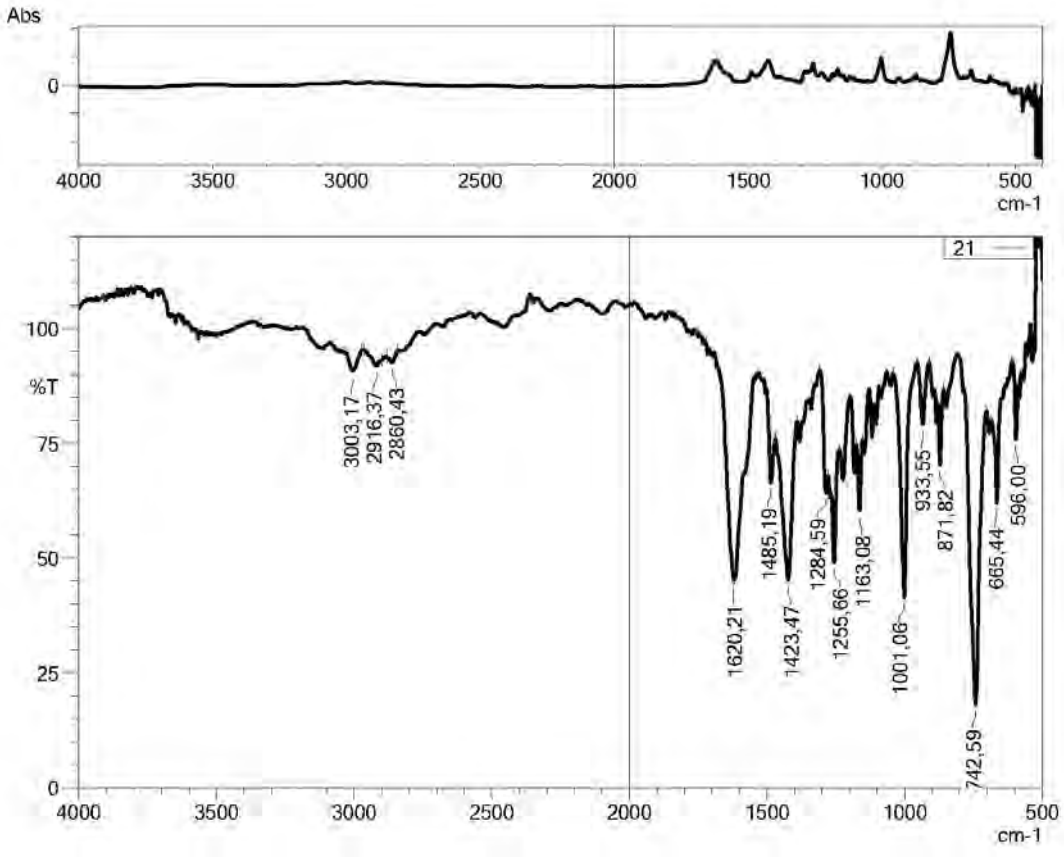


**Figure 5.15.** *IR spectrum of compound **D2***

### 5.1.4.3. *(3-methylbenzofuran-2-yl)(4-methylpiperazin-1-yl)methanone (D3)*

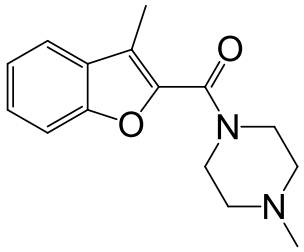


**Figure 5.16.** *Molecular structure of compound **D3***

**Physical Properties: Texture:** dense liquid, **Color:** dark-brown, **Yield:** 83%.

IR (ATR) $\upsilon_{max}$ ($cm^{-1}$): 2937-2791 ($SP^3$ C-H stretching, methylenes of piperazine, and 4-methyl piperazine), 1625 (C=O stretching, amide), 1435 (C=C stretching, aromatic), 1294-1261 (C-O stretching, ether), 1166-1138, 1016-1001 (C-N stretching, tertiary amine and/or ether), 871-667 (C-H aromatic out-of-plane bending).

$^1$H NMR (300 MHz) (DMSO-$d_6$) $\delta$ (ppm): 2.20 (s, 3H, **4-methyl**piperazine), 2.33 (s, 3H, **3-methyl**benzofuran), 2.35 (t, *J*= 4.52 Hz, 4H, piperazine-3, 5), 3.59 (brs, 4H, piperazine-2, 6), 7.32 (t, *J*= 7.45 Hz, 1H, benzofuran-5), 7.43 (t, *J*= 7.04 Hz, 1H, benzofuran-6), 7.59 (d, *J*= 8.23 Hz, 1H, benzofuran-7), 7.70 (d, *J*= 7.19 Hz, 1H, benzofuran-4),

$^{13}$C NMR (300 MHz) (DMSO-$d_6$) $\delta$ (ppm): 8.92 (**3-methyl**benzofuran), 42.41 (piperazine), 46.06 (**4-methyl**piperazine), 46.84 (piperazine), 55.16 (piperazine), 112.02, 119.24, 121.14, 123.64, 126.84, 128.92, 144.31, 153.38, 160.26 (benzofuran-**CO**-piperazine).

**HRMS (ESI) (m/z) $[M+1]^+$:** for $C_{15}H_{18}N_2O_2$ calculated: 259.1441; found: 259.1441.

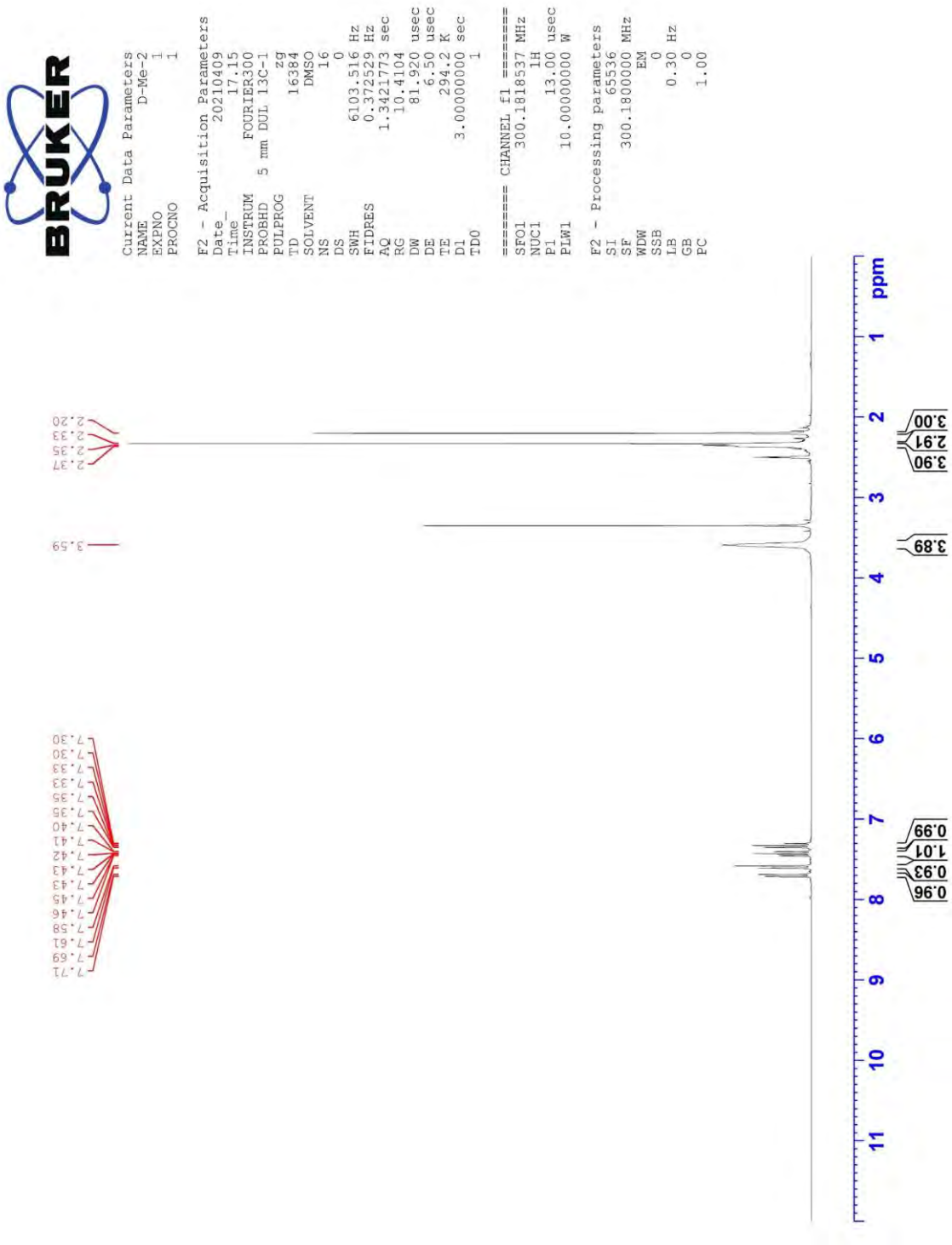


**Figure 5.17.** *1H NMR spectrum of compound **D3***

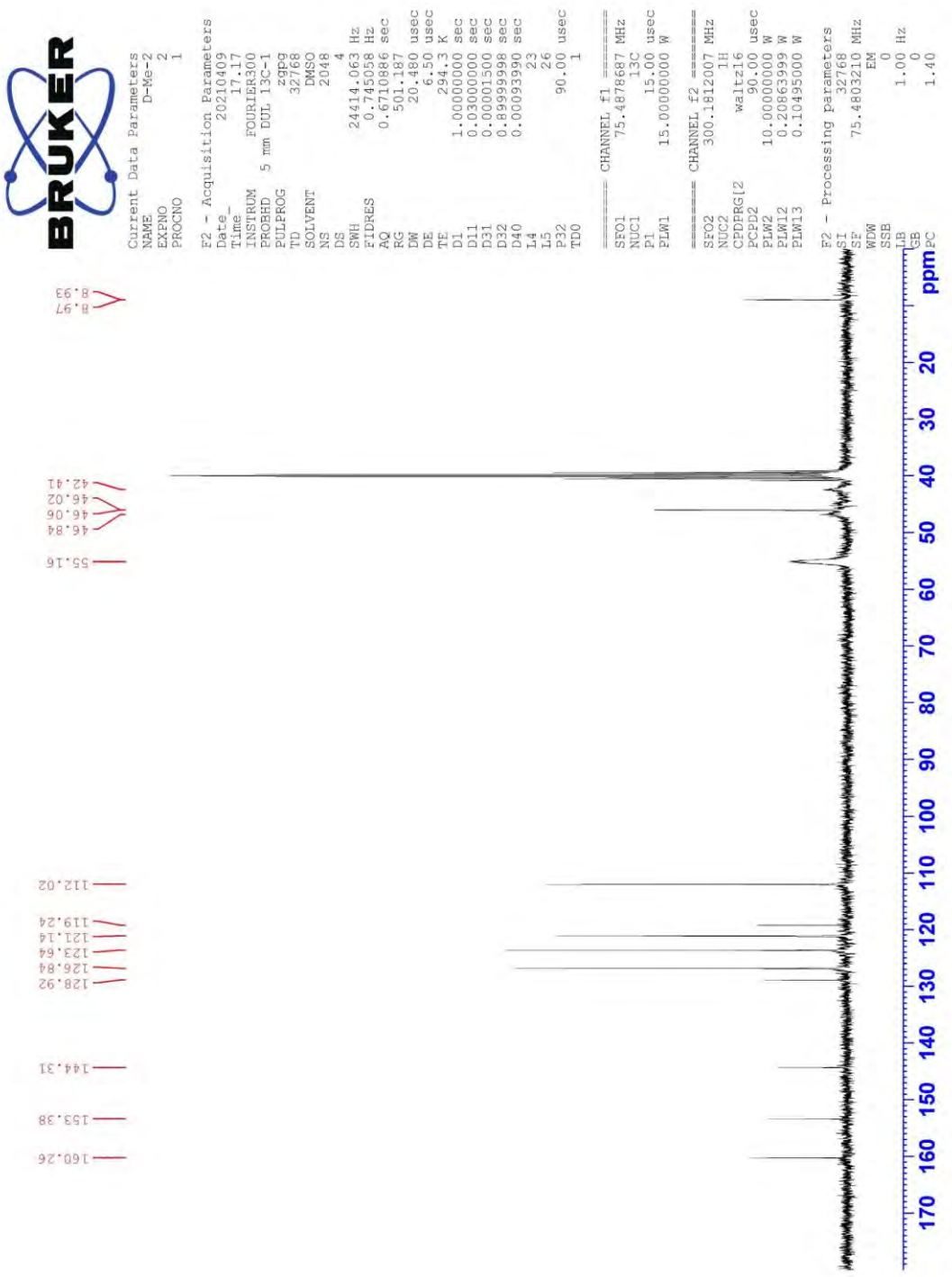


**Figure 5.18.** *$^{13}$C NMR spectrum of compound **D3***

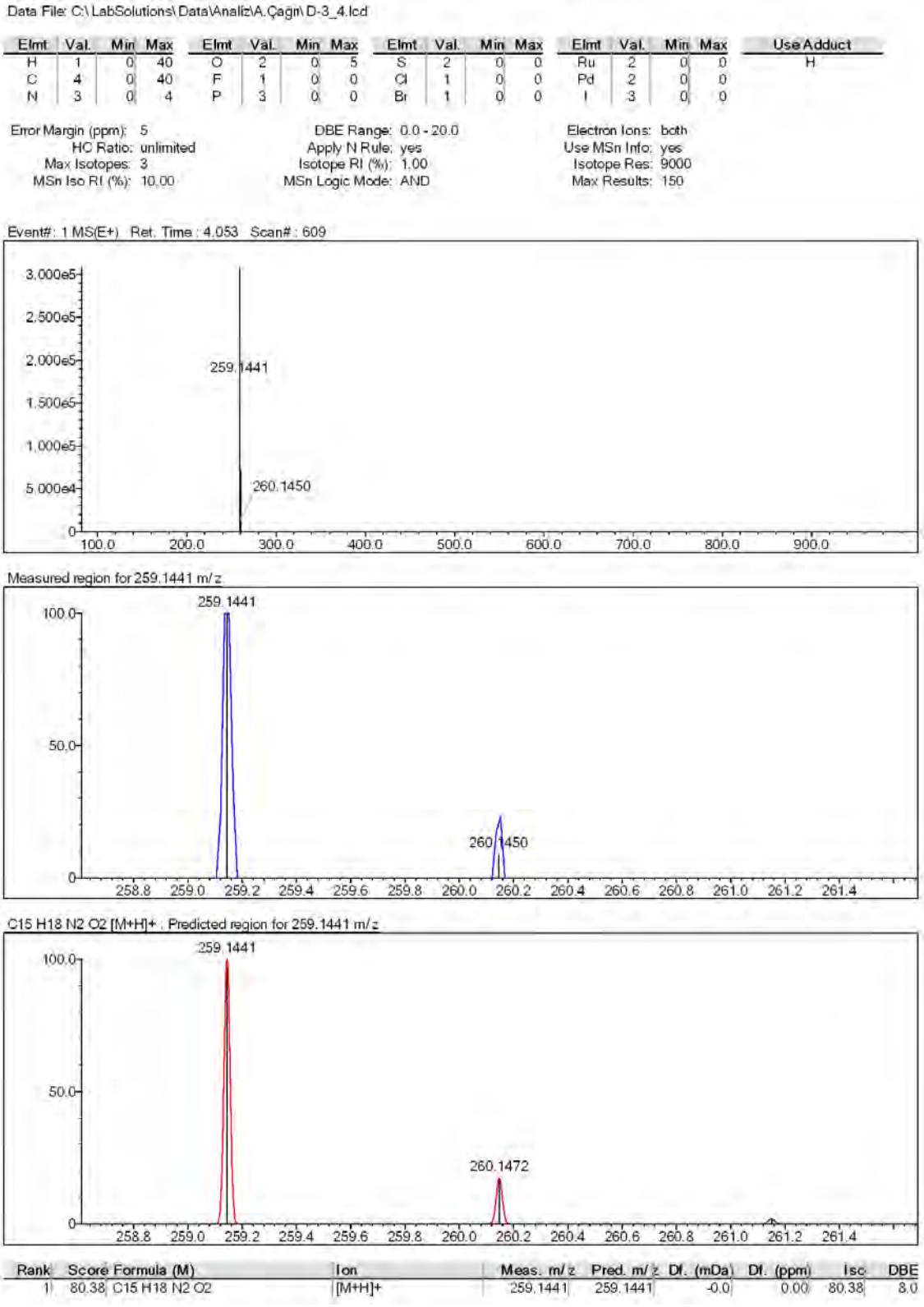


**Figure 5.19.** *High-resolution mass spectrum of compound* ***D3***

DOPNALAB

| | Item | Value |
|---|---|---|
| | Acquired Date&Time | 27.05.2021 15:04:29 |
| | Acquired by | System Administrator |
| | Filename | C:\Users\dopnalab\Desktop\sa\31.ispd |
| | Spectrum name | 31 |
| | Sample name | 3 |
| | Sample ID | |
| | Option | |
| | Comment | |
| | No. of Scans | 15 |
| | Resolution | 4 [cm-1] |
| | Apodization | Happ-Genzel |

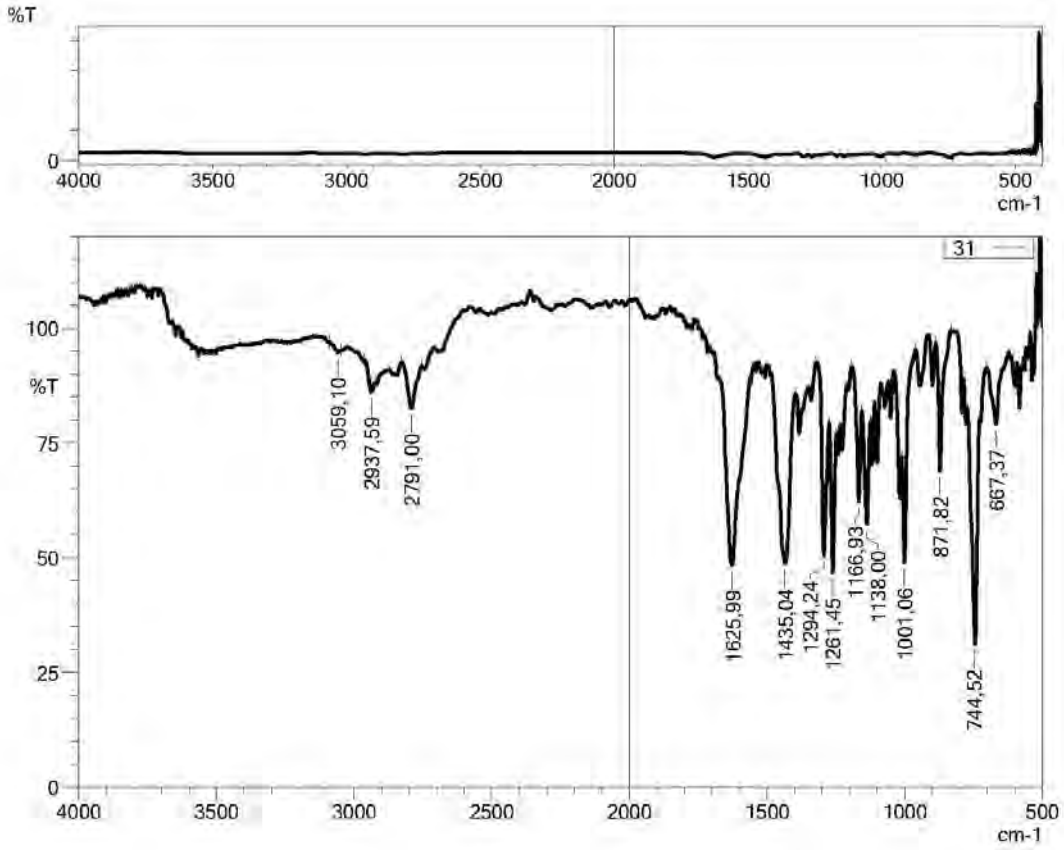


**Figure 5.20.** *IR spectrum of compound **D3***

### 5.1.4.4. *(4-ethylpiperazin-1-yl)(3-methylbenzofuran-2-yl)methanone (D4)*

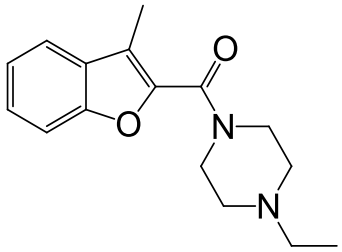


**Figure 5.21.** *Molecular structure of compound **D4***

**Physical Properties: Texture:** dense liquid, **Colour:** dark brown, **Yield:** 60%.

IR (ATR) $\upsilon_{max}$ ($cm^{-1}$): 3070 ($SP^2$ C-H stretching, aromatic), 2968-2767 ($SP^3$ C-H stretching, methylenes of piperazine, and ethyl-methyl piperazine), 1627 (C=O stretching, amide), 1435 (C=C stretching, aromatic), 1296-1253 (C-O stretching, ether), 1163-1122, 1012 (C-N stretching, tertiary amine and/or C-O stretching, ether), 869-669 (C-H aromatic out-of-plane bending).

$^1$H NMR (300 MHz) (DMSO-$d_6$) $\delta$ (ppm): 1.00 (t, $J$= 7.17 Hz, 3H, piperazine-$CH_2$-**$CH_3$**) 2.31-2.42 (m, 9H, **3-methyl**benzofuran, piperazine-3, 5 and piperazine-**$CH_2$**-$CH_3$), 3.59 (brs, 4H, piperazine-2, 6), 7.33 (t, $J$= 7.46 Hz, 1H, benzofuran-5), 7.43 (t, $J$= 7.04 Hz, 1H, benzofuran-6), 7.59 (d, $J$= 8.23 Hz, 1H, benzofuran-7), 7.70 (d, $J$= 7.12 Hz, 1H, benzofuran-4).

$^{13}$C NMR (300 MHz) (DMSO-$d_6$) $\delta$ (ppm): 8.94 (**3-methyl**benzofuran), 12.35 (piperazine-$CH_2$-**$CH_3$**), 42.45 (piperazine), 46.82 (piperazine), 51.90 (piperazine-**$CH_2$**-$CH_3$), 53.02 (piperazine), 112.00, 119.25, 121.13, 123.63, 126.83, 128.92, 144.33, 153.37, 160.18 (benzofuran-**CO**-piperazine).

**HRMS (ESI) (m/z) $[M+1]^+$:** for $C_{16}H_{20}N_2O_2$ calculated: 273.1598; found: 273.1598.

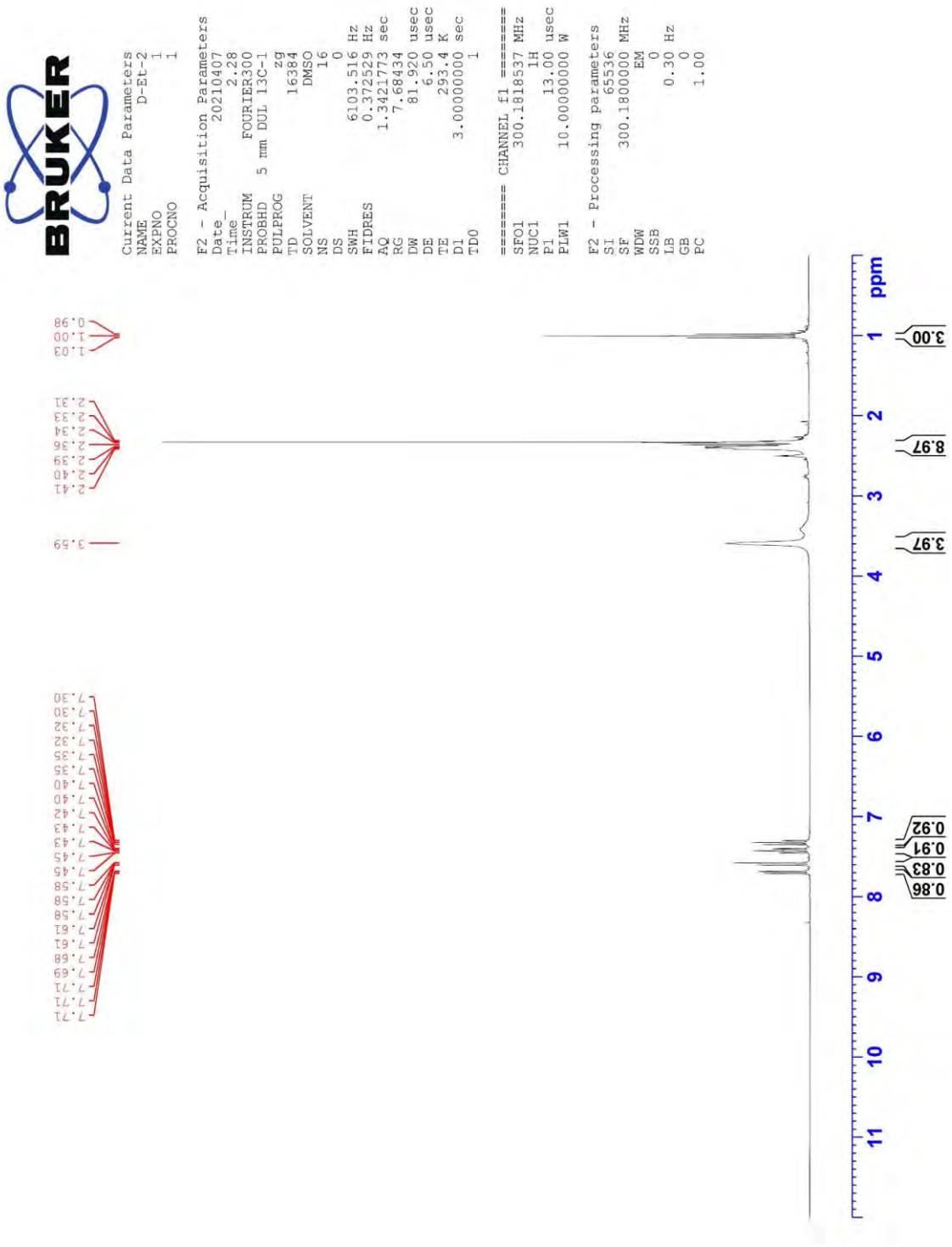


**Figure 5.22.** *[1]H NMR spectrum of compound **D4***

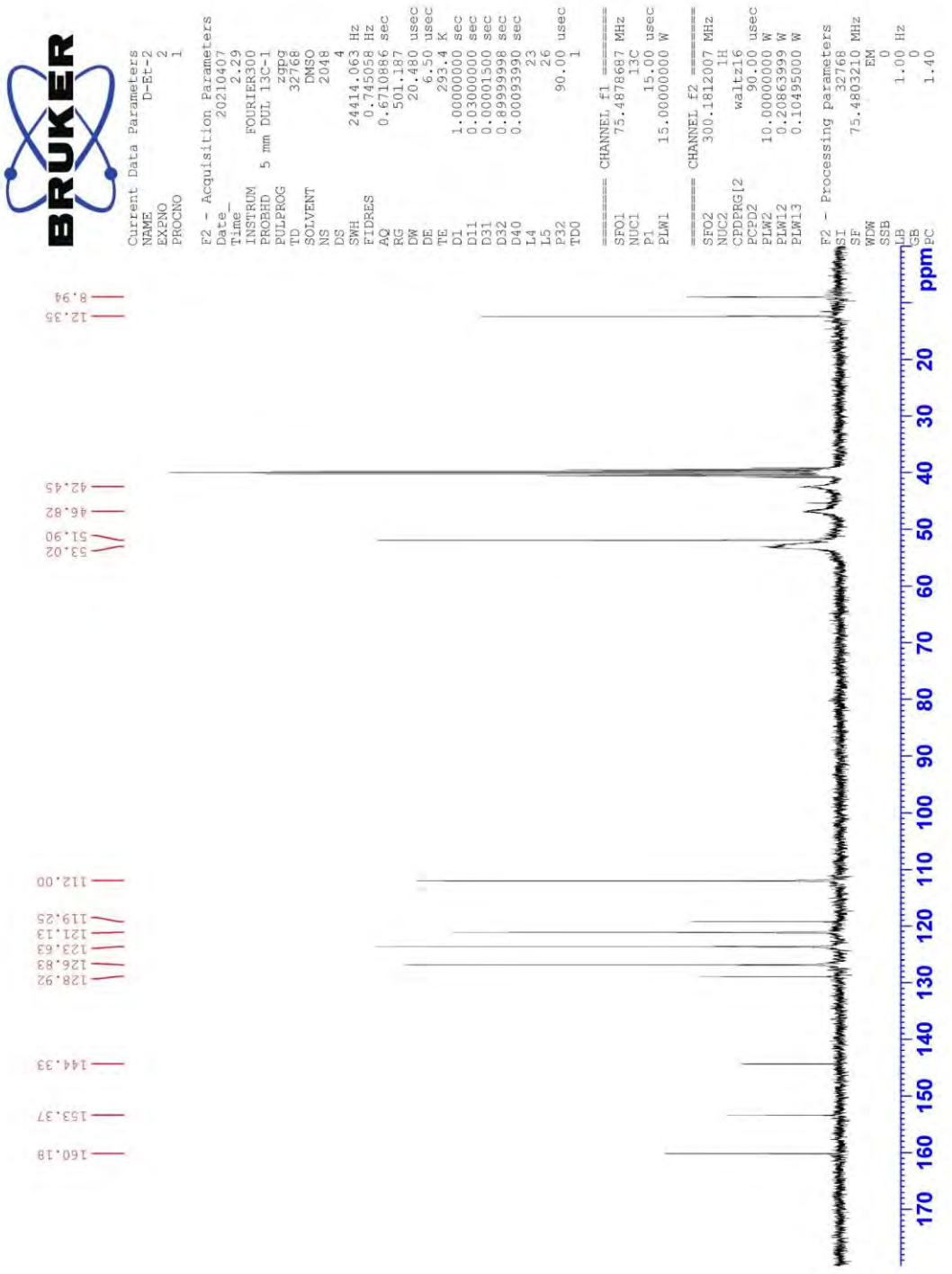


**Figure 5.23.** *$^{13}$C NMR spectrum of compound **D4***

Data File: C:\LabSolutions\Data\Analiz\Asaf\D-4_79.lcd

| Elmt | Val. | Min | Max | Elmt | Val. | Min | Max | Elmt | Val. | Min | Max | Elmt | Val. | Min | Max | Use Adduct |
|---|---|---|---|---|---|---|---|---|---|---|---|---|---|---|---|---|
| H | 1 | 0 | 40 | O | 2 | 1 | 5 | S | 2 | 0 | 0 | Ru | 2 | 0 | 0 | H |
| C | 4 | 0 | 40 | F | 1 | 0 | 0 | Cl | 1 | 0 | 0 | Pd | 2 | 0 | 0 | |
| N | 3 | 2 | 6 | P | 3 | 0 | 0 | Br | 1 | 0 | 0 | I | 3 | 0 | 0 | |

Error Margin (ppm): 10
HC Ratio: unlimited
Max Isotopes: 3
MSn Iso RI (%): 10.00

DBE Range: 5.0 - 20.0
Apply N Rule: yes
Isotope RI (%): 1.00
MSn Logic Mode: AND

Electron Ions: both
Use MSn Info: yes
Isotope Res: 9000
Max Results: 150

Event#: 1 MS(E+) Ret. Time: 1.627 -> 2.040 Scan#: 245 -> 307

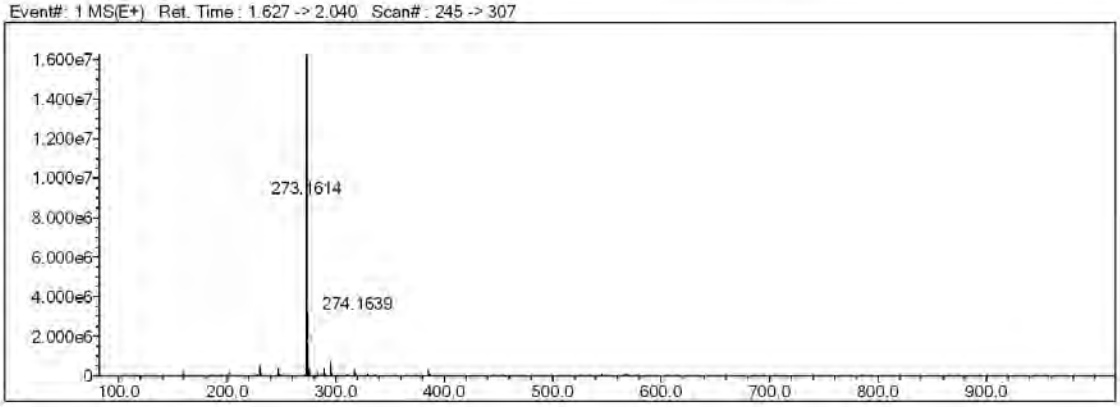


Measured region for 273.1614 m/z

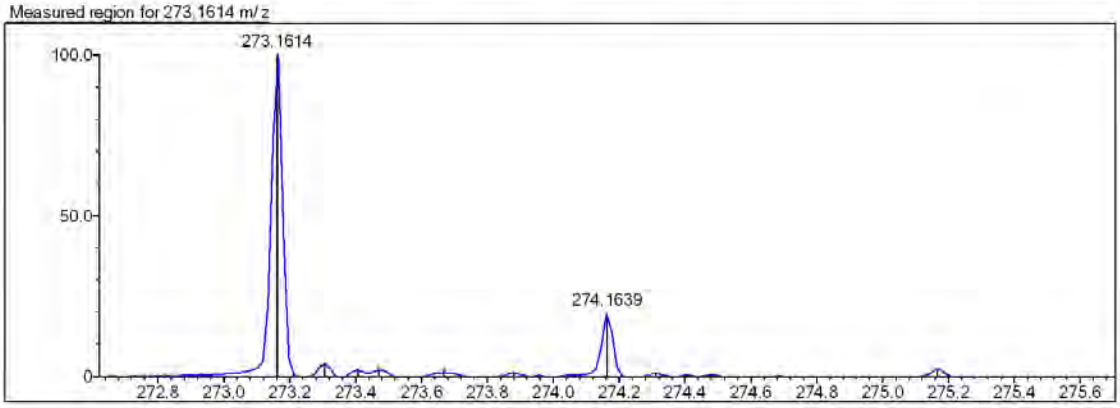


C16 H20 N2 O2 [M+H]+ : Predicted region for 273.1598 m/z

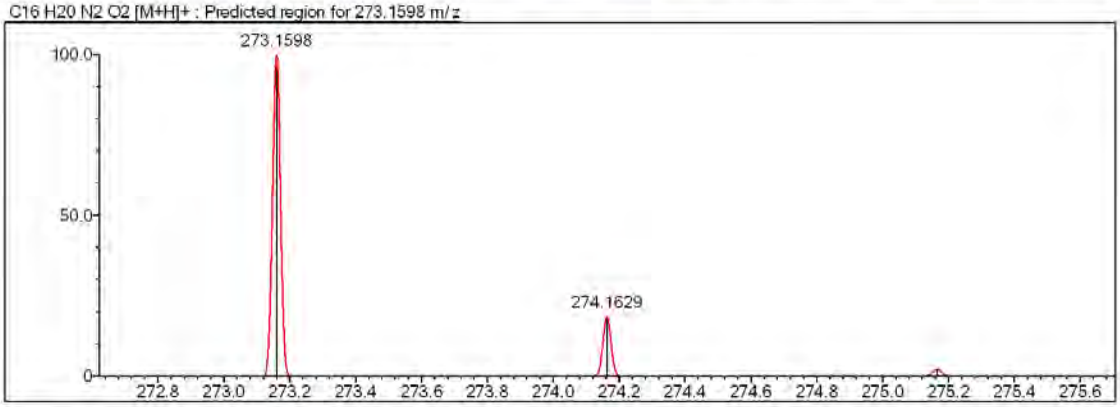


| Rank | Score | Formula (M) | Ion | Meas. m/z | Pred. m/z | Df. (mDa) | Df. (ppm) | Isc | DBE |
|---|---|---|---|---|---|---|---|---|---|
| 1 | 62.85 | C16 H20 N2 O2 | [M+H]+ | 273.1614 | 273.1598 | 1.6 | 5.86 | 77.21 | 8.0 |

**Figure 5.24.** *High-resolution mass spectrum of compound* ***D4***

DOPNALAB

| | Item | Value |
|---|---|---|
| | Acquired Date&Time | 27.05.2021 15:10:22 |
| | Acquired by | System Administrator |
| | Filename | C:\Users\dopnalab\Desktop\sa\41.ispd |
| | Spectrum name | 41 |
| | Sample name | 4 |
| | Sample ID | |
| | Option | |
| | Comment | |
| | No. of Scans | 15 |
| | Resolution | 4 [cm-1] |
| | Apodization | Happ-Genzel |

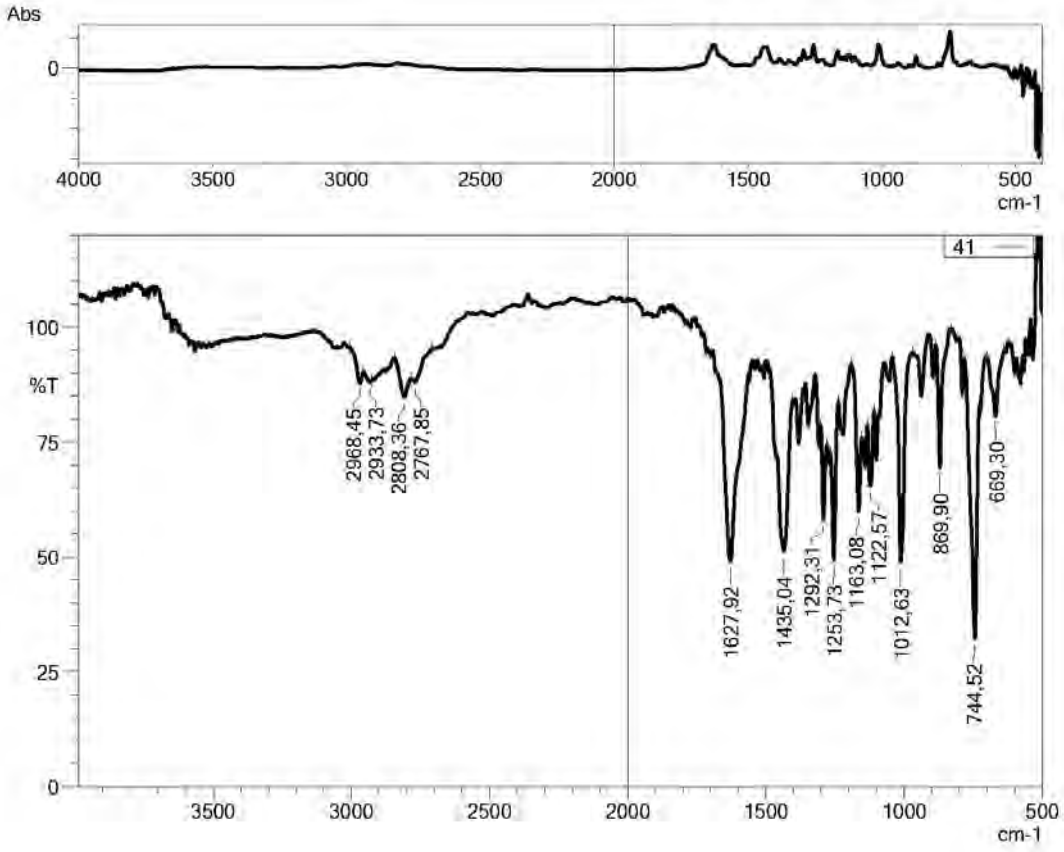


**Figure 5.25.** *IR spectrum of compound **D4***

### 5.1.4.5. *(4-(2-(dimethylamino)ethyl)piperazin-1-yl)(3-methylbenzofuran-2-yl)methanone (D5)*

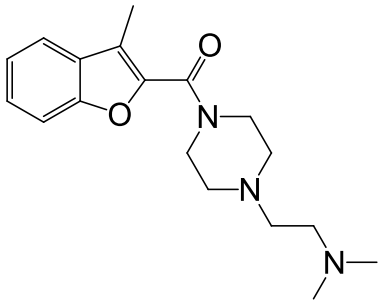


**Figure 5.26.** *Molecular structure of compound **D5***

**Physical Properties: Texture:** dense liquid, **Colour:** dark brown, **Yield:** 82%%.

IR (ATR) $\upsilon_{max}$ ($cm^{-1}$): 3070 ($SP^2$ C-H stretching, aromatic), 2939-2767 ($SP^3$ C-H stretching, methylenes of piperazine, and dimethylaminoethyl-piperazine), 1627 (C=O stretching, amide), 1435 (C=C stretching, aromatic), 1292-1253 (C-O stretching, ether), 1165-1132, 1095-1001 (C-N stretching, tertiary amine and/or C-O stretching, ether), 871-669 (C-H aromatic out-of-plane bending).

$^1$H NMR (300 MHz) (DMSO-$d_6$) $\delta$ (ppm): 2.12 (s, 6H, -N(**$CH_3$**)$_2$), 2.33-2.42 (m, 7H, **3-methyl**benzofuran and piperazine-(**$CH_2$**)$_2$-N), 2.44 (t, *J*= 4.44 Hz, 4H, piperazine-3, 5), 3.58 (brs, 4H, piperazine-2, 6), 7.33 (t, *J*= 7.46 Hz, 1H, benzofuran-5), 7.43 (t, *J*= 7.70 Hz, 1H, benzofuran-6), 7.59 (d, *J*= 8.23 Hz, 1H, benzofuran-7), 7.70 (d, *J*= 7.60 Hz, 1H, benzofuran-4).

$^{13}$C NMR (300 MHz) (DMSO-$d_6$) $\delta$ (ppm): 8.95 (**3-methyl**benzofuran), 42.34 (piperazine), 45.97 (-N(**$CH_3$**)$_2$), 46.82 (piperazine), 53.56 (piperazine), 56.04 (piperazine-(**$CH_2$**)$_2$-N), 57.03 (piperazine-(**$CH_2$**)$_2$-N), 112.01, 119.26, 121.14, 123.63, 126.84, 128.92, 144.31, 153.37, 160.17 (benzofuran-**CO**-piperazine).

**HRMS (ESI) (m/z) $[M+1]^+$:** for $C_{18}H_{25}N_3O_2$ calculated: 316.2020; found: 316.2029.

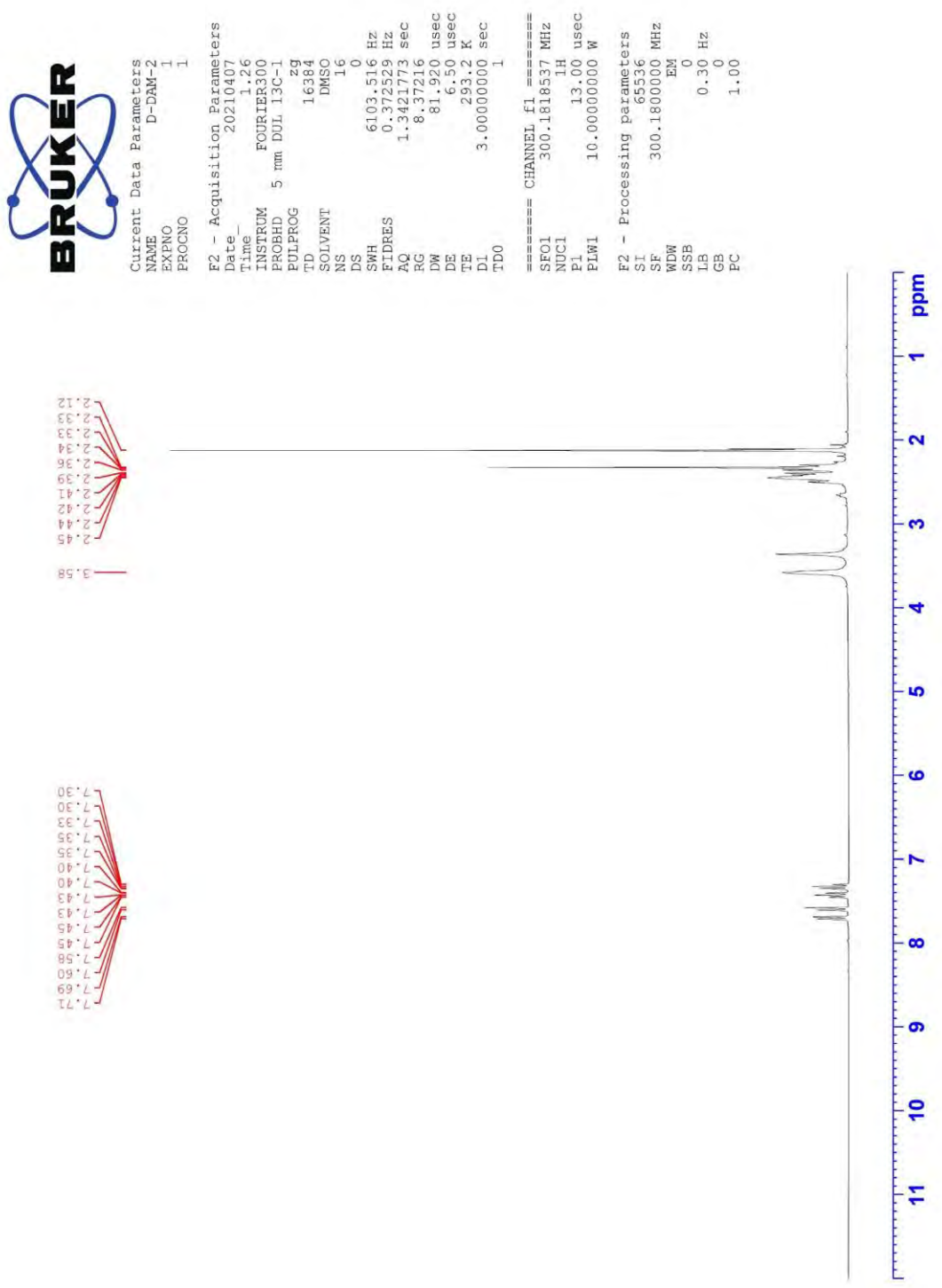


**Figure 5.27.** *$^{1}H$ NMR spectrum of compound **D5***

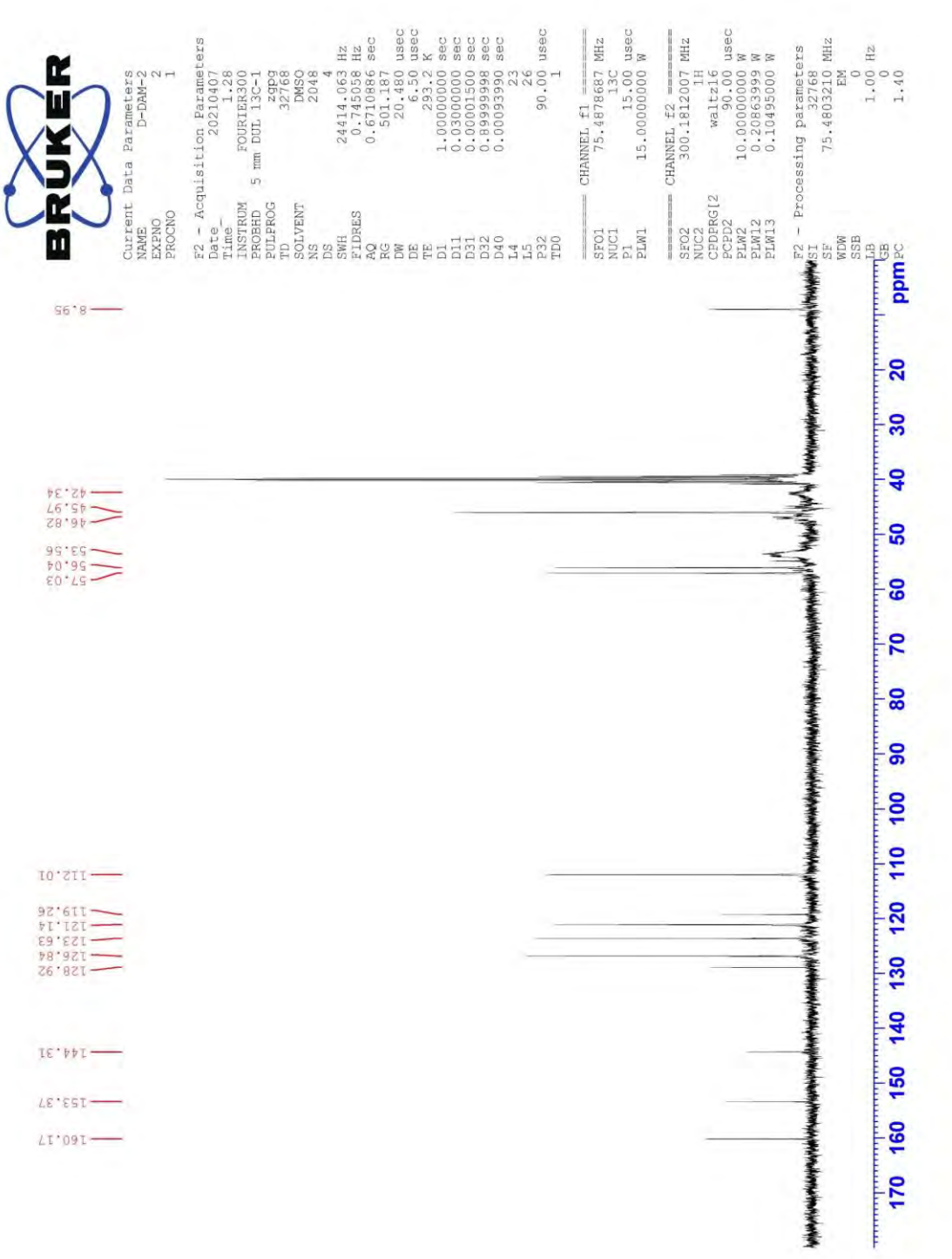


**Figure 5.28.** *$^{13}$C NMR spectrum of compound **D5***

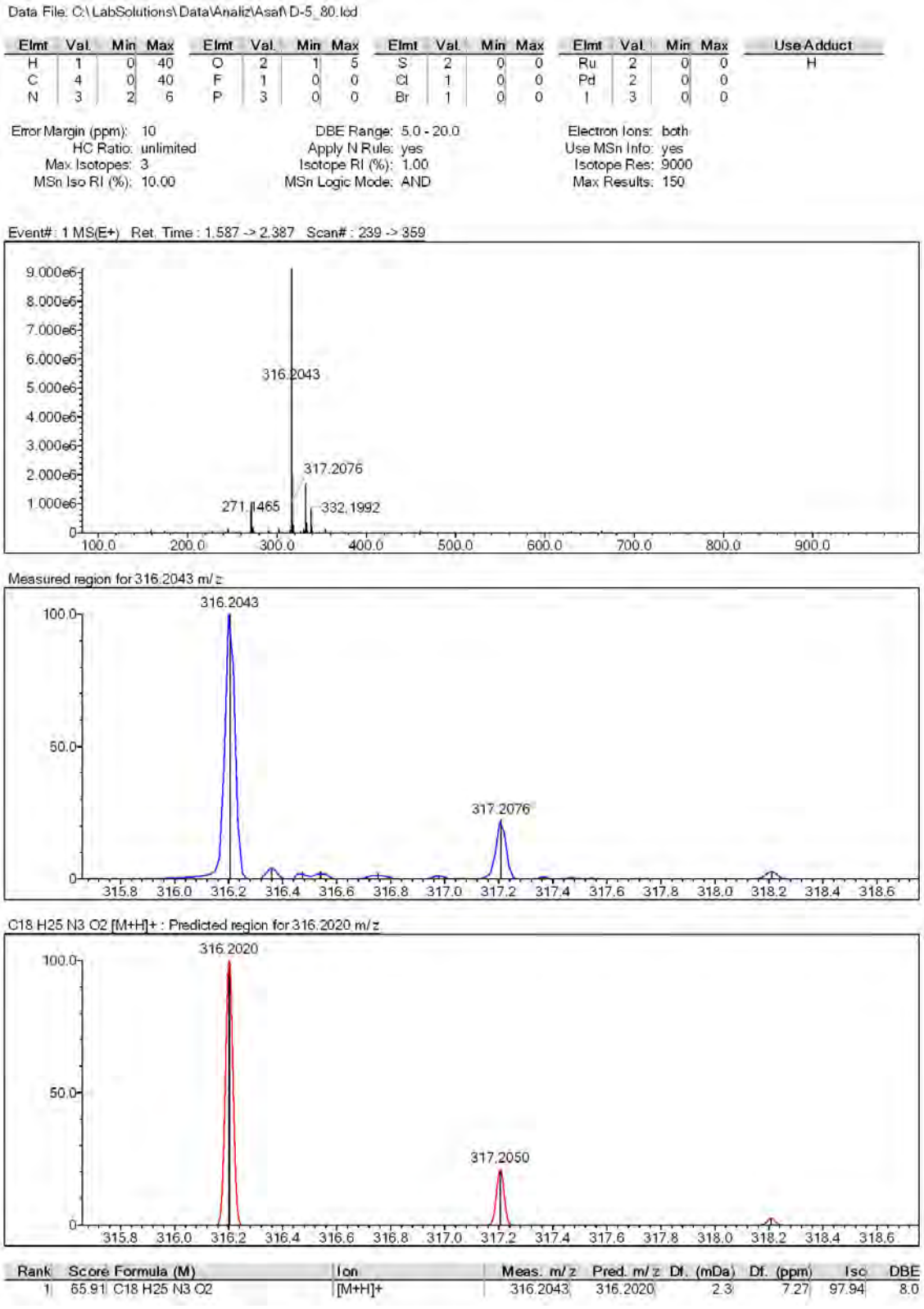


**Figure 5.29.** *High-resolution mass spectrum of compound* ***D5***

DOPNALAB

| | Item | Value |
|---|---|---|
| | Acquired Date&Time | 27.05.2021 15:15:35 |
| | Acquired by | System Administrator |
| | Filename | C:\Users\dopnalab\Desktop\sa\51.ispd |
| | Spectrum name | 51 |
| | Sample name | 5 |
| | Sample ID | |
| | Option | |
| | Comment | |
| | No. of Scans | 15 |
| | Resolution | 4 [cm-1] |
| | Apodization | Happ-Genzel |

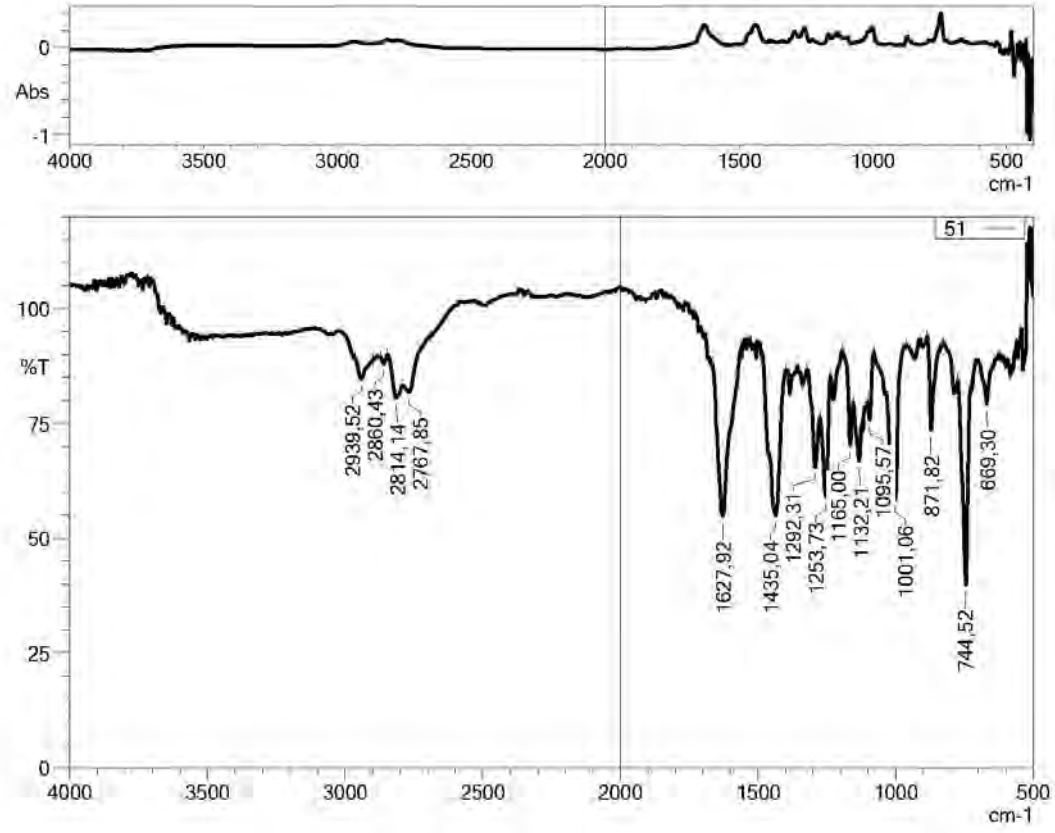


**Figure 5.30.** *IR spectrum of compound **D5***

### 5.1.4.6. *benzofuran-2-yl(4-phenylpiperazin-1-yl)methanone (D6)*

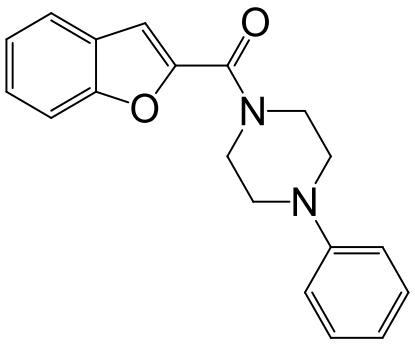


**Figure 5.31.** *Molecular structure of compound* ***D6***

**Physical Properties: Texture:** solid crystals, **Color:** white, **M.P.:** 175-176ºC**, Yield:** 84%.

**IR (ATR) $\upsilon_{max}$ ($cm^{-1}$):** 3105-3059 ($SP^2$ C-H stretching, aromatic), 2819 ($SP^3$ C-H stretching, methylenes of piperazine), 1610 (C=O stretching, amide), 1566-1504 (C-H bending, indicative of non-substituted benzofuran at position 3), 1438 (C=C stretching, aromatic), 1292-1224 (C-O stretching, ether), 1178-1153, 1014 (C-N stretching, tertiary amine and/or ether), 947-675 (C-H aromatic out-of-plane bending, prominent peak at 947 and more peaks between 870-830 indicate non-substituted benzofuran at position 3).

**$^1$H NMR (300 MHz) (DMSO-$d_6$) $\delta$ (ppm):** 3.24 (t, *J*= 5.13 Hz, 4H, piperazine-3, 5), 3.87 (brs, 4H, piperazine-2, 6), 6.83 (t, *J*= 7.25 Hz, 1H, phenyl-4), 6.97 (d, *J*= 7.89, 2H, phenyl-2, 6), 7.25 (t, *J*= 7.97 Hz, 2H, phenyl-3,5), 7.35 (t, *J*= 7.49 Hz, 1H, benzofuran-5), 7.46 (s fused with t, *J*= 7.76 Hz, 2H, benzofuran-3 (s), benzofuran- 6 (t)), 7.69 (d, *J*= 8.30 Hz, 1H, benzofuran-7), 7.77 (d, *J*= 7.30Hz, 1H, benzofuran-4).

**$^{13}$C NMR (300 MHz) (DMSO-$d_6$) $\delta$ (ppm):** 42.75 (piperazine), 46.54 (piperazine), 49.03 (piperazine), 111.47, 112.28, 116.35, 119.89, 122.94, 124.20, 127.04, 127.16, 129.49, 148.66, 151.14, 154.40, 159.32 (benzofuran-**CO-**piperazine).

**HRMS (ESI) (m/z) $[M+1]^+$:** for $C_{19}H_{18}N_2O_2$ calculated: 307.1441; found: 307.1434.

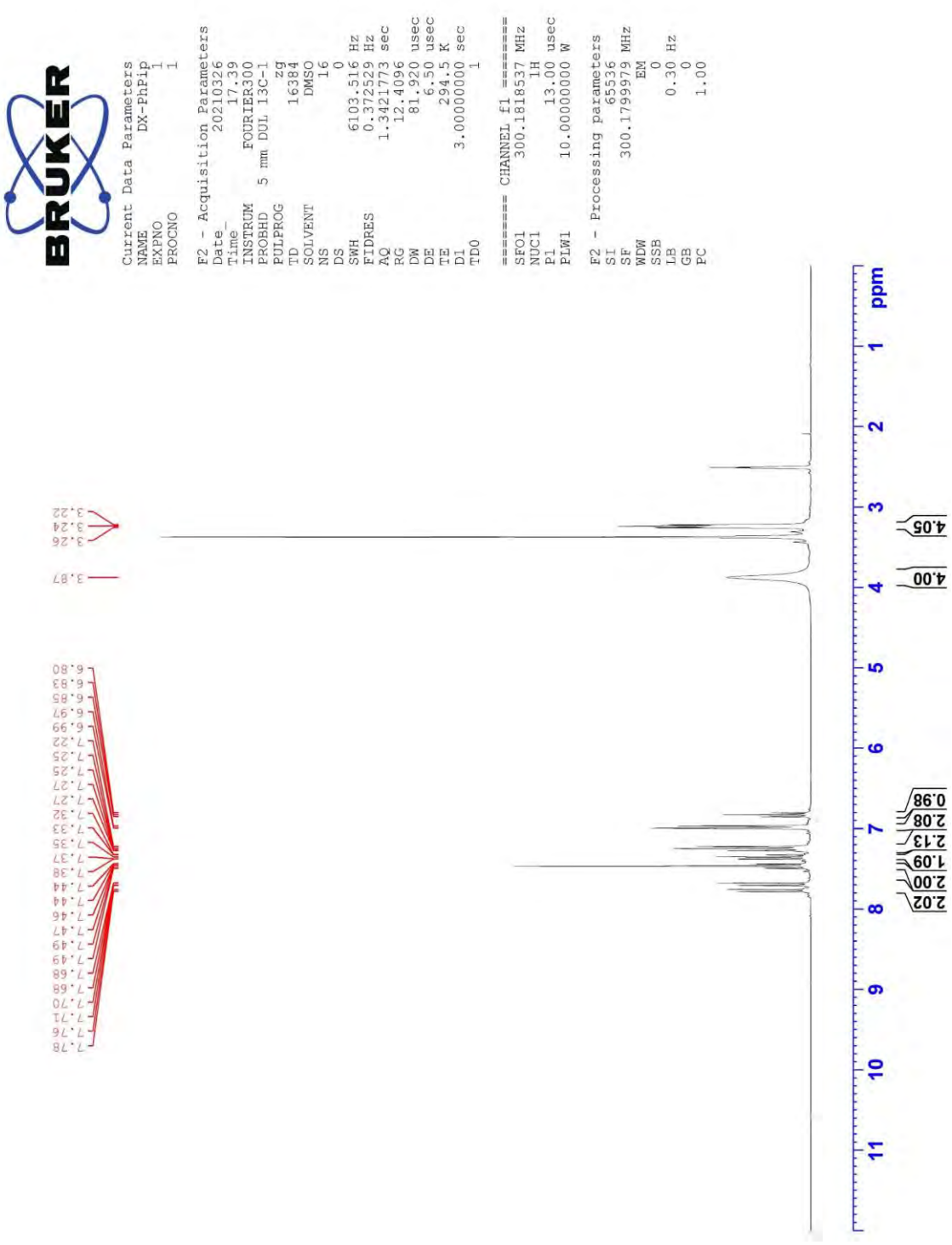


**Figure 5.32.** *$^{1}H$ NMR spectrum of compound **D6***

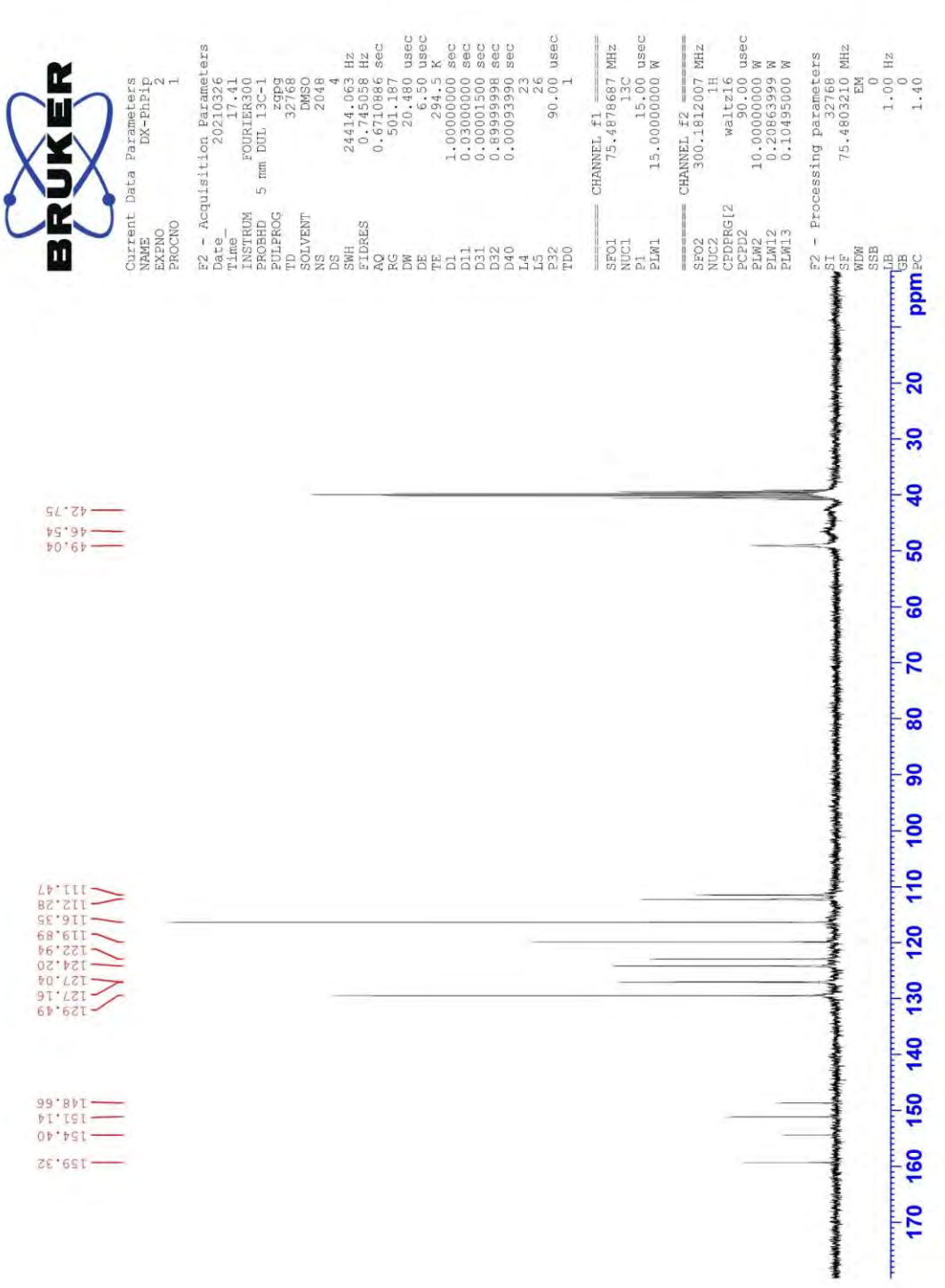


**Figure 5.33.** *$^{13}$C NMR of compound **D6***

Data File: C:\LabSolutions\Data\Analiz\Asaf\D-6-C_95.lcd

| Elmt | Val. | Min | Max | Elmt | Val. | Min | Max | Elmt | Val. | Min | Max | Elmt | Val. | Min | Max | Use Adduct |
|---|---|---|---|---|---|---|---|---|---|---|---|---|---|---|---|---|
| H | 1 | 0 | 40 | O | 2 | 0 | 5 | S | 2 | 0 | 2 | Ru | 2 | 0 | 0 | H |
| C | 4 | 0 | 40 | F | 1 | 0 | 0 | Cl | 1 | 0 | 1 | Pd | 2 | 0 | 0 | |
| N | 3 | 0 | 7 | P | 3 | 0 | 0 | Br | 1 | 0 | 0 | I | 3 | 0 | 0 | |

Error Margin (ppm): 5
HC Ratio: unlimited
Max Isotopes: 3
MSn Iso RI (%): 10.00

DBE Range: 10.0 - 25.0
Apply N Rule: yes
Isotope RI (%): 1.00
MSn Logic Mode: AND

Electron Ions: both
Use MSn Info: yes
Isotope Res: 9000
Max Results: 150

Event#: 1 MS(E+) Ret. Time : 6.240 -> 6.507 Scan# : 937 -> 977

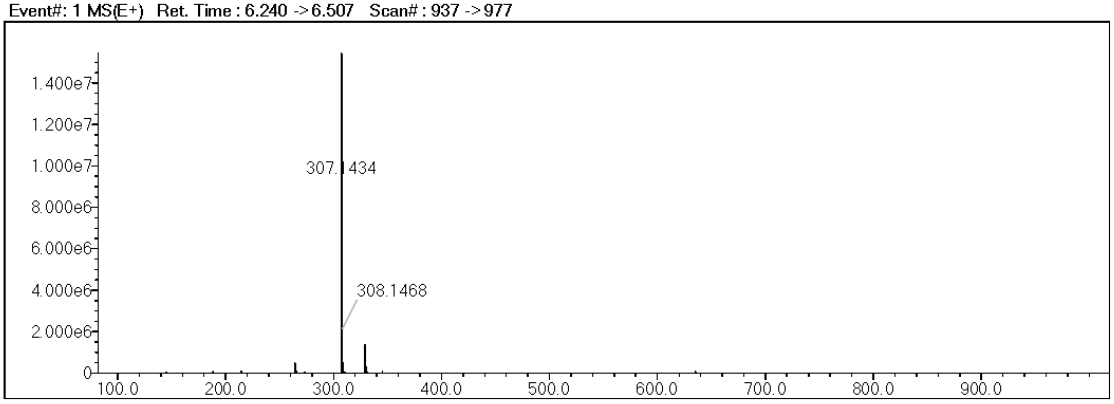


Measured region for 307.1434 m/z

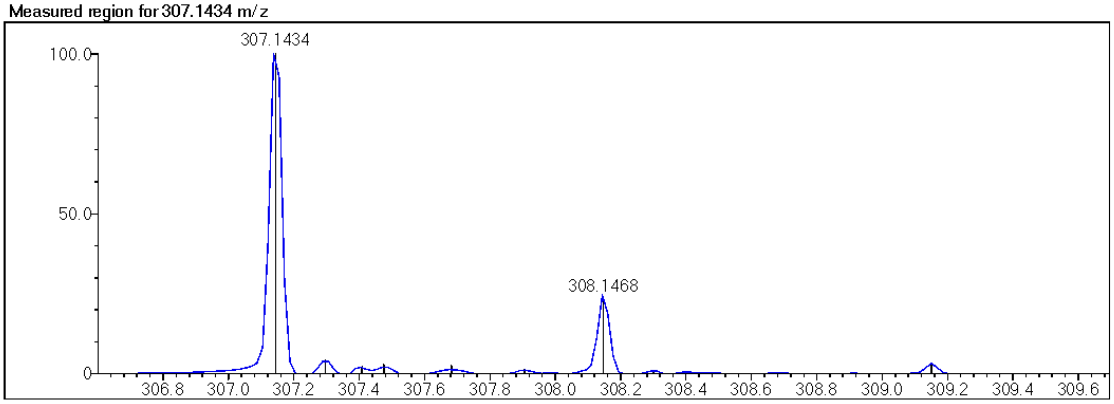


C19 H18 N2 O2 [M+H]+ : Predicted region for 307.1441 m/z

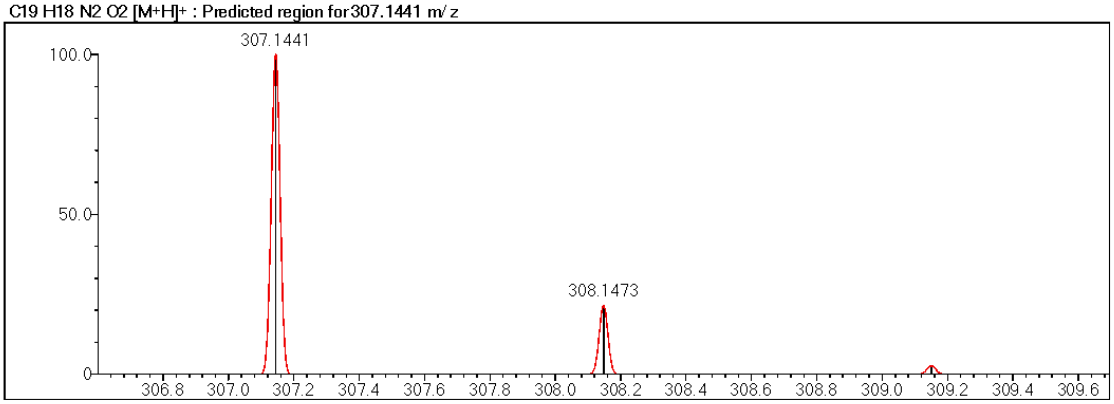


| Rank | Score | Formula (M) | Ion | Meas. m/z | Pred. m/z | Df. (mDa) | Df. (ppm) | Iso | DBE |
|---|---|---|---|---|---|---|---|---|---|
| 1 | 96.80 | C19 H18 N2 O2 | [M+H]+ | 307.1434 | 307.1441 | -0.7 | -2.28 | 100.00 | 12.0 |

**Figure 5.34.** *High-resolution mass spectrum of compound* ***D6***

DOPNALAB

| | Item | Value |
|---|---|---|
| | Acquired Date&Time | 27.05.2021 15:22:52 |
| | Acquired by | System Administrator |
| | Filename | C:\Users\dopnalab\Desktop\sa\61.ispd |
| | Spectrum name | 61 |
| | Sample name | 6 |
| | Sample ID | |
| | Option | |
| | Comment | |
| | No. of Scans | 16 |
| | Resolution | 4 [cm-1] |
| | Apodization | Happ-Genzel |

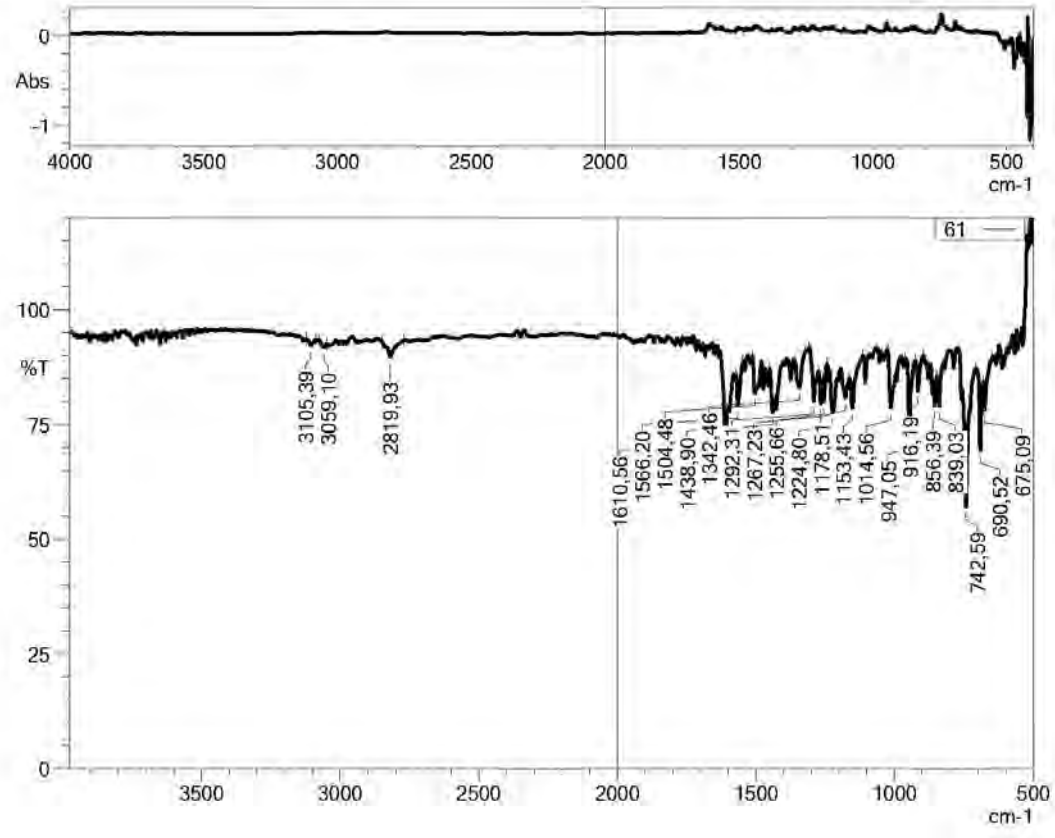


**Figure 5.35.** *IR spectrum of compound **D6***

### 5.1.4.7. *(4-(benzofuran-2-carbonyl)piperazin-1-yl)(furan-2-yl)methanone (D7)*

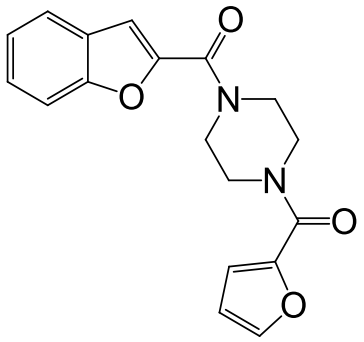

**Figure 5.36.** *Molecular structure of compound **D7***

**Physical Properties: Texture:** solid crystals, **Colour:** white, **M.P.:** 104-105ºC**, Yield:** 84%.

**IR (ATR) $\upsilon_{max}$ ($cm^{-1}$):** 3132-3061 ($SP^2$ C-H stretching, aromatic), 2860 ($SP^3$ C-H stretching, methylenes of piperazine), 1614 (C=O stretching, amide), 1566 (C-H bending, indicative of non-substituted benzofuran at position 3), 1485-1423 (C=C stretching, aromatic), 1255-1222 (C-O stretching, ether), 1178, 1001 (C-N stretching, tertiary amine and/or ether), 933-675 (C-H aromatic out-of-plane bending).

**$^1$H NMR (300 MHz) (DMSO-$d_6$) $\delta$ (ppm):** 3.81 (brs, 8H, piperazine-2, 3, 5, 6), 6.66 (dd, *J*= 3.46, 1.76 Hz, 1H, furan-4), 7.06 (d, *J*= 3.45 Hz, 1H, furan-3), 7.35 (t, *J*= 7.03 Hz, 1H, benzofuran-5), 7.47 (s fused with t, *J*= 7.76 Hz, 2H, benzofuran-3 (s), benzofuran-6 (t)), 7.68 (d, *J*= 8.30 Hz, 1H, benzofuran-7), 7.77 (d, *J*= 7.40 Hz, 1H, benzofuran-4), 7.86 (dd, *J*= 1.68, 0.73 Hz, 1H, furan-5).

**$^{13}$C NMR (300 MHz) (DMSO-$d_6$) $\delta$ (ppm):** 42.70 (piperazine), 46.48 (piperazine), 111.69, 111.87, 112.29, 116.47, 122.96, 124.21, 127.11, 145.42, 147.21, 148.44, 154.43, 158.94 (piperazine-**CO**-furan), 159.54 (benzofuran-**CO**-piperazine).

**HRMS (ESI) (m/z) $[M+1]^+$:** for $C_{18}H_{16}N_2O_4$ calculated: 325.1183; found: 325.1174.

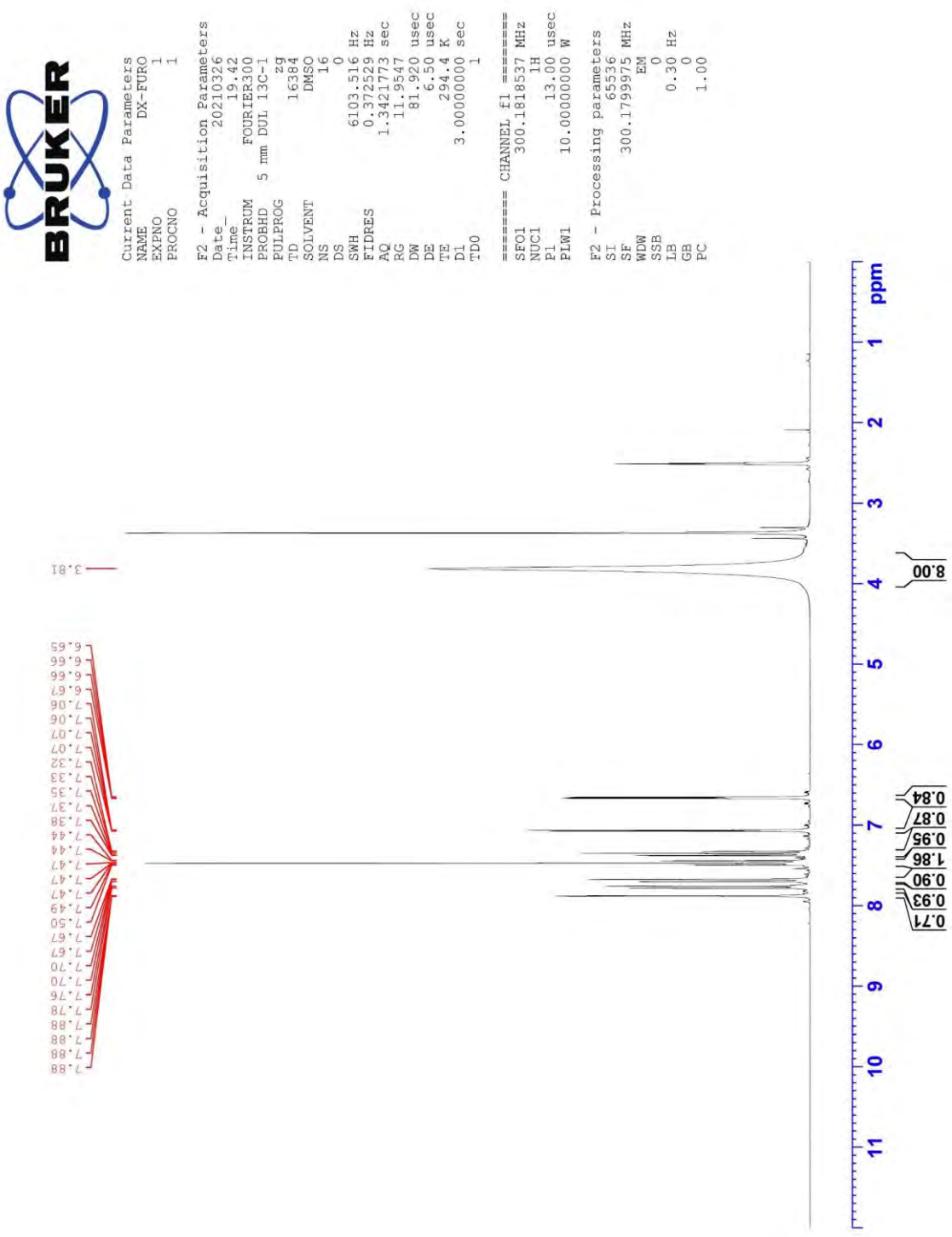


**Figure 5.37.** *$^{1}H$ NMR spectrum of compound **D7***

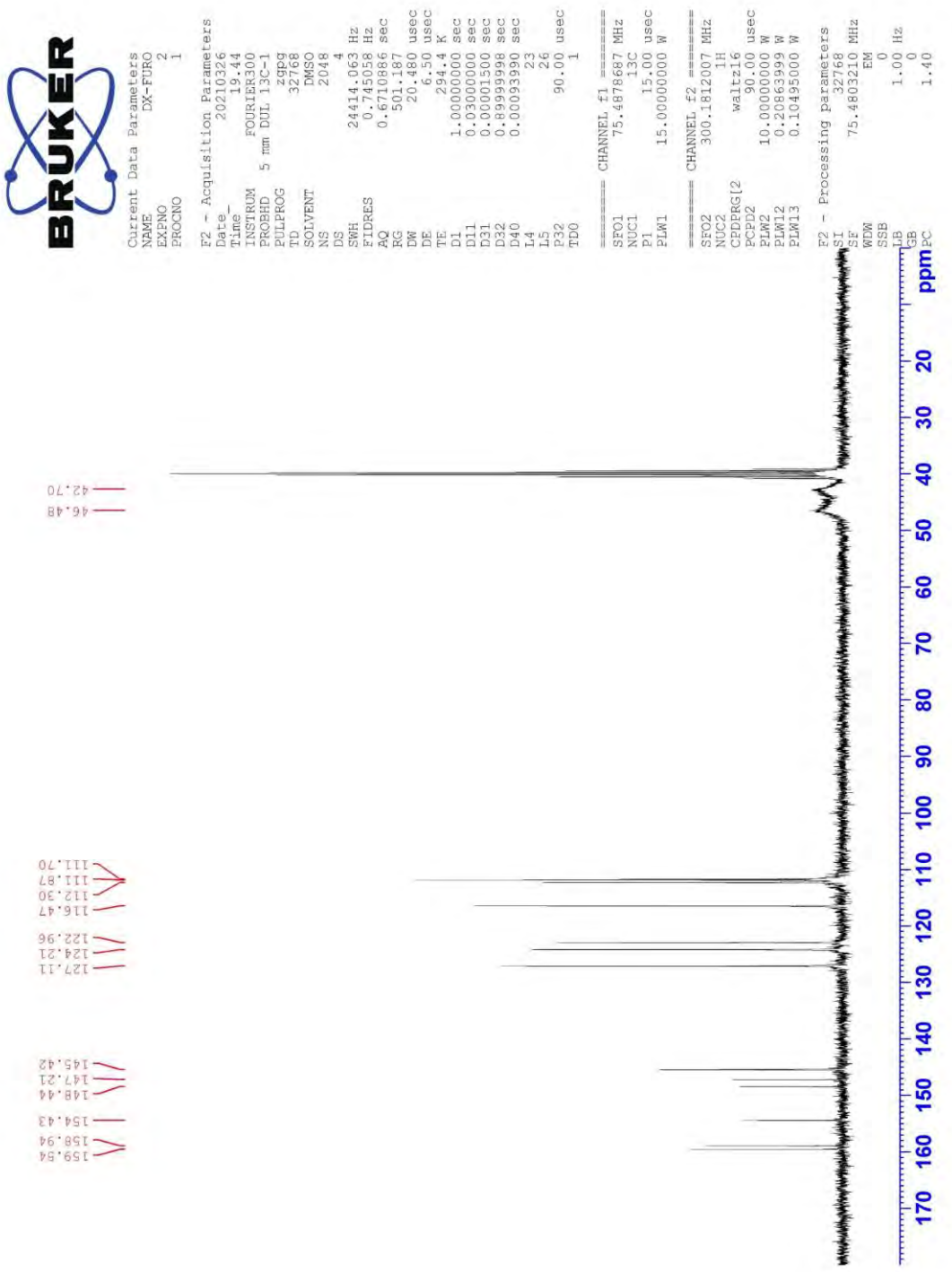


**Figure 5.38.** *$^{13}C$ NMR of compound **D7***

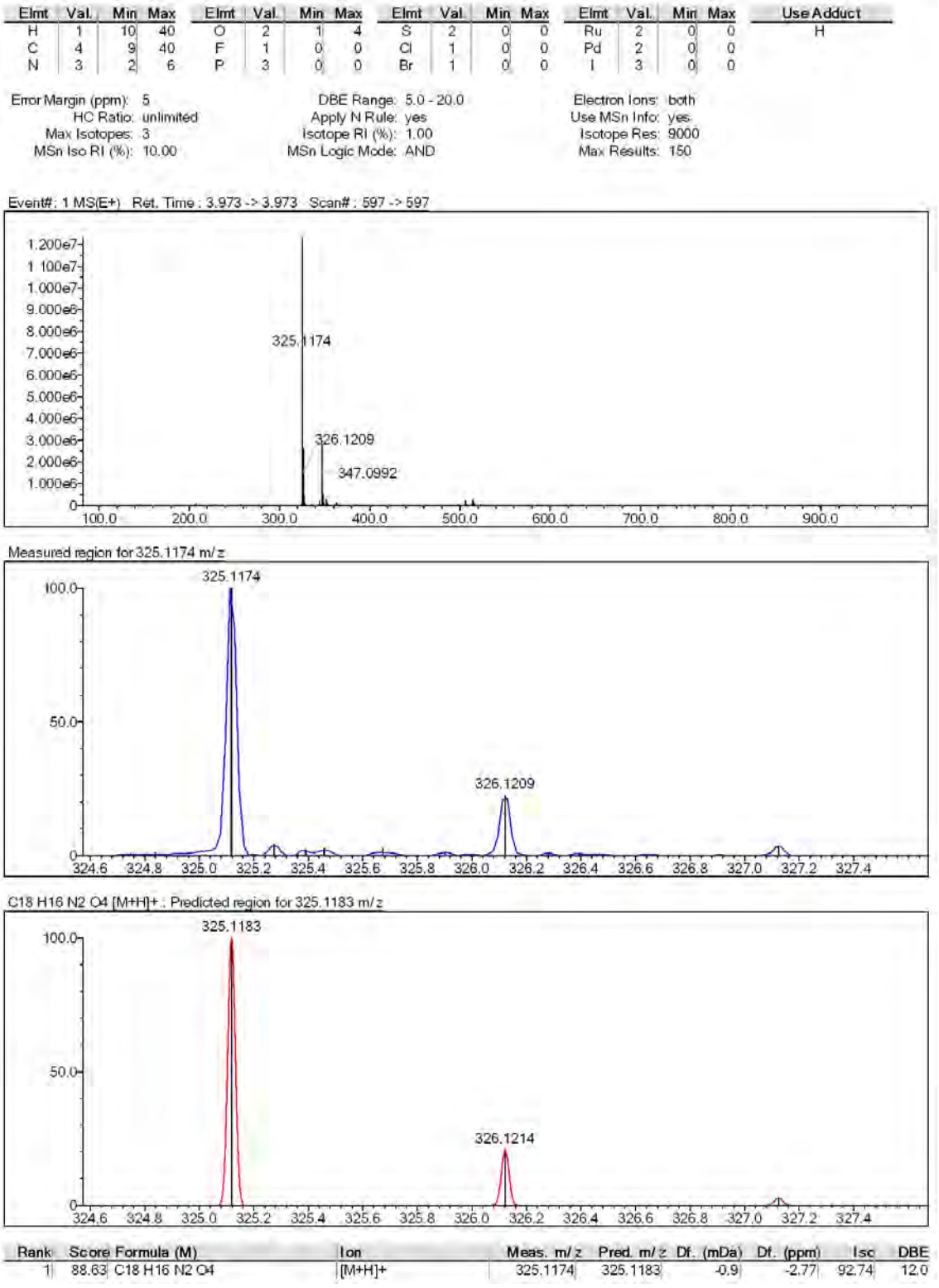


**Figure 5.39.** *High-resolution mass spectrum of compound **D7***

DOPNALAB

| | Item | Value |
|---|---|---|
| | Acquired Date&Time | 27.05.2021 15:29:55 |
| | Acquired by | System Administrator |
| | Filename | C:\Users\dopnalab\Desktop\sa\71.ispd |
| | Spectrum name | 71 |
| | Sample name | 7 |
| | Sample ID | |
| | Option | |
| | Comment | |
| | No. of Scans | 16 |
| | Resolution | 4 [cm-1] |
| | Apodization | Happ-Genzel |

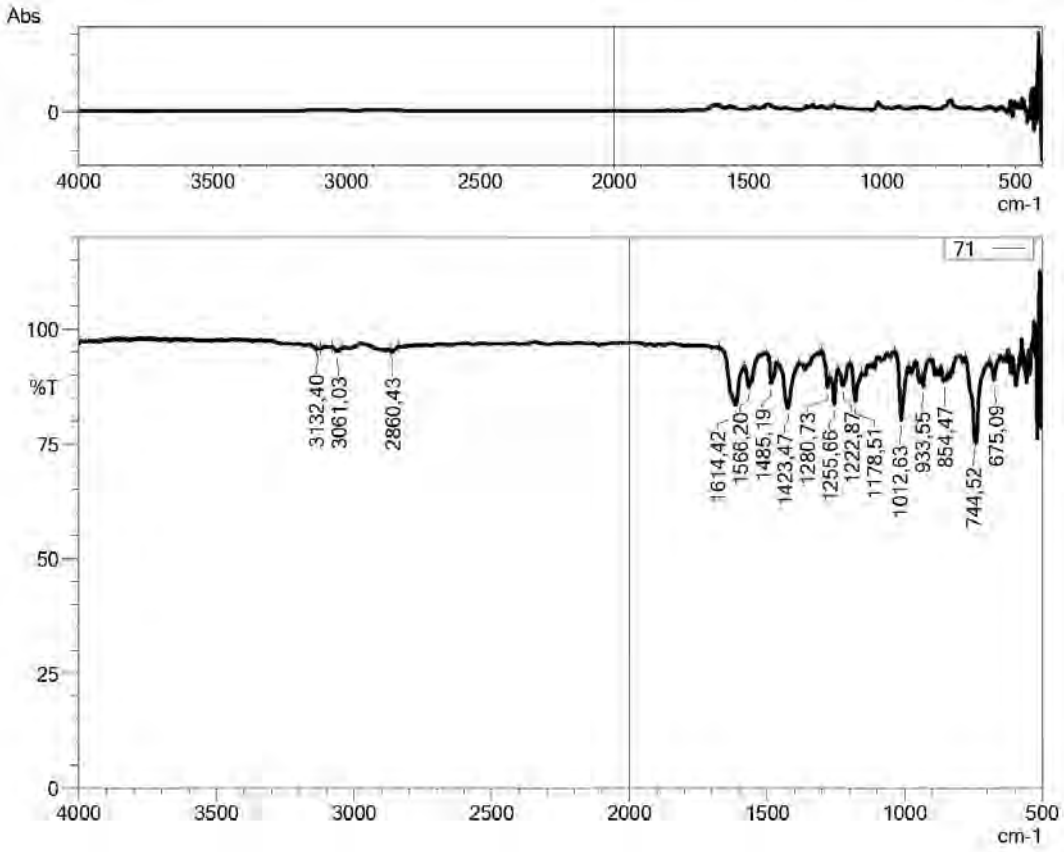


**Figure 5.40.** *IR spectrum of compound **D7***

### 5.1.4.8. *benzofuran-2-yl(4-methylpiperazin-1-yl)methanone (D8)*

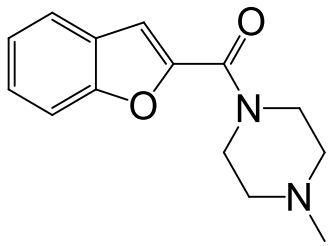


**Figure 5.41.** *Molecular structure of compound* ***D8***

**Physical Properties: Texture:** liquid, **Color:** yellow, **Yield:** 81%.

**IR (ATR) $\upsilon_{max}$ ($cm^{-1}$):** 2937-2791 ($SP^3$ C-H stretching, methylenes of piperazine, and 4-methyl piperazine), 1631 (C=O stretching, amide), 1562 (C-H bending, indicative of non-substituted benzofuran at position 3), 1429 (C=C stretching, aromatic), 1294-1226 (C-O stretching, ether), 1168-1141, 1022-1001 (C-N stretching, tertiary amine and/or ether), 933-675 (C-H aromatic out-of-plane bending).

**$^1$H NMR (300 MHz) (DMSO-$d_6$) $\delta$ (ppm):** 2.20 (s, 3H, **4-methyl**piperazine), 2.37 (t, *J*= 5.05 Hz, 4H, piperazine-3, 5), 3.69 (brs, 4H, piperazine-2, 6), 7.33 (t, *J*= 7.46 Hz, 1H, benzofuran-5), 7.38 (s, 1H, benzofuran-3), 7.43 (t, *J*= 7.75 Hz, 1H, benzofuran-6), 7.65 (d, *J*= 8.29 Hz, 1H, benzofuran-7), 7.74 (d, *J*= 7.68 Hz, 1H, benzofuran-4).

**$^{13}$C NMR (300 MHz) (DMSO-$d_6$) $\delta$ (ppm):** 42.62 (piperazine), 46.00 (**4-methyl**piperazine), 46.82 (piperazine), 55.03 (piperazine), 111.18, 112.23, 122.87, 124.14, 126.93, 127.16, 148.73, 154.33, 159.31 (benzofuran-**CO-**piperazine).

**HRMS (ESI) (m/z) $[M+1]^+$:** for $C_{14}H_{16}N_2O_2$ calculated: 245.1285; found: 245.1275.

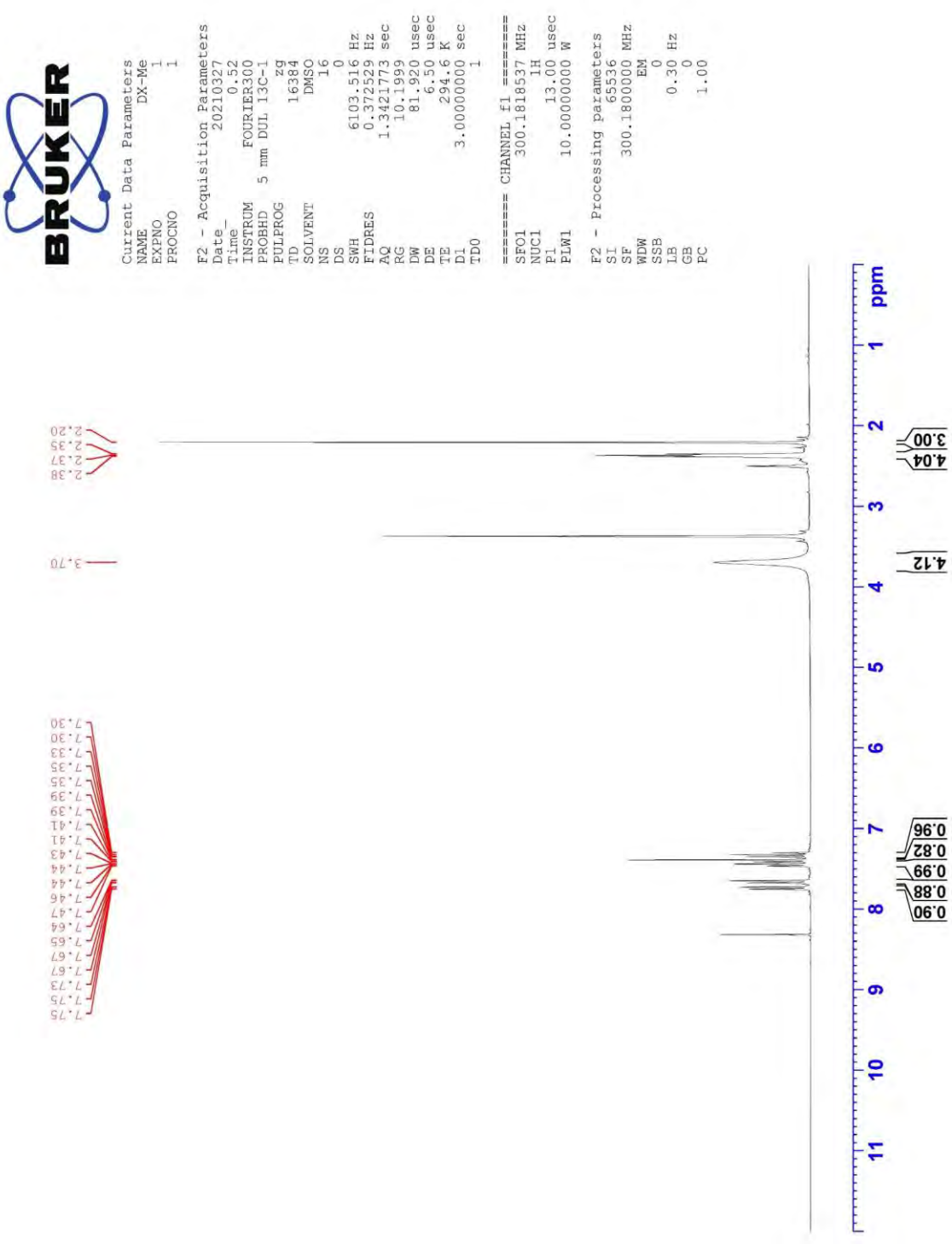


**Figure 5.42.** *$^{1}H$ NMR spectrum of compound **D8***

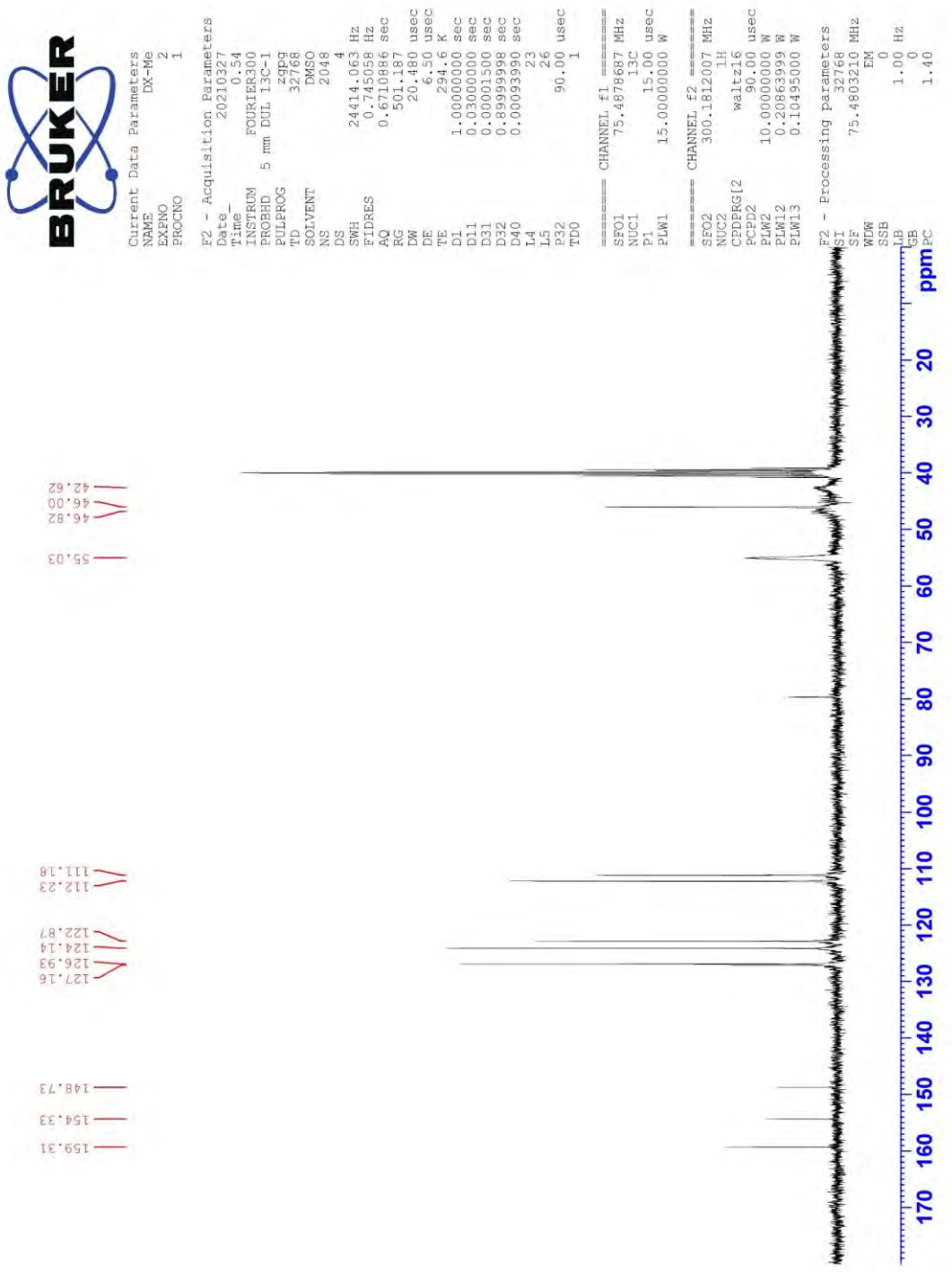


**Figure 5.43.** *$^{1}$H NMR spectrum of compound **D8***

| Elmt | Val. | Min | Max | Elmt | Val. | Min | Max | Elmt | Val. | Min | Max | Elmt | Val. | Min | Max | Use Adduct |
|---|---|---|---|---|---|---|---|---|---|---|---|---|---|---|---|---|
| H | 1 | 10 | 40 | O | 2 | 1 | 4 | S | 2 | 0 | 0 | Ru | 2 | 0 | 0 | H |
| C | 4 | 9 | 40 | F | 1 | 0 | 0 | Cl | 1 | 0 | 0 | Pd | 2 | 0 | 0 | |
| N | 3 | 2 | 6 | P | 3 | 0 | 0 | Br | 1 | 0 | 0 | I | 3 | 0 | 0 | |

Error Margin (ppm): 5
HC Ratio: unlimited
Max Isotopes: 3
MSn Iso RI (%): 10.00

DBE Range: 5.0 - 20.0
Apply N Rule: yes
Isotope RI (%): 1.00
MSn Logic Mode: AND

Electron Ions: both
Use MSn Info: yes
Isotope Res: 9000
Max Results: 150

Event#: 1 MS(E+) Ret. Time: 1.733 -> 1.733 - 2.893 -> 2.900 Scan#: 261 -> 261 - 435 -> 435

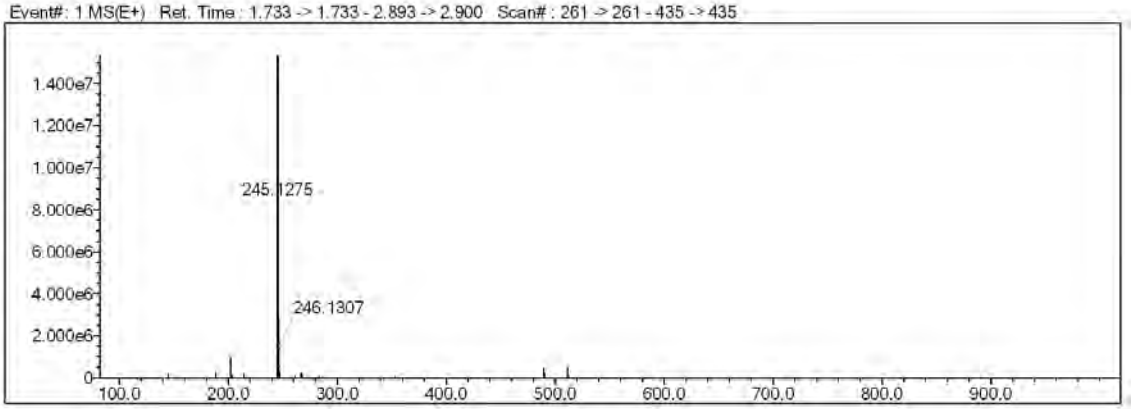


Measured region for 245.1275 m/z

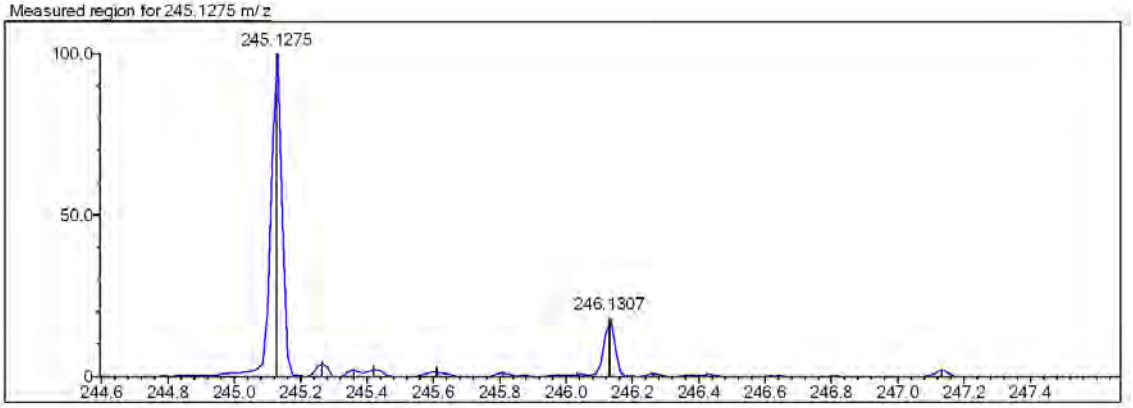


C14 H16 N2 O2 [M+H]+ : Predicted region for 245.1285 m/z

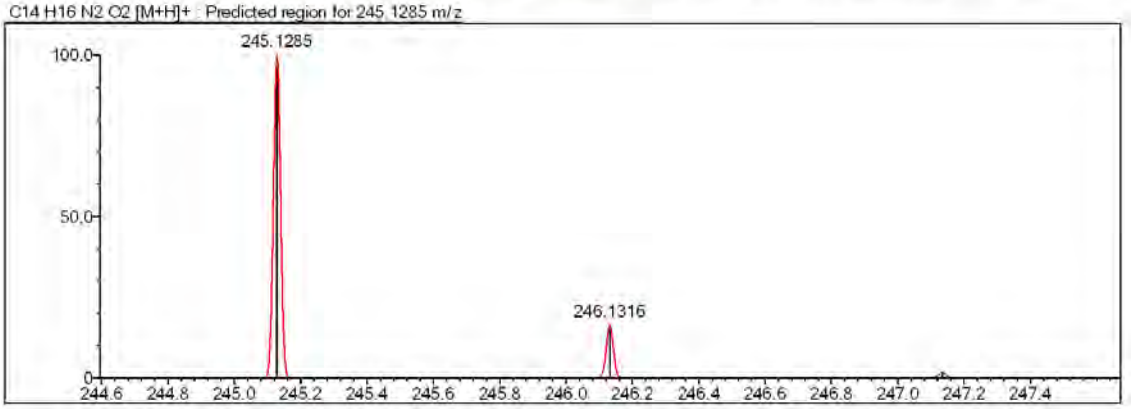


| Rank | Score | Formula (M) | Ion | Meas. m/z | Pred. m/z | Df. (mDa) | Df. (ppm) | Isc | DBE |
|---|---|---|---|---|---|---|---|---|---|
| 1 | 75.42 | C14 H16 N2 O2 | [M+H]+ | 245.1275 | 245.1285 | -1.0 | -4.08 | 81.72 | 8.0 |

**Figure 5.44.** *High-resolution mass spectrum of compound **D8***

DOPNALAB

| | Item | Value |
|---|---|---|
| | Acquired Date&Time | 27.05.2021 15:34:34 |
| | Acquired by | System Administrator |
| | Filename | C:\Users\dopnalab\Desktop\sa\81.ispd |
| | Spectrum name | 81 |
| | Sample name | 8 |
| | Sample ID | |
| | Option | |
| | Comment | |
| | No. of Scans | 16 |
| | Resolution | 4 [cm-1] |
| | Apodization | Happ-Genzel |

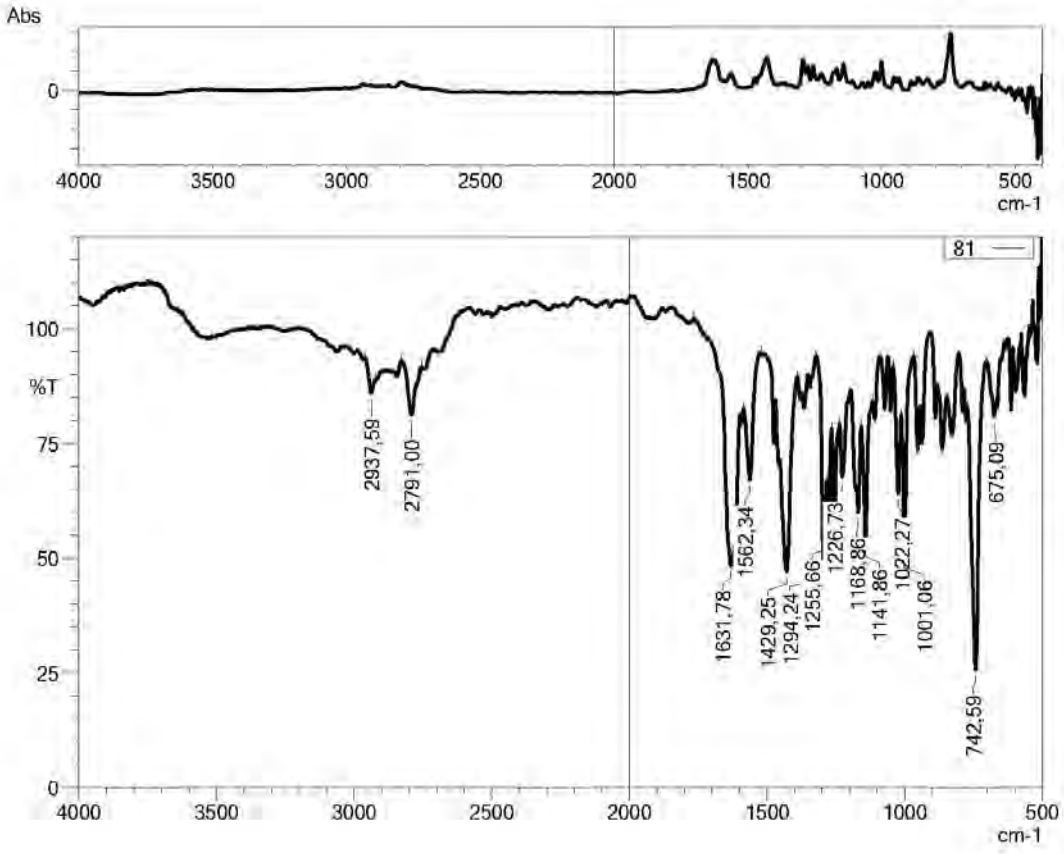


**Figure 5.45.** *IR spectrum of compound **D8***

### 5.1.4.9. *benzofuran-2-yl(4-ethylpiperazin-1-yl)methanone (D9)*

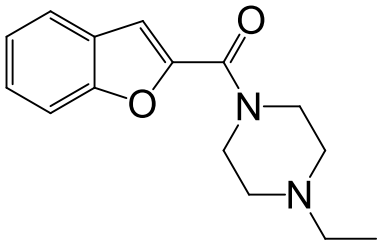


**Figure 5.46.** *Molecular structure of compound **D9***

**Physical Properties: Texture:** solid crystals, **Color:** light brown, **M.P.:** 56-57ºC**, Yield:** 77%.

**IR (ATR) $\upsilon_{max}$ ($cm^{-1}$):** 3070 ($SP^2$ C-H stretching, aromatic), 2964-2765 ($SP^3$ C-H stretching, methylenes of piperazine, and ethyl-methyl piperazine), 1625 (C=O stretching, amide), 1566 (C-H bending, indicative of non-substituted benzofuran at position 3), 1431 (C=C stretching, aromatic), 1290-1228 (C-O stretching, ether), 1161-1128, 1016 (C-N stretching, tertiary amine and/or C-O stretching, ether), 947-690 (C-H aromatic out-of-plane bending, prominent peak at 947 and more peaks between 870-830 indicate non-substituted benzofuran at position 3).

**$^1$H NMR (300 MHz) (DMSO-$d_6$) $\delta$ (ppm):** 1.02 (t, *J*= 7.17 Hz, 3H, piperazine-$CH_2$-**$CH_3$**) 2.37 (q, *J*= 14.43, 7.25 Hz, 2H, piperazine-**$CH_2$**-$CH_3$), 2.42 (t, *J*= 5.08 Hz, 4H, piperazine-3, 5), 3.71 (brs, 4H, piperazine-2, 6), 7.32 (t, *J*= 7.01 Hz, 1H, benzofuran-5), 7.40 (s, 1H, benzofuran-3), 7.45 (t, *J*= 7.08 Hz, 1H, benzofuran-6), 7.67 (d, *J*= 8.32 Hz, 1H, benzofuran-7), 7.75 (d, *J*= 7.31 Hz, 1H, benzofuran-4).

**$^{13}$C NMR (300 MHz) (DMSO-$d_6$) $\delta$ (ppm):** 12.33 (piperazine-$CH_2$-**$CH_3$**), 42.72 (piperazine), 46.75 (piperazine), 51.89 (piperazine-**$CH_2$**-$CH_3$), 52.68 (piperazine), 111.18, 112.24, 122.87, 124.15, 126.93, 127.15, 148.74, 154.32, 159.24 (benzofuran-**CO**-piperazine).

**HRMS (ESI) (m/z) $[M+1]^+$:** for $C_{15}H_{18}N_2O_2$ calculated: 259.1441; found: 259.1441.

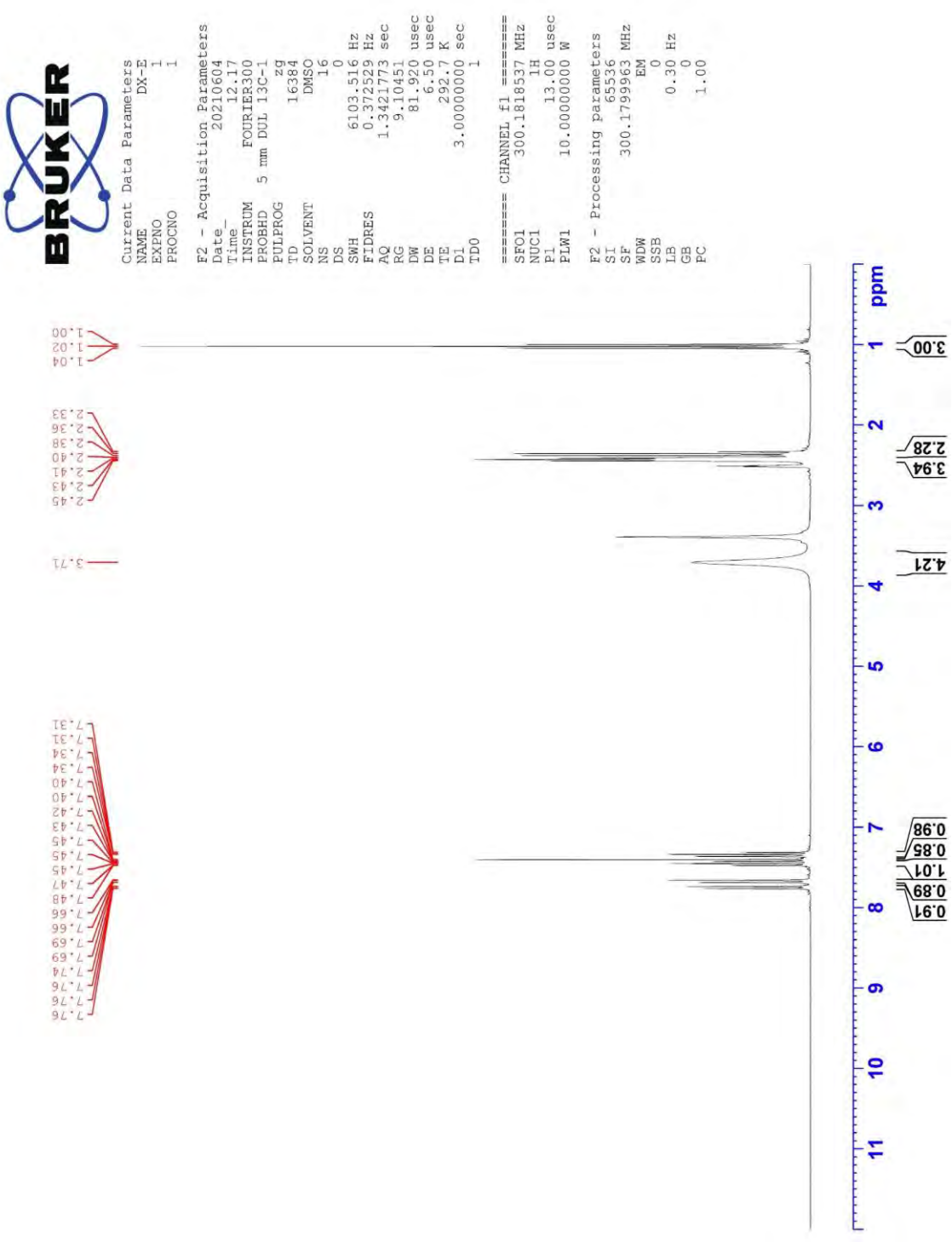


**Figure 5.47.** *$^{1}H$ NMR spectrum of compound **D9***

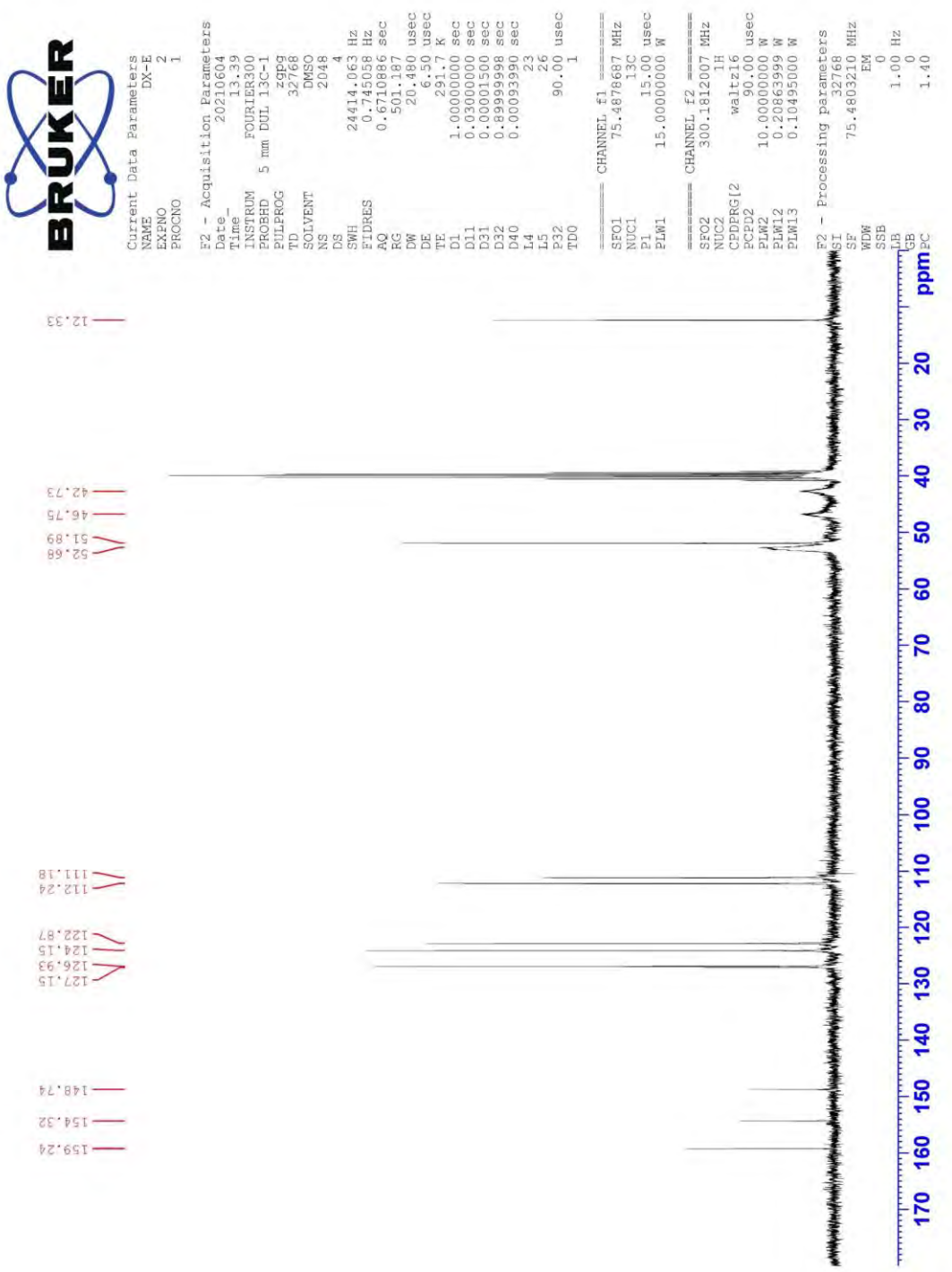


**Figure 5.48.** *$^{13}$C NMR spectrum of compound **D9***

Data File: C:\LabSolutions\Data\Analiz\A.Çagri\D-9_3.lcd

| Elmt | Val. | Min | Max | Elmt | Val. | Min | Max | Elmt | Val. | Min | Max | Elmt | Val. | Min | Max | Use Adduct |
|---|---|---|---|---|---|---|---|---|---|---|---|---|---|---|---|---|
| H | 1 | 0 | 40 | O | 2 | 2 | 5 | S | 2 | 0 | 4 | Ru | 2 | 0 | 0 | H |
| C | 4 | 0 | 40 | F | 1 | 0 | 0 | Cl | 1 | 0 | 0 | Pd | 2 | 0 | 0 | |
| N | 3 | 2 | 4 | P | 3 | 0 | 0 | Br | 1 | 0 | 0 | I | 3 | 0 | 0 | |

Error Margin (ppm): 5
HC Ratio: unlimited
Max Isotopes: 3
MSn Iso RI (%): 10.00

DBE Range: 0.0 - 20.0
Apply N Rule: yes
Isotope RI (%): 1.00
MSn Logic Mode: AND

Electron Ions: both
Use MSn Info: yes
Isotope Res: 9000
Max Results: 150

Event#: 1 MS(E+) Ret. Time : 1.547 -> 2.467 Scan# : 233 -> 371

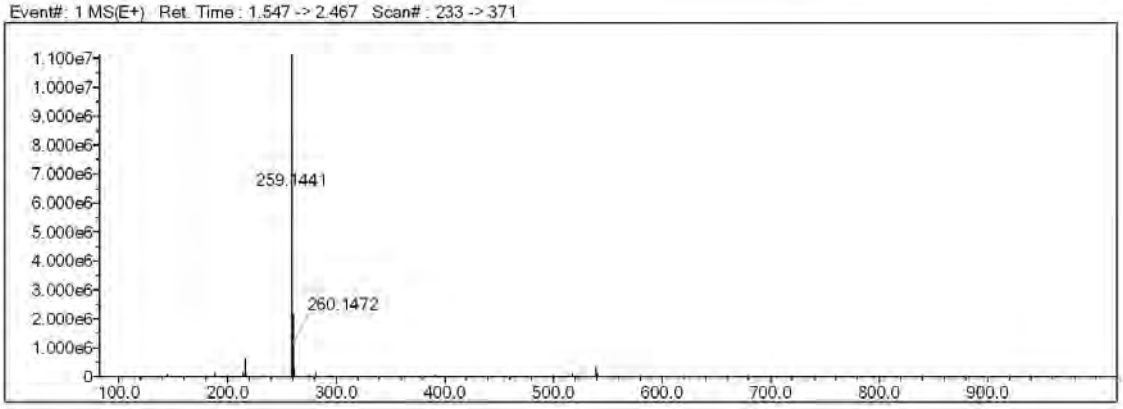


Measured region for 259.1441 m/z

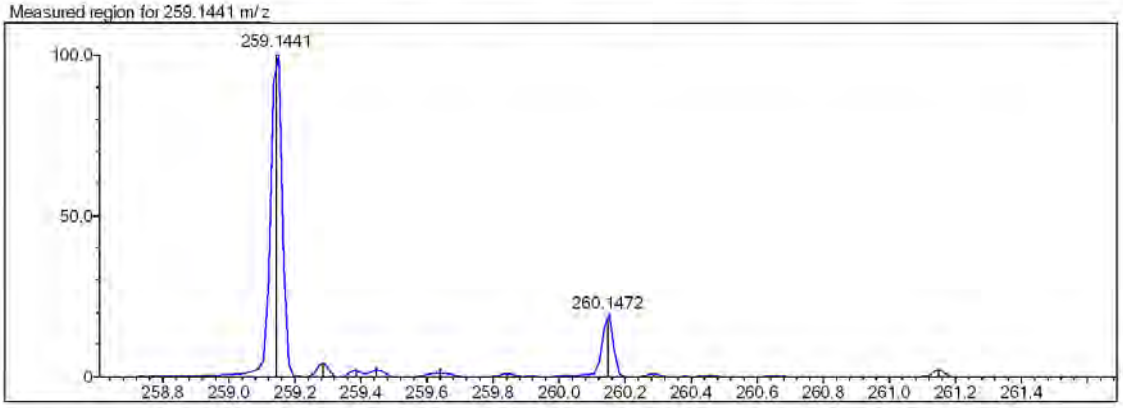


C15 H18 N2 O2 [M+H]+ : Predicted region for 259.1441 m/z

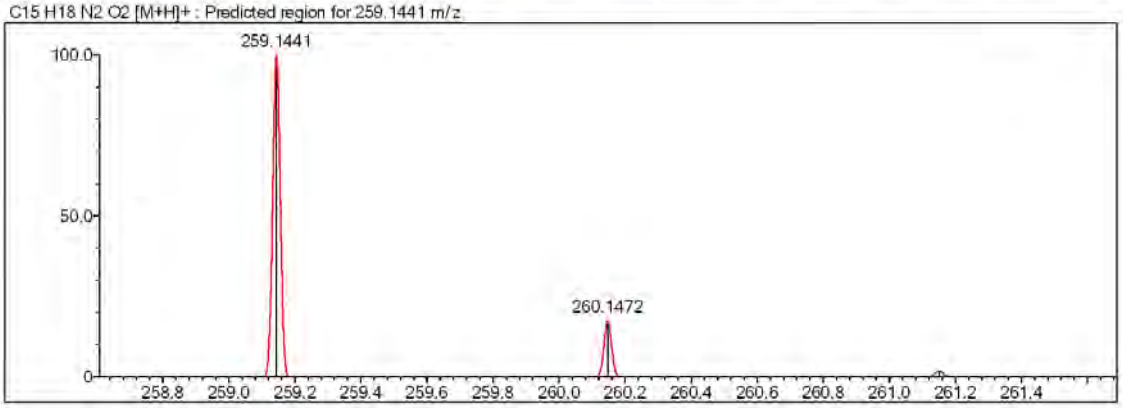


| Rank | Score | Formula (M) | Ion | Meas. m/z | Pred. m/z | Df. (mDa) | Df. (ppm) | Isc | DBE |
|---|---|---|---|---|---|---|---|---|---|
| 1 | 100.00 | C15 H18 N2 O2 | [M+H]+ | 259.1441 | 259.1441 | -0.0 | 0.00 | 100.00 | 8.0 |

**Figure 5.49.** *High-resolution mass spectrum of compound **D9***

DOPNALAB

| | Item | Value |
|---|---|---|
| | Acquired Date&Time | 27.05.2021 15:39:48 |
| | Acquired by | System Administrator |
| | Filename | C:\Users\dopnalab\Desktop\sa\91.ispd |
| | Spectrum name | 91 |
| | Sample name | 9 |
| | Sample ID | |
| | Option | |
| | Comment | |
| | No. of Scans | 15 |
| | Resolution | 4 [cm-1] |
| | Apodization | Happ-Genzel |

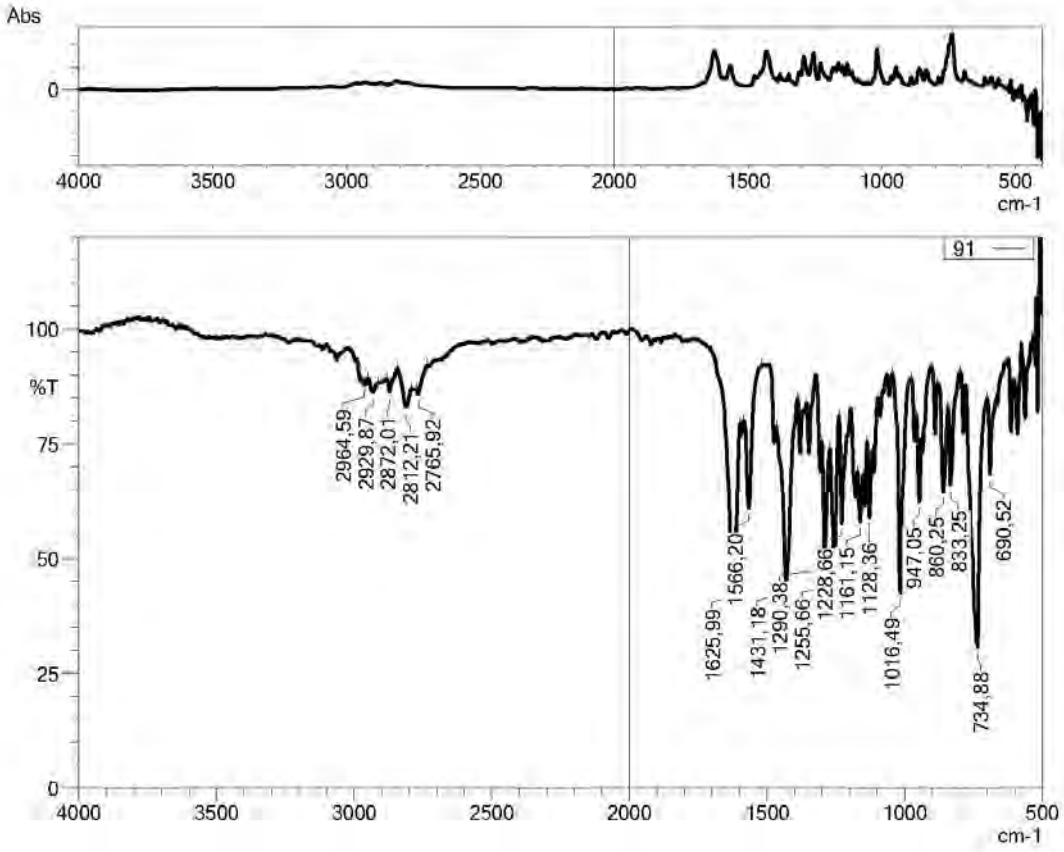


**Figure 5.50.** *IR spectrum of compound **D9***

### 5.1.4.10. *benzofuran-2-yl(4-(2-(dimethylamino)ethyl)piperazin-1-yl)methanone (D10)*

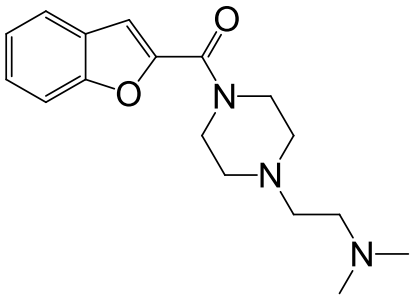


**Figure 5.51.** *Molecular structure of compound **D10***

**Physical Properties: Texture:** solid crystals, **Color:** yellowish white, **M.P.:** 59-61ºC**, Yield:** 75%.

**IR (ATR) $\upsilon_{max}$ ($cm^{-1}$):** 3070 ($SP^2$ C-H stretching, aromatic), 2956-2765 ($SP^3$ C-H stretching, methylenes of piperazine, and dimethylaminoethyl-piperazine), 1625 (C=O stretching, amide), 1566 (C-H bending, indicative of non-substituted benzofuran at position 3), 1431 (C=C stretching, aromatic), 1290-1228 (C-O stretching, ether), 1161-1128, 1016 (C-N stretching, tertiary amine and/or C-O stretching, ether), 947-690 (C-H aromatic out-of-plane bending prominent peak at 947 and more peaks between 870-830 indicate non-substituted benzofuran at position 3).

**$^1$H NMR (300 MHz) (DMSO-$d_6$) $\delta$ (ppm):** 2.13 (s, 6H, -N(**$CH_3$**)$_2$), 2.32-2.43 (m, 4H, piperazine-(**$CH_2$**)$_2$-N), 2.47 (t, *J*= 5.09 Hz, 4H, piperazine-3, 5), 3.69 (brs, 4H, piperazine-2, 6), 7.34 (t, *J*= 7.95 Hz, 1H, benzofuran-5), 7.40 (s, 1H, benzofuran-3), 7.44 (t, *J*= 7.08 Hz, 1H, benzofuran-6), 7.67 (d, *J*= 8.32 Hz, 1H, benzofuran-7), 7.75 (d, *J*= 7.30 Hz, 1H, benzofuran-4).

**$^{13}$C NMR (300 MHz) (DMSO-$d_6$) $\delta$ (ppm):** 42.68 (piperazine), 45.99 (-N(**$CH_3$**)$_2$), 46.81 (piperazine), 53.57 (piperazine), 56.04 (piperazine-(**$CH_2$**)$_2$-N), 57.03 (piperazine-(**$CH_2$**)$_2$-N), 111.17, 112.24, 122.87, 124.14, 126.93, 127.15, 148.72, 154.32, 159.22 (benzofuran-**CO**-piperazine).

**HRMS (ESI) (m/z) $[M+1]^+$:** for $C_{17}H_{23}N_3O_2$ calculated: 302.1863; found: 302.1869.

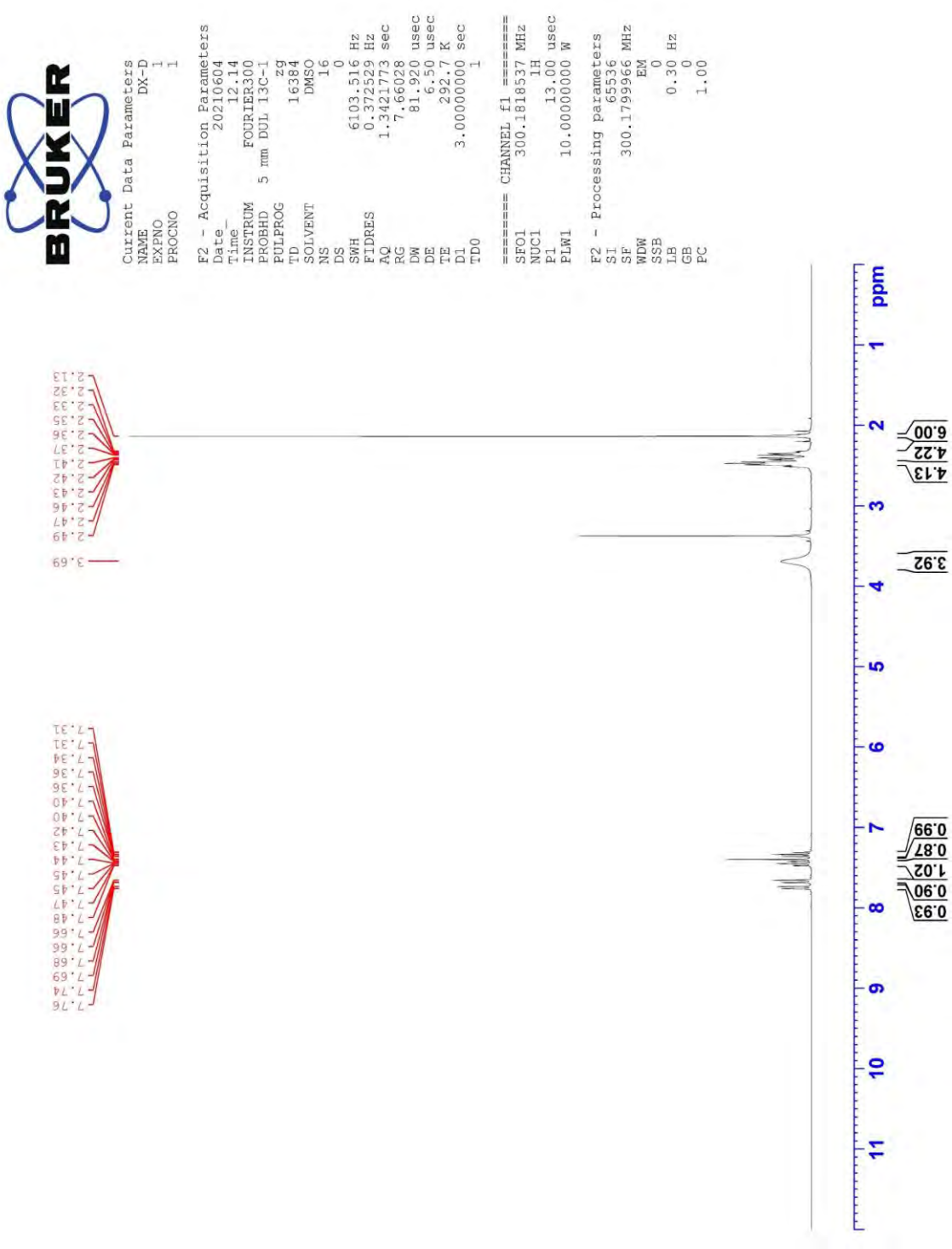


**Figure 5.52.** *$^{1}H$ NMR spectrum of compound **D10***

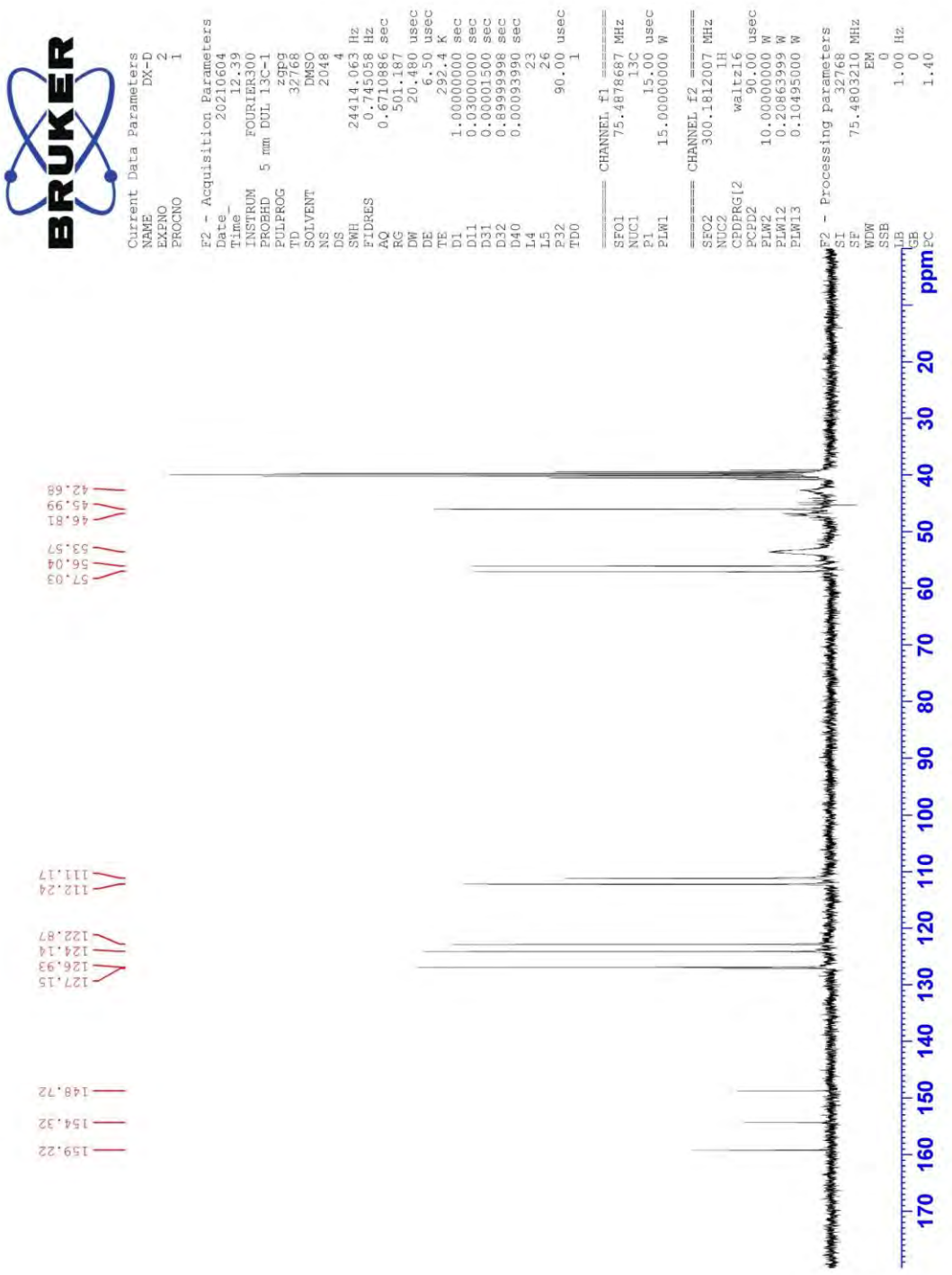


**Figure 5.53.** *$^{13}$C NMR spectrum of compound **D10***

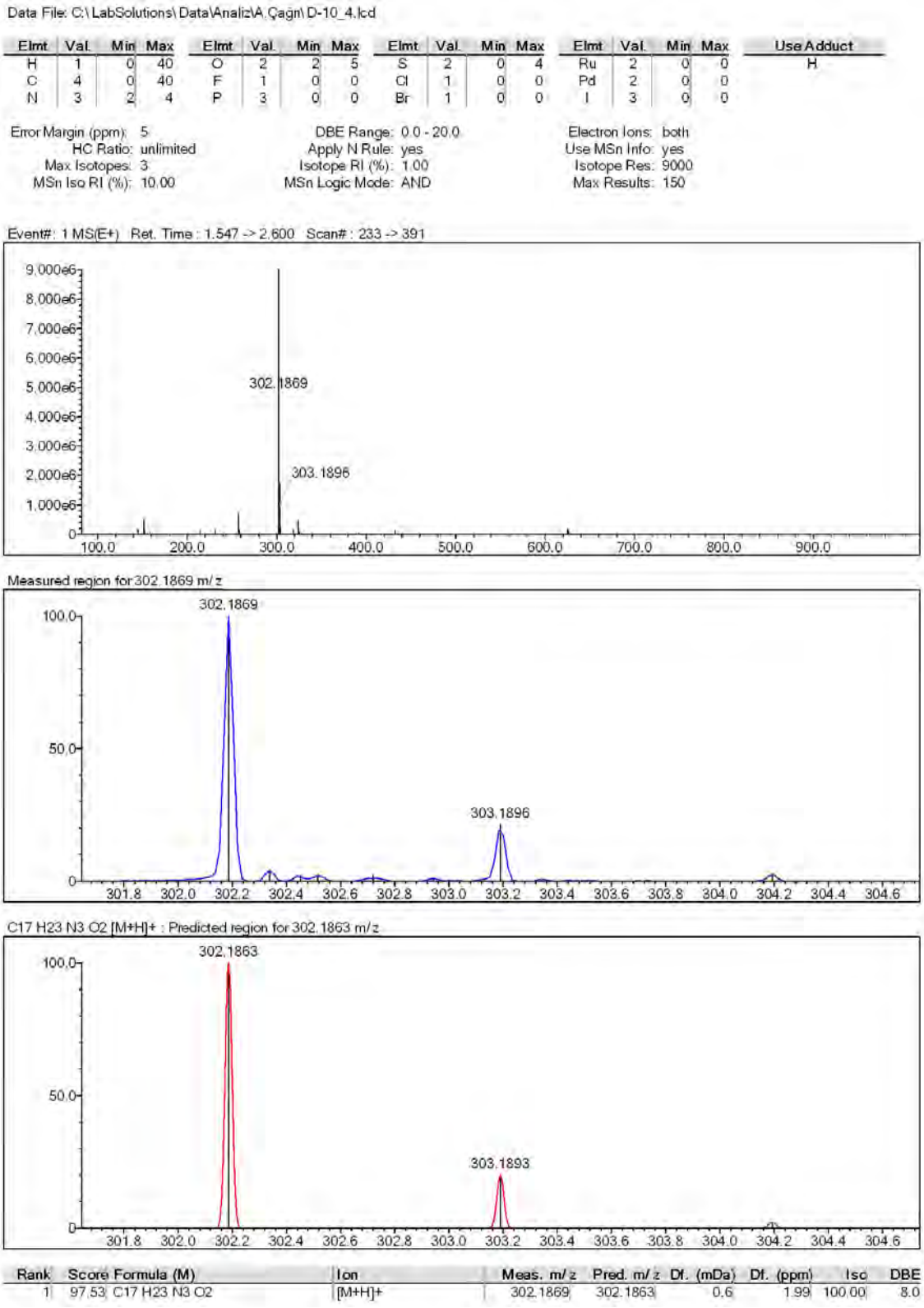


**Figure 5.54.** *High-resolution mass spectrum of compound* ***D10***

DOPNALAB

| | Item | Value |
|---|---|---|
| | Acquired Date&Time | 27.05.2021 15:44:54 |
| | Acquired by | System Administrator |
| | Filename | C:\Users\dopnalab\Desktop\sa\101.ispd |
| | Spectrum name | 101 |
| | Sample name | 10 |
| | Sample ID | |
| | Option | |
| | Comment | |
| | No. of Scans | 15 |
| | Resolution | 4 [cm-1] |
| | Apodization | Happ-Genzel |

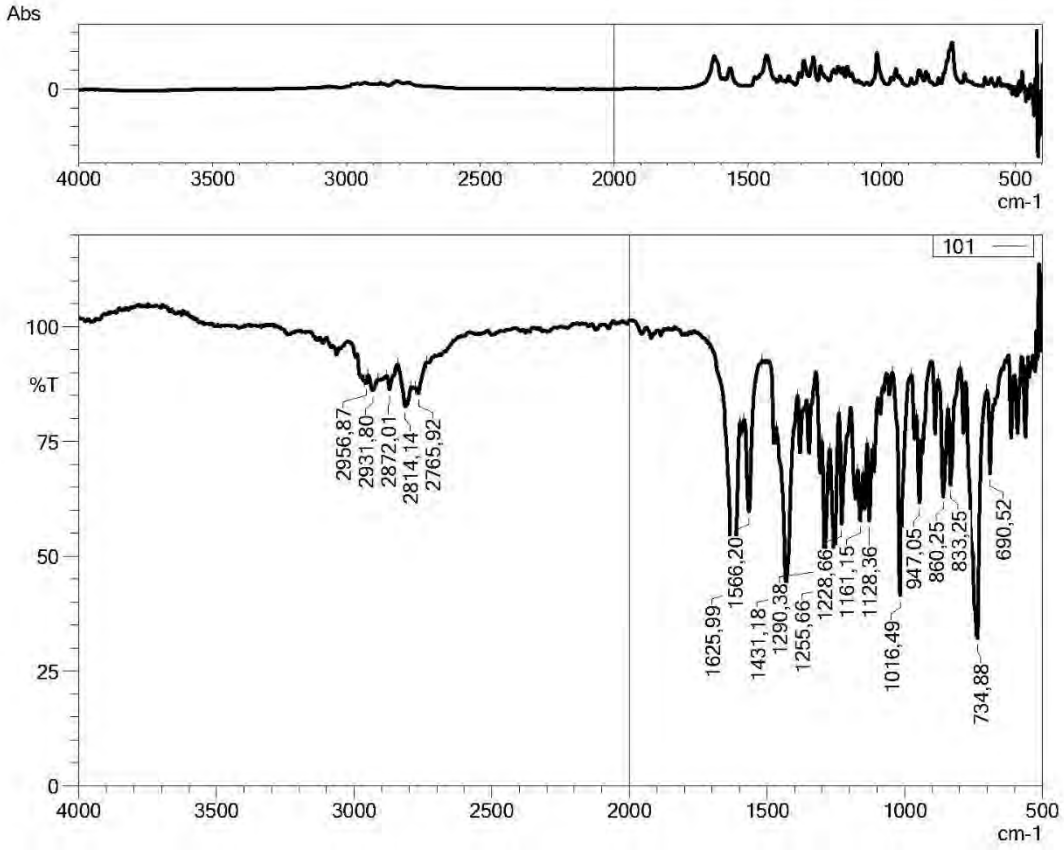


**Figure 5.55.** *IR spectrum of compound **D10***

### 5.1.4.11. *(5-chloro-3-methylbenzofuran-2-yl)(4-phenylpiperazin-1-yl)methanone (D11)*

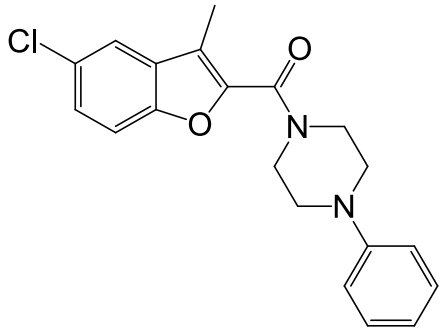


**Figure 5.56.** *Molecular structure of compound **D11***

**Physical Properties: Texture:** solid crystals, **Color:** yellowish white, **M.P.:** 142-143ºC**, Yield:** 75%.

**IR (ATR) $\upsilon_{max}$ ($cm^{-1}$):** 3026 ($SP^2$ C-H stretching, aromatic), 2953-2816 ($SP^3$ C-H stretching, 3-methylbenzofuran and methylenes of piperazine), 1622 (C=O stretching, amide), 1598-1502, 1442 (C=C stretching, aromatic), 1236 (C-O stretching, ether), 1155, 1010 (C-N stretching, tertiary amine and/or ether), 900-632 (C-H aromatic out-of-plane bending).

**$^1$H NMR (300 MHz) (DMSO-$d_6$) $\delta$ (ppm):** 2.35 (s, 3H, **3-methyl**benzofuran), 3.22 (brs, 4H, piperazine-3, 5), 3.76 (brs, 4H, piperazine-2, 6), 6.83 (t, *J*= 7.25 Hz, 1H, phenyl-4), 6.97 (d, *J*= 7.87, 2H, phenyl-2, 6), 7.24 (t, *J*= 8.58 Hz, 2H, phenyl-3,5), 7.47 (dd, *J*= 8.78, 2.19 Hz, 1H, benzofuran-6), 7.67 (d, *J*= 8.78 Hz, 1H, benzofuran-7), 7.84 (d, *J*= 2.01 Hz, 1H, benzofuran-4).

**$^{13}$C NMR (300 MHz) (DMSO-$d_6$) $\delta$ (ppm):** 8.91 (**3-methyl**benzofuran), 42.53 (piperazine), 46.55 (piperazine), 49.14 (piperazine), 113.77, 116.44, 119.31, 119.95, 120.85, 126.86, 128.20, 129.48, 130.61, 145.62, 151.14, 151.93, 159.82 (benzofuran-**CO-**piperazine).

**HRMS (ESI) (m/z) $[M+1]^+$:** for $C_{20}H_{19}ClN_2O_2$ calculated: 355.1208; found: 355.1218.

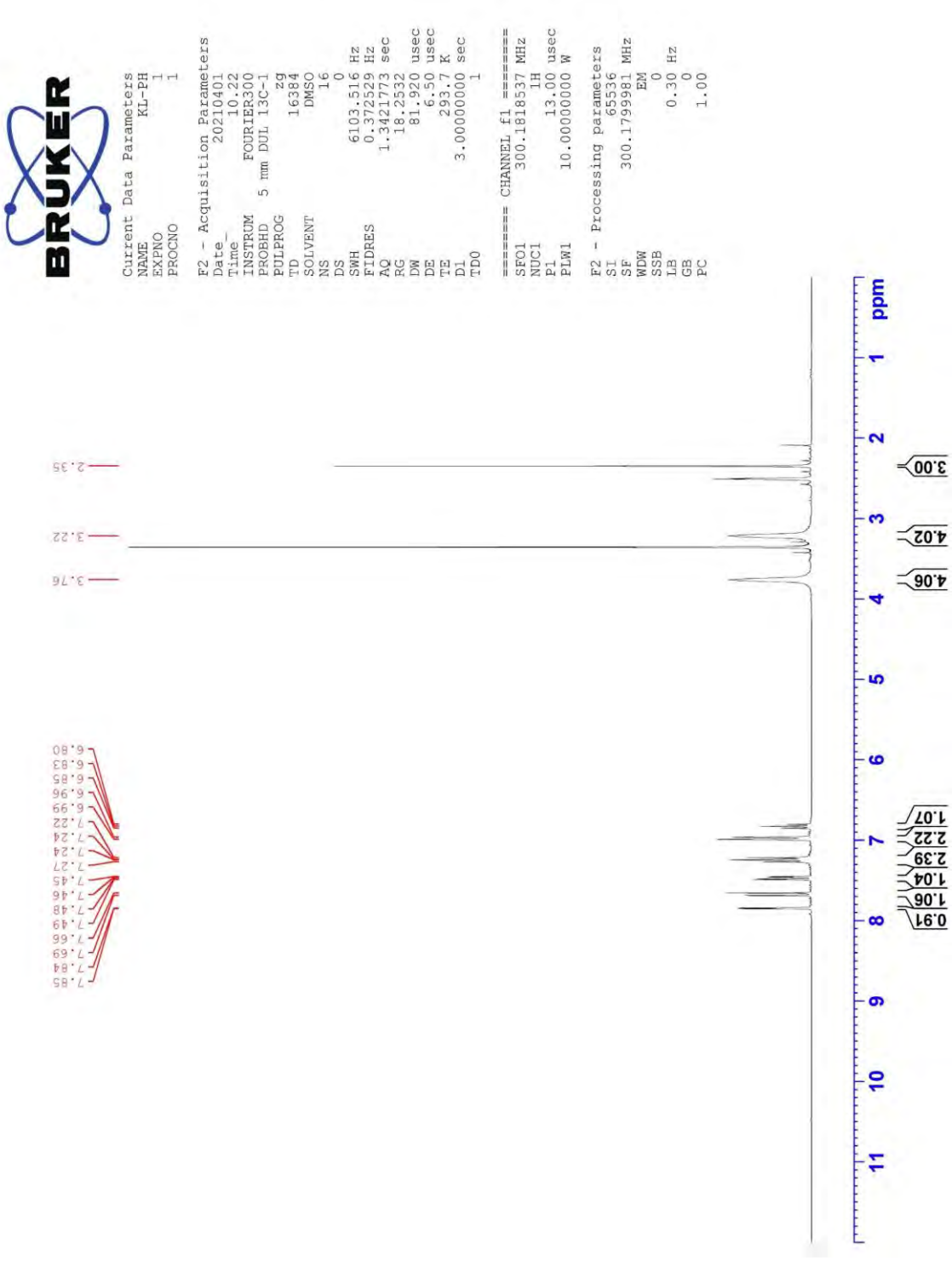


**Figure 5.57.** *$^{1}H$ NMR spectrum of compound **D11***

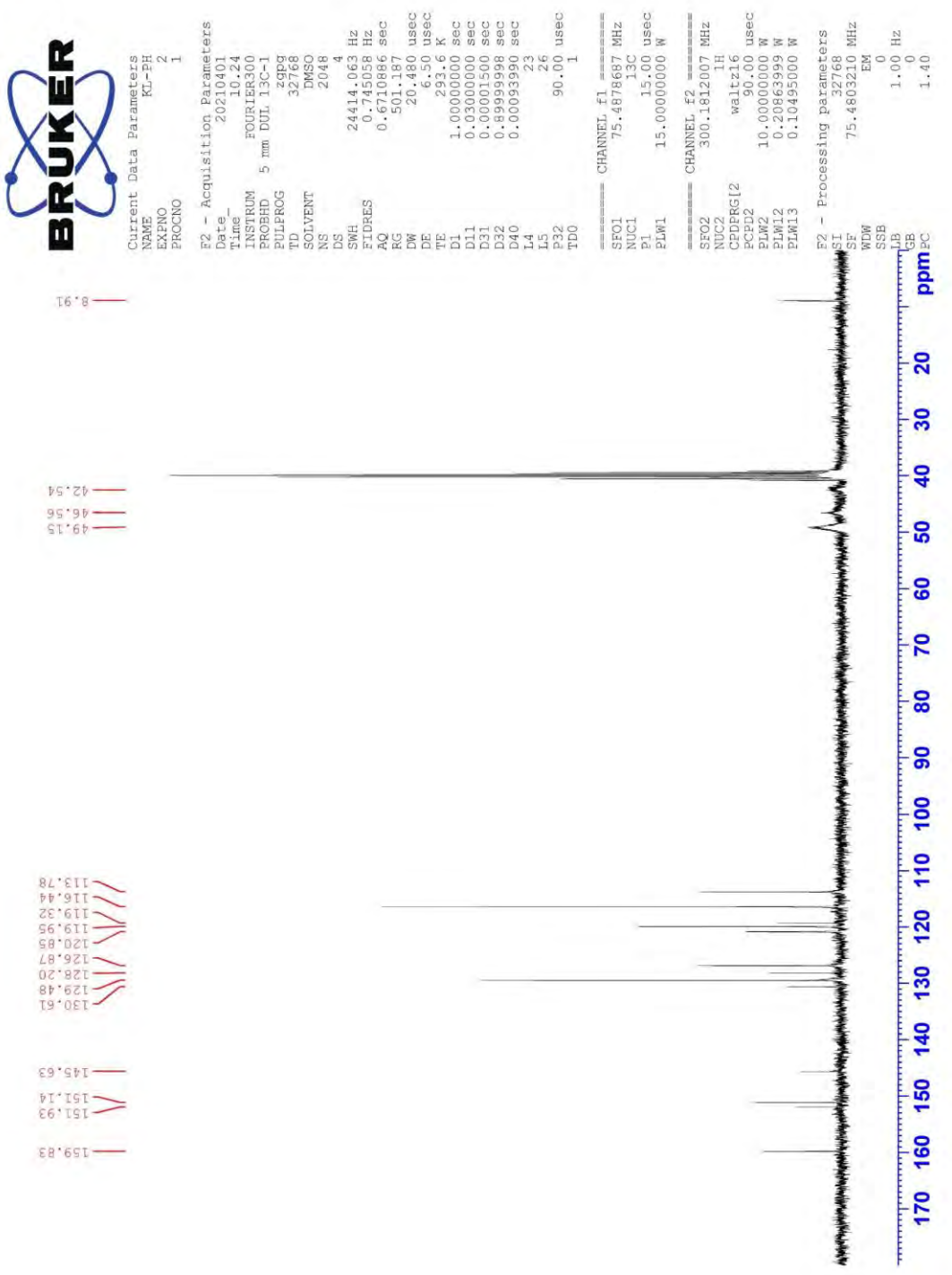


**Figure 5.58.** *$^{13}C$ NMR spectrum of compound **D11***

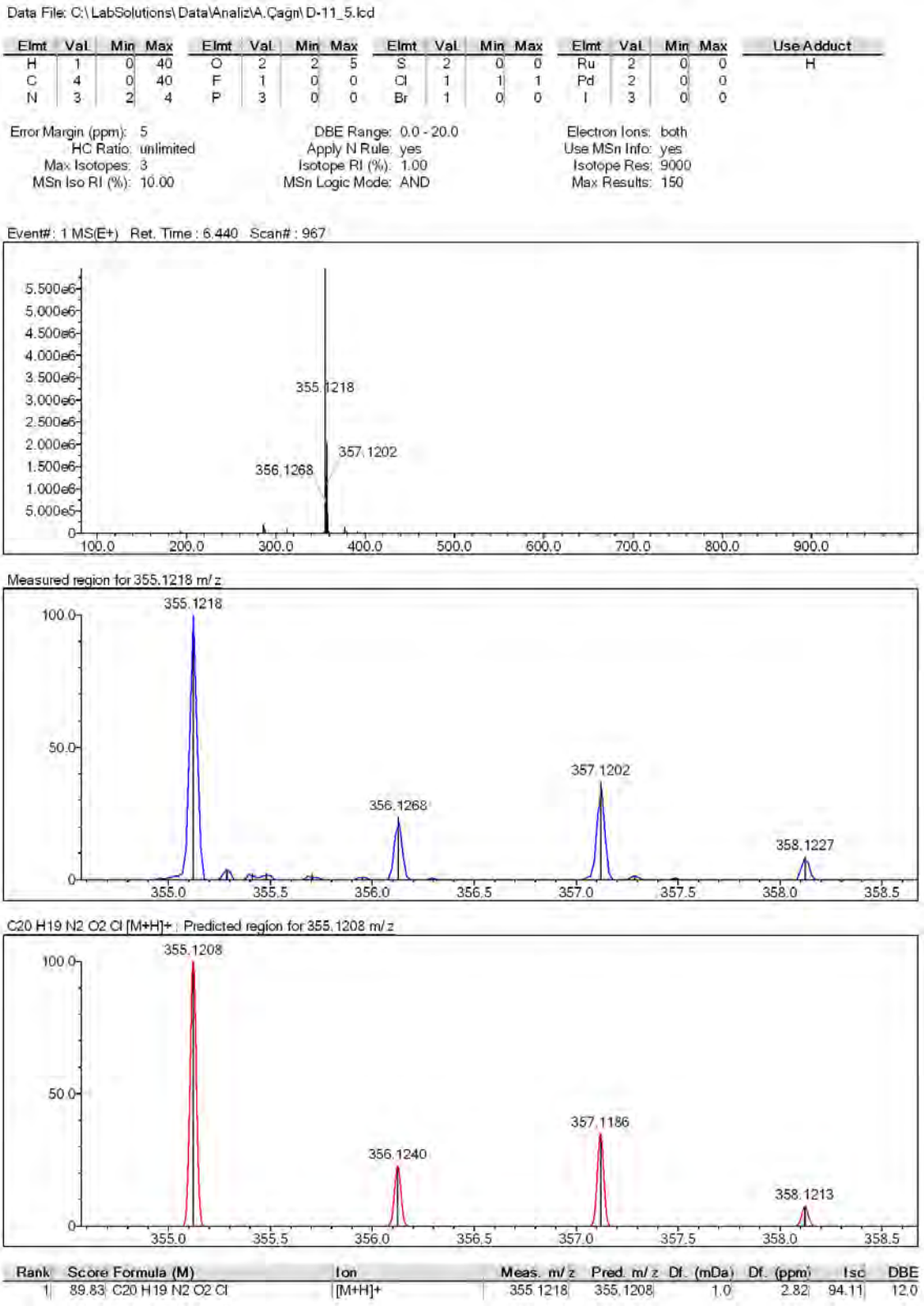


**Figure 5.59.** *High-resolution mass spectrum of compound* ***D11***

DOPNALAB

| | Item | Value |
|---|---|---|
| | Acquired Date&Time | 27.05.2021 15:50:51 |
| | Acquired by | System Administrator |
| | Filename | C:\Users\dopnalab\Desktop\sa\111.ispd |
| | Spectrum name | 111 |
| | Sample name | 11 |
| | Sample ID | |
| | Option | |
| | Comment | |
| | No. of Scans | 15 |
| | Resolution | 4 [cm-1] |
| | Apodization | Happ-Genzel |

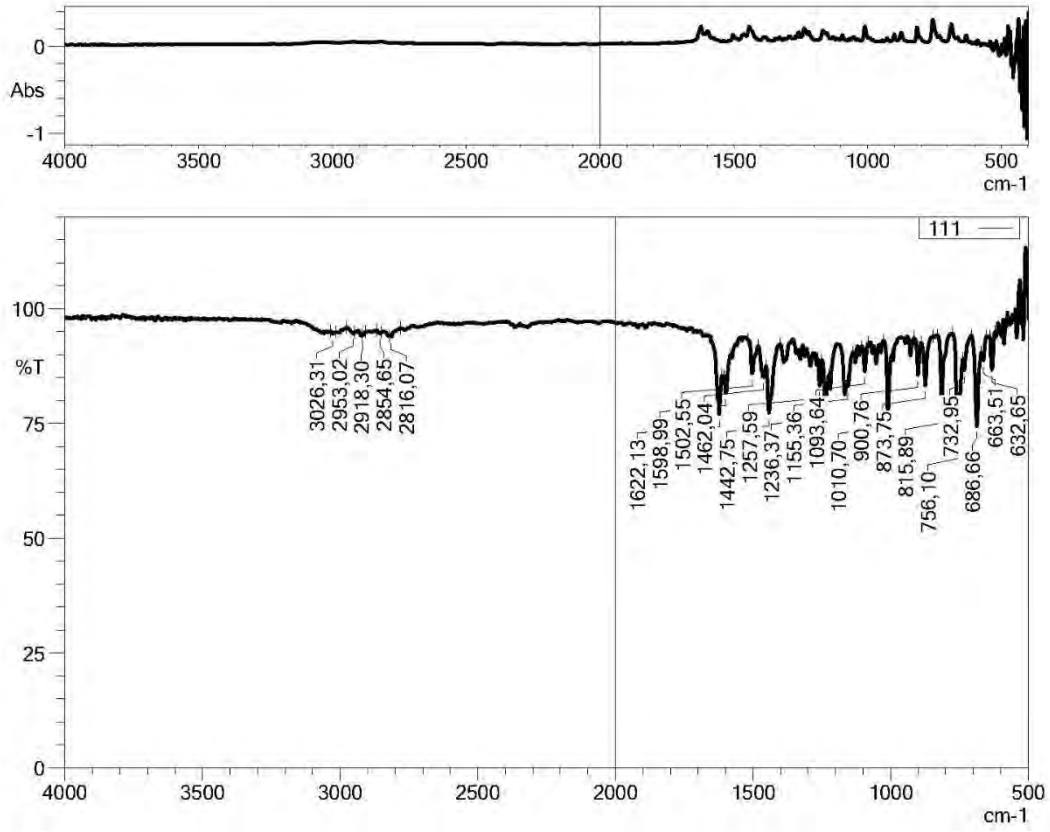


**Figure 5.60.** *IR spectrum of compound **D11***

### 5.1.4.12. *(4-(5-chloro-3-methylbenzofuran-2-carbonyl)piperazin-1-yl)(furan-2-yl)methanone (D12)*

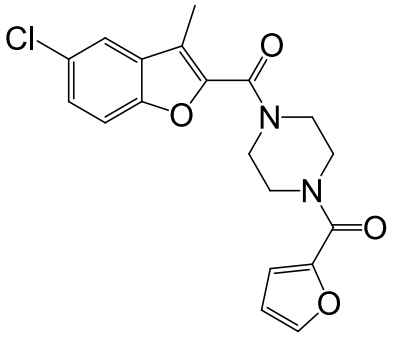


**Figure 5.61.** *Molecular structure of compound **D12***

**Physical Properties: Texture:** solid crystals, **Color:** white, **M.P.:** 119-120ºC**, Yield:** 54%.

**IR (ATR) $\upsilon_{max}$ ($cm^{-1}$):** 3120-3007 ($SP^2$ C-H stretching, aromatic), 2922-2904 ($SP^3$ C-H stretching, methylenes of piperazine and 3-methylbenzofuran), 1637 (C=O, carbonyl of furoyl), 1612 (C=O stretching, amide), 1487-1423 (C=C stretching, aromatic), 1259 (C-O stretching, ether), 1165, 1002 (C-N stretching, tertiary amine and/or ether), 800 (C-Cl stretching), 750-630 (C-H aromatic out-of-plane bending).

**$^1$H NMR (300 MHz) (DMSO-$d_6$) $\delta$ (ppm):** 2.35 (s, 3H, **3-methyl**benzofuran), 3.71-3.77 (m, 8H, piperazine-2, 3, 5, 6), 6.65 (dd, *J*= 3.45, 1.77 Hz, 1H, furan-4), 7.05 (d, *J*= 3.46 Hz, 1H, furan-3), 7.47 (dd, *J*= 8.79, 2.21 Hz, 1H, benzofuran-6), 7.66 (d, *J*= 8.80 Hz, 1H, benzofuran-7), 7.84-7.92 (m, 2H, benzofuran-4 and furan-5).

**$^{13}$C NMR (300 MHz) (DMSO-$d_6$) $\delta$ (ppm):** 8.94 (**3-methyl**benzofuran), 42.74 (piperazine), 46.65 (piperazine), 111.86, 113.81, 114.09, 116.46, 119.66, 120.86, 121.58, 126.94, 128.20, 130.59, 145.41, 147.17, 151.95, 158.91 (piperazine-**CO**-furan), 160.04 (benzofuran-**CO**-piperazine).

**HRMS (ESI) (m/z) $[M+1]^+$:** for $C_{19}H_{17}ClN_2O_4$ calculated: 373.0950; found: 373.0966.

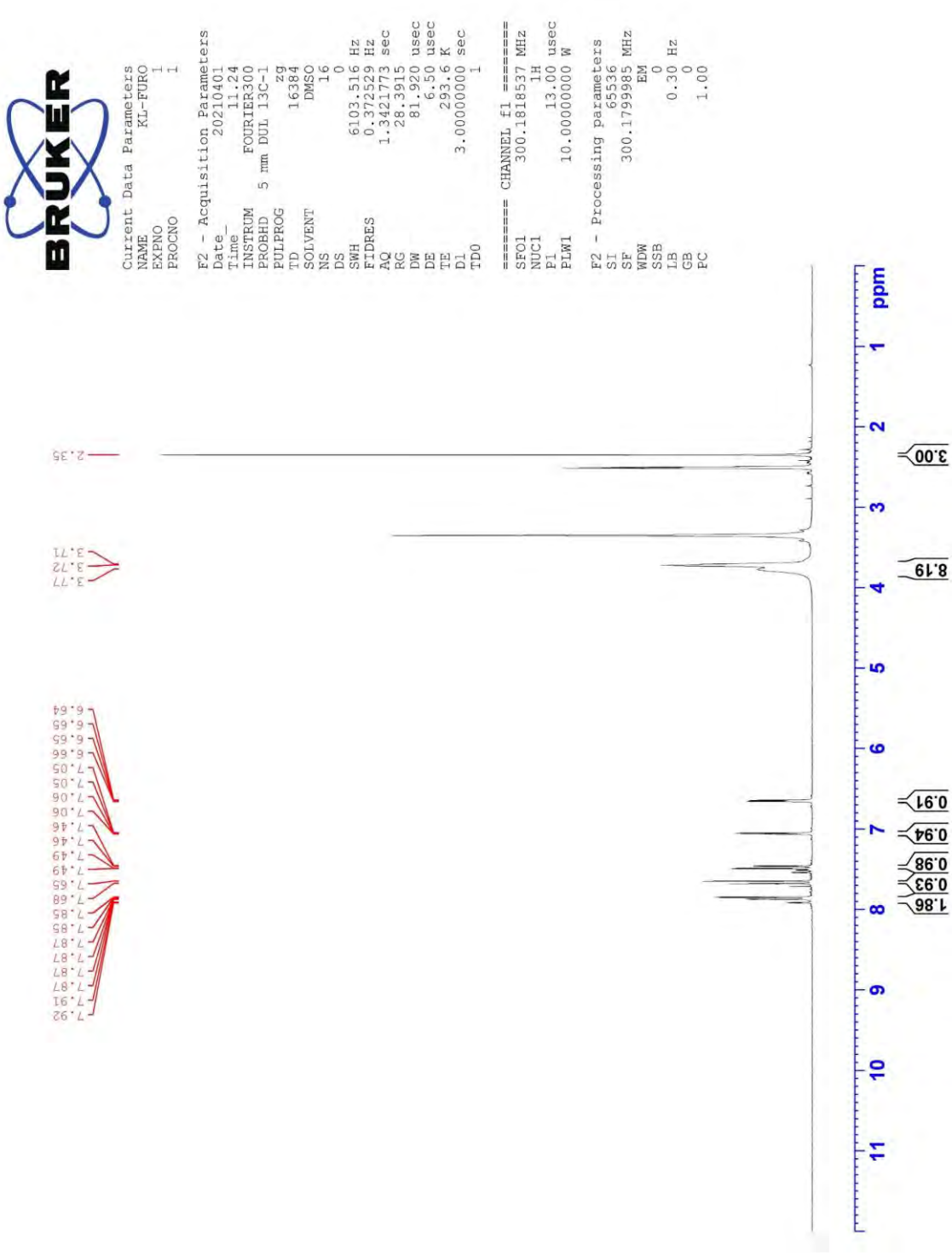


**Figure 5.62.** *[1]H NMR spectrum of compound **D12***

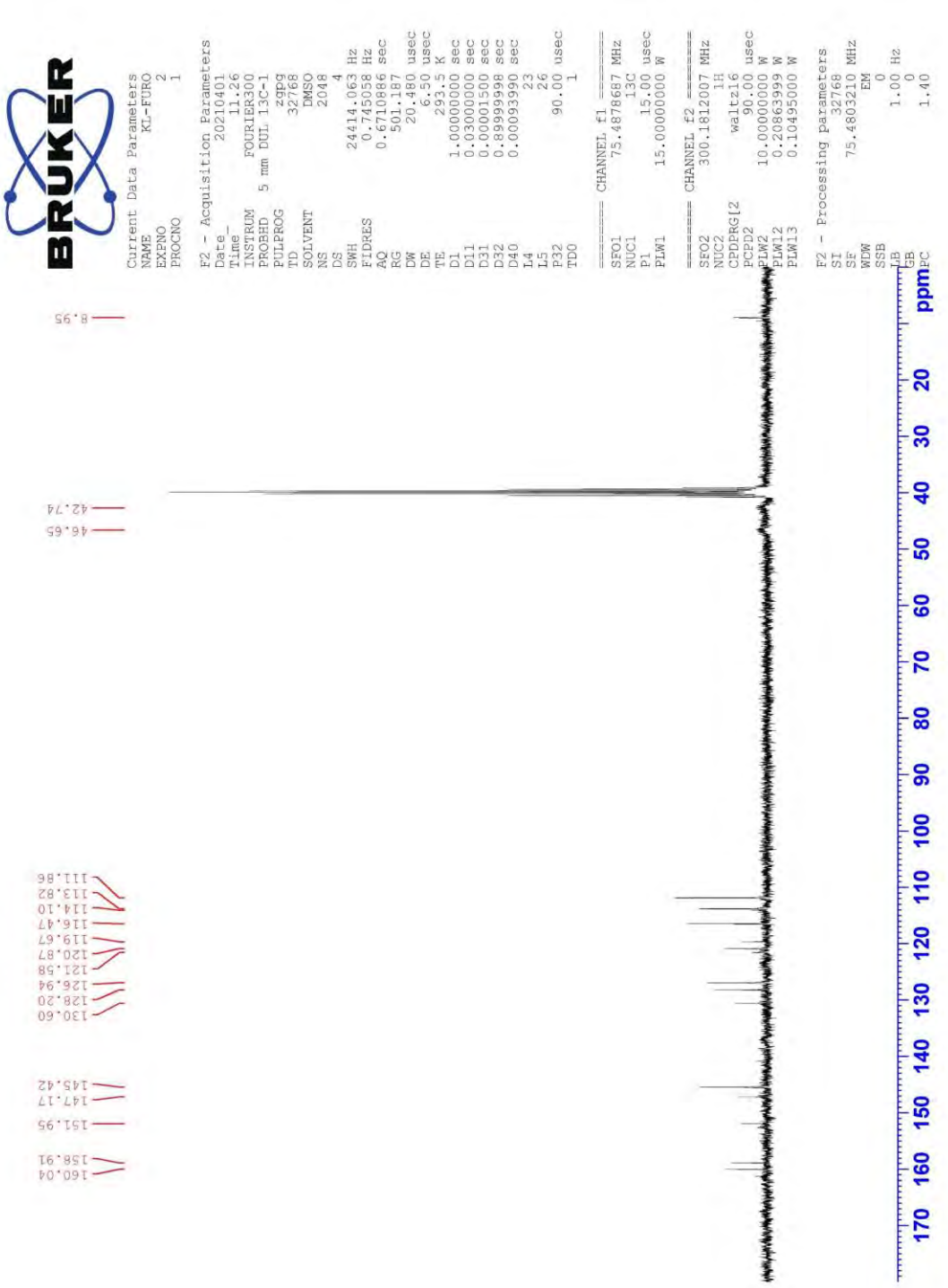


**Figure 5.63.** *$^{13}$C NMR spectrum of compound **D12***

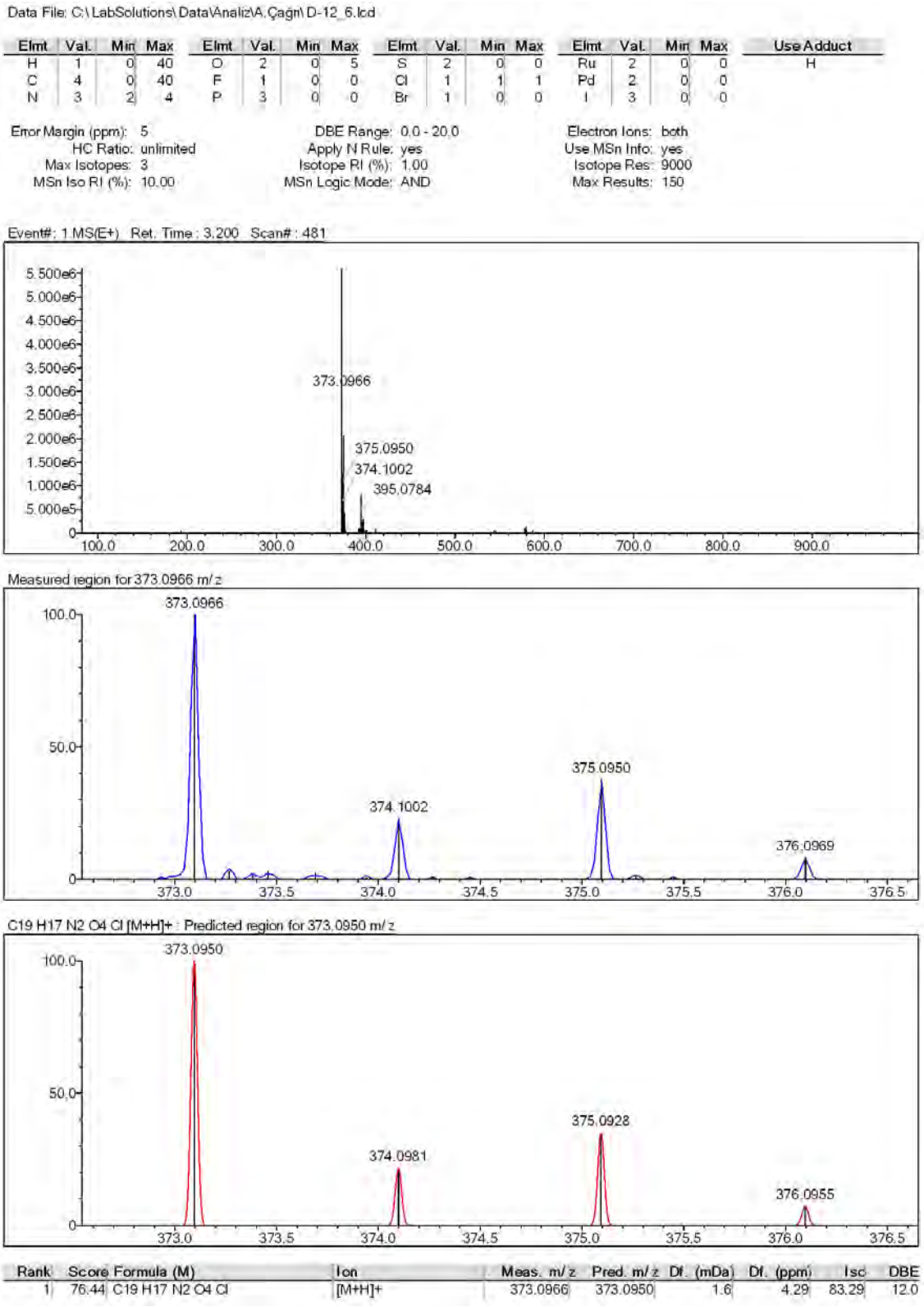


**Figure 5.64.** *High-resolution mass spectrum of compound* ***D12***

DOPNALAB

| | Item | Value |
|---|---|---|
| | Acquired Date&Time | 27.05.2021 15:56:57 |
| | Acquired by | System Administrator |
| | Filename | C:\Users\dopnalab\Desktop\sa\121.ispd |
| | Spectrum name | 121 |
| | Sample name | 12 |
| | Sample ID | |
| | Option | |
| | Comment | |
| | No. of Scans | 16 |
| | Resolution | 4 [cm-1] |
| | Apodization | Happ-Genzel |

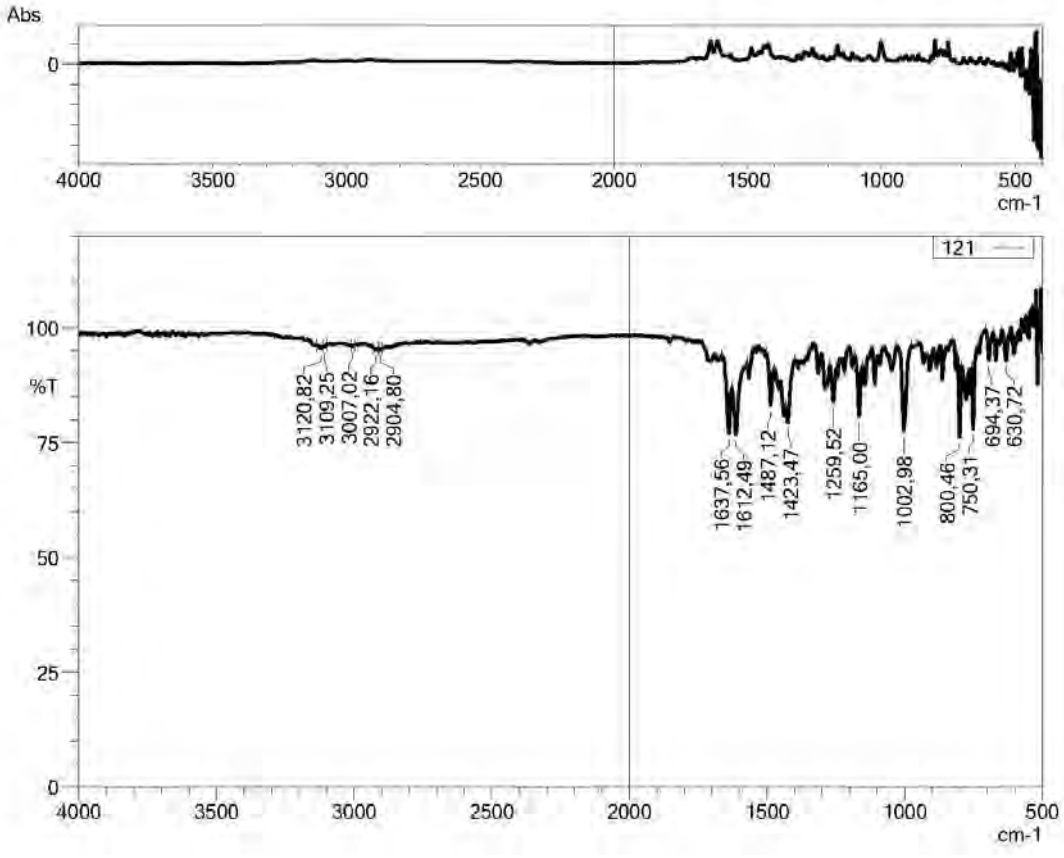


**Figure 5.65.** *IR spectrum of compound **D12***

### 5.1.4.13. *(5-chloro-3-methylbenzofuran-2-yl)(4-methylpiperazin-1-yl)methanone (D13)*

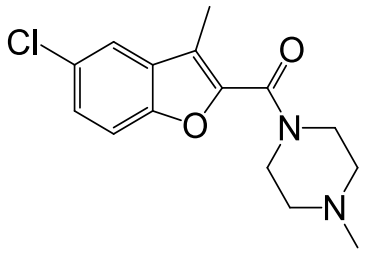


**Figure 5.66.** *Molecular structure of compound **D13***

**Physical Properties: Texture:** solid crystals, **Color:** yellowish white, **M.P.:** 100-102ºC**, Yield:** 69%.

**IR (ATR) $\upsilon_{max}$ ($cm^{-1}$):** 3120 ($SP^2$ C-H stretching, aromatic), 2937-2796 ($SP^3$ C-H stretching, 4-methyl piperazine, methylenes of piperazine, and 3-methylbenzofuran), 1625 (C=O stretching, amide), 1435 (C=C stretching, aromatic), 1292-1261 (C-O stretching, ether), 1165-1136, 1014-997 (C-N stretching, tertiary amine and/or ether), 813 (C-Cl stretching), 759-688 (C-H aromatic out-of-plane bending).

**$^1$H NMR (300 MHz) (DMSO-$d_6$) $\delta$ (ppm):** 2.20 (s, 3H, **4-methyl**piperazine), 2.29 (s, 3H, **3-methyl**benzofuran), 2.35 (t, *J*= 5.91 Hz, 4H, piperazine-3, 5), 3.58 (brs, 4H, piperazine-2, 6), 7.44 (dd, *J*= 8.78, 2.19 Hz, 1H, benzofuran-6), 7.64 (d, *J*= 8.77 Hz, 1H, benzofuran-7), 7.81 (d, *J*= 2.05 Hz, 1H, benzofuran-4).

**$^{13}$C NMR (300 MHz) (DMSO-$d_6$) $\delta$ (ppm):** 8.81 (**3-methyl**benzofuran), 42.29 (piperazine), 46.00 (**4-methyl**piperazine), 46.82 (piperazine), 54.86 (piperazine), 113.73, 118.79, 120.77, 126.72, 128.14, 130.58, 145.76, 151.91, 159.79 (benzofuran-**CO**-piperazine).

**HRMS (ESI) (m/z) $[M+1]^+$:** for $C_{15}H_{17}ClN_2O_2$ calculated: 293.1051; found: 293.1056.

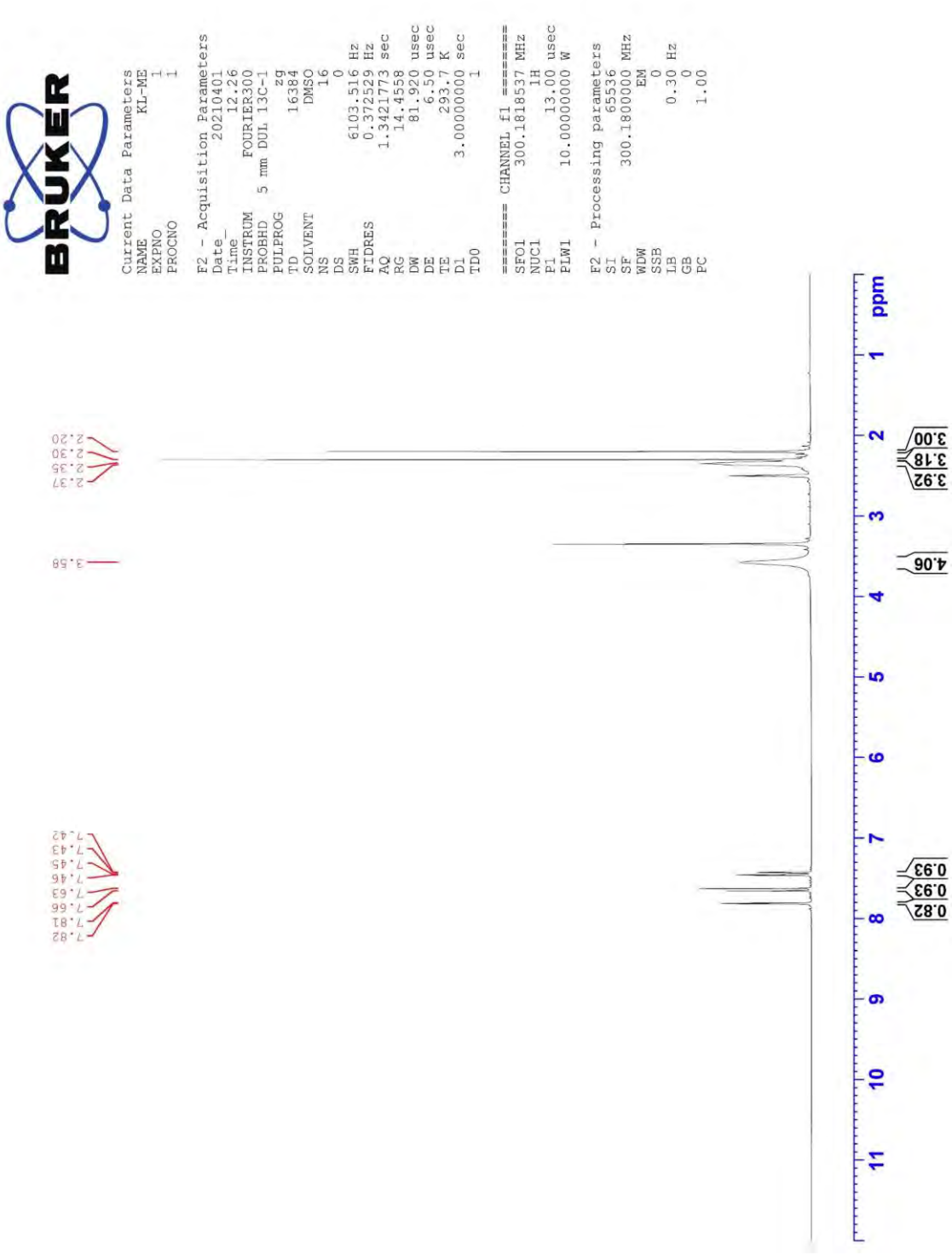


**Figure 5.67.** *$^{1}H$ NMR spectrum of compound **D13***

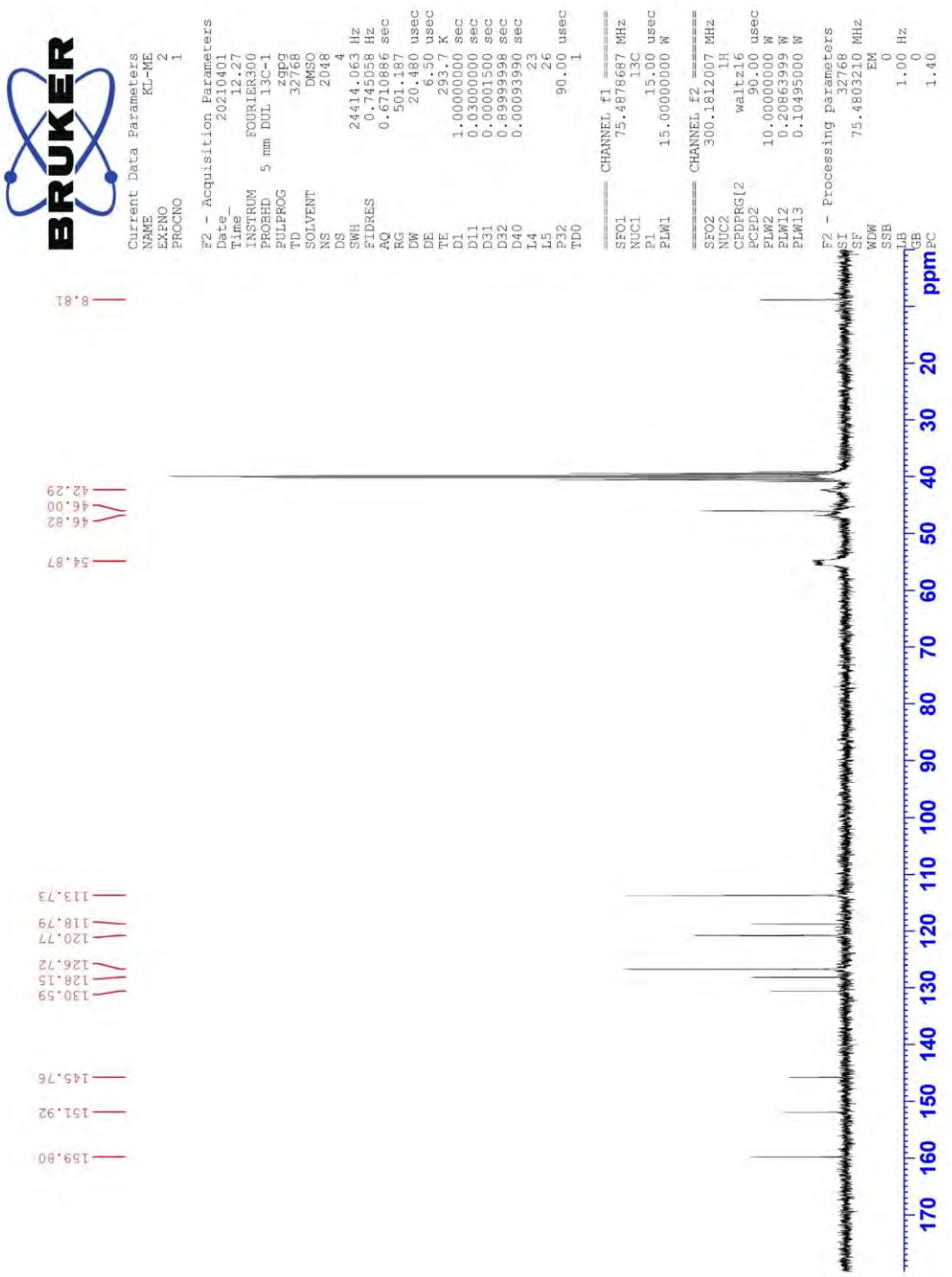


**Figure 5.68.** *$^{13}$C NMR spectrum of compound **D13***

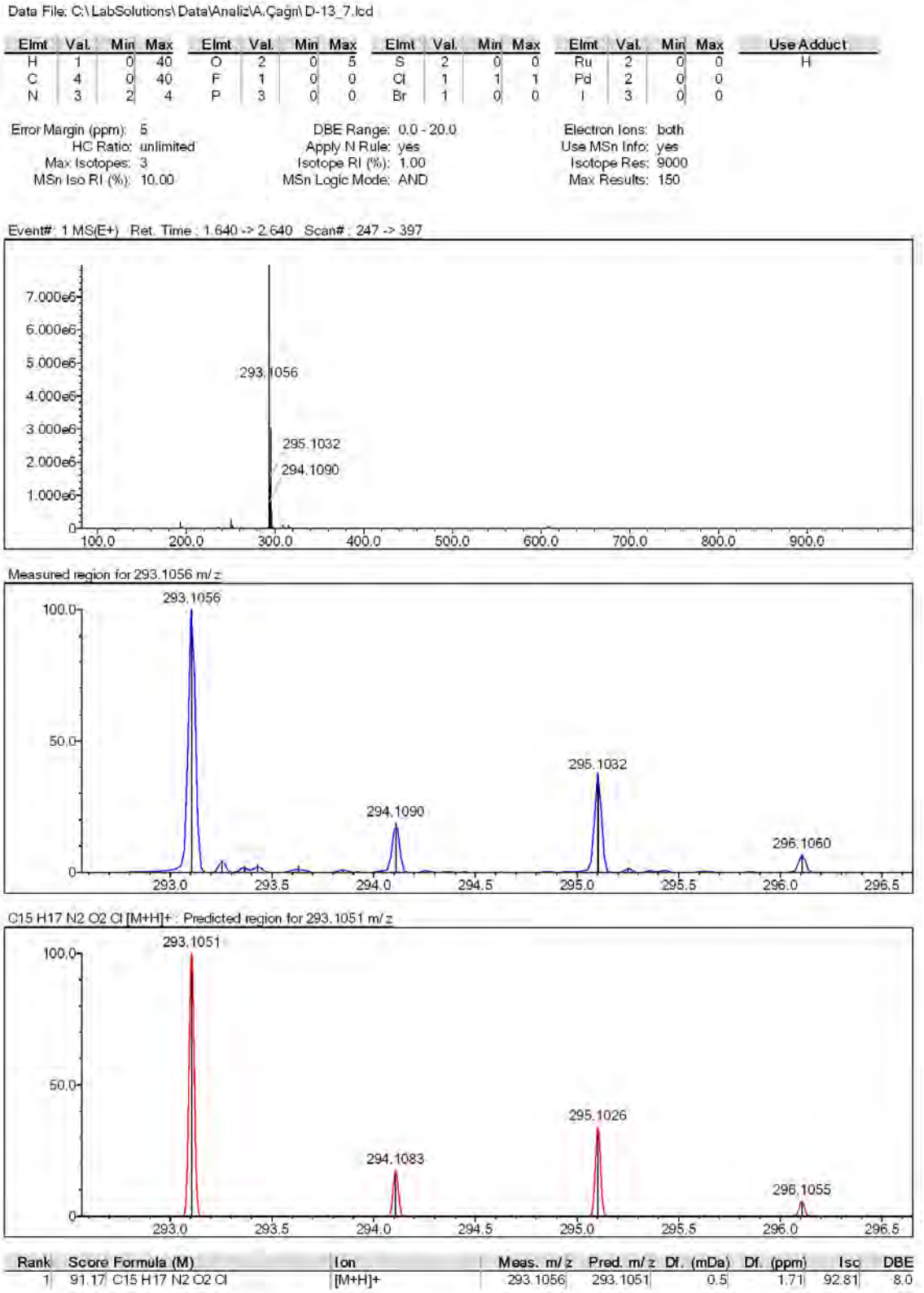


**Figure 5.69.** *High-resolution mass spectrum of compound* ***D13***

DOPNALAB

| | Item | Value |
|---|---|---|
| | Acquired Date&Time | 27.05.2021 16:03:11 |
| | Acquired by | System Administrator |
| | Filename | C:\Users\dopnalab\Desktop\sa\131.ispd |
| | Spectrum name | 131 |
| | Sample name | 13 |
| | Sample ID | |
| | Option | |
| | Comment | |
| | No. of Scans | 15 |
| | Resolution | 4 [cm-1] |
| | Apodization | Happ-Genzel |

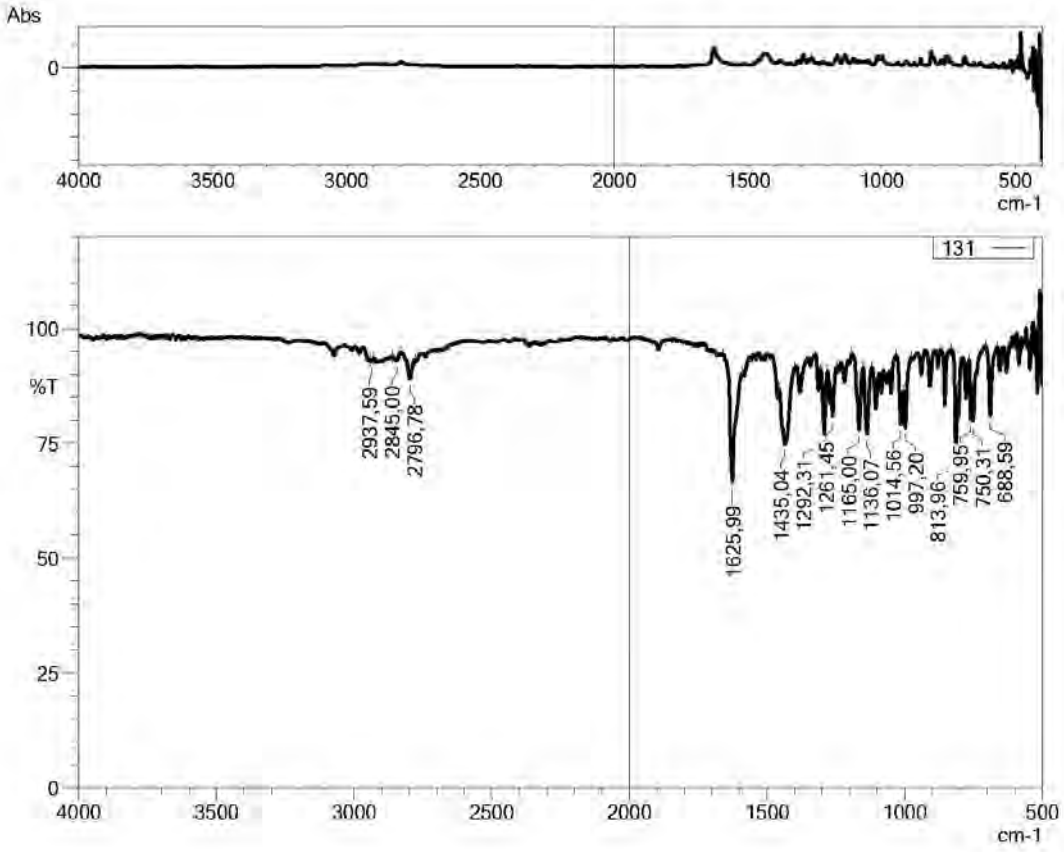


**Figure 5.70.** *IR spectrum of compound **D13***

### 5.1.4.14. *(5-chloro-3-methylbenzofuran-2-yl)(4-ethylpiperazin-1-yl)methanone (D14)*

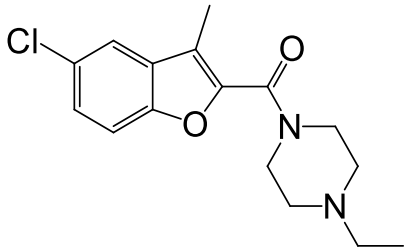


**Figure 5.71.** *Molecular structure of compound **D14***

**Physical Properties: Texture:** liquid, **Colour:** brown, **Yield:** 68%.

**IR (ATR) $\upsilon_{max}$ ($cm^{-1}$):** 2970-2769 ($SP^3$ C-H stretching, methylenes of piperazine, ethyl-methyl piperazine, and 3-methylbenzofuran), 1631 (C=O stretching, amide), 1436 (C=C stretching, aromatic), 1255 (C-O stretching, ether), 1163-1105, 1010 (C-N stretching, tertiary amine and/or C-O stretching, ether), 802 (C-Cl stretching), 750-690 (C-H aromatic out-of-plane bending).

**$^1$H NMR (300 MHz) (DMSO-$d_6$) $\delta$ (ppm):** 1.03 (t, *J*= 7.17 Hz, 3H, piperazine-$CH_2$-**$CH_3$**) 2.30 (s, 3H, **3-methyl**benzofuran), 2.36 (q, *J*= 14.44, 7.25 Hz, 2H, piperazine-**$CH_2$**-$CH_3$), 2.40 (brs, 4H, piperazine-3, 5), 3.58 (brs, 4H, piperazine-2, 6), 7.45 (dd, *J*= 8.78, 2.20 Hz, 1H, benzofuran-6), 7.65 (d, *J*= 8.77 Hz, 1H, benzofuran-7), 7.82 (d, *J*= 2.08 Hz, 1H, benzofuran-4).

**$^{13}$C NMR (300 MHz) (DMSO-$d_6$) $\delta$ (ppm):** 8.82 (**3-methyl**benzofuran), 12.34 (piperazine-$CH_2$-**$CH_3$**), 42.40 (piperazine), 46.74 (piperazine), 51.88 (piperazine-**$CH_2$**-$CH_3$), 52.44 (piperazine), 53.30 (piperazine), 113.73, 118.79, 120.78, 126.73, 128.15, 130.59, 145.77, 151.91, 159.73 (benzofuran-**CO**-piperazine).

**HRMS (ESI) (m/z) $[M+1]^+$:** for $C_{16}H_{19}ClN_2O_2$ calculated: 307.1208; found: 307.1216.

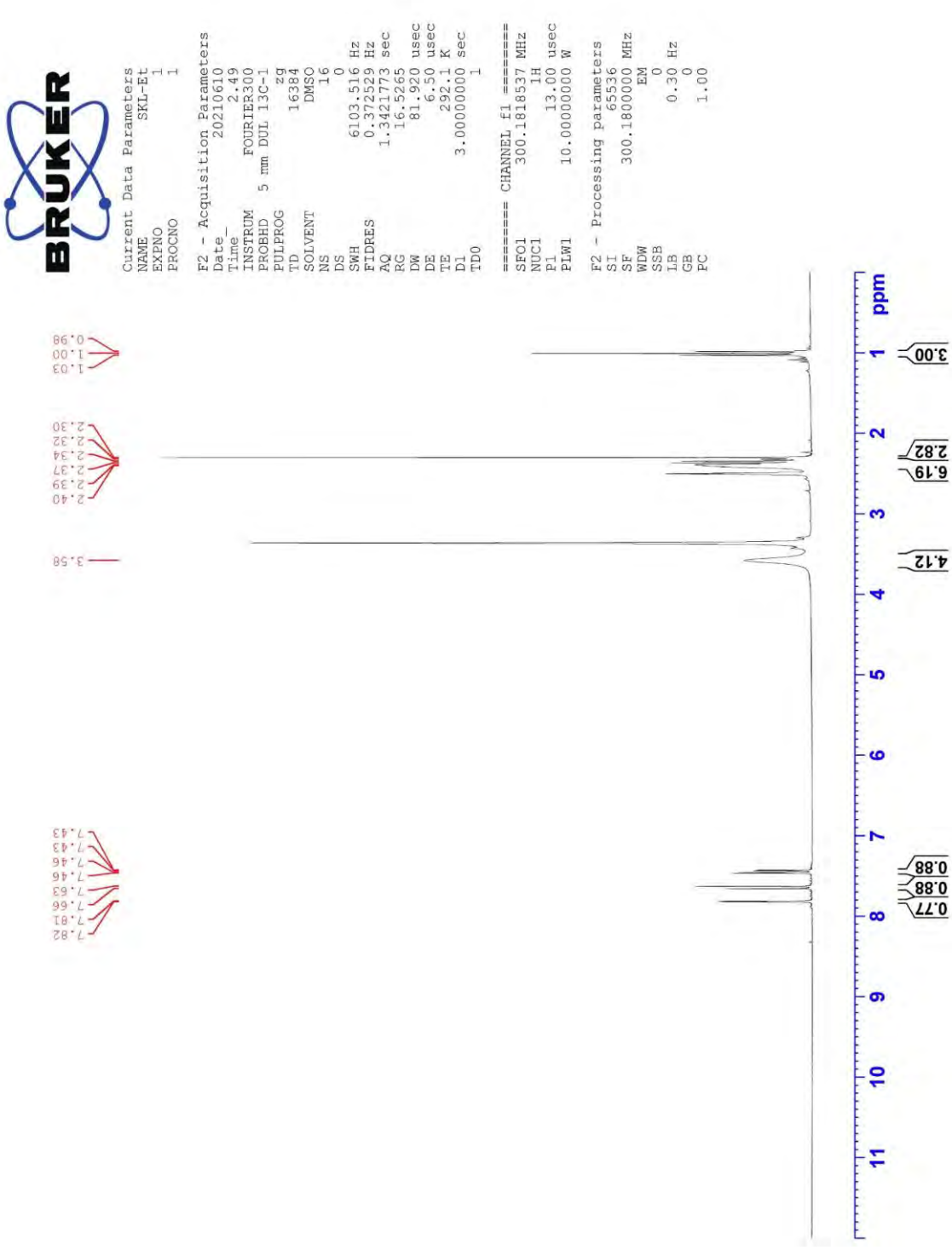


**Figure 5.72.** *[1]H NMR spectrum of compound **D14***

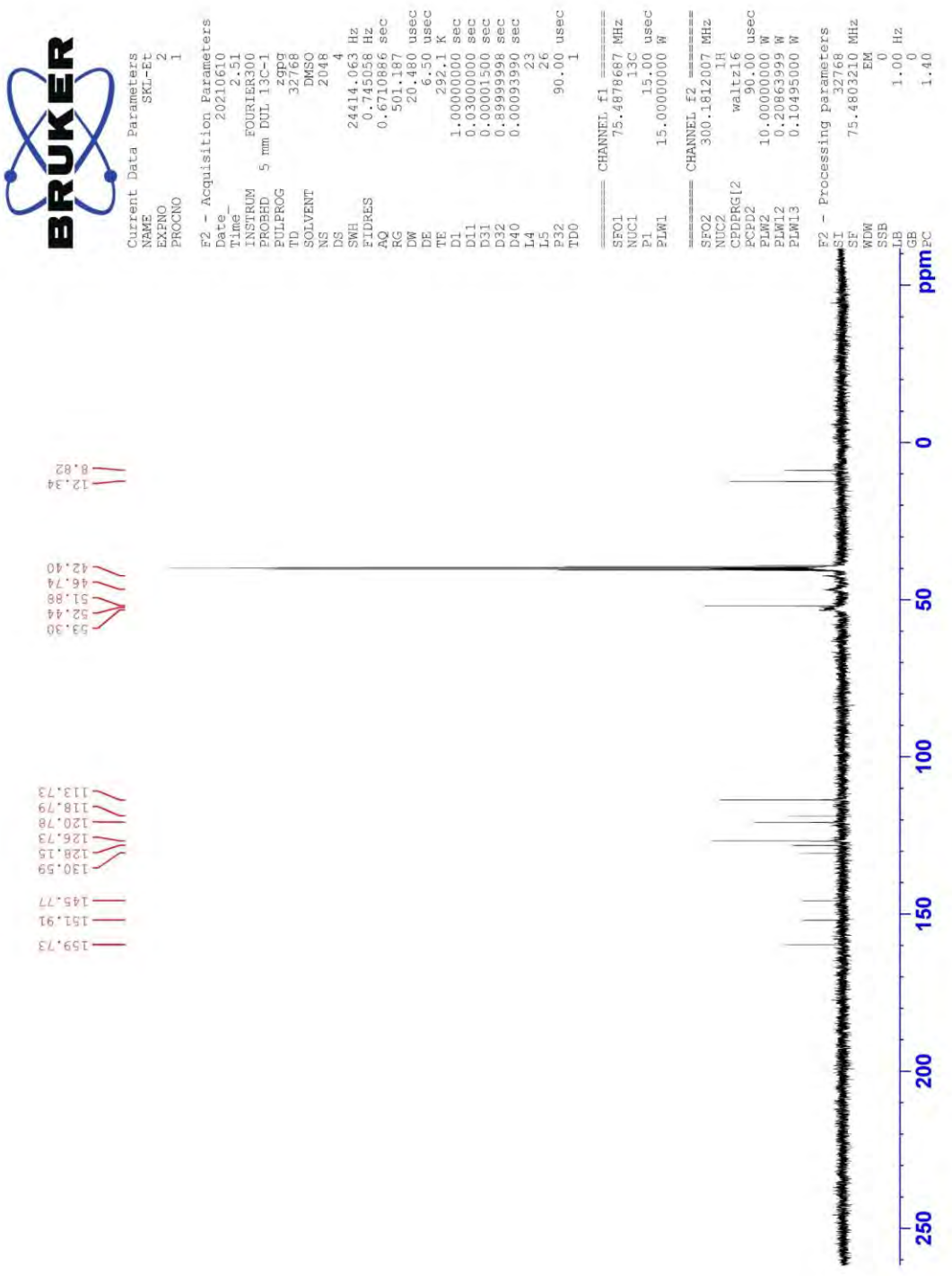


**Figure 5.73.** *$^{13}$C NMR spectrum of compound **D14***

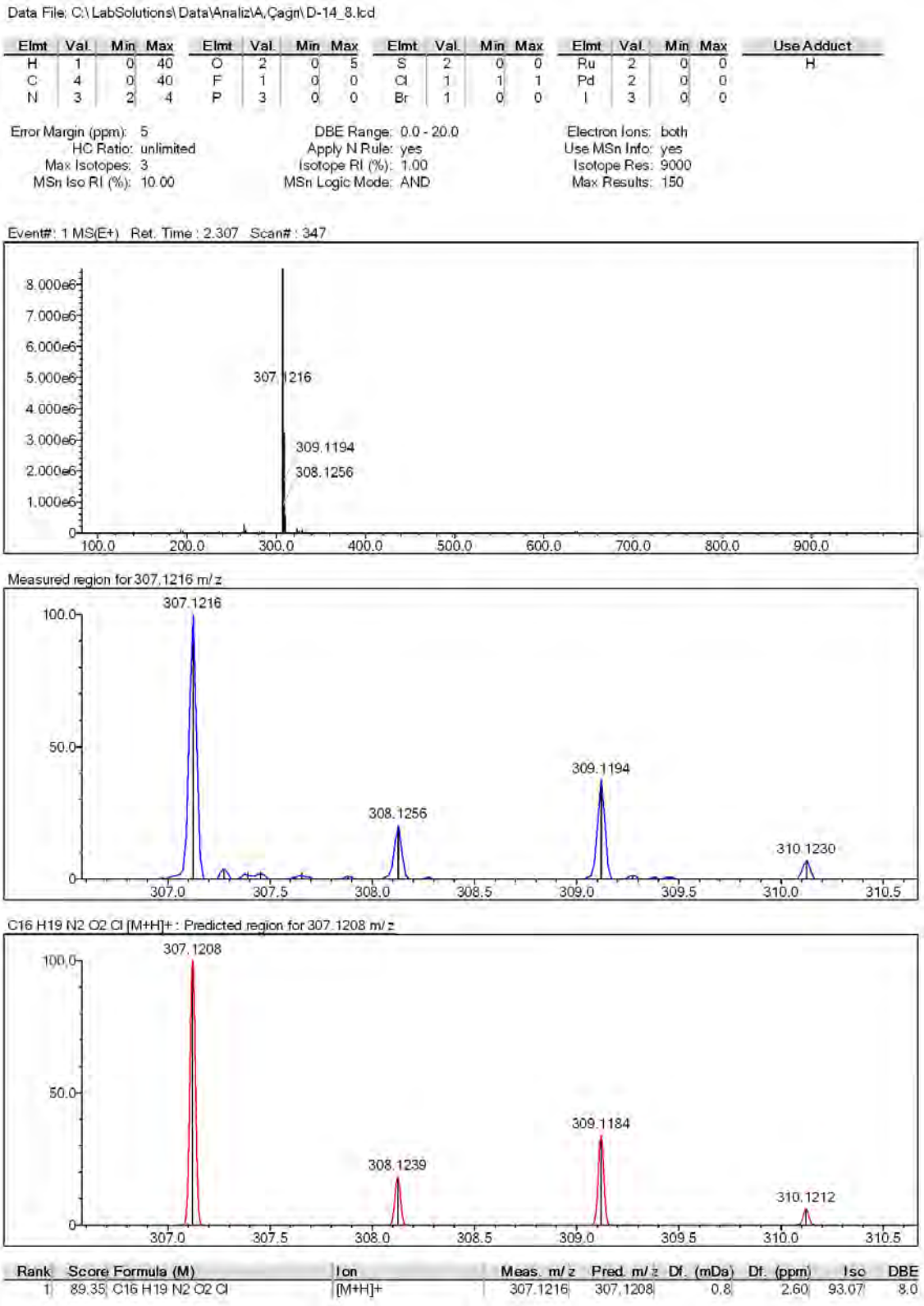


**Figure 5.74.** *High-resolution mass spectrum of compound* ***D14***

DOPNALAB

| | Item | Value |
|---|---|---|
| | Acquired Date&Time | 27.05.2021 16:11:32 |
| | Acquired by | System Administrator |
| | Filename | C:\Users\dopnalab\Desktop\sa\141.ispd |
| | Spectrum name | 141 |
| | Sample name | 14 |
| | Sample ID | |
| | Option | |
| | Comment | |
| | No. of Scans | 15 |
| | Resolution | 4 [cm-1] |
| | Apodization | Happ-Genzel |

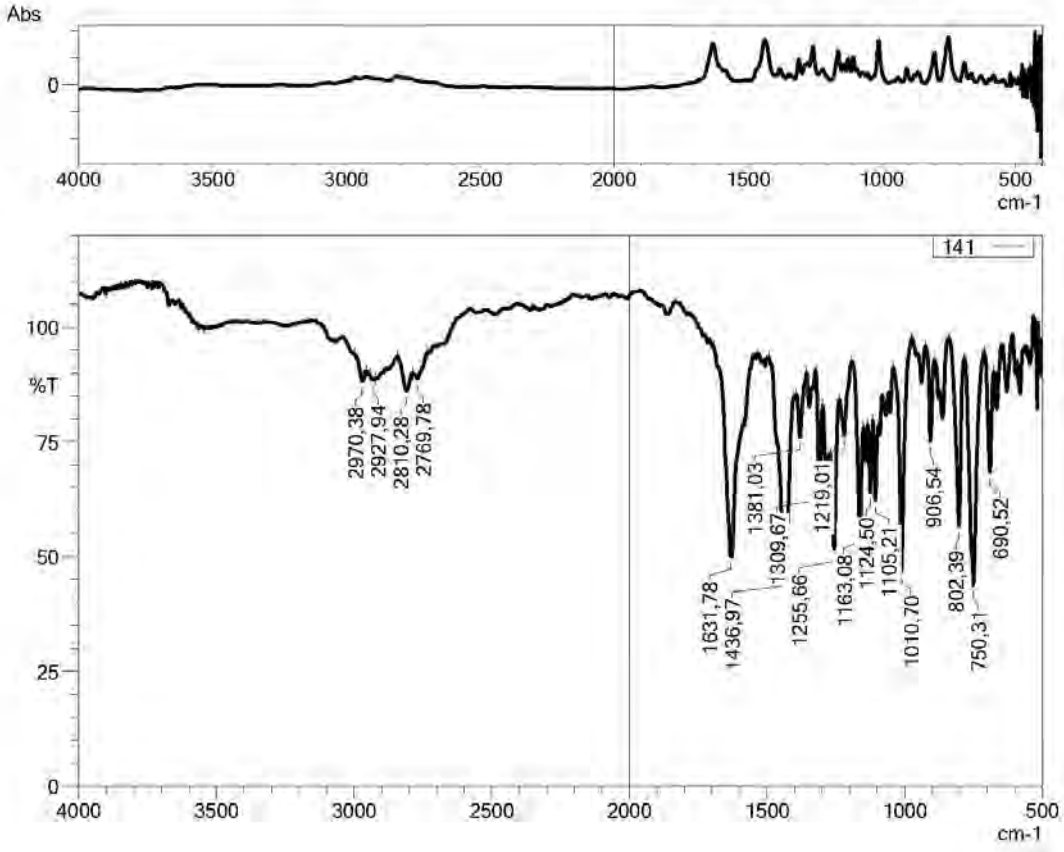


**Figure 5.75.** *IR spectrum of compound **D14***

### 5.1.4.15. *(5-chloro-3-methylbenzofuran-2-yl)(4-(2-(dimethylamino)ethyl)piperazin-1-yl)methanone (D15)*

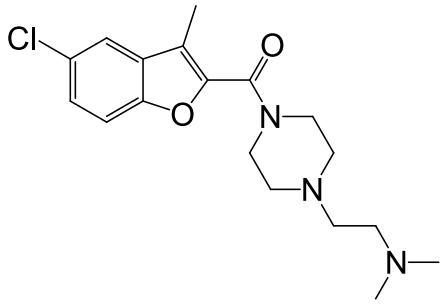


**Figure 5.76.** *Molecular structure of compound* ***D15***

**Physical Properties: Texture:** liquid, **Colour:** brown, **Yield:** 66%.

**IR (ATR) $\upsilon_{max}$ ($cm^{-1}$):** 2939-2765 ($SP^3$ C-H stretching, methylenes of piperazine, dimethylaminoethyl-piperazine, and 3-benzofuran), 1629 (C=O stretching, amide), 1436 (C=C stretching, aromatic), 1257 (C-O stretching, ether), 1161-1099, 1001 (C-N stretching, tertiary amine and/or C-O stretching, ether), 804 (C-Cl stretching), 862-690 (C-H aromatic out-of-plane bending).

**$^1$H NMR (300 MHz) (DMSO-$d_6$) $\delta$ (ppm):** 2.12 (s, 6H, -N**($CH_3$)$_2$**), 2.30 (s, 3H, **3-methyl**benzofuran), 2.33-2.44 (m, 8H, piperazine-3, 5 and piperazine-(**$CH_2$)$_2$**-N), 3.57 (brs, 4H, piperazine-2, 6), 7.44 (dd, *J*= 8.78, 2.20 Hz, 1H, benzofuran-6), 7.64 (d, *J*= 8.77 Hz, 1H, benzofuran-7), 7.81 (d, *J*= 2.07 Hz, 1H, benzofuran-4).

**$^{13}$C NMR (300 MHz) (DMSO-$d_6$) $\delta$ (ppm):** 8.82 (**3-methyl**benzofuran), 42.33 (piperazine), 45.96 (-N**($CH_3$)$_2$**), 46.79 (piperazine), 54.01 (piperazine), 56.01 (piperazine-(**$CH_2$)$_2$**-N), 57.02 (piperazine-(**$CH_2$)$_2$**-N), 113.72, 118.79, 120.77, 126.72, 128.15, 130.59, 145.77, 151.91, 159.71 (benzofuran-**CO-**piperazine).

**HRMS (ESI) (m/z) [M + 1]+:** for $C_{18}H_{24}ClN_3O_2$ calculated: 350.1630; found: 350.1642.

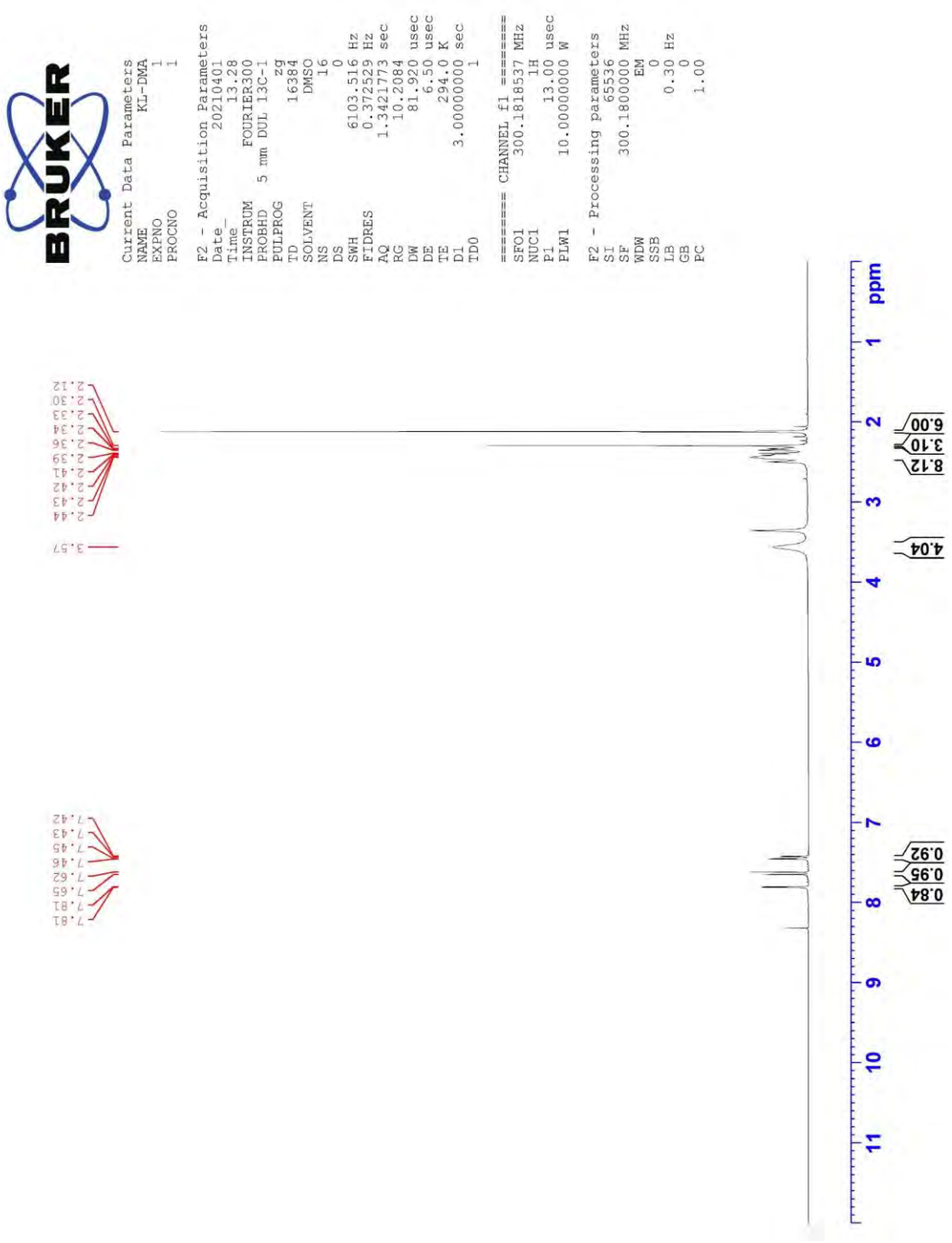


**Figure 5.77.** *$^{1}H$ NMR spectrum of compound **D15***

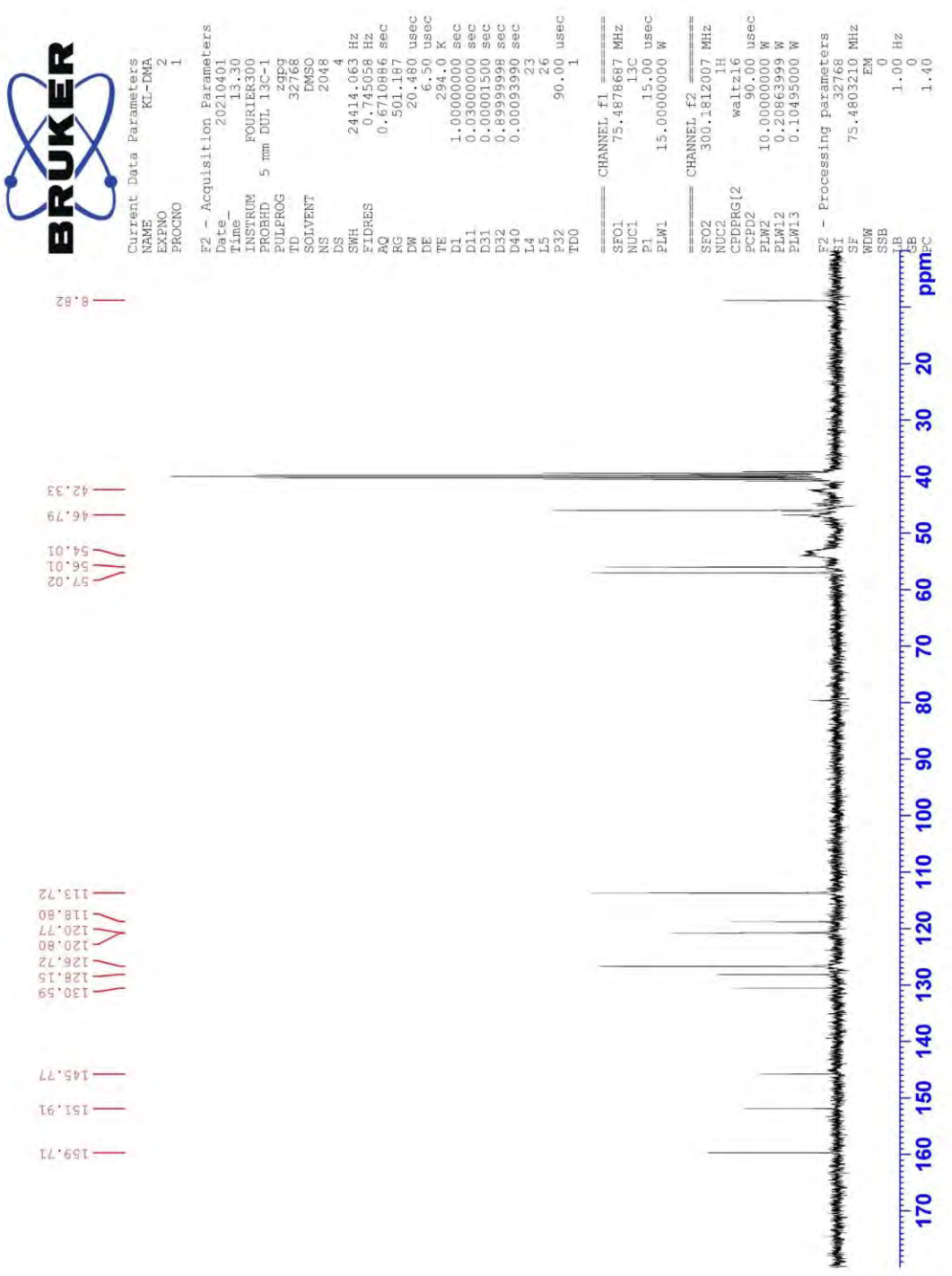


**Figure 5.78.** *$^{13}$C NMR spectrum of compound **D15***

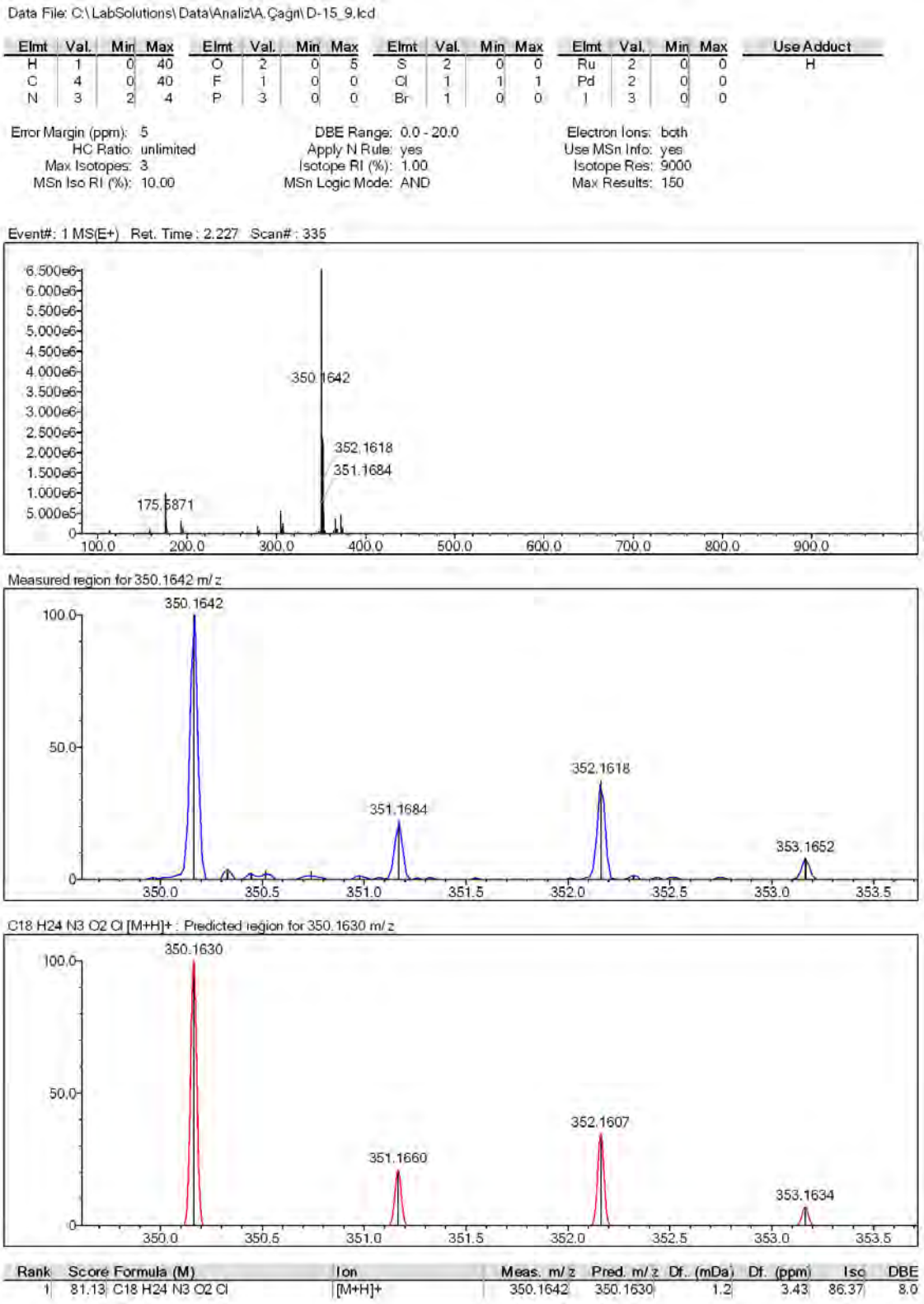


**Figure 5.79.** *High-resolution mass spectrum of compound* ***D15***

DOPNALAB

| Item | Value |
|---|---|
| Acquired Date&Time | 27.05.2021 16:18:11 |
| Acquired by | System Administrator |
| Filename | C:\Users\dopnalab\Desktop\sa\151.ispd |
| Spectrum name | 151 |
| Sample name | 15 |
| Sample ID | |
| Option | |
| Comment | |
| No. of Scans | 15 |
| Resolution | 4 [cm-1] |
| Apodization | Happ-Genzel |

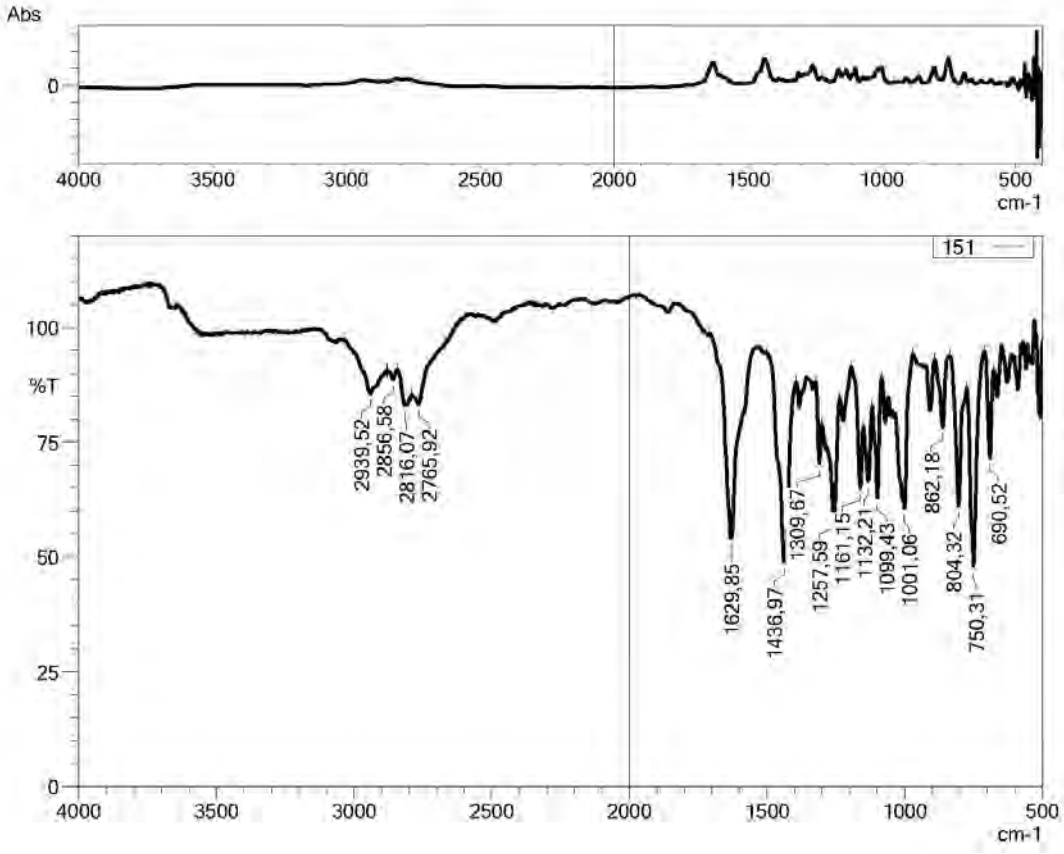


**Figure 5.80.** *IR spectrum of compound **D15***

### 5.1.4.16. *(5-chlorobenzofuran-2-yl)(4-phenylpiperazin-1-yl)methanone (D16)*

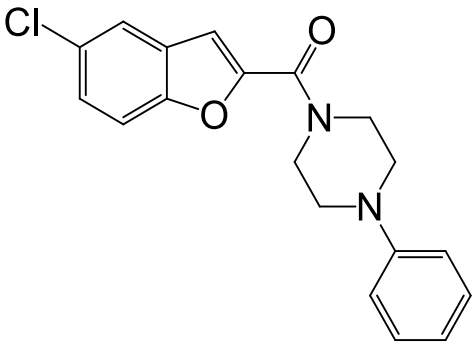


**Figure 5.81.** *Molecular structure of compound **D16***

**Physical Properties: Texture:** solid crystals, **Color:** yellowish white, **M.P.:** 173-175ºC**, Yield:** 87%.

**IR (ATR) $\upsilon_{max}$ ($cm^{-1}$):** 3111-3066 ($SP^2$ C-H stretching, aromatic), 2980-2819 ($SP^3$ C-H stretching, methylenes of piperazine), 1612 (C=O stretching, amide), 1558 (C-H bending, indicative of non-substituted benzofuran at position 3), 1438-1429 (C=C stretching, aromatic), 1219 (C-O stretching, ether), 1178-1153, 1060-1014 (C-N stretching, tertiary amine and/or ether), 806 (C-Cl stretching), 947-688 (C-H aromatic out-of-plane bending).

**$^1$H NMR (300 MHz) (DMSO-$d_6$) $\delta$ (ppm):** 3.23 (t, *J*= 5.04 Hz, 4H, piperazine-3, 5), 3.85 (brs, 4H, piperazine-2, 6), 6.82 (t, *J*= 7.25 Hz, 1H, phenyl-4), 6.97 (d, *J*= 7.90 Hz, 2H, phenyl-2, 6), 7.24 (t, *J*= 8.54 Hz, 2H, phenyl-3,5), 7.42 (s, 1H, benzofuran-3), 7.47 (dd, *J*= 8.84, 2.22 Hz, 1H, benzofuran-6), 7.73 (d, *J*= 8.83 Hz, 1H, benzofuran-7), 7.83 (d, *J*= 2.09 Hz, 1H, benzofuran-4).

**$^{13}$C NMR (300 MHz) (DMSO-$d_6$) $\delta$ (ppm):** 42.61 (piperazine), 46.67 (piperazine), 48.97 (piperazine), 110.92, 113.99, 116.36, 119.90, 122.27, 126.99, 128.52, 128.79, 129.49, 150.08, 151.10, 152.91, 158.90 (benzofuran-**CO-**piperazine).

**HRMS (ESI) (m/z) $[M+1]^+$:** for $C_{19}H_{17}ClN_2O_2$ calculated: 341.1051; found: 341.1058.

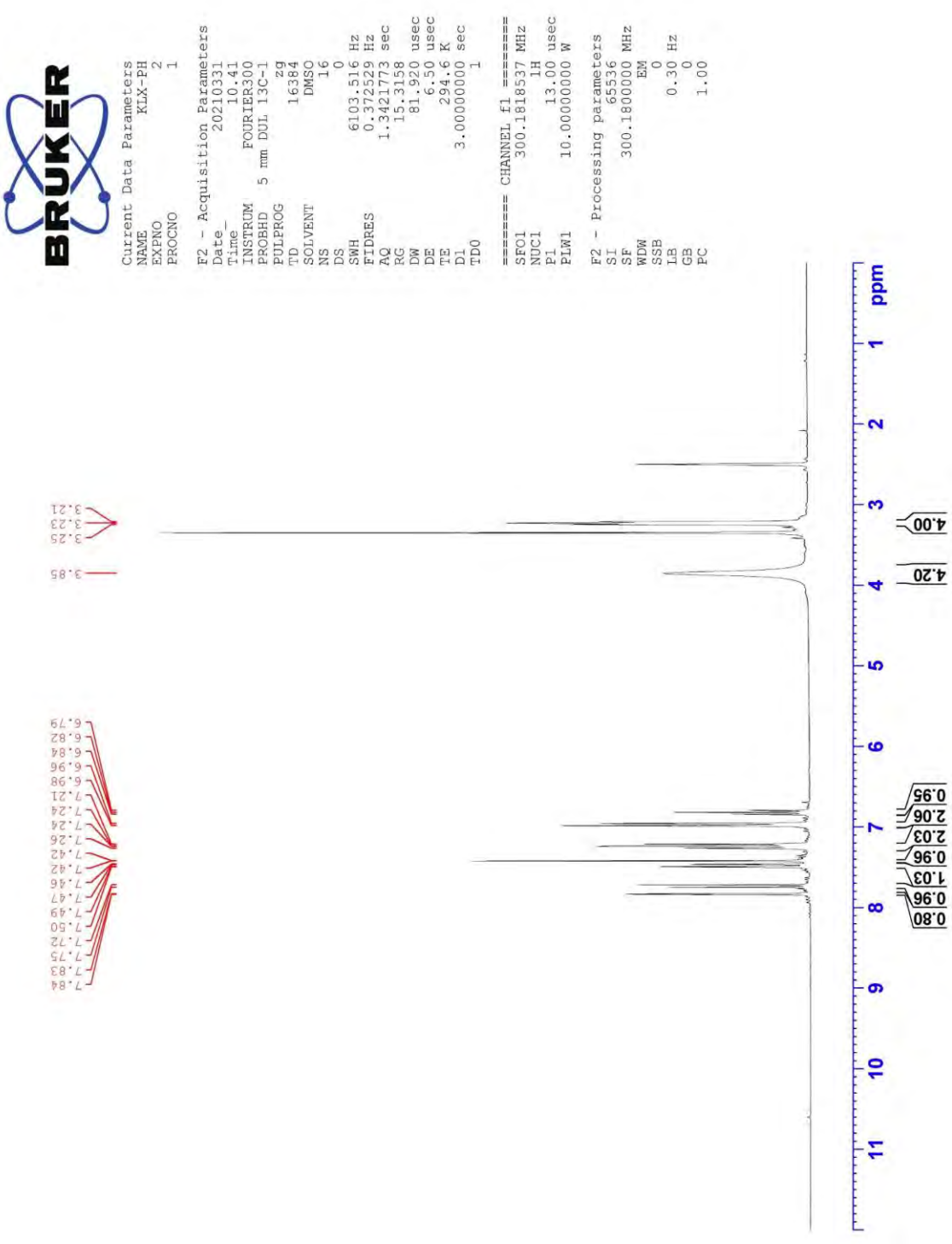


**Figure 5.82.** *$^{1}H$ NMR spectrum of compound **D16***

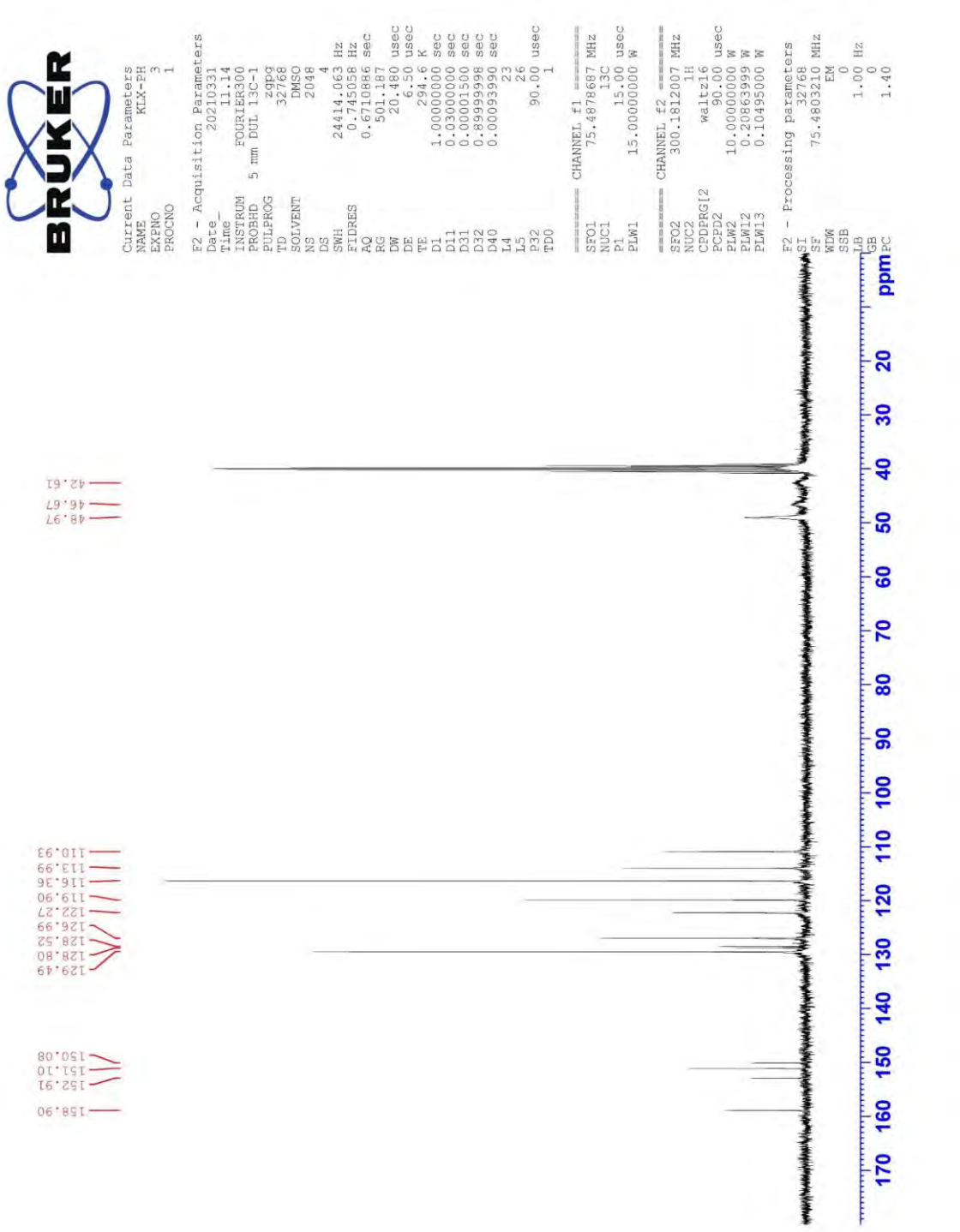


**Figure 5.83.** *$^{13}$C NMR spectrum of compound **D16***

Data File: C:\LabSolutions\Data\Analiz\Asaf\D-16-C_82.lcd

| Elmt | Val. | Min | Max | Elmt | Val. | Min | Max | Elmt | Val. | Min | Max | Elmt | Val. | Min | Max | Use Adduct |
|---|---|---|---|---|---|---|---|---|---|---|---|---|---|---|---|---|
| H | 1 | 0 | 40 | O | 2 | 1 | 5 | S | 2 | 0 | 0 | Ru | 2 | 0 | 0 | H |
| C | 4 | 0 | 40 | F | 1 | 0 | 0 | Cl | 1 | 0 | 1 | Pd | 2 | 0 | 0 | |
| N | 3 | 2 | 6 | P | 3 | 0 | 0 | Br | 1 | 0 | 0 | I | 3 | 0 | 0 | |

Error Margin (ppm): 10
HC Ratio: unlimited
Max Isotopes: 3
MSn Iso RI (%): 10.00

DBE Range: 5.0 - 20.0
Apply N Rule: yes
Isotope RI (%): 1.00
MSn Logic Mode: AND

Electron Ions: both
Use MSn Info: yes
Isotope Res: 9000
Max Results: 150

Event#: 1 MS(E+) Ret. Time: 4.787 -> 5.507 Scan#: 719 -> 827

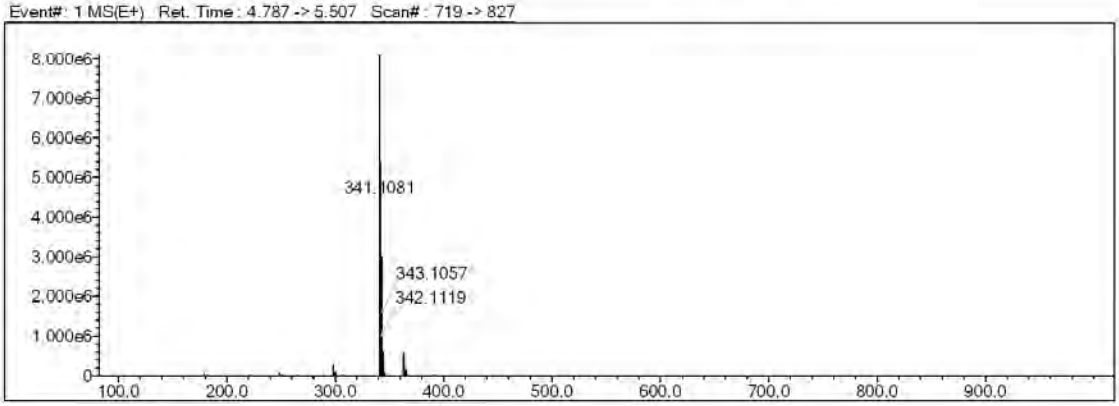


Measured region for 341.1081 m/z

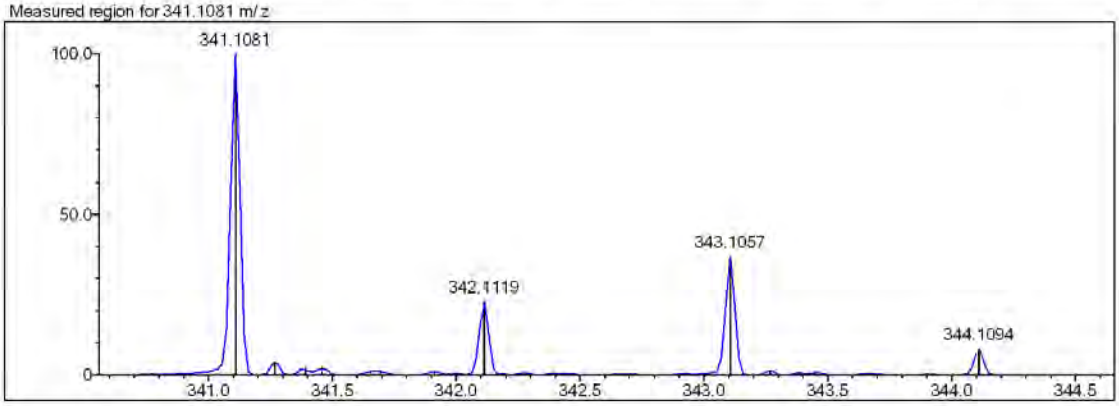


C19 H17 N2 O2 Cl [M+H]+ : Predicted region for 341.1051 m/z

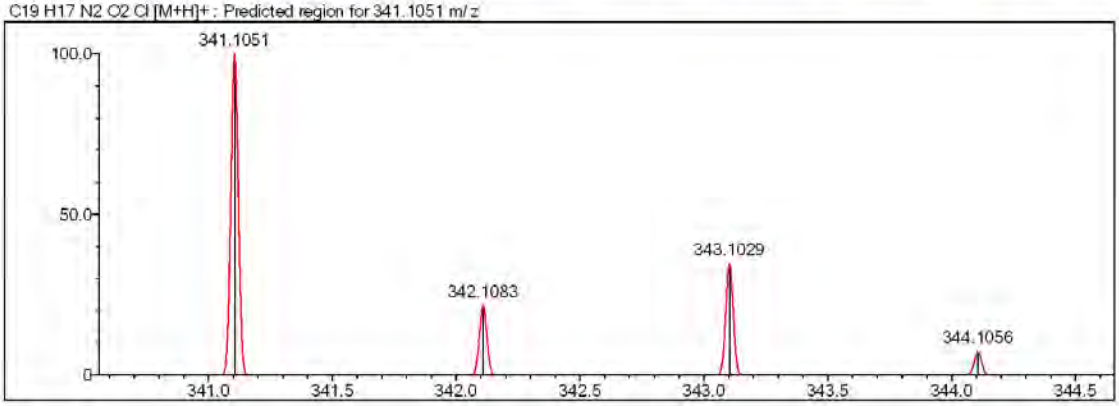


| Rank | Score | Formula (M) | Ion | Meas. m/z | Pred. m/z | Df. (mDa) | Df. (ppm) | Isc | DBE |
|---|---|---|---|---|---|---|---|---|---|
| 1 | 43.48 | C19 H17 N2 O2 Cl | [M+H]+ | 341.1081 | 341.1051 | 3.0 | 8.79 | 83.46 | 12.0 |

**Figure 5.84.** *High-resolution mass spectrum of compound* ***D16***

DOPNALAB

| | Item | Value |
|---|---|---|
| | Acquired Date&Time | 27.05.2021 16:23:48 |
| | Acquired by | System Administrator |
| | Filename | C:\Users\dopnalab\Desktop\sa\161.ispd |
| | Spectrum name | 161 |
| | Sample name | 16 |
| | Sample ID | |
| | Option | |
| | Comment | |
| | No. of Scans | 15 |
| | Resolution | 4 [cm-1] |
| | Apodization | Happ-Genzel |

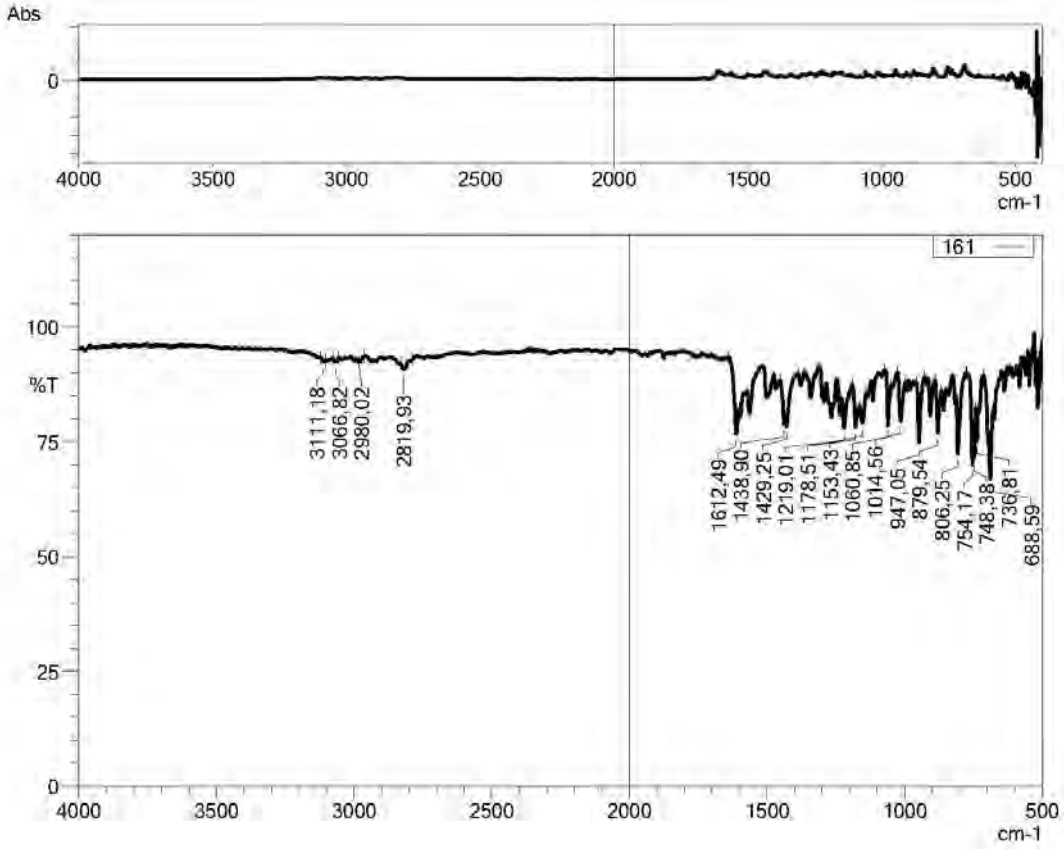


**Figure 5.85.** *IR spectrum of compound **D16***

### 5.1.4.17. *(4-(5-chlorobenzofuran-2-carbonyl)piperazin-1-yl)(furan-2-yl)methanone (D17)*

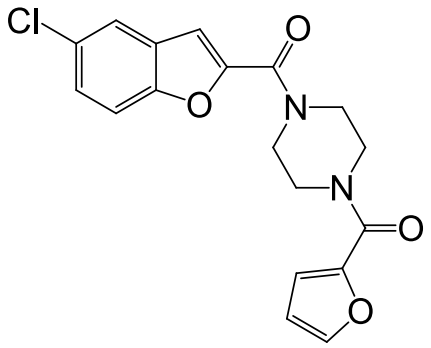


**Figure 5.86.** *Molecular structure of compound **D17***

**Physical Properties: Texture:** solid crystals, **Color:** white, **M.P.:** 112-114ºC**, Yield:** 95%.

**IR (ATR) $\upsilon_{max}$ ($cm^{-1}$):** 3140 ($SP^2$ C-H stretching, aromatic), 2924-2868 ($SP^3$ C-H stretching, methylenes of piperazine), 1631 (C=O stretching, amide, and furoyl), 1558 (C-H bending, indicative of non-substituted benzofuran at position 3), 1483-1421 (C=C stretching, aromatic), 1257 (C-O stretching, ether), 1178, 1012-1001 (C-N stretching, tertiary amine and/or ether), 866-694 (C-H aromatic out-of-plane bending).

**$^1$H NMR (300 MHz) (DMSO-$d_6$) $\delta$ (ppm):** 3.79 (brs, 8H, piperazine-2, 3, 5, 6), 6.65 (dd, *J*= 3.45, 1.76 Hz, 1H, furan-4), 7.05 (d, *J*= 1.72 Hz, 1H, furan-3), 7.43 (s, 1H, benzofuran-3), 7.47 (dd, *J*= 8.84, 2.22 Hz, 1H, benzofuran-6), 7.72 (d, *J*= 8.82 Hz, 1H, benzofuran-7), 7.84 (d, *J*= 2.08 Hz, 1H, benzofuran-4), 7.87 (d, *J*= 0.96 Hz, 1H, furan-5).

**$^{13}$C NMR (300 MHz) (DMSO-$d_6$) $\delta$ (ppm):** 42.71 (piperazine), 46.33 (piperazine), 111.09, 111.88, 114.01, 116.49, 122.27, 127.05, 128.52, 128.77, 145.43, 147.20, 149.87, 152.93, 158.93 (piperazine-**CO**-furan), 159.12 (benzofuran-**CO**-piperazine).

**HRMS (ESI) (m/z) $[M+1]^+$:** for $C_{18}H_{15}ClN_2O_4$ calculated: 359.0793; found: 359.0802.

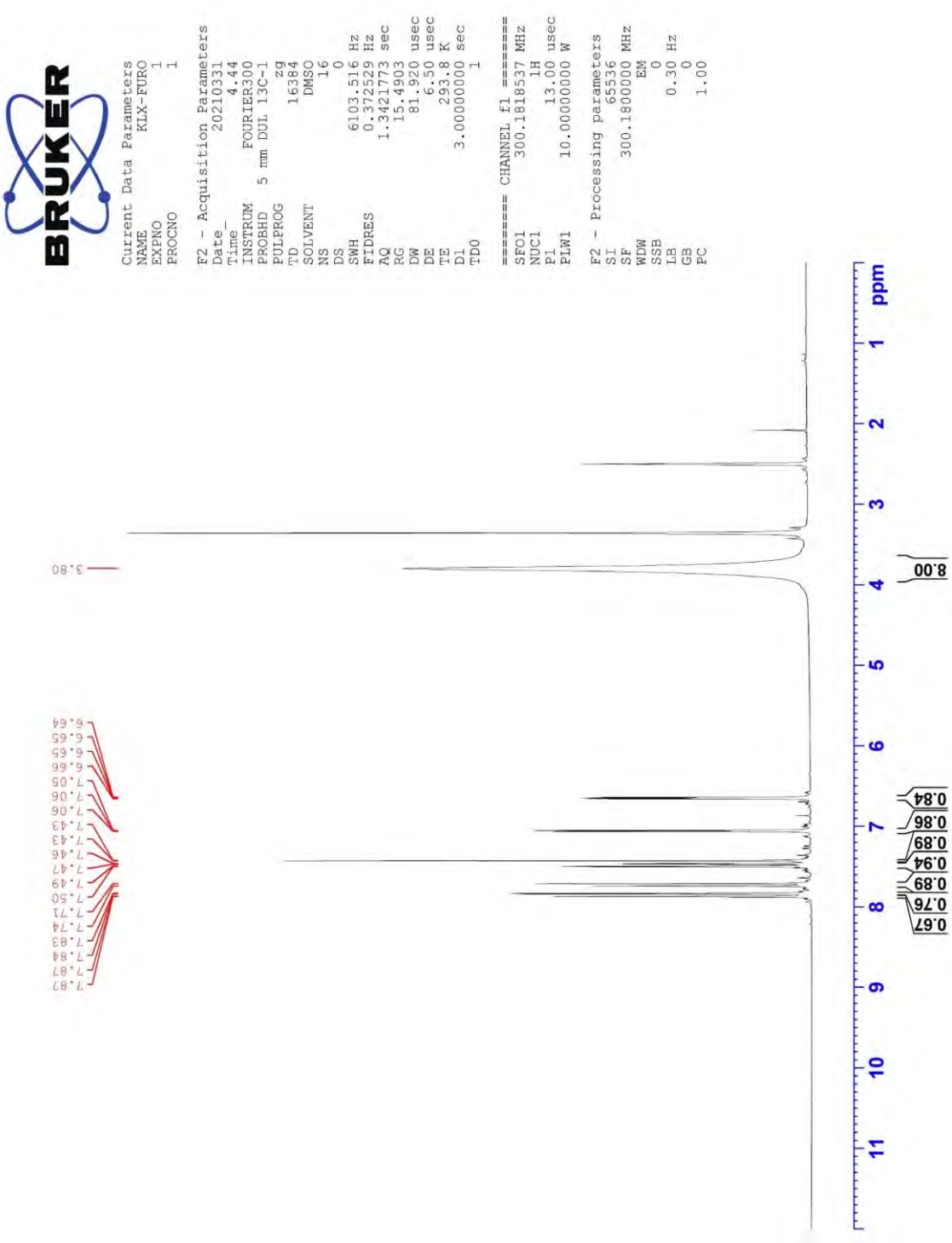


**Figure 5.87.** *[1]H NMR spectrum of compound **D17***

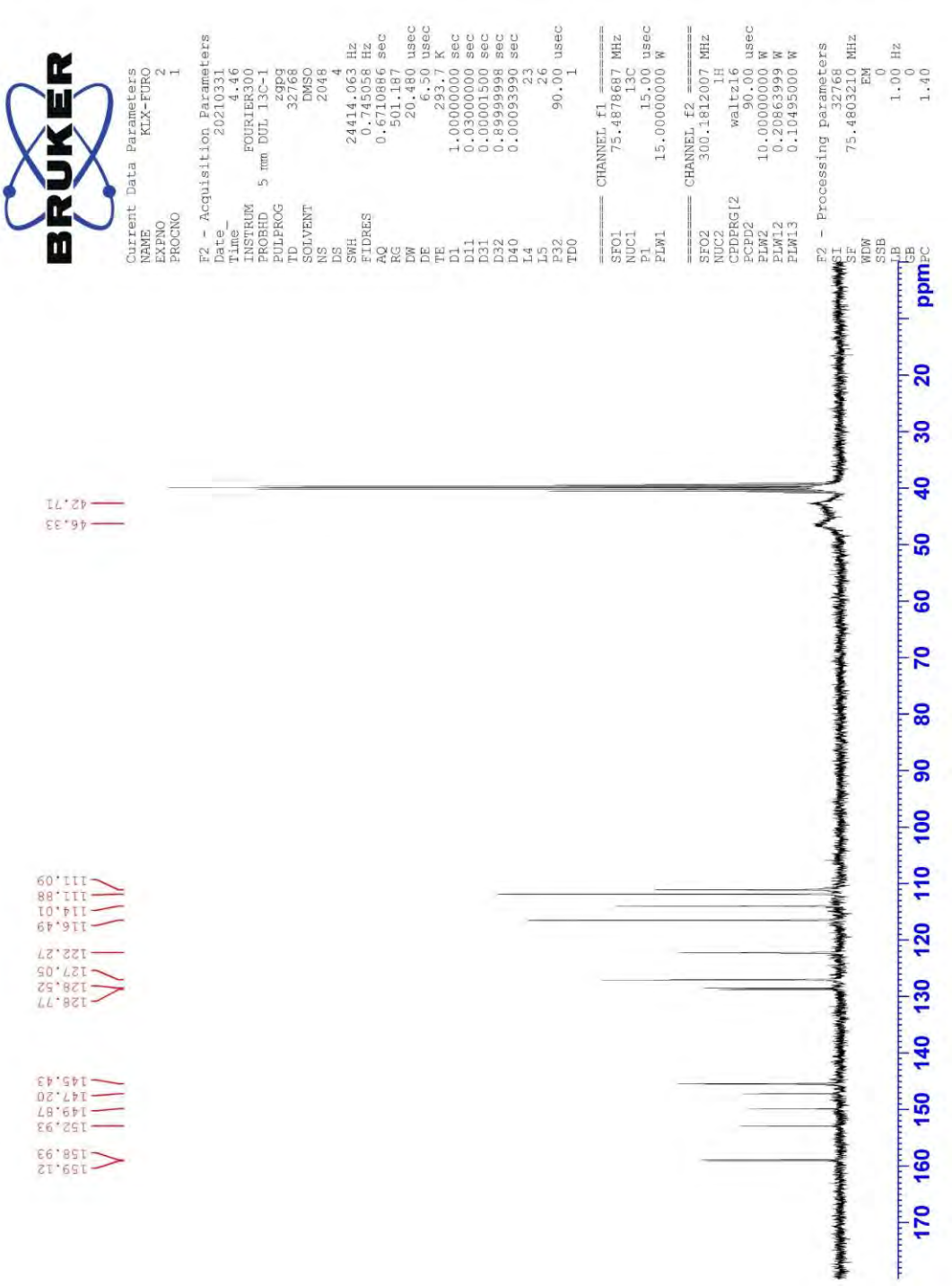


**Figure 5.88.** *$^{13}$C NMR spectrum of compound **D17***

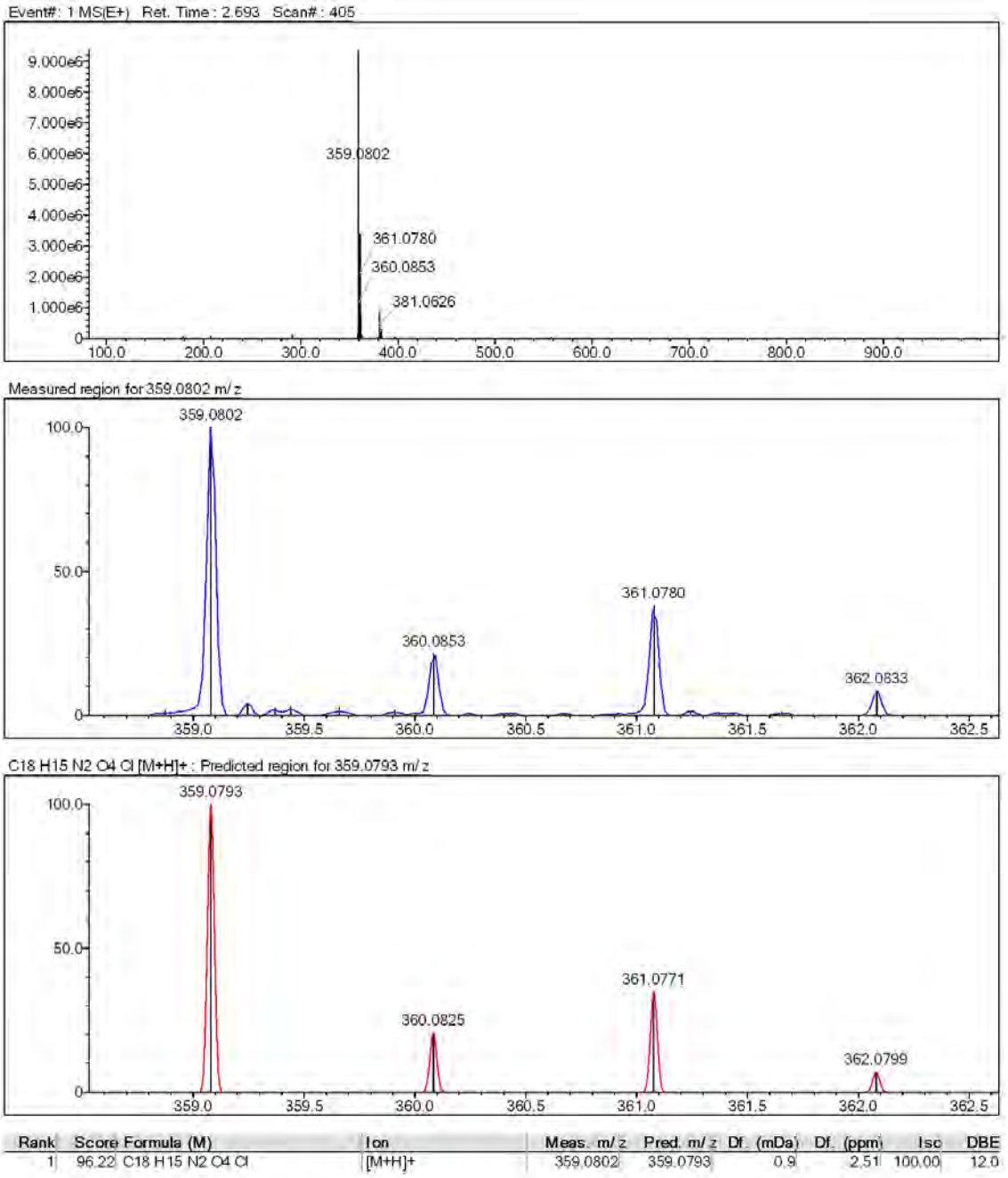


| Rank | Score | Formula (M) | Ion | Meas. m/z | Pred. m/z | Df. (mDa) | Df. (ppm) | Isc | DBE |
|---|---|---|---|---|---|---|---|---|---|
| 1 | 96.22 | C18 H15 N2 O4 Cl | [M+H]+ | 359.0802 | 359.0793 | 0.9 | 2.51 | 100.00 | 12.0 |

**Figure 5.89.** *High-resolution mass spectrum of compound **D17***

DOPNALAB

| | Item | Value |
|---|---|---|
| | Acquired Date&Time | 27.05.2021 16:30:32 |
| | Acquired by | System Administrator |
| | Filename | C:\Users\dopnalab\Desktop\sa\171.ispd |
| | Spectrum name | 171 |
| | Sample name | 17 |
| | Sample ID | |
| | Option | |
| | Comment | |
| | No. of Scans | 15 |
| | Resolution | 4 [cm-1] |
| | Apodization | Happ-Genzel |

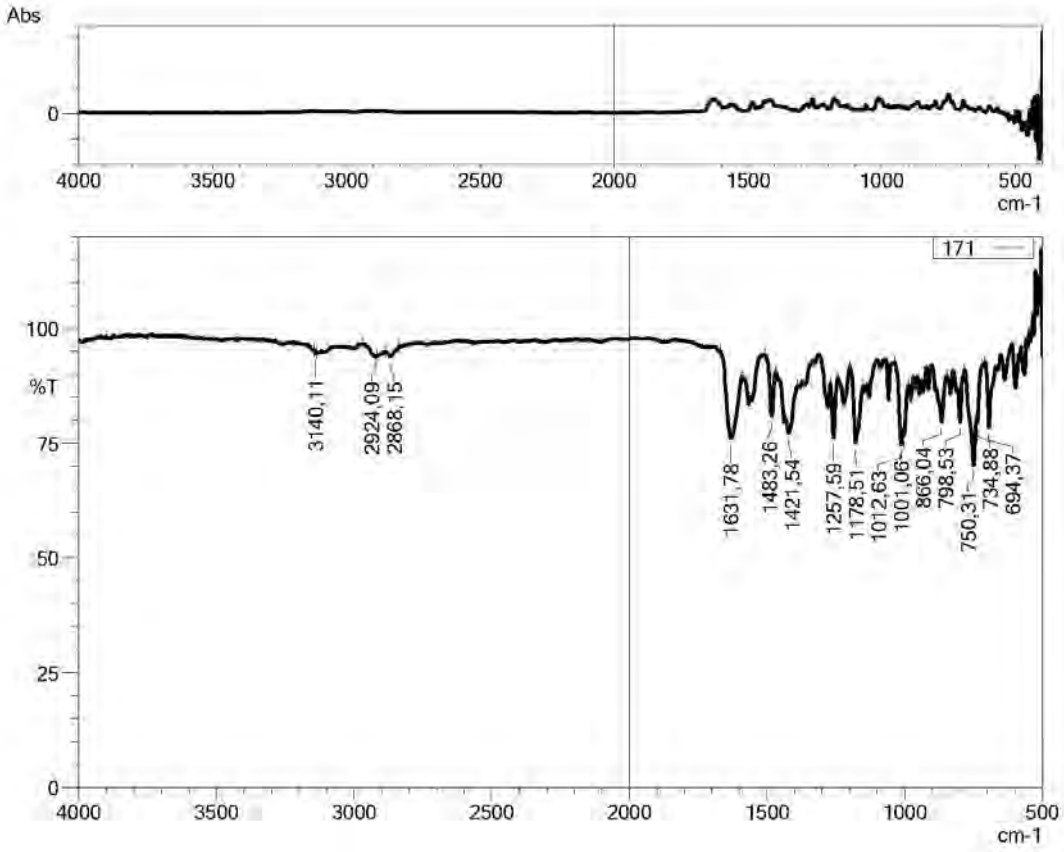


**Figure 5.90.** *IR spectrum of compound **D17***

### 5.1.4.18. *(5-chlorobenzofuran-2-yl)(4-methylpiperazin-1-yl)methanone (D18)*

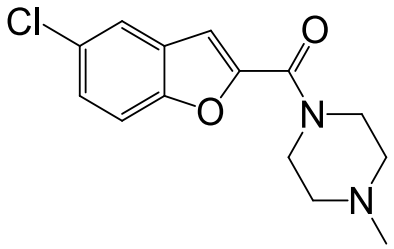


**Figure 5.91.** *Molecular structure of compound **D18***

**Physical Properties: Texture:** semisolid, **Color:** brown, **M.P.:** 53-55ºC**, Yield:** 68%.

**IR (ATR) $\upsilon_{max}$ ($cm^{-1}$):** 3088 ($SP^2$ C-H stretching, aromatic), 2939-2775 ($SP^3$ C-H stretching, methylenes of piperazine, and 4-methyl piperazine), 1635 (C=O stretching, amide), 1566 (C-H bending, indicative of non-substituted benzofuran at position 3), 1433 (C=C stretching, aromatic), 1288-1257 (C-O stretching, ether), 1176-1143, 1029-997 (C-N stretching, tertiary amine and/or ether), 873 (C-H aromatic out-of-plane bending, one peak, non-substituted benzofuran at position 3), 817 (C-Cl stretching), 746-694 (C-H aromatic out-of-plane bending).

**$^1$H NMR (300 MHz) (DMSO-$d_6$) $\delta$ (ppm):** 2.20 (s, 3H, **4-methyl**piperazine), 2.36 (t, *J*= 5.05 Hz, 4H, piperazine-3, 5), 3.68 (brs, 4H, piperazine-2, 6), 7.35 (d, *J*= 0.87 Hz, 1H, benzofuran-3), 7.45 (dd, *J*= 8.84, 2.25 Hz, 1H, benzofuran-6), 7.70 (d, *J*= 8.84 Hz, 1H, benzofuran-7), 7.81 (d, *J*= 2.02 Hz, 1H, benzofuran-4).

**$^{13}$C NMR (300 MHz) (DMSO-$d_6$) $\delta$ (ppm):** 42.59 (piperazine), 45.99 (**4-methyl**piperazine), 46.81 (piperazine), 55.02 (piperazine), 110.63, 113.95, 122.18, 122.22, 126.87, 128.47, 128.79, 150.14, 152.84, 158.88 (benzofuran-**CO**-piperazine).

**HRMS (ESI) (m/z) $[M+1]^+$:** for $C_{14}H_{15}ClN_2O_2$ calculated: 279.0895; found: 279.0897.

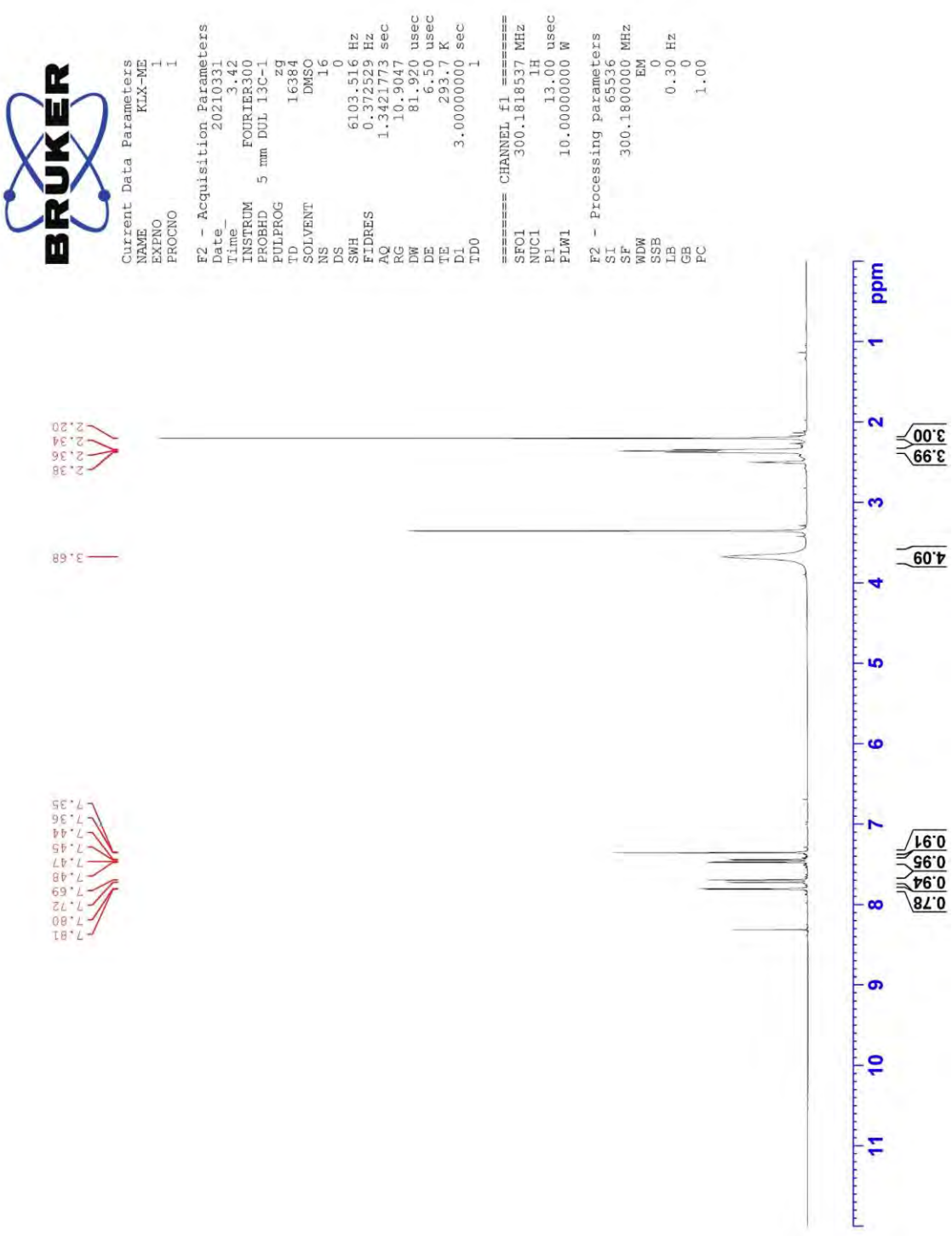


**Figure 5.92.** *[1]H NMR spectrum of compound **D18***

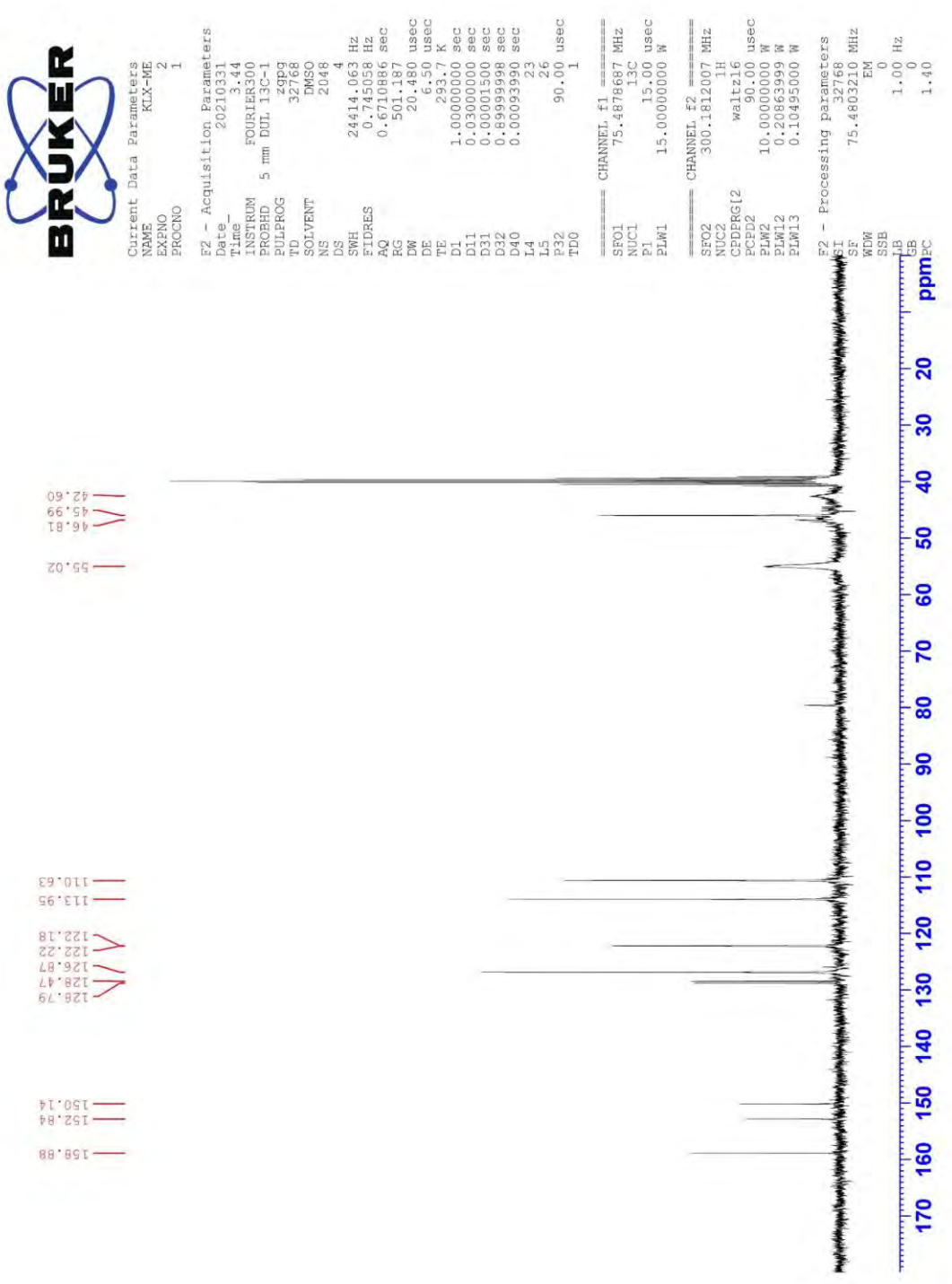


**Figure 5.93.** *$^{13}$C NMR spectrum of compound **D18***

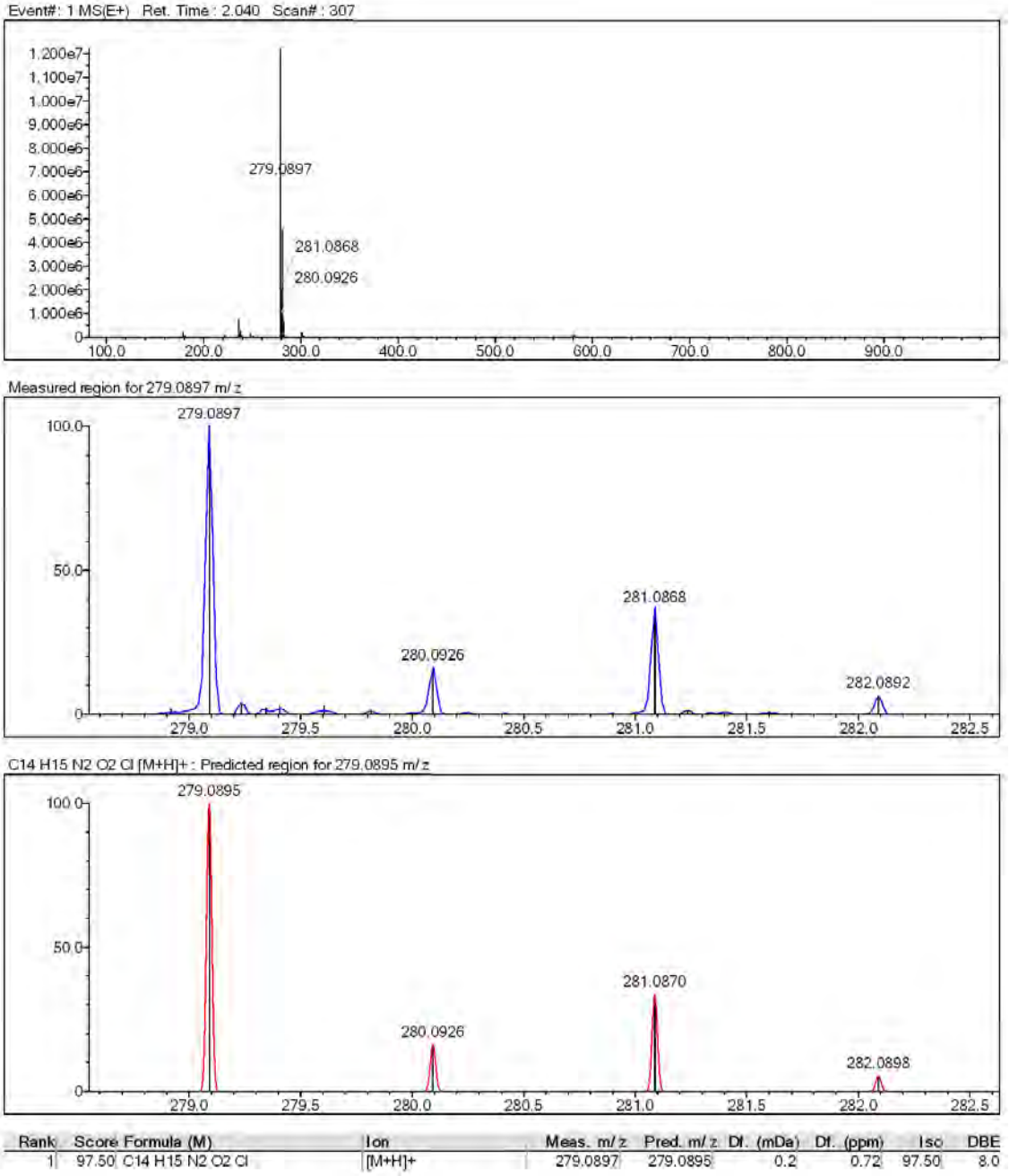


**Figure 5.94.** *High-resolution mass spectrum of compound* ***D18***

DOPNALAB

| | Item | Value |
|---|---|---|
| | Acquired Date&Time | 27.05.2021 16:38:01 |
| | Acquired by | System Administrator |
| | Filename | C:\Users\dopnalab\Desktop\sa\181.ispd |
| | Spectrum name | 181 |
| | Sample name | 18 |
| | Sample ID | |
| | Option | |
| | Comment | |
| | No. of Scans | 15 |
| | Resolution | 4 [cm-1] |
| | Apodization | Happ-Genzel |

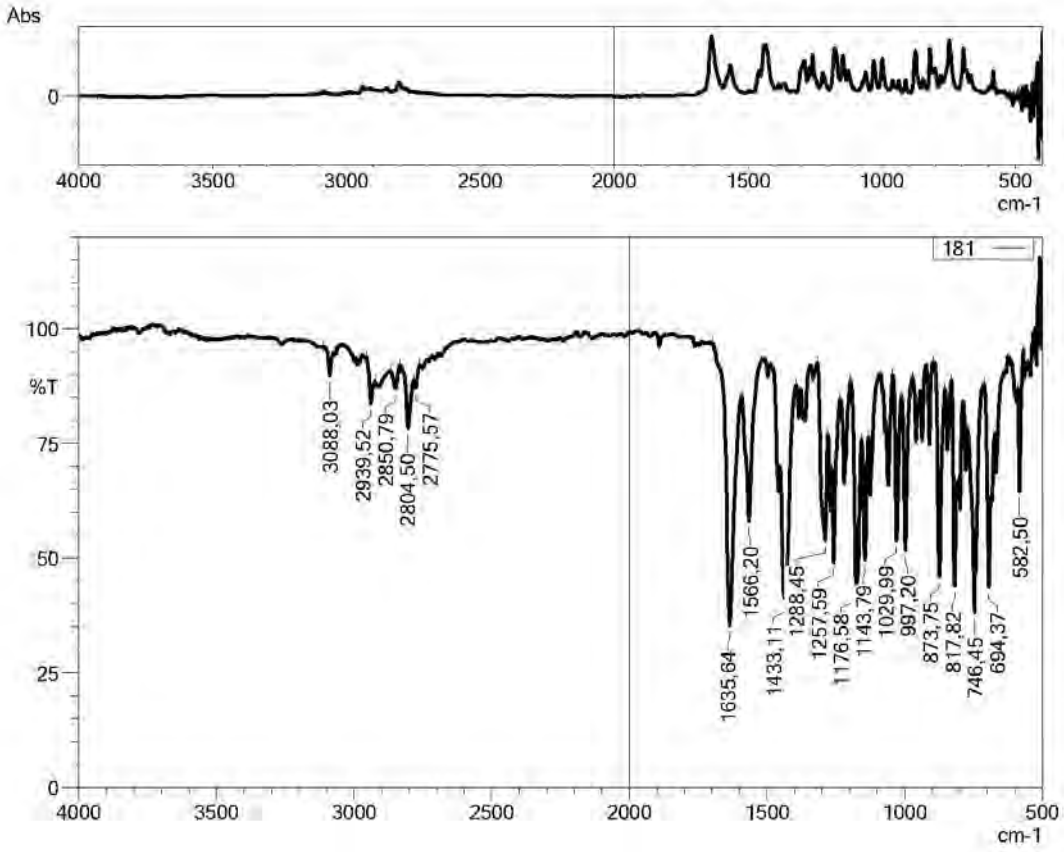


**Figure 5.95.** *IR spectrum of compound **D18***

### 5.1.4.19. *(5-chlorobenzofuran-2-yl)(4-ethylpiperazin-1-yl)methanone (D19)*

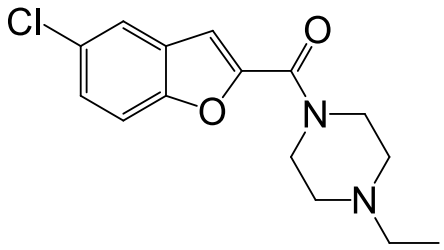


**Figure 5.96.** *Molecular structure of compound **D19***

**Physical Properties: Texture:** solid crystals, **Color:** white, **M.P.:** 89-90ºC**, Yield:** 75%.

**IR (ATR) $\upsilon_{max}$ ($cm^{-1}$):** 3099 (($SP^2$ C-H stretching, aromatic), 2970-2796 ($SP^3$ C-H stretching, methylenes of piperazine, and ethyl-methyl piperazine), 1635 (C=O stretching, amide), 1568 (C-H bending, indicative of non-substituted benzofuran at position 3), 1440 (C=C stretching, aromatic), 1296, 1255 (C-O stretching, ether), 1166, 1014 (C-N stretching, tertiary amine and/or C-O stretching, ether), 877 (C-H aromatic out-of-plane bending, one peak, non-substituted benzofuran at position 3), 819 (C-Cl stretching), 746-694 (C-H aromatic out-of-plane bending).

**$^1$H NMR (300 MHz) (DMSO-$d_6$) $\delta$ (ppm):** 1.00 (t, *J*= 7.17 Hz, 3H, piperazine-$CH_2$-**$CH_3$**), 2.35 (q, *J*= 14.44, 7.11 Hz, 2H, piperazine-**$CH_2$**-$CH_3$), 2.41 (t, *J*= 5.08 Hz, 4H, piperazine-3, 5), 3.68 (brs, 4H, piperazine-2, 6), 7.35 (s, 1H, benzofuran-3), 7.46 (dd, *J*= 8.83, 2.21 Hz, 1H, benzofuran-6), 7.71 (d, *J*= 8.84 Hz, 1H, benzofuran-7), 7.81 (d, *J*= 2.06 Hz, 1H, benzofuran-4).

**$^{13}$C NMR (300 MHz) (DMSO-$d_6$) $\delta$ (ppm):** 12.33 (piperazine-$CH_2$-**$CH_3$**), 42.64 (piperazine), 46.86 (piperazine), 51.87 (piperazine-**$CH_2$**-$CH_3$), 53.01 (piperazine), 110.59, 113.95, 122.19, 126.87, 128.47, 128.79, 150.16, 152.84, 158.81 (benzofuran-**CO**-piperazine).

**HRMS (ESI) (m/z) $[M+1]^+$:** for $C_{15}H_{17}ClN_2O_2$ calculated: 293.1051; found: 293.1056.

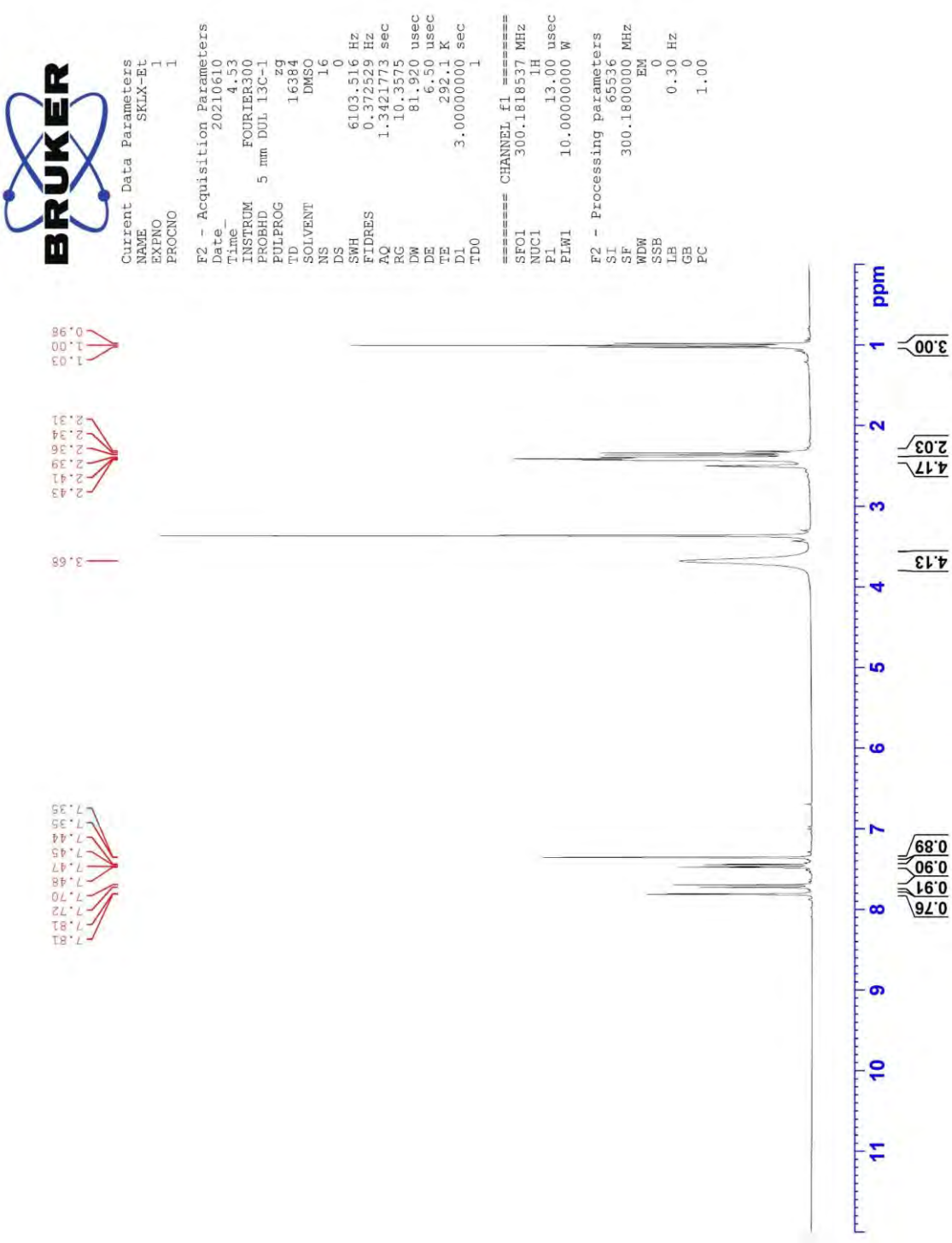


**Figure 5.97.** *[1]H NMR spectrum of compound **D19***

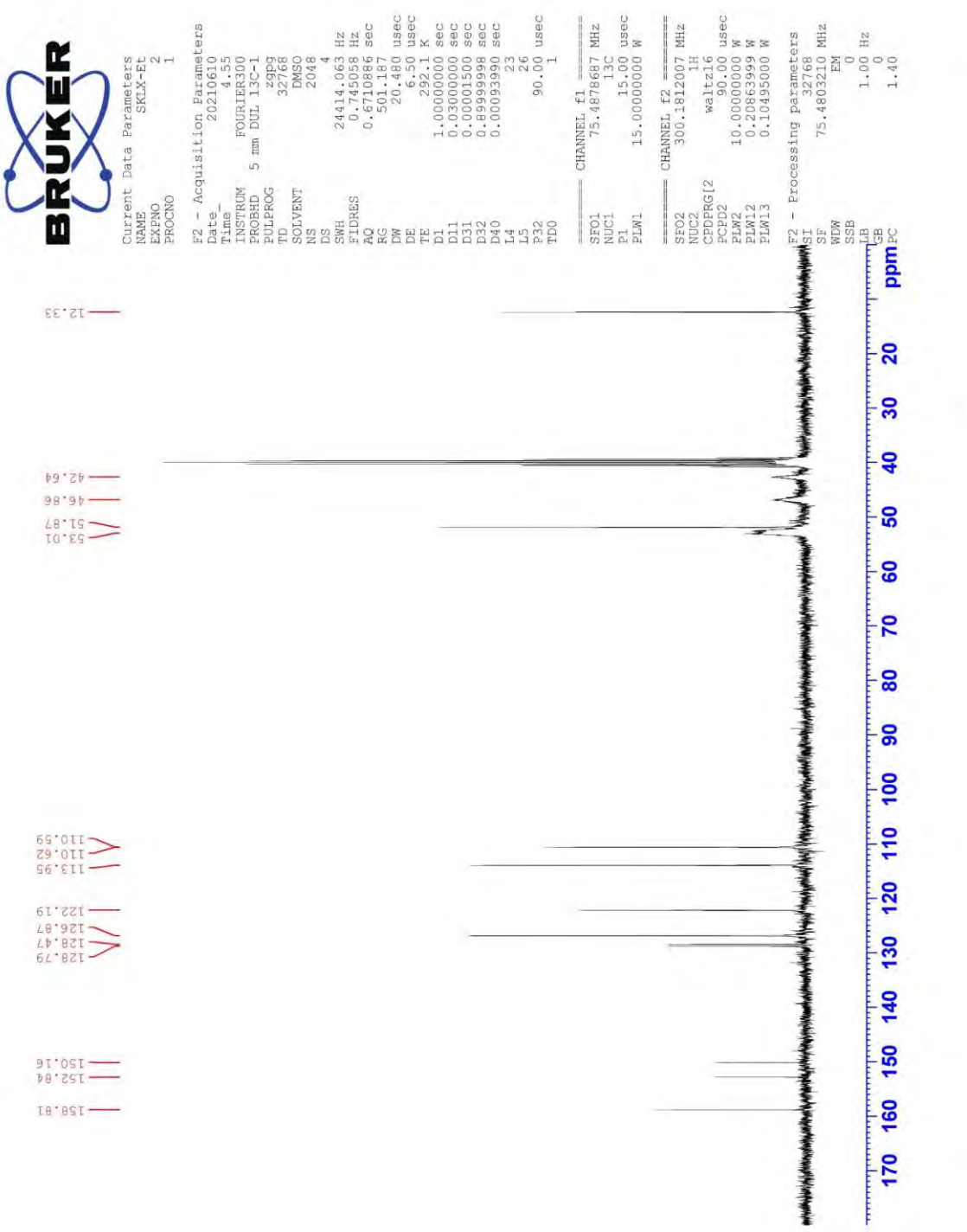


**Figure 5.98.** *$^{13}$C NMR spectrum of compound **D19***

Data File: C:\LabSolutions\Data\Analiz\A.Çağrı\D-19_13.lcd

| Elmt | Val. | Min | Max | Elmt | Val. | Min | Max | Elmt | Val. | Min | Max | Elmt | Val. | Min | Max | Use Adduct |
|---|---|---|---|---|---|---|---|---|---|---|---|---|---|---|---|---|
| H | 1 | 0 | 40 | O | 2 | 0 | 5 | S | 2 | 0 | 0 | Ru | 2 | 0 | 0 | H |
| C | 4 | 0 | 40 | F | 1 | 0 | 0 | Cl | 1 | 1 | 1 | Pd | 2 | 0 | 0 | |
| N | 3 | 2 | 4 | P | 3 | 0 | 0 | Br | 1 | 0 | 0 | I | 3 | 0 | 0 | |

Error Margin (ppm): 5
HC Ratio: unlimited
Max Isotopes: 3
MSn Iso RI (%): 10.00

DBE Range: 0.0 - 20.0
Apply N Rule: yes
Isotope RI (%): 1.00
MSn Logic Mode: AND

Electron Ions: both
Use MSn Info: yes
Isotope Res: 9000
Max Results: 150

Event#: 1 MS(E+) Ret. Time: 1.587 -> 2.693 Scan#: 239 -> 405

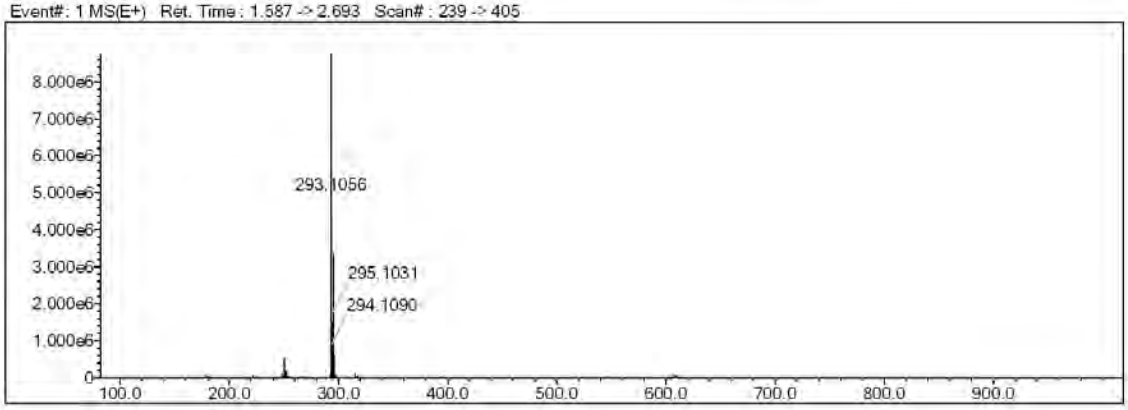


Measured region for 293.1056 m/z

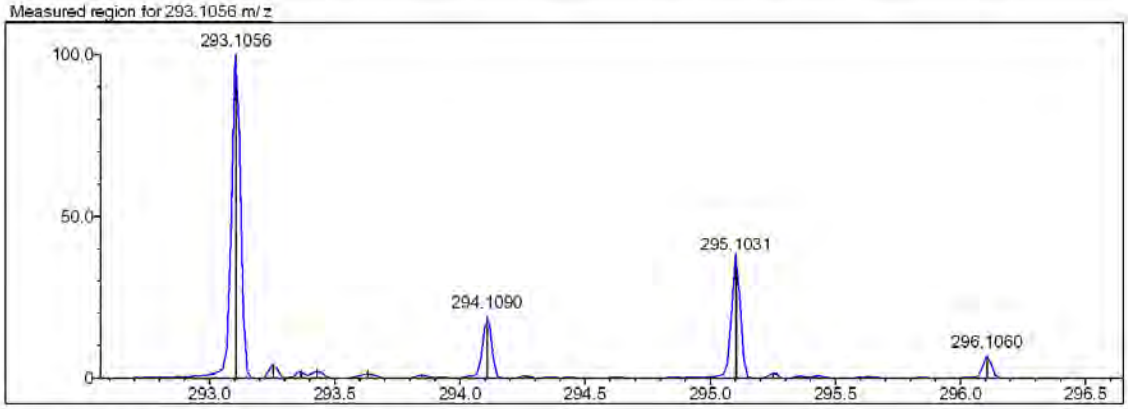


C15 H17 N2 O2 Cl [M+H]+ : Predicted region for 293.1051 m/z

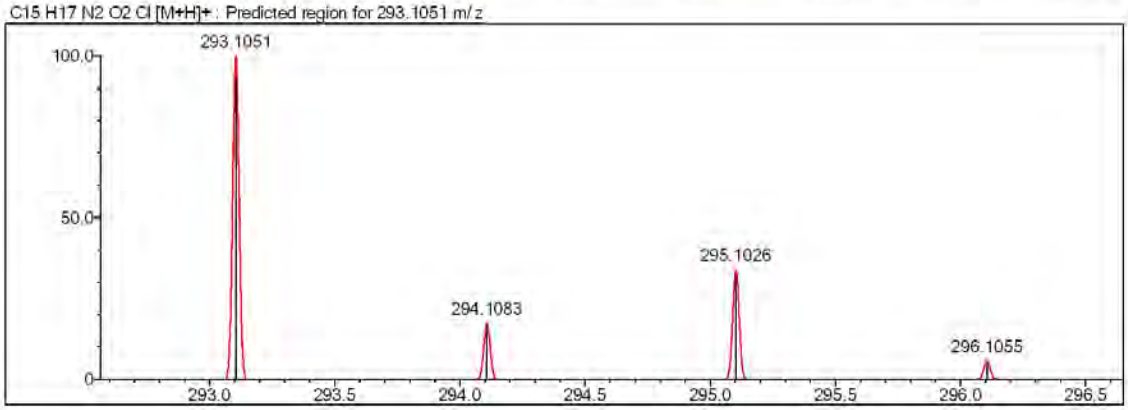


| Rank | Score | Formula (M) | Ion | Meas. m/z | Pred. m/z | Df. (mDa) | Df. (ppm) | Isc | DBE |
|---|---|---|---|---|---|---|---|---|---|
| 1 | 90.55 | C15 H17 N2 O2 Cl | [M+H]+ | 293.1056 | 293.1051 | 0.5 | 1.71 | 92.19 | 8.0 |

**Figure 5.99.** *High-resolution mass spectrum of compound* ***D19***

DOPNALAB

| | Item | Value |
|---|---|---|
| | Acquired Date&Time | 27.05.2021 16:44:27 |
| | Acquired by | System Administrator |
| | Filename | C:\Users\dopnalab\Desktop\sa\191.ispd |
| | Spectrum name | 191 |
| | Sample name | 19 |
| | Sample ID | |
| | Option | |
| | Comment | |
| | No. of Scans | 15 |
| | Resolution | 4 [cm-1] |
| | Apodization | Happ-Genzel |

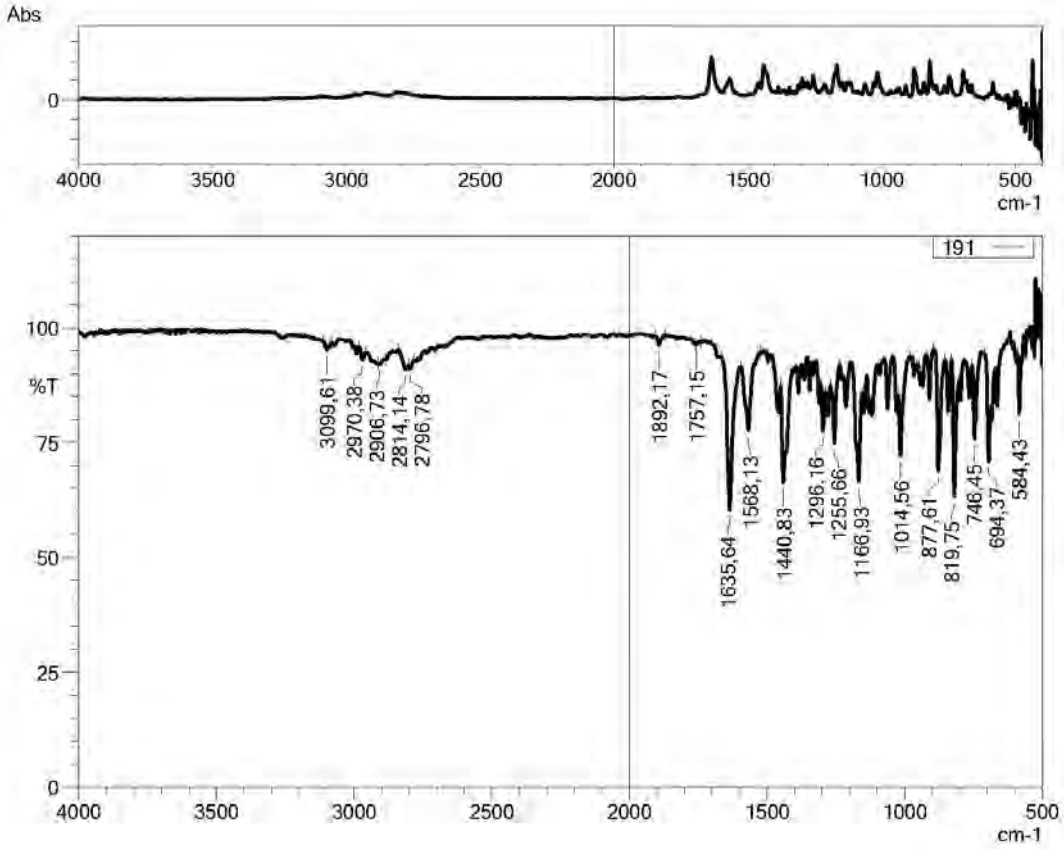


**Figure 5.100.** *IR spectrum of compound **D19***

### 5.1.4.20. *(5-chlorobenzofuran-2-yl)(4-(2-(dimethylamino)ethyl)piperazin-1-yl)methanone (D20)*

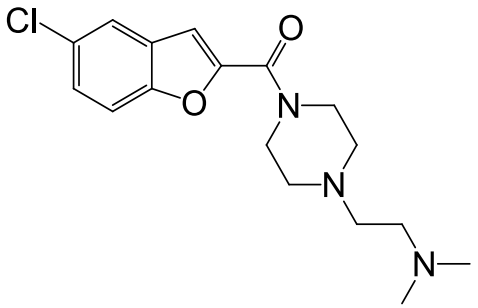


**Figure 5.101.** *Molecular structure of compound* ***D20***

**Physical Properties: Texture:** solid crystals, **Color:** yellow, **M.P.:** 65-67ºC**, Yield:** 70%.

**IR (ATR) $\upsilon_{max}$ ($cm^{-1}$):** 2978-2767 ($SP^3$ C-H stretching, methylenes of piperazine, dimethylaminoethyl-piperazine), 1614 (C=O stretching, amide), 1560 (C-H bending, indicative of non-substituted benzofuran at position 3), 1438-1421 (C=C stretching, aromatic), 1294-1217 (C-O stretching, ether), 1174, 1036-1020 (C-N stretching, tertiary amine and/or C-O stretching, ether), 939-694 (C-H aromatic out-of-plane bending), 873 (C-H aromatic out-of-plane bending, one peak, non-substituted benzofuran at position 3), 808 (C-Cl stretching).

**$^1$H NMR (300 MHz) (DMSO-$d_6$) $\delta$ (ppm):** 2.12 (s, 6H, -N**($CH_3$)$_2$**), 2.34-2.42 (m, 4H, piperazine-(**$CH_2$)$_2$**-N), 2.46 (t, *J*= 5.05 Hz, 4H, piperazine-3, 5), 3.67 (brs, 4H, piperazine-2, 6), 7.35 (s, 1H, benzofuran-3), 7.46 (dd, *J*= 8.83, 2.25 Hz, 1H, benzofuran-6), 7.71 (d, *J*= 8.84 Hz, 1H, benzofuran-7), 7.81 (d, *J*= 2.07 Hz, 1H, benzofuran-4).

**$^{13}$C NMR (300 MHz) (DMSO-$d_6$) $\delta$ (ppm):** 42.67 (piperazine), 46.02 (-N**($CH_3$)$_2$**), 46.82 (piperazine), 53.62 (piperazine), 56.00 (piperazine-(**$CH_2$)$_2$**-N), 57.02 (piperazine-(**$CH_2$)$_2$**-N), 110.63, 113.95, 122.18, 126.87, 128.46, 128.79, 150.15, 152.84, 158.79 (benzofuran-**CO-**piperazine).

**HRMS (ESI) (m/z) $[M+1]^+$:** for $C_{17}H_{22}ClN_3O_2$ calculated: 336.1473; found: 336.1488.

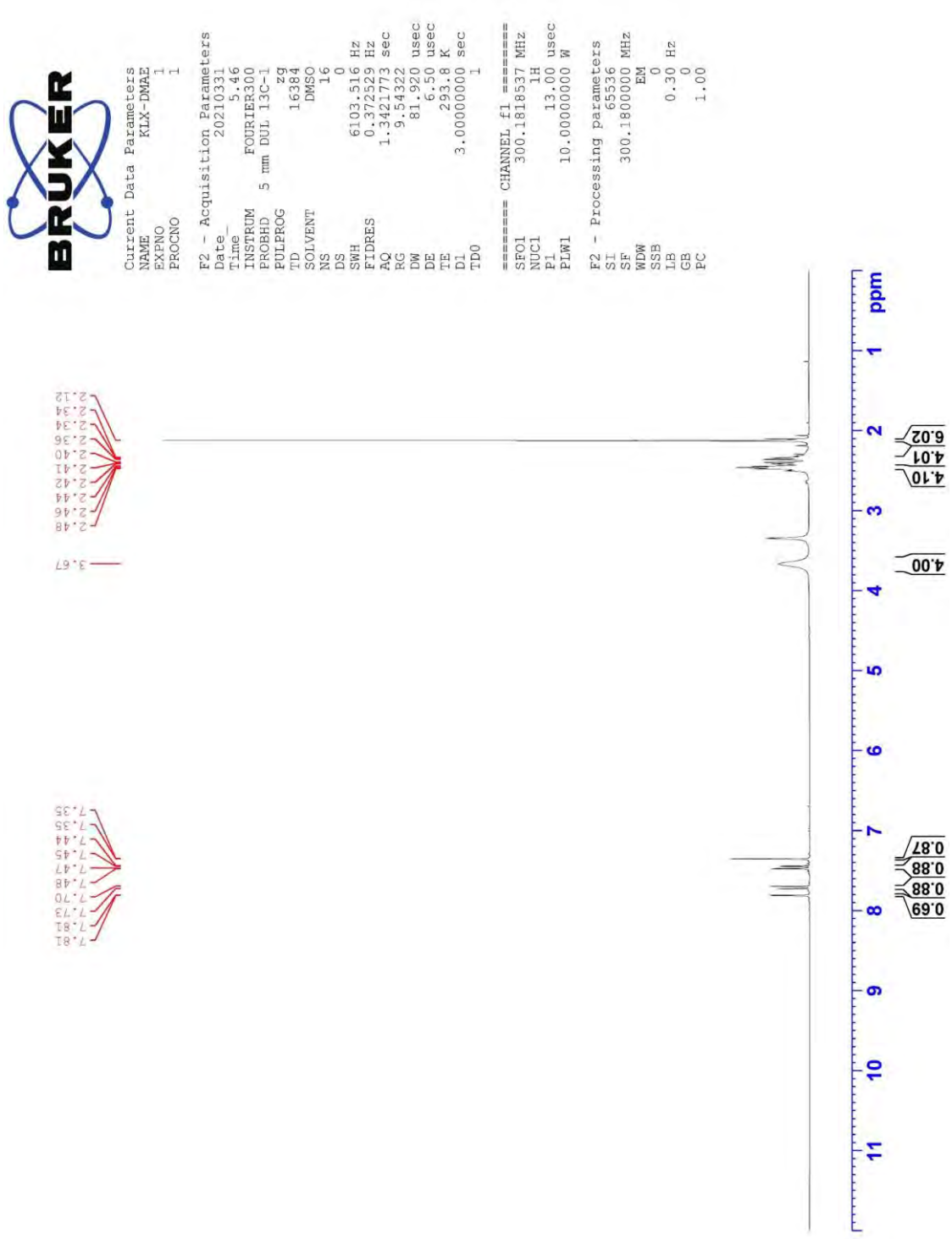


**Figure 5.102.** *[1]H NMR spectrum of compound **D20***

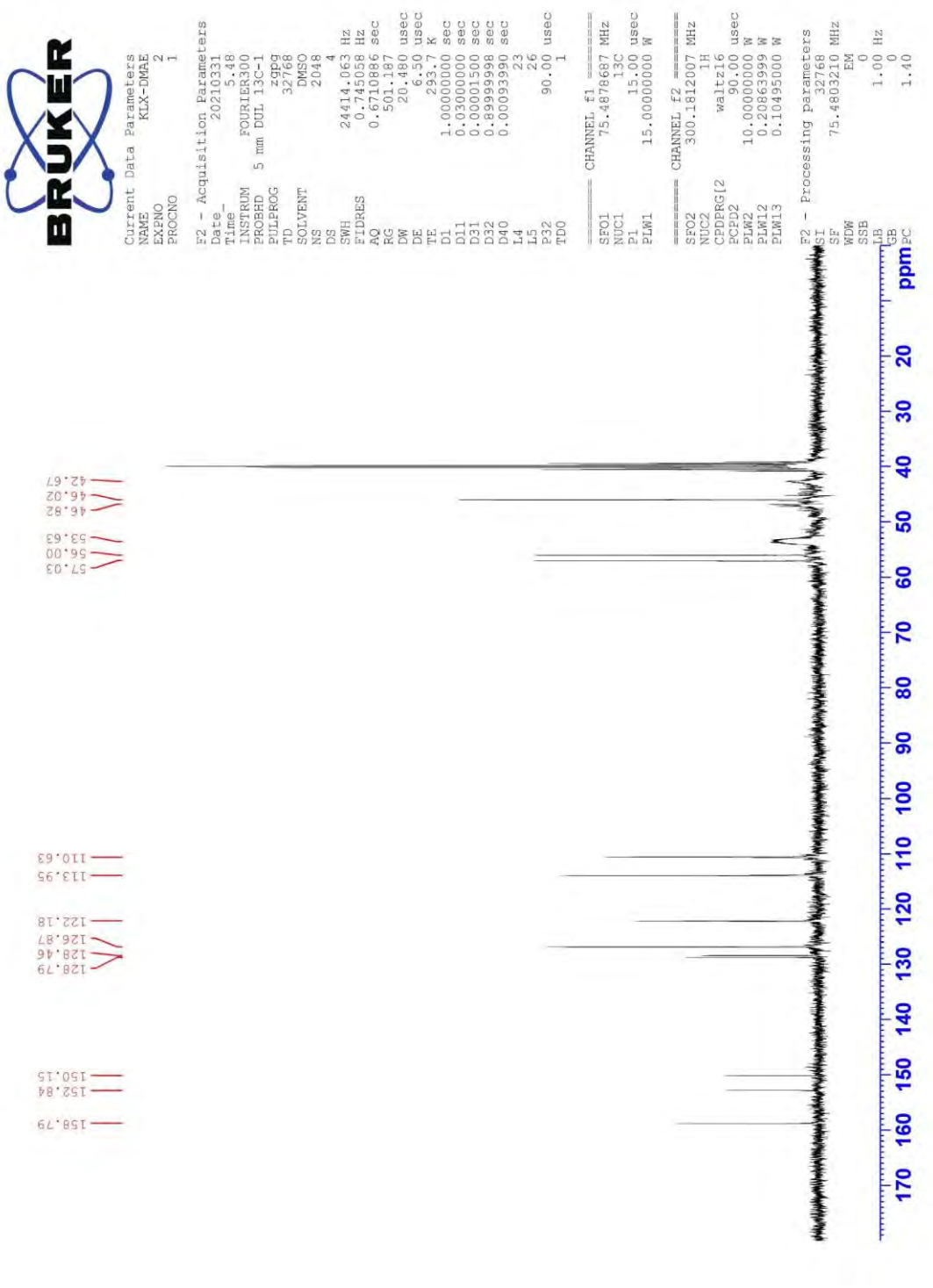


**Figure 5.103.** *$^{13}$C NMR spectrum of compound **D20***

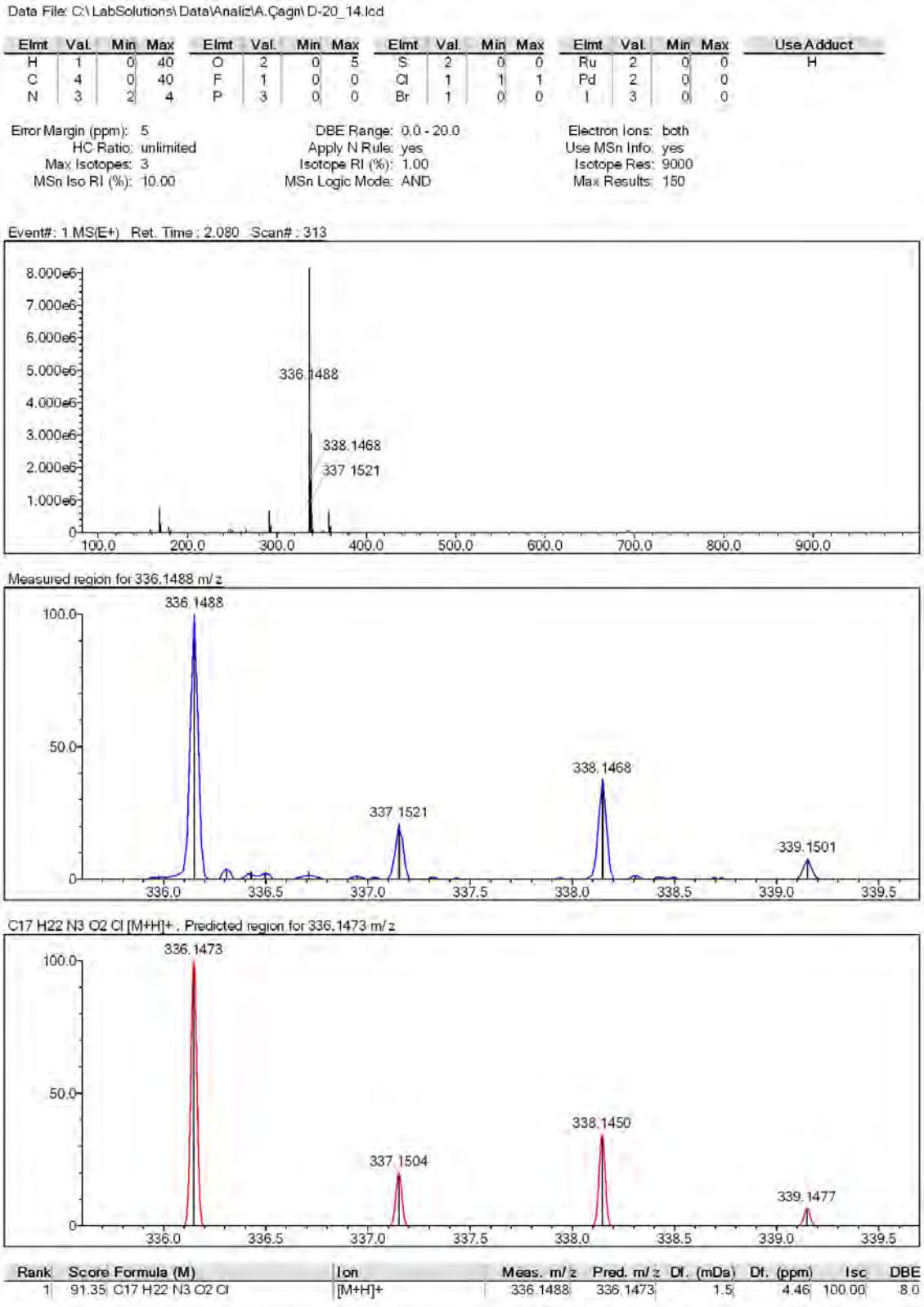


**Figure 5.104.** *High-resolution mass spectrum of compound* ***D20***

DOPNALAB

| | Item | Value |
|---|---|---|
| | Acquired Date&Time | 27.05.2021 16:49:34 |
| | Acquired by | System Administrator |
| | Filename | C:\Users\dopnalab\Desktop\sa\201.ispd |
| | Spectrum name | 201 |
| | Sample name | 20 |
| | Sample ID | |
| | Option | |
| | Comment | |
| | No. of Scans | 15 |
| | Resolution | 4 [cm-1] |
| | Apodization | Happ-Genzel |

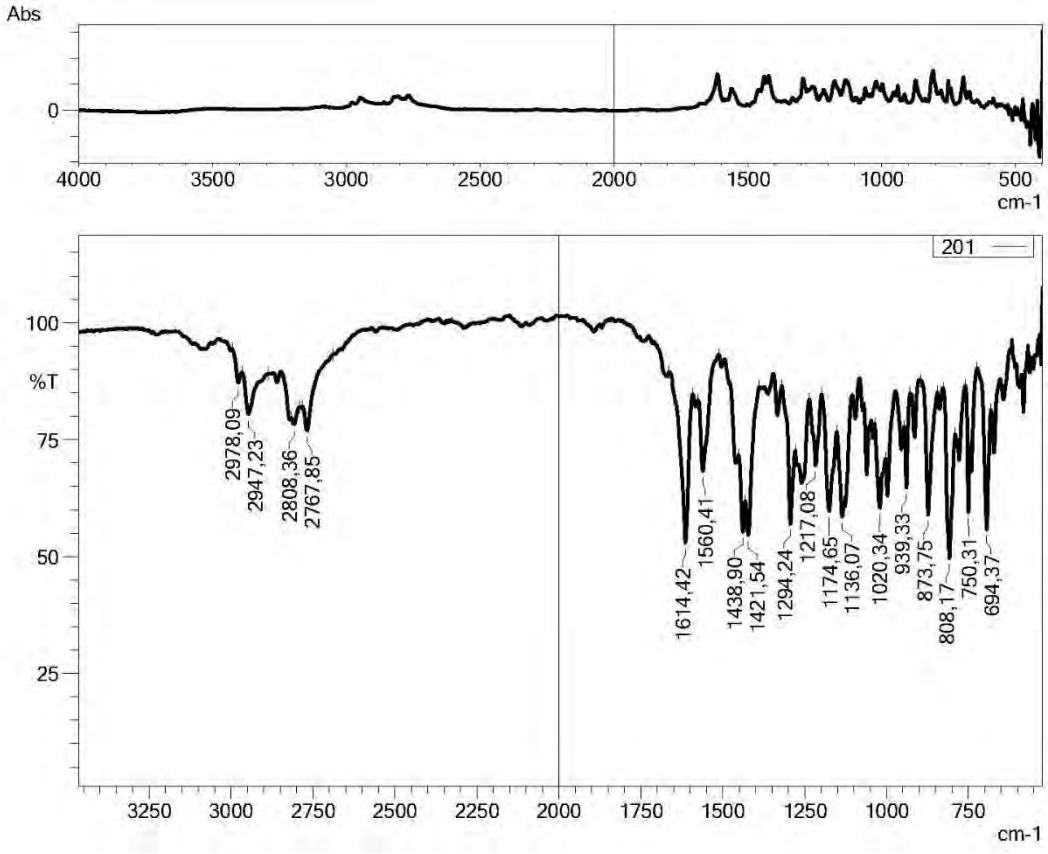


**Figure 5.105.** *IR spectrum of compound **D20***

### 5.1.4.21. *(3-methyl-5-nitrobenzofuran-2-yl)(4-phenylpiperazin-1-yl)methanone (D21)*

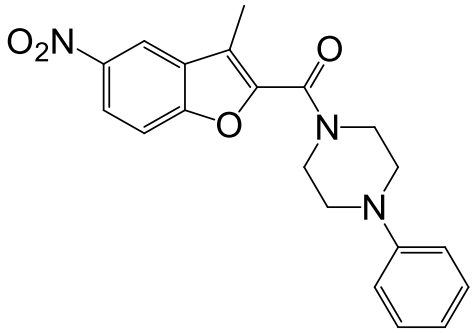


**Figure 5.106.** *Molecular structure of compound **D21***

**Physical Properties: Texture:** amorphous solid particles, **Color:** brown, **M.P.:** 199-201ºC**, Yield:** 70%.

**IR (ATR) $\upsilon_{max}$ ($cm^{-1}$):** 2943-2812 ($SP^3$ C-H stretching, 3-methylbenzofuran and methylenes of piperazine), 1633 (C=O stretching, amide), 1597-1521 (N-O asymmetric stretching, nitro group), 1440 (C=C stretching, aromatic), 1338 (N-O symmetric stretching, nitro group), 1278-1226 (C-O stretching, ether), 1012 (C-N stretching, tertiary amine and/or ether), 881-694 (C-H aromatic out-of-plane bending).

**$^1$H NMR (300 MHz) (DMSO-$d_6$) $\delta$ (ppm):** 2.43 (s, 3H, **3-methyl**benzofuran), 3.81 (brs, 8H, piperazine-2, 3, 5, 6), 6.87 (t, *J*= 7.22 Hz, 1H, phenyl-4), 7.03 (d, *J*= 8.25, 2H, phenyl-2, 6), 7.28 (t, *J*= 8.52 Hz, 2H, phenyl-3,5), 7.87 (d, *J*= 9.09 Hz, 1H, benzofuran-7), 8.32 (dd, *J*= 9.09, 2.41 Hz, 1H, benzofuran-6), 8.71 (d, *J*= 2.33 Hz, 1H, benzofuran-4).

**$^{13}$C NMR (300 MHz) (DMSO-$d_6$) $\delta$ (ppm):** 8.87 (**3-methyl**benzofuran), 43.09 (piperazine), 49.38 (piperazine), 113.23, 116.87, 118.08, 120.40, 120.70, 122.41, 129.58, 144.41, 146.98, 156.36, 159.37 (benzofuran-**CO-**piperazine).

**HRMS (ESI) (m/z) $[M+1]^+$:** for $C_{20}H_{19}N_3O_4$ calculated: 366.1448; found: 366.1458.

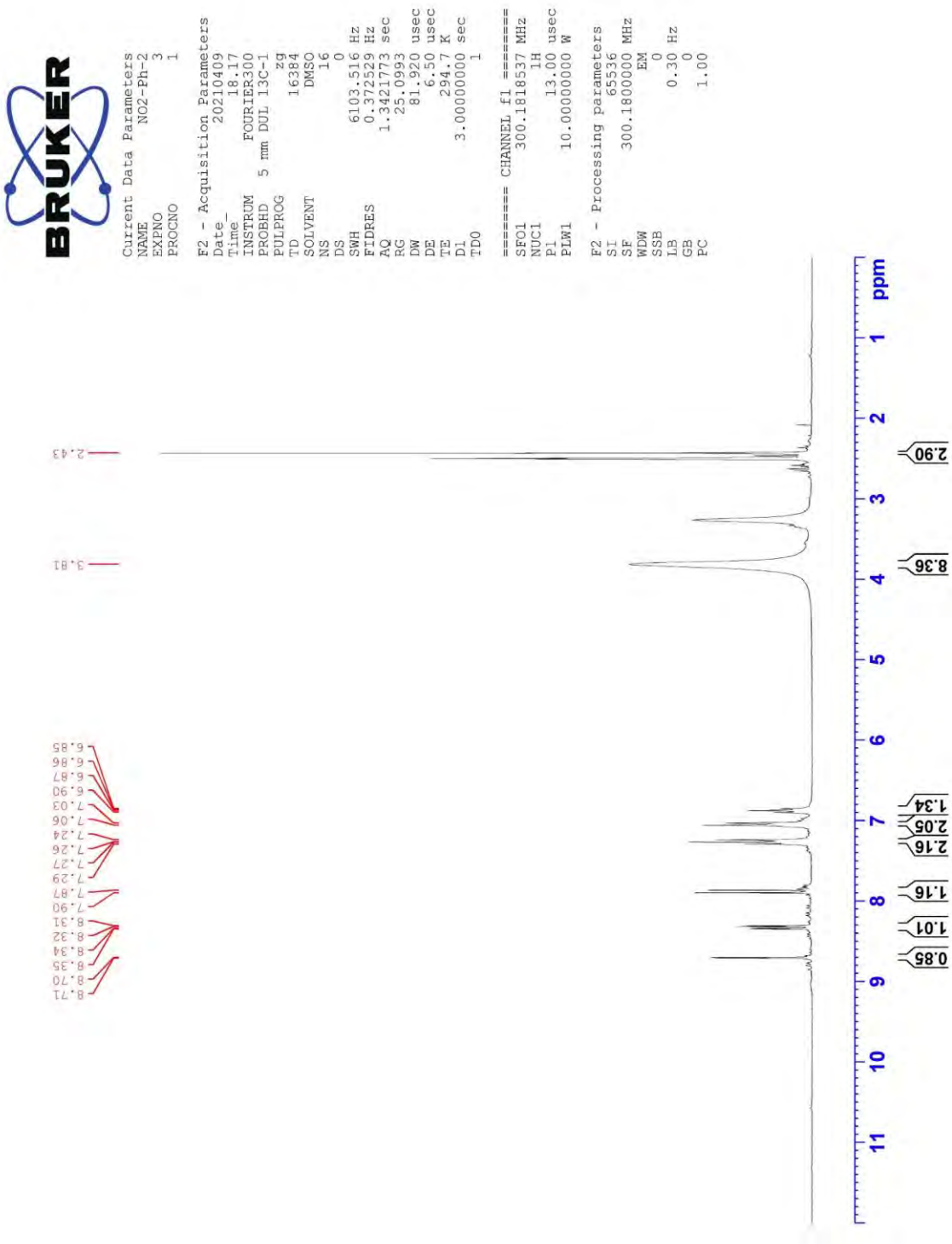


**Figure 5.107.** *$^{1}H$ NMR spectrum of compound **D21***

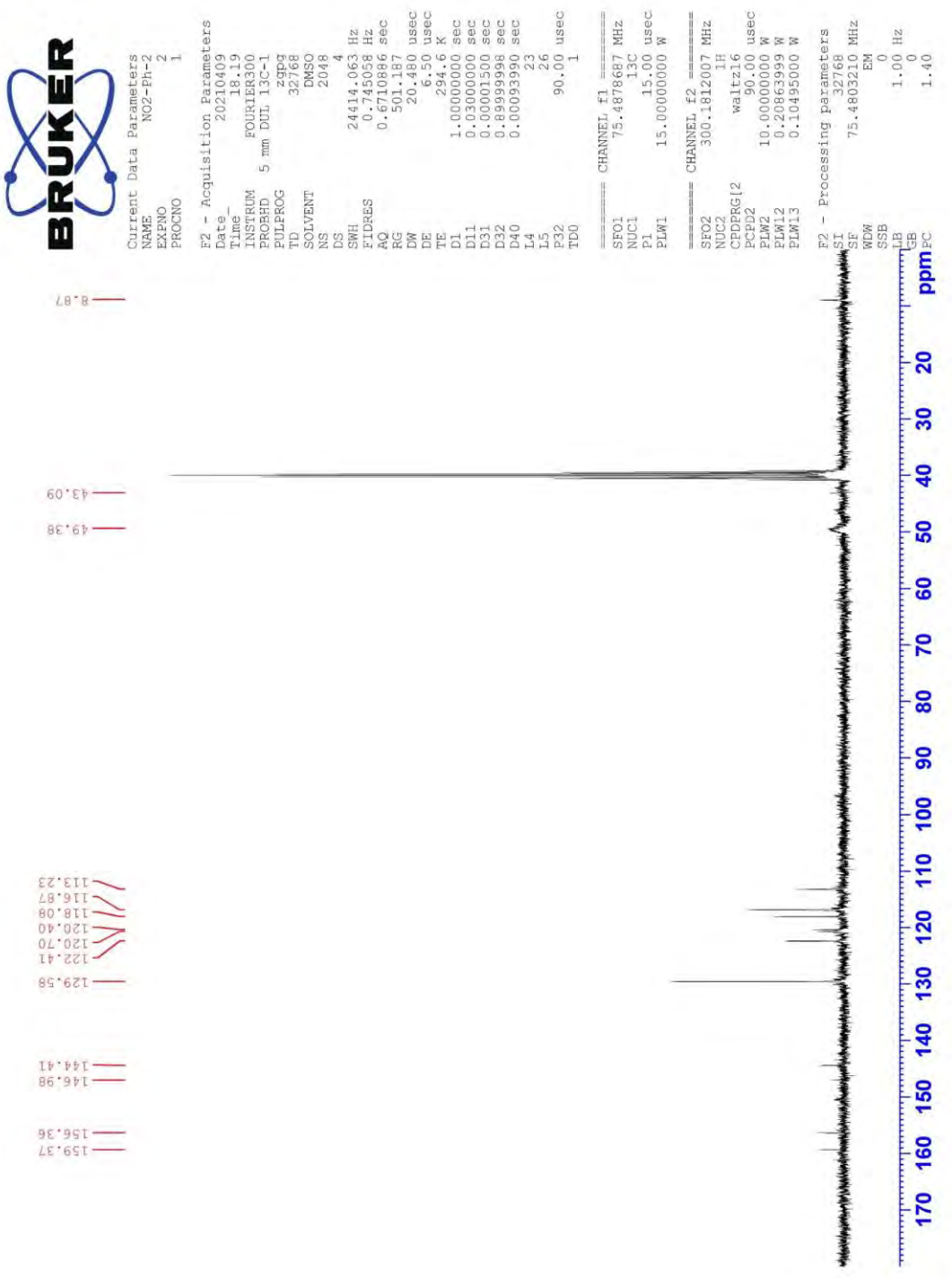


**Figure 5.108.** *$^{13}$C NMR spectrum of compound **D21***

Data File: C:\LabSolutions\Data\Analiz\Asafi D-21-C_84.lcd

| Elmt | Val. | Min | Max | Elmt | Val. | Min | Max | Elmt | Val. | Min | Max | Elmt | Val. | Min | Max | Use Adduct |
|---|---|---|---|---|---|---|---|---|---|---|---|---|---|---|---|---|
| H | 1 | 0 | 40 | O | 2 | 1 | 5 | S | 2 | 0 | 0 | Ru | 2 | 0 | 0 | H |
| C | 4 | 0 | 40 | F | 1 | 0 | 0 | Cl | 1 | 0 | 1 | Pd | 2 | 0 | 0 | |
| N | 3 | 2 | 6 | P | 3 | 0 | 0 | Br | 1 | 0 | 0 | I | 3 | 0 | 0 | |

Error Margin (ppm): 12
HC Ratio: unlimited
Max Isotopes: 3
MSn Iso RI (%): 10.00

DBE Range: 5.0 - 20.0
Apply N Rule: yes
Isotope RI (%): 1.00
MSn Logic Mode: AND

Electron Ions: both
Use MSn Info: yes
Isotope Res: 9000
Max Results: 150

Event#: 1 MS(E+) Ret. Time: 4.013 -> 4.827 Scan#: 603 -> 725

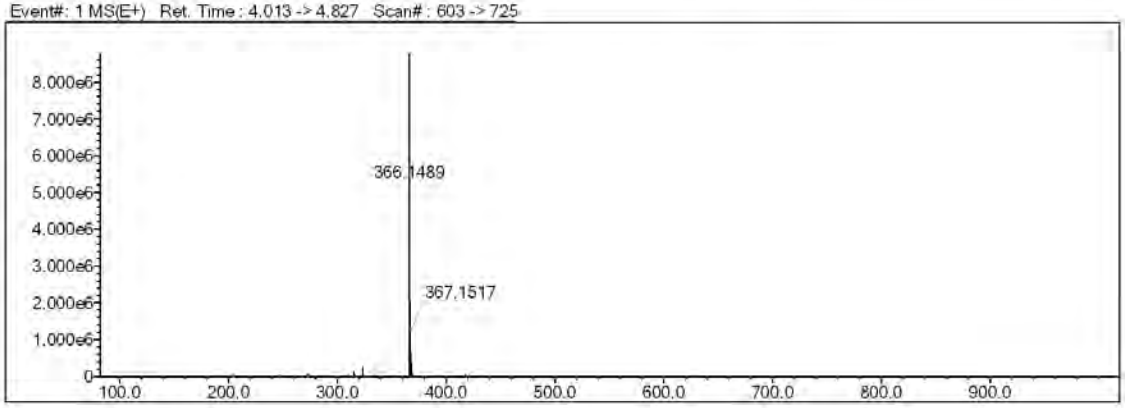


Measured region for 366.1489 m/z

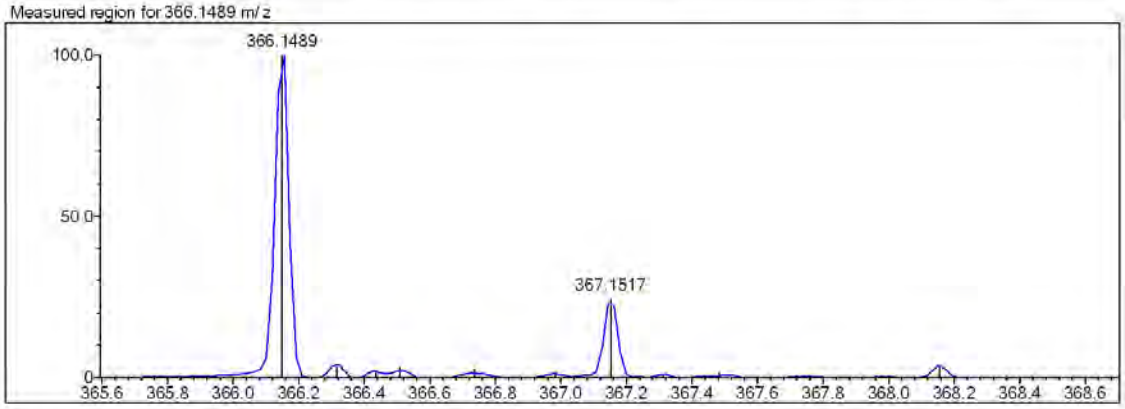


C20 H19 N3 O4 [M+H]+ : Predicted region for 366.1448 m/z

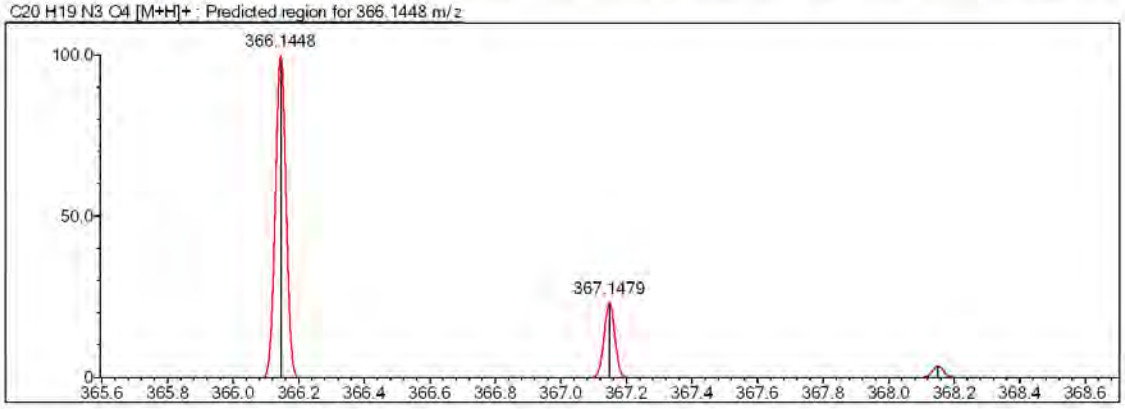


| Rank | Score | Formula (M) | Ion | Meas. m/z | Pred. m/z | Df. (mDa) | Df. (ppm) | Isc | DBE |
|---|---|---|---|---|---|---|---|---|---|
| 1 | 29.02 | C20 H19 N3 O4 | [M+H]+ | 366.1489 | 366.1448 | 4.1 | 11.20 | 78.87 | 13.0 |

**Figure 5.109.** *High-resolution mass spectrum of compound* ***D21***

DOPNALAB

| | Item | Value |
|---|---|---|
| | Acquired Date&Time | 27.05.2021 16:59:09 |
| | Acquired by | System Administrator |
| | Filename | C:\Users\dopnalab\Desktop\sa\211.ispd |
| | Spectrum name | 211 |
| | Sample name | 21 |
| | Sample ID | |
| | Option | |
| | Comment | |
| | No. of Scans | 15 |
| | Resolution | 4 [cm-1] |
| | Apodization | Happ-Genzel |

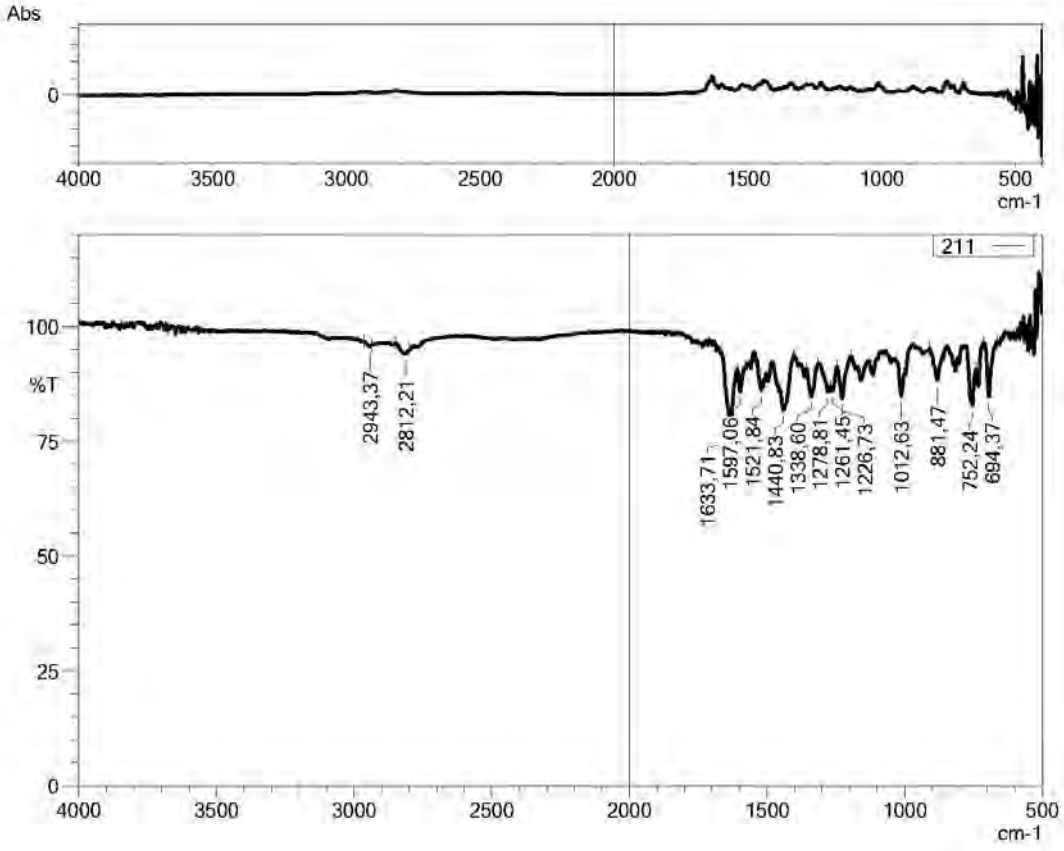


**Figure 5.110.** *IR spectrum of compound* ***D21***

### 5.1.4.22. *(4-(furan-2-carbonyl)piperazin-1-yl)(3-methyl-5-nitrobenzofuran-2-yl)methanone (D22)*

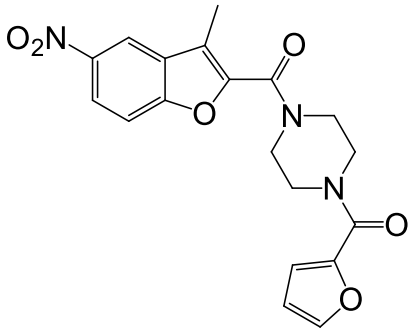

**Figure 5.111.** *Molecular structure of compound* ***D22***

**Physical Properties: Texture:** solid powder, **Color:** brown, **M.P.:** 144-146ºC**, Yield:** 28%.

**IR (ATR) $\upsilon_{max}$ ($cm^{-1}$):** 3099 ($SP^2$ C-H stretching, aromatic), 2922-2862 ($SP^3$ C-H stretching, methylenes of piperazine and 3-methylbenzofuran), 1633 (C=O stretching, amide), 1521 (N-O asymmetric stretching, nitro group), 1425 (C=C stretching, aromatic), 1346 (N-O symmetric stretching, nitro group), 1257 (C-O stretching, ether), 1161, 1002 (C-N stretching, tertiary amine and/or ether), 883-738 (C-H aromatic out-of-plane bending).

**$^1$H NMR (300 MHz) (DMSO-$d_6$) $\delta$ (ppm):** 2.44 (s, 3H, **3-methyl**benzofuran), 3.74 (brs, 8H, piperazine-2, 3, 5, 6), 6.65 (dd, *J*= 3.44, 1.75 Hz, 1H, furan-4), 7.07 (d, *J*= 2.80 Hz, 1H, furan-3), 7.86-7.89 (m, 2H, benzofuran-7 and furan-5), 8.33 (dd, J= 9.08, 2.41 Hz, 2H, benzofuran-6), 8.70 (d, *J*= 2.24 Hz, 1H, benzofuran-4).

**$^{13}$C NMR (300 MHz) (DMSO-$d_6$) $\delta$ (ppm):** 8.89 (**3-methyl**benzofuran), 42.56 (piperazine), 46.70 (piperazine), 111.88, 113.25, 116.51, 118.08, 120.65, 122.44, 129.55, 144.39, 145.44, 145.48, 146.82, 147.16, 156.36, 158.91 (piperazine-**CO**-furan), 159.58 (benzofuran-**CO**-piperazine).

**HRMS (ESI) (m/z) $[M+1]^+$:** for $C_{19}H_{17}N_3O_6$ calculated: 384.1190; found: 384.1206.

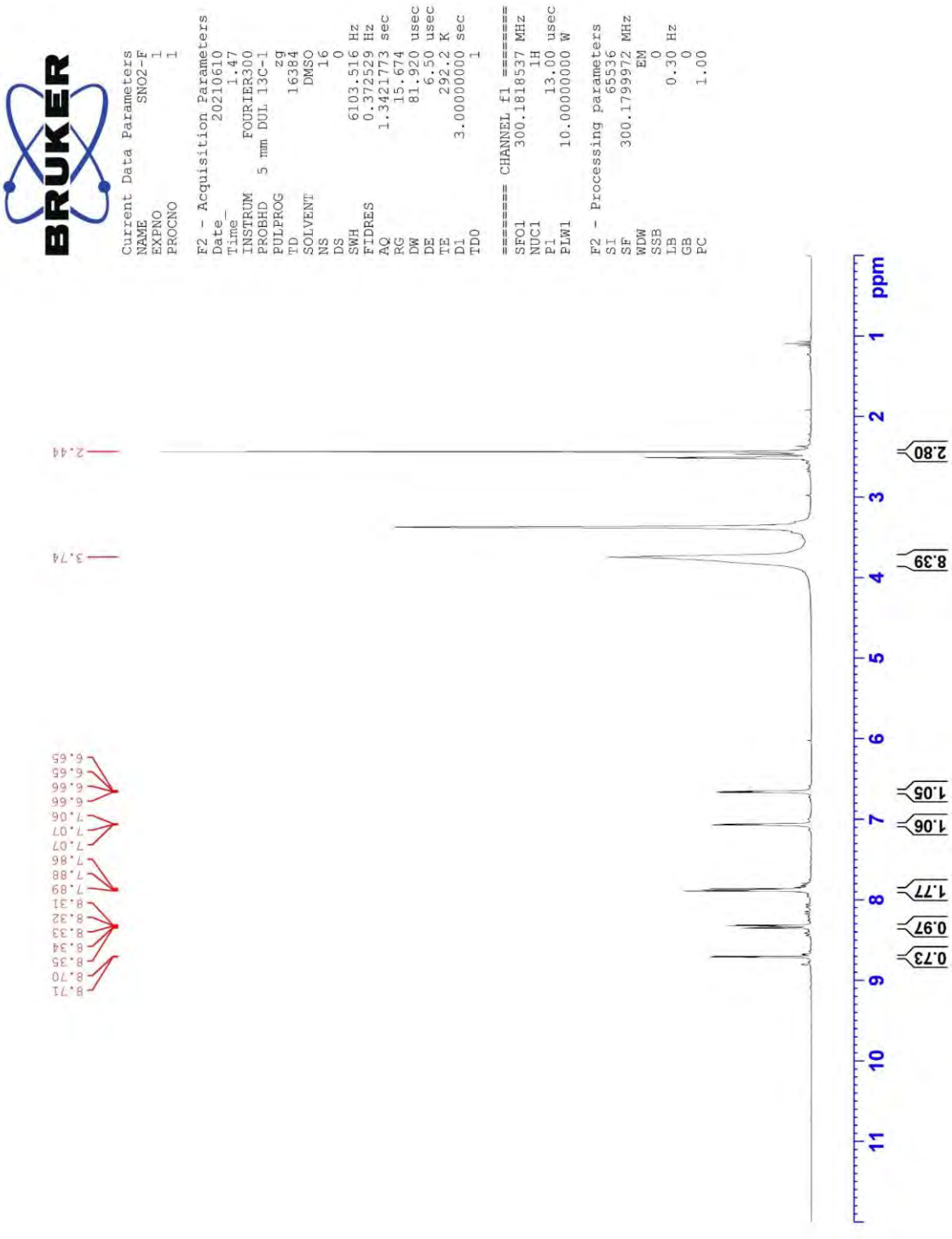


**Figure 5.112.** *$^{1}H$ NMR spectrum of compound **D22***

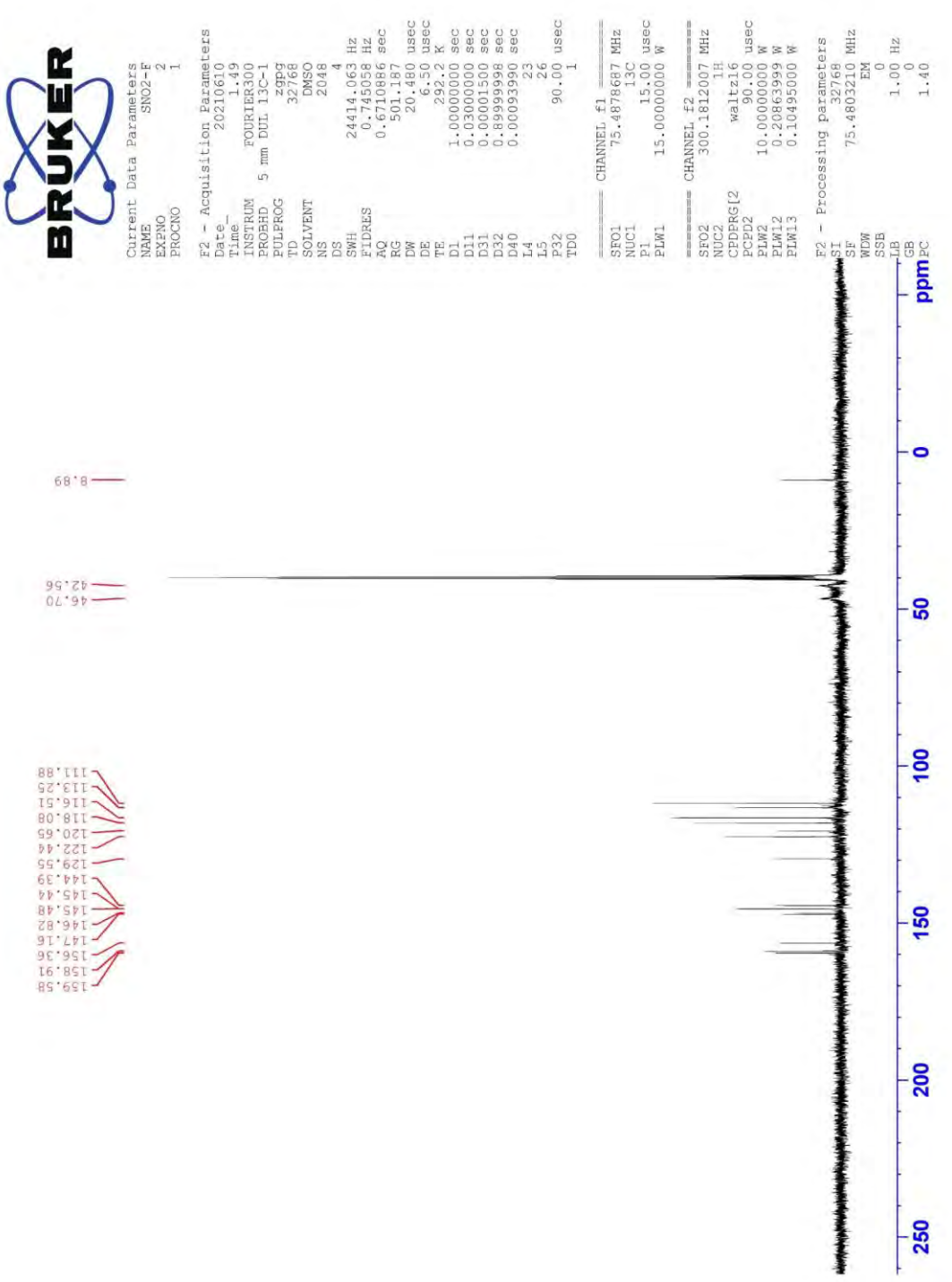


**Figure 5.113.** *$^{13}$C NMR spectrum of compound **D22***

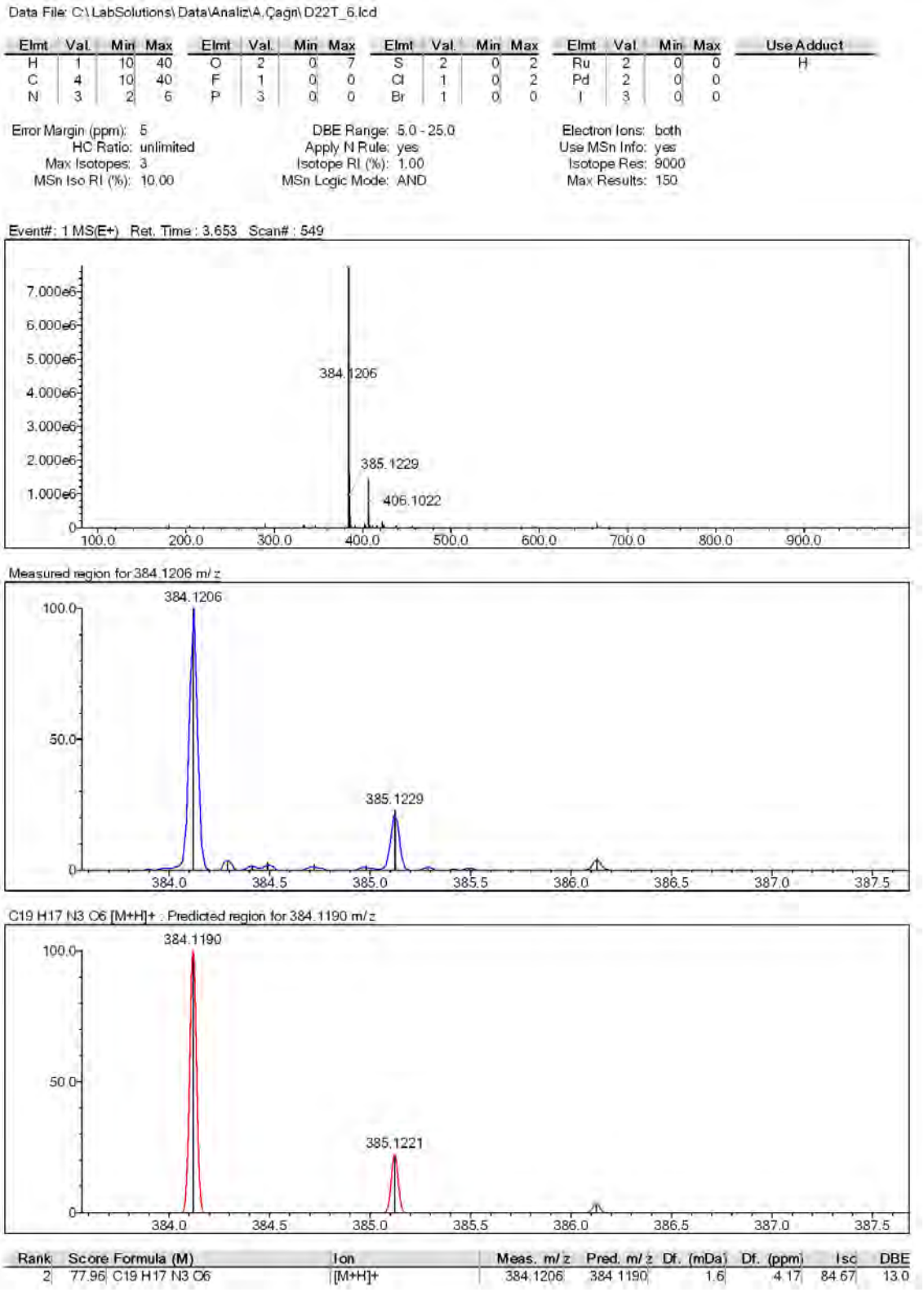


**Figure 5.114.** *High-resolution mass spectrum of compound* ***D22***

DOPNALAB

| | Item | Value |
|---|---|---|
| | Acquired Date&Time | 27.05.2021 17:04:29 |
| | Acquired by | System Administrator |
| | Filename | C:\Users\dopnalab\Desktop\sa\221.ispd |
| | Spectrum name | 221 |
| | Sample name | 22 |
| | Sample ID | |
| | Option | |
| | Comment | |
| | No. of Scans | 15 |
| | Resolution | 4 [cm-1] |
| | Apodization | Happ-Genzel |

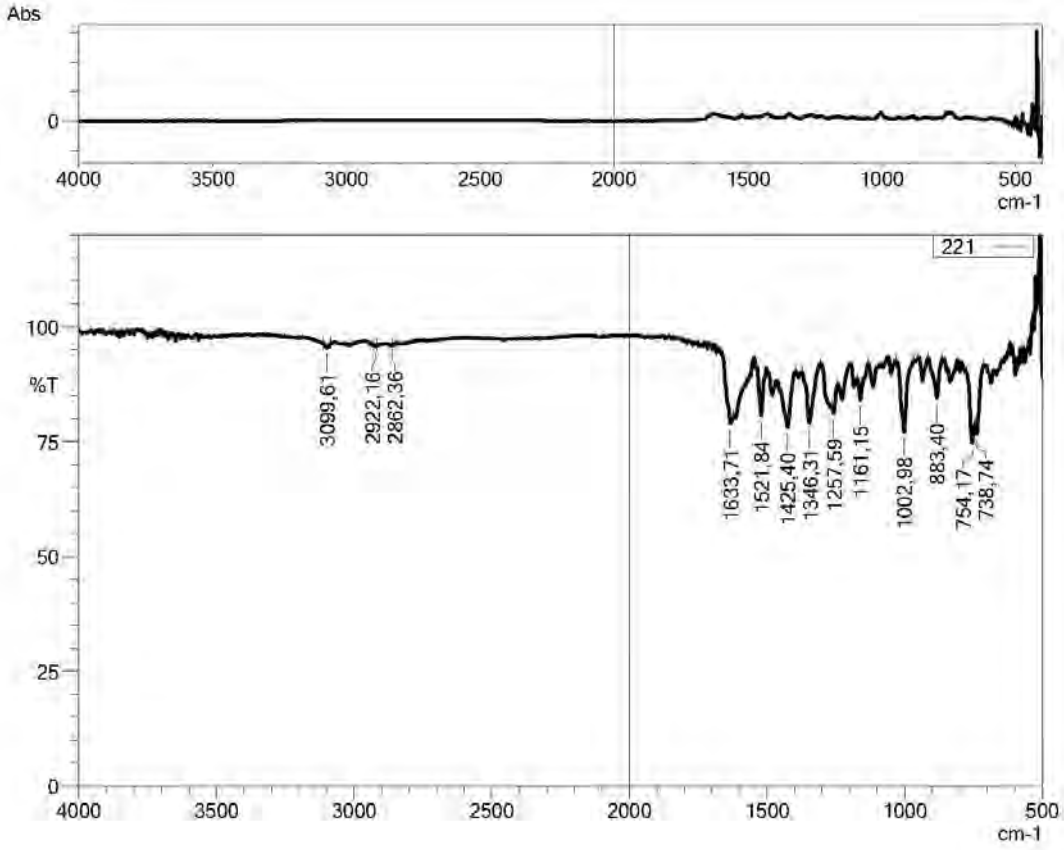


**Figure 5.115.** *IR spectrum of compound **D22***

### 5.1.4.23. *(3-methyl-5-nitrobenzofuran-2-yl)(4-methylpiperazin-1-yl)methanone (D23)*

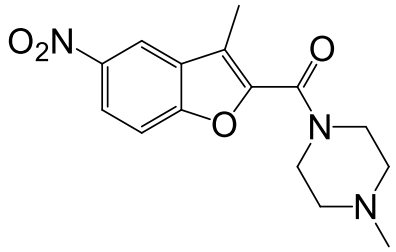

**Figure 5.116.** *Molecular structure of compound* ***D23***

**Physical Properties: Texture:** semisolid, **Color:** dark brown, **M.P.:** 102-104ºC**, Yield:** 54%.

**IR (ATR) $\upsilon_{max}$ ($cm^{-1}$):** 3099 ($SP^2$ C-H stretching, aromatic), 2937-2792 ($SP^3$ C-H stretching, 4-methyl piperazine, methylenes of piperazine, and 3-methylbenzofuran), 1631 (C=O stretching, amide), 1523 (N-O asymmetric stretching, nitro group), 1435 (C=C stretching, aromatic), 1344 (N-O symmetric stretching, nitro group), 1292-1267 (C-O stretching, ether), 1138, 999 (C-N stretching, tertiary amine and/or ether), 887-665 (C-H aromatic out-of-plane bending).

**$^1$H NMR (300 MHz) (DMSO-$d_6$) $\delta$ (ppm):** 2.21 (s, 3H, **4-methyl**piperazine), 2.38-2.42 (m, 7H, **3-methyl**benzofuran and piperazine-3, 5), 3.61 (brs, 4H, piperazine-2, 6), 7.85 (d, *J*= 9.09 Hz, 1H, benzofuran-7), 8.29-8.33 (m, 1H, benzofuran-6), 8.67 (d, *J*= 2.27 Hz, 1H, benzofuran-4).

**$^{13}$C NMR (300 MHz) (DMSO-$d_6$) $\delta$ (ppm):** 8.76 (**3-methyl**benzofuran), 42.39 (piperazine), 46.01 (**4-methyl**piperazine), 46.79 (piperazine), 54.68 (piperazine), 55.47 (piperazine), 113.18, 117.98, 119.79, 122.26, 129.55, 144.36, 147.17, 156.36, 159.31 (benzofuran-**CO**-piperazine).

**HRMS (ESI) (m/z) $[M+1]^+$:** for $C_{15}H_{17}N_3O_4$ calculated: 304.1292; found: 304.1302.

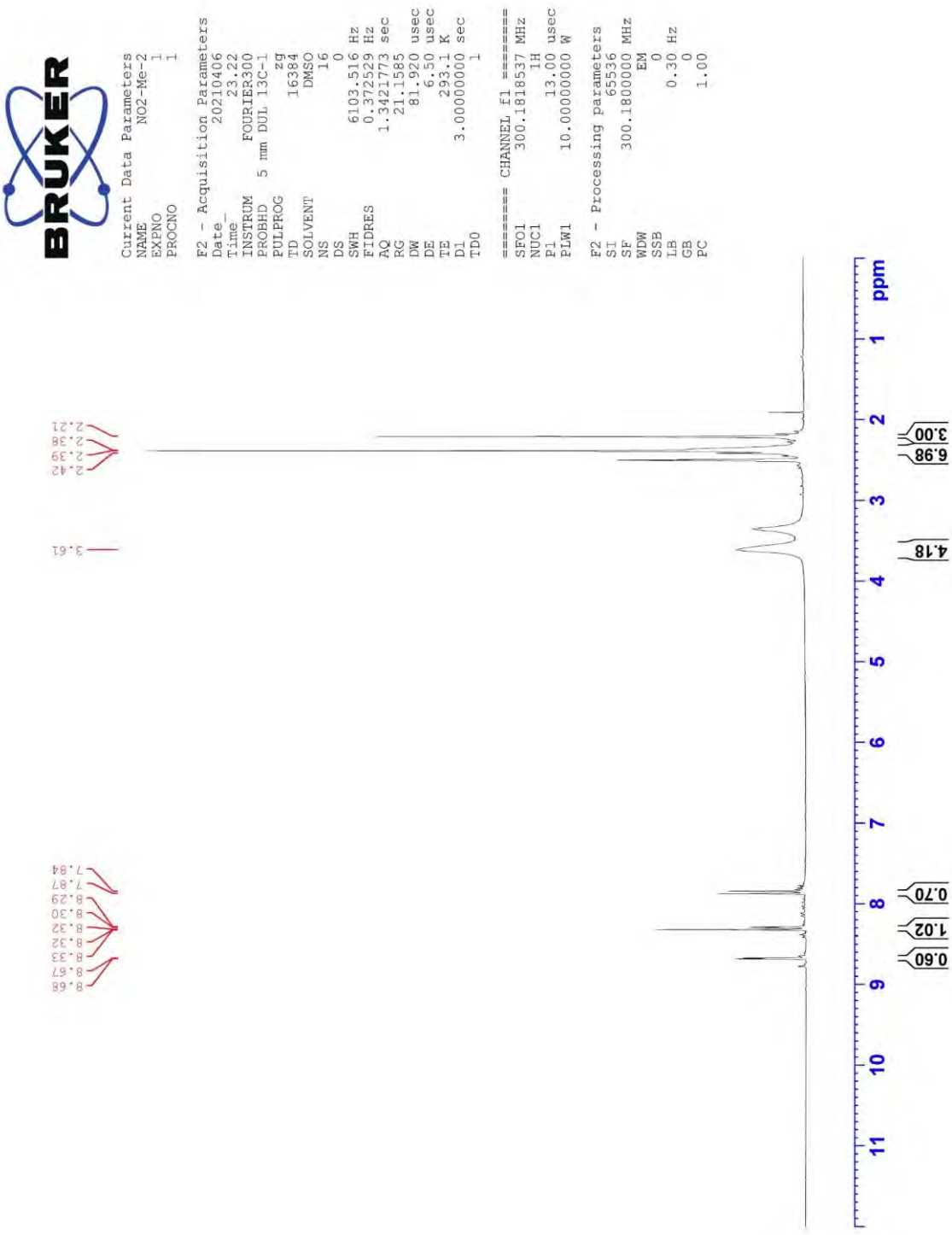


**Figure 5.117.** *$^{1}H$ NMR spectrum of compound **D23***

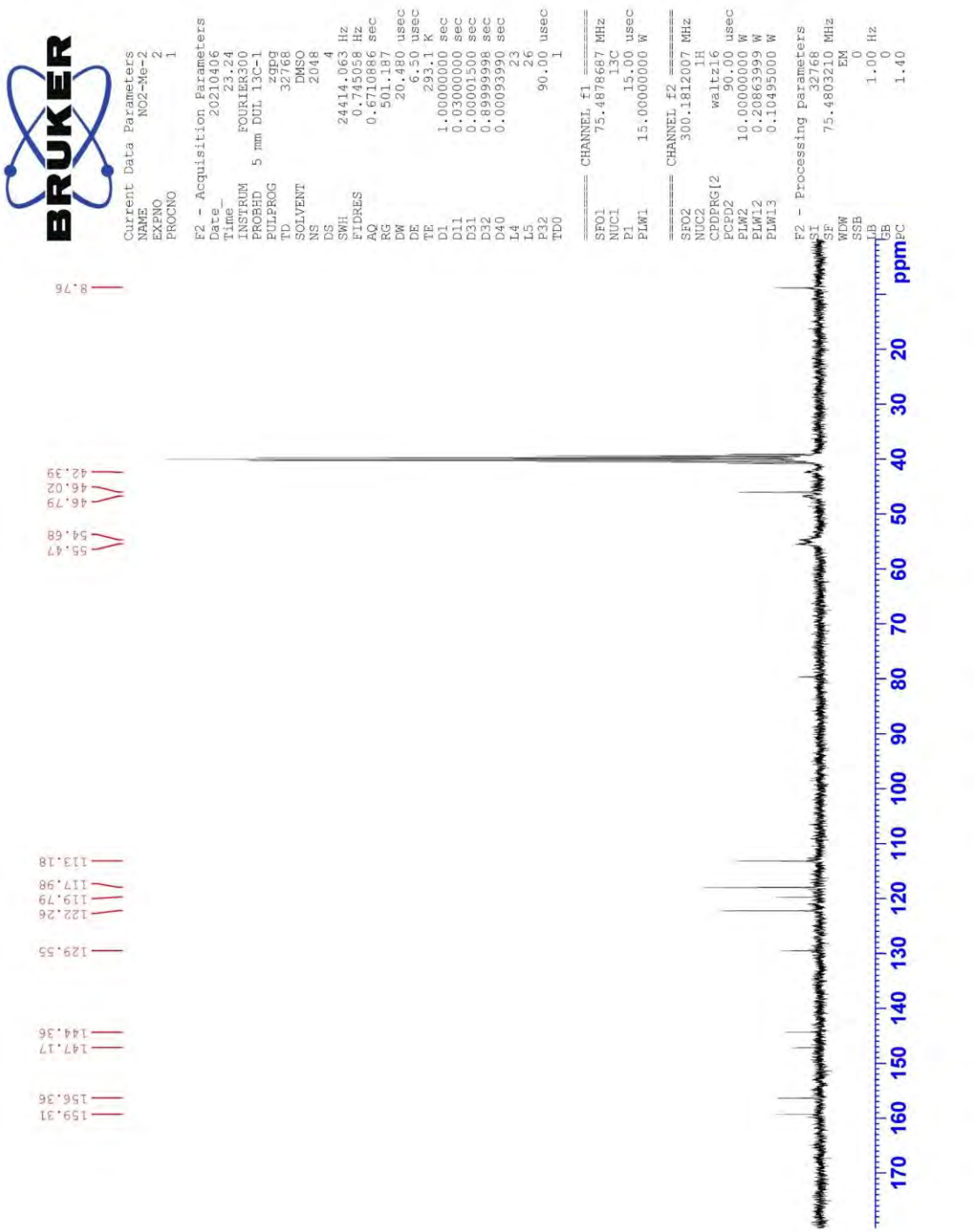


**Figure 5.118.** *$^{13}$C NMR spectrum of compound **D23***

| Elmt | Val. | Min | Max | Elmt | Val. | Min | Max | Elmt | Val. | Min | Max | Elmt | Val. | Min | Max | Use Adduct |
|---|---|---|---|---|---|---|---|---|---|---|---|---|---|---|---|---|
| H | 1 | 0 | 40 | O | 2 | 0 | 6 | S | 2 | 0 | 2 | Ru | 2 | 0 | 0 | H |
| C | 4 | 0 | 40 | F | 1 | 0 | 0 | Cl | 1 | 0 | 0 | Pd | 2 | 0 | 0 | |
| N | 3 | 0 | 7 | P | 3 | 0 | 0 | Br | 1 | 0 | 0 | I | 3 | 0 | 0 | |

Error Margin (ppm): 5
HC Ratio: unlimited
Max Isotopes: 3
MSn Iso RI (%): 10.00

DBE Range: 5.0 - 25.0
Apply N Rule: yes
Isotope RI (%): 1.00
MSn Logic Mode: AND

Electron Ions: both
Use MSn Info: yes
Isotope Res: 9000
Max Results: 150

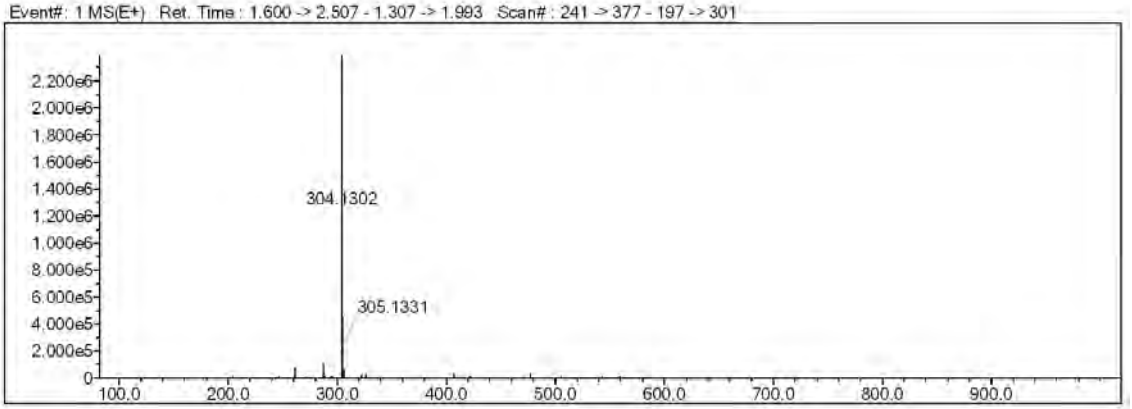


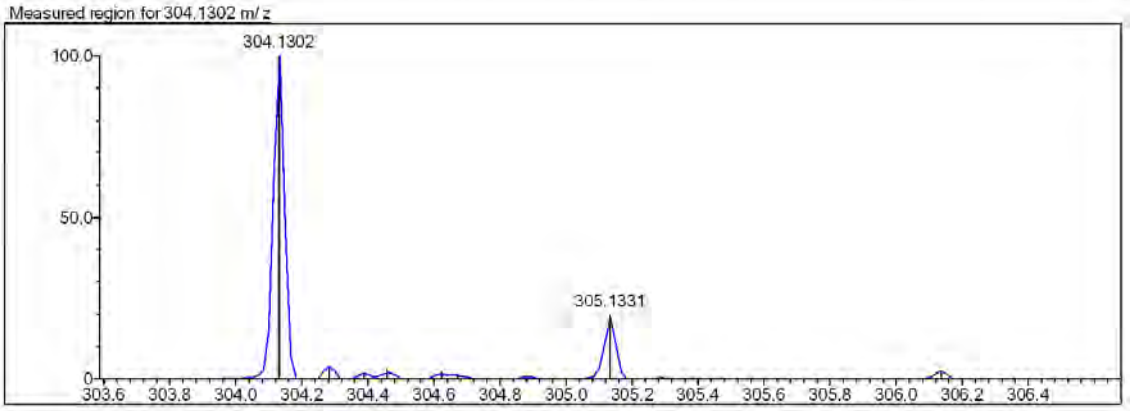


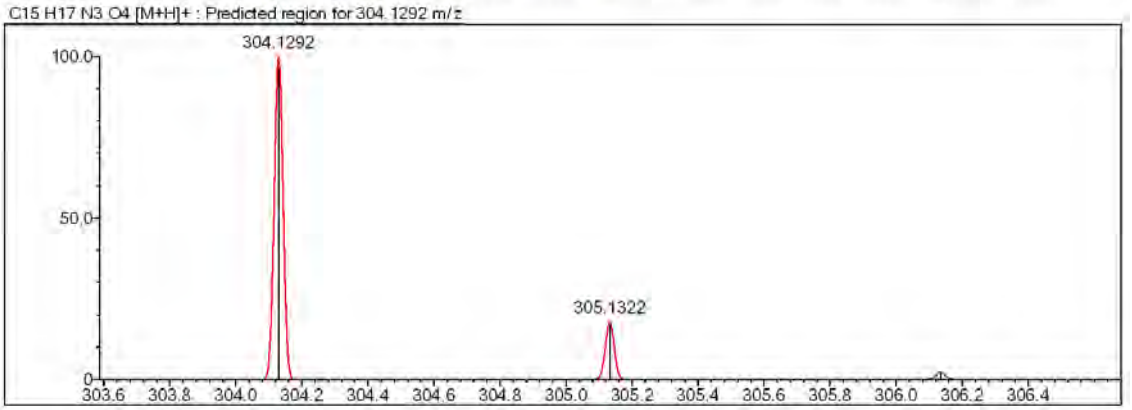


| Rank | Score | Formula (M) | Ion | Meas. m/z | Pred. m/z | Df. (mDa) | Df. (ppm) | Iso | DBE |
|---|---|---|---|---|---|---|---|---|---|
| 2 | 80.45 | C15 H17 N3 O4 | [M+H]+ | 304.1302 | 304.1292 | 1.0 | 3.29 | 85.34 | 9.0 |

**Figure 5.119.** *High-resolution mass spectrum of compound* ***D23***

DOPNALAB

| | Item | Value |
|---|---|---|
| | Acquired Date&Time | 27.05.2021 17:09:51 |
| | Acquired by | System Administrator |
| | Filename | C:\Users\dopnalab\Desktop\sa\231.ispd |
| | Spectrum name | 231 |
| | Sample name | 23 |
| | Sample ID | |
| | Option | |
| | Comment | |
| | No. of Scans | 15 |
| | Resolution | 4 [cm-1] |
| | Apodization | Happ-Genzel |

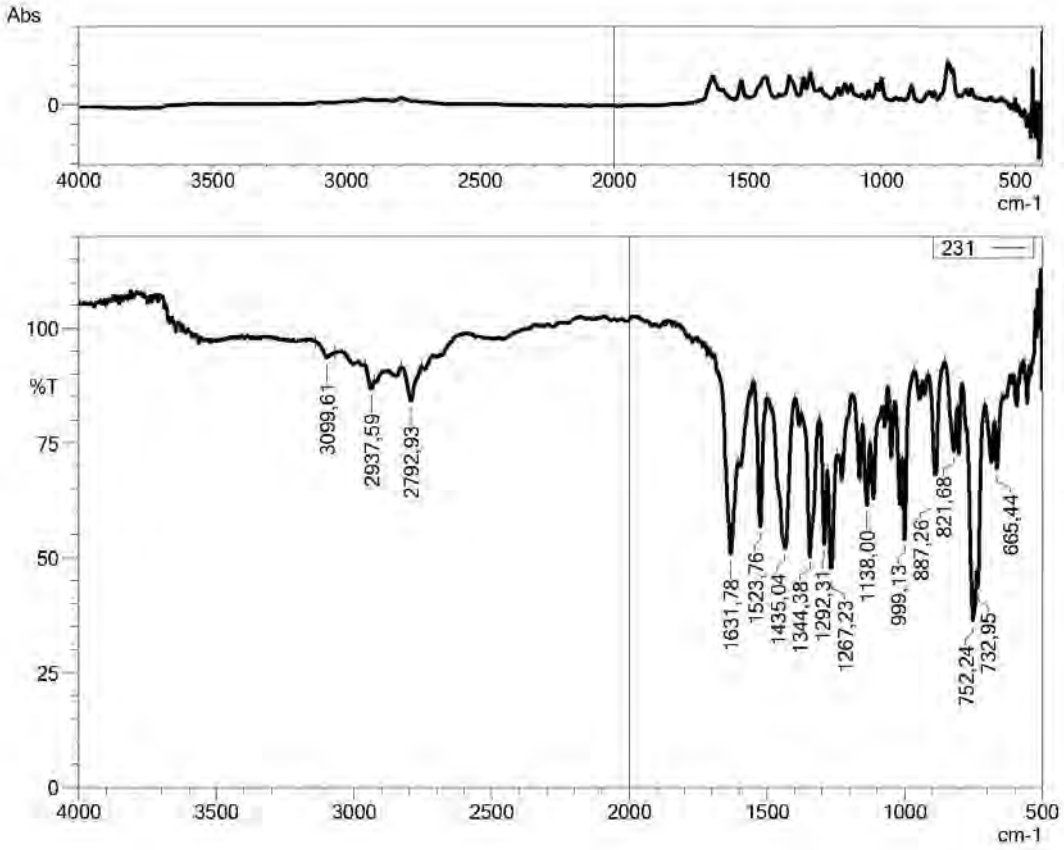


**Figure 5.120.** *IR spectrum of compound **D23***

### 5.1.4.24. *(4-ethylpiperazin-1-yl)(3-methyl-5-nitrobenzofuran-2-yl)methanone (D24)*

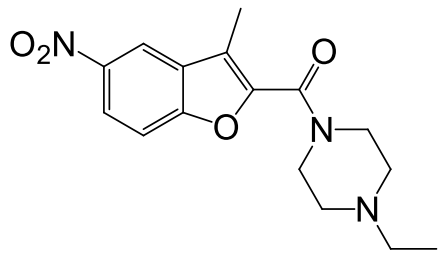


**Figure 5.121.** *Molecular structure of compound **D24***

**Physical Properties: Texture:** solid crystals, **Color:** brown, **M.P.:** 86-88ºC**, Yield:** 36%.

**IR (ATR) $\upsilon_{max}$ ($cm^{-1}$):** 3098 ($SP^2$ C-H stretching, aromatic), 2972-2769 ($SP^3$ C-H stretching, methylenes of piperazine, ethyl-methyl piperazine, and 3-methylbenzofuran), 1631 (C=O stretching, amide), 1523 (N-O asymmetric stretching, nitro group), 1436 (C=C stretching, aromatic), 1344 (N-O symmetric stretching, nitro group), 1259 (C-O stretching, ether), 1161-1114, 1010 (C-N stretching, tertiary amine and/or C-O stretching, ether), 885-732 (C-H aromatic out-of-plane bending).

**$^1$H NMR (300 MHz) (DMSO-$d_6$) $\delta$ (ppm):** 1.01 (t, *J*= 7.16 Hz, 3H, piperazine-$CH_2$-**$CH_3$**), 2.33-2.42 (m, 9H, **3-methyl**benzofuran, piperazine-**$CH_2$**-$CH_3$ and piperazine-3, 5), 3.62 (brs, 4H, piperazine-2, 6), 7.86 (d, *J*= 9.03 Hz, 1H, benzofuran-7), 8.31 (dd, J= 9.08, 2.26 Hz, 1H, benzofuran-6), 8.68 (d, *J*= 2.29 Hz, 1H, benzofuran-4).

**$^{13}$C NMR (300 MHz) (DMSO-$d_6$) $\delta$ (ppm):** 8.80 (**3-methyl**benzofuran), 12.34 (piperazine-$CH_2$-**$CH_3$**), 42.45 (piperazine), 46.89 (piperazine), 51.86 (piperazine-**$CH_2$**-$CH_3$), 52.40 (piperazine), 113.16, 117.98, 119.78, 122.26, 129.55, 144.36, 147.18, 156.35, 159.25 (benzofuran-**CO**-piperazine).

**HRMS (ESI) (m/z) $[M+1]^+$:** for $C_{16}H_{19}N_3O_4$ calculated: 318.1448; found: 318.1453.

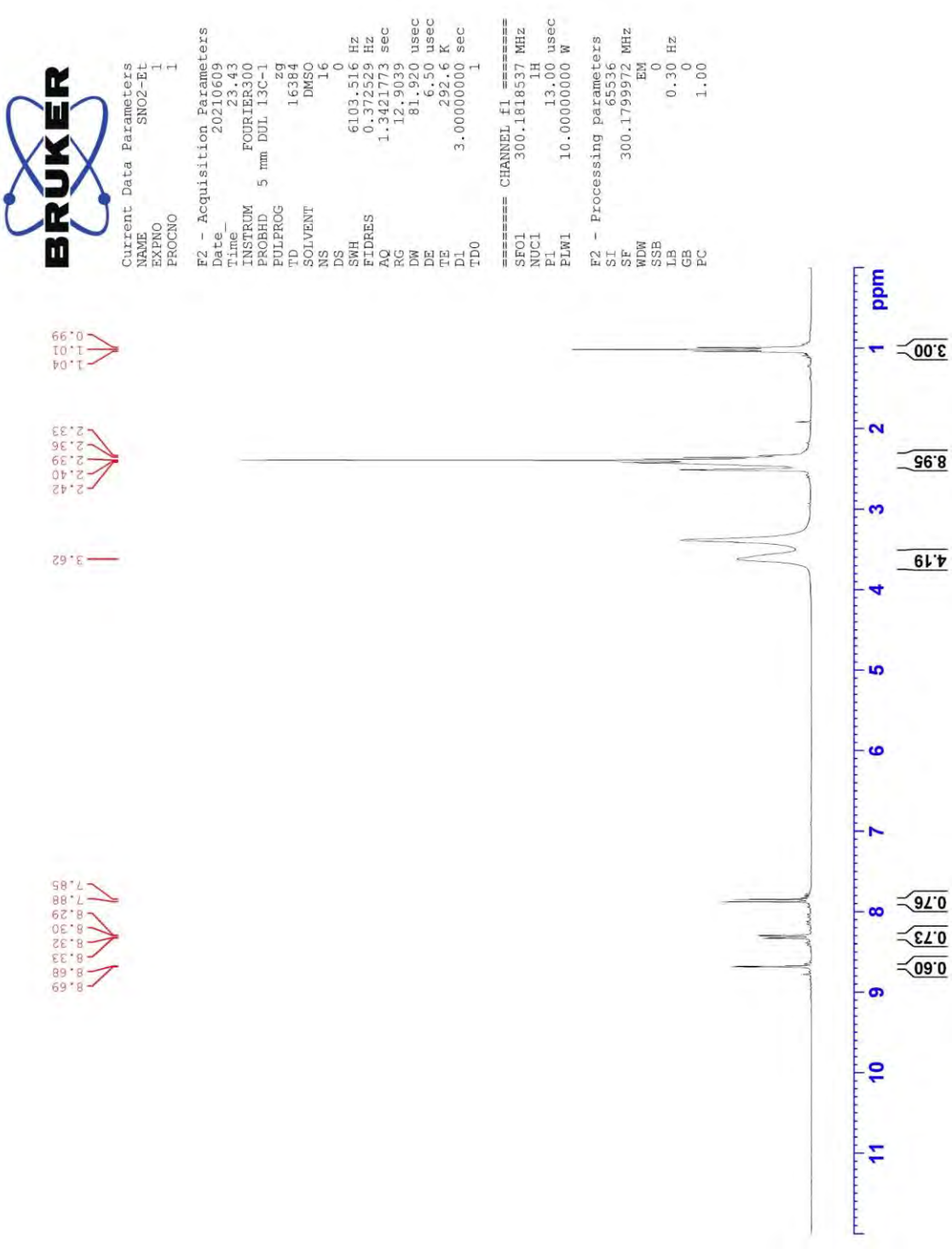


**Figure 5.122.** *$^{1}H$ NMR spectrum of compound **D24***

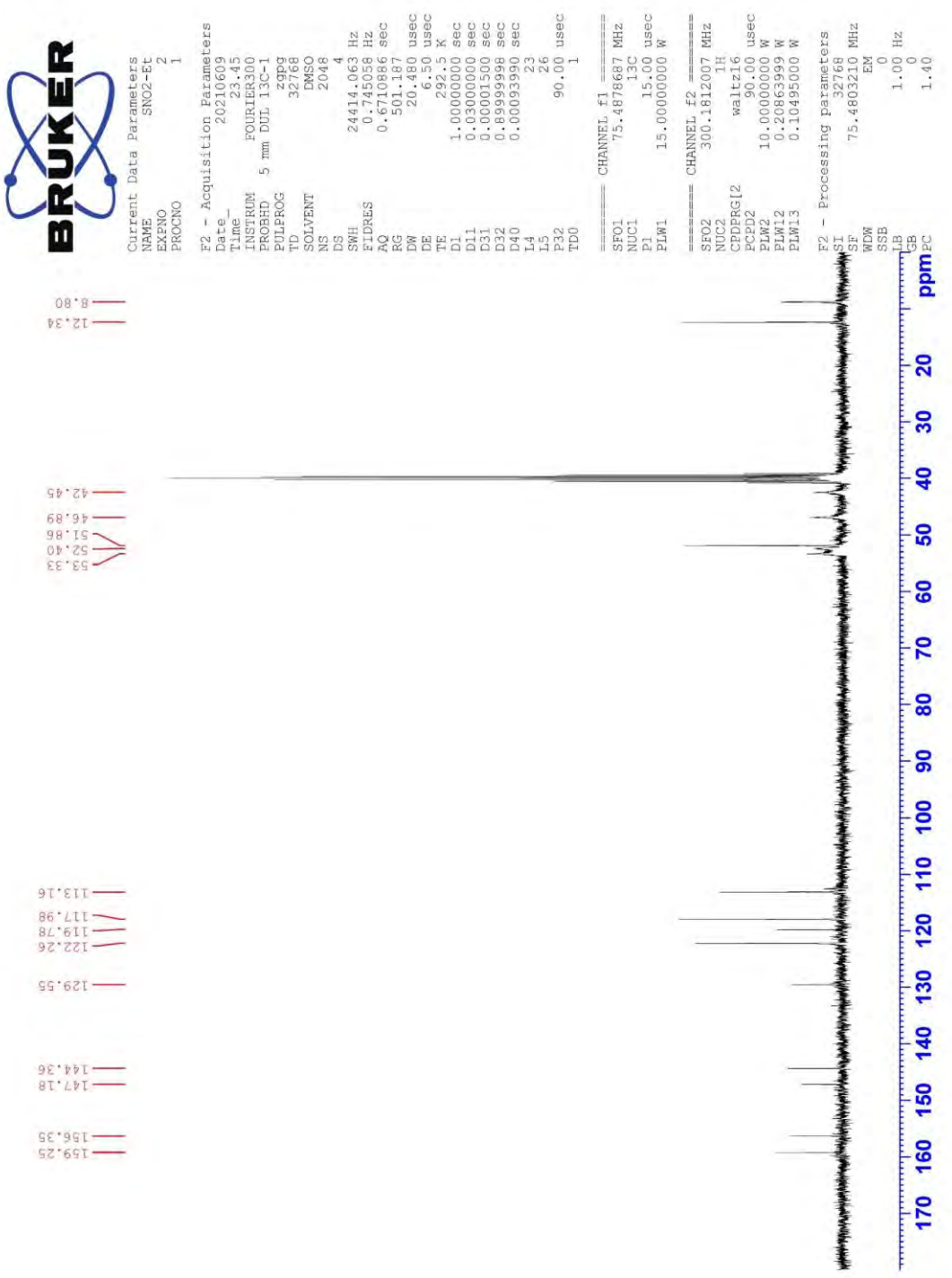


**Figure 5.123.** *$^{13}$C NMR spectrum of compound **D24***

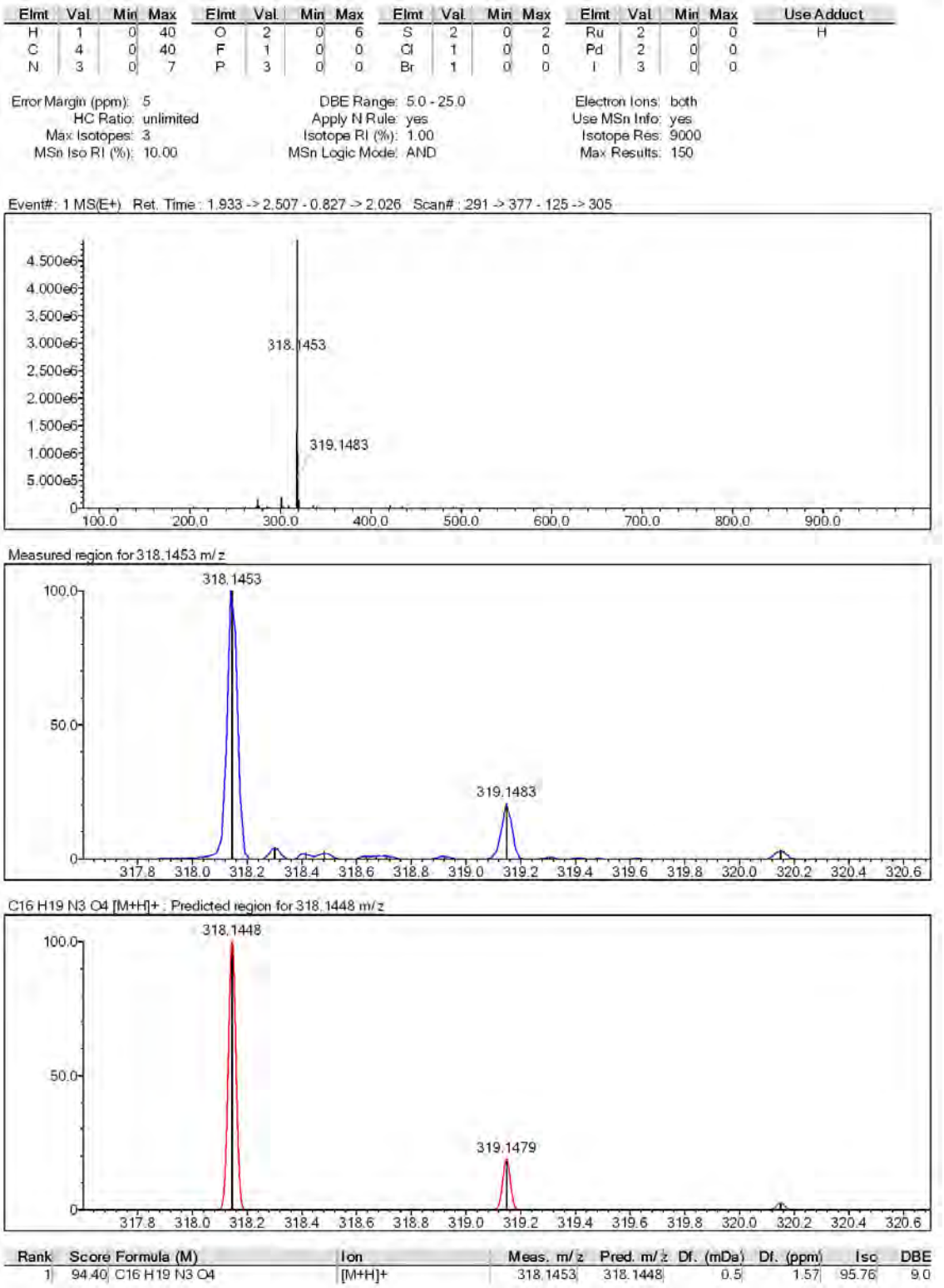


**Figure 5.124.** *High-resolution mass spectrum of compound* ***D24***

DOPNALAB

| | Item | Value |
|---|---|---|
| | Acquired Date&Time | 27.05.2021 17:16:09 |
| | Acquired by | System Administrator |
| | Filename | C:\Users\dopnalab\Desktop\sa\241.ispd |
| | Spectrum name | 241 |
| | Sample name | 24 |
| | Sample ID | |
| | Option | |
| | Comment | |
| | No. of Scans | 15 |
| | Resolution | 4 [cm-1] |
| | Apodization | Happ-Genzel |

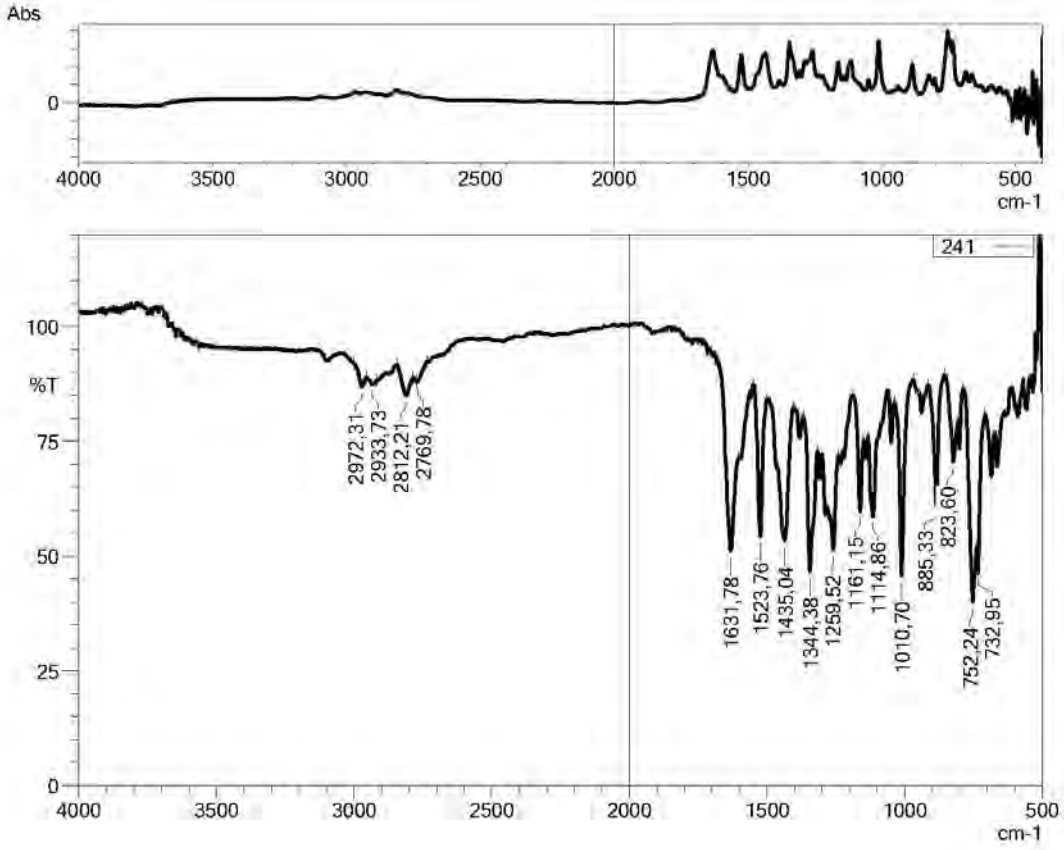


**Figure 5.125.** *IR spectrum of compound **D24***

### 5.1.4.25. *(4-(2-(dimethylamino)ethyl)piperazin-1-yl)(3-methyl-5-nitrobenzofuran-2-yl)methanone (D25)*

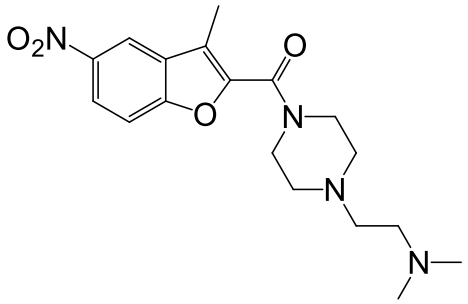

**Figure 5.126.** *Molecular structure of compound* ***D25***

**Physical Properties: Texture:** liquid, **Colour:** dark-brown, **Yield:** 47%.

**IR (ATR) $\upsilon_{max}$ ($cm^{-1}$):** 3095 ($SP^2$ C-H stretching, aromatic), 2941-2769 ($SP^3$ C-H stretching, methylenes of piperazine, dimethylaminoethyl-piperazine, and 3-benzofuran), 1678 (C=O stretching, amide), 1525 ((N-O asymmetric stretching, nitro group), 1436 (C=C stretching, aromatic), 1344 (N-O symmetric stretching, nitro group), 1244 (C-O stretching, ether), 1132, 999 (C-N stretching, tertiary amine and/or C-O stretching, ether), 889-684 (C-H aromatic out-of-plane bending).

**$^1$H NMR (300 MHz) (DMSO-$d_6$) $\delta$ (ppm):** 2.13 (s, 6H, -N(**$CH_3$**)$_2$), 2.30-2.46 (m, 11H, **3-methyl**benzofuran, piperazine-3, 5 and piperazine-(**$CH_2$**)$_2$-N), 3.59 (brs, 4H, piperazine-2, 6), 7.44 (d, *J*= 9.08 Hz, 1H, benzofuran-7), 8.30 (dd, *J*= 9.09, 2.42 Hz, 1H, benzofuran-6), 8.68 (d, *J*= 2.34 Hz, 1H, benzofuran-4).

**$^{13}$C NMR (300 MHz) (DMSO-$d_6$) $\delta$ (ppm):** 8.79 (**3-methyl**benzofuran), 42.39 (piperazine), 45.99 (-N(**$CH_3$**)$_2$), 46.86 (piperazine), 53.26 (piperazine), 55.97 (piperazine-(**$CH_2$**)$_2$-N), 57.02 (piperazine-(**$CH_2$**)$_2$-N), 113.16, 117.96, 119.77, 122.25, 129.56, 144.38, 147.19, 156.35, 159.24 (benzofuran-**CO**-piperazine).

**HRMS (ESI) (m/z) $[M+1]^+$:** for $C_{18}H_{24}N_4O_4$ calculated: 361.1870; found: 361.1887.

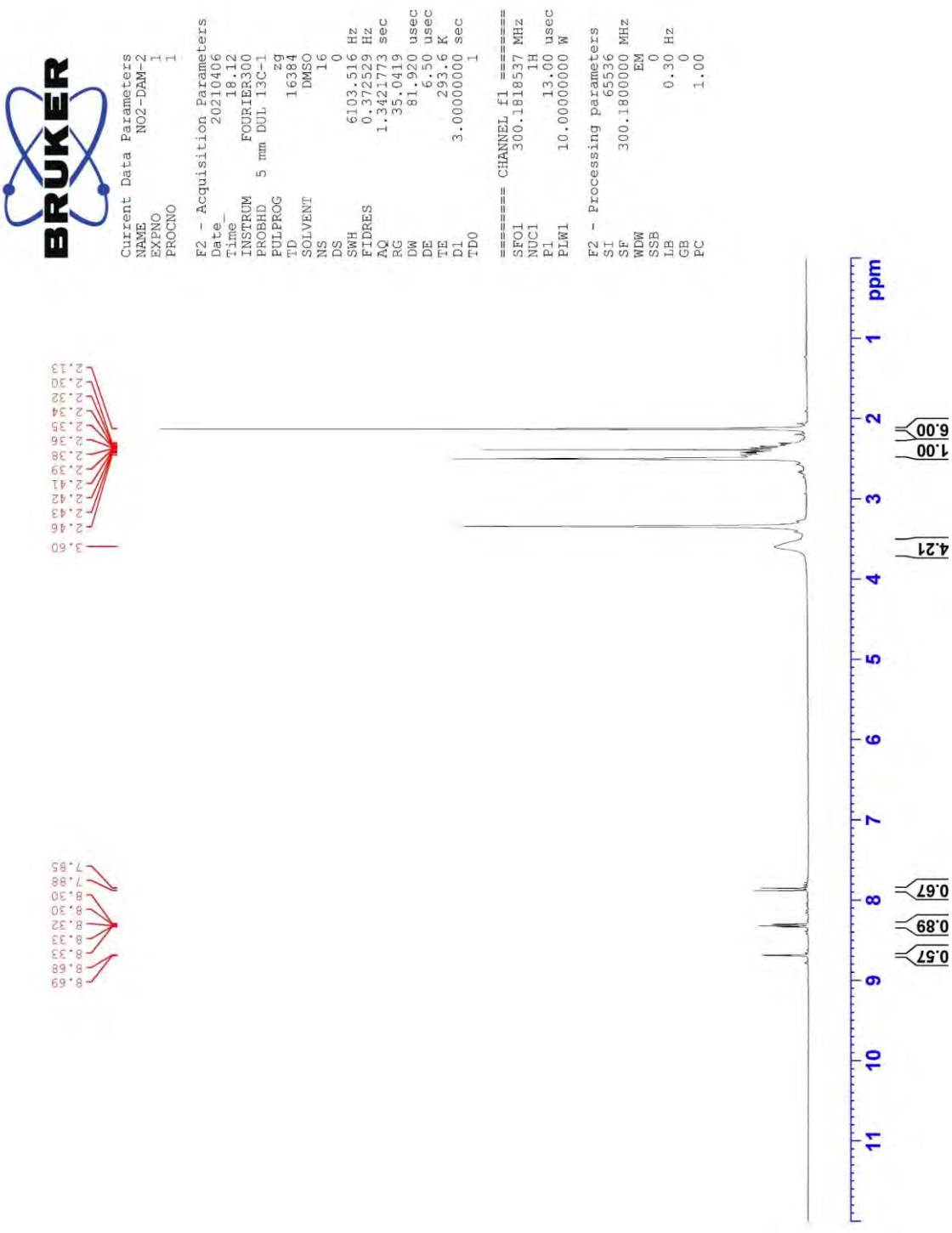


**Figure 5.127.** *$^{1}H$ NMR spectrum of compound **D25***

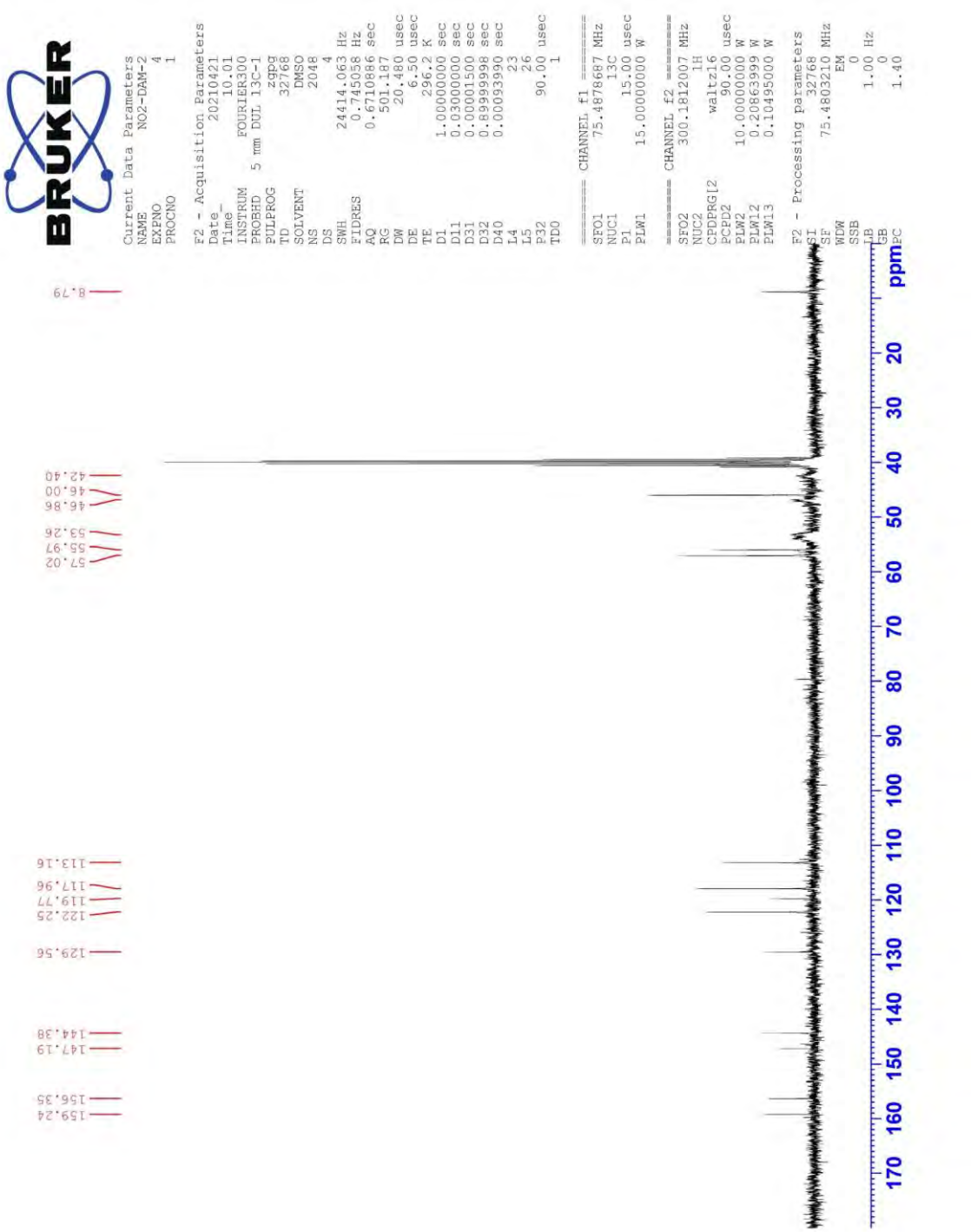


**Figure 5.128.** *$^{13}$C NMR spectrum of compound **D25***

| Elmt | Val. | Min | Max | Elmt | Val. | Min | Max | Elmt | Val. | Min | Max | Elmt | Val. | Min | Max | Use Adduct |
|---|---|---|---|---|---|---|---|---|---|---|---|---|---|---|---|---|
| H | 1 | 10 | 40 | O | 2 | 0 | 7 | S | 2 | 0 | 2 | Ru | 2 | 0 | 0 | H |
| C | 4 | 10 | 40 | F | 1 | 0 | 0 | Cl | 1 | 0 | 2 | Pd | 2 | 0 | 0 | |
| N | 3 | 2 | 6 | P | 3 | 0 | 0 | Br | 1 | 0 | 0 | I | 3 | 0 | 0 | |

Error Margin (ppm): 5
HC Ratio: unlimited
Max Isotopes: 3
MSn Iso RI (%): 10.00

DBE Range: 5.0 - 25.0
Apply N Rule: yes
Isotope RI (%): 1.00
MSn Logic Mode: AND

Electron Ions: both
Use MSn Info: yes
Isotope Res: 9000
Max Results: 150

Event#: 1 MS(E+) Ret. Time: 3.093 -> 3.507 - 2.040 -> 2.984 Scan#: 465 -> 527 - 307 -> 449

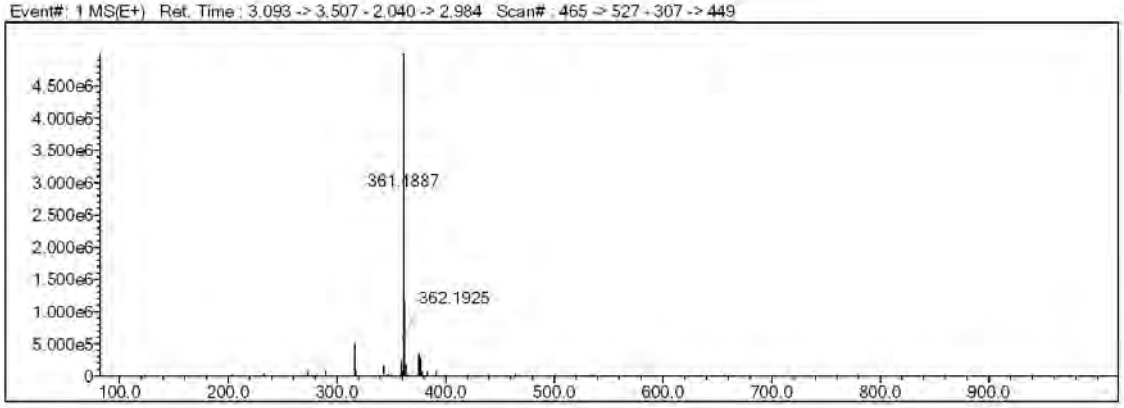


Measured region for 361.1887 m/z

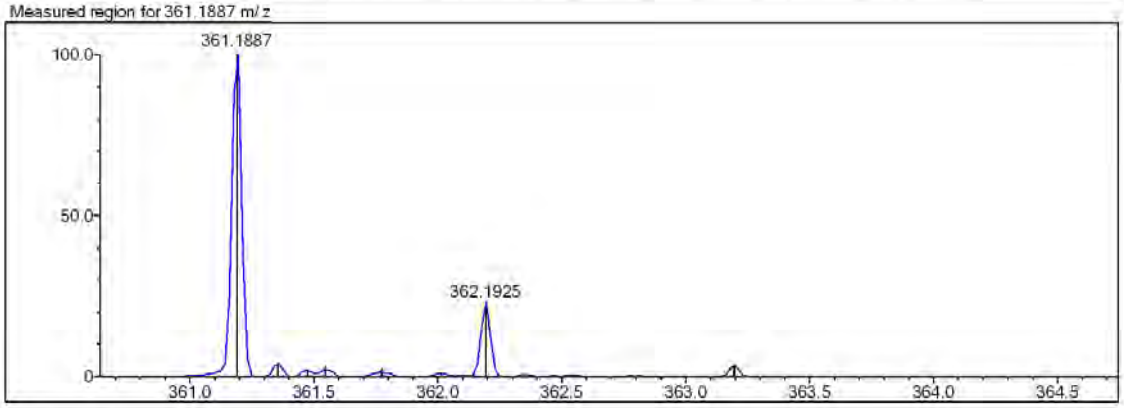


C18 H24 N4 O4 [M+H]+ : Predicted region for 361.1870 m/z

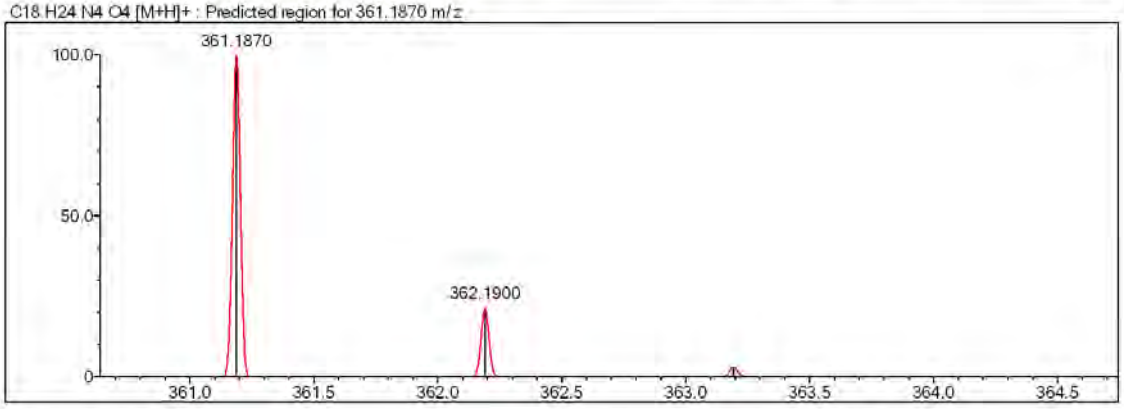


| Rank | Score | Formula (M) | Ion | Meas. m/z | Pred. m/z | Df. (mDa) | Df. (ppm) | Isc | DBE |
|---|---|---|---|---|---|---|---|---|---|
| 1 | 83.36 | C18 H24 N4 O4 | [M+H]+ | 361.1887 | 361.1870 | 1.7 | 4.71 | 91.88 | 9.0 |

**Figure 5.129.** *High-resolution mass spectrum of compound* ***D25***

DOPNALAB

| | Item | Value |
|---|---|---|
| | Acquired Date&Time | 27.05.2021 17:21:55 |
| | Acquired by | System Administrator |
| | Filename | C:\Users\dopnalab\Desktop\sa\251.ispd |
| | Spectrum name | 251 |
| | Sample name | 25 |
| | Sample ID | |
| | Option | |
| | Comment | |
| | No. of Scans | 16 |
| | Resolution | 4 [cm-1] |
| | Apodization | Happ-Genzel |

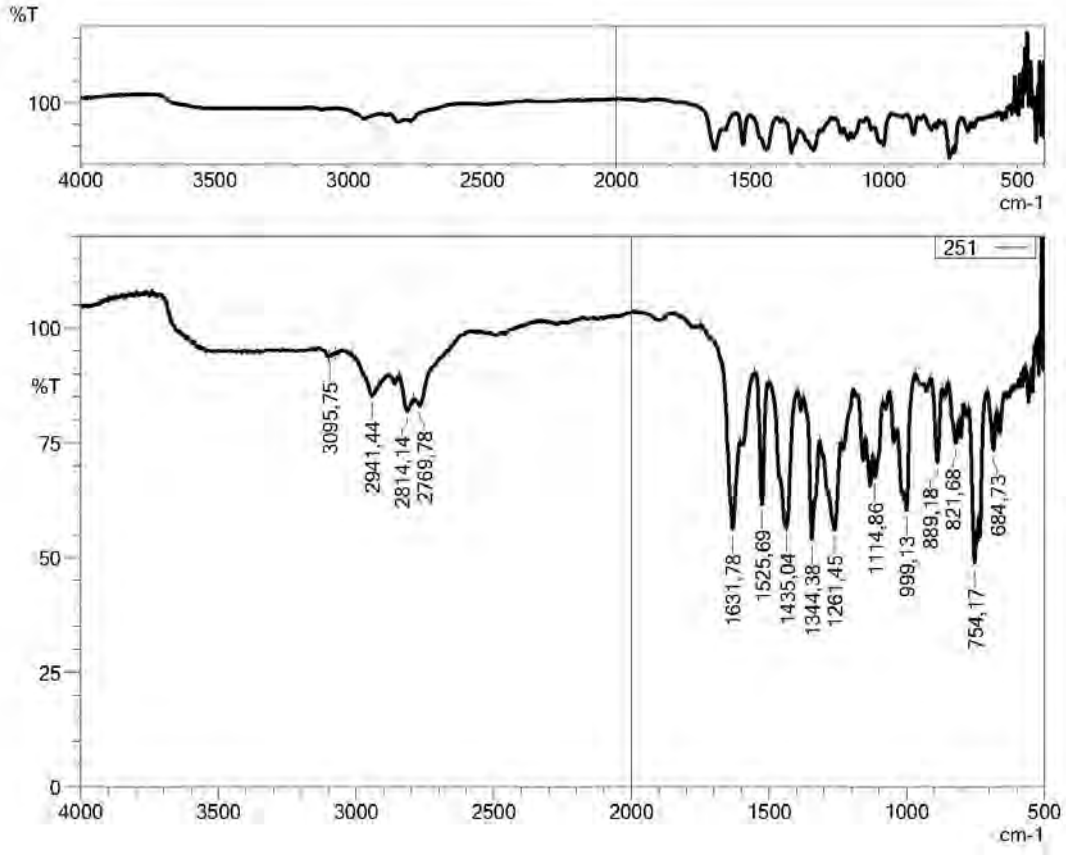


**Figure 5.130.** *IR spectrum of compound **D25***

### 5.1.4.26. *(5-nitrobenzofuran-2-yl)(4-phenylpiperazin-1-yl)methanone (D26)*

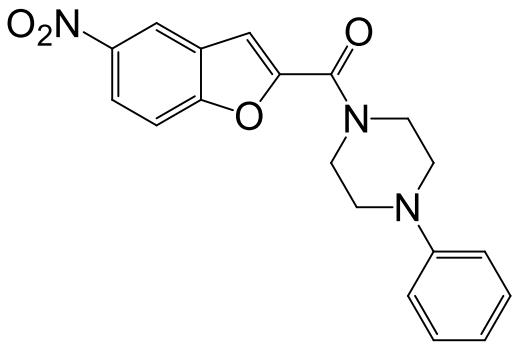


**Figure 5.131.** *Molecular structure of compound* ***D26***

**Physical Properties: Texture:** solid crystals, **Color:** brown, **M.P.:** 239-241ºC**, Yield:** 74%.

**IR (ATR) $\upsilon_{max}$ ($cm^{-1}$):** 3101 ($SP^2$ C-H stretching, aromatic), 2906-2814 ($SP^3$ C-H stretching, methylenes of piperazine), 1612 (C=O stretching, amide), 1566 (N-O asymmetric stretching, nitro group), 1442 (C=C stretching, aromatic), 1342 (N-O symmetric stretching, nitro group), 1267-1228 (C-O stretching, ether), 1153, 1018 (C-N stretching, tertiary amine and/or ether), 947-690 (C-H aromatic out-of-plane bending).

**$^1$H NMR (300 MHz) (DMSO-$d_6$) $\delta$ (ppm):** 3.27 (brs, 4H, piperazine- 3, 5), 3.88 (brs, 4H, piperazine-2, 6), 6.83 (t, *J*= 7.22 Hz, 1H, phenyl-4), 7.00 (d, *J*= 8.04, 2H, phenyl-2, 6), 7.25 (t, *J*= 7.84 Hz, 2H, phenyl-3,5), 7.62-7.66 (m, 1H, benzofuran-3), 7.84-7.97 (m, 1H, benzofuran-7), 8.32-8.45 (m, 1H, benzofuran-6), 8.73-8.93 (m, 1H, benzofuran-4).

**HRMS (ESI) (m/z) $[M+1]^+$:** for $C_{19}H_{17}N_3O_4$ calculated: 352.1292; found: 352.1307.

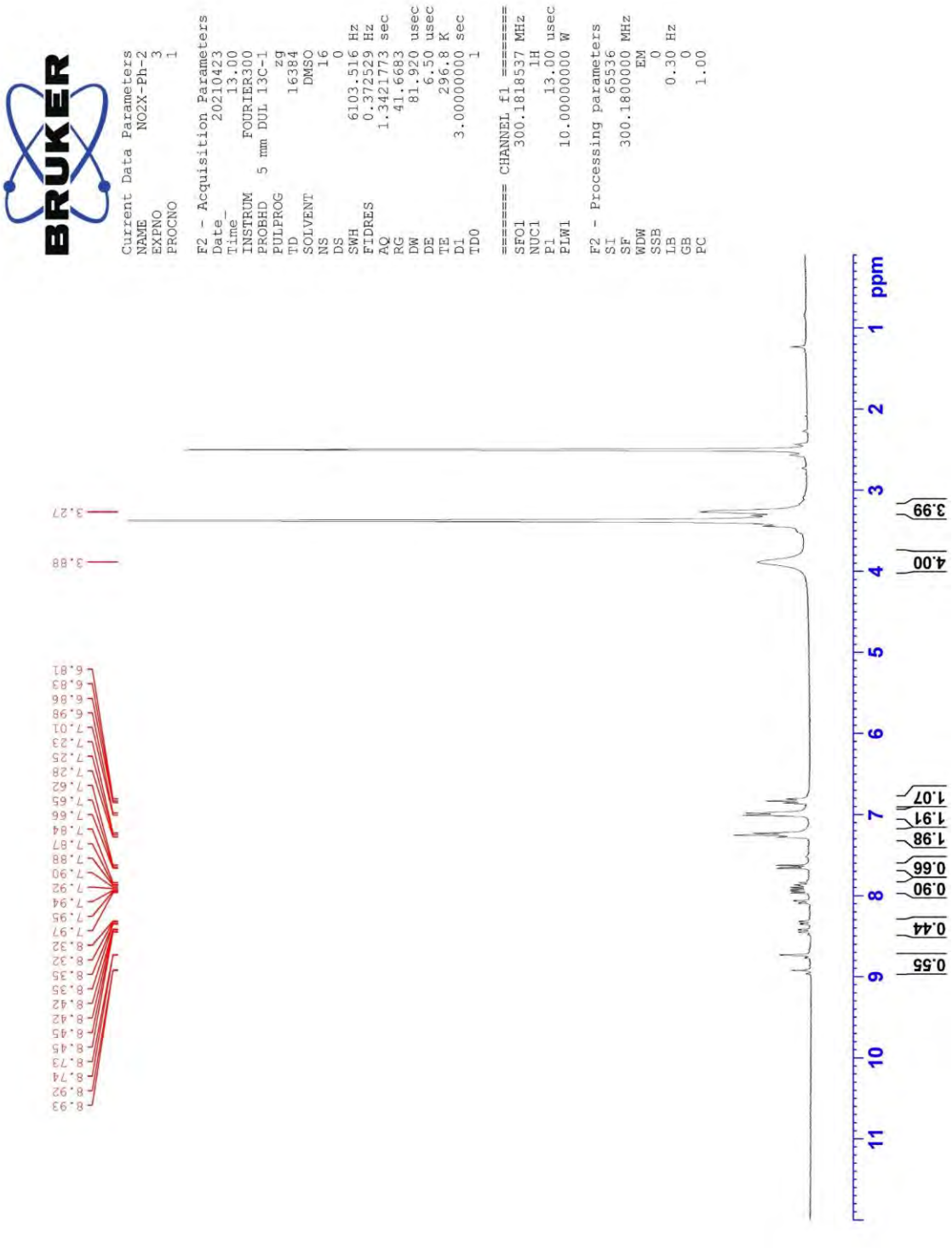


**Figure 5.132.** *[1]H NMR spectrum of compound **D26***

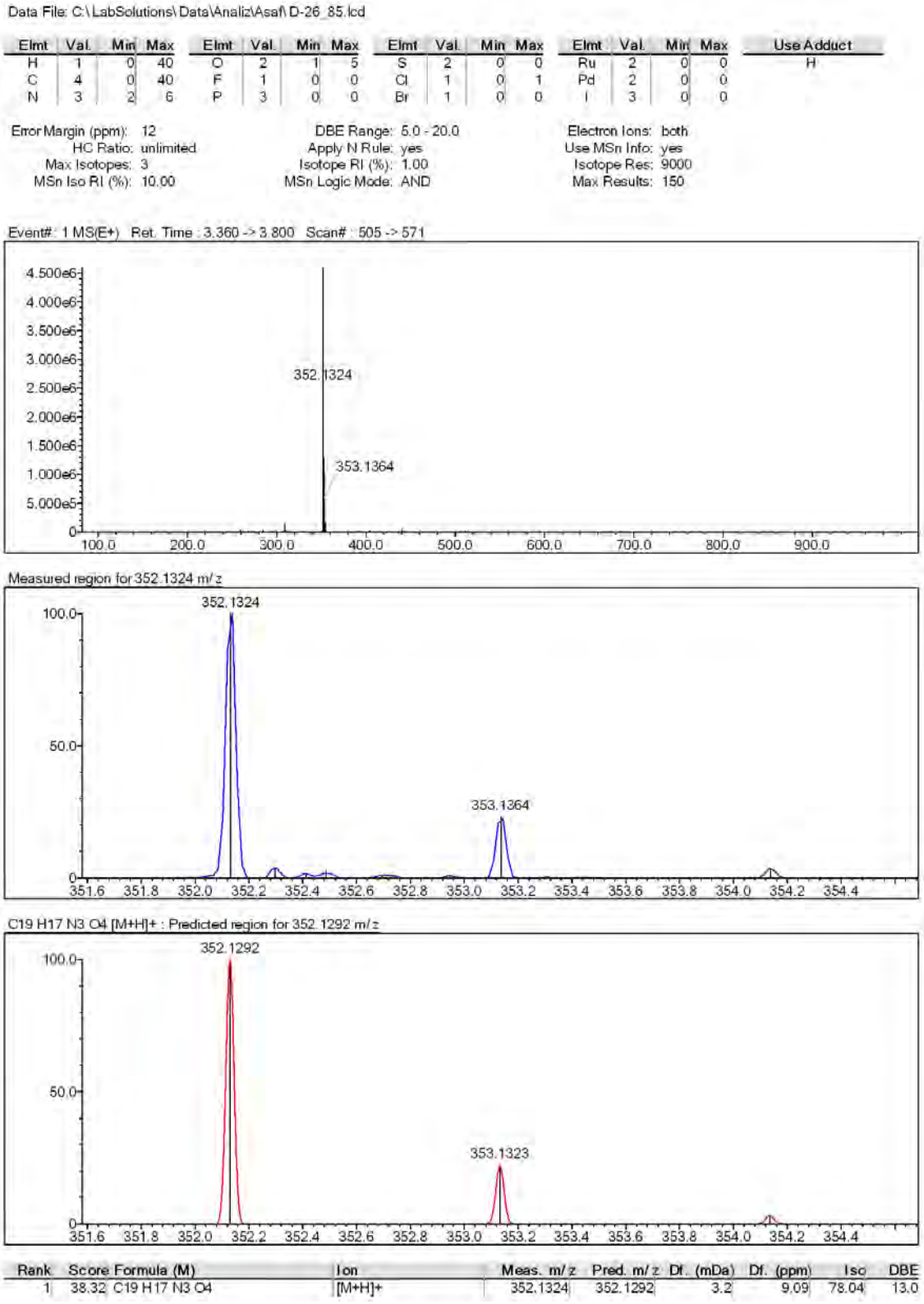


**Figure 5.133.** *High-resolution mass spectrum of compound* ***D26***

DOPNALAB

| | Item | Value |
|---|---|---|
| | Acquired Date&Time | 27.05.2021 17:27:11 |
| | Acquired by | System Administrator |
| | Filename | C:\Users\dopnalab\Desktop\sa\261.ispd |
| | Spectrum name | 261 |
| | Sample name | 26 |
| | Sample ID | |
| | Option | |
| | Comment | |
| | No. of Scans | 16 |
| | Resolution | 4 [cm-1] |
| | Apodization | Happ-Genzel |

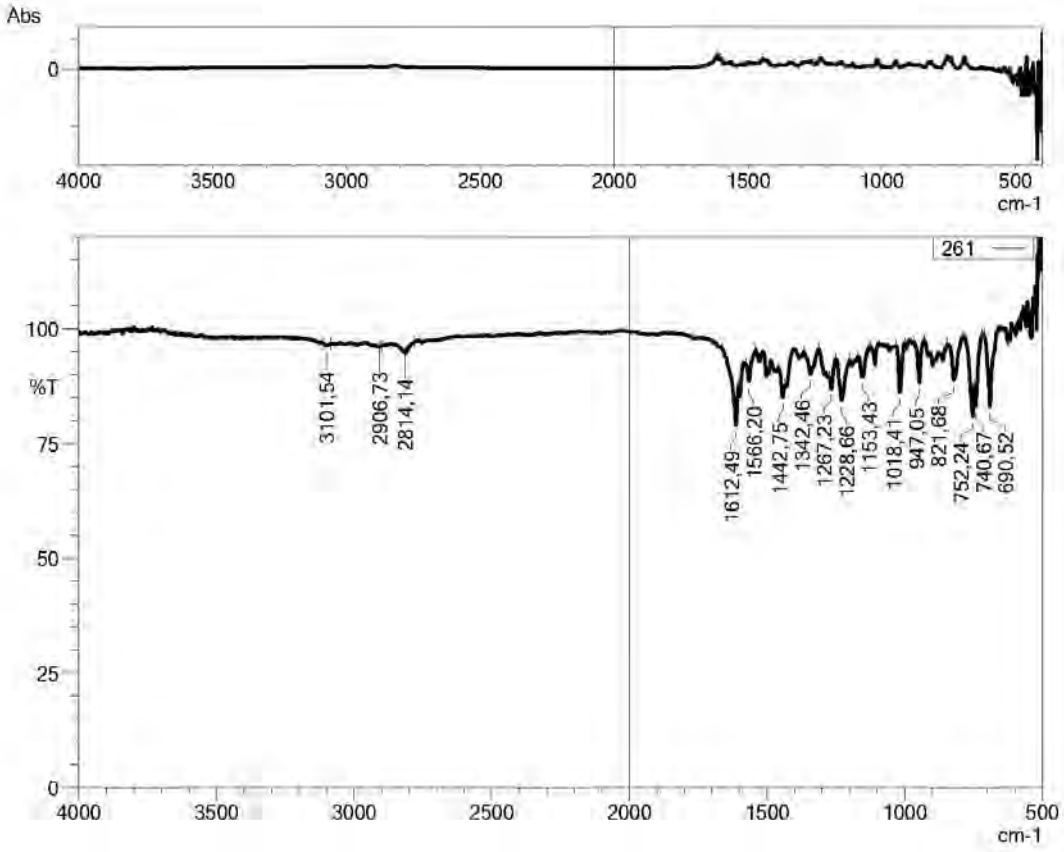


**Figure 5.134.** *IR spectrum of compound **D26***

### 5.1.4.27. *(4-(furan-2-carbonyl)piperazin-1-yl)(5-nitrobenzofuran-2-yl)methanone (D27)*

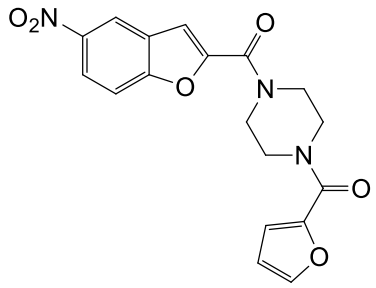

**Figure 5.135.** *Molecular structure of compound **D27***

**Physical Properties: Texture:** solid crystals, **Color:** brown, **M.P.:** 102-103ºC**, Yield:** 71%.

**IR (ATR) $\upsilon_{max}$ ($cm^{-1}$):** 3101 ($SP^2$ C-H stretching, aromatic), 1614 (C=O stretching, amide), 1566 (N-O asymmetric stretching, nitro group), 1427 (C=C stretching, aromatic), 1342 (N-O symmetric stretching, nitro group), 1261-1232 (C-O stretching, ether), 1176, 1014 (C-N stretching, tertiary amine and/or ether), 877-682 (C-H aromatic out-of-plane bending).

**$^1$H NMR (300 MHz) (DMSO-$d_6$) $\delta$ (ppm):** 3.81 (m, 8H, piperazine-2, 3, 5, 6), 6.65 (dd, *J*= 3.46, 1.75 Hz, 1H, furan-4), 7.06 (d, *J*= 3.41 Hz, 1H, furan-3), 7.65 (s, 1H, benzofuran-3), 7.88 (d, *J*= 0.99 Hz, 1H, furan-5), 7.93 (d, *J*= 9.15 Hz, 1H, benzofuran-7), 8.34 (dd, *J*= 9.12, 2.46 Hz, 1H, benzofuran-6), 8.73 (d, *J*= 2.36 Hz, 1H, benzofuran-4).

**$^{13}$C NMR (300 MHz) (DMSO-$d_6$) $\delta$ (ppm):** 42.75 (piperazine), 46.69 (piperazine), 111.89, 112.13, 113.43, 116.52, 119.62, 122.45, 127.81, 144.63, 145.46, 147.19, 151.23, 157.14, 158.74 (piperazine-**CO**-furan), 158.94 (benzofuran-**CO**-piperazine).

**HRMS (ESI) (m/z) $[M+1]^+$:** for $C_{18}H_{15}N_3O_6$ calculated: 370.1034; found: 370.1035.

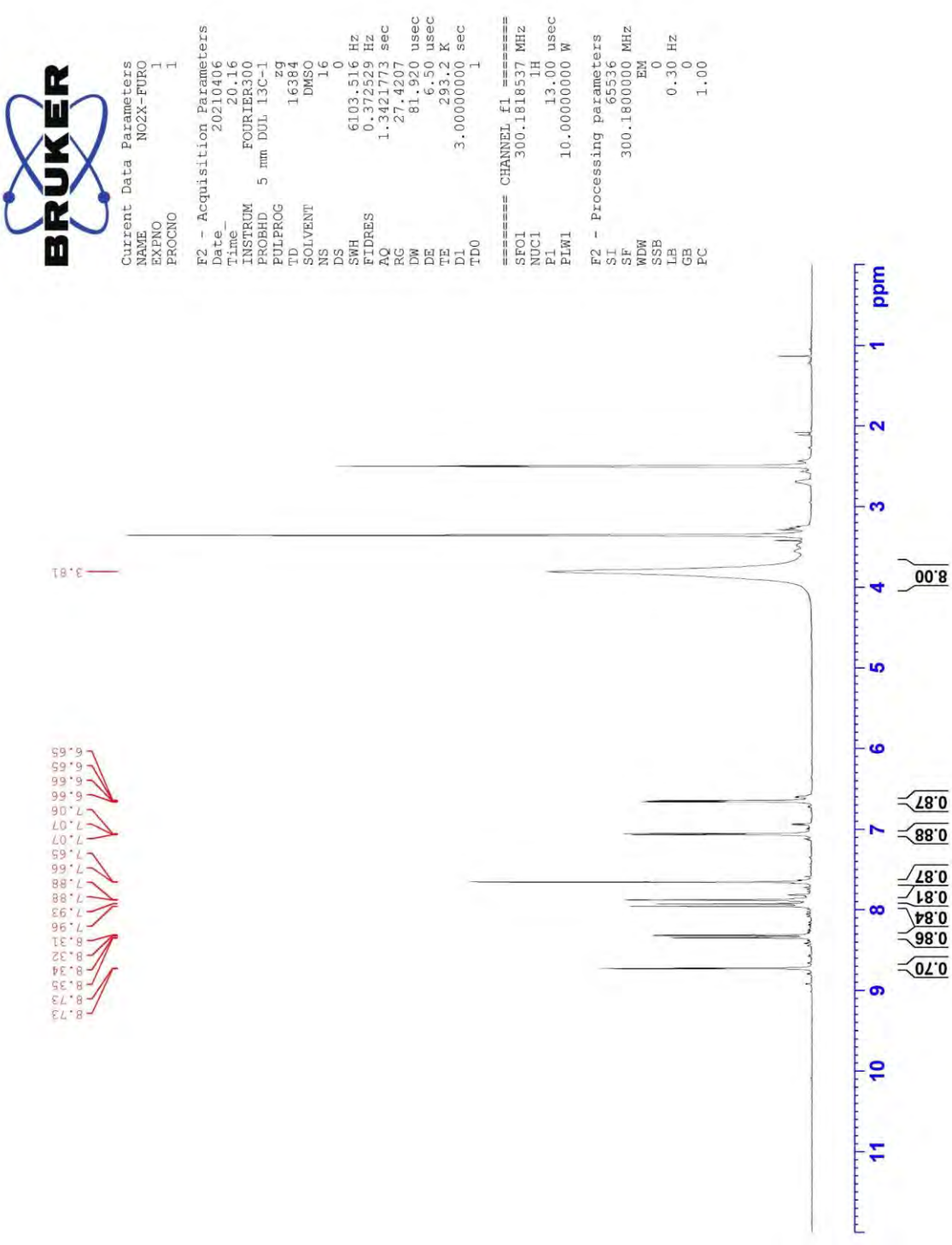


**Figure 5.136.** *[1]H NMR spectrum of compound **D27***

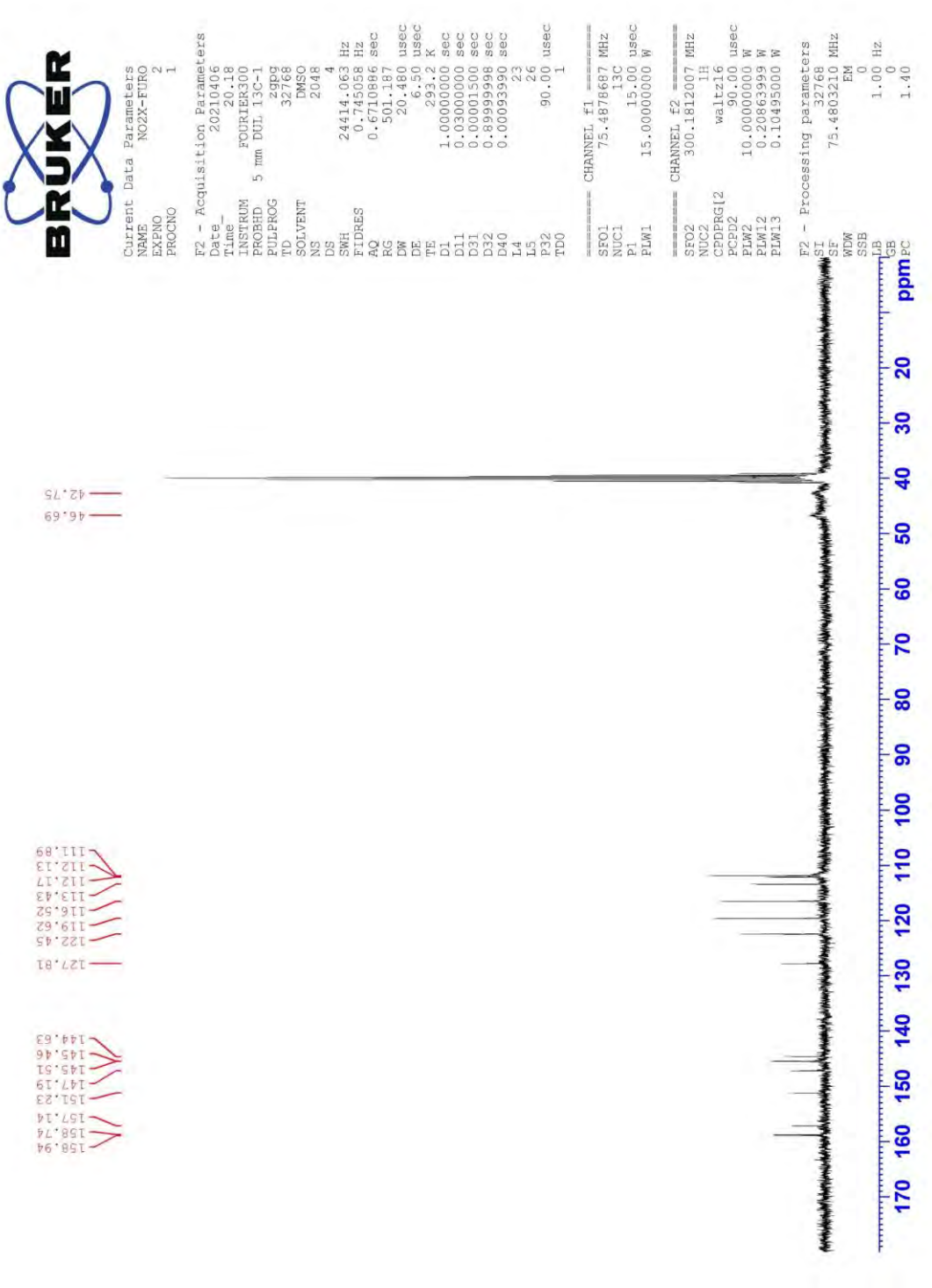


**Figure 5.137.** *$^{13}$C NMR spectrum of compound **D27***

| Elmt | Val. | Min | Max | Elmt | Val. | Min | Max | Elmt | Val. | Min | Max | Elmt | Val. | Min | Max | Use Adduct |
|---|---|---|---|---|---|---|---|---|---|---|---|---|---|---|---|---|
| H | 1 | 0 | 40 | O | 2 | 0 | 6 | S | 2 | 0 | 2 | Ru | 2 | 0 | 0 | H |
| C | 4 | 0 | 40 | F | 1 | 0 | 0 | Cl | 1 | 0 | 0 | Pd | 2 | 0 | 0 | |
| N | 3 | 0 | 7 | P | 3 | 0 | 0 | Br | 1 | 0 | 0 | I | 3 | 0 | 0 | |

Error Margin (ppm): 5
HC Ratio: unlimited
Max Isotopes: 3
MSn Iso RI (%): 10.00

DBE Range: 5.0 - 25.0
Apply N Rule: yes
Isotope RI (%): 1.00
MSn Logic Mode: AND

Electron Ions: both
Use MSn Info: yes
Isotope Res: 9000
Max Results: 150

Event#: 1 MS(E+) Ret. Time: 3.320 - 3.387 -> 4.959 Scan#: 499 - 509 -> 745

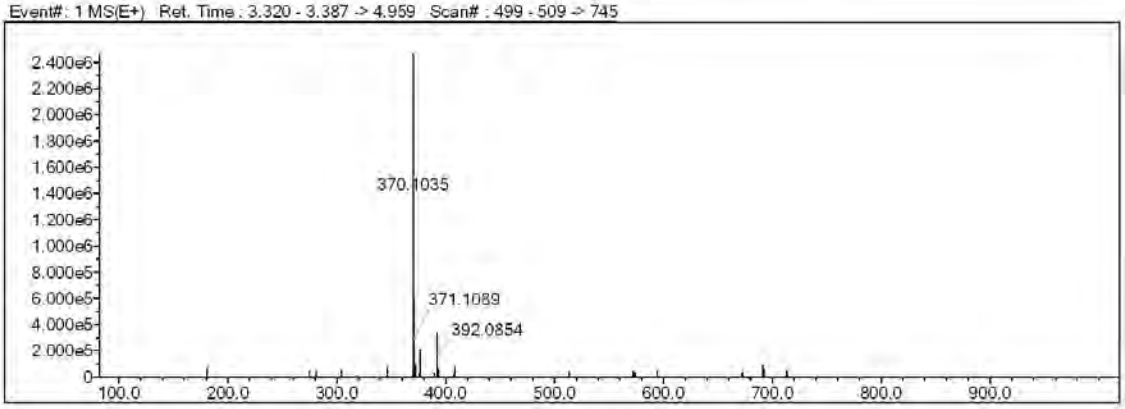


Measured region for 370.1035 m/z

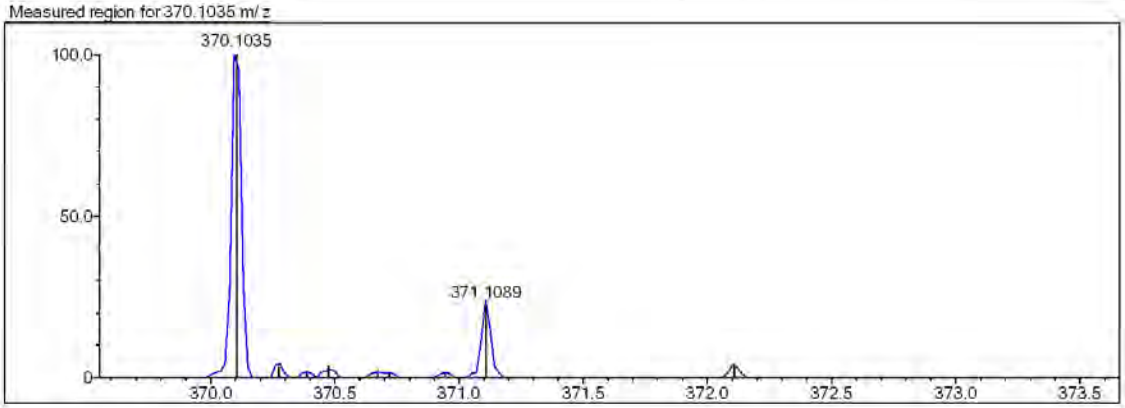


C18 H15 N3 O6 [M+H]+ : Predicted region for 370.1034 m/z

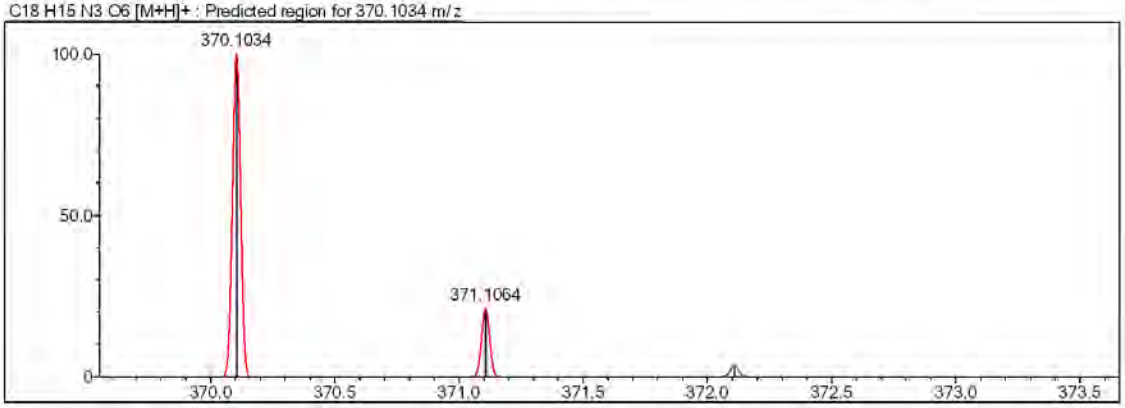


| Rank | Score | Formula (M) | Ion | Meas. m/z | Pred. m/z | Df. (mDa) | Df. (ppm) | Isc | DBE |
|---|---|---|---|---|---|---|---|---|---|
| 1 | 100.00 | C18 H15 N3 O6 | [M+H]+ | 370.1035 | 370.1034 | 0.1 | 0.27 | 100.00 | 13.0 |

**Figure 5.138.** *High-resolution mass spectrum of compound* ***D27***

DOPNALAB

| | Item | Value |
|---|---|---|
| | Acquired Date&Time | 27.05.2021 17:31:59 |
| | Acquired by | System Administrator |
| | Filename | C:\Users\dopnalab\Desktop\sa\271.ispd |
| | Spectrum name | 271 |
| | Sample name | 27 |
| | Sample ID | |
| | Option | |
| | Comment | |
| | No. of Scans | 16 |
| | Resolution | 4 [cm-1] |
| | Apodization | Happ-Genzel |

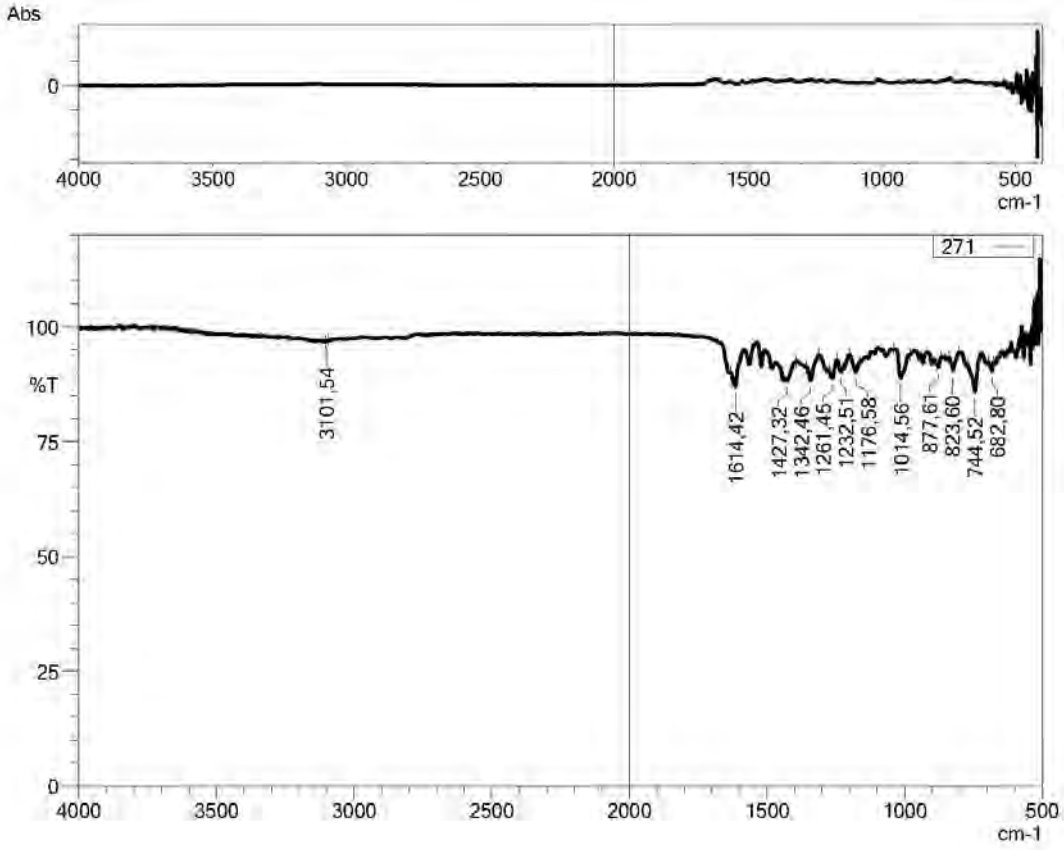


**Figure 5.139.** *IR spectrum of compound **D27***

### 5.1.4.28. *(4-methylpiperazin-1-yl)(5-nitrobenzofuran-2-yl)methanone (28)*

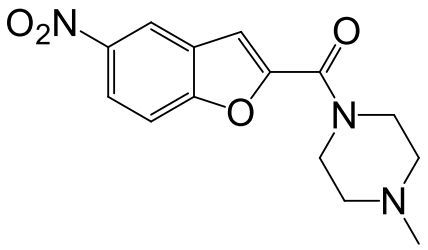


**Figure 5.140.** *Molecular structure of compound **D28***

**Physical Properties: Texture:** solid powder, **Color:** brown, **M.P.:** 136-138ºC**, Yield:** 43%.

**IR (ATR) $\upsilon_{max}$ ($cm^{-1}$):** 3101 ($SP^2$ C-H stretching, aromatic), 2931-2798 ($SP^3$ C-H stretching, 4-methyl piperazine, methylenes of piperazine, and 3-methylbenzofuran), 1631 (C=O stretching, amide), 1521 (N-O asymmetric stretching, nitro group), 1438 (C=C stretching, aromatic), 1342 (N-O symmetric stretching, nitro group), 1288-1265 (C-O stretching, ether), 1143, 1022-999 (C-N stretching, tertiary amine and/or ether), 898-684 (C-H aromatic out-of-plane bending).

**$^1$H NMR (300 MHz) (DMSO-$d_6$) $\delta$ (ppm):** 2.21 (s, 3H, **4-methyl**piperazine), 2.38 (t, *J*= 4.99, 4H, piperazine-3, 5), 3.69 (brs, 4H, piperazine-2, 6), 7.58 (s, 1H, benzofuran-3), 7.92 (d, *J*= 9.13 Hz, 1H, benzofuran-7), 8.32 (dd, *J*= 9.13, 2.46 Hz, 1H, benzofuran-6), 8.70 (d, *J*= 2.37 Hz, 1H, benzofuran-4).

**$^{13}$C NMR (300 MHz) (DMSO-$d_6$) $\delta$ (ppm):** 42.51 (piperazine), 45.99 (**4-methyl**piperazine), 46.81 (piperazine), 54.80 (piperazine), 111.62, 113.37, 119.52, 122.29, 127.84, 144.59, 151.47, 157.09, 158.49 (benzofuran-**CO-**piperazine).

**HRMS (ESI) (m/z) $[M+1]^+$:** for $C_{14}H_{15}N_3O_4$ calculated: 290.1135; found: 290.1138.

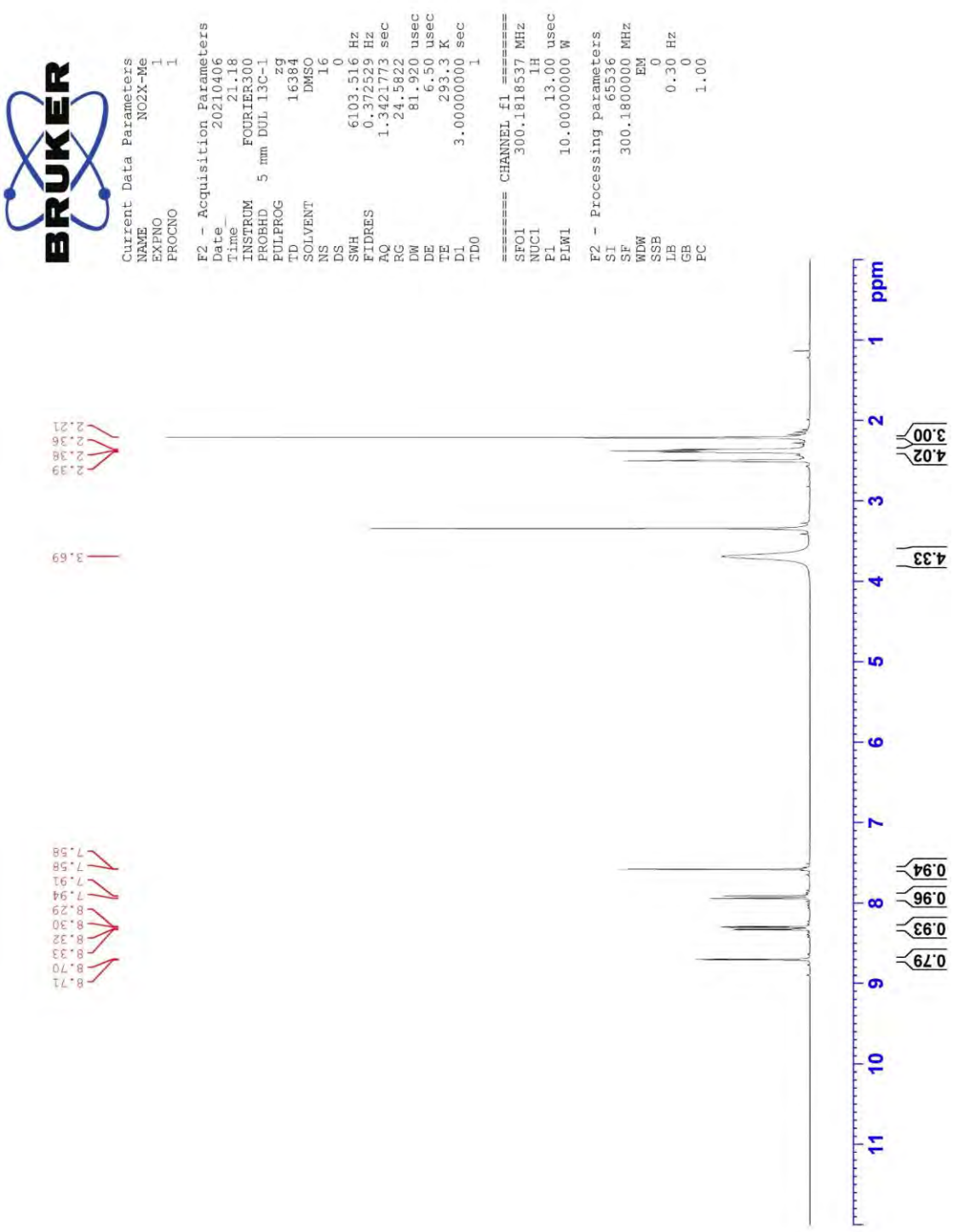


**Figure 5.141.** *[1]H NMR spectrum of compound* ***D28***

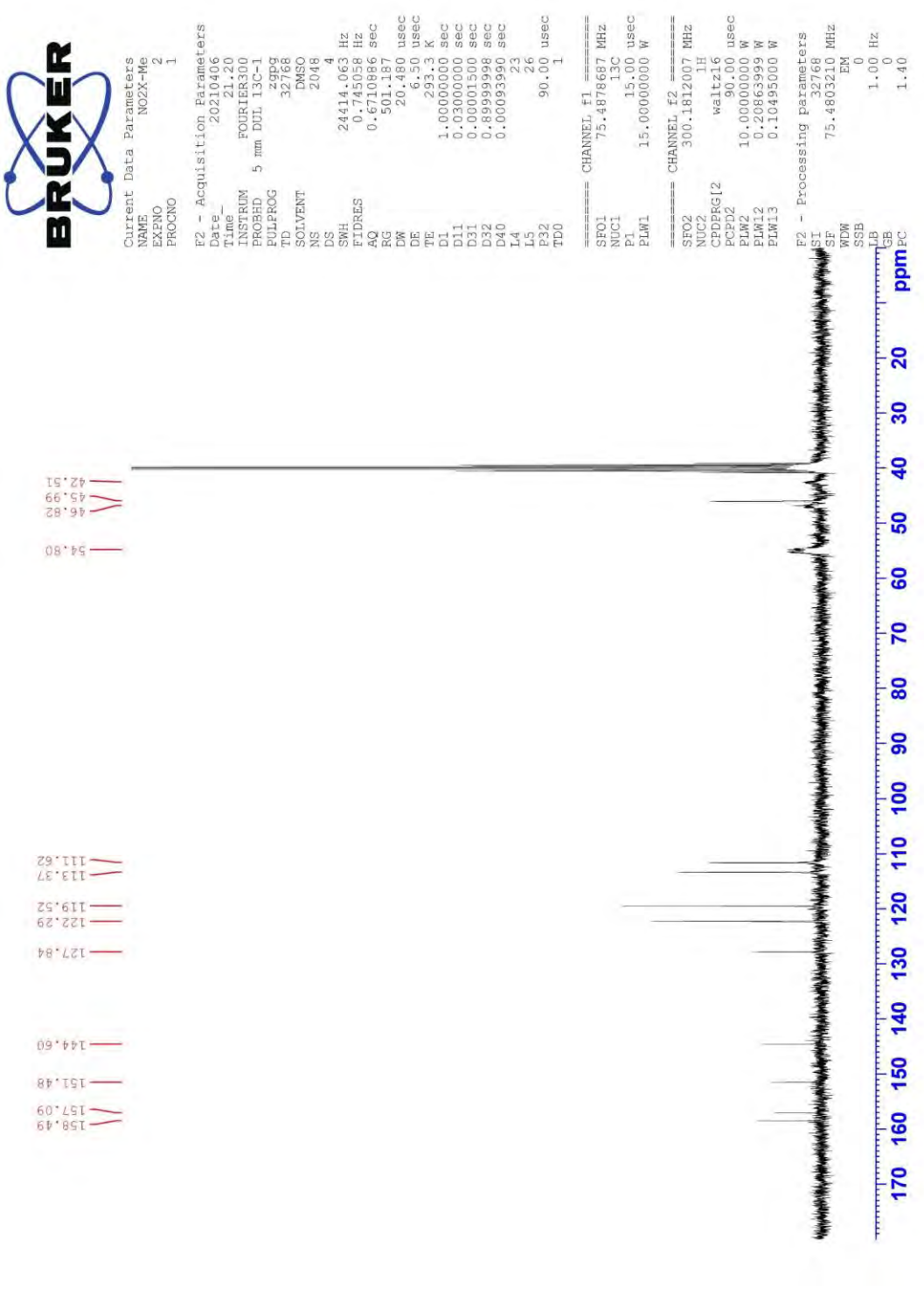


**Figure 5.142.** *$^{13}$C NMR spectrum of compound **D28***

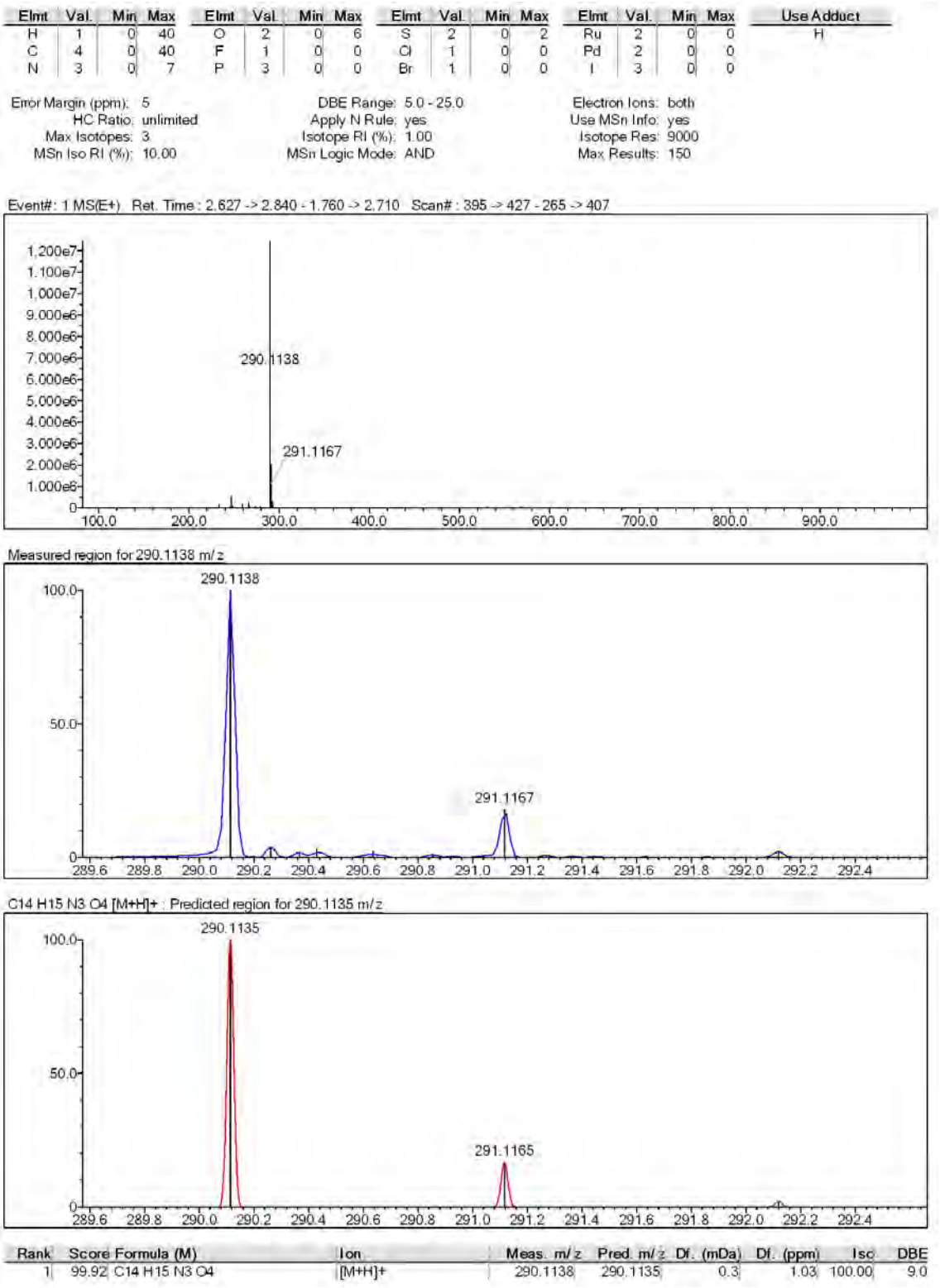


**Figure 5.143.** *High-resolution mass spectrum of compound* ***D28***

DOPNALAB

| | Item | Value |
|---|---|---|
| | Acquired Date&Time | 27.05.2021 17:35:58 |
| | Acquired by | System Administrator |
| | Filename | C:\Users\dopnalab\Desktop\sa\281.ispd |
| | Spectrum name | 281 |
| | Sample name | 28 |
| | Sample ID | |
| | Option | |
| | Comment | |
| | No. of Scans | 15 |
| | Resolution | 4 [cm-1] |
| | Apodization | Happ-Genzel |

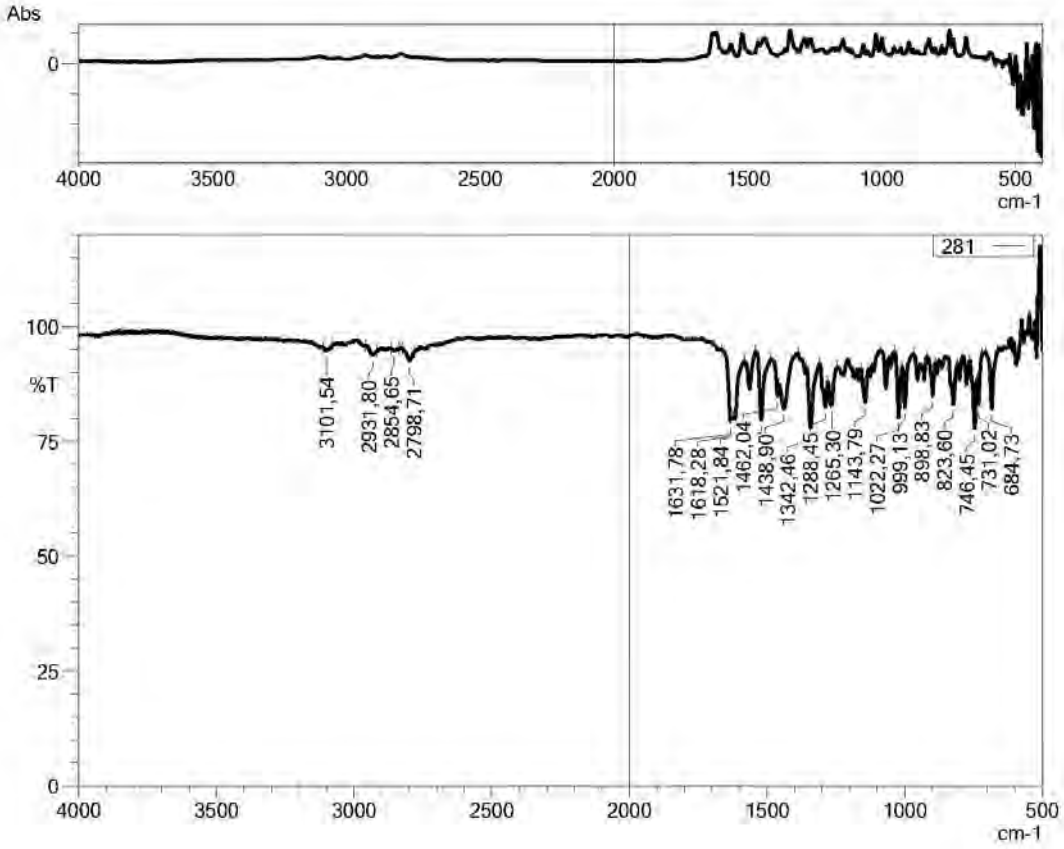


**Figure 5.144.** *IR spectrum of compound* ***D28***

### 5.1.4.29. *(4-ethylpiperazin-1-yl)(5-nitrobenzofuran-2-yl)methanone (D29)*

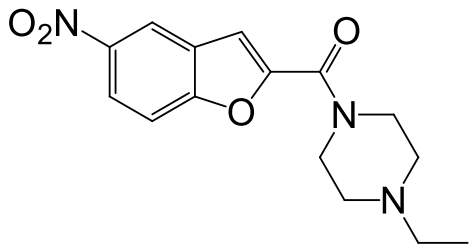


**Figure 5.145.** *Molecular structure of compound **D28***

**Physical Properties: Texture:** amorphous powder, **Color:** brown, **M.P.:** 108-110ºC**, Yield:** 42%.

**IR (ATR) $\upsilon_{max}$ ($cm^{-1}$):** 3093 ($SP^2$ C-H stretching, aromatic), 2937-2767 ($SP^3$ C-H stretching, methylenes of piperazine, and ethyl-methyl piperazine), 1620 (C=O stretching, amide), 1517 (N-O asymmetric stretching, nitro group), 1431 (C=C stretching, aromatic), 1344 (N-O symmetric stretching, nitro group), 1294-1228 (C-O stretching, ether), 1178, 1016 (C-N stretching, tertiary amine and/or C-O stretching, ether), 891-684 (C-H aromatic out-of-plane bending).

**$^1$H NMR (300 MHz) (DMSO-$d_6$) $\delta$ (ppm):** 1.01 (t, *J*= 7.17 Hz, 3H, piperazine-$CH_2$-**$CH_3$**), 2.36 (q, *J*= 14.44, 7.25 Hz, 2H, piperazine-**$CH_2$**-$CH_3$), 2.42 (t, *J*= 4.97, 4H, piperazine-3, 5), 3.69 (brs, 4H, piperazine-2, 6), 7.58 (s, 1H, benzofuran-3), 7.92 (d, *J*= 9.14 Hz, 1H, benzofuran-7), 8.31 (dd, *J*= 9.22, 2.36 Hz, 1H, benzofuran-6), 8.70 (d, *J*= 2.36 Hz, 1H, benzofuran-4).

**$^{13}$C NMR (300 MHz) (DMSO-$d_6$) $\delta$ (ppm):** 12.34 (piperazine-$CH_2$-**$CH_3$**), 42.73 (piperazine), 46.94 (piperazine), 51.86 (piperazine-**$CH_2$**-$CH_3$), 52.37 (piperazine), 53.16 (piperazine) 111.61, 113.36, 119.52, 122.29, 127.84, 144.59, 151.50, 157.08, 158.43 (benzofuran-**CO**-piperazine).

**HRMS (ESI) (m/z) $[M+1]^+$:** for $C_{15}H_{17}N_3O_4$ calculated: 304.1292; found: 304.1296.

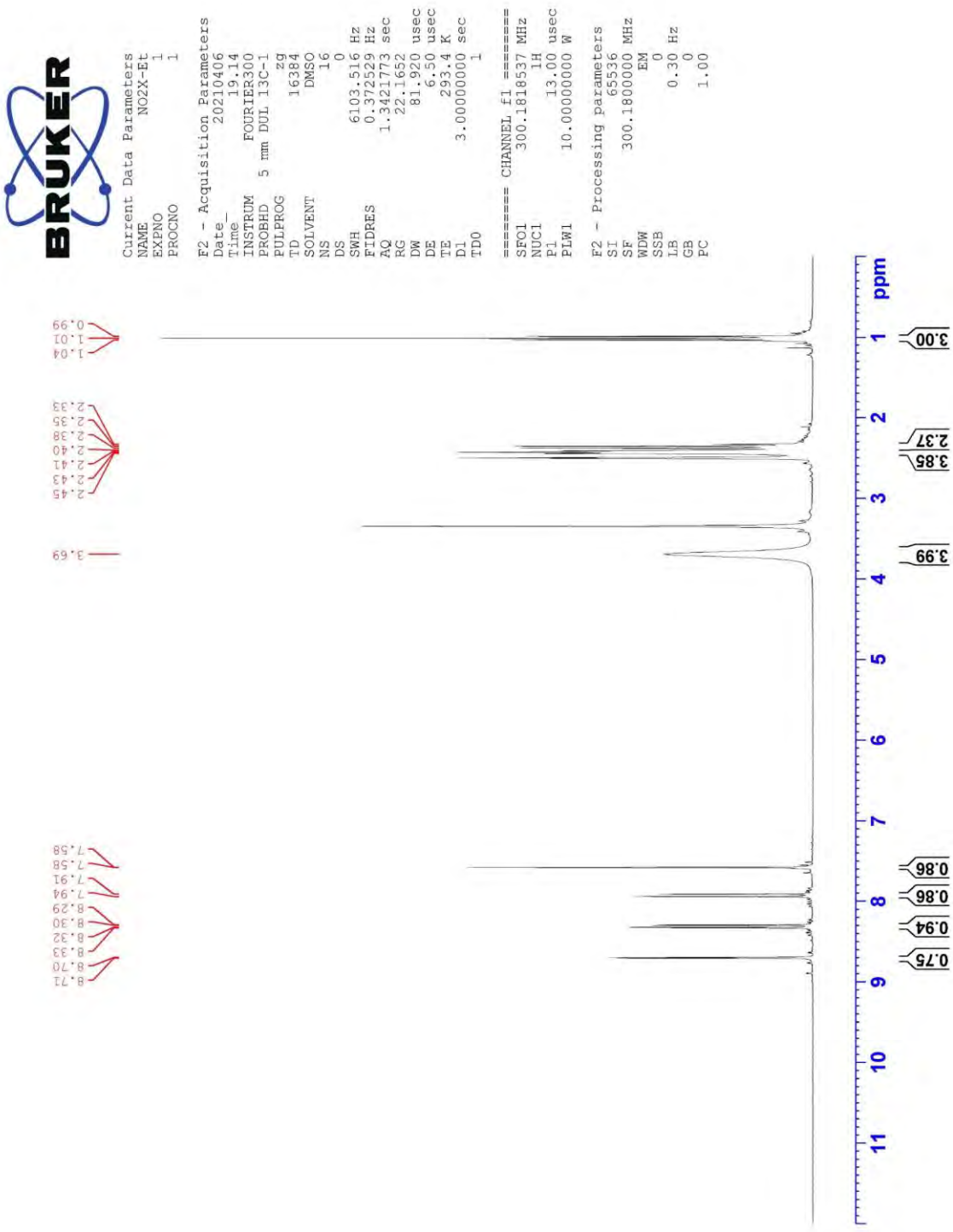


**Figure 5.146.** *$^{1}H$ NMR spectrum of compound **D29***

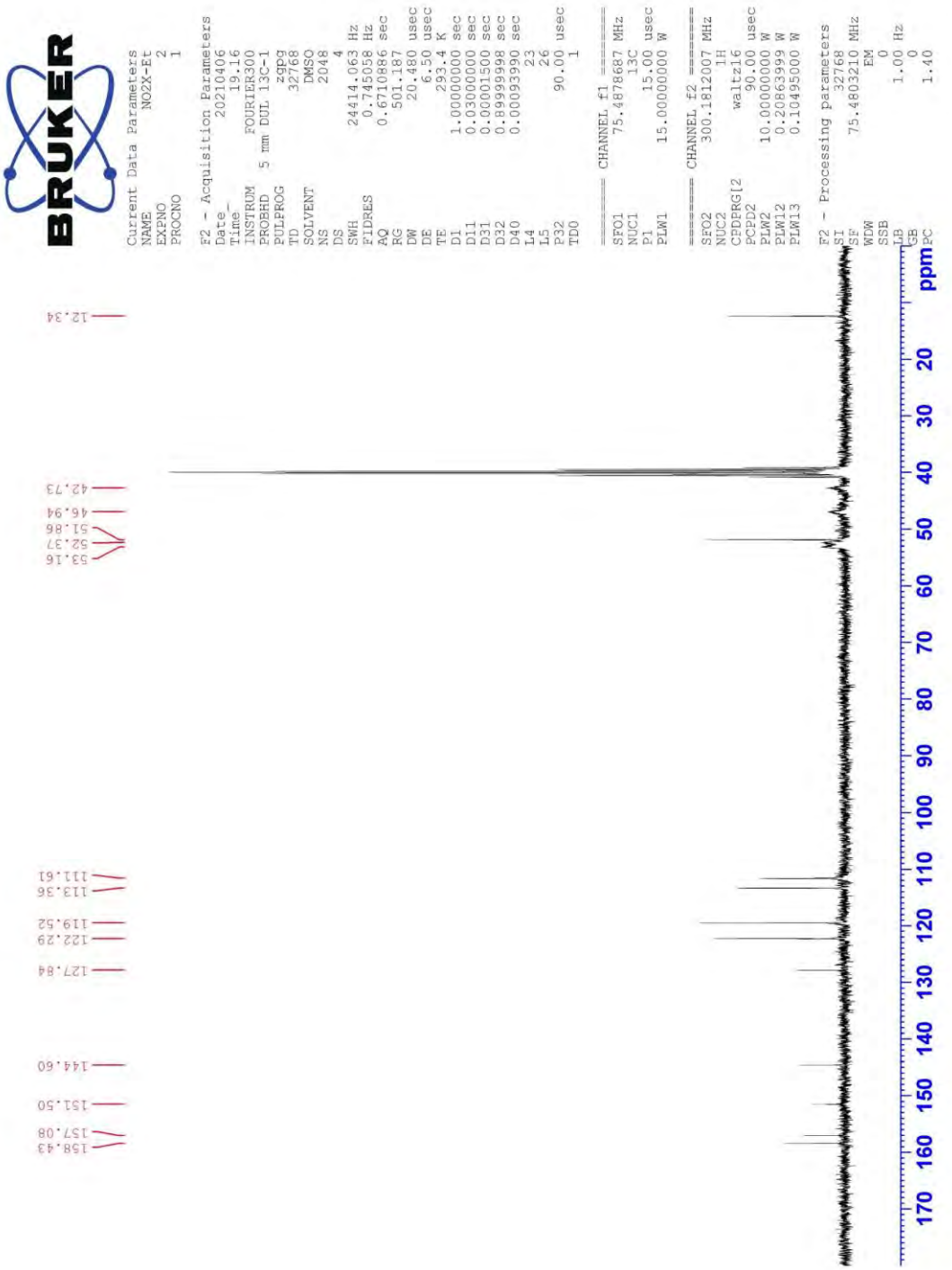


**Figure 5.147.** *$^{13}$C NMR spectrum of compound **D29***

| Elmt | Val. | Min | Max | Elmt | Val. | Min | Max | Elmt | Val. | Min | Max | Elmt | Val. | Min | Max | Use Adduct |
|---|---|---|---|---|---|---|---|---|---|---|---|---|---|---|---|---|
| H | 1 | 0 | 40 | O | 2 | 0 | 6 | S | 2 | 0 | 2 | Ru | 2 | 0 | 0 | H |
| C | 4 | 0 | 40 | F | 1 | 0 | 0 | Cl | 1 | 0 | 0 | Pd | 2 | 0 | 0 | |
| N | 3 | 0 | 7 | P | 3 | 0 | 0 | Br | 1 | 0 | 0 | I | 3 | 0 | 0 | |

Error Margin (ppm): 5
HC Ratio: unlimited
Max Isotopes: 3
MSn Iso RI (%): 10.00

DBE Range: 5.0 - 25.0
Apply N Rule: yes
Isotope RI (%): 1.00
MSn Logic Mode: AND

Electron Ions: both
Use MSn Info: yes
Isotope Res: 9000
Max Results: 150

Event#: 1 MS(E+) Ret. Time: 2.560 -> 3.187 - 2.040 -> 2.694 Scan#: 385 -> 479 - 307 -> 405

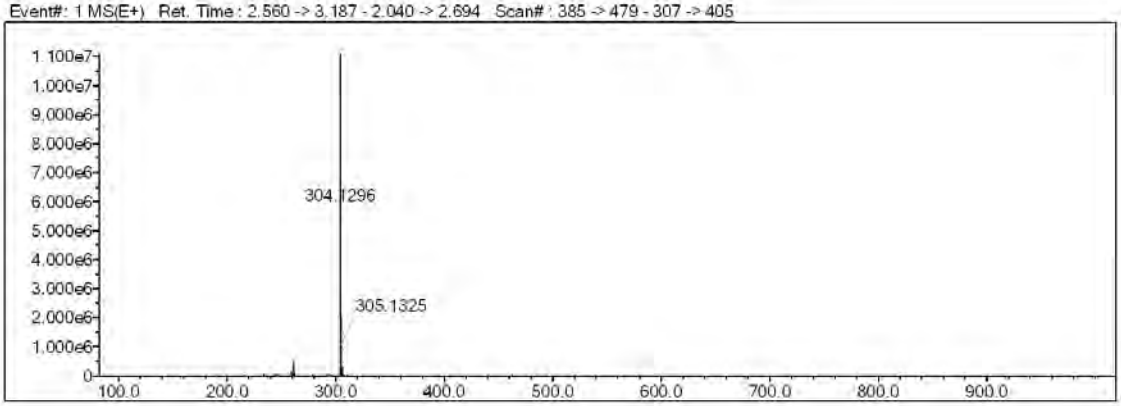


Measured region for 304.1296 m/z

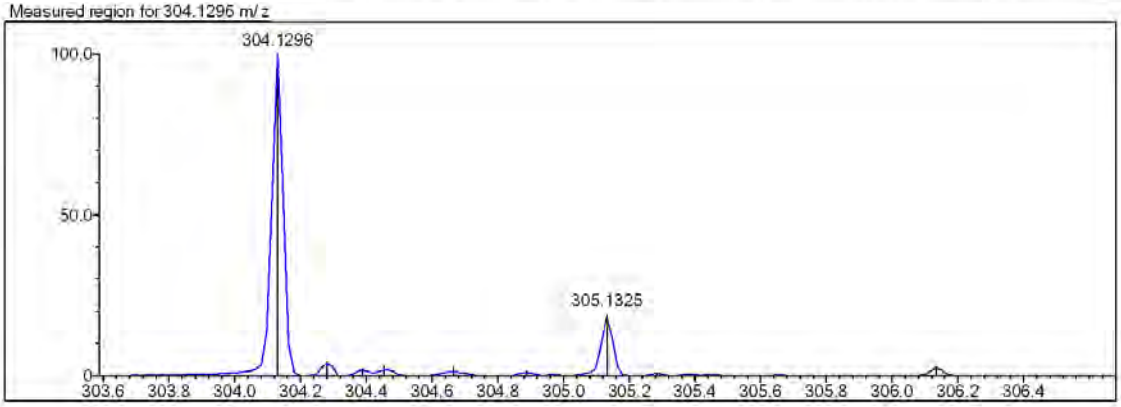


C15 H17 N3 O4 [M+H]+ : Predicted region for 304.1292 m/z

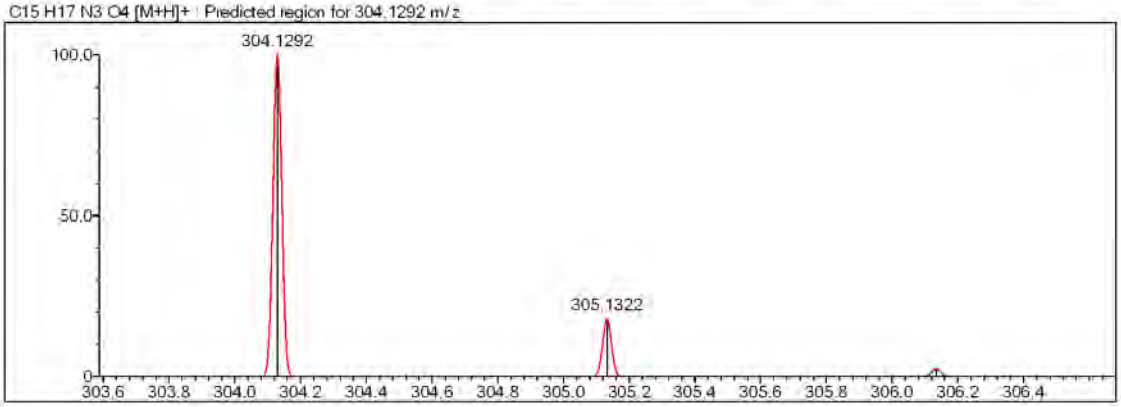


| Rank | Score | Formula (M) | Ion | Meas. m/z | Pred. m/z | Df. (mDa) | Df. (ppm) | Isc | DBE |
|---|---|---|---|---|---|---|---|---|---|
| 1 | 99.20 | C15 H17 N3 O4 | [M+H]+ | 304.1296 | 304.1292 | 0.4 | 1.32 | 100.00 | 9.0 |

**Figure 5.148.** *High-resolution mass spectrum of compound* ***D29***

DOPNALAB

| Item | Value |
|---|---|
| Acquired Date&Time | 27.05.2021 17:40:23 |
| Acquired by | System Administrator |
| Filename | C:\Users\dopnalab\Desktop\sa\291.ispd |
| Spectrum name | 291 |
| Sample name | 29 |
| Sample ID | |
| Option | |
| Comment | |
| No. of Scans | 15 |
| Resolution | 4 [cm-1] |
| Apodization | Happ-Genzel |

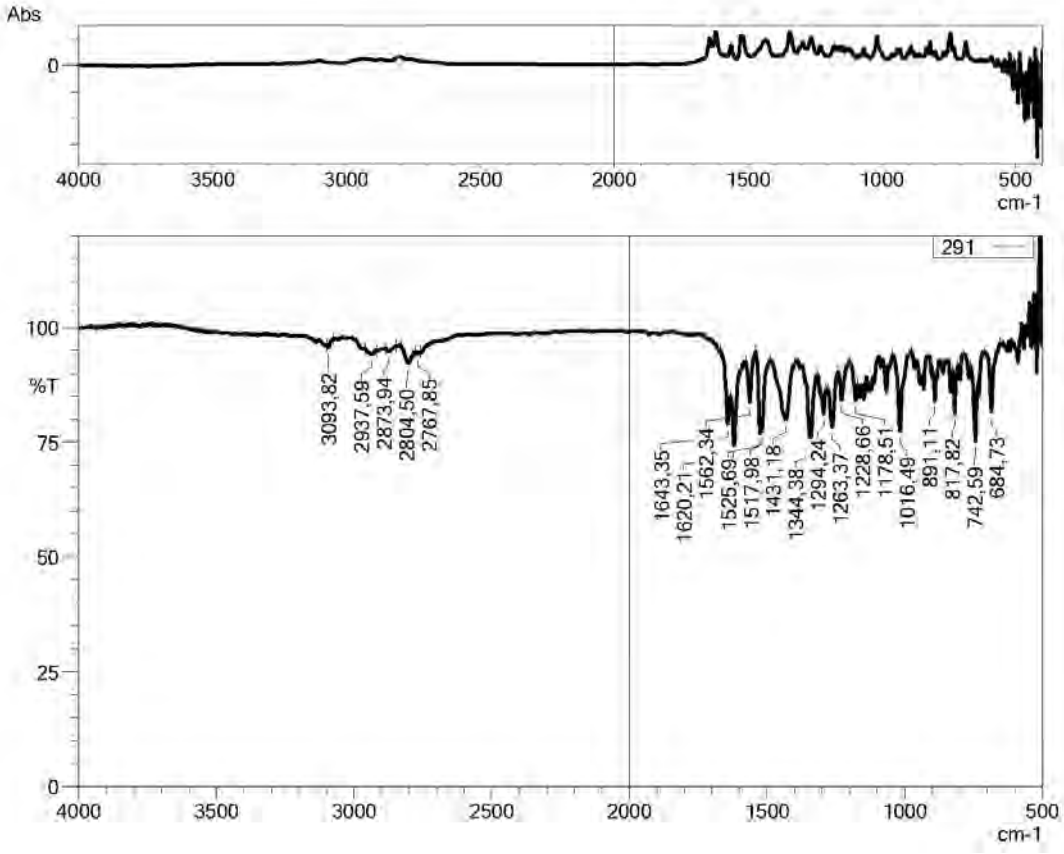


**Figure 5.149.** *IR spectrum of compound **D29***

### 5.1.4.30. *(4-(2-(dimethylamino)ethyl)piperazin-1-yl)(5-nitrobenzofuran-2-yl)methanone (30)*

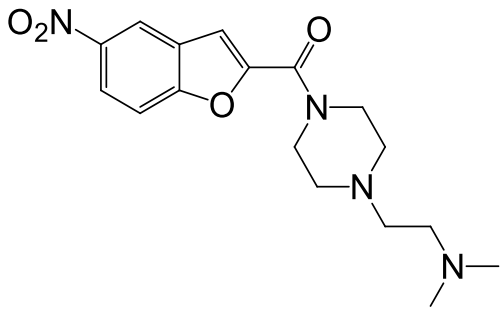

**Figure 5.150.** *Molecular structure of compound **D30***

**Physical Properties: Texture:** amorphous powder, **Color:** brown, **M.P.:** 71-73ºC**, Yield:** 63%.

**IR (ATR) $\upsilon_{max}$ ($cm^{-1}$):** 3109 ($SP^2$ C-H stretching, aromatic), 2937-2765 ($SP^3$ C-H stretching, methylenes of piperazine, and dimethylaminoethyl-piperazine), 1631 (C=O stretching, amide), 1519 ((N-O asymmetric stretching, nitro group), 1431 (C=C stretching, aromatic), 1340 (N-O symmetric stretching, nitro group), 1271 (C-O stretching, ether), 1130, 1024-997 (C-N stretching, tertiary amine and/or C-O stretching, ether), 883-684 (C-H aromatic out-of-plane bending).

**$^1$H NMR (300 MHz) (DMSO-$d_6$) $\delta$ (ppm):** 2.13 (s, 6H, -N**($CH_3$)$_2$**), 2.30-2.48 (m, 8H, piperazine-3, 5 and piperazine-(**$CH_2$)$_2$**-N), 3.68 (brs, 4H, piperazine-2, 6), 7.58 (s, 1H, benzofuran-3), 7.92 (d, *J*= 9.14 Hz, 1H, benzofuran-7), 8.31 (dd, *J*= 9.10, 2.49 Hz, 1H, benzofuran-6), 8.70 (d, *J*= 2.37 Hz, 1H, benzofuran-4).

**$^{13}$C NMR (300 MHz) (DMSO-$d_6$) $\delta$ (ppm):** 42.81 (piperazine), 45.99 (-N**($CH_3$)$_2$**), 46.82 (piperazine), 53.15 (piperazine), 55.97 (piperazine-(**$CH_2$)$_2$**-N), 57.02 (piperazine-(**$CH_2$)$_2$**-N), 111.63, 113.37, 119.53, 122.30, 127.84, 144.59, 151.47, 157.09, 158.41 (benzofuran-**CO**-piperazine).

**HRMS (ESI) (m/z) $[M+1]^+$:** for $C_{17}H_{22}N_4O_4$ calculated: 347.1714; found: 347.1720.

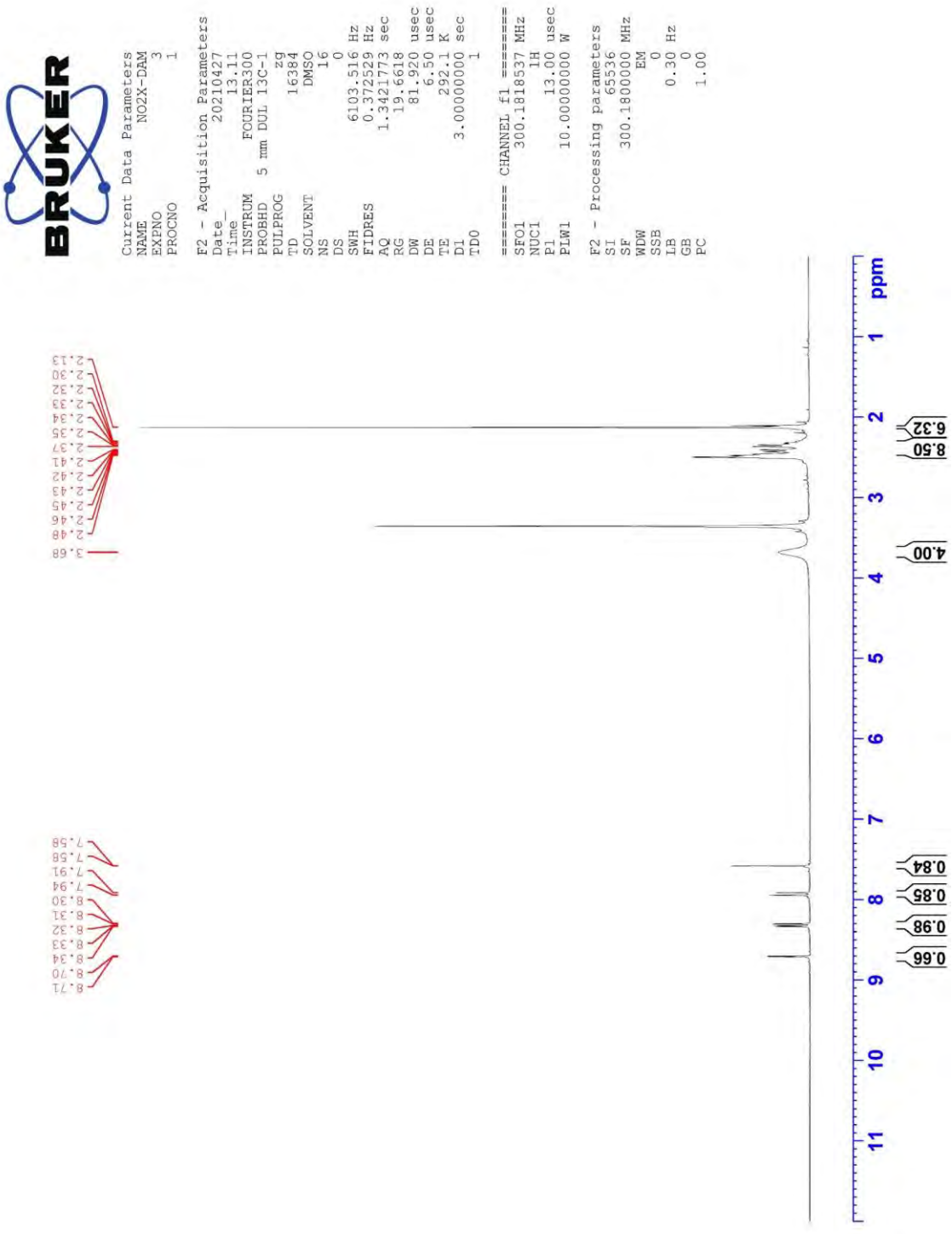


**Figure 5.151.** *[1]H NMR spectrum of compound **D30***

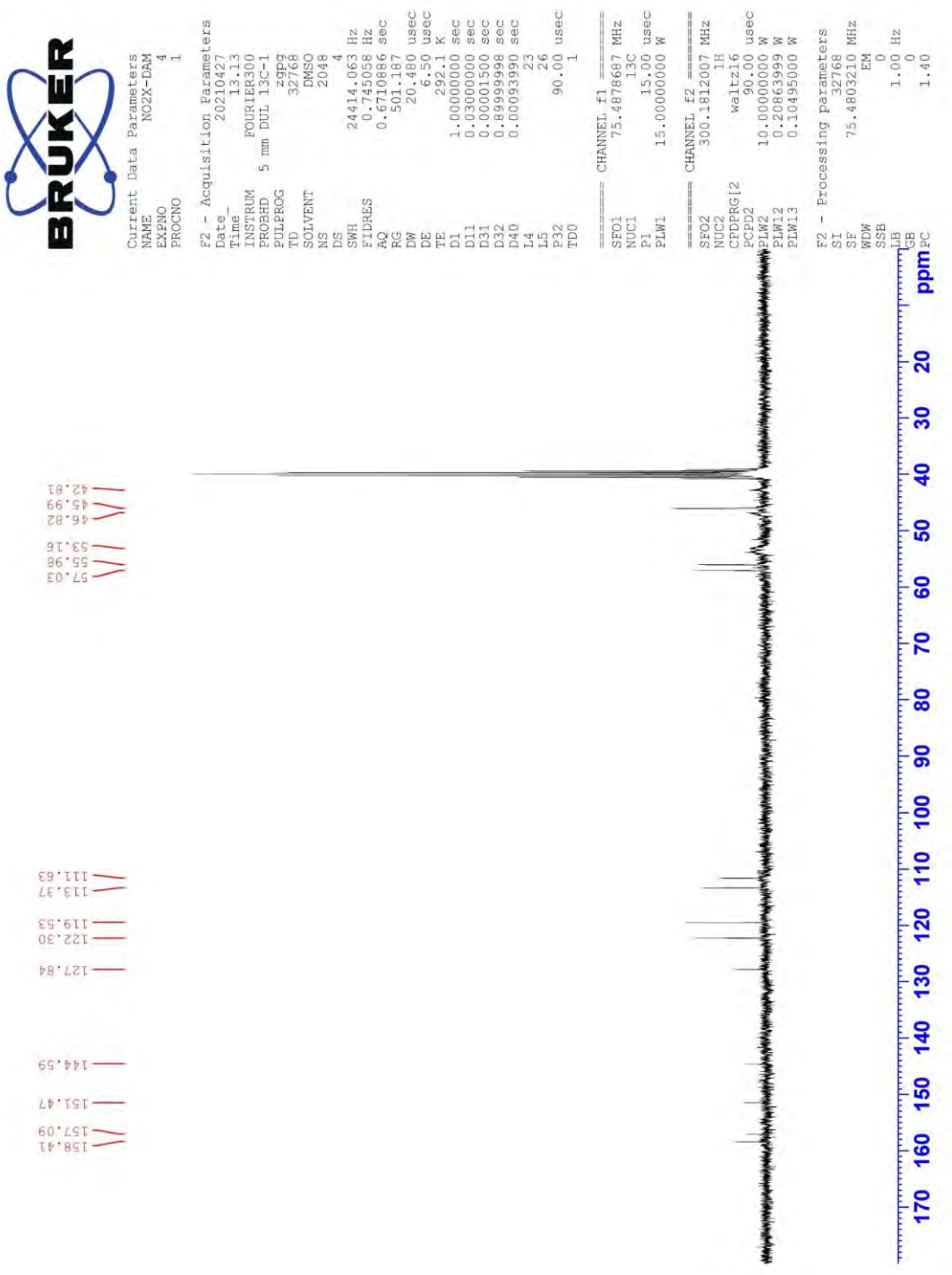


**Figure 5.152.** *[13]C NMR spectrum of compound **D30***

| Elmt | Val. | Min | Max | Elmt | Val. | Min | Max | Elmt | Val. | Min | Max | Elmt | Val. | Min | Max | Use Adduct |
|---|---|---|---|---|---|---|---|---|---|---|---|---|---|---|---|---|
| H | 1 | 0 | 40 | O | 2 | 0 | 6 | S | 2 | 0 | 2 | Ru | 2 | 0 | 0 | H |
| C | 4 | 0 | 40 | F | 1 | 0 | 0 | Cl | 1 | 0 | 0 | Pd | 2 | 0 | 0 | |
| N | 3 | 0 | 7 | P | 3 | 0 | 0 | Br | 1 | 0 | 0 | I | 3 | 0 | 0 | |

Error Margin (ppm): 5
HC Ratio: unlimited
Max Isotopes: 3
MSn Iso RI (%): 10.00

DBE Range: 5.0 - 25.0
Apply N Rule: yes
Isotope RI (%): 1.00
MSn Logic Mode: AND

Electron Ions: both
Use MSn Info: yes
Isotope Res: 9000
Max Results: 150

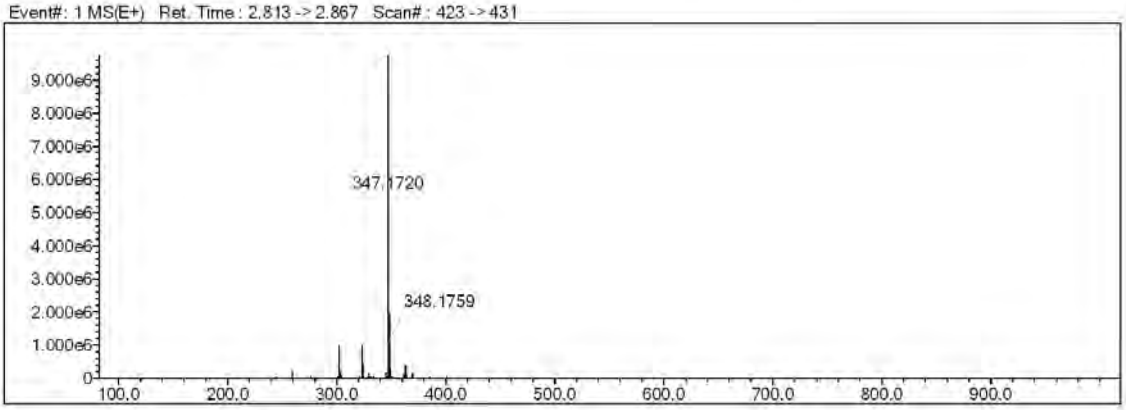


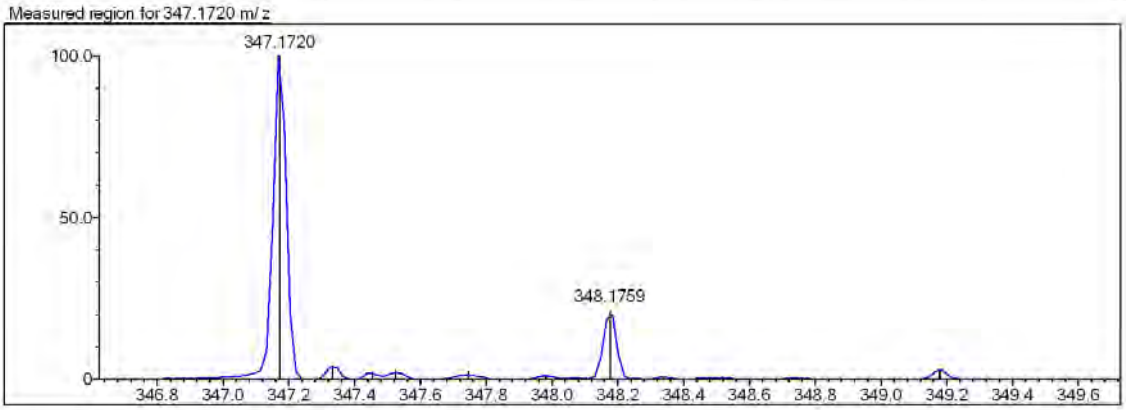


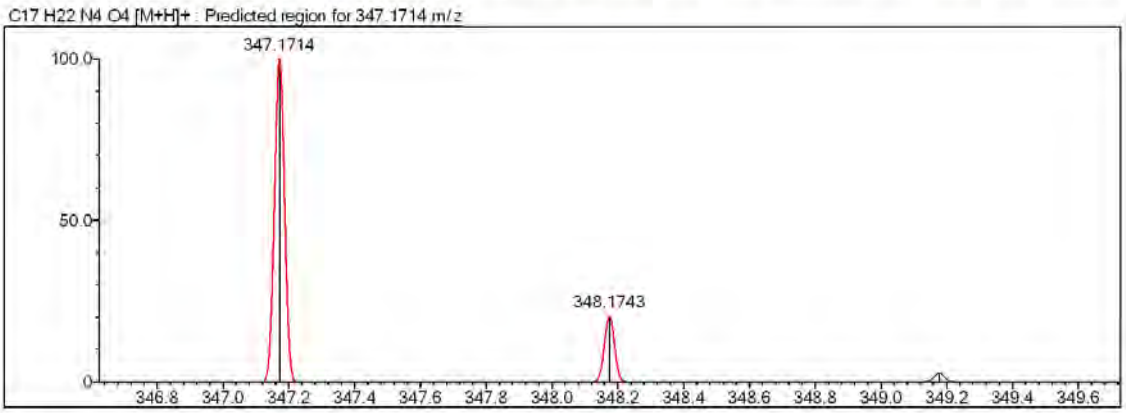


| Rank | Score | Formula (M) | Ion | Meas. m/z | Pred. m/z | Df. (mDa) | Df. (ppm) | Isc | DBE |
|---|---|---|---|---|---|---|---|---|---|
| 1 | 95.80 | C17 H22 N4 O4 | [M+H]+ | 347.1720 | 347.1714 | 0.6 | 1.73 | 97.58 | 9.0 |

**Figure 5.153.** *High-resolution mass spectrum of compound* ***D30***

DOPNALAB

| | Item | Value |
|---|---|---|
| | Acquired Date&Time | 27.05.2021 17:44:57 |
| | Acquired by | System Administrator |
| | Filename | C:\Users\dopnalab\Desktop\sa\301.ispd |
| | Spectrum name | 301 |
| | Sample name | 30 |
| | Sample ID | |
| | Option | |
| | Comment | |
| | No. of Scans | 15 |
| | Resolution | 4 [cm-1] |
| | Apodization | Happ-Genzel |

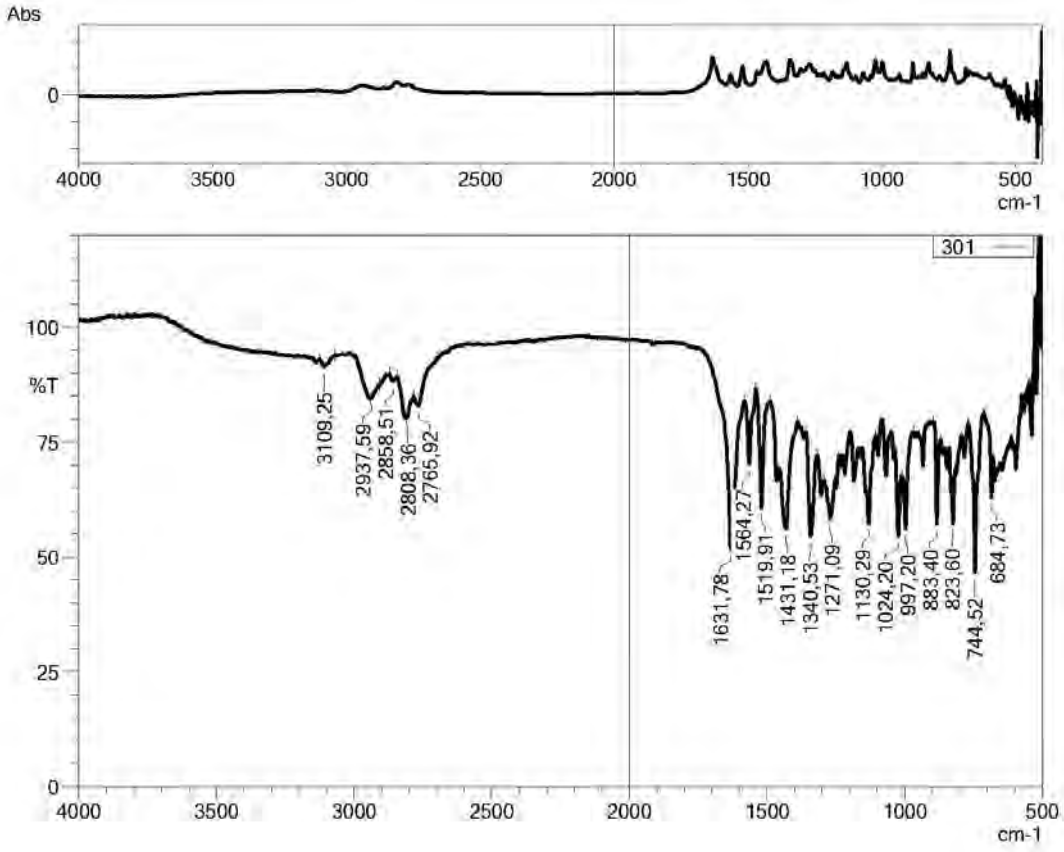


**Figure 5.154.** *IR spectrum of compound **D30***

### 5.1.4.31. *(5-methoxy-3-methylbenzofuran-2-yl)(4-phenylpiperazin-1-yl)methanone (D31)*

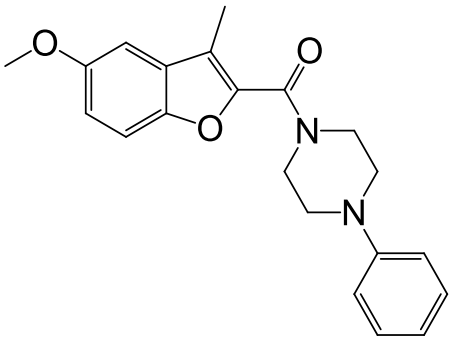

**Figure 5.155.** *Molecular structure of compound* ***D31***

**Physical Properties: Texture:** solid crystals, **Color:** light brown, **M.P.:** 114-116ºC**, Yield:** 51%.

**IR (ATR) $\upsilon_{max}$ ($cm^{-1}$):** 3053 ($SP^2$ C-H stretching, aromatic), 2945-2808 ($SP^3$ C-H stretching, methoxy and methylenes of piperazine), 1622 (C=O stretching, amide), 1458-1431 (C=C stretching, aromatic), 1230-1209 (C-O stretching, ether), 1168, 1010 (C-N stretching, tertiary amine and/or ether), 821-690 (C-H aromatic out-of-plane bending).

**$^1$H NMR (300 MHz) (DMSO-$d_6$) $\delta$ (ppm):** 2.34 (s, 3H, **3-methyl**benzofuran), 3.20 (brs, 4H, piperazine-3, 5), 3.75 (t, *J*= 4.58 Hz, 4H, piperazine-2, 6), 3.82 (s, 3H, **5-methoxy**benzofuran), 6.82 (t, *J*= 7.25 Hz, 1H, phenyl-4), 6.97 (d, *J*= 7.85, 2H, phenyl-2, 6), 7.02 (dd, *J*= 8.98, 2.61 Hz, 1H, benzofuran-6), 7.20-7.26 (m, 3H, phenyl-3,5 and benzofuran-4), 7.52 (d, *J*= 8.97 Hz, 1H, benzofuran-7).

**$^{13}$C NMR (300 MHz) (DMSO-$d_6$) $\delta$ (ppm):** 9.19 (**3-methyl**benzofuran), 42.69 (piperazine), 46.83 (piperazine), 49.24 (piperazine), 56.16 (**5-methoxy**benzofuran), 102.95, 112.74, 116.07, 116.43, 119.94, 120.10, 129.48, 144.87, 148.20, 151.18, 156.34, 160.24 (benzofuran-**CO**-piperazine).

**HRMS (ESI) (m/z) $[M+1]^+$:** for $C_{21}H_{22}N_2O_3$ calculated: 351.1703; found: 351.1732.

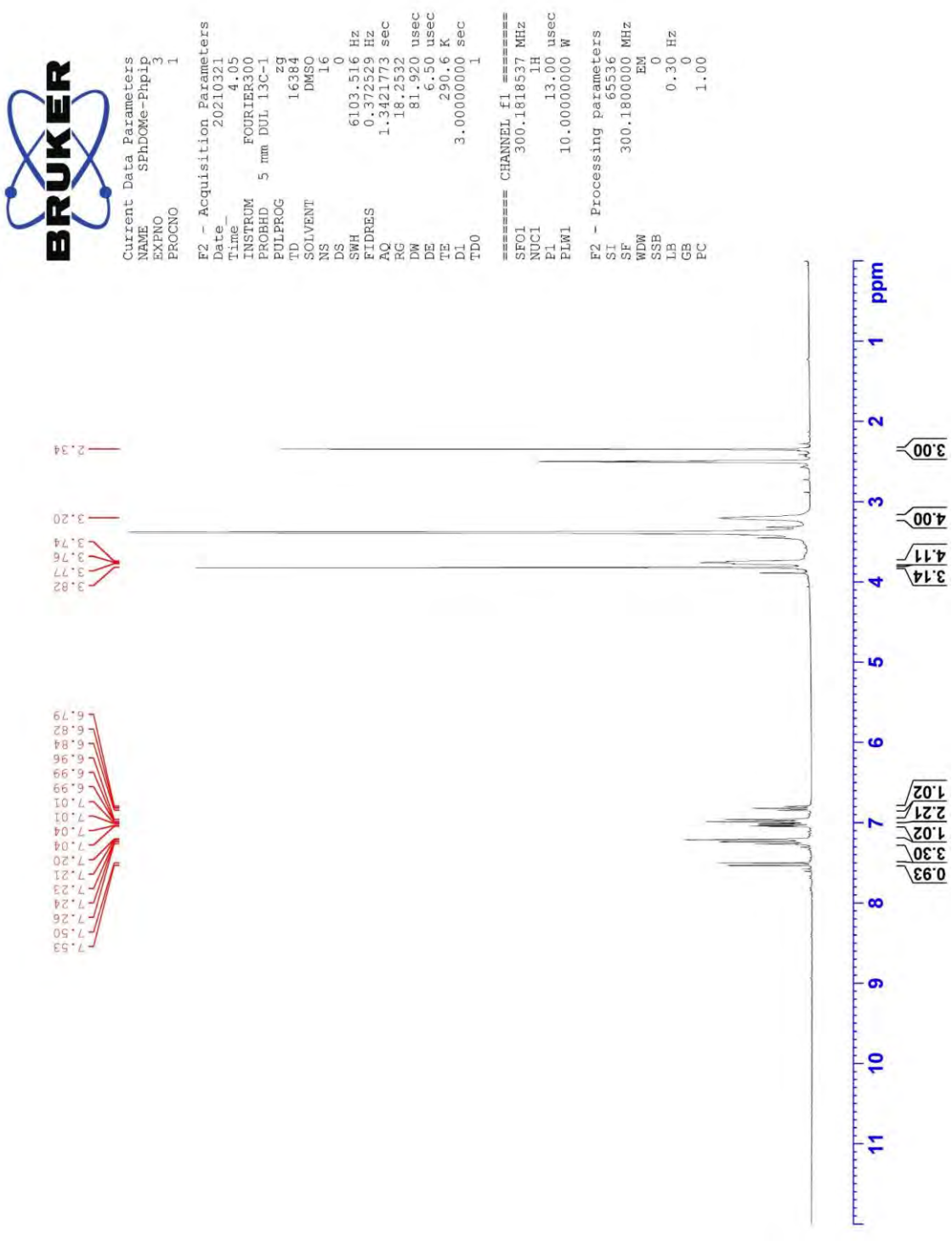


**Figure 5.156.** *[1]H NMR spectrum of compound **D31***

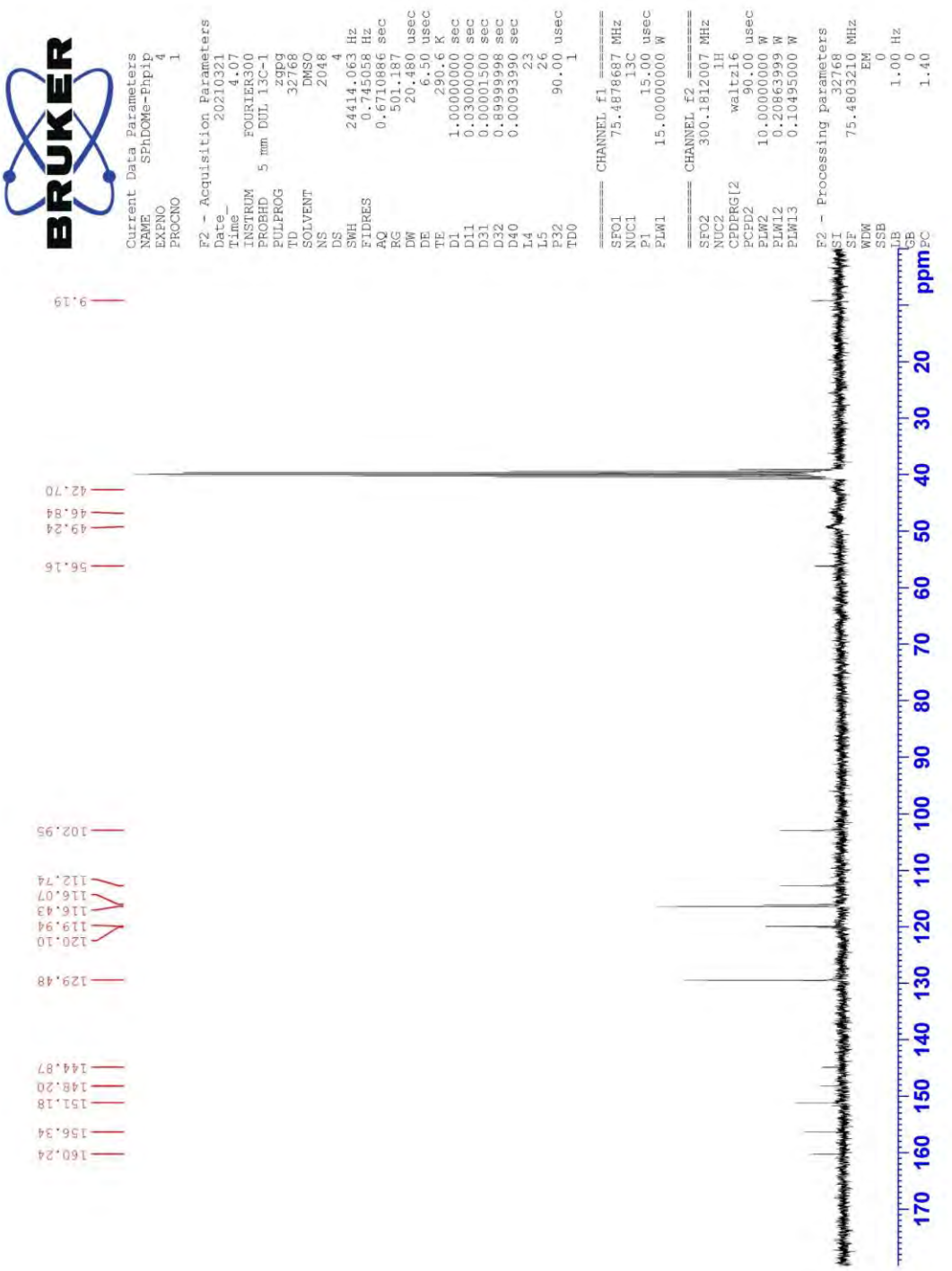


**Figure 5.157.** *$^{13}$C NMR spectrum of compound **D31***

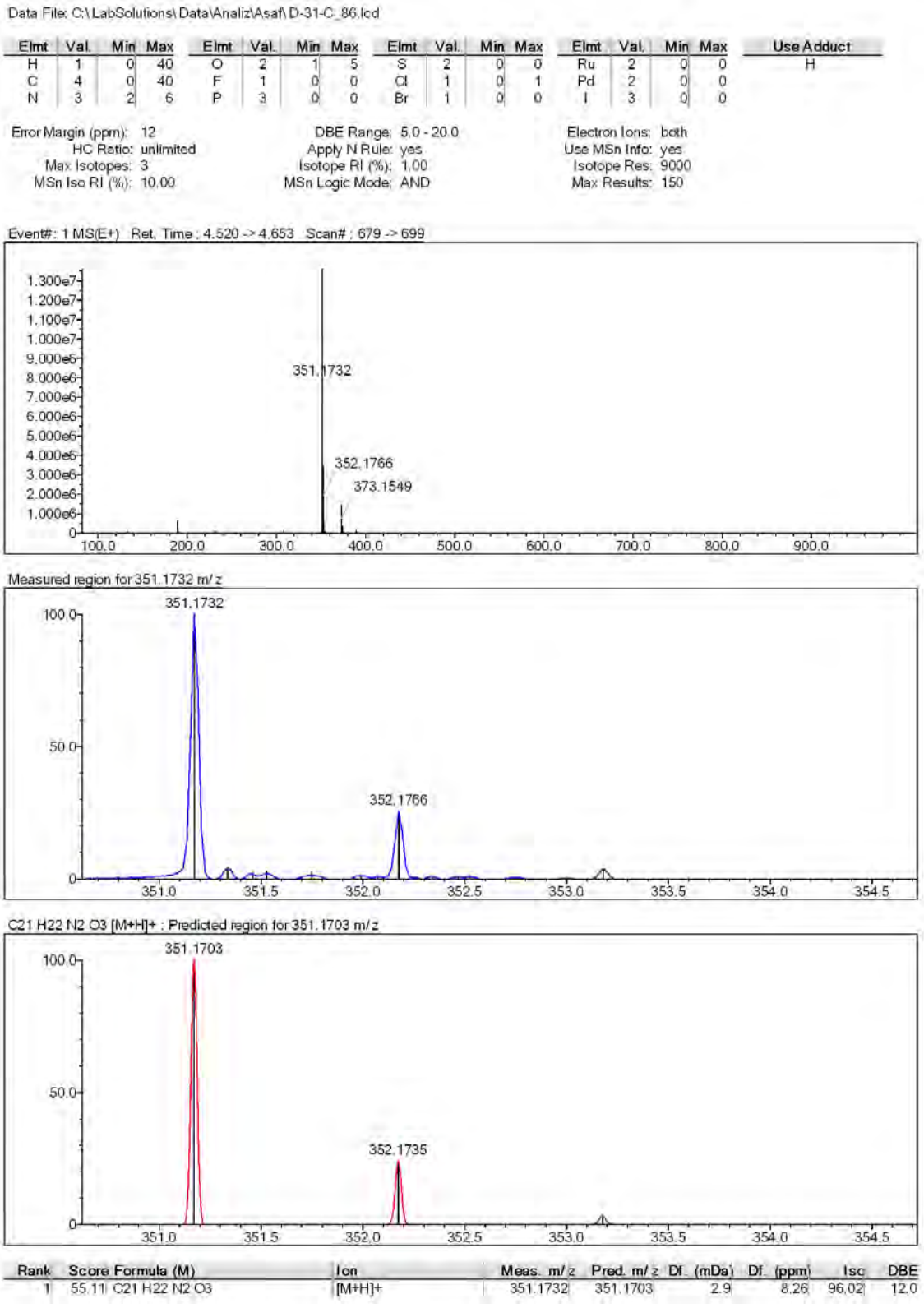


**Figure 5.158.** *High-resolution mass spectrum of compound* ***D31***

DOPNALAB

| | Item | Value |
|---|---|---|
| | Acquired Date&Time | 27.05.2021 13:08:14 |
| | Acquired by | System Administrator |
| | Filename | C:\Users\dopnalab\Desktop\sa\311.ispd |
| | Spectrum name | 311 |
| | Sample name | 31 |
| | Sample ID | |
| | Option | |
| | Comment | |
| | No. of Scans | 15 |
| | Resolution | 4 [cm-1] |
| | Apodization | Happ-Genzel |

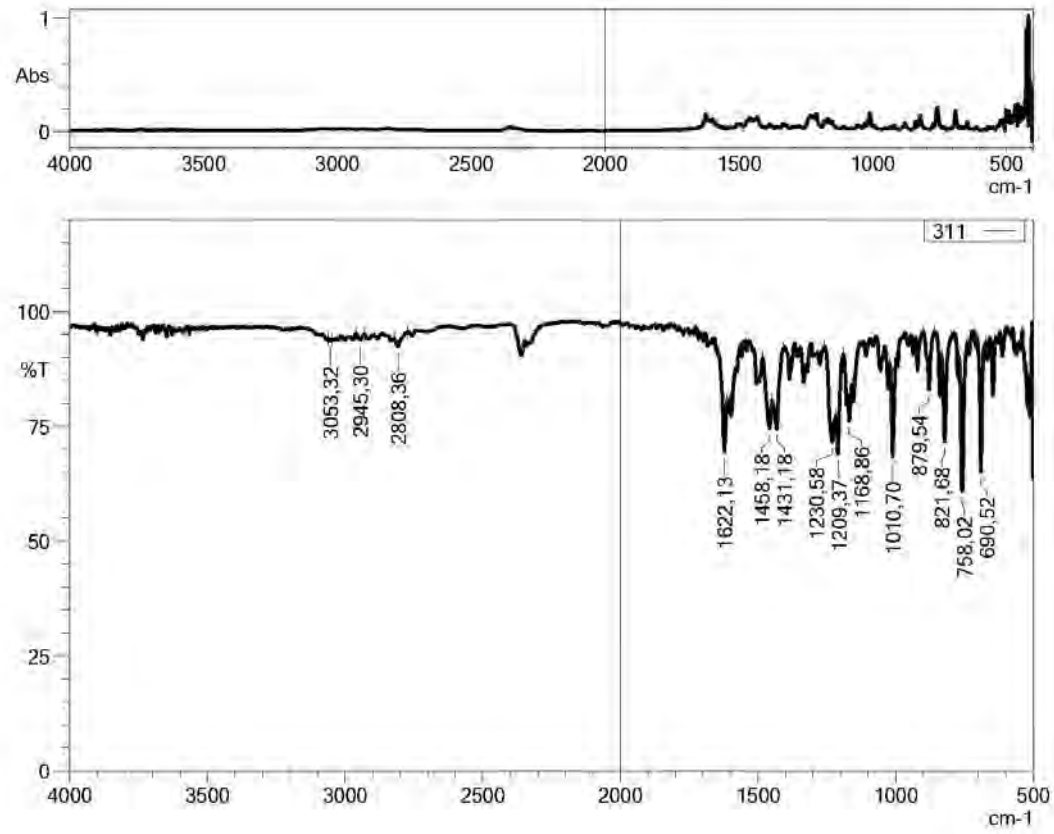


**Figure 5.159.** *IR spectrum of compound **D31***

### 5.1.4.32. *(4-(furan-2-carbonyl)piperazin-1-yl)(5-methoxy-3-methylbenzofuran-2-yl)methanone (D32)*

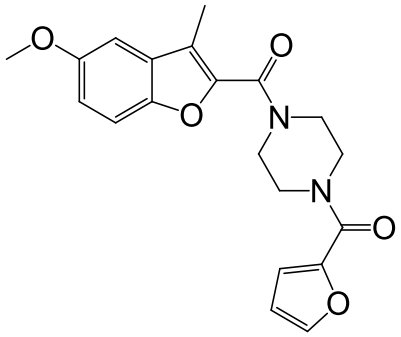

**Figure 5.160.** *Molecular structure of compound* ***D32***

**Physical Properties: Texture:** solid crystals, **Color:** light brown, **M.P.:** 122-124ºC**, Yield:** 49%.

**IR (ATR) $\upsilon_{max}$ ($cm^{-1}$):** 3061 ($SP^2$ C-H stretching, aromatic), 2933-2808 ($SP^3$ C-H stretching, methylenes of piperazine and methoxy), 1622 (C=O stretching, amide), 1429 (C=C stretching, aromatic), 1273-1209 (C-O stretching, ether), 1180, 1004 (C-N stretching, tertiary amine and/or ether), 829-750 (C-H aromatic out-of-plane bending).

**$^1$H NMR (300 MHz) (DMSO-$d_6$) $\delta$ (ppm):** 2.35 (s, 3H, **3-methyl**benzofuran), 3.72-3.75 (m, 8H, piperazine-2, 3, 5, 6), 3.82 (s, 3H, **5-methoxy**benzofuran), 6.64 (dd, *J*= 3.42, 1.74 Hz, 1H, furan-4), 7.01-7.05 (m, 2H, benzofuran-6 and furan-4), 7.20 (d, *J*= 2.49 Hz, 1H, benzofuran-4), 7.50 (d, *J*= 8.97 Hz, 1H, benzofuran-7), 7.86 (d, *J*= 0.88 Hz, 1H, furan-5).

**$^{13}$C NMR (300 MHz) (DMSO-$d_6$) $\delta$ (ppm):** 9.17 (**3-methyl**benzofuran), 42.80 (piperazine), 46.74 (piperazine), 56.20 (**5-methoxy**benzofuran), 102.99, 111.85, 112.76, 116.15, 116.44, 120.45, 129.56, 144.68, 145.41, 147.17, 148.25, 156.37, 158.92 (piperazine-**CO**-furan), 160.47 (benzofuran-**CO**-piperazine).

**HRMS (ESI) (m/z) $[M+1]^+$:** for $C_{20}H_{20}N_2O_5$ calculated: 369.1445; found: 369.1446.

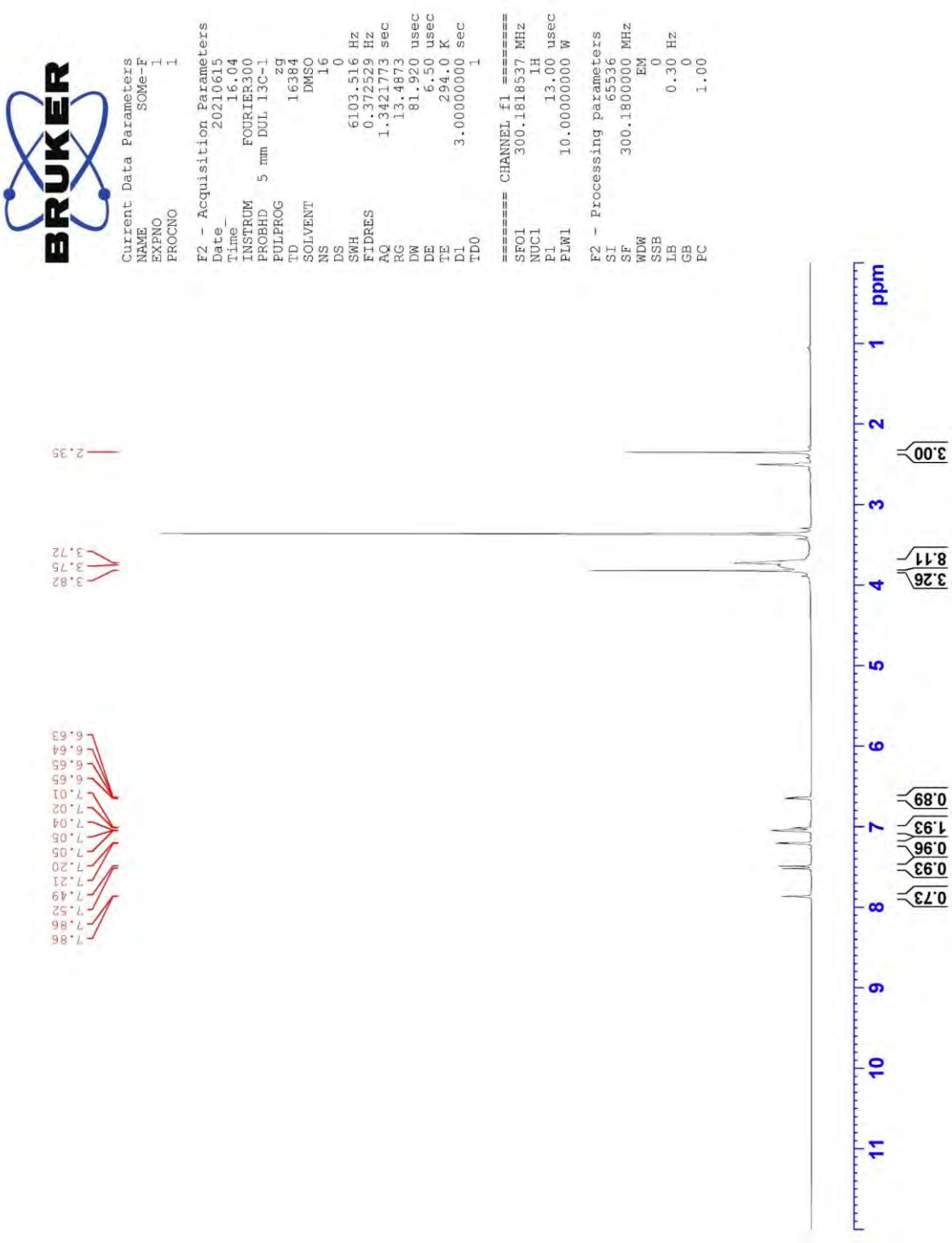


**Figure 5.161.** *$^{1}H$ NMR spectrum of compound **D32***

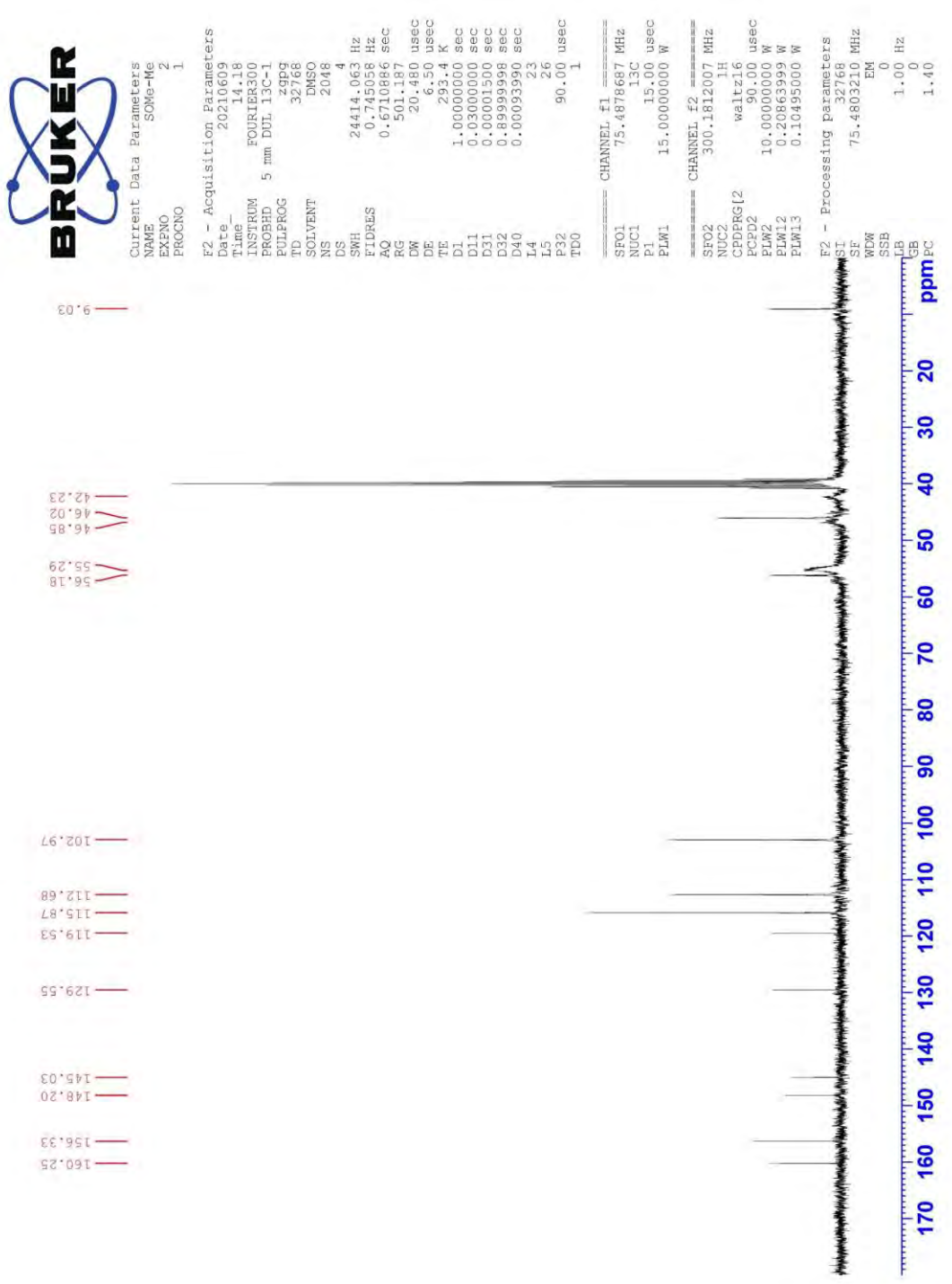


**Figure 5.162.** *[13]C NMR spectrum of compound **D32***

Data File: C:\LabSolutions\Data\Analiz\A.Çağrı\D32T_2.lcd

| Elmt | Val. | Min | Max | Elmt | Val. | Min | Max | Elmt | Val. | Min | Max | Elmt | Val. | Min | Max | Use Adduct |
|---|---|---|---|---|---|---|---|---|---|---|---|---|---|---|---|---|
| H | 1 | 0 | 40 | O | 2 | 0 | 5 | S | 2 | 0 | 2 | Ru | 2 | 0 | 0 | H |
| C | 4 | 0 | 40 | F | 1 | 0 | 0 | Cl | 1 | 0 | 1 | Pd | 2 | 0 | 0 | |
| N | 3 | 0 | 7 | P | 3 | 0 | 0 | Br | 1 | 0 | 0 | I | 3 | 0 | 0 | |

Error Margin (ppm): 5
HC Ratio: unlimited
Max Isotopes: 3
MSn Iso RI (%): 10.00

DBE Range: 10.0 - 25.0
Apply N Rule: yes
Isotope RI (%): 1.00
MSn Logic Mode: AND

Electron Ions: both
Use MSn Info: yes
Isotope Res: 9000
Max Results: 150

Event#: 1 MS(E+) Ret. Time: 3.613 -> 4.133 Scan#: 543 -> 621

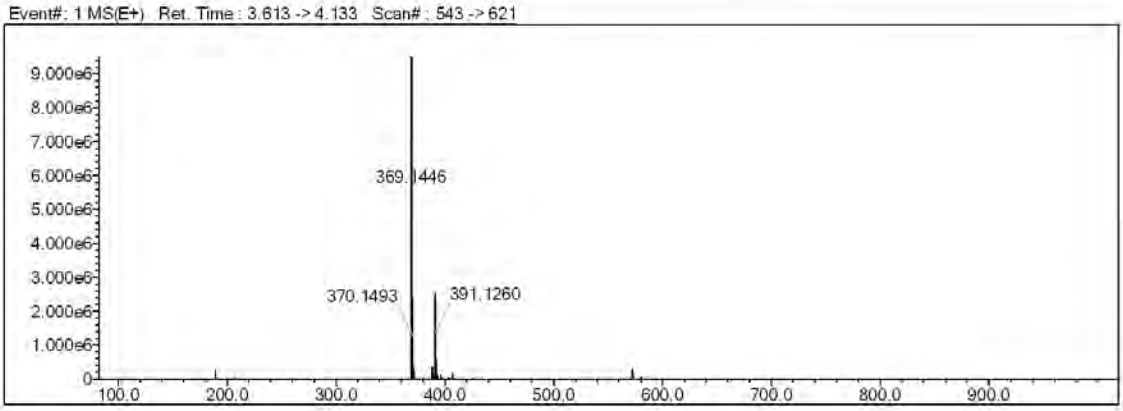


Measured region for 369.1446 m/z

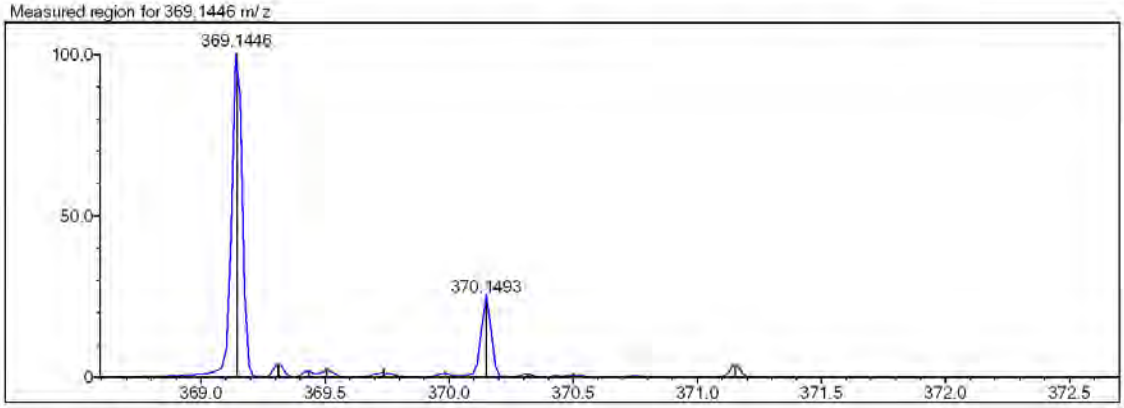


C20 H20 N2 O5 [M+H]+ : Predicted region for 369.1445 m/z

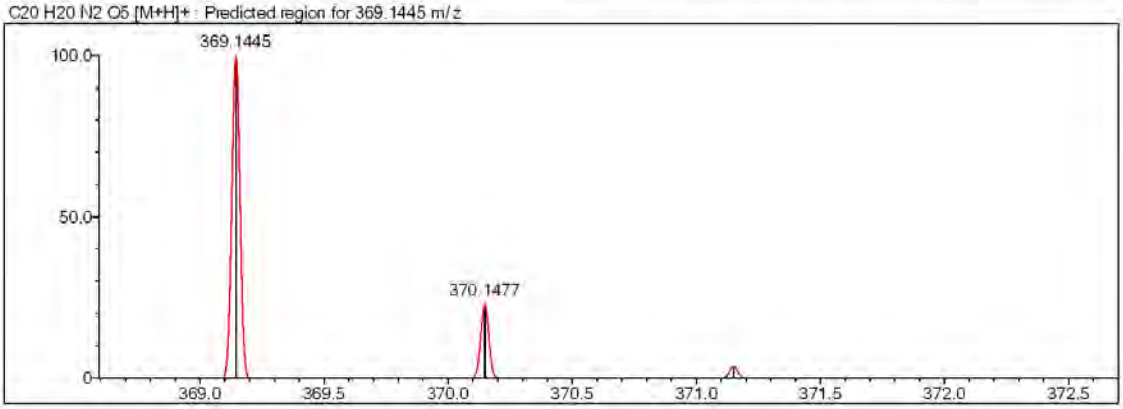


| Rank | Score | Formula (M) | Ion | Meas. m/z | Pred. m/z | Df. (mDa) | Df. (ppm) | Isc | DBE |
|---|---|---|---|---|---|---|---|---|---|
| 1 | 97.77 | C20 H20 N2 O5 | [M+H]+ | 369.1446 | 369.1445 | 0.1 | 0.27 | 97.77 | 12.0 |

**Figure 5.163.** *High-resolution mass spectrum of compound* ***D32***

DOPNALAB

| | Item | Value |
|---|---|---|
| | Acquired Date&Time | 27.05.2021 13:17:28 |
| | Acquired by | System Administrator |
| | Filename | C:\Users\dopnalab\Desktop\sa\321.ispd |
| | Spectrum name | 321 |
| | Sample name | 32 |
| | Sample ID | |
| | Option | |
| | Comment | |
| | No. of Scans | 16 |
| | Resolution | 4 [cm-1] |
| | Apodization | Happ-Genzel |

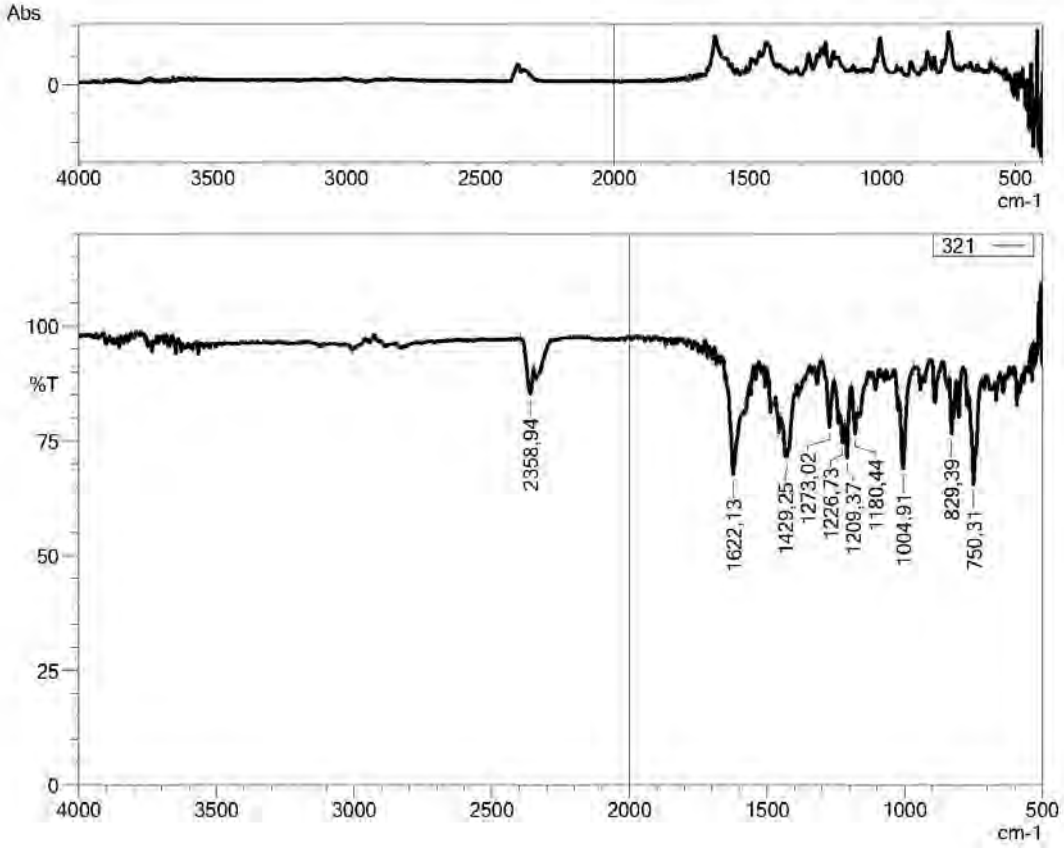


**Figure 5.164.** *IR spectrum of compound **D32***

### 5.1.4.33. *(5-methoxy-3-methylbenzofuran-2-yl)(4-methylpiperazin-1-yl)methanone (D33)*

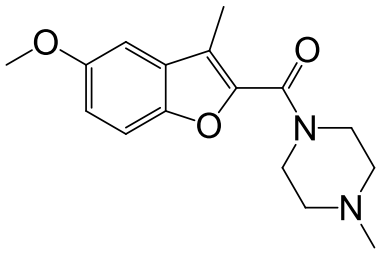


**Figure 5.165.** *Molecular structure of compound **D33***

**Physical Properties: Texture:** semisolid, **Color:** black, **M.P.:** 73-75ºC**, Yield:** 57%.

**IR (ATR) $\upsilon_{max}$ ($cm^{-1}$):** 3065 ($SP^2$ C-H stretching, aromatic), 2939-2792 ($SP^3$ C-H stretching, methylenes of piperazine, 4-methyl piperazine, and methoxy), 1622 (C=O stretching, amide), 1429 (C=C stretching, aromatic), 1226-1209 (C-O stretching, ether), 1180, 1002 (C-N stretching, tertiary amine and/or ether), 829-752 (C-H aromatic out-of-plane bending).

**$^1$H NMR (300 MHz) (DMSO-$d_6$) $\delta$ (ppm):** 2.21 (s, 3H, **4-methyl**piperazine), 2.31 (s, 3H, **3-methyl**benzofuran), 2.35 (t, *J*= 4.47 Hz, 4H, piperazine-3, 5), 3.59 (brs, 4H, piperazine-2, 6), 3.82 (s, 3H, **5-methoxy**benzofuran), 7.01 (dd, *J*= 8.97, 2.61 Hz, 1H, benzofuran-6), 7.19 (s, 1H, benzofuran-4), 7.50 (d, *J*= 8.96 Hz, 1H, benzofuran-7).

**$^{13}$C NMR (300 MHz) (DMSO-$d_6$) $\delta$ (ppm):** 9.03 (**3-methyl**benzofuran), 42.23 (piperazine), 46.02 (**4-methyl**piperazine), 46.85 (piperazine), 55.29 (piperazine), 56.18 (**5-methoxy**benzofuran), 102.97, 112.68, 115.87, 119.53, 129.55, 145.03, 148.20, 156.33, 160.25 (benzofuran-**CO-**piperazine).

**HRMS (ESI) (m/z) $[M+1]^+$:** for $C_{16}H_{20}N_2O_3$ calculated: 289.1547; found: 289.1537.

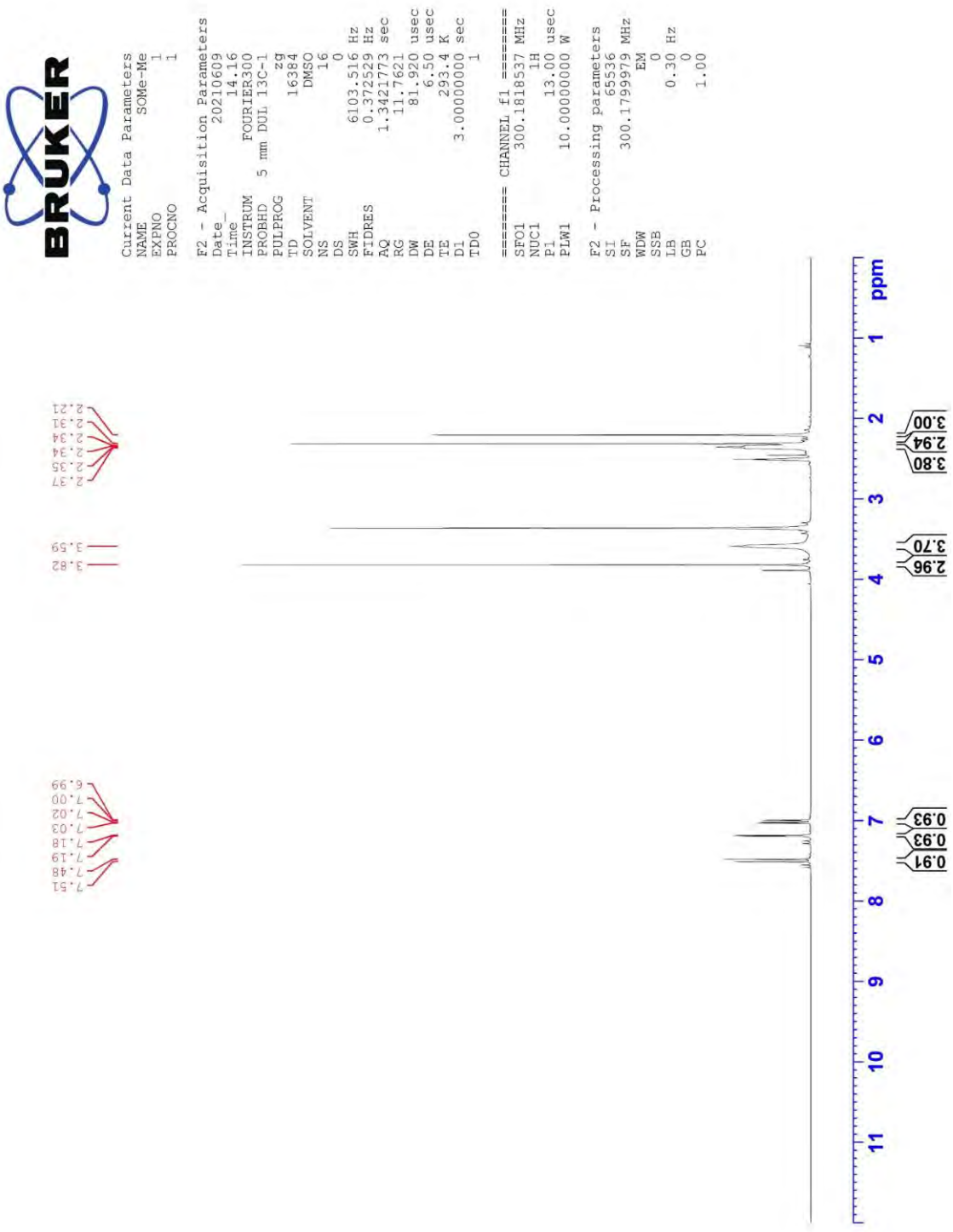


**Figure 5.166.** *[1]H NMR spectrum of compound **D33***

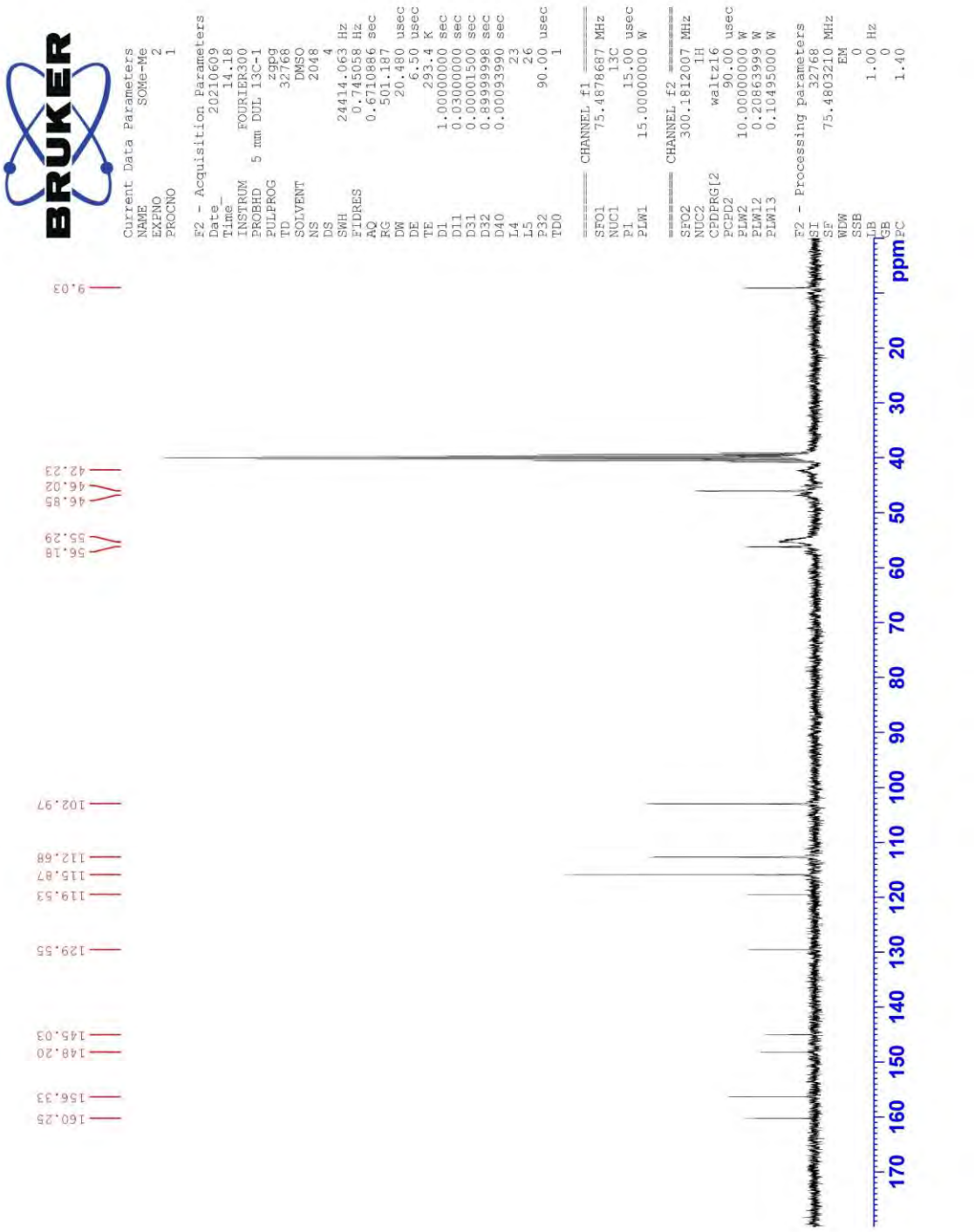


**Figure 5.167.** *$^{13}$C NMR spectrum of compound **D33***

| Elmt | Val. | Min | Max | Elmt | Val. | Min | Max | Elmt | Val. | Min | Max | Elmt | Val. | Min | Max | Use Adduct |
|---|---|---|---|---|---|---|---|---|---|---|---|---|---|---|---|---|
| H | 1 | 10 | 40 | O | 2 | 1 | 4 | S | 2 | 0 | 0 | Ru | 2 | 0 | 0 | H |
| C | 4 | 9 | 40 | F | 1 | 0 | 0 | Cl | 1 | 0 | 0 | Pd | 2 | 0 | 0 | |
| N | 3 | 2 | 6 | P | 3 | 0 | 0 | Br | 1 | 0 | 0 | I | 3 | 0 | 0 | |

Error Margin (ppm): 5
HC Ratio: unlimited
Max Isotopes: 3
MSn Iso RI (%): 10.00

DBE Range: 5.0 - 20.0
Apply N Rule: yes
Isotope RI (%): 1.00
MSn Logic Mode: AND

Electron Ions: both
Use MSn Info: yes
Isotope Res: 9000
Max Results: 150

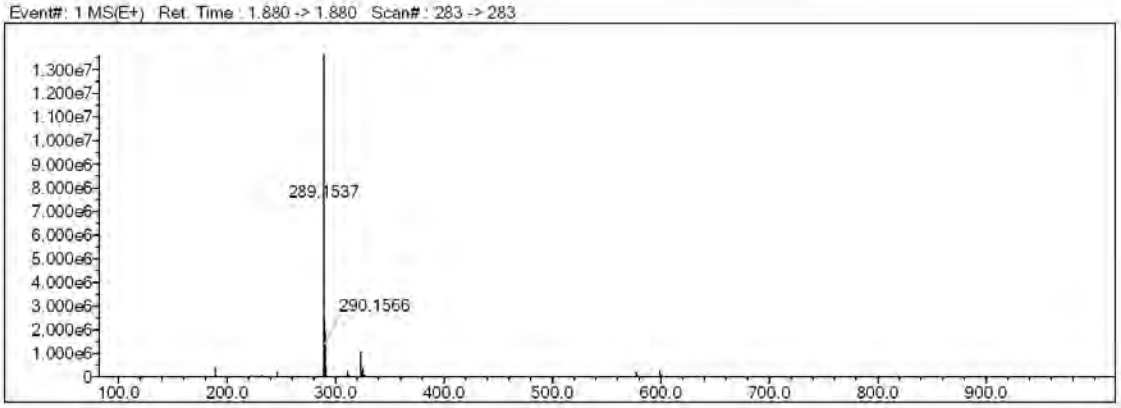


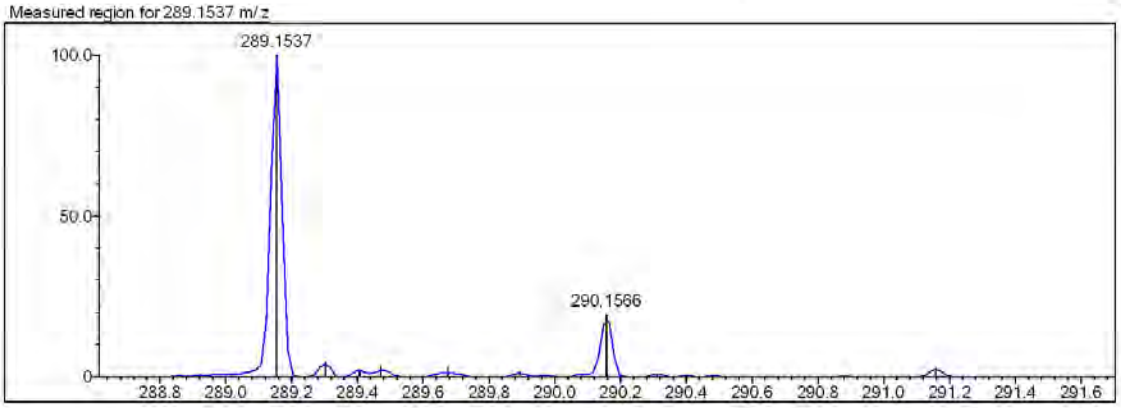


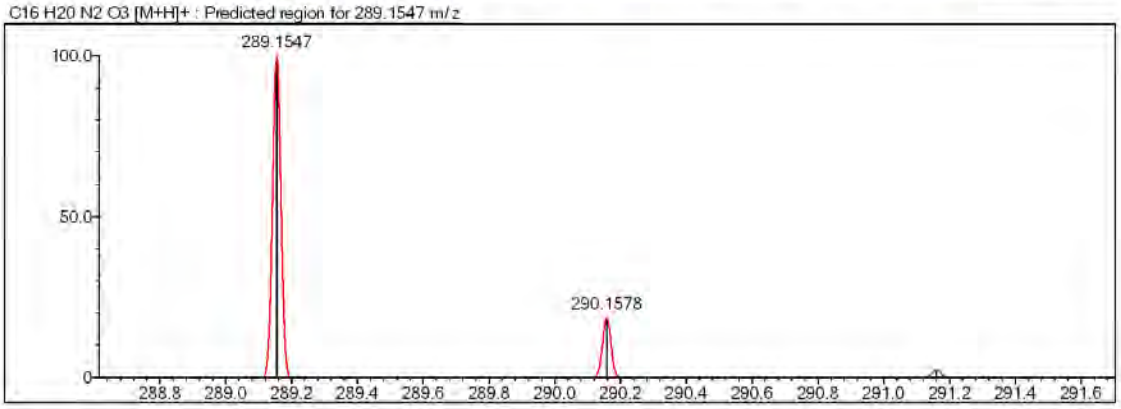


| Rank | Score | Formula (M) | Ion | Meas. m/z | Pred. m/z | Df. (mDa) | Df. (ppm) | Isc | DBE |
|---|---|---|---|---|---|---|---|---|---|
| 1 | 93.85 | C16 H20 N2 O3 | [M+H]+ | 289.1537 | 289.1547 | -1.0 | -3.46 | 100.00 | 8.0 |

**Figure 5.168.** *High-resolution mass spectrum of compound **D33***

DOPNALAB

| | Item | Value |
|---|---|---|
| | Acquired Date&Time | 27.05.2021 13:28:02 |
| | Acquired by | System Administrator |
| | Filename | C:\Users\dopnalab\Desktop\sa\331.ispd |
| | Spectrum name | 331 |
| | Sample name | 33 |
| | Sample ID | |
| | Option | |
| | Comment | |
| | No. of Scans | 15 |
| | Resolution | 4 [cm-1] |
| | Apodization | Happ-Genzel |

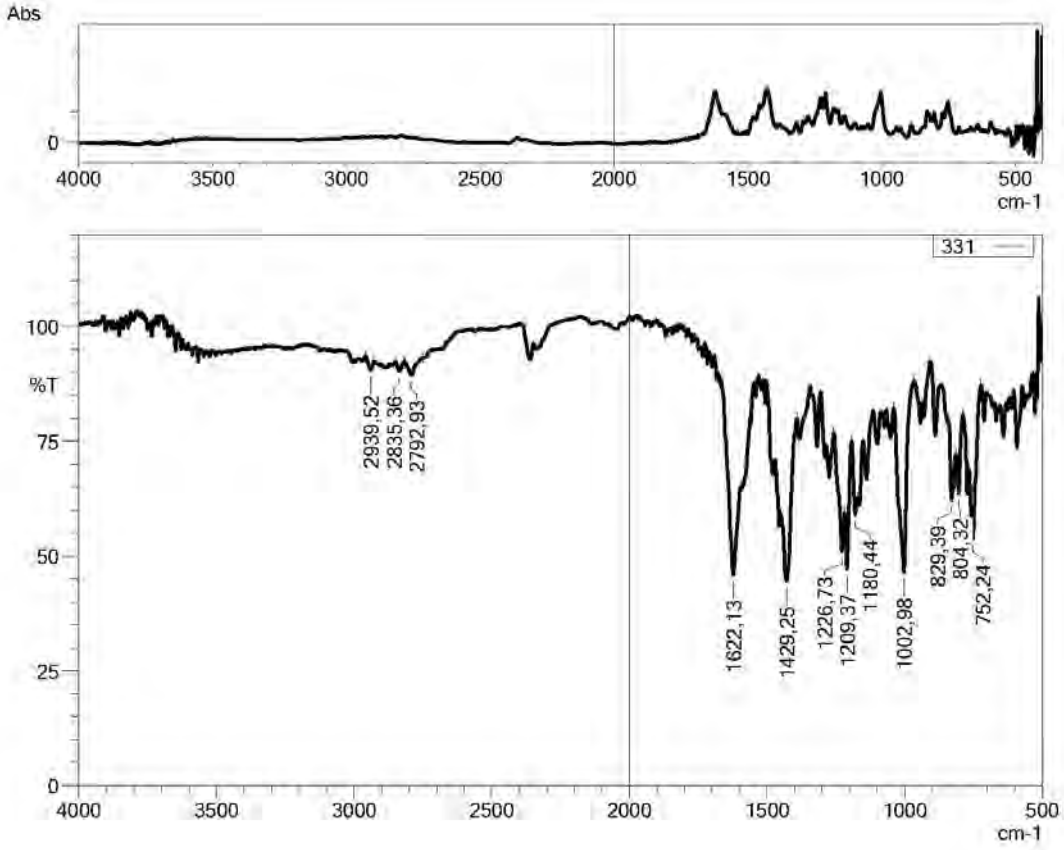


**Figure 5.169.** *IR spectrum of compound **D33***

### 5.1.4.34. *(4-ethylpiperazin-1-yl)(5-methoxy-3-methylbenzofuran-2-yl)methanone (D34)*

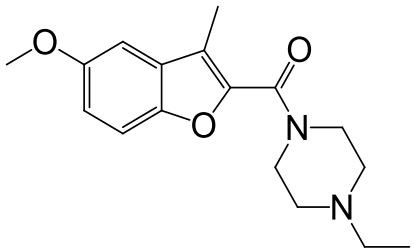

**Figure 5.170.** *Molecular structure of compound* ***D34***

**Physical Properties: Texture:** liquid, **Color:** black, **Yield:** 54%.

**IR (ATR) $\upsilon_{max}$ ($cm^{-1}$):** 2970-2767 ($SP^3$ C-H stretching, methylenes of piperazine, ethyl-methyl piperazine, and methoxy), 1625 (C=O stretching, amide), 1431 (C=C stretching, aromatic), 1236-1211 (C-O stretching, ether), 1163, 1010 (C-N stretching, tertiary amine and/or C-O stretching, ether), 823-754 (C-H aromatic out-of-plane bending).

**$^1$H NMR (300 MHz) (DMSO-$d_6$) $\delta$ (ppm):** 1.01 (t, *J*= 7.17 Hz, 3H, piperazine-$CH_2$-**$CH_3$**) 2.31 (s, 3H, **3-methyl**benzofuran), 2.36 (q, *J*= 14.36, 7.13 Hz, 2H, piperazine-**$CH_2$**-$CH_3$), 2.41 (t, *J*= 4.56 Hz, 4H, piperazine-3, 5), 3.59 (t, *J*= 4.51 Hz, 4H, piperazine-2, 6), 3.82 (s, 3H, **5-methoxy**benzofuran), 7.01 (dd, *J*= 8.97, 2.61 Hz, 1H, benzofuran-6), 7.19 (d, *J*= 2.55 Hz, 1H, benzofuran-4), 7.49 (d, *J*= 8.96 Hz, 1H, benzofuran-7).

**$^{13}$C NMR (300 MHz) (DMSO-$d_6$) $\delta$ (ppm):** 9.04 (**3-methyl**benzofuran), 12.35 (piperazine-$CH_2$-**$CH_3$**) 42.40 (piperazine), 46.95 (piperazine), 51.90 (piperazine-**$CH_2$**-$CH_3$), 52.69 (piperazine), 56.17 (**5-methoxy**benzofuran), 102.96, 112.67, 115.87, 119.52, 129.55, 145.05, 148.19, 156.33, 160.18 (benzofuran-**CO**-piperazine).

**HRMS (ESI) (m/z) $[M+1]^+$:** for $C_{17}H_{22}N_2O_3$ calculated: 303.1703; found: 303.1690.

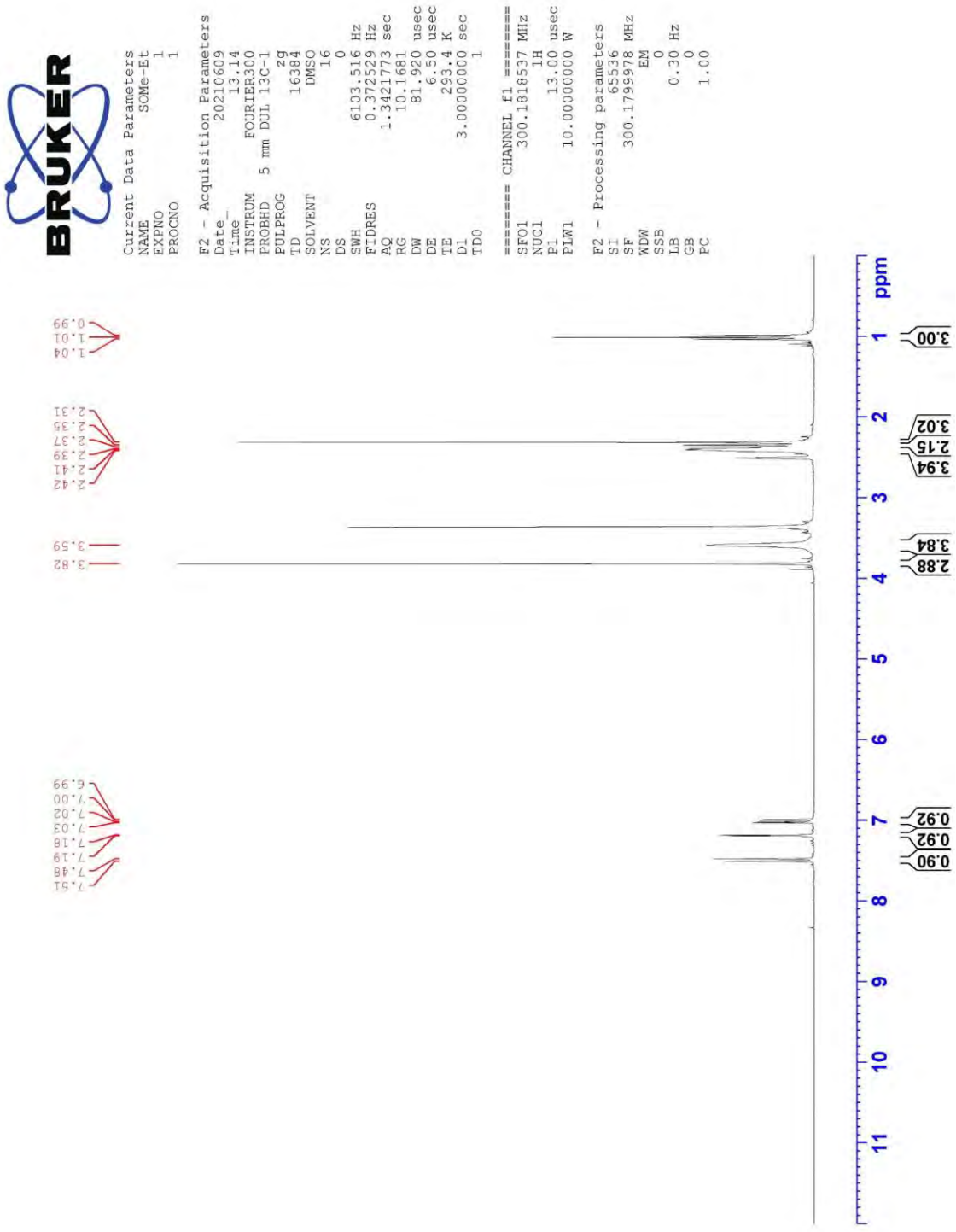


**Figure 5.171.** *[1]H NMR spectrum of compound **D34***

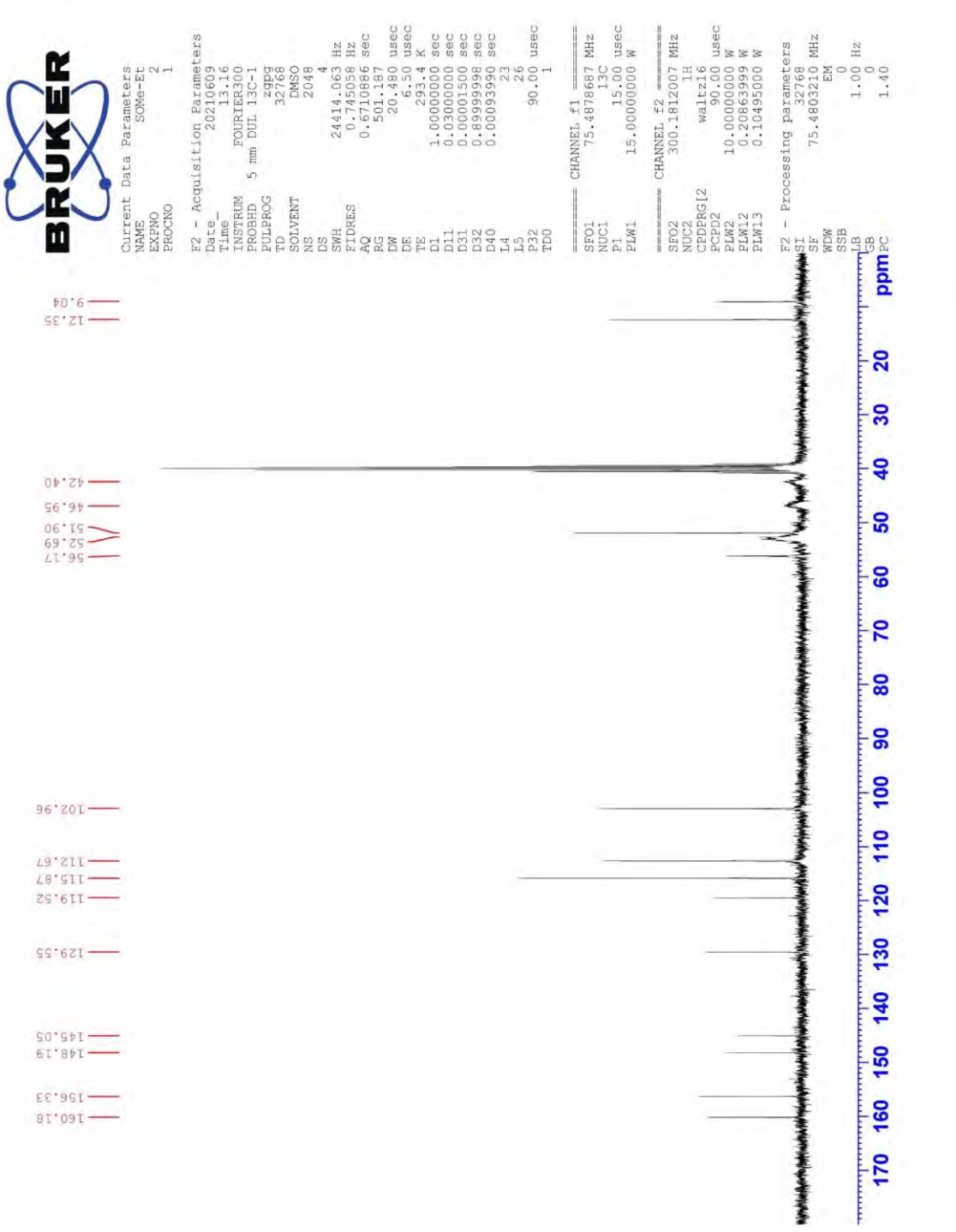


**Figure 5.172.** *$^{13}$C NMR spectrum of compound **D34***

| Elmt | Val. | Min | Max | Elmt | Val. | Min | Max | Elmt | Val. | Min | Max | Elmt | Val. | Min | Max | Use Adduct |
|---|---|---|---|---|---|---|---|---|---|---|---|---|---|---|---|---|
| H | 1 | 10 | 40 | O | 2 | 1 | 4 | S | 2 | 0 | 0 | Ru | 2 | 0 | 0 | H |
| C | 4 | 9 | 40 | F | 1 | 0 | 0 | Cl | 1 | 0 | 0 | Pd | 2 | 0 | 0 | |
| N | 3 | 2 | 6 | P | 3 | 0 | 0 | Br | 1 | 0 | 0 | I | 3 | 0 | 0 | |

Error Margin (ppm): 5
HC Ratio: unlimited
Max Isotopes: 3
MSn Iso RI (%): 10.00

DBE Range: 5.0 - 20.0
Apply N Rule: yes
Isotope RI (%): 1.00
MSn Logic Mode: AND

Electron Ions: both
Use MSn Info: yes
Isotope Res: 9000
Max Results: 150

Event#: 1 MS(E+) Ret. Time: 1.787 -> 1.787 Scan#: 269 -> 269

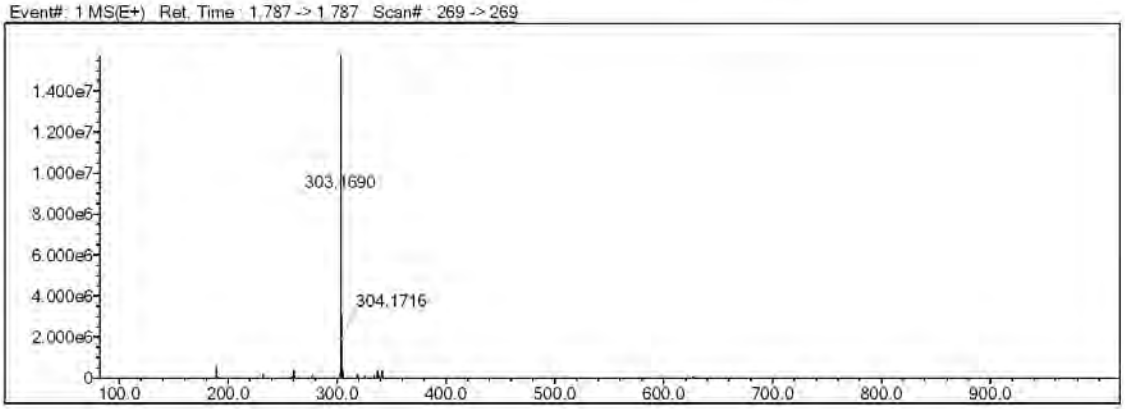


Measured region for 303.1690 m/z

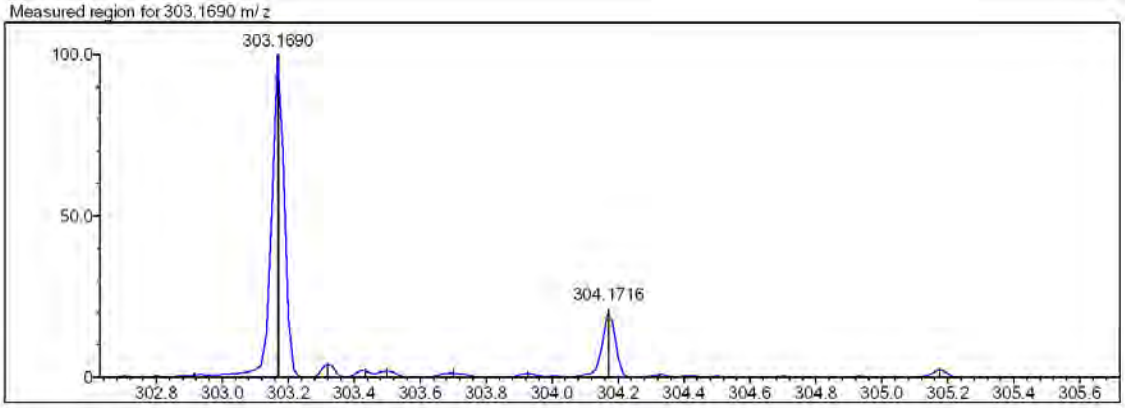


C17 H22 N2 O3 [M+H]+ : Predicted region for 303.1703 m/z

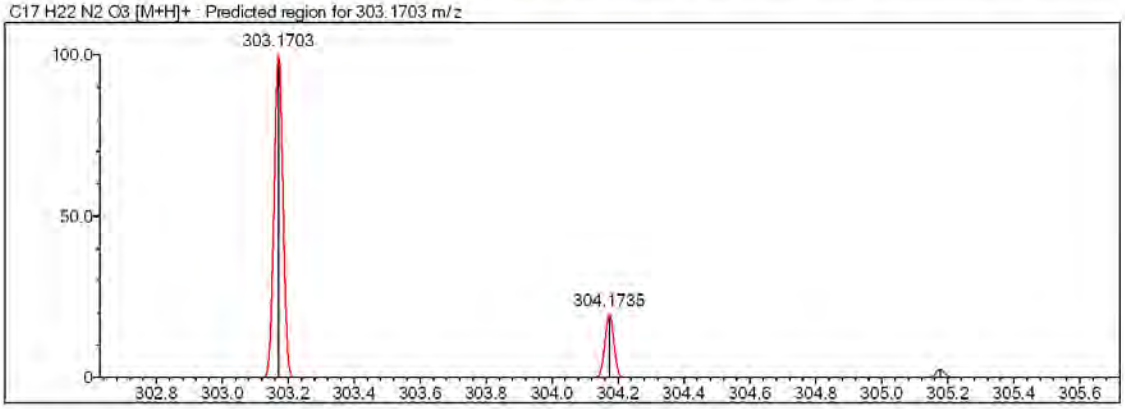


| Rank | Score | Formula (M) | Ion | Meas. m/z | Pred. m/z | Df. (mDa) | Df. (ppm) | Isc | DBE |
|---|---|---|---|---|---|---|---|---|---|
| 1 | 82.45 | C17 H22 N2 O3 | [M+H]+ | 303.1690 | 303.1703 | -1.3 | -4.29 | 89.84 | 8.0 |

**Figure 5.173.** *High-resolution mass spectrum of compound* ***D34***

DOPNALAB

| | Item | Value |
|---|---|---|
| | Acquired Date&Time | 27.05.2021 13:36:25 |
| | Acquired by | System Administrator |
| | Filename | C:\Users\dopnalab\Desktop\sa\341.ispd |
| | Spectrum name | 341 |
| | Sample name | 34 |
| | Sample ID | |
| | Option | |
| | Comment | |
| | No. of Scans | 16 |
| | Resolution | 4 [cm-1] |
| | Apodization | Happ-Genzel |

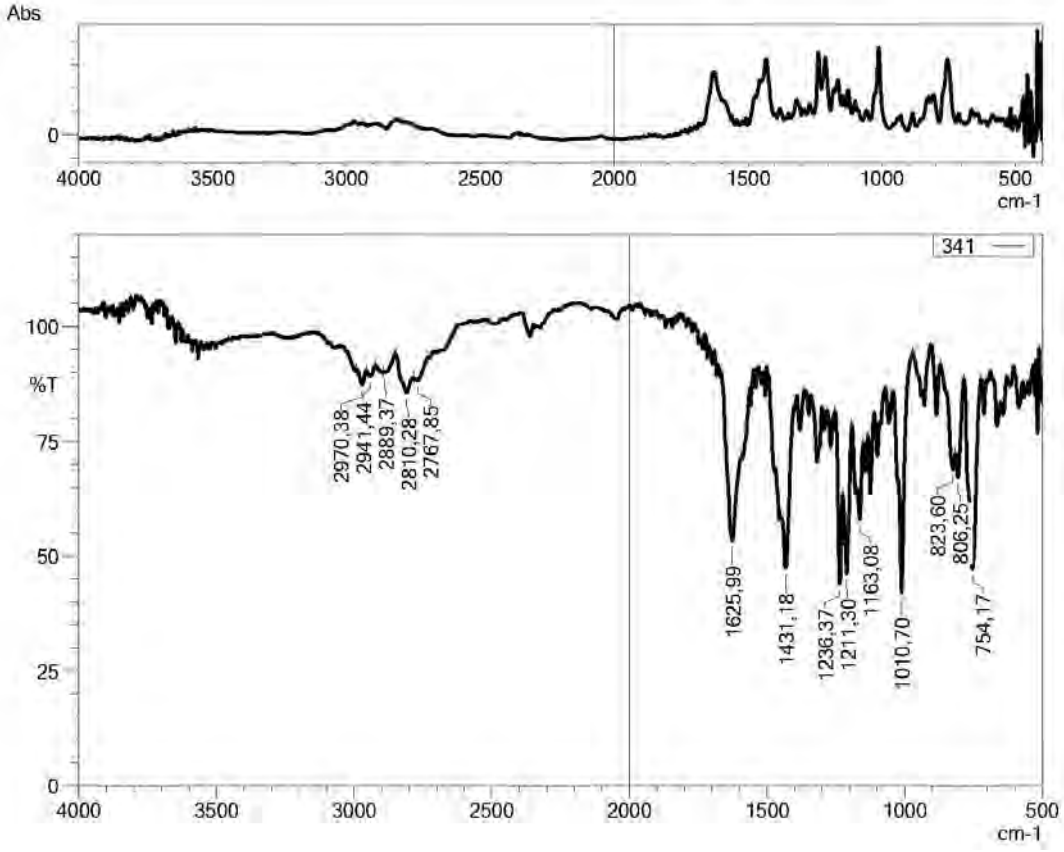


**Figure 5.174.** *IR spectrum of compound **D34***

### 5.1.4.35. *(4-(2-(dimethylamino)ethyl)piperazin-1-yl)(5-methoxy-3-methylbenzofuran-2-yl)methanone (D35)*

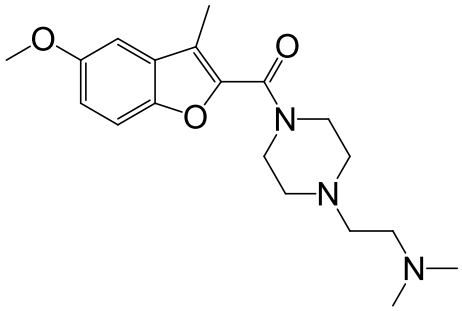

**Figure 5.175.** *Molecular structure of compound* ***D35***

**Physical Properties: Texture:** liquid, **Color:** black, **Yield:** 75%.

**IR (ATR) $\upsilon_{max}$ ($cm^{-1}$):** 2972-2767 ($SP^3$ C-H stretching, methylenes of piperazine, dimethylaminoethyl-piperazine, and methoxy), 1625 (C=O stretching, amide), 1456-1433 (C=C stretching, aromatic), 1234-1211 (C-O stretching, ether), 1132, 1008 (C-N stretching, tertiary amine and/or C-O stretching, ether), 823-752 (C-H aromatic out-of-plane bending).

**$^1$H NMR (300 MHz) (DMSO-$d_6$) $\delta$ (ppm):** 2.12 (s, 6H, -N**($CH_3$)$_2$**), 2.30 (s, 3H, **3-methyl**benzofuran), 2.33-2.41 (m, 4H, piperazine-(**$CH_2$)$_2$**-N), 2.44 (t, *J*= 4.64 Hz, 4H, piperazine-), 3.57 (brs, 4H, piperazine-2, 6), 3.81 (s, 3H, **5-methoxy**benzofuran), 7.00 (dd, *J*= 8.96, 2.57 Hz, 1H, benzofuran-6), 7.18 (d, *J*= 2.42 Hz, 1H, benzofuran-4), 7.48 (d, *J*= 8.96 Hz, 1H, benzofuran-7).

**$^{13}$C NMR (300 MHz) (DMSO-$d_6$) $\delta$ (ppm):** 9.04 (**3-methyl**benzofuran), 42.56 (piperazine), 45.99 (-N**($CH_3$)$_2$**), 46.76 (piperazine), 53.55 (piperazine), 56.02 (**5-methoxy**benzofuran), 56.99 (piperazine-(**$CH_2$)$_2$**-N), 102.95, 112.66, 115.86, 119.55, 129.55, 145.03, 148.19, 156.33, 160.16 (benzofuran-**CO-**piperazine).

**HRMS (ESI) (m/z) $[M+1]^+$:** for $C_{19}H_{27}N_3O_3$ calculated: 346.2125; found: 346.2125.

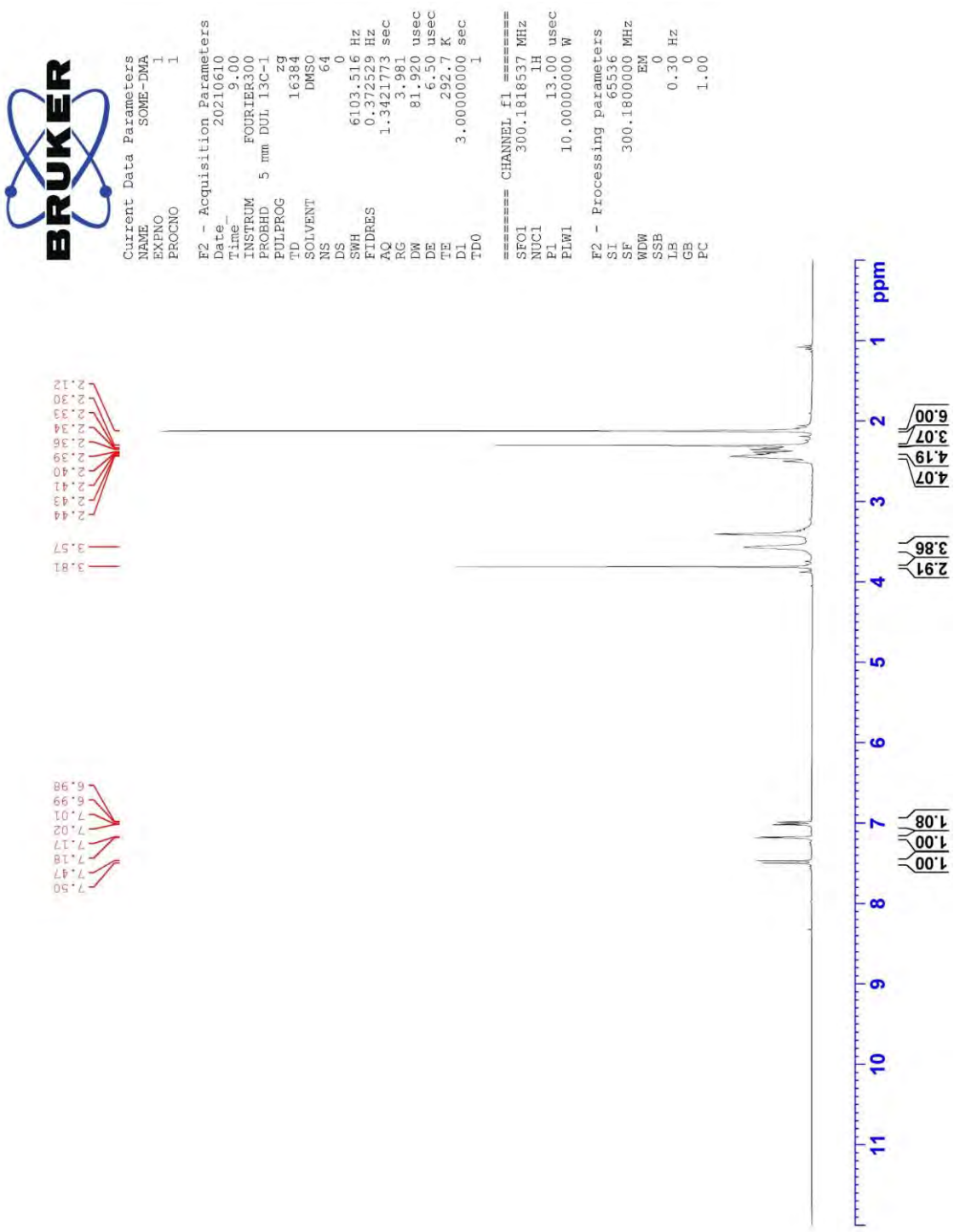


**Figure 5.176.** *$^{1}H$ NMR spectrum of compound **D35***

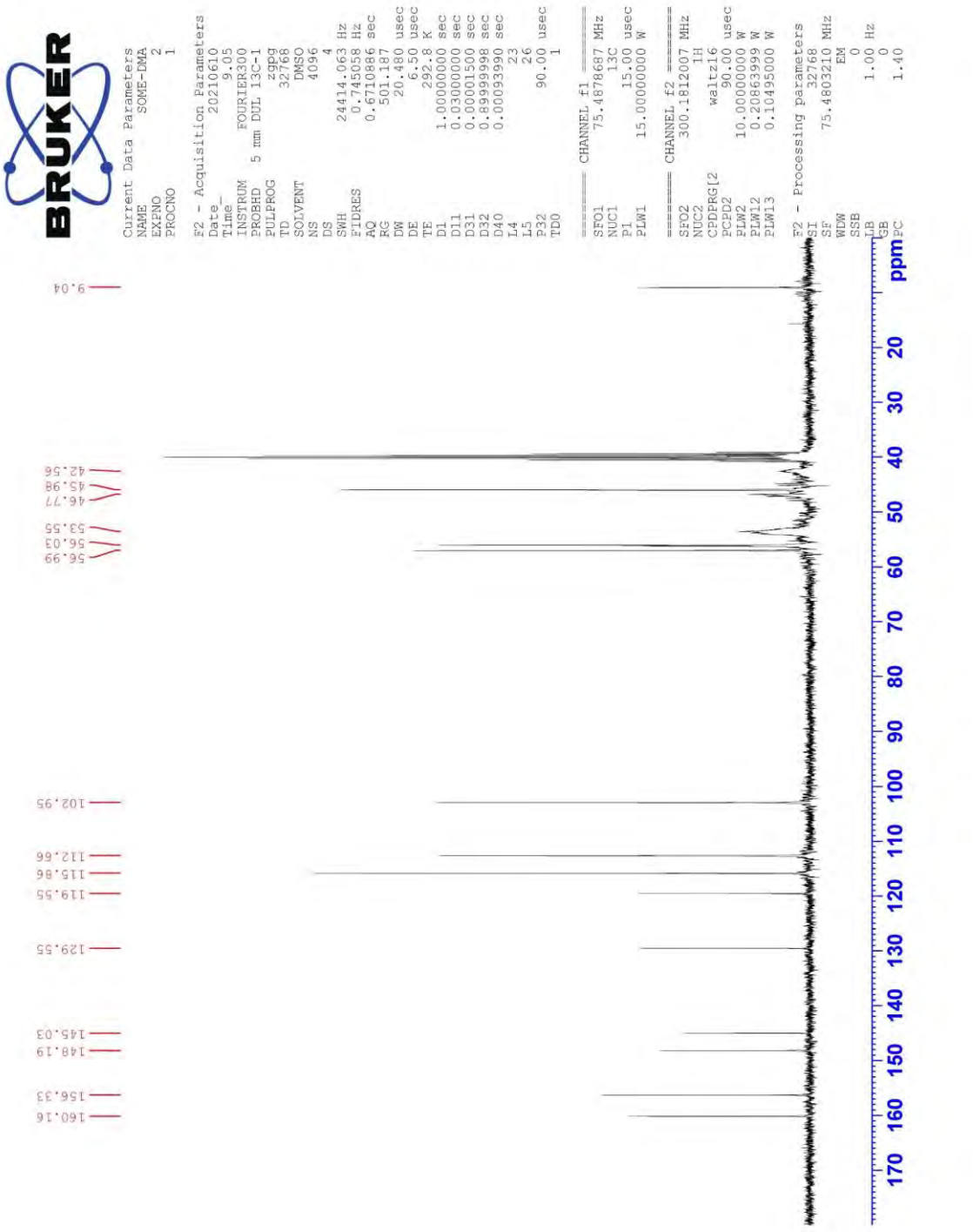


**Figure 5.177.** *$^{13}$C NMR spectrum of compound **D35***

Data File: C:\LabSolutions\Data\Analiz\A.Çağrı\D-35_15.lcd

| Elmt | Val. | Min | Max | Elmt | Val. | Min | Max | Elmt | Val. | Min | Max | Elmt | Val. | Min | Max | Use Adduct |
|---|---|---|---|---|---|---|---|---|---|---|---|---|---|---|---|---|
| H | 1 | 0 | 40 | O | 2 | 0 | 5 | S | 2 | 0 | 0 | Ru | 2 | 0 | 0 | H |
| C | 4 | 0 | 40 | F | 1 | 0 | 0 | Cl | 1 | 0 | 0 | Pd | 2 | 0 | 0 | |
| N | 3 | 0 | 4 | P | 3 | 0 | 0 | Br | 1 | 0 | 0 | I | 3 | 0 | 0 | |

Error Margin (ppm): 5
HC Ratio: unlimited
Max Isotopes: 3
MSn Iso RI (%): 10.00

DBE Range: 0.0 - 20.0
Apply N Rule: yes
Isotope RI (%): 1.00
MSn Logic Mode: AND

Electron Ions: both
Use MSn Info: yes
Isotope Res: 9000
Max Results: 150

Event#: 1 MS(E+) Ret. Time: 1.920 Scan#: 289

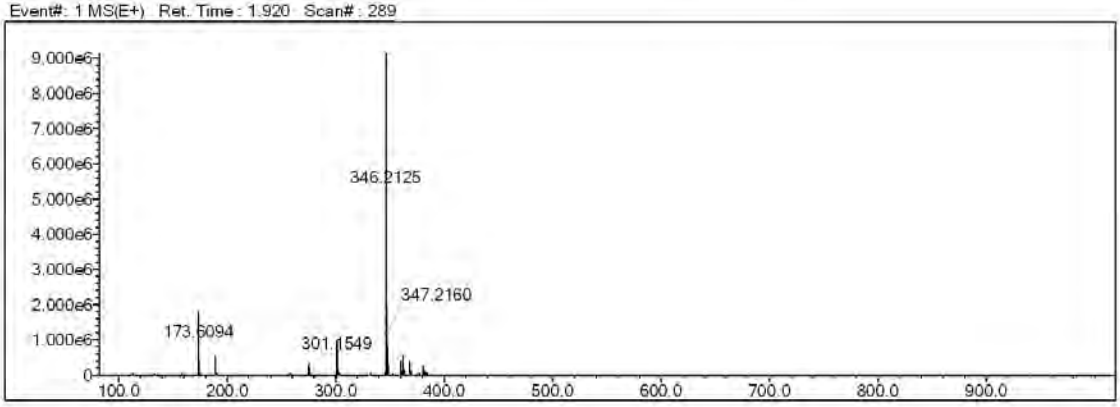


Measured region for 346.2125 m/z

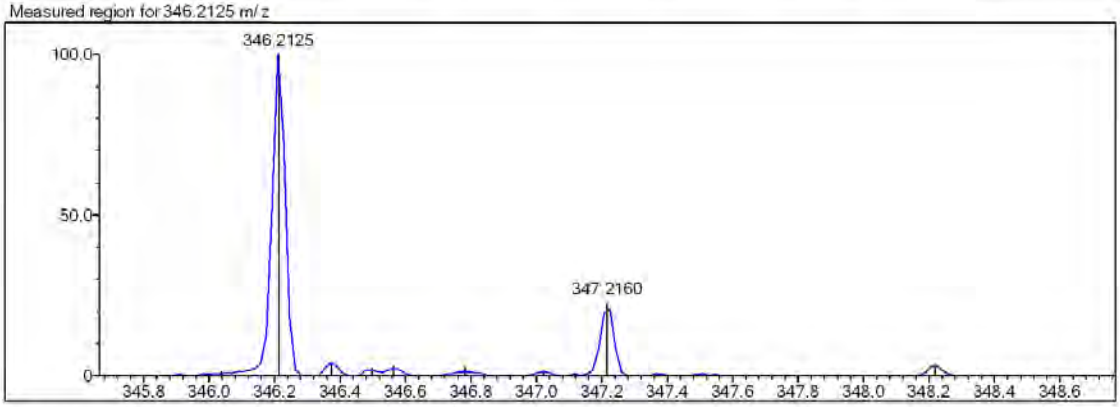


C19 H27 N3 O3 [M+H]+ : Predicted region for 346.2125 m/z

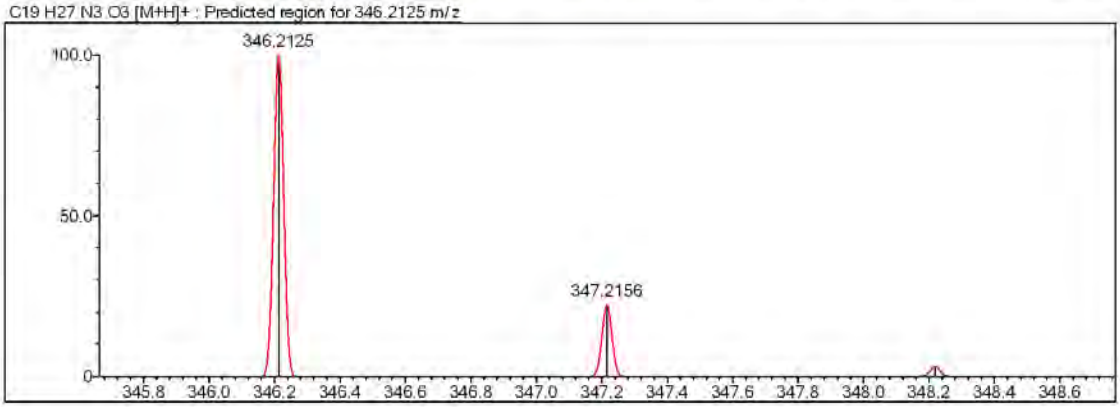


| Rank | Score | Formula (M) | Ion | Meas. m/z | Pred. m/z | Df. (mDa) | Df. (ppm) | Isc | DBE |
|---|---|---|---|---|---|---|---|---|---|
| 1 | 99.87 | C19 H27 N3 O3 | [M+H]+ | 346.2125 | 346.2125 | -0.0 | 0.00 | 99.87 | 8.0 |

**Figure 5.178.** *High-resolution mass spectrum of compound **D35***

DOPNALAB

| | Item | Value |
|---|---|---|
| | Acquired Date&Time | 27.05.2021 13:43:46 |
| | Acquired by | System Administrator |
| | Filename | C:\Users\dopnalab\Desktop\sa\352.ispd |
| | Spectrum name | 352 |
| | Sample name | 35 |
| | Sample ID | |
| | Option | |
| | Comment | |
| | No. of Scans | 16 |
| | Resolution | 4 [cm-1] |
| | Apodization | Happ-Genzel |

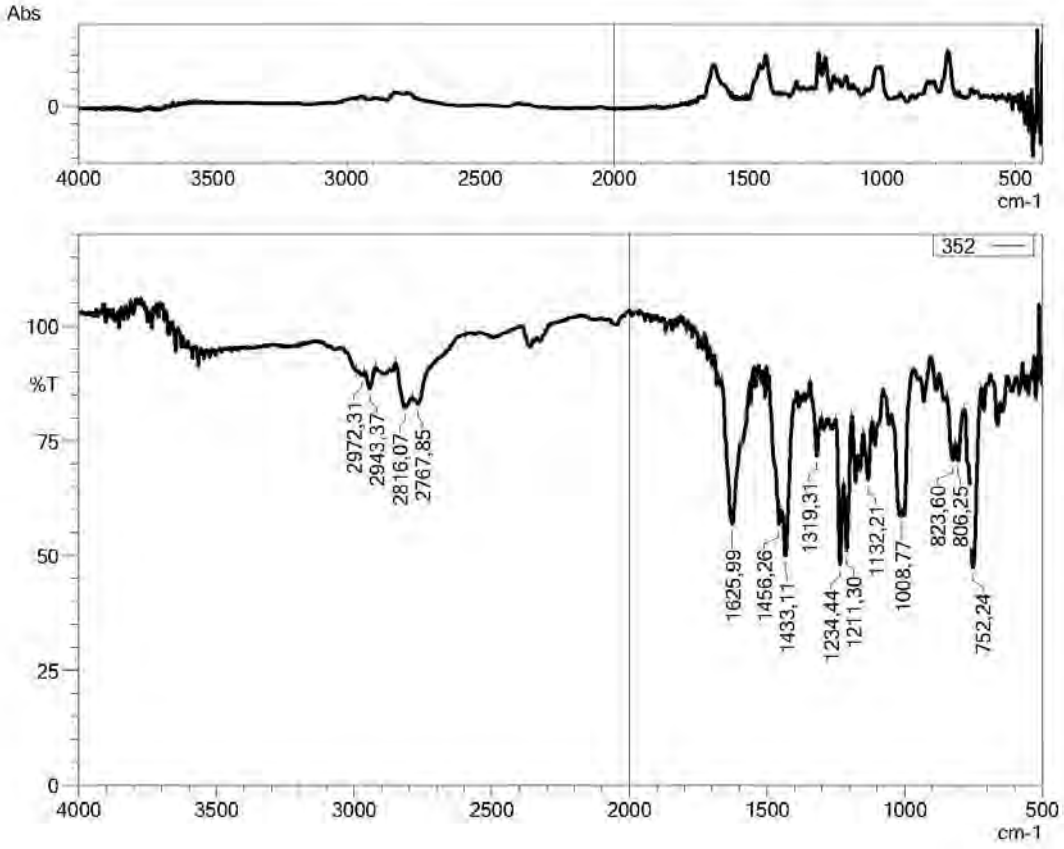


**Figure 5.179.** *IR spectrum of compound **D35***

### 5.1.4.36. *(4-benzylpiperazin-1-yl)(5-methoxy-3-methylbenzofuran-2-yl)methanone (D36)*

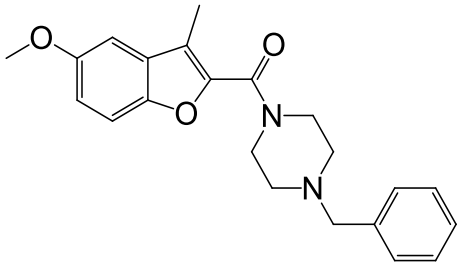

**Figure 5.180.** *Molecular structure of compound **D36***

**Physical Properties: Texture:** liquid, **Color:** black, **Yield:** 62%.

**IR (ATR) $\upsilon_{max}$ ($cm^{-1}$):** 3061 ($SP^2$ C-H stretching, aromatic), 2933-2808 ($SP^3$ C-H stretching, methoxy, and methylenes of piperazine and benzyl), 1625 (C=O stretching, amide), 1431 (C=C stretching, aromatic), 1230-1211 (C-O stretching, ether), 1018-999 (C-N stretching, tertiary amine and/or ether), 804-698 (C-H aromatic out-of-plane bending).

**$^1$H NMR (300 MHz) (DMSO-$d_6$) $\delta$ (ppm):** 2.30 (s, 3H, **3-methyl**benzofuran), 2.42 (t, *J*= 4.46 Hz, 4H, piperazine-3, 5), 3.52 (s, 2H, phenyl-**$CH_2$**-piperazine), 3.60 (t, *J*= 4.50 Hz, 4H, piperazine-2, 6), 3.81 (s, 3H, **5-methoxy**benzofuran), 7.00 (dd, *J*= 8.97, 2.61 Hz, 1H, benzofuran-6), 7.18 (d, *J*= 2.55 Hz, 1H, benzofuran-4), 7.25-7.28 (m, 1H, phenyl-4), 7.32-7.34 (m, 4H, phenyl-2,3,5,6), 7.48 (d, *J*= 8.97 Hz, 1H, benzofuran-7).

**$^{13}$C NMR (300 MHz) (DMSO-$d_6$) $\delta$ (ppm):** 9.09 (**3-methyl**benzofuran), 42.60 (piperazine), 47.04 (piperazine), 52.93 (piperazine), 56.18 (**5-methoxy**benzofuran), 62.23 (phenyl-**$CH_2$**-piperazine), 102.98, 112.68, 115.87, 119.53, 127.52, 128.69, 129.38, 129.54, 138.23, 145.01, 148.21, 156.33, 160.22 (benzofuran-**CO**-piperazine).

**HRMS (ESI) (m/z) $[M+1]^+$:** for $C_{22}H_{24}N_2O_3$ calculated: 365.1860; found: 365.1869.

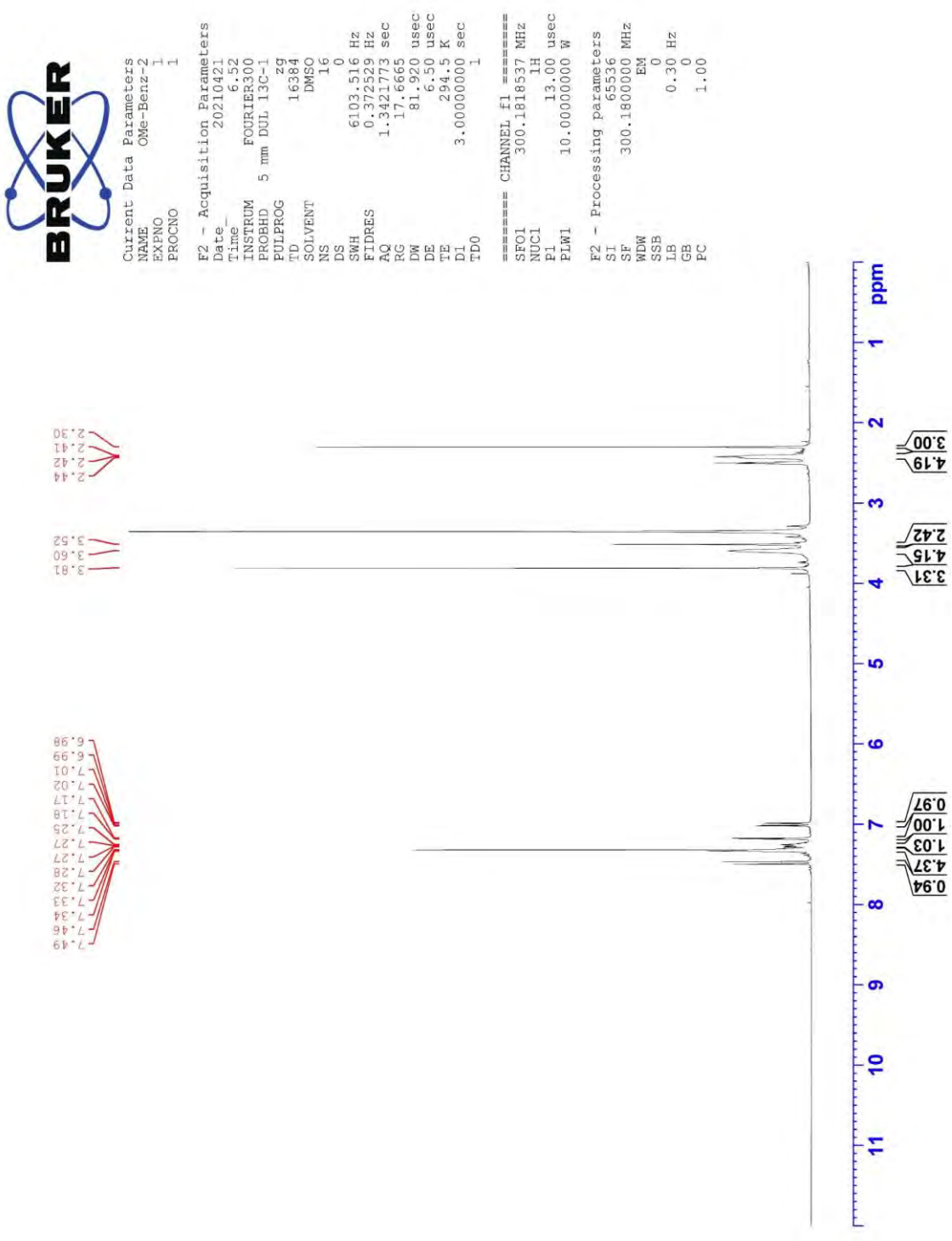


**Figure 5.181.** *[1]H NMR spectrum of compound **D36***

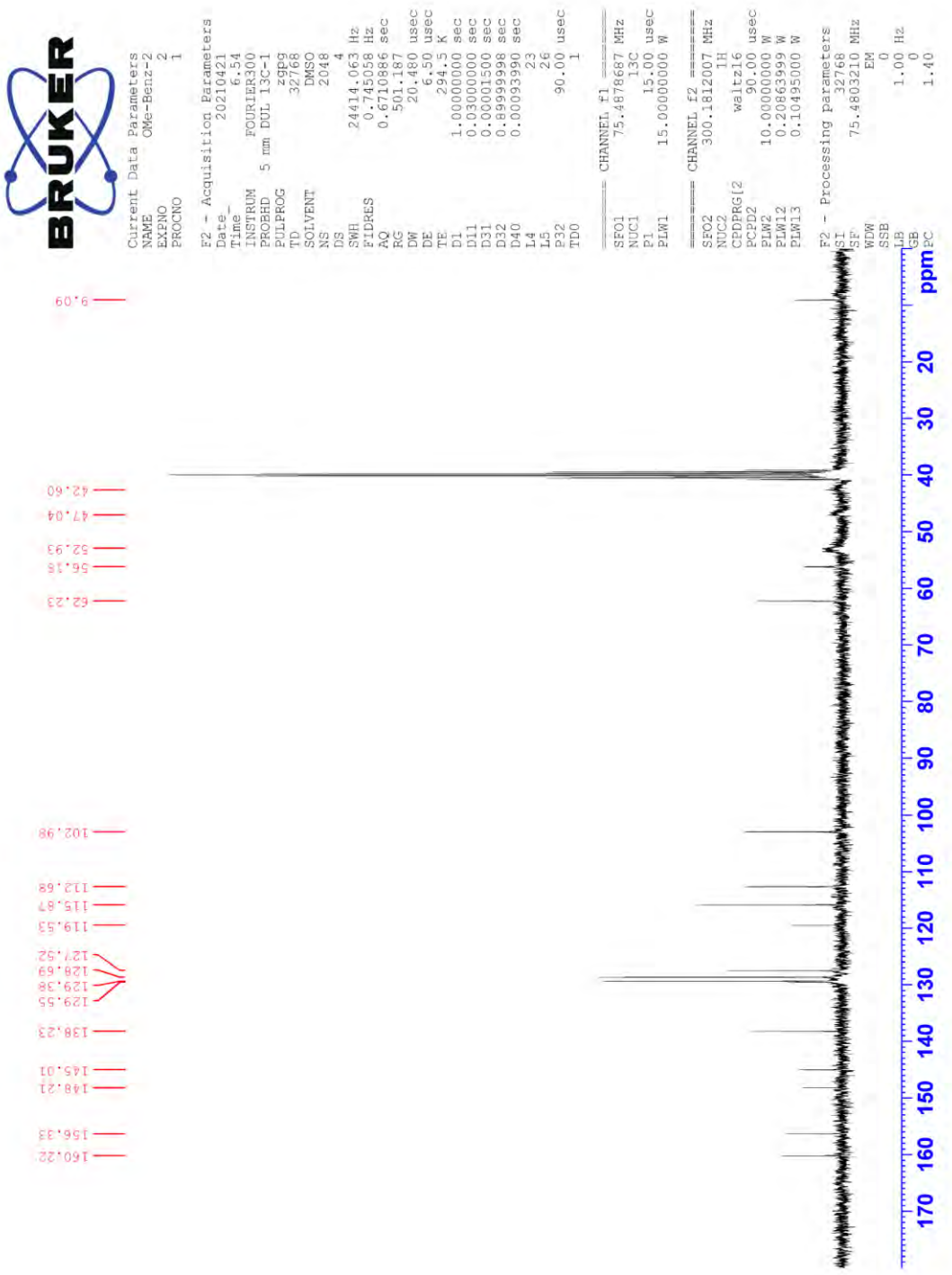


**Figure 5.182.** *$^{13}$C NMR spectrum of compound **D36***

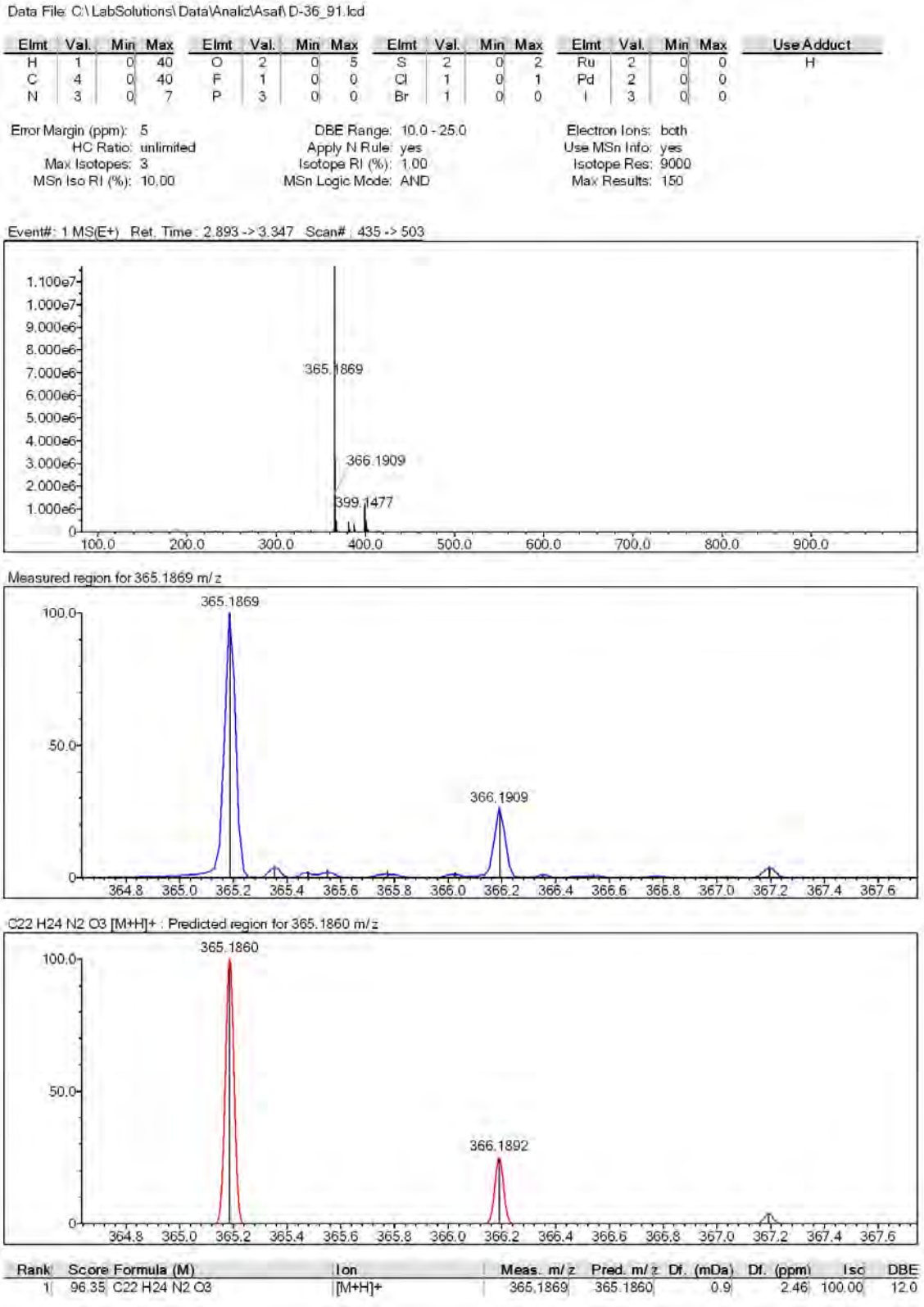


**Figure 5.183.** *High-resolution mass spectrum of compound* ***D36***

DOPNALAB

| Item | Value |
|---|---|
| Acquired Date&Time | 27.05.2021 13:02:09 |
| Acquired by | System Administrator |
| Filename | C:\Users\dopnalab\Desktop\sa\361.ispd |
| Spectrum name | 361 |
| Sample name | 36 |
| Sample ID | |
| Option | |
| Comment | |
| No. of Scans | 16 |
| Resolution | 4 [cm-1] |
| Apodization | Happ-Genzel |

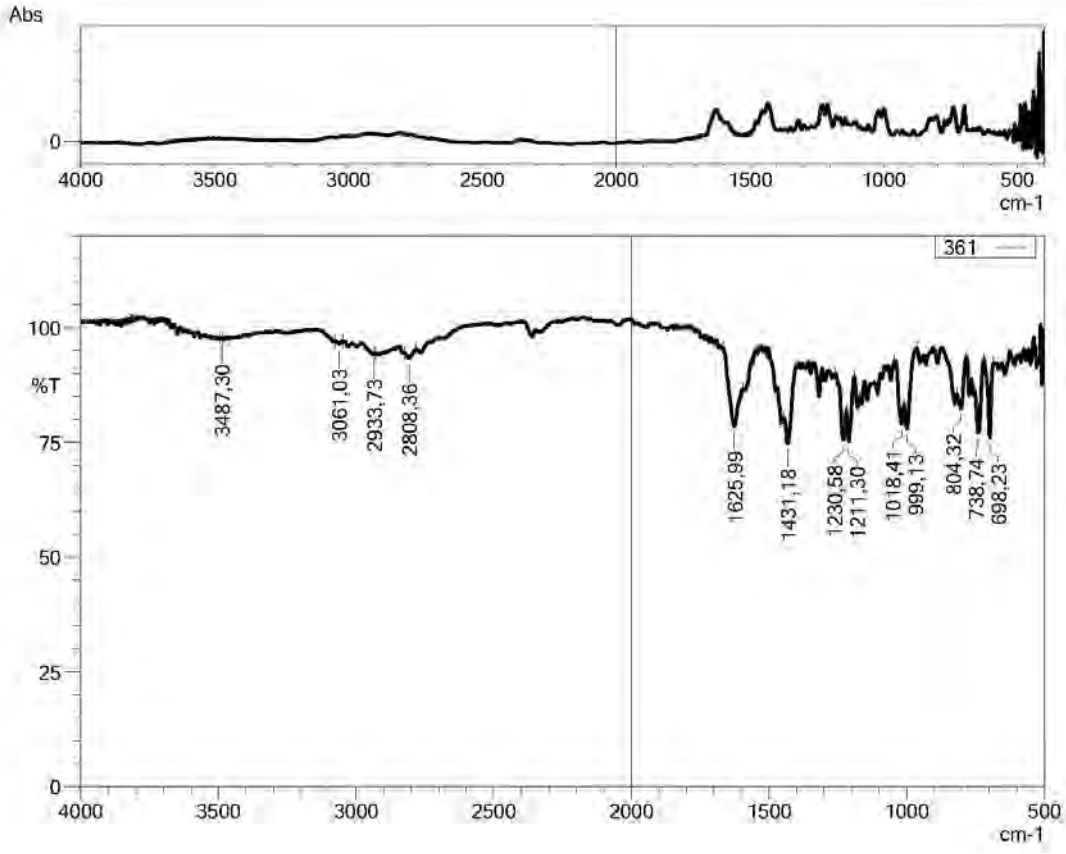


**Figure 5.184.** *IR spectrum of compound **D36***

### 5.1.4.37. *(5-methoxybenzofuran-2-yl)(4-phenylpiperazin-1-yl)methanone (D37)*

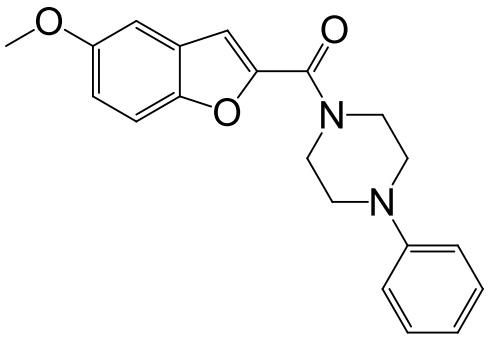

**Figure 5.185.** *Molecular structure of compound **D37***

**Physical Properties: Texture:** solid crystals, **Color:** light yellow, **M.P.:** 197-199ºC**, Yield:** 61%.

**IR (ATR) $\upsilon_{max}$ ($cm^{-1}$):** 3100 ($SP^2$ C-H stretching, aromatic), 2814-2767 ($SP^3$ C-H stretching, methoxy and methylenes of piperazine), 1633 (C=O stretching, amide), 1558 (C-H bending, indicative of non-substituted benzofuran at position 3), 1456-1429 (C=C stretching, aromatic), 1226-1209 (C-O stretching, ether), 1155, 1026 (C-N stretching, tertiary amine and/or ether), 808 (C-H aromatic out-of-plane bending, one peak, non-substituted benzofuran at position 3), 750-702 (C-H aromatic out-of-plane bending).

**$^1$H NMR (300 MHz) (DMSO-$d_6$) $\delta$ (ppm):** 3.22 (t, *J*= 4.70 Hz, 4H, piperazine-3, 5), 3.79 (s, 3H, **5-methoxy**benzofuran), 3.87 (brs, 4H, piperazine-2, 6), 6.82 (t, *J*= 7.26 Hz, 1H, phenyl-4), 6.98 (d, *J*= 7.89, 2H, phenyl-2, 6), 7.02 (dd, *J*= 9.02, 2.61 Hz, 1H, benzofuran-6), 7.21-7.27 (m, 3H, phenyl-3,5 and benzofuran-4), 7.38 (s, 1H, benzofuran-3), 7.59 (d, *J*= 9.02 Hz, 1H, benzofuran-7).

**$^{13}$C NMR (300 MHz) (DMSO-$d_6$) $\delta$ (ppm):** 49.05 (piperazine), 56.07 (**5-methoxy**benzofuran), 104.36, 111.79, 112.95, 116.28, 116.35, 119.89, 127.78, 129.49, 149.38, 151.14, 156.49, 159.24 (benzofuran-**CO**-piperazine).

**HRMS (ESI) (m/z) $[M+1]^+$:** for $C_{20}H_{20}N_2O_3$ calculated: 337.1547; found: 337.1551.

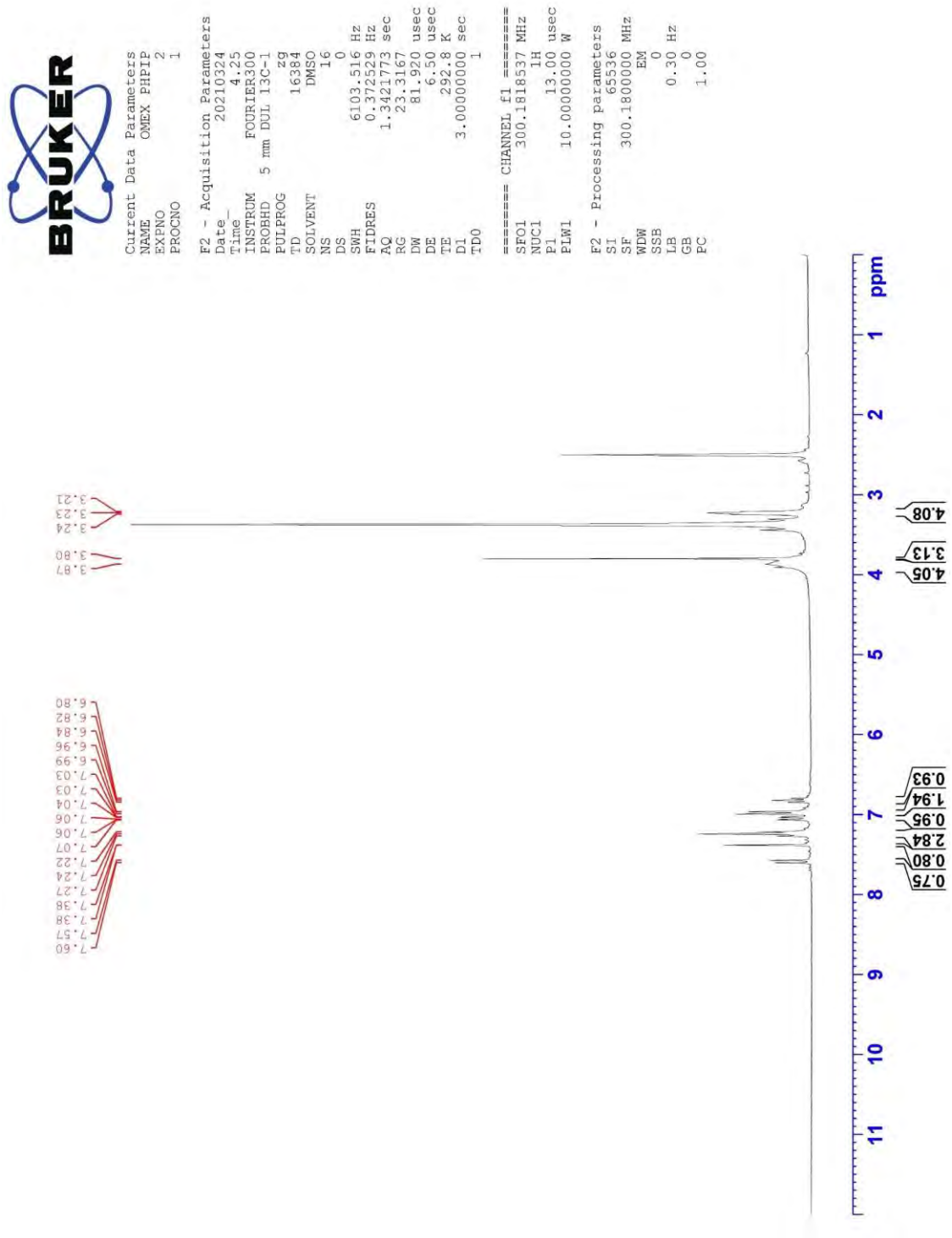


**Figure 5.186.** *[1]H NMR spectrum of compound **D37***

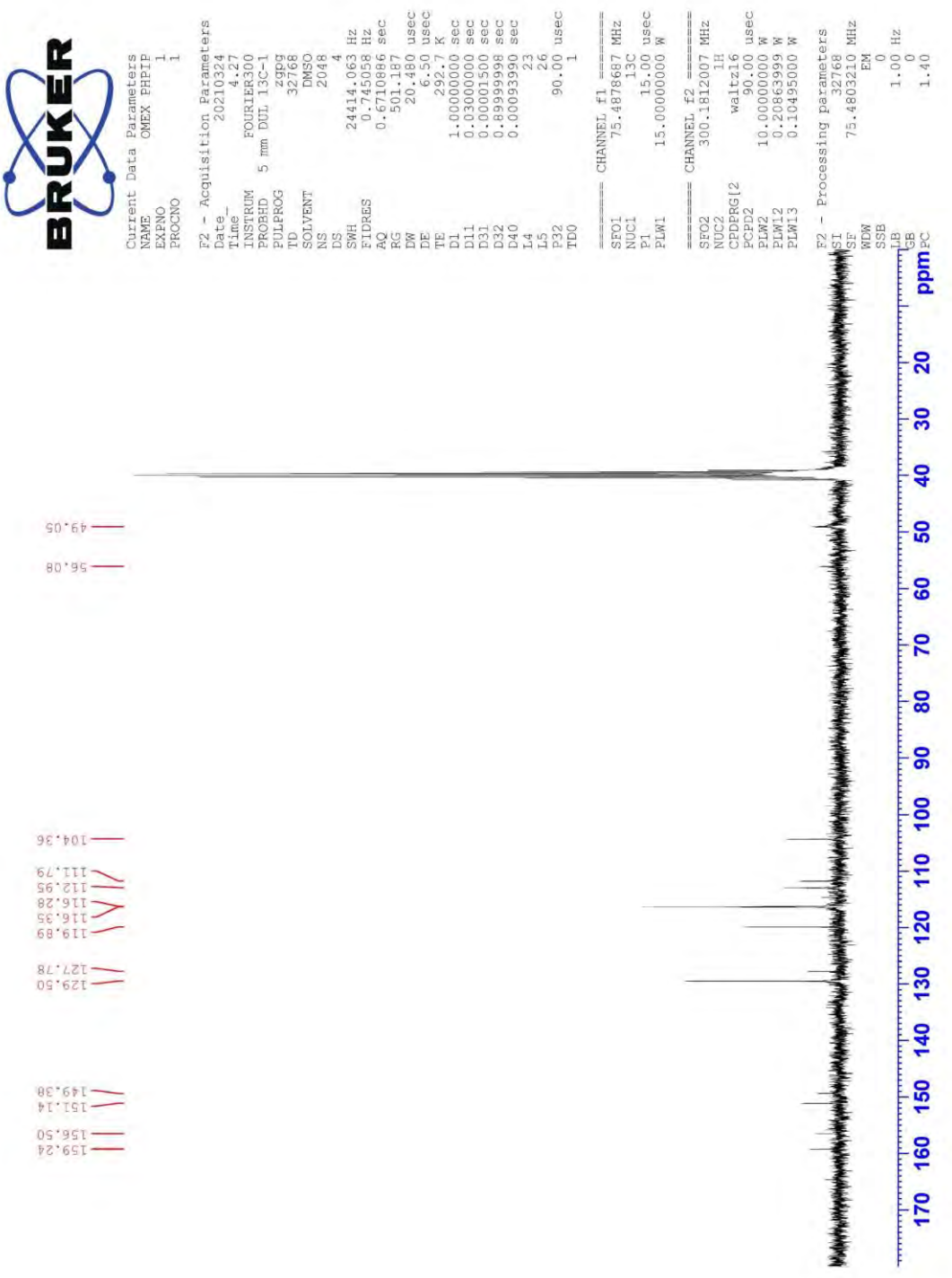


**Figure 5.187.** *[13]C NMR spectrum of compound **D37***

Data File: C:\LabSolutions\Data\Analiz\A.Çağrı\D-37_18.lcd

| Elmt | Val. | Min | Max | Elmt | Val. | Min | Max | Elmt | Val. | Min | Max | Elmt | Val. | Min | Max | Use Adduct |
|---|---|---|---|---|---|---|---|---|---|---|---|---|---|---|---|---|
| H | 1 | 0 | 40 | O | 2 | 0 | 5 | S | 2 | 0 | 0 | Ru | 2 | 0 | 0 | H |
| C | 4 | 0 | 40 | F | 1 | 0 | 0 | Cl | 1 | 0 | 0 | Pd | 2 | 0 | 0 | |
| N | 3 | 0 | 4 | P | 3 | 0 | 0 | Br | 1 | 0 | 0 | I | 3 | 0 | 0 | |

Error Margin (ppm): 5
HC Ratio: unlimited
Max Isotopes: 3
MSn Iso RI (%): 10.00

DBE Range: 0.0 - 20.0
Apply N Rule: yes
Isotope RI (%): 1.00
MSn Logic Mode: AND

Electron Ions: both
Use MSn Info: yes
Isotope Res: 9000
Max Results: 150

Event#: 1 MS(E+) Ret. Time : 4.093 Scan# : 615

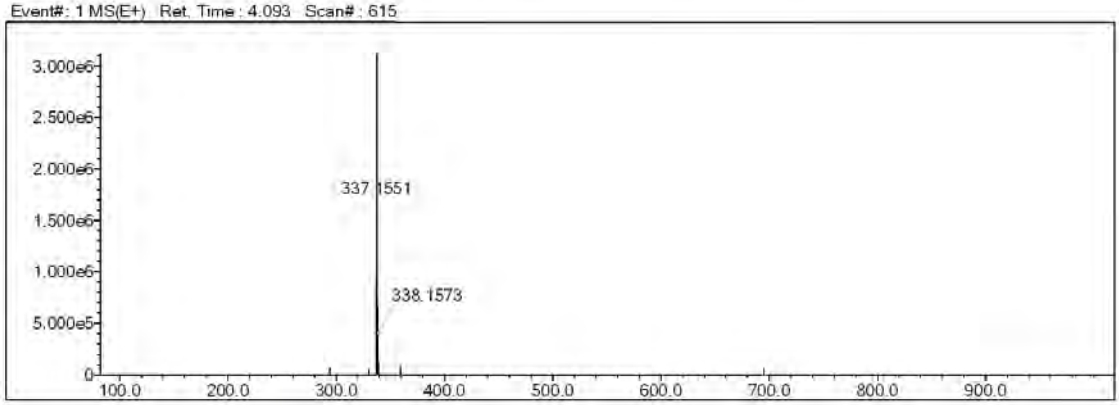


Measured region for 337.1551 m/z

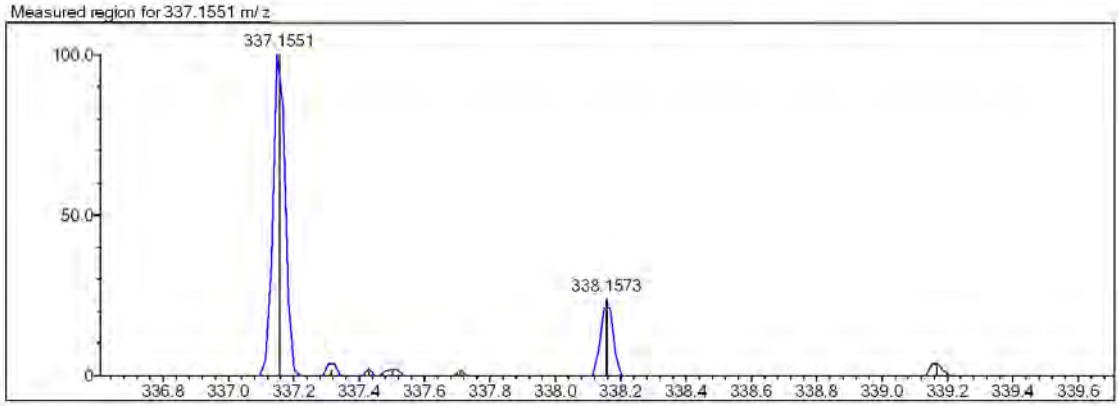


C20 H20 N2 O3 [M+H]+ : Predicted region for 337.1547 m/z

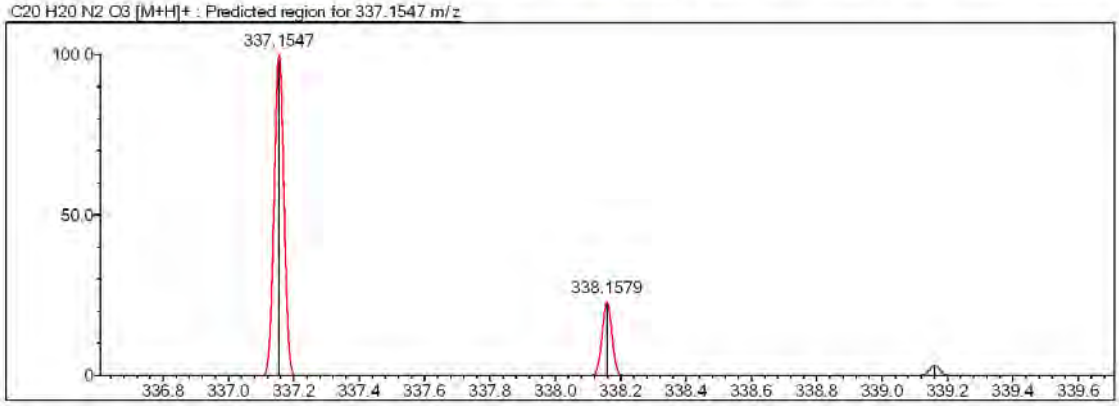


| Rank | Score | Formula (M) | Ion | Meas. m/z | Pred. m/z | Df. (mDa) | Df. (ppm) | Isc | DBE |
|---|---|---|---|---|---|---|---|---|---|
| 1 | 80.41 | C20 H20 N2 O3 | [M+H]+ | 337.1551 | 337.1547 | 0.4 | 1.19 | 80.79 | 12.0 |

**Figure 5.188.** *High-resolution mass spectrum of compound **D37***

DOPNALAB

| | Item | Value |
|---|---|---|
| | Acquired Date&Time | 27.05.2021 14:00:14 |
| | Acquired by | System Administrator |
| | Filename | C:\Users\dopnalab\Desktop\sa\371.ispd |
| | Spectrum name | 371 |
| | Sample name | 37 |
| | Sample ID | |
| | Option | |
| | Comment | |
| | No. of Scans | 15 |
| | Resolution | 4 [cm-1] |
| | Apodization | Happ-Genzel |

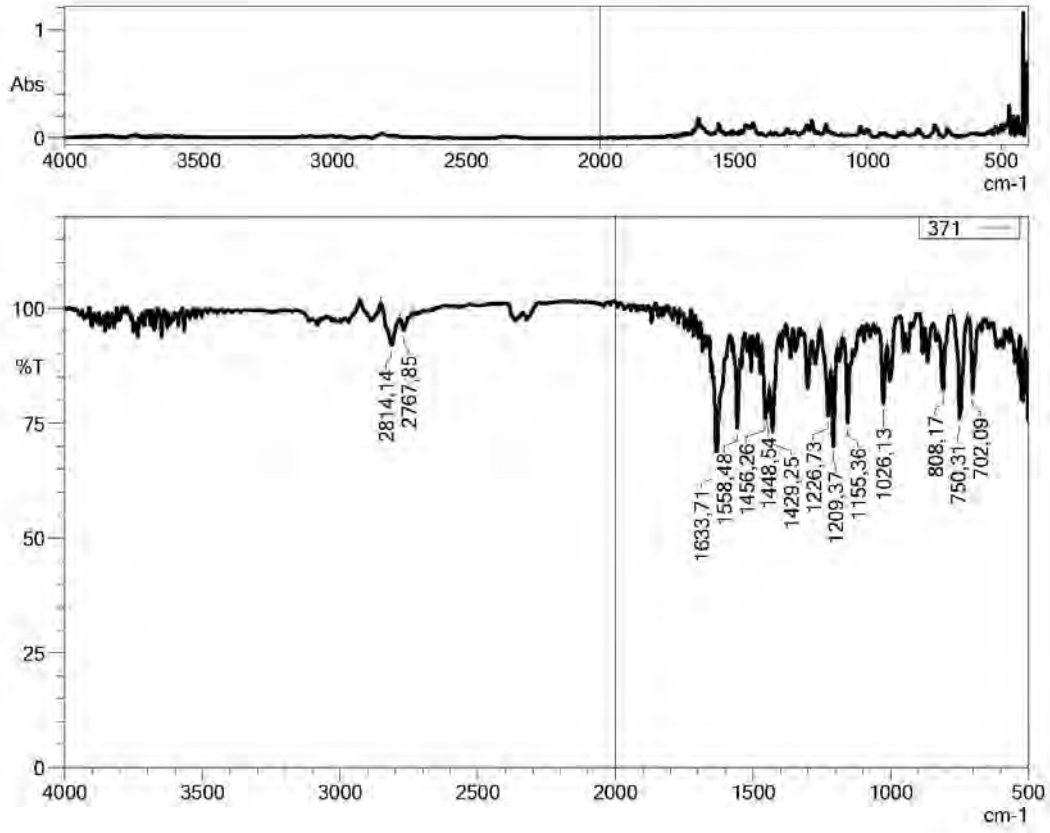


**Figure 5.189.** *IR spectrum of compound **D37***

### 5.1.4.38. *(4-(furan-2-carbonyl)piperazin-1-yl)(5-methoxybenzofuran-2-yl)methanone (D38)*

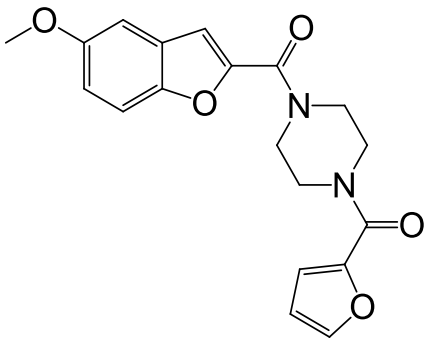

**Figure 5.190.** *Molecular structure of compound **D38***

**Physical Properties: Texture:** solid crystals, **Color:** white, **M.P.:** 124.5-125ºC**, Yield:** 44%.

**IR (ATR) $\upsilon_{max}$ ($cm^{-1}$):** 3028 ($SP^2$ C-H stretching, aromatic), 2831-2765 ($SP^3$ C-H stretching, methylenes of piperazine and methoxy), 1622 (C=O stretching, amide), 1558 (C-H bending, indicative of non-substituted benzofuran at position 3), 1429 (C=C stretching, aromatic), 1209 (C-O stretching, ether), 1182, 1002 (C-N stretching, tertiary amine and/or ether), 829 (C-H aromatic out-of-plane bending, one peak, non-substituted benzofuran at position 3) 738-700 (C-H aromatic out-of-plane bending).

**$^1$H NMR (300 MHz) (DMSO-$d_6$) $\delta$ (ppm):** 3.73-3.91 (m, 11H, piperazine-2, 3, 5, 6 and **5-methoxy**benzofuran), 6.65 (dd, *J*= 3.47, 1.74 Hz, 1H, furan-4), 7.03-7.07 (m, 2H, benzofuran-6 and furan-3), 7.23 (d, *J*= 2.57 Hz, 1H, benzofuran-4), 7.38 (s, 1H, benzofuran-3), 7.58 (d, *J*= 9.04 Hz, 1H, benzofuran-7), 7.86 (dd, *J*= 1.71, 0.75 Hz, 1H, furan-5).

**$^{13}$C NMR (300 MHz) (DMSO-$d_6$) $\delta$ (ppm):** 42.59 (piperazine), 46.73 (piperazine), 56.08 (**5-methoxy**benzofuran), 104.35, 111.89, 112.01, 112.98, 116.49, 127.75, 145.45, 147.17, 149.16, 149.38, 156.49, 158.93 (piperazine-**CO**-furan), 159.46 (benzofuran-**CO**-piperazine).

**HRMS (ESI) (m/z) $[M+1]^+$:** for $C_{19}H_{18}N_2O_5$ calculated: 355.1288; found: 355.1293.

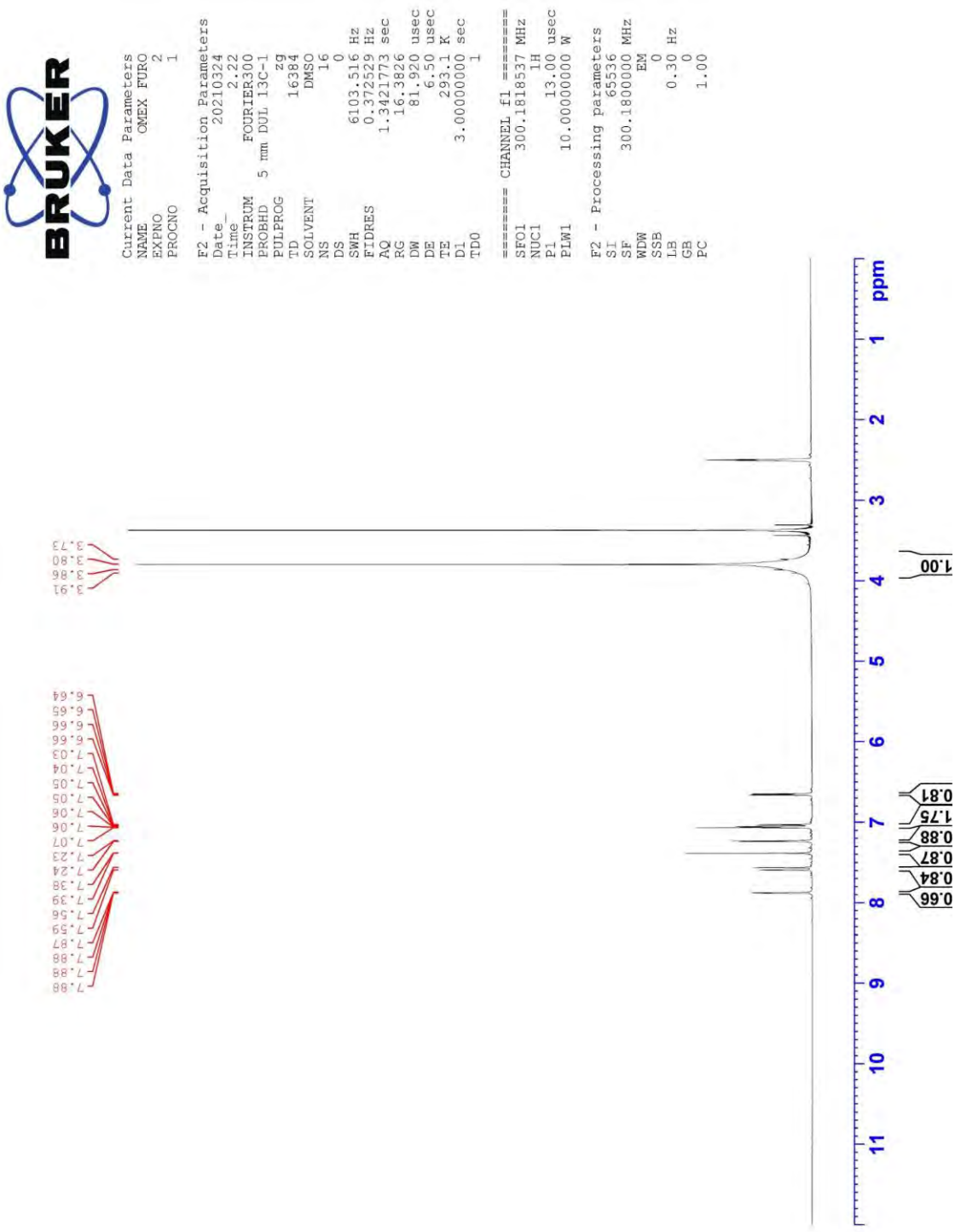


**Figure 5.191.** *$^{1}H$ NMR spectrum of compound **D38***

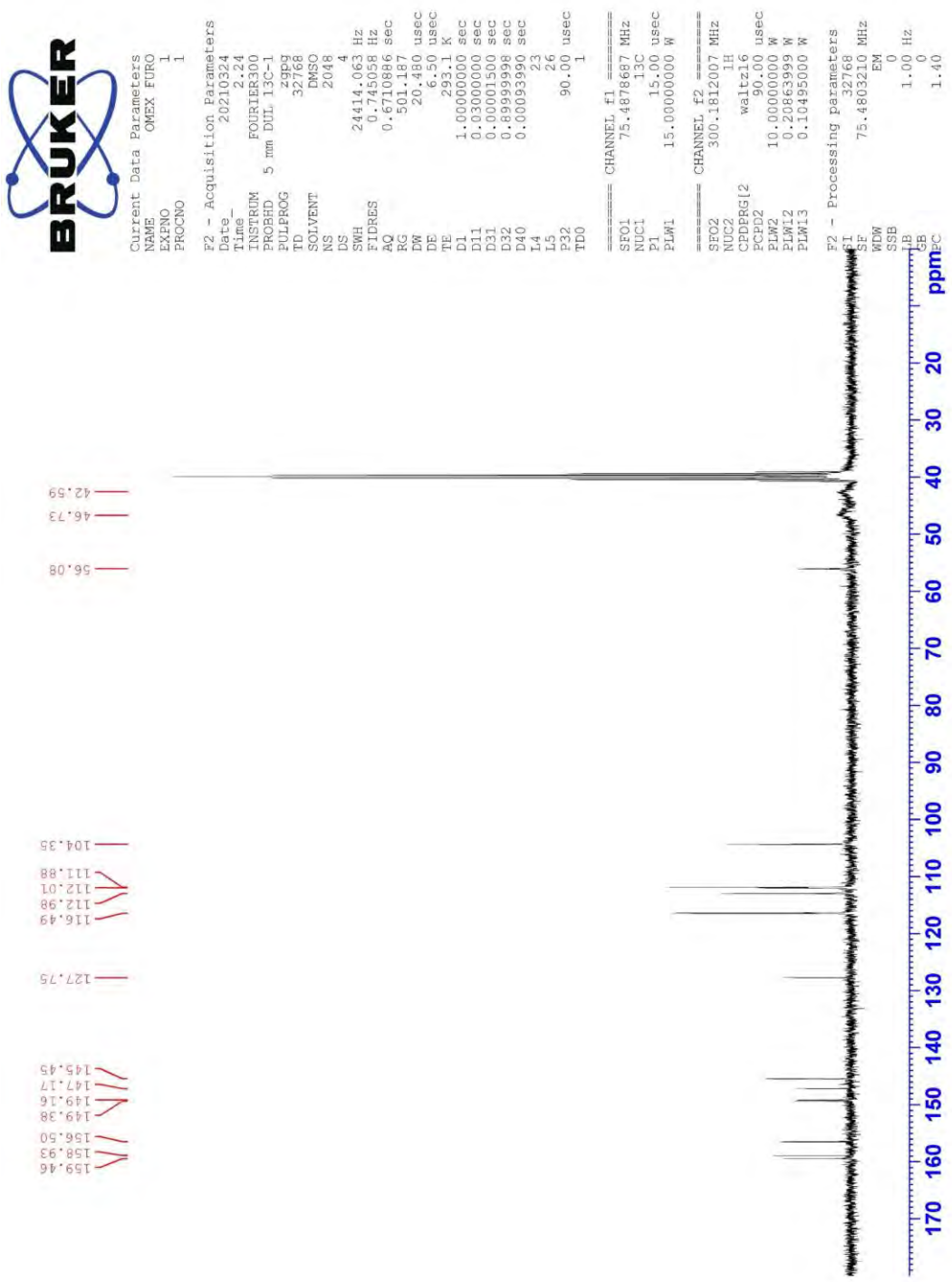


**Figure 5.192.** *$^{13}$C NMR spectrum of compound **D38***

Data File: C:\LabSolutions\Data\Analiz\A.Çağın\D-38_19.lcd

| Elmt | Val. | Min | Max | Elmt | Val. | Min | Max | Elmt | Val. | Min | Max | Elmt | Val. | Min | Max | Use Adduct |
|---|---|---|---|---|---|---|---|---|---|---|---|---|---|---|---|---|
| H | 1 | 0 | 40 | O | 2 | 0 | 5 | S | 2 | 0 | 0 | Ru | 2 | 0 | 0 | H |
| C | 4 | 0 | 40 | F | 1 | 0 | 0 | Cl | 1 | 0 | 0 | Pd | 2 | 0 | 0 | |
| N | 3 | 0 | 4 | P | 3 | 0 | 0 | Br | 1 | 0 | 0 | I | 3 | 0 | 0 | |

Error Margin (ppm): 5
HC Ratio: unlimited
Max Isotopes: 3
MSn Iso RI (%): 10.00

DBE Range: 0.0 - 20.0
Apply N Rule: yes
Isotope RI (%): 1.00
MSn Logic Mode: AND

Electron Ions: both
Use MSn Info: yes
Isotope Res: 9000
Max Results: 150

Event#: 1 MS(E+) Ret. Time: 2.133 Scan#: 321

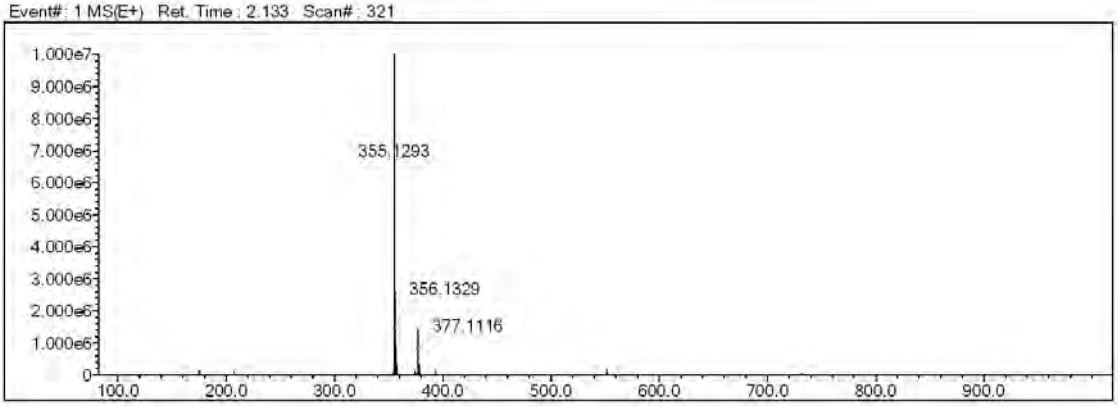


Measured region for 355.1293 m/z

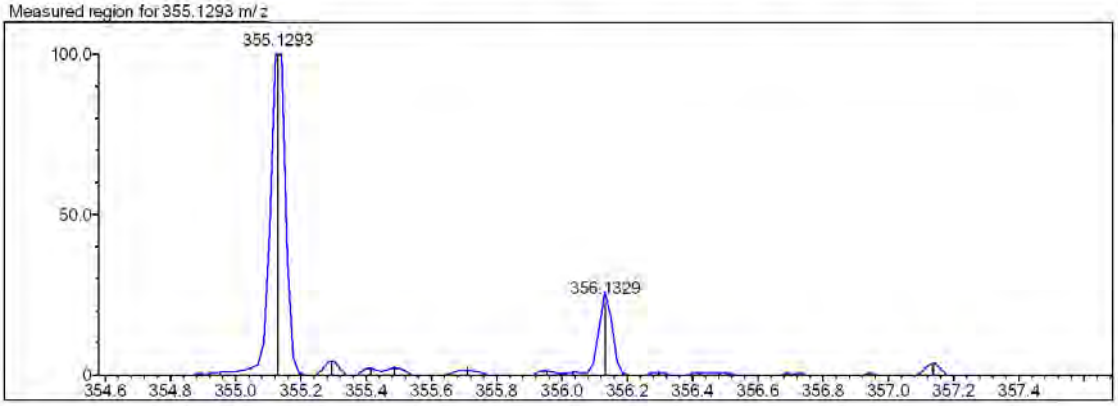


C19 H18 N2 O5 [M+H]+ : Predicted region for 355.1288 m/z

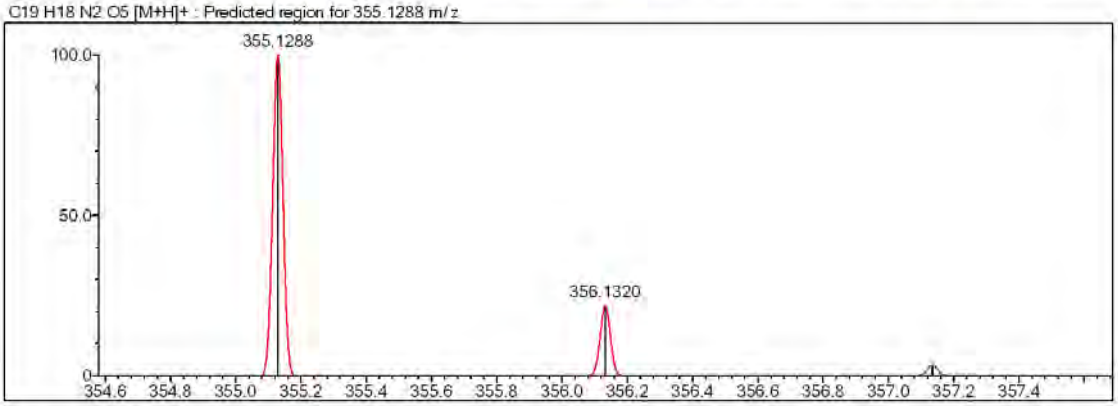


| Rank | Score | Formula (M) | Ion | Meas. m/z | Pred. m/z | Df. (mDa) | Df. (ppm) | Isc | DBE |
|---|---|---|---|---|---|---|---|---|---|
| 1 | 98.97 | C19 H18 N2 O5 | [M+H]+ | 355.1293 | 355.1288 | 0.5 | 1.41 | 100.00 | 12.0 |

**Figure 5.193.** *High-resolution mass spectrum of compound* ***D38***

DOPNALAB

| | Item | Value |
|---|---|---|
| | Acquired Date&Time | 27.05.2021 14:04:14 |
| | Acquired by | System Administrator |
| | Filename | C:\Users\dopnalab\Desktop\sa\381.ispd |
| | Spectrum name | 381 |
| | Sample name | 38 |
| | Sample ID | |
| | Option | |
| | Comment | |
| | No. of Scans | 15 |
| | Resolution | 4 [cm-1] |
| | Apodization | Happ-Genzel |

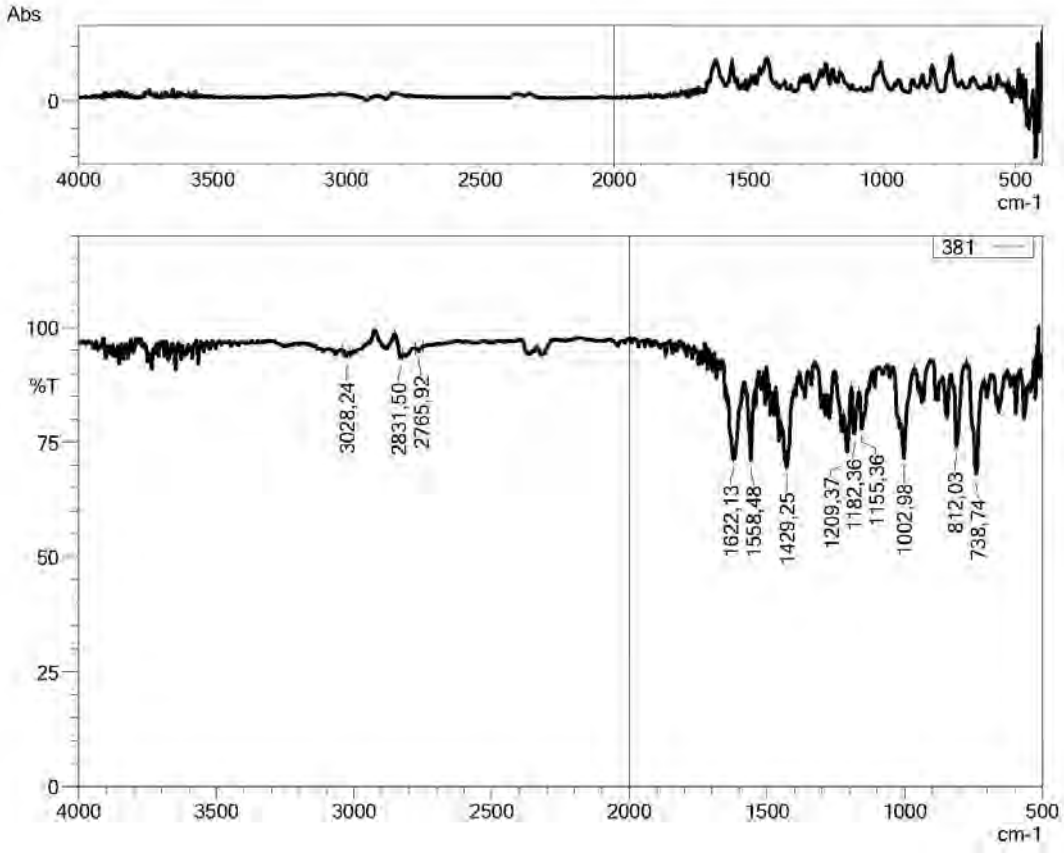


**Figure 5.194.** *IR spectrum of compound **D38***

### 5.1.4.39. *(5-methoxybenzofuran-2-yl)(4-methylpiperazin-1-yl)methanone (D39)*

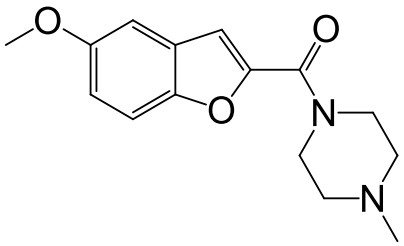


**Figure 5.195.** *Molecular structure of compound **D39***

**Physical Properties: Texture:** liquid, **Color:** yellow, **Yield:** 66%.

**IR (ATR) $\upsilon_{max}$ ($cm^{-1}$):** 3095 ($SP^2$ C-H stretching, aromatic), 2939-2792 ($SP^3$ C-H stretching, methylenes of piperazine, 4-methyl piperazine, and methoxy), 1624 (C=O stretching, amide), 1558 (C-H bending, indicative of non-substituted benzofuran at position 3), 1427 (C=C stretching, aromatic), 1296-1203 (C-O stretching, ether), 1161-1141, 1024-002 (C-N stretching, tertiary amine and/or ether), 806 (C-H aromatic out-of-plane bending, one peak, non-substituted benzofuran at position 3), 746 (C-H aromatic out-of-plane bending).

**$^1$H NMR (300 MHz) (DMSO-$d_6$) $\delta$ (ppm):** 2.20 (s, 3H, **4-methyl**piperazine), 2.36 (t, *J*= 5.04 Hz, 4H, piperazine-3, 5), 3.69 (brs, 4H, piperazine-2, 6), 3.79 (s, 3H, **5-methoxy**benzofuran), 7.02 (dd, *J*= 9.02, 2.64 Hz, 1H, benzofuran-6), 7.21 (d, *J*= 2.58 Hz, 1H, benzofuran-4), 7.30 (s, 1H, benzofuran-3), 7.56 (d, *J*= 9.03 Hz, 1H, benzofuran-7).

**$^{13}$C NMR (300 MHz) (DMSO-$d_6$) $\delta$ (ppm):** 42.79 (piperazine), 46.01 (**4-methyl**piperazine) 46.82 (piperazine), 55.09 (piperazine), 56.07 (**5-methoxy**benzofuran), 104.35, 111.49, 112.89, 116.12, 127.78, 149.29, 156.48, 159.24 (benzofuran-**CO**-piperazine).

**HRMS (ESI) (m/z) $[M+1]^+$:** for $C_{15}H_{18}N_2O_3$ calculated: 275.1390; found: 275.1389.

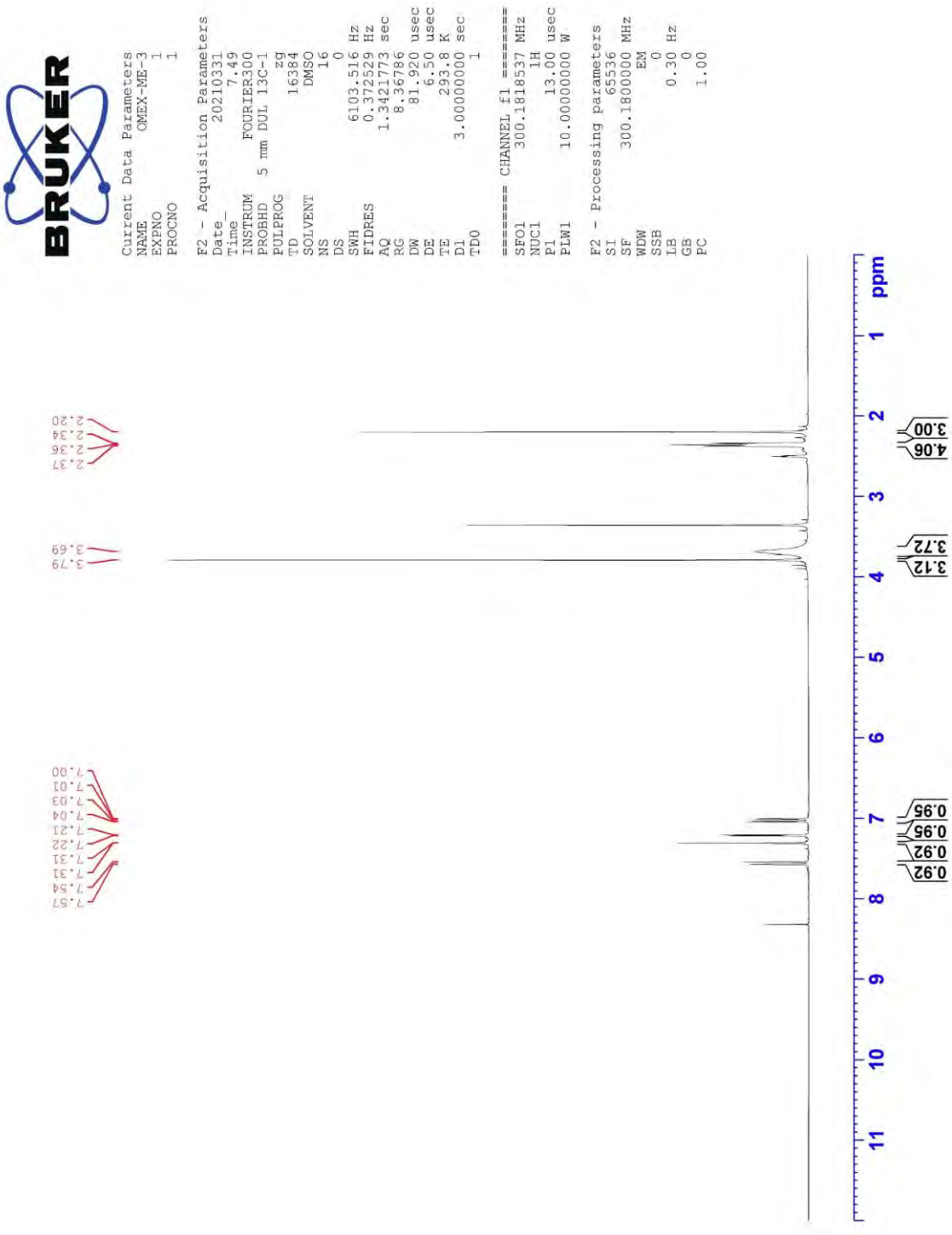


**Figure 5.196.** *$^{1}H$ NMR spectrum of compound **D39***

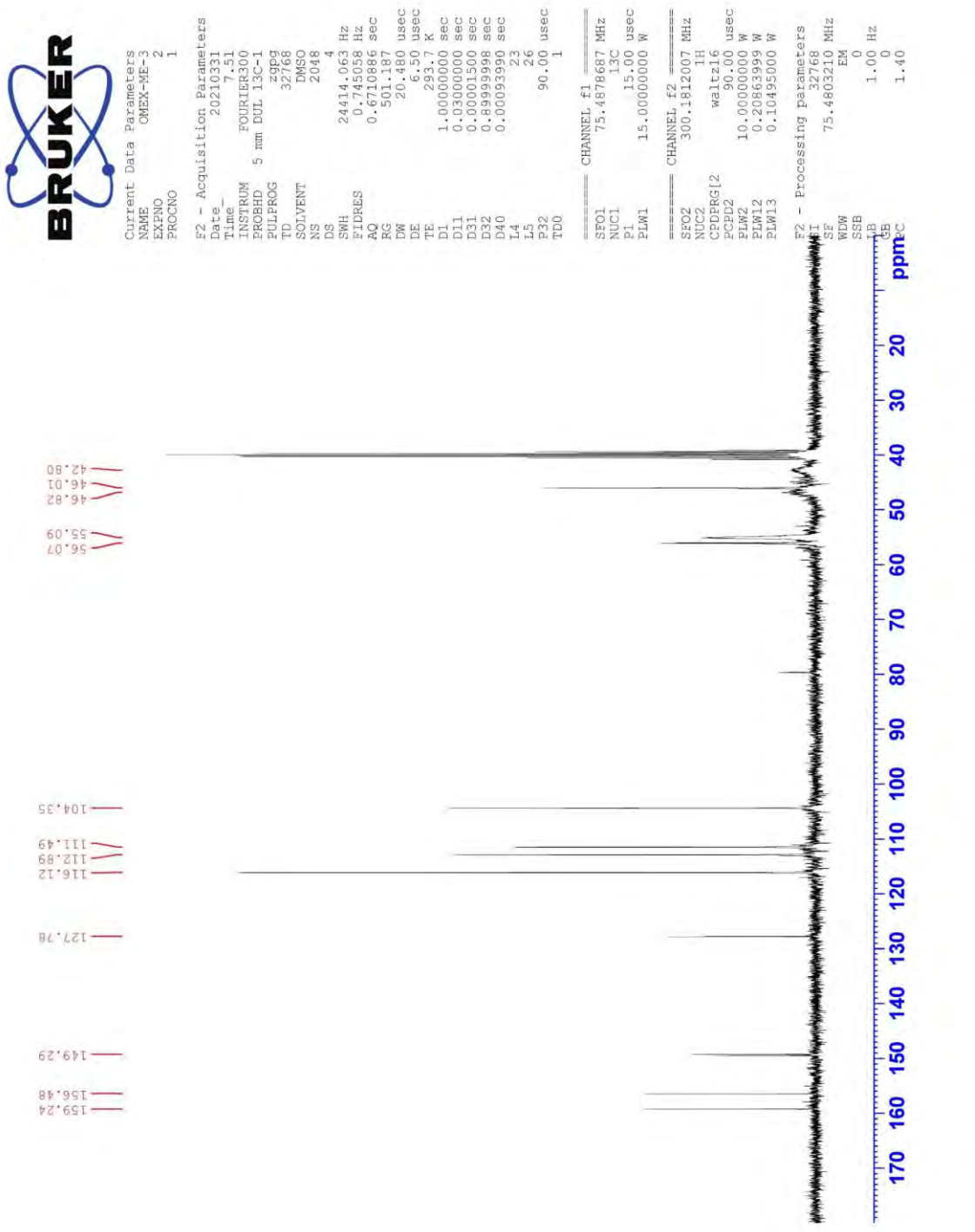


**Figure 5.197.** *$^{13}$C NMR spectrum of compound **D39***

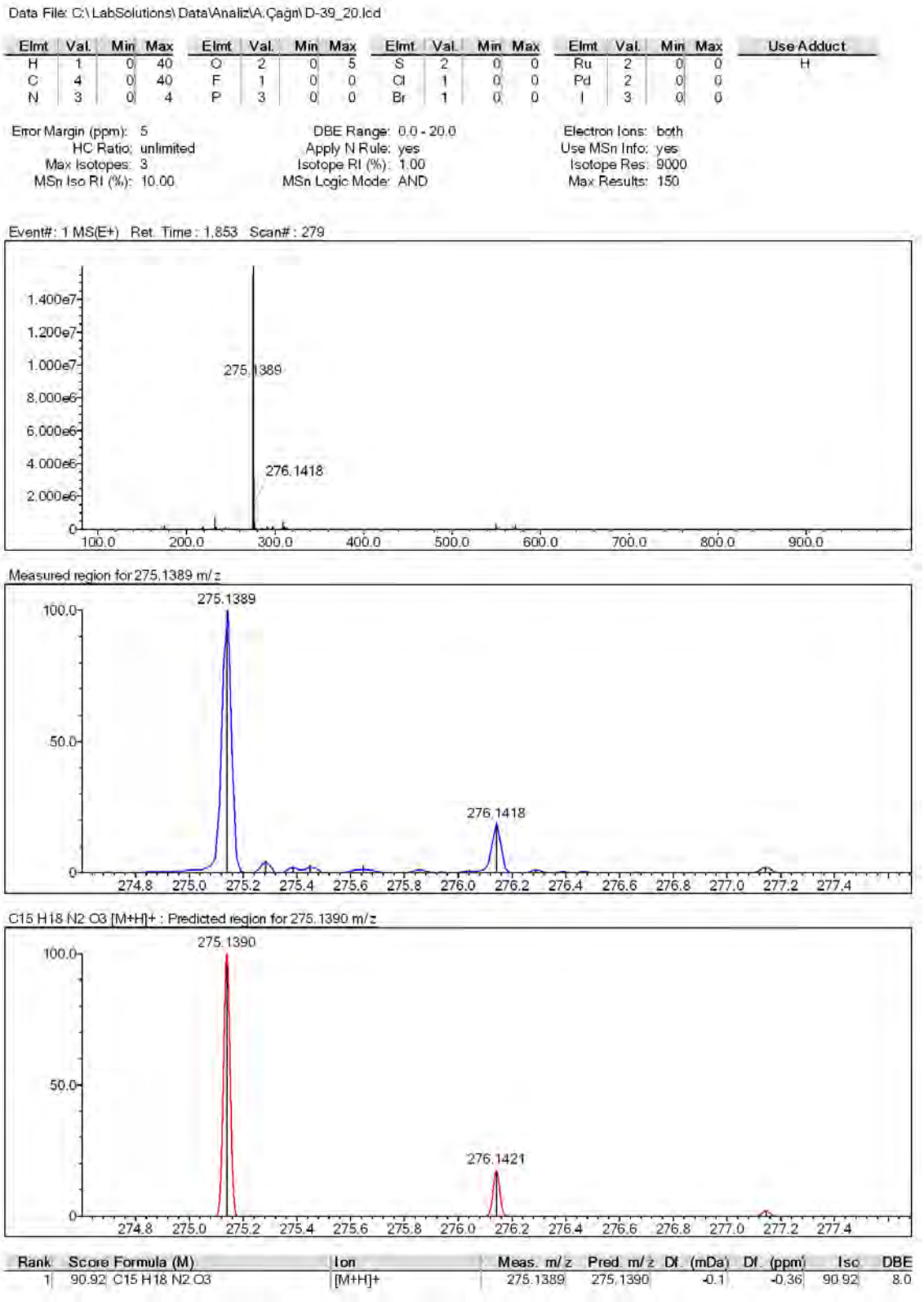


**Figure 5.198.** *High-resolution mass spectrum of compound **D39***

DOPNALAB

| | Item | Value |
|---|---|---|
| | Acquired Date&Time | 27.05.2021 14:13:32 |
| | Acquired by | System Administrator |
| | Filename | C:\Users\dopnalab\Desktop\sa\391.ispd |
| | Spectrum name | 391 |
| | Sample name | 39 |
| | Sample ID | |
| | Option | |
| | Comment | |
| | No. of Scans | 15 |
| | Resolution | 4 [cm-1] |
| | Apodization | Happ-Genzel |

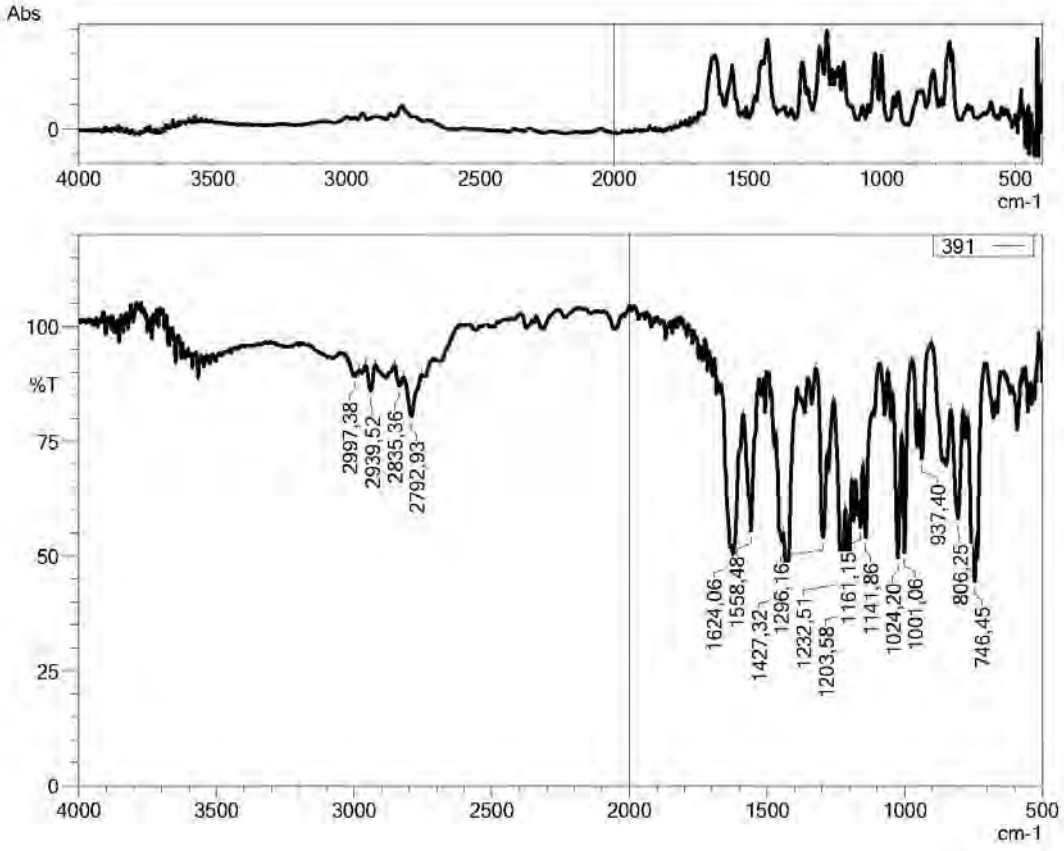


**Figure 5.199.** *IR spectrum of compound **D39***

### 5.1.4.40. *(4-ethylpiperazin-1-yl)(5-methoxybenzofuran-2-yl)methanone (D40)*

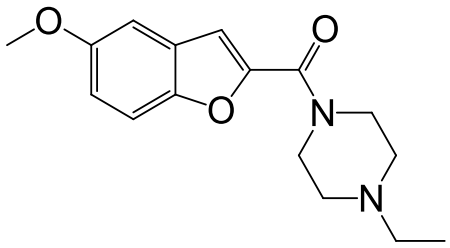

**Figure 5.200.** *Molecular structure of compound* ***D40***

**Physical Properties: Texture:** liquid, **Color:** brown, **Yield:** 54%.

**IR (ATR) $\upsilon_{max}$ ($cm^{-1}$):** 2968-2810 ($SP^3$ C-H stretching, methylenes of piperazine, ethyl-methyl piperazine, and methoxy), 1624 (C=O stretching, amide), 1558 (C-H bending, indicative of non-substituted benzofuran at position 3), 1427 (C=C stretching, aromatic), 1300, 1232-1203 (C-O stretching, ether), 1016 (C-N stretching, tertiary amine and/or C-O stretching, ether), 933-734 (C-H aromatic out-of-plane bending), 806 (C-H aromatic out-of-plane bending, one peak, non-substituted benzofuran at position 3).

**$^1$H NMR (300 MHz) (DMSO-$d_6$) $\delta$ (ppm):** 1.01 (t, *J*= 7.17 Hz, 3H, piperazine-$CH_2$-**$CH_3$**), 2.35 (q, *J*= 14.28, 7.12 Hz, 2H, piperazine-**$CH_2$**-$CH_3$), 2.41 (t, *J*= 5.08 Hz, 4H, piperazine-3, 5), 3.69 (brs, 4H, piperazine-2, 6), 3.79 (s, 3H, **5-methoxy**benzofuran), 7.00 (dd, *J*= 9.03, 2.64 Hz, 1H, benzofuran-6), 7.21 (d, *J*=2.57 Hz, 1H, benzofuran-4), 7.31 (s, 1H, benzofuran-3), 7.56 (d, *J*= 9.03 Hz, 1H, benzofuran-7).

**$^{13}$C NMR (300 MHz) (DMSO-$d_6$) $\delta$ (ppm):** 12.35 (piperazine-$CH_2$-**$CH_3$**), 42.73 (piperazine), 46.98 (piperazine), 51.90 (piperazine-**$CH_2$**-$CH_3$), 52.97 (piperazine), 56.05 (**5-methoxy**benzofuran), 104.31, 111.50, 112.90, 116.14, 127.78, 149.27, 149.47, 156.46, 159.18 (benzofuran-**CO**-piperazine).

**HRMS (ESI) (m/z) $[M+1]^+$:** for $C_{16}H_{20}N_2O_3$ calculated: 289.1547; found: 289.1545.

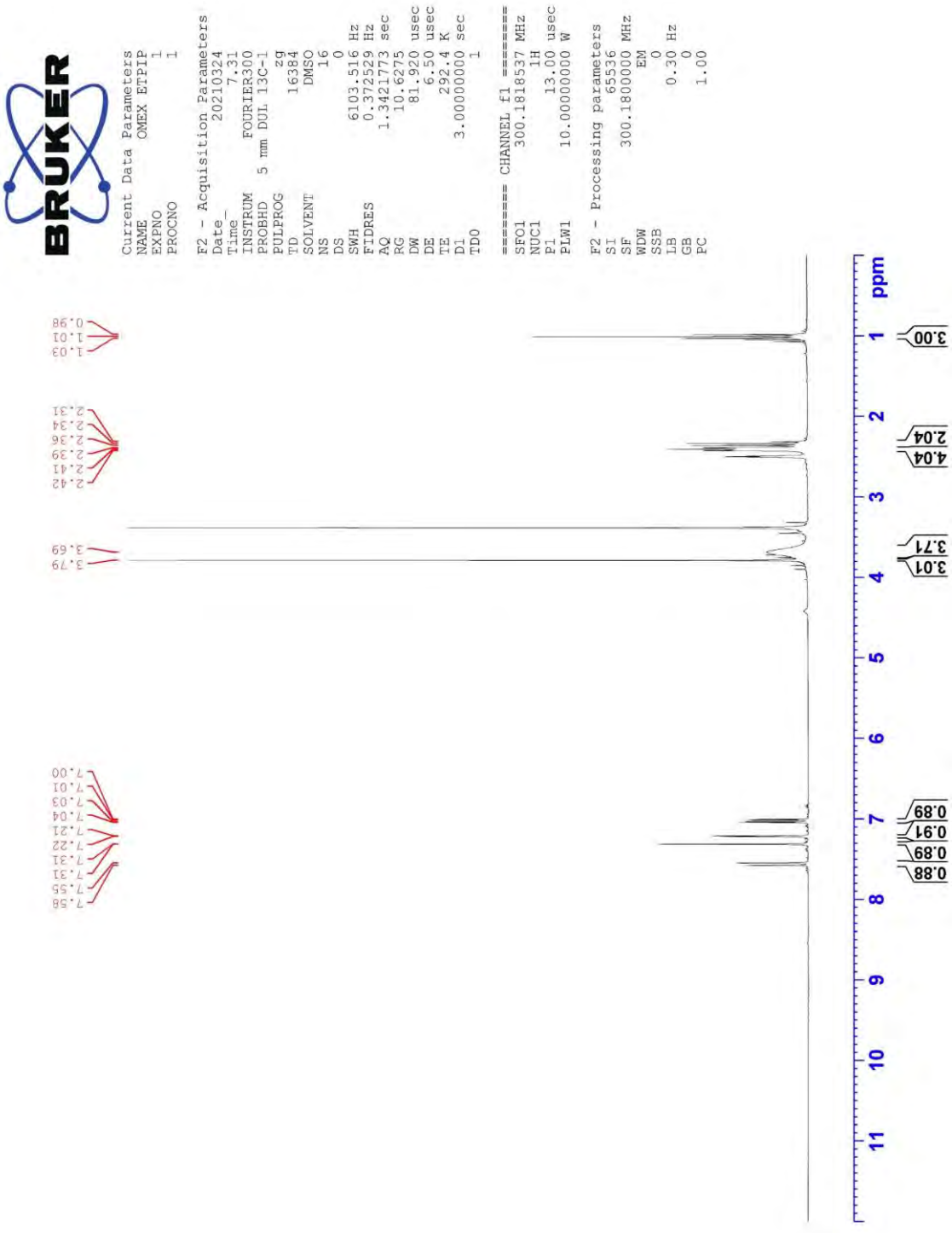


**Figure 5.201.** *Molecular structure of compound **D40***

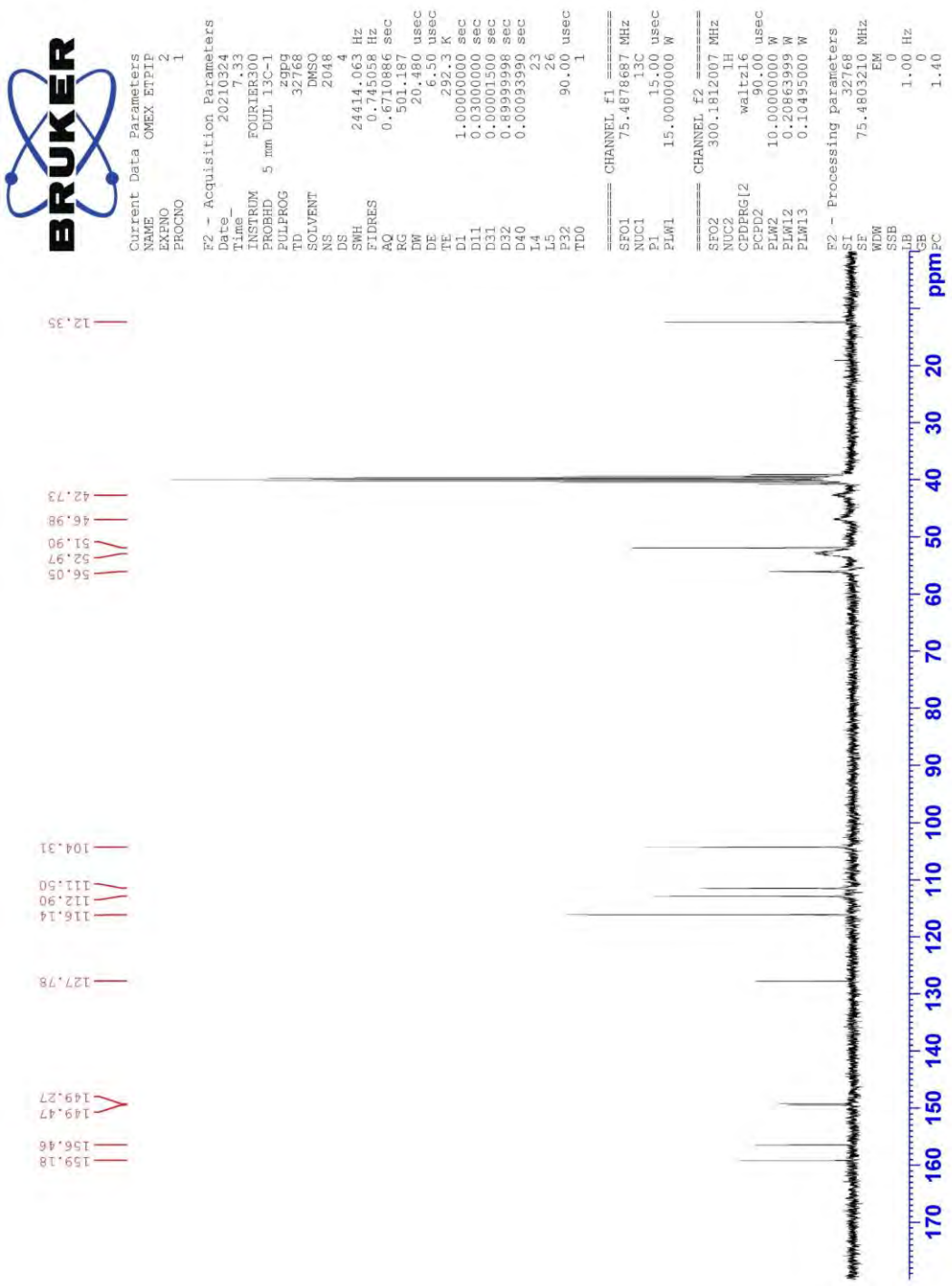


**Figure 5.202.** *$^{13}$C NMR spectrum of compound **D40***

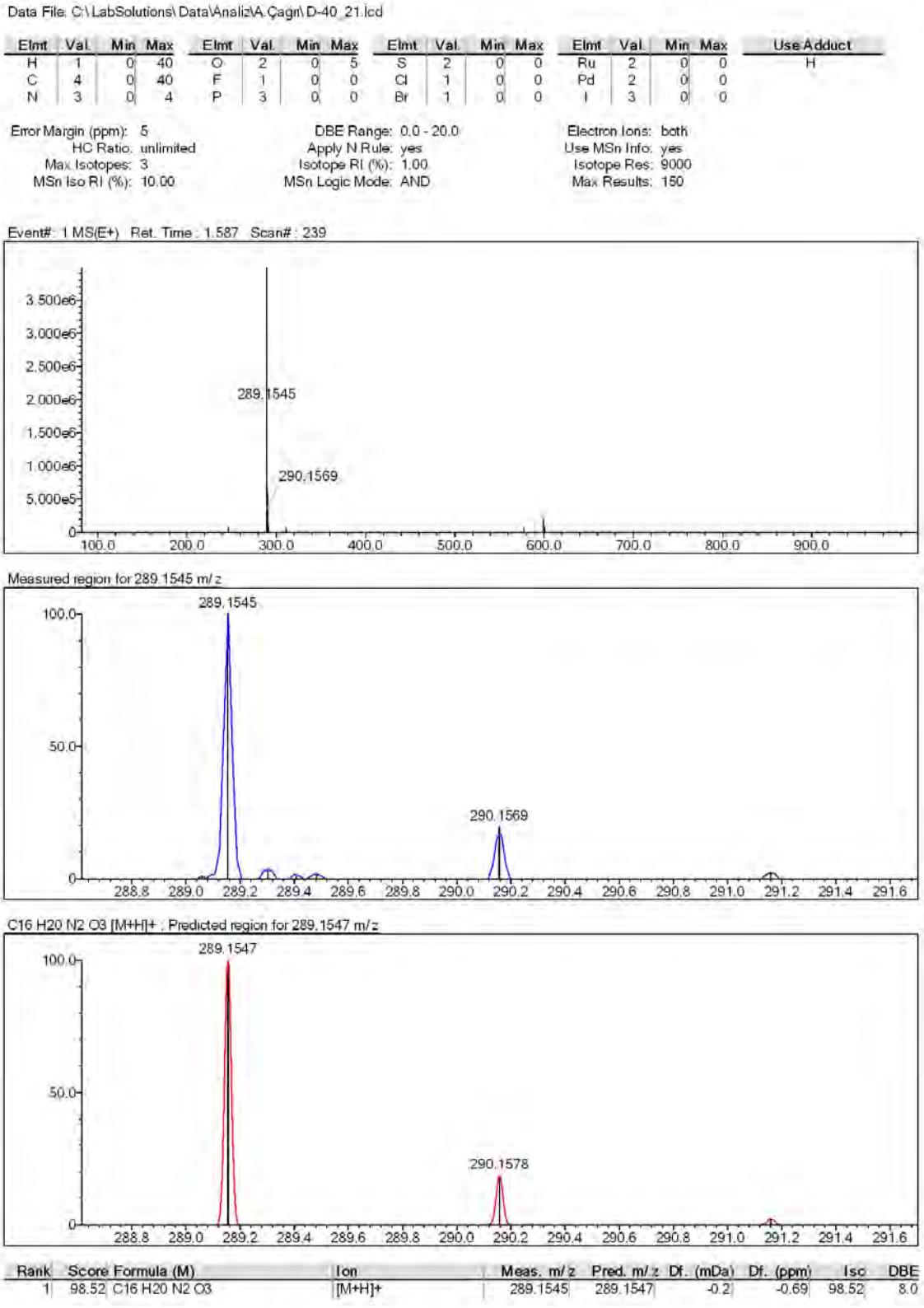


**Figure 5.203.** *High-resolution mass spectrum of compound* ***D40***

DOPNALAB

| | Item | Value |
|---|---|---|
| | Acquired Date&Time | 27.05.2021 14:22:52 |
| | Acquired by | System Administrator |
| | Filename | C:\Users\dopnalab\Desktop\sa\401.ispd |
| | Spectrum name | 401 |
| | Sample name | 40 |
| | Sample ID | |
| | Option | |
| | Comment | |
| | No. of Scans | 15 |
| | Resolution | 4 [cm-1] |
| | Apodization | Happ-Genzel |

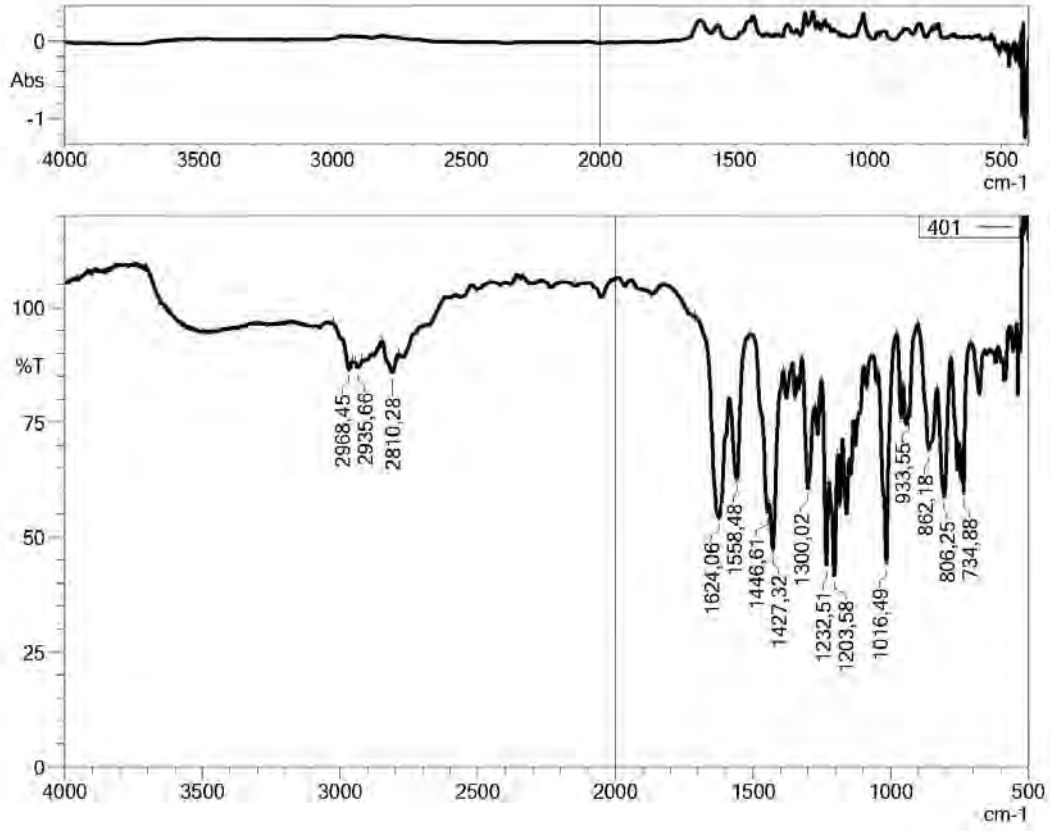


**Figure 5.204.** *IR spectrum of compound **D40***

### 5.1.4.41. *(4-(2-(dimethylamino)ethyl)piperazin-1-yl)(5-methoxybenzofuran-2-yl)methanone (D41)*

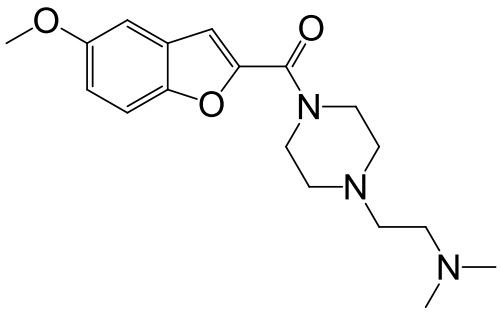

**Figure 5.205.** *Molecular structure of compound* ***D41***

**Physical Properties: Texture:** liquid**, Color:** brown, **Yield:** 51%.

**IR (ATR) $\upsilon_{max}$ ($cm^{-1}$):** 2939-2767 ($SP^3$ C-H stretching, methylenes of piperazine, dimethylaminoethyl-piperazine, and methoxy), 1625 (C=O stretching, amide), 1558 (C-H bending, indicative of non-substituted benzofuran at position 3), 1456-1429 (C=C stretching, aromatic), 1300, 1232-1205 (C-O stretching, ether), 1024-1001 (C-N stretching, tertiary amine and/or C-O stretching, ether), 939-734 (C-H aromatic out-of-plane bending), 806 (C-H aromatic out-of-plane bending, one peak, non-substituted benzofuran at position 3).

**$^1$H NMR (300 MHz) (DMSO-$d_6$) $\delta$ (ppm):** 2.12 (s, 6H, -N**($CH_3$)$_2$**), 2.30-2.42 (m, 4H, piperazine-**($CH_2$)$_2$**-N), 2.46 (t, *J*= 4.90 Hz, 4H, piperazine-3, 5), 3.67 (brs, 4H, piperazine-2, 6), 3.79 (s, 3H, **5-methoxy**benzofuran), 7.02 (dd, *J*= 9.03, 2.64 Hz, 1H, benzofuran-6), 7.21 (d, *J*= 2.57 Hz, 1H, benzofuran-4), 7.31 (s, 1H, benzofuran-3), 7.56 (d, *J*= 9.03 Hz, 1H, benzofuran-7).

**$^{13}$C NMR (300 MHz) (DMSO-$d_6$) $\delta$ (ppm):** 42.62 (piperazine), 46.03 (-N**($CH_3$)$_2$**), 46.80 (piperazine), 53.56 (piperazine), 56.03 (**5-methoxy**benzofuran), 57.02 (piperazine-**($CH_2$)$_2$**-N), 104.34, 111.50, 112.90, 116.13, 127.78, 149.28, 149.47, 156.47, 159.17 (benzofuran-**CO**-piperazine).

**HRMS (ESI) (m/z) $[M+1]^+$:** for $C_{18}H_{25}N_3O_3$ calculated: 332.1969; found: 332.1970.

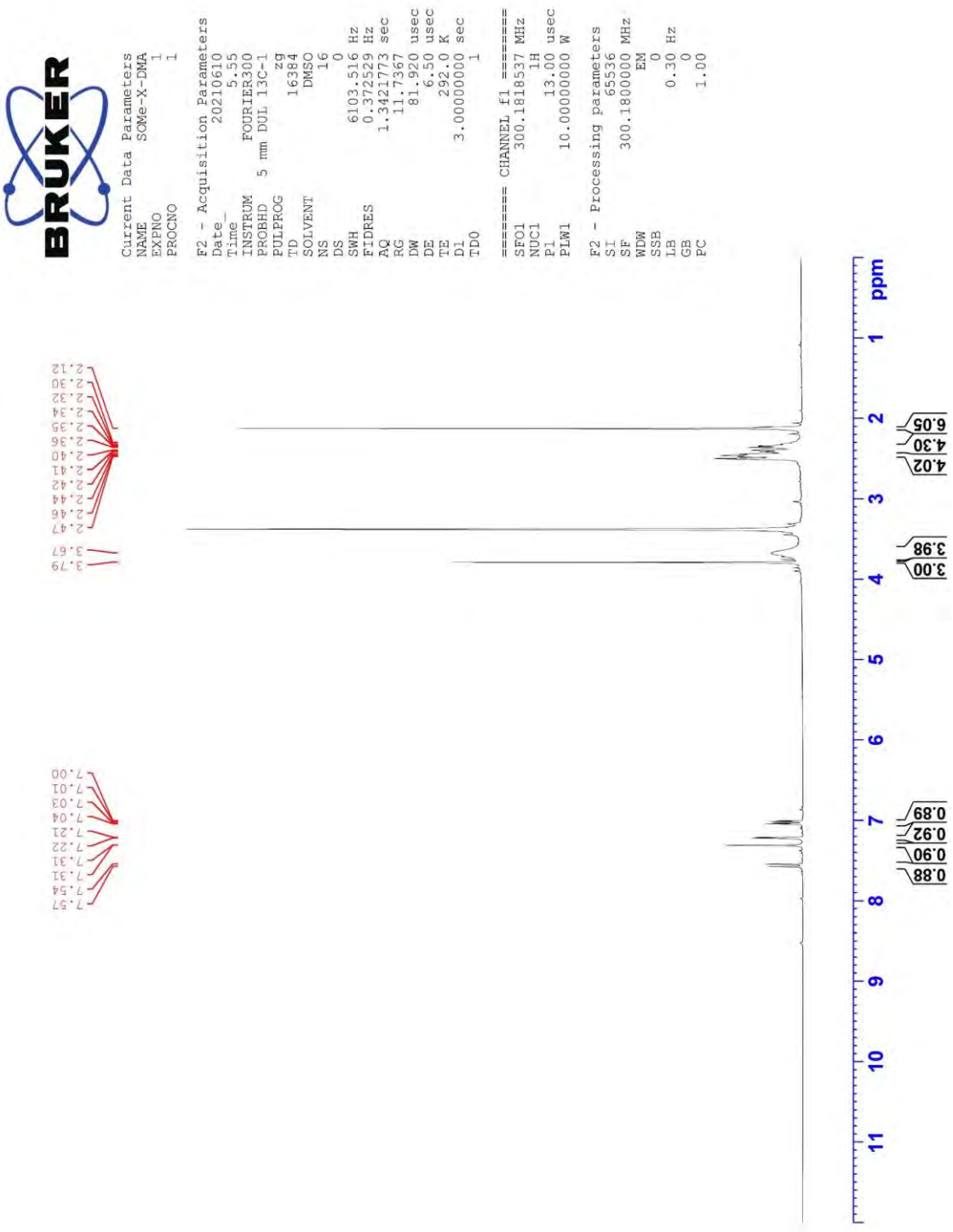


**Figure 5.206.** *$^{1}H$ NMR spectrum of compound **D41***

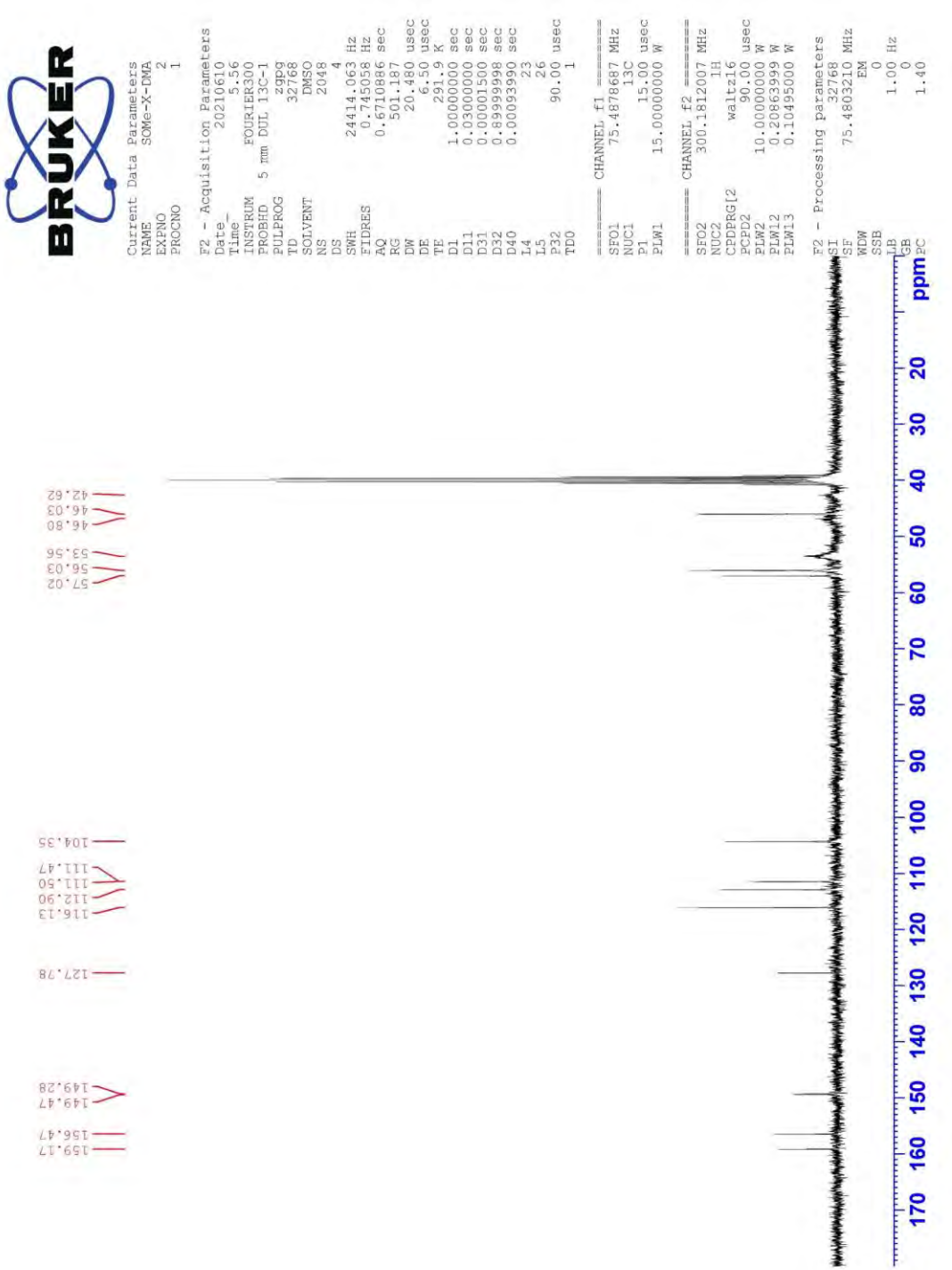


**Figure 5.207.** *$^{13}$C NMR spectrum of compound **D41***

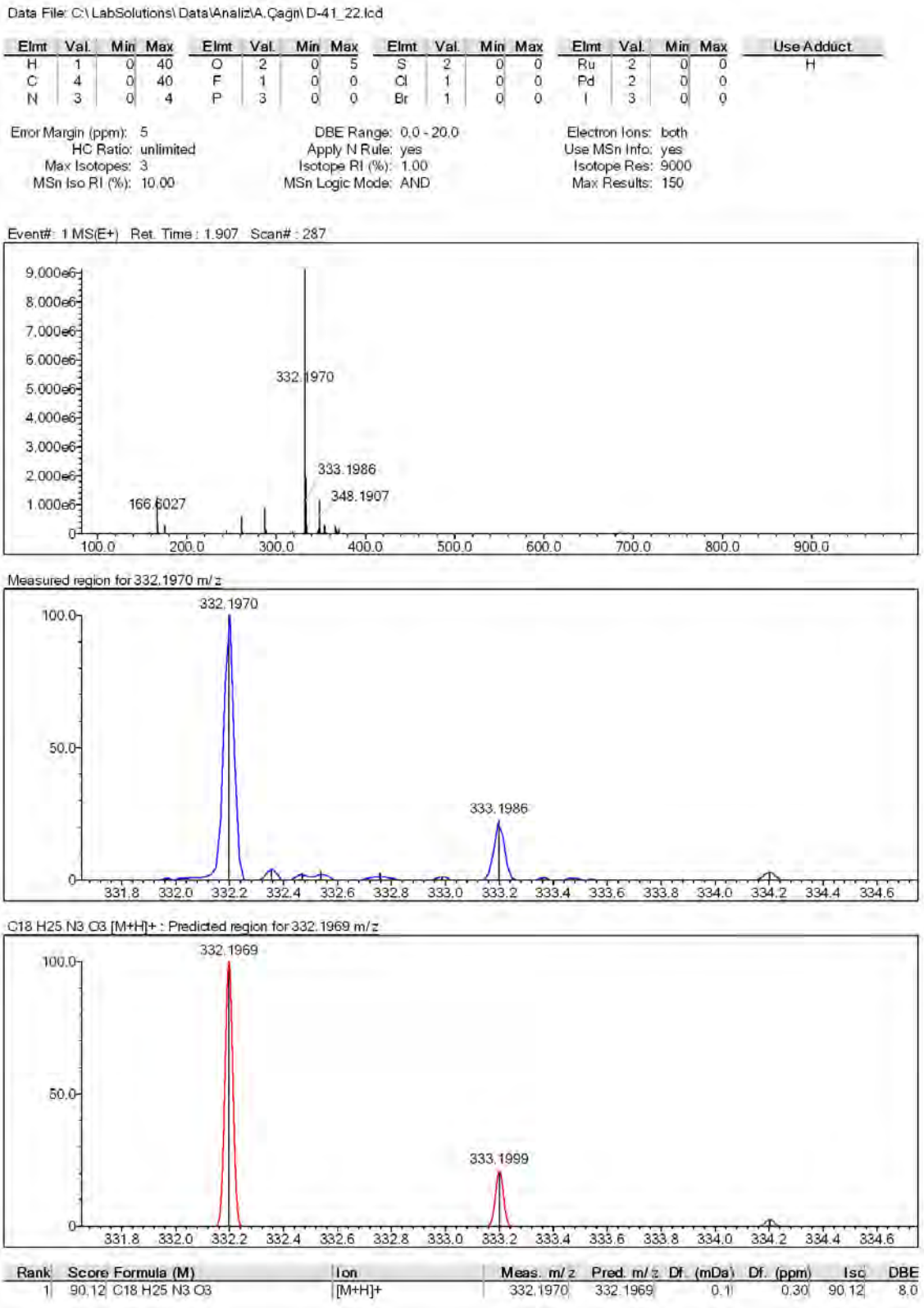


**Figure 5.208.** *High-resolution mass spectrum of compound* ***D41***

DOPNALAB

| | Item | Value |
|---|---|---|
| | Acquired Date&Time | 27.05.2021 14:26:40 |
| | Acquired by | System Administrator |
| | Filename | C:\Users\dopnalab\Desktop\sa\411.ispd |
| | Spectrum name | 411 |
| | Sample name | 41 |
| | Sample ID | |
| | Option | |
| | Comment | |
| | No. of Scans | 15 |
| | Resolution | 4 [cm-1] |
| | Apodization | Happ-Genzel |

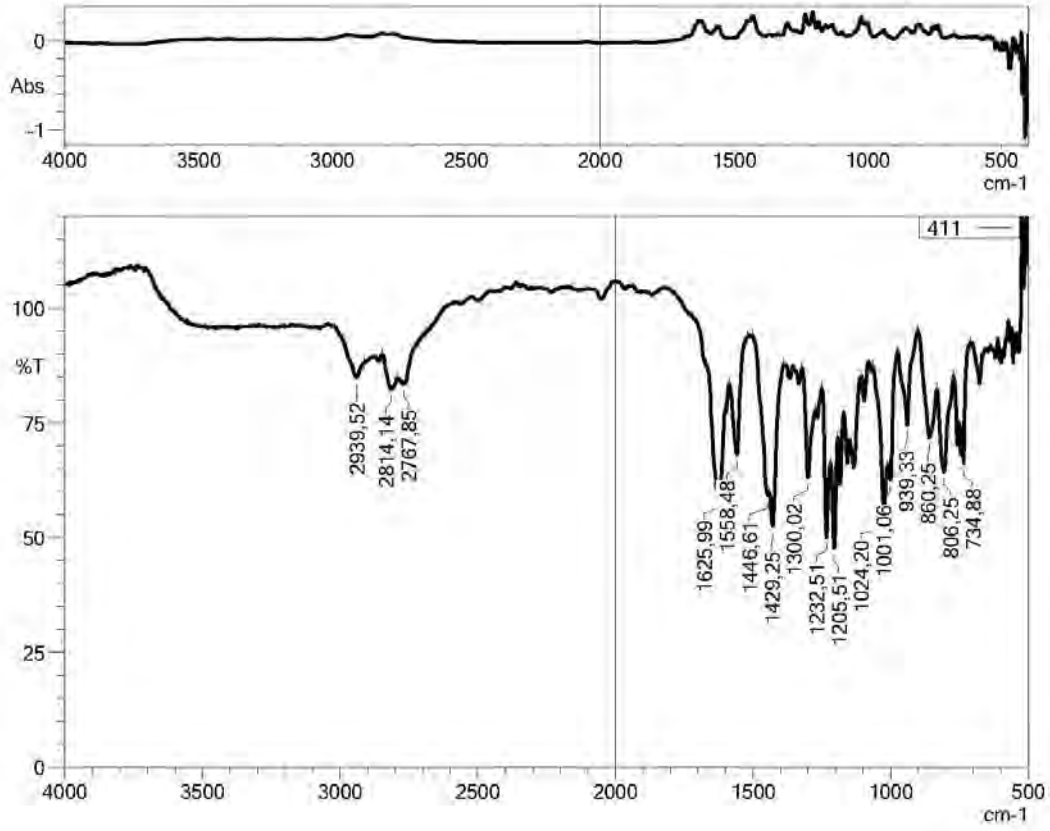


**Figure 5.209.** *IR spectrum of compound **D41***

### 5.1.4.42. *(4-benzylpiperazin-1-yl)(5-methoxybenzofuran-2-yl)methanone (D42)*

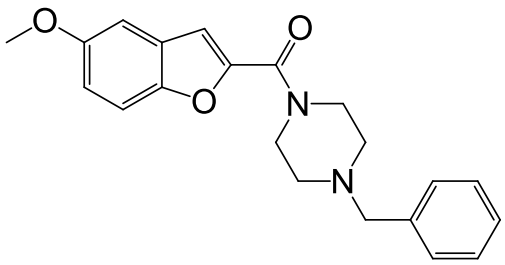

**Figure 5.210.** *Molecular structure of compound* ***D42***

**Physical Properties: Texture: solid** crystals, **Color:** white, **M.P.:** 78.5-79ºC**, Yield:** 59%.

**IR (ATR) $\upsilon_{max}$ ($cm^{-1}$):** 3061 ($SP^2$ C-H stretching, aromatic), 2810-2767 ($SP^3$ C-H stretching, methoxy, and methylenes of piperazine and benzyl), 1633 (C=O stretching, amide), 1558 (C-H bending, indicative of non-substituted benzofuran at position 3), 1456-1427 (C=C stretching, aromatic), 1224-1207 (C-O stretching, ether), 1155, 1026 (C-N stretching, tertiary amine and/or ether), 808 (C-H aromatic out-of-plane bending, one peak, non-substituted benzofuran at position 3) 748-702 (C-H aromatic out-of-plane bending).

**$^1$H NMR (300 MHz) (DMSO-$d_6$) $\delta$ (ppm):** 2.43 (t, *J*= 4.88 Hz, 4H, piperazine-3, 5), 3.50 (s, 2H, phenyl-**$CH_2$**-piperazine), 3.69 (brs, 4H, piperazine-2, 6), 3.78 (s, 3H, **5-methoxy**benzofuran), 7.00 (dd, *J*= 9.03, 2.63 Hz, 1H, benzofuran-6), 7.21 (d, *J*= 2.55 Hz, 1H, benzofuran-4), 7.25-7.28 (m, 1H, phenyl-4), 7.30-7.33 (m, 5H, phenyl-2,3,5,6 and benzofuran-3), 7.55 (d, *J*= 9.04 Hz, 1H, benzofuran-7).

**$^{13}$C NMR (300 MHz) (DMSO-$d_6$) $\delta$ (ppm):** 42.84 (piperazine), 46.87 (piperazine), 53.00 (piperazine), 56.07 (**5-methoxy**benzofuran), 62.22 (phenyl-**$CH_2$**-piperazine), 104.38, 111.51, 112.88, 116.13, 127.52, 127.78, 128.69, 129.38, 138.19, 149.29, 149.46, 156.48, 159.22 (benzofuran-**CO**-piperazine).

**HRMS (ESI) (m/z) $[M+1]^+$:** for $C_{21}H_{22}N_2O_3$ calculated: 351.1703; found: 351.1703.

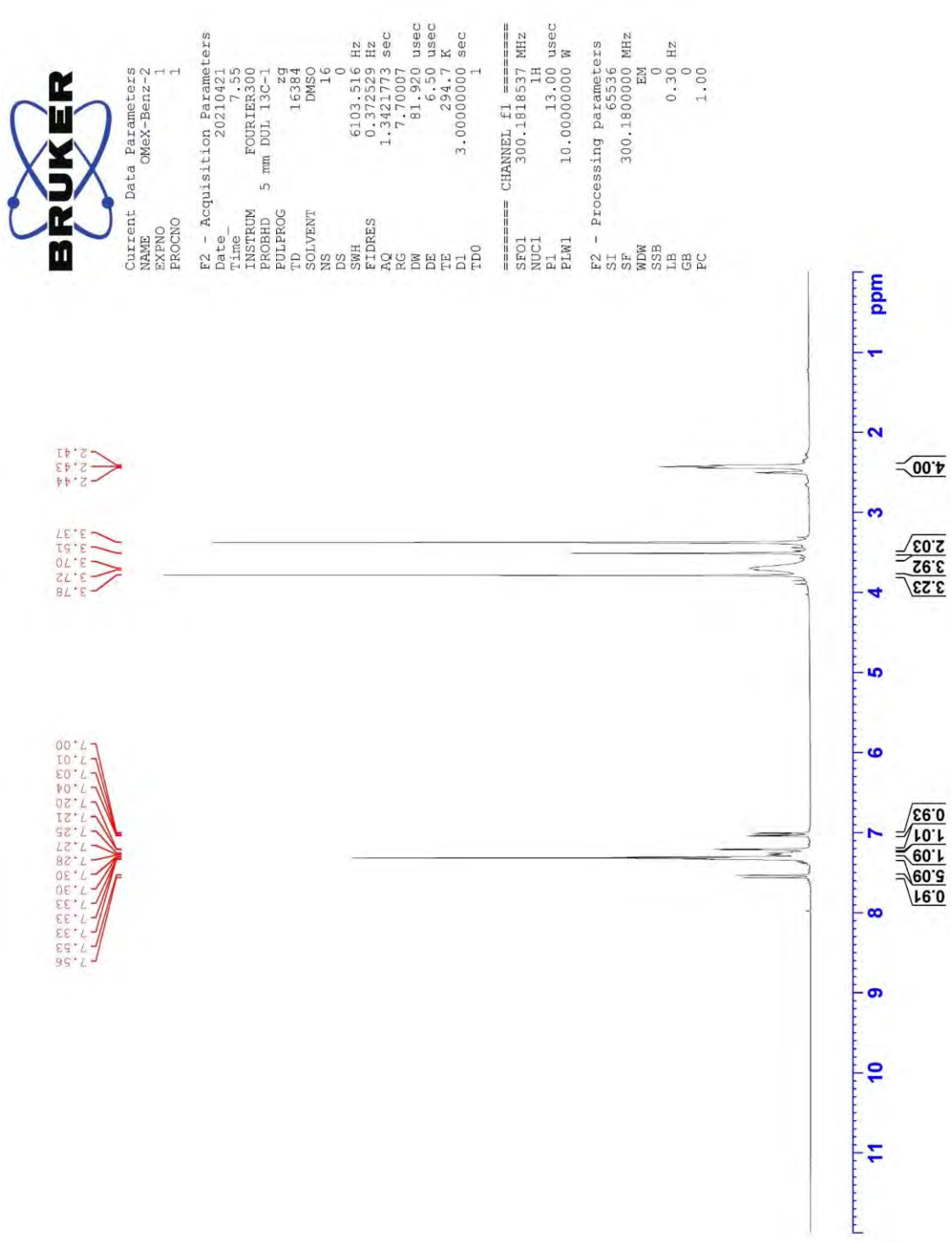


**Figure 5.211.** *[1]H NMR spectrum of compound **D42***

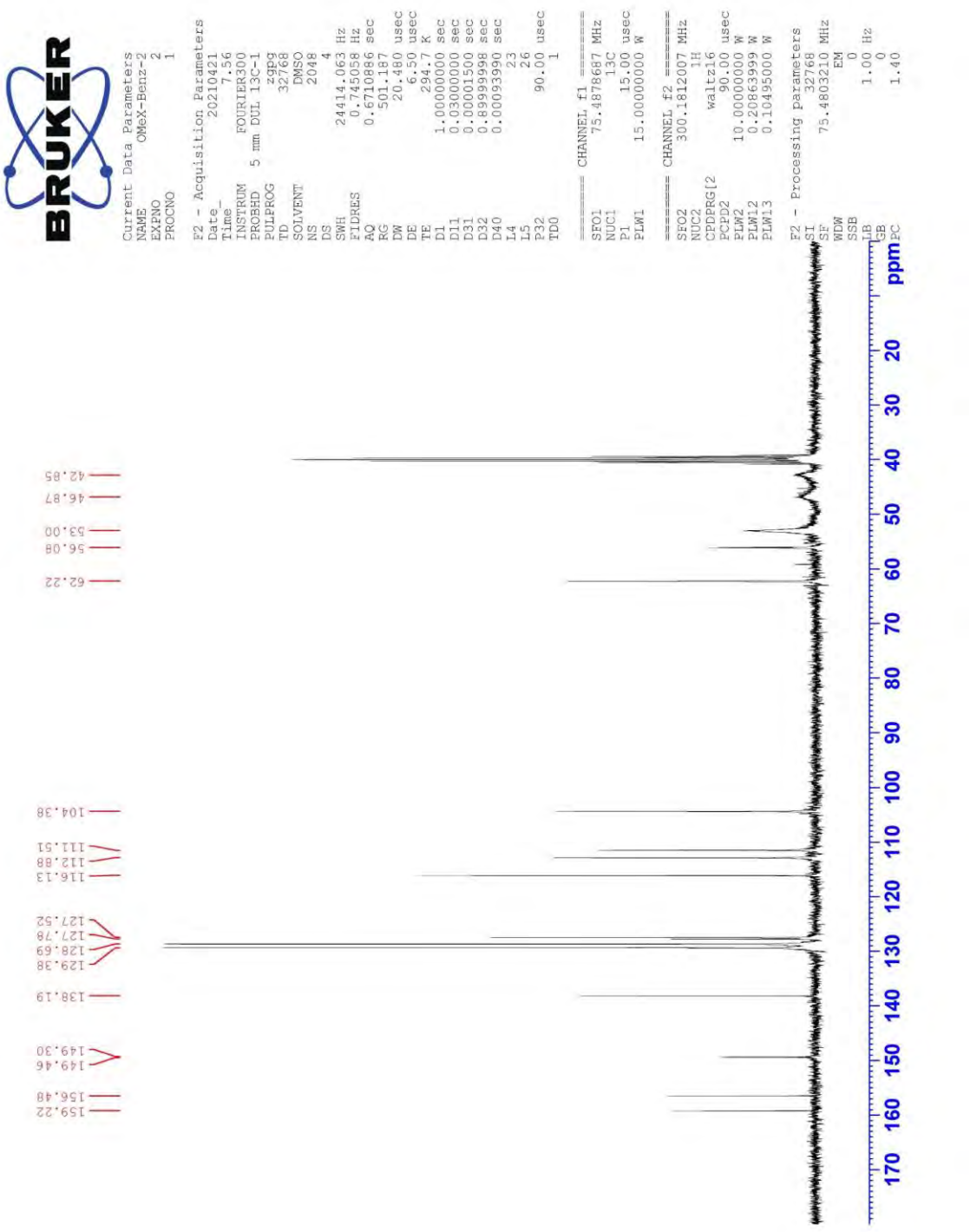


**Figure 5.212.** *$^{13}$C NMR spectrum of compound **D42***

Data File: C:\LabSolutions\Data\Analiz\A.Çağrı\D-42_23.lcd

| Elmt | Val. | Min | Max | Elmt | Val. | Min | Max | Elmt | Val. | Min | Max | Elmt | Val. | Min | Max | Use Adduct |
|---|---|---|---|---|---|---|---|---|---|---|---|---|---|---|---|---|
| H | 1 | 0 | 40 | O | 2 | 0 | 5 | S | 2 | 0 | 0 | Ru | 2 | 0 | 0 | H |
| C | 4 | 0 | 40 | F | 1 | 0 | 0 | Cl | 1 | 0 | 0 | Pd | 2 | 0 | 0 | |
| N | 3 | 0 | 4 | P | 3 | 0 | 0 | Br | 1 | 0 | 0 | I | 3 | 0 | 0 | |

Error Margin (ppm): 5
HC Ratio: unlimited
Max Isotopes: 3
MSn Iso RI (%): 10.00

DBE Range: 0.0 - 20.0
Apply N Rule: yes
Isotope RI (%): 1.00
MSn Logic Mode: AND

Electron Ions: both
Use MSn Info: yes
Isotope Res: 9000
Max Results: 150

Event#: 1 MS(E+) Ret. Time : 2.213 Scan# : 333

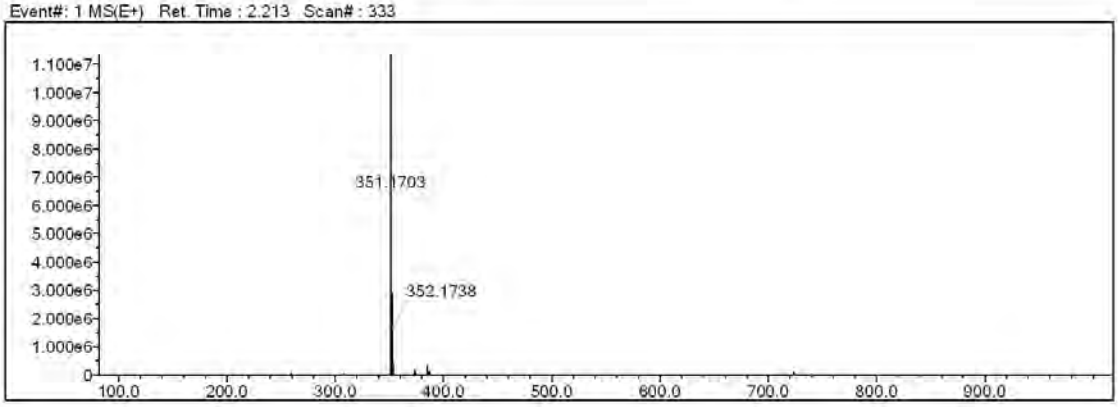


Measured region for 351.1703 m/z

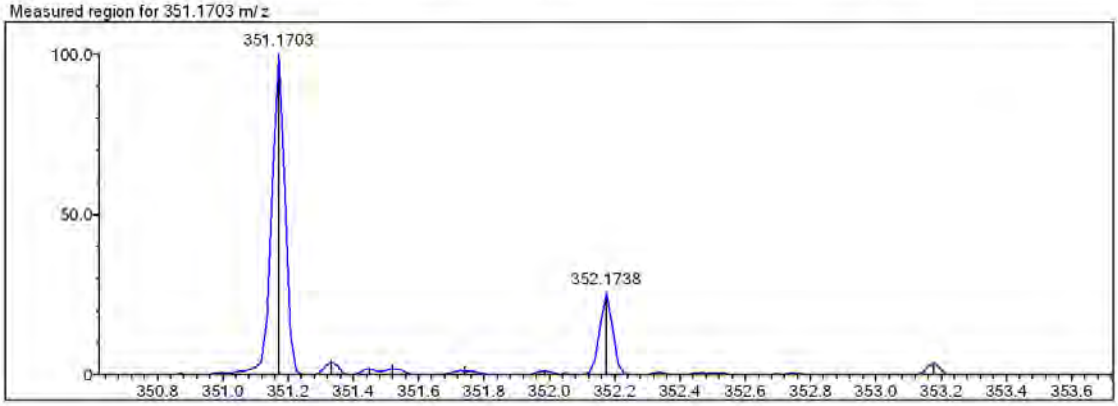


C21 H22 N2 O3 [M+H]+ : Predicted region for 351.1703 m/z

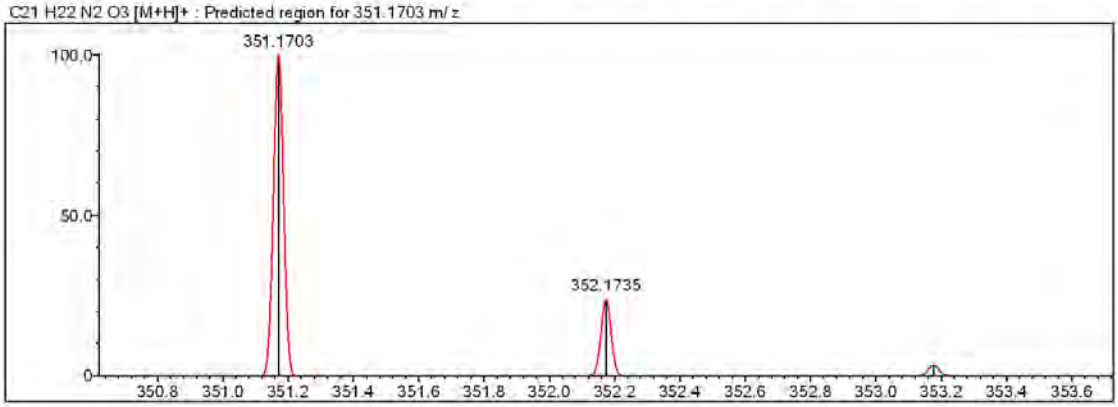


| Rank | Score | Formula (M) | Ion | Meas. m/z | Pred. m/z | Df. (mDa) | Df. (ppm) | Iso | DBE |
|---|---|---|---|---|---|---|---|---|---|
| 1 | 100.00 | C21 H22 N2 O3 | [M+H]+ | 351.1703 | 351.1703 | -0.0 | 0.00 | 100.00 | 12.0 |

**Figure 5.213.** *High-resolution mass spectrum of compound* ***D42***

DOPNALAB

| | Item | Value |
|---|---|---|
| | Acquired Date&Time | 27.05.2021 13:53:20 |
| | Acquired by | System Administrator |
| | Filename | C:\Users\dopnalab\Desktop\sa\422.ispd |
| | Spectrum name | 422 |
| | Sample name | 42 |
| | Sample ID | |
| | Option | |
| | Comment | |
| | No. of Scans | 15 |
| | Resolution | 4 [cm-1] |
| | Apodization | Happ-Genzel |

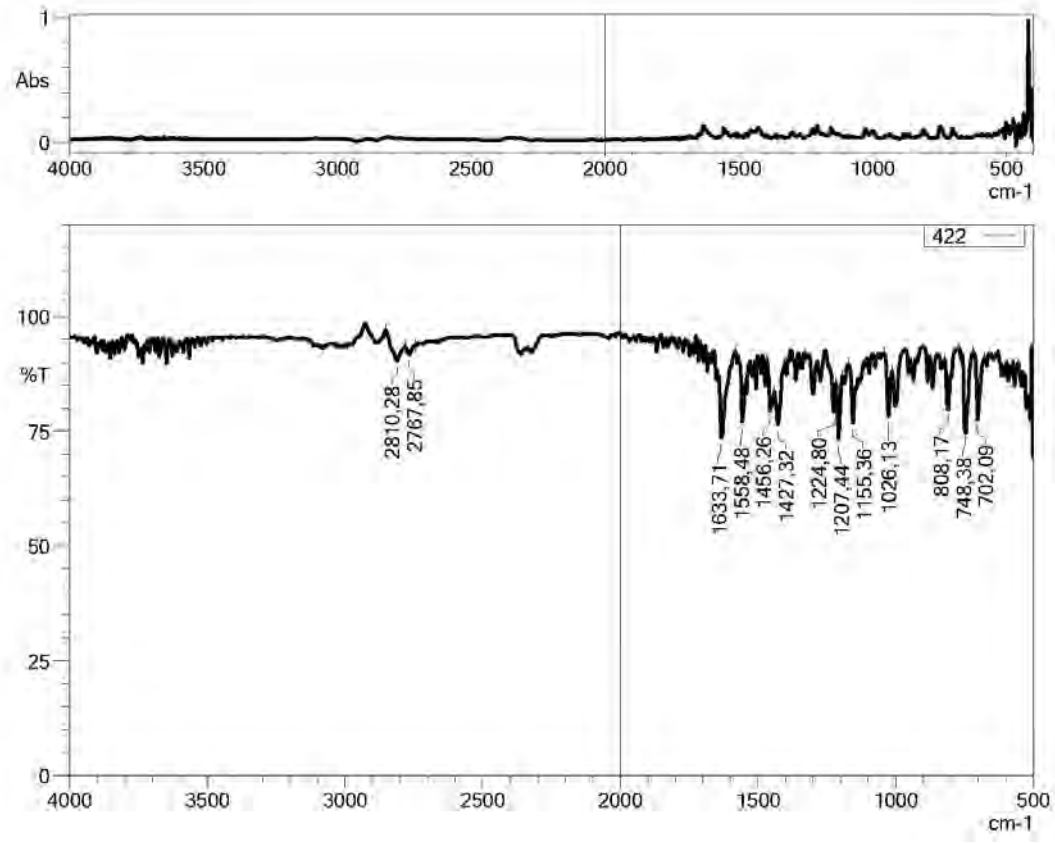


**Figure 5.214.** *IR spectrum of compound **D42***

## 5.2. Chemical Analysis Results

### 5.2.1. Mass spectrometry

The mass spectra of the synthesized compounds were obtained *via* LCMS-IT-TOF using electron spray ionization. The ionization mode was set to detect only the positive ions. At the same time, liquid chromatography was achieved to detect any impurities. As a result, all the chromatograms showed little to no impurities. The mass analysis was then achieved for the products coming out of the chromatograph and fed into the spray ionization unit of the instrument.

The mass analysis involved the detection of mass/charge (m/z) values of each compound. The theoretical values were calculated and compared to the obtained results. Each analysis showed a score of more than 90% accuracy with an error margin set to 0.05. This means that the identity of the compounds is confirmed and complies with the NMR and IR results. By analyzing the spectra, each compound has a parent peak $[M+1]^+$ respective to its molecular weight. All the spectra and analytical data were reported in the analytical monographs of the compounds.

### 5.2.2. $^1$H NMR analysis results

$^1$H NMR analysis was achieved using Bruker UltraShield 300 MHz. All of the samples were prepared in DMSO-$d_6$ and the chemical shifts ($\delta$) were provided in ppm. About 10 mg of each substance was solved with 500 µL of DMSO inside NMR tubes. NMR spectrometer finished the $^1$H NMR analysis in 1 minute for each sample. It should be noted that the peak of hydrogenated DMSO appeared in all of the analytical spectra. DMSO appeared as a quintet at 2.5 ppm. Additionally, a strong singlet appeared in most of the compounds' spectra at around 3.36 ppm which indicates protons of water with no relation to the synthesized compounds.

All of the compounds are composed of a benzofuran ring as the central nucleus from which various derivatives were designed by changing the groups at positions 2, 3 and 5 of the ring. When considering the benzofuran without substituents at positions 3 and 5, the chemical shifts of protons in 3, 4, 5, 6 and 7 of the benzofuran ring were recognized at around 7.38, 7.74, 7.33, 7.43, and 7.65 ppm, respectively. This can be clearly seen in compounds **D8**-**D10**. Substitution of the proton in position 3 with a methyl group was approved by the disappearance of the peak of the aromatic proton at around 7.38 ppm and the appearance of a singlet peak of methyl in the aliphatic region at 2.2-

2.45 ppm in the spectra of 3-methylated compounds. Similarly, substituting the proton at position 5 of benzofuran with different groups lead to the disappearance of the peak of the aromatic proton at around 7.33 ppm.

5-methoxy benzofuran derivatives have a singlet peak of the methoxy group protons at around 3.81 ppm. In compounds **D37**-**D42**, the protons of benzofuran at positions 3, 4, 6, and 7 were recognized at around 7.35, 7.21, 7.02, and 7.56 ppm respectively. The 3-methylated compounds **D31**-**D36**, have a singlet peak for the protons of the methyl group at around 2.30 ppm. The protons at positions 4, 6, and 7 have approximately similar shifts to those of the unmethylated derivatives. The correlation between the peaks and their respective protons was concluded from the coupling constant (*J*). The benzofuran-4 proton showed a doublet (d) with *J* value equals to one of the *J* values of the doublet of doublet (dd) of the benzofuran-6 proton. Hence, the position of the protons' respective chemical shifts (δ) was assigned accordingly.

5-chlorobenzofuran derivatives have different chemical shifts for their protons in comparison to those of the 5-methoxy derivatives. In compounds **D16**-**D20**, the chemical shifts of protons at positions 3, 4, 6, and 7 of the benzofuran were detectable at around 7.35, 7.81, 7.47, and 7.71 respectively. The methyl group at position 3 of compounds **D11**-**D15** have a chemical shift at around 2.30 ppm like those of the 5-methoxy and 5-unsubstituted benzofuran derivatives. The protons of compounds **D11**-**D15** at positions 4, 6, and 7 have close chemical shifts to those of their 3-unmethylated counterparts. It is observable that the chemical shifts of the benzofuran ring's protons of the 5-chlorobenzofuran derivatives are very close to those of the 5-unsubstituted ones. Similar to the 5-methoxybenzofuran derivatives, the chemical shifts of the 4, 6, and 7 protons were determined relying on the *J* values.

5-nitrobenzofuran derivatives, **D26**-**D30**, have chemical shifts of their protons at positions 3, 4, 6, and 7 at around 7.60, 8.70, 8.32, and 7.92 ppm, respectively. The protons of the 3-methylated counterparts, **D21**-**D25**, at positions 4, 6, and 7 have almost similar chemical shifts except for compounds **D25** which has a different chemical shift for the proton at position 7 of the ring at 7.44 ppm. The nitro group at position 5 affected the resonance of the protons of the benzofuran ring obviously. The strong electron-withdrawing property of the nitro group causes the protons of the benzofuran ring to be deshielded. Hence, the resonance of the protons shifted downfield to higher chemical

shifts. Also similar to the 5-methoxy, and 5-chlorobenzofuran derivatives, the chemical shifts of the 4, 6, and 7 protons were assigned relying on the *J* values.

The protons of the piperazine ring showed a variation in the chemical shifts in most of the derivatives. In general, the peaks of the methylenes of piperazine appeared as triplets in some of the compounds and as a broad singlet in others. This might be due to the lower 300 MHz power of the instrument used which could not give an optimum resolution in some of the compounds. The protons of piperazine's methylenes number 2 and 6 displayed peaks at around 3.60 ppm for 4-benzyl, methyl, ethyl, and dimethylaminoethyl piperazine derivatives of 3-methylbenzofurans. While the 3-unsubstituted benzofuran derivatives of the same piperazine counterparts had their peaks appearing around 3.69 ppm. This indicates that the 3-methyl group of benzofuran influences the configuration of the compound particularly the amidic linkage which contributes to the electronic and magnetic fields in that area. It is likely that the methyl group attenuates the electron-withdrawing ability of the amidic group leading to a weak shielding of the protons at positions 2 and 6 of piperazine and inducing an upfield shift compared to that of the 3-unsubstituted benzofuran derivatives. The piperazine's protons at 2 and 6 of the phenyl derivatives showed a resonance at 3.75-3.88 ppm. The furoyl derivatives showed a broad sharp singlet of their 2, 3, 5, and 6 methylene's protons at a range of 3.71-3.91 ppm. The protons of the furoyl derivatives of piperazine resolved in a single peak because both of the piperazine nitrogen atoms are bonded into carbonyl groups forming amidic functionality. Thus, the protons are affected equally by the symmetric amide sides.

The piperazine's methylenes number 3 and 5 had their protons resonating at different chemical shifts in most of the derivatives. The protons of 3 and 5 methylenes of benzylpiperazine derivatives showed triplets at around 2.42 ppm. Those of the phenylpiperazine derivatives were shifted downfield to around 3.25 ppm except 3-nitrobenzofuran derivatives which showed peaks at around 3.81 ppm. The furoyl derivatives had their 3 and 5 methylenes' protons shifted as broad singlets together with those of methylenes number 2 and 6. The protons of 4-methyl, ethyl, and dimethylaminoethylpiperazine derivatives displayed peaks at around 3.35, 2.40, and 2.44 ppm, respectively.

Finally, the substituents at 4-piperazine showed well-resolved shifts mostly. The protons of the 4-methyl group displayed singlets at around 2.20 ppm in all the derivatives.

The methyl group of the 4-ethyl substituent showed triplets at around 1.01 ppm, and the methylene group exhibited quartets at approximately 2.36 ppm in all the derivatives. The two terminal methyl groups of the 4-dimethylaminoethyl substituent exhibited broad singlet for the protons of both at around 2.12 ppm, while the protons of the aminoethyl had multiplets at approximately 2.30-2.48 ppm for all the derivatives.

### 5.2.3. $^{13}$C NMR analysis results

$^{13}$C NMR analysis was achieved using Bruker UltraShield instrument and for the same samples prepared previously for $^{1}$H NMR, see **section 5.2.2**. The analysis was achieved at 75 MHz. The NMR spectrometer required 1 hour for each sample to carry out the $^{13}$C NMR analysis. The septet peak appearing at around 39.95 ppm belongs to DMSO.

The data shown in Table 5.1 were concluded from 1D and 2D NMR analysis. Compounds **D3**, **D18**, **D25**, and **D41** only were analyzed using 2D NMR in addition to their 1D NMR. The 2D data of their counterparts were extrapolated and interpreted inferentially.

In the benzofuran ring, the carbons bonded directly to the oxygen are the most deshielded, hence they displayed peaks in the far downfield region but not farther than the carbonyl carbon. C7a was more deshielded in comparison to C2 due to all the bonds of C7a being inside the aromatic cycle while one bond of C2 is outside the ring to an electron-withdrawing group which contributes to reorder the deshielded electron clouds between itself and the aromatic ring and hence induces a weak shielding effect on C2. The presence of methyl group in position 3 had a shielding effect on C3 generally which induced a decrease in the value of the chemical shift. In contrast, the 3-methyl group caused deshielding on C2 and increased the chemical shift accordingly.

The chemical shift of C5 was affected by the presence of substituents bonded directly to it. A chlorine substituent has a deshielding effect on C5 causing a downfield shift observed by the increased value of the chemical shift and caused no significant effect on C4 and C6. On the other hand, a stronger deshielding effect was observed by the presence of a nitro group bonded to C5 and a slight shielding on C4 and C6 was observed by the decreased chemical shifts toward the upfield. Moreover, the presence of 5-methoxy group caused even a stronger deshielding than that caused by the nitro group and a stronger shielding effect on C4 and C6. Slight differences are observed between the remaining carbons of benzofuran. It should be noted that the results and interpretations

of the compounds in **Table 5.1** are comparable to the rest of the synthesized compounds with only minor differences.

**Table 5.1.** *Chemical shifts of carbons of benzofuran*

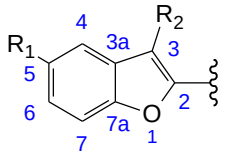


| Substituents | | | δ (ppm)[1] | | | | | | | |
|---|---|---|---|---|---|---|---|---|---|---|
| **R1** | **R2** | **Cpd[2]** | **C2** | **C3** | **C4** | **C5** | **C6** | **C7** | **C3a** | **C7a** |
| **H** | **CH3** | **D3** | 144.4 | 119.24 | 121.14 | 123.64 | 126.83 | 112.02 | 128.99 | 153.38 |
| | **H** | **D8** | 148.73 | 111.18 | 122.87 | 124.14 | 126.93 | 112.23 | 128.82 | 154.33 |
| **Cl** | **CH3** | **D13** | 145.76 | 118.79 | 120.77 | 128.14 | 126.72 | 113.73 | 130.58 | 151.91 |
| | **H** | **D18** | 150.19 | 110.64 | 122.2 | 128.53 | 126.87 | 113.95 | 128.82 | 152.87 |
| **NO2** | **CH3** | **D25** | 147.26 | 119.83 | 118.01 | 144.5 | 122.31 | 113.22 | 129.7 | 156.5 |
| | **H** | **D30** | 151.47 | 111.63 | 119.53 | 144.59 | 122.30 | 113.37 | 127.84 | 157.09 |
| **OCH3** | **CH3** | **D53** | 145.03 | 119.55 | 102.95 | 156.33 | 115.86 | 112.66 | 129.55 | 148.19 |
| | **H** | **D41** | 149.28 | 111.56 | 104.46 | 156.52 | 116.27 | 112.90 | 127.81 | 149.28 |

[1]chemical shift, [2]compound's code

The carbons of phenyl piperazine in general showed signals in chemical shifts similar to those reported by Alver *et al*. (2007) [159]. The C2 and C6 of piperazine showed signals at around 46 ppm with a weak signal also appearing at 42 ppm which indicates that each carbon might have its own signal but cannot be assigned individually, while the signal of C3 and C5 kept appearing at approximate chemical shift around 49 ppm. The phenyl group showed peaks at around 116 ppm for both its C2 and C6, 129 ppm for C3 and C5, 151 ppm for C1, and 119 ppm for C4.

The peaks of C3 and C5 in furoyl piperazine in compound **D2** and its similar derivatives were shifted altogether with those of C2 and C6 in the same region at around 46 ppm. The peaks of bonded protons to these carbons also appeared in the same chemical shift in $^{1}$H NMR. The similarity in chemical shifts of protons and carbons of furoyl piperazine derivatives is explained by the symmetry of the piperazine ring due to its bonded carbonyl groups on both sides. The approximate chemical shifts of the carbons of the furan ring were 111, 116, 145, and 147 ppm for C4, C3, C5, and C2, respectively.

In methyl piperazine derivatives, the carbon of the methyl group in position 4 showed a signal at around 46 ppm concomitantly with those of C2 and C6 of piperazine. In addition, the peaks of C3 and C5 in piperazine were shifted downfield to around 55 ppm in methyl piperazine as in compounds **D3**, **D8**, **D13**, **D18**, **D23**, **D28**, **D33,** and **D39**. These data are in line with those reported in the literature [160].

In ethyl piperazine, C2 and C6 of piperazine showed their peaks as usual at around 42 and 46 ppm whereas C3 and C5 had their peaks at 53 ppm. The methylene bridge of the ethyl group have a signal at around 52 ppm, while the terminal methyl showed its carbon's signal at around 12 ppm. These results comply with those reported in the literature [161].

In piperazine derivatives containing dimethylaminoethyl side chain, the carbons of the two terminal methyl groups showed signals at around 46 ppm. The carbon of methylene bonded directly to the piperazine ring showed its peak at around 56 ppm while that bonded to the amine nitrogen was observed at 57 ppm. In the piperazine ring, the C2 and C6 showed their peaks as usual at around 42 and 46 ppm and they are undifferentiated from each other. While the C3 and C5 have signals at around 53 ppm. These data are confirmed by 2D NMR analysis reported in Table 5.4 and Table 5.5.

Finally, the benzylpiperazine derivatives **D36** and **D42** have signals of piperazine C2 and C6 at around 42 and 47 ppm, and C3 and C5 at 53 ppm. The benzylic methylene appeared at 62 ppm. The phenylic C2 and C6 showed signals at 129 ppm, C3 and C5 at 128 ppm, C1 at 138 ppm, and C4 at 126 ppm. These results are comparable to those reported in the literature [162].

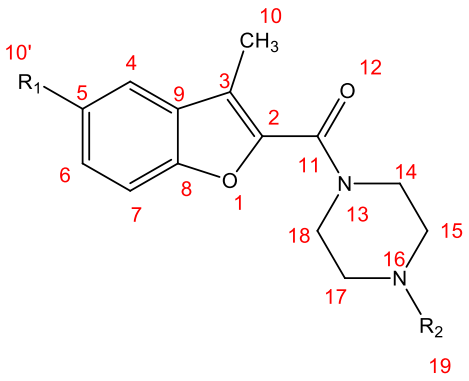


**Figure 5.215.** *The common nucleus of all the synthesized compounds*

### 5.2.4. 2D NMR results

To confirm the spectroscopical results, 2D NMR spectroscopy analysis was carried out for compounds **D3**, **D18**, **D25**, and **D41**. The four compounds were targeted as their substituents on the benzofuran ring are different while considering the most active compounds **D25** and **D41** to be fully analyzed by various spectroscopical means.

2D NMR techniques including HSQC (Heteronuclear Single Quantum Correlation) and HMBS (Heteronuclear Multiple Bond Correlation) were used to determine the correlation between the protons and their directly (HSQC) and indirectly (HMBC) bonded carbons. The relation between protons and carbons of the analyzed molecules was elucidated clearly and the results are shown in **Table 5.2** to **Table 5.5** and **Figure 5.216** to **Figure 5.225**.

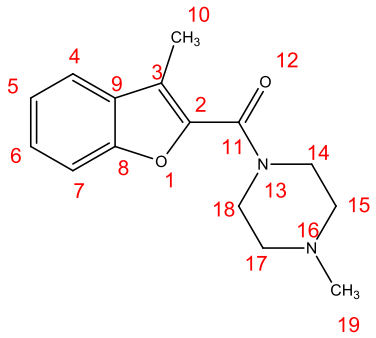


**Figure 5.216.** *Numbering of compound **D3** for illustration of 2D NMR results*

**Table 5.2.** *2D NMR results of compound **D3***

| **Chemical Identity** | **HSQC[1]** | | | **HMBC[2]** | |
|---|---|---|---|---|---|
| | **Hydrogen and carbon site** | **$^{1}$H δ (ppm)** | **$^{13}$C δ (ppm)** | **Correlated carbon site** | **$^{13}$C δ (ppm)** |
| **Benzofuran-3** | 10 | 2.33 | 8.93 | 3 | 119 |
| | | | | 9 | 128.9 |
| | | | | 2 | 144.4 |
| | | | | 11 | 160.27 |
| **4-Methyl piperazine** | 19 | 2.20 | 46.02 | 15 and 17 | 55 |
| **Pipeerazine-3,5** | 15 and 17 | 2.36 | 55.17 | 19 | 46 |
| **Piperazine-2,6** | 14 or 18 | 3.60 | 42.41 | 15 and 17 | 55 |
| | | | | 11 | 160 |
| **Piperazine-2,6** | 14 or 18 | 3.60 | 46.58 | - | - |
| **Benzofuran-5** | 5 | 7.33 | 123.64 | 7 | 112 |
| | | | | 9 | 128.99 |
| **Benzofuran-6** | 6 | 7.43 | 126.83 | 4 | 121 |
| | | | | 8 | 153 |
| **Benzofuran-7** | 7 | 7.59 | 112.02 | 5 | 123.64 |
| | | | | 9 | 128.99 |
| | | | | 8 | 153 |
| **Benzofuran-4** | 4 | 7.70 | 121.14 | 6 | 126.9 |
| | | | | 3 | 119.24 |
| | | | | 8 | 153 |

[1]results which illustrate which hydrogen bonded to which carbon directly, [2] correlations of carbons in a distance of two or three bonds from the respective hydrogen.

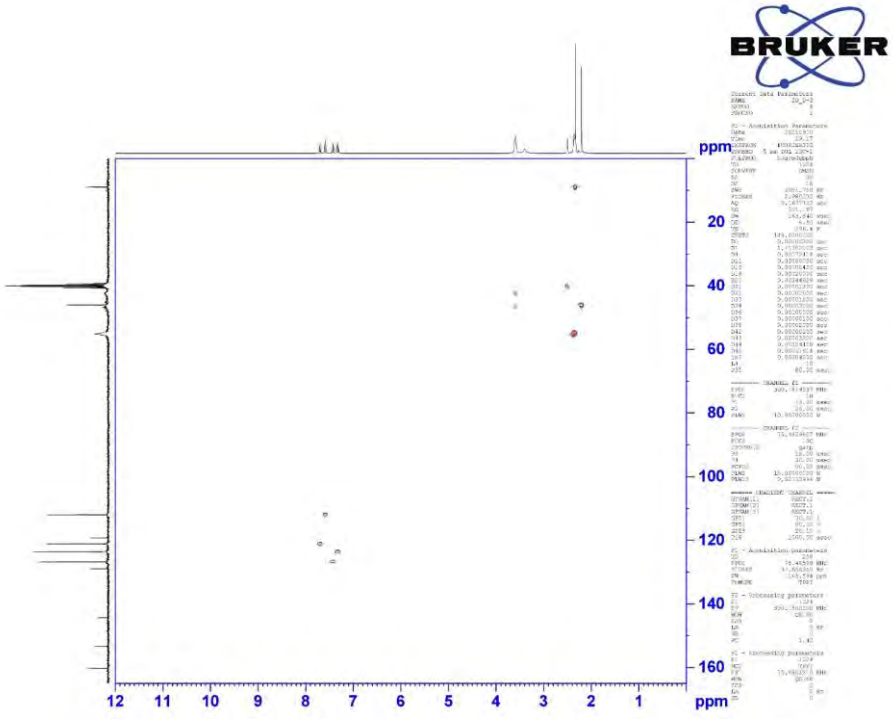


**Figure 5.217.** *HSQC NMR spectrum of compound* ***D3***

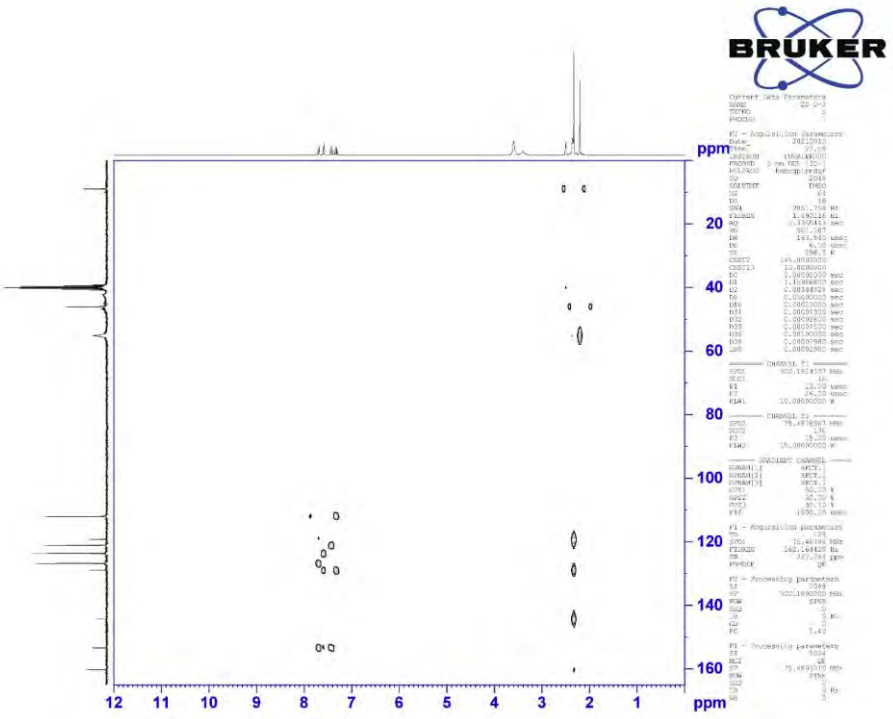


**Figure 5.218.** *HMBC NMR spectrum of compound* ***D3***

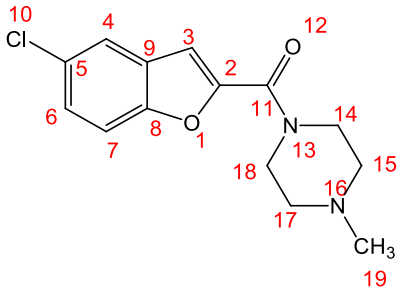


**Figure 5.219.** *Numbering of compound **D18** for illustration of 2D NMR results*

**Table 5.3.** *2D NMR results of compound **D18***

| **Chemical Identity** | **HSQC[1]** | | | **HMBC[2]** | |
|---|---|---|---|---|---|
| | **Hydrogen and carbon site** | **$^{1}$H δ (ppm)** | **$^{13}$C δ (ppm)** | **Correlated carbon site** | **$^{13}$C δ (ppm)** |
| **4-Methyl piperazine** | 19 | 2.19 | 46.02 | 15 and 17 | 55.06 |
| **Pipeerazine-3,5** | 15 and 17 | 2.36 | 55.08 | 19 | 46.02 |
| | | | | | 55.06 |
| **Piperazine-2,6** | 14 or 18 | 3.67 | 42.65 | - | - |
| **Piperazine-2,6** | 14 or 18 | 3.67 | 46.82 | - | - |
| **Benzofuran-3** | 3 | 7.35 | 110.64 | 9 | 128.82 |
| | | | | 2 | 150.19 |
| | | | | 8 | 152.87 |
| | | | | 4 | 122.21 |
| **Benzofuran-6** | 6 | 7.45 | 126.87 | 4 | 122.26 |
| | | | | 5 | 128.53 |
| | | | | 8 | 152.87 |
| **Benzofuran-7** | 7 | 7.69 | 113.95 | 5 | 128.53 |
| **Benzofuran-4** | 4 | 7.79 | 122.2 | 6 | 126.97 |
| | | | | 3 | 110.68 |

[1]results which illustrate which hydrogen bonded to which carbon directly, [2] correlations of carbons in a distance equivalent to two or three bonds from the respective hydrogen.

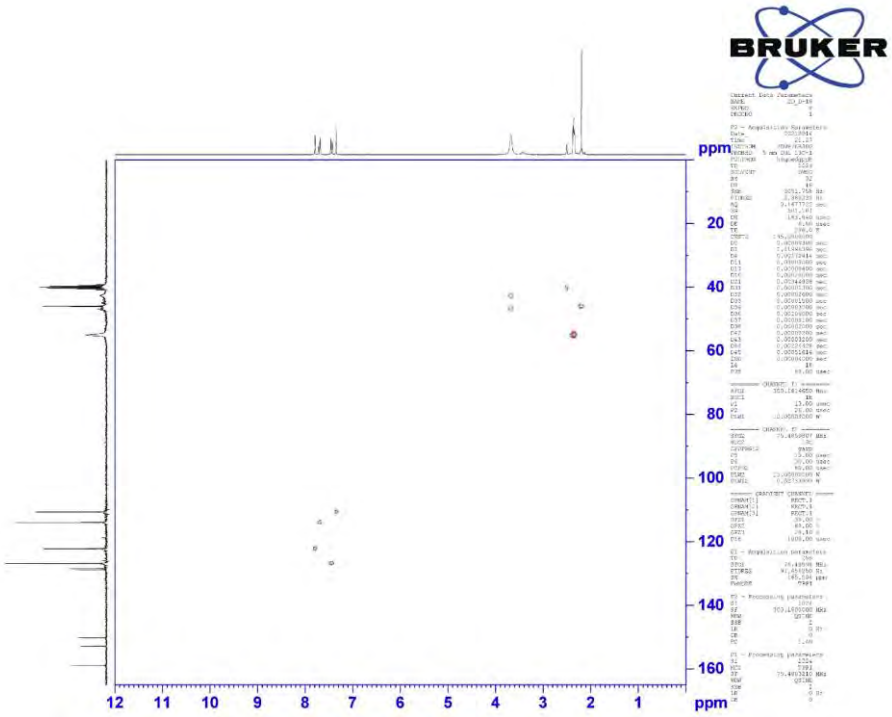


**Figure 5.220.** *HSQC NMR spectrum of compound* ***D18***

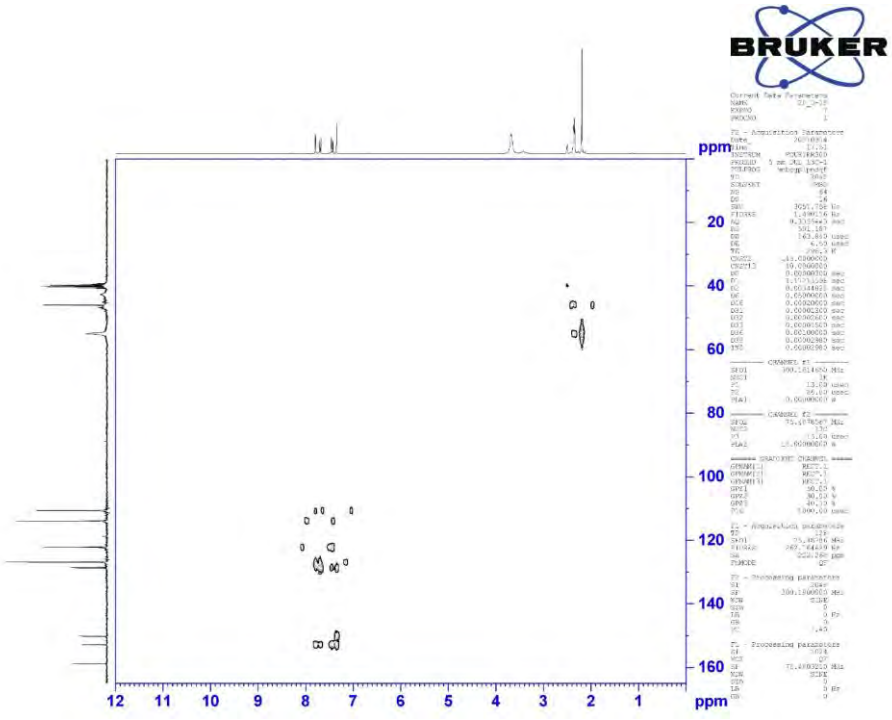


**Figure 5.221.** *HMBC NMR spectrum of compound* ***D18***

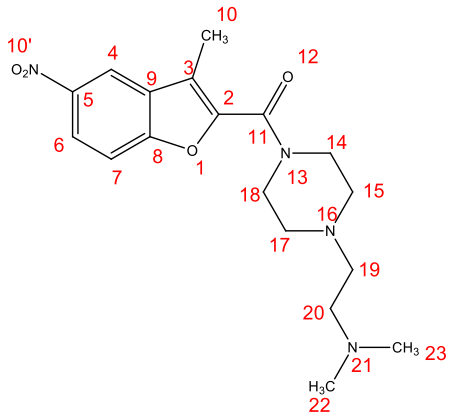


**Figure 5.222.** *Numbering of compound **D25** for illustration of 2D NMR results*

**Table 5.4.** *2D NMR results of compound **D25***

| **Chemical Identity** | **HSQC[1]** | | | **HMBC[2]** | |
|---|---|---|---|---|---|
| | **Hydrogen and carbon site** | **$^{1}$H δ (ppm)** | **$^{13}$C δ (ppm)** | **Correlated carbon site** | **$^{13}$C δ (ppm)** |
| **-N(CH$_3$)$_2$** | 22 and 23 | 2.13 | 46 | 20 | 57.11 |
| **3-Methyl benzofuran** | 10 | 2.38 | 8.9 | 3 | 119.38 |
| | | | | 9 | 129.68 |
| | | | | 2 | 147.26 |
| **-CH$_2$-N(CH$_3$)$_2$** | 20 | 2.33 | 57.11 | 22 and 23 | 46 |
| | | | | 19 | 56 |
| **Pip-CH$_2$-** | 19 | 2.42 | 56 | 20 | 57.11 |
| **Piperazine-3,5** | 15 and 17 | 2.46 | 53.4 | - | - |
| **Piperazine-2,6** | 14 or 18 | 3.59 | 42.39 | - | - |
| **Piperazine-2,6** | 14 or 18 | 3.59 | 46.98 | - | - |
| **Benzofuran-7** | 7 | 7.86 | 113.22 | 9 | 129.7 |
| | | | | 5 | 144.5 |
| **Benzofuran-6** | 6 | 8.31 | 122.31 | 4 | 118.01 |
| | | | | 8 | 156.5 |
| **Benzofuran-4** | 4 | 8.68 | 118.01 | 5 | 144.5 |
| | | | | 8 | 156.5 |

[1] results which illustrate which hydrogen bonded to which carbon directly, [2] correlations of carbons in a distance of two or three bonds from the respective hydrogen.

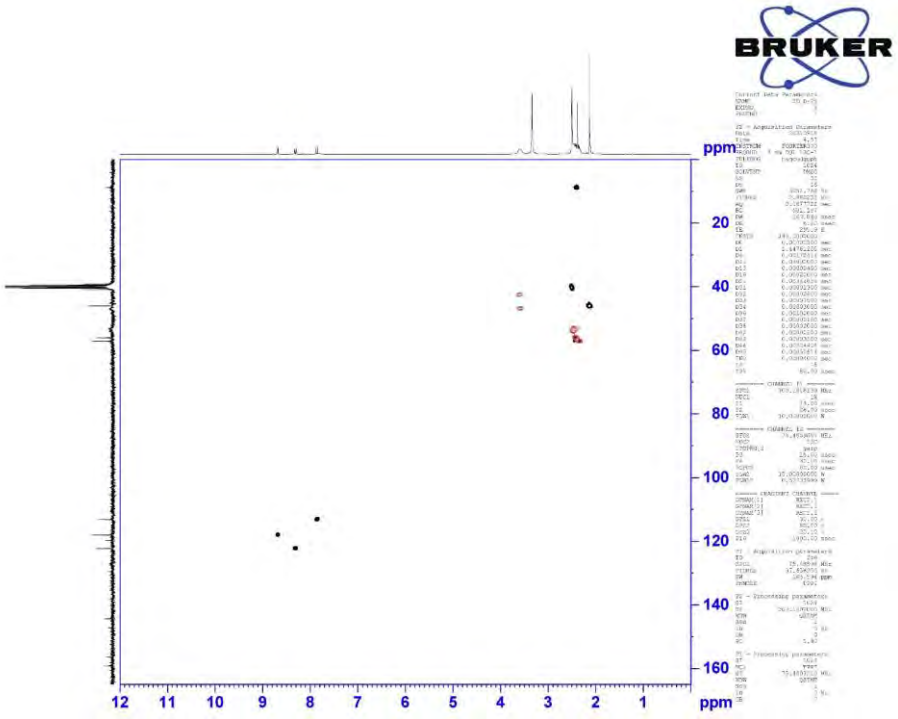


**Figure 5.223.** *HSQC NMR spectrum of compound* ***D25***

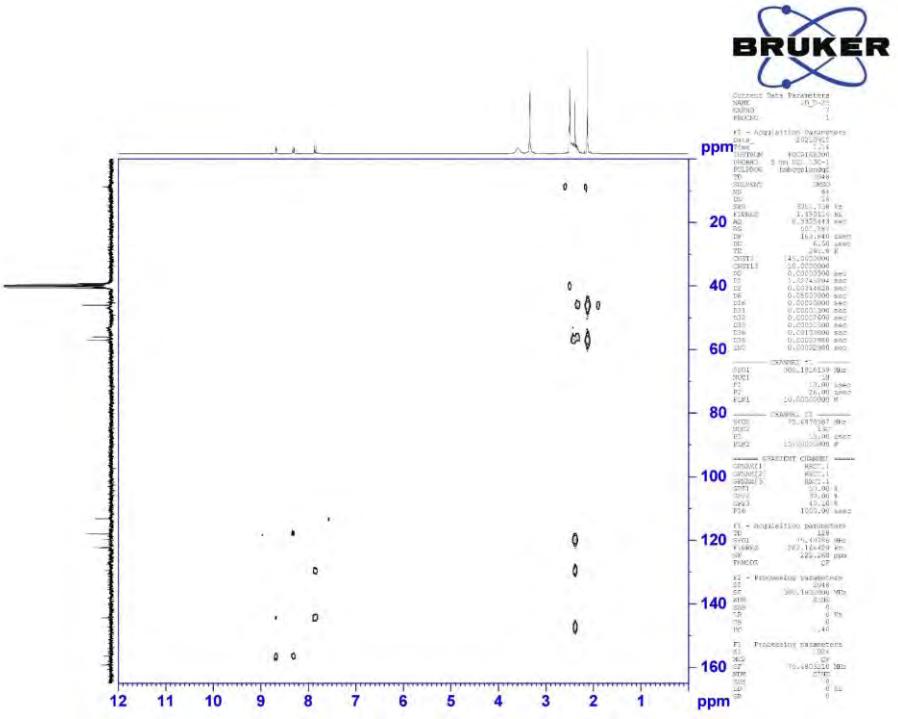


**Figure 5.224.** *HMBC NMR spectrum of compound* ***D25***

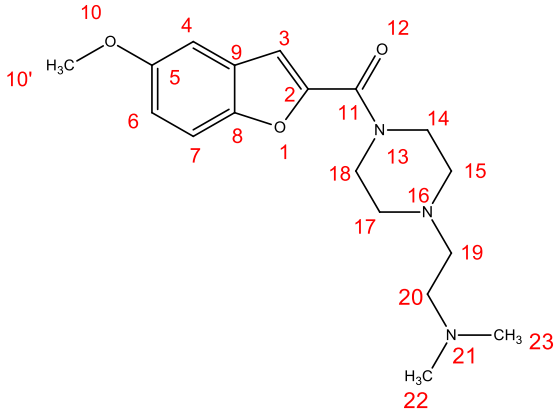


**Figure 5.225.** *Numbering of compound **D41** for illustration of 2D NMR results*

**Table 5.5.** *2D NMR results of compound **D41***

| **Chemical Identity** | **HSQC[1]** | | | **HMBC[2]** | |
|---|---|---|---|---|---|
| | **Hydrogen and carbon site** | **$^{1}$H δ (ppm)** | **$^{13}$C δ (ppm)** | **Correlated carbon site** | **$^{13}$C δ (ppm)** |
| **-N(CH$_3$)$_2$** | 22 and 23 | 2.12 | 46.14 | 20 | 57.18 |
| **-CH$_2$-N(CH$_3$)$_2$** | 20 | 2.33 | 57.18 | 22 and 23 | 46.14 |
| | | | | 19 | 57.18 |
| **Pip-CH$_2$-** | 19 | 2.41 | 56.18 | 20 | 57.18 |
| **Piperazine-3,5** | 15 and 17 | 2.46 | 53.61 | - | - |
| **Piperazine-2,6** | 14 or 18 | 3.67 | 42.75 | - | - |
| **Piperazine-2,6** | 14 or 18 | 3.67 | 46.86 | - | - |
| **5-Methoxybenzofuran** | 10’ | 3.79 | 56.1 | 5 | 156.52 |
| **Benzofuran-6** | 6 | 7.02 | 116.27 | 4 | 104.46 |
| | | | | 8 | 149.28 |
| **Benzofuran-4** | 4 | 7.21 | 104.46 | 6 | 116.27 |
| | | | | 8 | 149.28 |
| **Benzofuran-3** | 3 | 7.31 | 111.56 | 9 | 127.81 |
| | | | | 8 | 149.28 |
| **Benzofuran-7** | 7 | 7.56 | 112.90 | 9 | 127.81 |
| | | | | 5 | 156.52 |

[1] results which illustrate which hydrogen bonded to which carbon directly, [2] correlations of carbons in a distance equivalent to two or three bonds from the respective hydrogen.

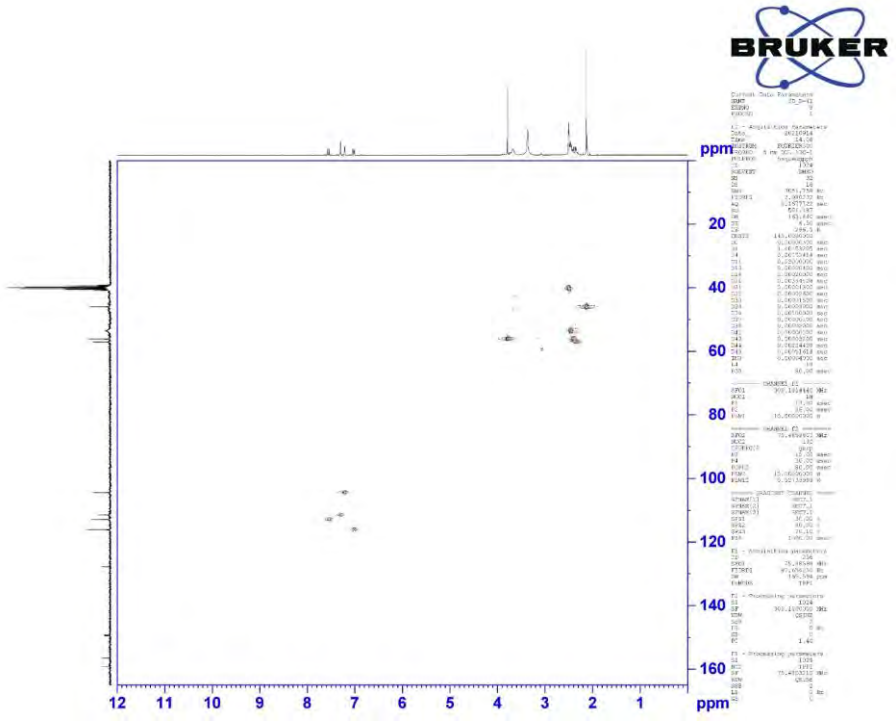


**Figure 5.226.** *HSQC NMR spectrum of compound* ***D41***

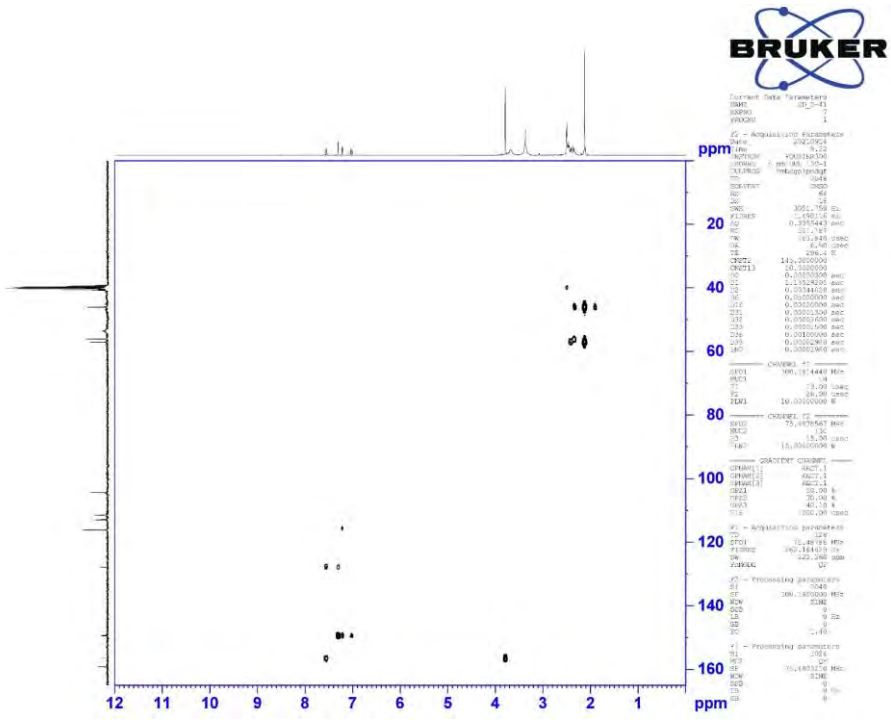


**Figure 5.227.** *HMBC NMR spectrum of compound* ***D41***

### 5.2.5. IR analysis results

The IR analysis was used to indicate the main functional groups in the synthesized molecules. The spectra were presented as a function of the percentage of transmittance versus wave number ($cm^{-1}$). A group of bands was seen above 3000 $cm^{-1}$ which indicates C-H stretching of $SP^2$ hybridized carbons which are basically the aromatic carbons. The region 3000-2750 included peaks indicative of $SP^3$ C-H stretching i.e., methylenes of piperazine, 4- methyl, 4-ethyl, 4-dimethylaminoethylpiperazine, 4-benzylpiperazine, 3-methyl, and 5-methoxy benzofuran.

The amidic functional group was recognized in the region 1633-1612 $cm^{-1}$ as a C=O stretching. The carbonyl group of 4-furoyl piperazine was seen at around 1637 $cm^{-1}$ (conjugated ketone) beside the amidic peak in some compounds while it was masked by the amidic group in others. The signals at 1200-1300 $cm^{-1}$ are indicative of the C-O stretching ether functionality of benzofuran. Similarly, the peaks that occurred in 1020-1000 $cm^{-1}$ might be indicative of ether or C-N stretching of a tertiary amine like the tertiary amine functional group of piperazine at position 4. Other peaks also were observed in different regions and described in the analytical monographs. A reference table of the regions of various functional groups is provided by Merck [163].

## 5.3. Results and Discussion of *In vitro* AChE and BChE Inhibition Tests

The synthesized compounds **D1**-**D42** were tested to evaluate their activity to inhibit both AChE and BChE. The tests involved colorimetric analysis of the ligand-enzyme-complex which was formed by reacting both parts under *in vitro* environment. The test method and the mechanism underlying the whole process of analysis are described by Sağlık [149]. The tests and analysis were achieved in two stages. Firstly, the % inhibition of all the compounds was calculated of the tested compounds in $10^{-3}$ and $10^{-4}$ M and the results are shown in Table 5.6 which represent inhibition percentage ± standard deviation (SD). Secondly, the compounds which displayed more than 50% inhibition activity in the tested concentrations were further tested in lower concentrations down to $10^{-9}$ M and the results are illustrated in Table 5.7. Donepezil and tacrine were used as standard reference compounds as inhibitors of AChE and BChE, respectively.

**Table 5.6.** *% Inhibition of the synthesized compounds, donepezil and tacrine against AChE and BChE*

| Compounds | AChE Inhibition %[1] | | BChE Inhibition %[1] | |
|---|---|---|---|---|
| | $10^{-3}$ M | $10^{-4}$ M | $10^{-3}$ M | $10^{-4}$ M |
| **D1** | 68.757±0.988 | 41.951±0.952 | 32.152±0.857 | 20.654±0.726 |
| **D2** | 62.662±1.124 | 44.528±0.937 | 35.098±0.759 | 25.748±0.674 |
| **D3** | 71.218±0.965 | 48.912±0.891 | 30.657±0.865 | 21.221±0.835 |
| **D4** | 69.092±0.872 | 42.473±0.837 | 28.552±0.809 | 18.645±0.616 |
| **D5** | 63.634±1.397 | 46.728±0.884 | 37.610±0.721 | 22.195±0.746 |
| **D6** | 69.905±0.918 | 47.365±0.995 | 39.671±0.832 | 26.375±0.899 |
| **D7** | 65.173±1.437 | 40.220±0.951 | 30.551±0.811 | 19.148±0.702 |
| **D8** | 68.789±1.046 | 44.848±0.962 | 38.735±0.715 | 23.037±0.854 |
| **D9** | 72.222±1.250 | 48.035±0.832 | 36.714±0.689 | 26.759±0.776 |
| **D10** | 76.014±0.989 | 40.512±0.764 | 40.649±0.852 | 22.614±0.834 |
| **D11** | 64.562±1.180 | 42.354±0.897 | 30.112±0.833 | 20.498±0.815 |
| **D12** | 69.341±1.026 | 47.722±0.926 | 28.649±0.721 | 19.006±0.697 |
| **D13** | 66.404±1.333 | 45.975±0.991 | 26.433±0.619 | 20.512±0.824 |
| **D14** | 73.766±1.254 | 41.192±0.824 | 25.148±0.778 | 17.498±0.616 |
| **D15** | 78.954±0.966 | 46.002±0.937 | 32.199±0.854 | 26.498±0.911 |
| **D16** | 69.171±1.417 | 43.545±0.853 | 38.603±0.908 | 29.367±0.946 |
| **D17** | 61.008±1.284 | 44.462±0.886 | 41.075±0.810 | 34.055±0.975 |
| **D18** | 67.099±1.192 | 40.675±0.819 | 39.123±0.746 | 30.975±0.892 |
| **D19** | 63.430±1.370 | 48.491±0.948 | 33.176±0.920 | 23.467±0.858 |
| **D20** | 66.640±0.917 | 42.848±0.961 | 35.024±0.887 | 21.528±0.734 |
| **D21** | 65.228±1.135 | 46.832±0.919 | 38.618±0.903 | 24.495±0.817 |
| **D22** | 78.164±1.287 | 43.161±0.937 | 34.759±0.945 | 26.375±0.885 |
| **D23** | 80.852±0.989 | 41.475±0.879 | 31.465±0.863 | 20.840±0.703 |
| **D24** | 79.375±1.120 | 47.619±0.731 | 29.077±0.874 | 18.988±0.644 |
| **D25** | 95.721±1.244 | 90.236±1.302 | 34.195±0.714 | 21.477±0.762 |
| **D26** | 82.418±1.266 | 48.504±0.937 | 38.203±0.969 | 30.912±0.872 |
| **D27** | 84.638±1.152 | 42.765±0.955 | 36.495±0.885 | 27.927±0.990 |
| **D28** | 86.246±1.389 | 40.002±0.803 | 40.035±0.935 | 20.367±0.704 |
| **D29** | 88.819±1.137 | 44.244±0.987 | 37.548±0.975 | 22.095±0.667 |
| **D30** | 93.527±1.388 | 89.621±1.247 | 32.465±0.715 | 26.792±0.712 |
| **D31** | 78.421±1.228 | 39.572±0.964 | 38.951±0.835 | 23.034±0.831 |
| **D32** | 79.077±1.138 | 47.103±0.951 | 33.744±0.897 | 19.517±0.754 |
| **D33** | 86.395±1.359 | 38.454±0.898 | 30.468±0.916 | 21.469±0.861 |
| **D34** | 80.885±1.164 | 46.889±0.775 | 32.023±0.834 | 20.647±.0.846 |
| **D35** | 89.920±1.217 | 44.690±0.934 | 35.677±0.816 | 25.331±0.945 |
| **D36** | 87.415±1.128 | 48.247±0.822 | 29.551±0.774 | 21.473±0.837 |
| **D37** | 82.667±1.192 | 43.420±0.961 | 34.656±0.684 | 23.618±0.719 |
| **D38** | 85.748±1.275 | 42.015±0.805 | 38.340±0.937 | 22.197±0.684 |
| **D39** | 88.592±1.136 | 40.381±0.980 | 31.798±0.819 | 17.288±0.762 |
| **D40** | 94.234±1.158 | 86.092±1.394 | 37.568±0.764 | 21.950±0.848 |
| **D41** | 95.348±1.457 | 91.751±1.385 | 39.621±0.902 | 24.735±0.912 |
| **D42** | 89.874±1.002 | 42.962±0.985 | 35.755±0.944 | 28.699±0.859 |
| **Donepezil** | 99.254±2.104 | 97.426±1.890 | - | - |
| **Tacrine** | - | - | 98.255±1.895 | 95.465±1.344 |

[1] inhibition % ± SD

**Table 5.7.** *$IC_{50}$ values of D25, D30, D40, D41 and donepezil against AChE*

| Compounds | AChE % Inhibition[1] | | | | | | | $IC_{50}$ (μM) [2] |
|---|---|---|---|---|---|---|---|---|
| | $10^{-3}$ M | $10^{-4}$ M | $10^{-5}$ M | $10^{-6}$ M | $10^{-7}$ M | $10^{-8}$ M | $10^{-9}$ M | |
| **D25** | 95.721 ±1.244 | 90.236 ±1.302 | 84.267 ±1.104 | 79.816 ±1.179 | 72.598 ±1.354 | 43.499 ±0.729 | 26.032 ±0.832 | 0.027 ±0.001 |
| **D30** | 93.527 ±1.388 | 89.621 ±1.247 | 77.234 ±1.106 | 68.190 ±1.385 | 62.526 ±1.402 | 43.058 ±0.978 | 21.677 ±0.852 | 0.047 ±0.002 |
| **D40** | 94.234 ±1.158 | 86.092 ±1.394 | 78.914 ±1.402 | 70.922 ±1.528 | 65.677 ±1.117 | 44.133 ±0.838 | 25.458 ±0.693 | 0.038 ±0.001 |
| **D41** | 95.348 ±1.457 | 91.751 ±1.385 | 81.695 ±1.166 | 74.207 ±1.578 | 70.689 ±1.022 | 45.819 ±0.942 | 23.738 ±0.811 | 0.023 ±0.001 |
| **Donepezil** | 99.254 ±2.104 | 97.426 ±1.890 | 92.258 ±1.510 | 90.318 ±1.104 | 81.365 ±1.104 | 43.875 ±0.601 | 21.418 ±0.548 | 0.021 ±0.001 |

[1]% inhibition ± SD, [2] $IC_{50}$ ± SD

The results of the first stage showed that four compounds have % inhibition against AChE of more than 50%. On the other hand, no activity in the determined limit of 50% was observed in the inhibition of BChE. Hence, no further investigations against BChE were made. In the inhibition of AChE, the active compounds were **D25**, **D30**, **D40**, and **D41**. Compounds **D25** and **D30** are derivatives of 5-nitrobenzofuran bridged through a carbonyl group to 4-(2-(dimethylamino)ethyl)piperazine, whereas compounds **D40** and **D41** are 5-methoxybenzofuran derivatives where **D40** is a 4-ethylpiperazine and **D41** is 4-(2-(dimethylamino)ethyl)piperazine hybrids. Albeit the activity of 5-unsubstituted (**D1**-**D10**) and 5-chloro (**D11**-**D20**) benzofurans was over 60% in $10^{-3}$ M, the activity was poor in $10^{-4}$ M. Thus, these derivatives were concluded to be inactive in inhibiting AChE. It is mainly due to a combination of the change in the functional groups bonded to the benzofuran ring with a contribution of the piperazine substituents. According to Cheung *et al*. (2012), pi-pi stacking of indanone in donepezil with trp-286 is essential for the compound to inhibit AChE [29]. While the carbonyl group in donepezil is part of the indanone scaffold, it is outside the benzofuran scaffold in the targeted products. Accordingly, the distance of the carbonyl from the key amino acid whom it will react might play a role in the changes of compounds' activity.

It was thought that compounds **D36** and **D42** would have good inhibitory activity against AChE due to the similarity in the main parts of the compounds to that of donepezil as illustrated in **Figure 5.228**. First, these compounds are derivatives of 5-methoxybenzofuran where compound **D36** has a methyl group in position 3 of benzofuran while **D42** has not. Second, the benzofuran ring can mimic indanone of donepezil in

forming hydrophobic bonds and pi-pi stacking with the surrounding amino acid residues in the active site of the enzyme. Third, the carbonyl group found in indanone was slightly shifted to the outside in the benzofuran derivatives, but it was expected to act as a hydrogen bond acceptor exactly like the carbonyl of indanone. Fourth, the equivalent of piperidine in donepezil is the piperazine ring in the title compounds of the thesis. Piperazine has one extra nitrogen atom which was thought it would participate in forming new bonds. Fifth, the benzyl group which forms a hydrophobic interaction with certain residues in the active site pocket of the enzyme is found in two of the synthesized compounds (**D36** and **D42**) and the reference compound donepezil. Unexpectedly, both compounds could not achieve the limit of 50% inhibition in $10^{-4}$ M despite the activity in $10^{-3}$ was 87.42±1.13% and 89.87±1.00% for **D36** and **D42**, respectively. The cause of such failure may be owed mainly to the variables in the benzofuran scaffold and its bonded side groups. Specifically, the difference in the aromaticity between indanone of the standard donepezil and the benzofuran of the target compounds and the change in positioning the carbonyl group to the outside of the ring. In addition, the carbonyl bridge in the benzofuran derivatives replaced the methylene bridge in donepezil which offers potential flexibility for the compound to form an optimum conformer for the binding site of AChE. The conformational isomerism around the methylene bridge of donepezil played a role in the inhibitory activity of the drug [29].

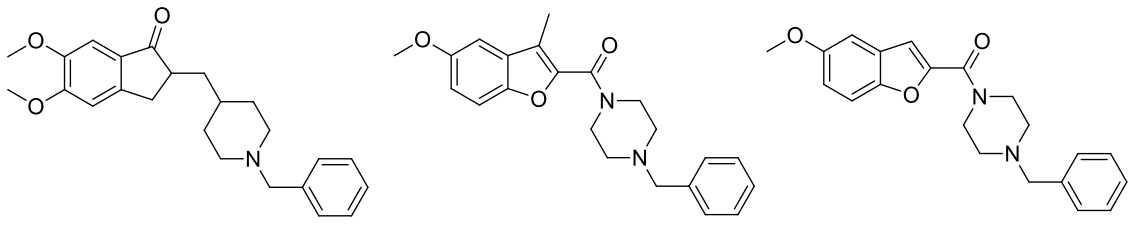


**Figure 5.228.** *Comparison of the chemical structures of compounds **D36** and **D42** with donepezil*

On the other hand, analogues of compound **D42** namely compounds **D40** and **D41** showed exquisite activities where their $IC_{50}$ values were 0.038±0.001 and 0.023±0.001, respectively. The difference in these compounds from **D42** is the piperazine derivatives used. Compound **D40** has a 4-ethyl substituent while compound **D41** has a 4-(2-(dimethylamino)ethyl) substituent on the piperazine ring. Additionally, the other two active 5-nitrobenzofuran derivatives **D25** and **D30** have the same piperazine side chain

as that of **D41** which is the dimethylamino ethyl. The chemical properties of the nitrogen in this group are similar to that of nitrogen number 4 of piperazine. This indicates that the nitrogen of dimethylamino group can act as a substitute to the nitrogen atom of piperazine since they both formed tertiary amines. As a result, the activity of compounds **D25**, **D30**, and **D41** is believed to occur due to certain interactions on the dimethylamino group instead of the nitrogen of piperazine.

### 5.4. β-Amyloid Aggregation Inhibitory Activity

The active compounds **D25**, **D30**, **D40**, and **D41** were tested for their capability to inhibit the aggregation of Aβ which is believed to be involved in the pathogenesis of AD. The results are illustrated in Table 5.8 and Figure 5.229. Various reviews and studies reported a non-cholinergic role of AChE which is mainly its involvement in Aβ aggregation [164–167]. AChE was investigated for its function in the formation of Aβ aggregates and indicated that its PAS basically promotes and propagates the formation of Aβ fibrils [168, 169]. As a result, from a postulation perspective, blocking the PAS of AChE can potentially prevent the enzyme from inducing the nucleation process of Aβ fibrillation. The agents synthesized in this thesis were designed to bind the active site of the enzyme by spanning both CAS and PAS similarly to donepezil. Hence, they are expected to inhibit the aggregation of Aβ.

**Table 5.8.** *Results of %inhibition of $A\beta_{1\text{-}42}$ aggregation by compounds **D25**, **D30**, **D40**, and **D41***

| | Control | D25 | D30 | D40 | D41 |
|---|---|---|---|---|---|
| **10 µM** | 92.895 | 85.001 | 68.423 | 66.844 | 80.398 |
| **1µM** | 85.498 | 69.607 | 59.131 | 55.136 | 68.415 |
| **0.1 µM** | 44.393 | 52.634 | 40.003 | 39.213 | 48.687 |
| **0.01 µM** | 32.898 | 31.516 | 28.343 | 22.635 | 32.898 |

The results showed that compounds **D25** and **D41** could inhibit the aggregation of Aβ in comparable percentage to that of the control used in the assay at the lowest concentration used 0.01 µM, where % inhibition was 32.89, 31.52, and 32.89 for the control, **D25** and **D41**, respectively. Both **D25** and **D41** showed more than 80% inhibition in 10 µM. Compounds **D30** and **D40** displayed inhibition of Aβ of more than 60% at 10 µM and more than 20% at 0.01 µM. Apparently, compounds **D25**, **D30**, **D40**, and **D41**

showed considerable Aβ aggregation inhibitory activity with **D25** and **D41** being comparable to the control inhibitor.

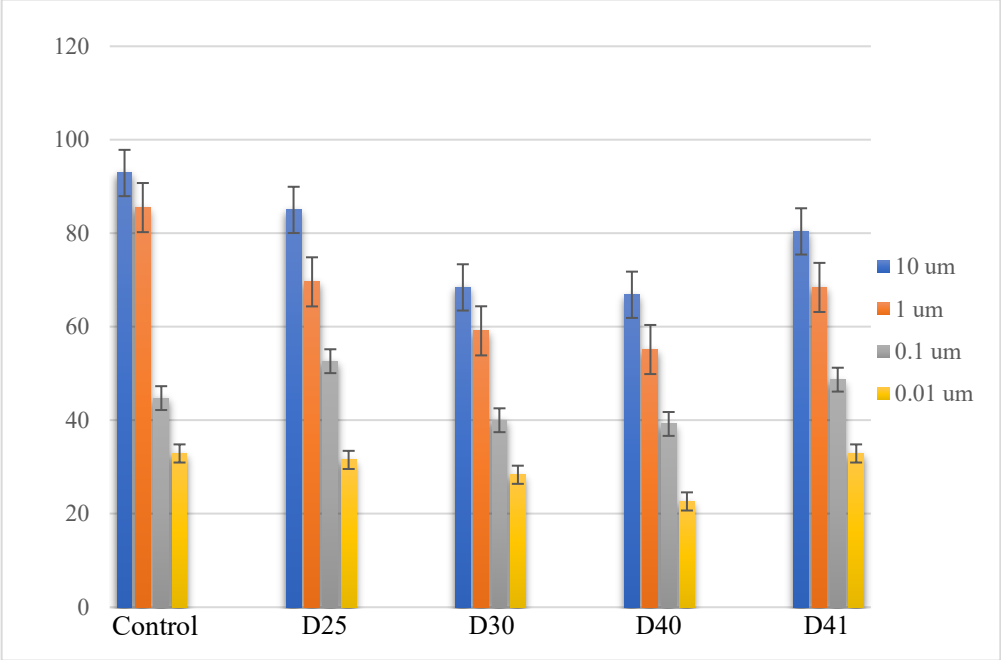


**Figure 5.229.** *Illustration of the inhibition of Aβ $_{1-42}$ aggregation*

## 5.5. Pharmacokinetic Profile

The prediction of the pharmacokinetic profile for compounds **D25**, **D30**, **D40**, **D41,** and the reference drug donepezil are illustrated in Table 5.9. All of the synthesized 42 compounds did not violate any rule of Lipinski's rule-of-five regarding the drug-likeness evaluation including the number of rotatable bonds and hydrogen-bond donors and acceptors. The remaining properties were calculated only for the active compounds.

The lipophilicity indicator $LogP_{o/w}$ was calculated and the results were in the required range as reported by Daina *et al*. [170], where the range is between -0.7 and 5. The lipophilicity values of the 5-nitrobenzofuran derivatives were apparently higher than those of their 5-methoxy analogues. Accordingly, this might contribute to the poor blood-brain barrier (BBB) permeability of compounds **D25** and **D30**. The lipophilicity of **D40** and **D41** is close to that of donepezil. On the other hand, the water solubility of the active compounds was higher than that of the standard. The recommended range of LogS values is -6.5 to 5. All of the four compounds displayed LogS values in the recommended range.

In predicting the absorbance and permeability in various body parts, the absorbance of the four compounds from the gastrointestinal tract (GIT) was expected to be highly

similar to that of the reference drug. Compounds **D40** and **D41** were predicted to be capable to permeate through BBB in contrast to **D25** and **D30**. The prediction model correlates between the polarity and lipophilicity of the compounds and finds their relation to the permeation through BBB [170, 171]. Topological polar surface area (TPSA) of compounds **D25** and **D30** was high enough to predict a poor BBB permeation in addition to the contribution of the lipophilicity.

As all of the designed compounds in this thesis were planned to target AChE in the central nervous system (CNS), the BBB permeability should be high or should be made high. One method to increase the bioavailability of compounds **D25** and **D30** in the CNS is by loading them on a drug delivery base permeable through the BBB. Nanotechnology is used to design such drug delivery systems and has solved a wide range of bioavailability problems [172].

The skin permeation indicator $LogK_p$ was also calculated for the active compounds to evaluate the safety issues while handling such compounds as they could be toxic by inhibiting AChE peripherally if absorbed through the skin. The range of $LogK_p$ that indicates a compound is skin permeable is between -8 and -1. All of the four compounds showed values indicative of their permeability through the skin. As a result, these compounds should be handled carefully not to have direct contact with the skin.

Regarding the metabolism, compounds **D25** and **D30** were predicted to be P-glycoprotein substrates similar to donepezil. In contrast, compounds **D40** and **D41** are predicted not to be targeted by P-glycoprotein. P-glycoprotein is a protein acting as a transmembrane efflux pump that ejects xenobiotics outside the cell. This protein can affect the success of drug therapy as it limits drug absorption, promotes its excretion *via* urine and bile, and decreases drugs penetration into certain tissues e.g. brain [173].

In this regard, BBB permeability of compounds **D25** and **D30** is affected by two factors, first is their polarity and lipophilicity profile and second is that they are substrates of P-glycoprotein. Again, the design of a drug delivery base *via* nanotechnology is believed to be the optimum solution to make the two compounds bioavailable in the CNS. Compounds **D40** and **D41** are not substrates of P-glycoprotein and are thought to have good bioavailability without any P-glycoprotein limitations. Another important point regarding the substrates of P-glycoprotein is that their toxicity is reduced as the protein enhances the excretion of xenobiotics including drugs. Despite the reduced cytotoxicity of compounds **D25** and **D41**, the toxicity of **D25** is further reduced by its enhanced

excretion profile. **D41** is very much safe on cells, but it is predicted to be a substrate of the metabolic enzymes CYP2C19 and CYP2D6 though.

Inferentially, compound **D41** seems to be elegant concerning all the required pharmacokinetic and pharmacodynamic properties. Compound **D40** has a comparable pharmacokinetic profile to that of **D41**, but its activity is less. On the other hand, compounds **D25** and **D30** both struggle in their success to achieve promising bioavailability but they are still good candidates as this issue can be solved as explained previously.

**Table 5.9.** *Pharmacokinetic profile of the active AChE inhibitor compounds*

| | **D25** | **D30** | **D40** | **D41** | **Donepezil** |
|---|---|---|---|---|---|
| **MW (g/mol)** | 360.41 | 346.38 | 288.34 | 331.41 | 379.49 |
| **RB[1]** | 6 | 6 | 4 | 6 | 6 |
| **HA[2]** | 6 | 6 | 4 | 5 | 4 |
| **HD[3]** | 0 | 0 | 0 | 0 | 0 |
| **TPSA[4] (Å$^2$)** | 85.75 | 85.75 | 45.92 | 49.16 | 38.77 |
| **Log $P_{o/w}$ [5] (XLOGP3)** | 2.16 | 1.80 | 2.27 | 1.94 | 4.28 |
| **Log S (ESOL) [6]** | -3.30, soluble | -2.99, soluble | -3.11, soluble | -3.00, soluble | -4.81, moderately soluble |
| **GI abs.[7]** | High | High | High | High | High |
| **BBB perm.[8]** | No | No | Yes | Yes | Yes |
| **P-GP sub.[9]** | Yes | Yes | No | No | Yes |
| **CYP P450[10]** | 1A2, 2C19, 2D6 | 1A2, 2C19 | 1A2, 2C19, 2D6 | 2C19, 2D6 | 2D6, 3A4 |
| **(Log $K_p$) cm/s[11]** | -6.96 | -7.13 | -6.45 | -6.94 | -5.58 |
| **NoV[12]** | 0 | 0 | 0 | 0 | 0 |

[1]Number of rotatable bonds, [2]number of hydrogen-bond acceptors, [3]number of hydrogen-bond donors, [4]topologica polar surface area, [5]octanol/water partition (lipophilicity descriptor), [6]water solubility, [7]absorption from the gastrointestinal tract, [8]blood-brain barrier permeability, [9]substrate of p-glycoprotien, [10]substrate of CYP P450 metabolic enzymes, [11]skin permeation, [12]Lipinski's rules violations number.

## 5.6. Results of Cytotoxicity Investigation

The effect of the most active compounds **D25, D30, D40,** and **D41** on the embryonic fibroblast NIH/3T3 cells was investigated. MTT method was used as described previously. The compounds were tested for a period of 24 h as illustrated in **Table 5.10**. The results showed that compounds **D40** and **D41** have an appreciated safety regarding the toxicity against healthy cells. Compound **D25** is considered safe too but not as much as **D40** and **D41**, but it is much safer than a wide range of AChE inhibitors reported in the literature. Compound **D30** showed the lowest cytotoxic safety among the active compounds. But it is also considered safer than a lot of compounds in the literature.

Compounds **D41** and **D25** were further tested for their cytotoxicity efficacy over a longer period of 48 hours. An only slight decrease in $IC_{50}$ was observed in the 48 h from that in the 24 h. In a comparison of the effective and toxic $IC_{50}$, the difference was calculated to be more than 9400 times for **D25** and more than 40000 times for **D41**. For compounds **D30** and **D40**, the toxic $IC_{50}$ values were approximately 2000 and 26000 times the effective $IC_{50}$, respectively, in a 24 h period. Thus, this is expected to result in a wide therapeutic window *via in vivo* and clinical settings.

**Table 5.10.** *Results of the cytotoxicity studies*

| Compound | NIH/3T3 $IC_{50}$ ± SD (μM) | |
|---|---|---|
| | 24 h | 48 h |
| **D25** | 265.552 ± 13.090 | 255.126 ± 12.410 |
| **D30** | 95.775±0.474 | - |
| **D40** | >1000 | - |
| **D41** | >1000 | 927.216 ± 21.590 |

## 5.7. Molecular Docking Analysis

Molecular docking was achieved to evaluate the interactions of the active compounds **D25**, **D30**, **D40**, and **D41** with the active site residues of AChE. Since there was no activity observed against BChE, molecular docking studies were unnecessary for this enzyme. Various inhibitors of AChE achieve their activity *via* binding to either the catalytic anionic site (CAS) or the peripheral anionic site (PAS) or both simultaneously by spanning through the whole active site region of the enzyme [149]. CAS includes key amino acids which are important binding targets for inhibitor agents and they are serin (ser)-203, glutamic acid (glu)-334, histidine (his)-447, tryptophan (trp)-86, tyrosine (tyr)-130, tyr-133, tyr-337, and phenylalanine (phe)-338. Whereas PAS includes tyr-72, aspartic acid (asp)-74, tyr-124, tyr-341, and trp-286 [149].

Cheung *et al*. (2012) reported the crystal structure of recombinant human AChE (rhAChE) complexed with donepezil [29]. They showed that trp-86 and trp-286 formed stacking interactions with indanone and benzyl ring of donepezil, respectively. In addition, the nitrogen of piperidine ring of donepezil could form a water-mediated hydrogen bond with tyrosine-341 (tyr-341) and tyr-377. They showed that one side of the piperidine (two carbons) packs tightly against hydrophobic sides of tyr-337, phenylalanine-330 (phe-330), and histidine-447 (his-447).

Ashani *et al*. (1993) reported the critical role of tyr-337 in inhibiting human AChE and the likelihood that phe-295 and trp-86 can form aromatic multi-contact interactions with certain ligands [174]. Castro and Martinez (2001) reviewed the significance of designing dual AChE inhibitors that bind both CAS and PAS of the enzyme and the role of trp-86 and trp-286 in the inhibition [164]. And according to this background, the interactions of the active molecules with the reported active site key amino acids will be evaluated.

The protocol of molecular docking was checked by redocking the reference compound donepezil is found previously complexed with the enzyme crystal used for this study (PDB: 4EY7). The redocking results showed a root-mean-square deviation (RMSD) value of 0.4040 which is totally acceptable since it is less than 2. RMSD values of more than 2 are indicative of poor protocols for molecular docking. The interactions of donepezil in the active site of the enzyme are illustrated in Figure 5.230, Figure 5.231, and Figure 5.232. Donepezil formed pi-pi stacking interactions with trp-286 and trp-86 which are key amino acids whose binding is critical for AChE inhibition. Other interactions included a hydrogen bond with phe-295 and a water-mediated hydrogen bond with ser-293 and trp-286.

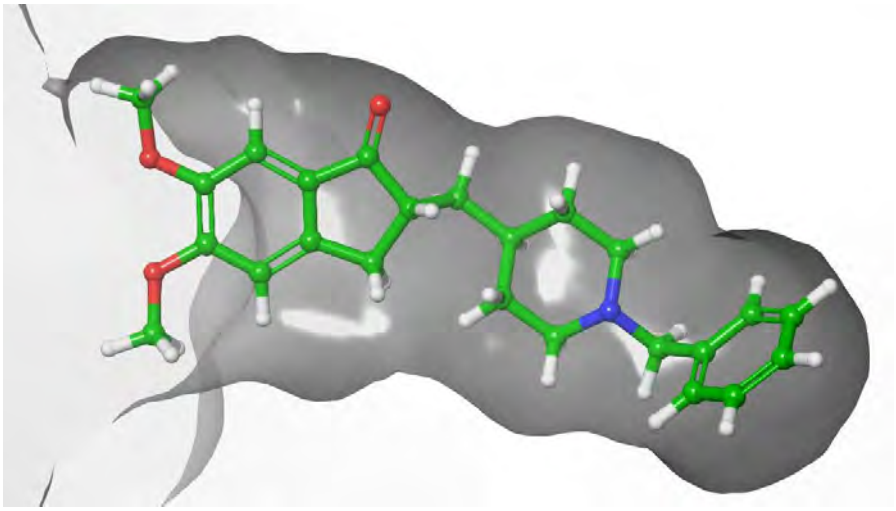

**Figure 5.230.** *Fitting of donepezil in the active site of AChE*

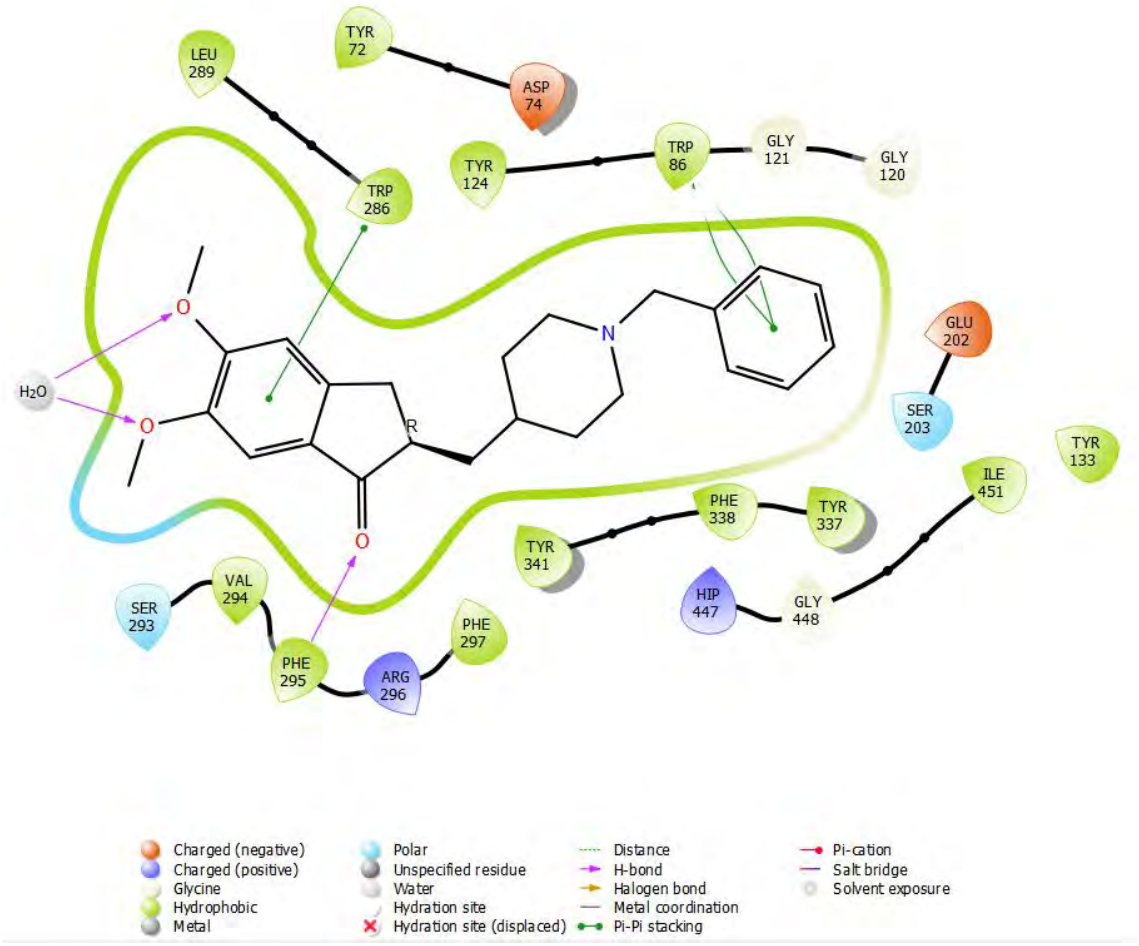


**Figure 5.231.** *Two-dimensional docked pose of donepezil in the active site of AChE*

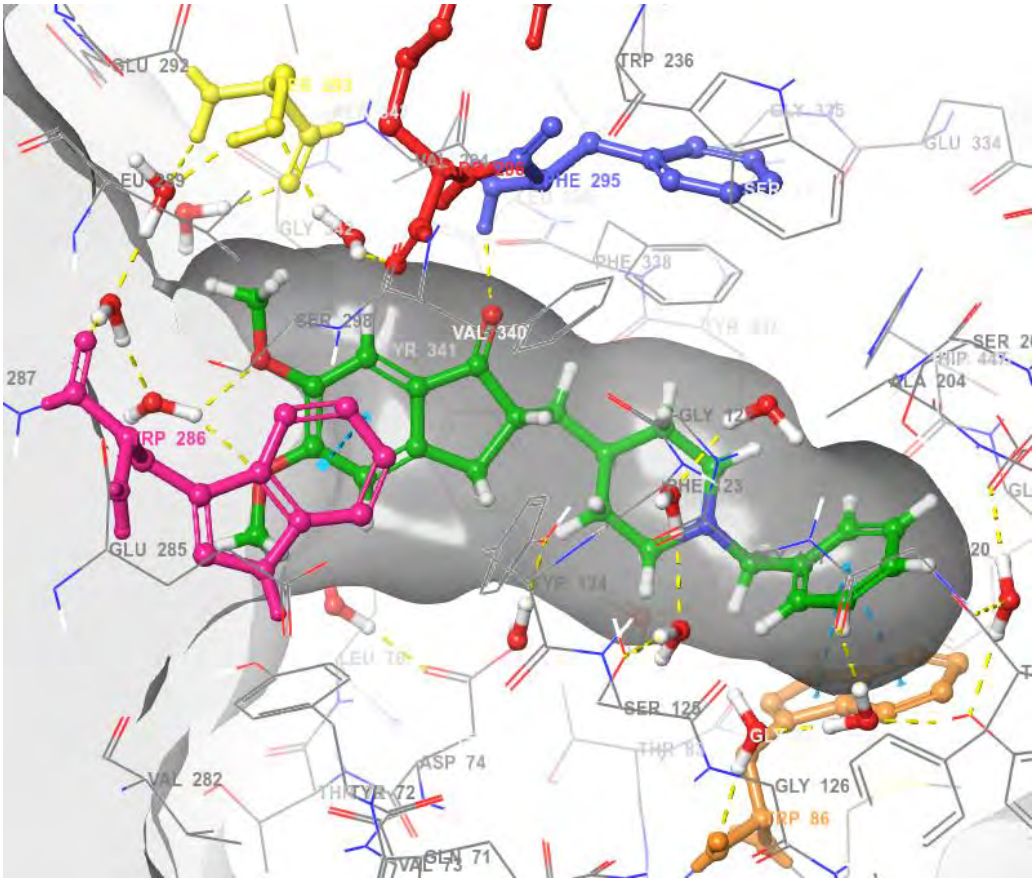


**Figure 5.232.** *Interactions of Donepezil with AChE binding site residues; trp-286 (purple), ser-293 (yellow), arg-296 (red), phe-295 (blue), trp-86 (orange).*

By investigating the docked pose of compound **D25** with that of donepezil as illustrated in Figure 5.233, the carbonyl groups of both compounds were superimposed and concluded that they have a critical role in propagating the molecule inside the active site pocket. Thus, the furan ring of the benzofuran in **D25** was retracted outward to match the position of the phenyl ring of donepezil instead of the cyclic pentanone ring. The noted positioning of compound **D25** might have the advantage of optimum placing the interacting groups from the key residues.

Regarding the ligand-enzyme interactions, Figure 5.234 and Figure 5.235 shows that compound **D25** formed a pi-cation stacking with the key amino acids trp-286 in PAS and trp-86 in CAS. Although these bonds are formed differently than those formed in donepezil they are still stacking bonds and such pi-cation interactions are known to occur with trp-286 and trp-86 [149, 175]. A hydrogen bond between the carbonyl group of compound **D25** and an aminic hydrogen atom of phe-295 was formed. This bond can stabilize the compound in the active site and might contribute to the observed activity of

**D25**. A water-mediated hydrogen bond between the terminal dimethylamino group of **D25** and tyr-337 was formed and is considered significant in enhancing the inhibitory activity against AChE [29].

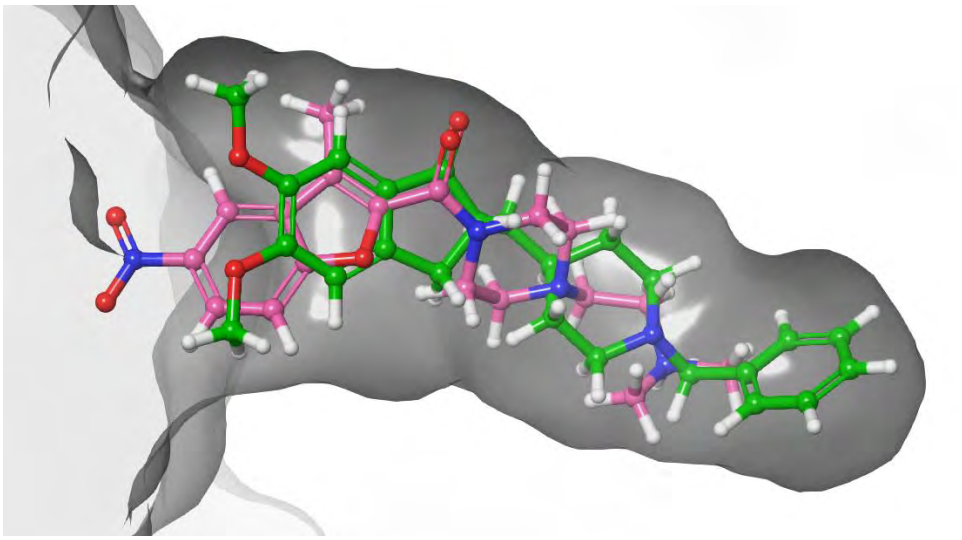

**Figure 5.233.** *Three-dimensional overlay of compound **D25** (pink) superimposed over donepezil (green)*

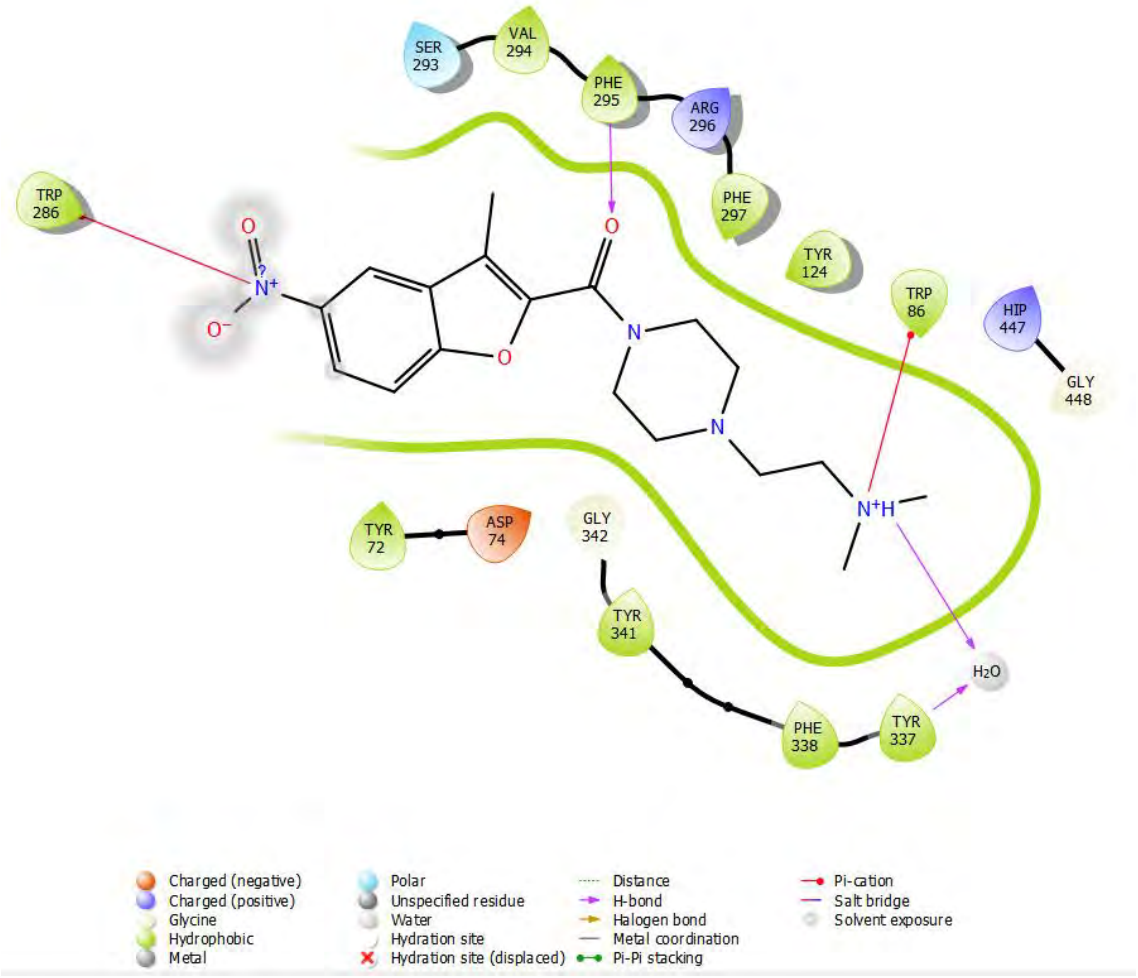


**Figure 5.234.** *Two-dimensional pose of compound **D25** and its interactions in AChE active site*

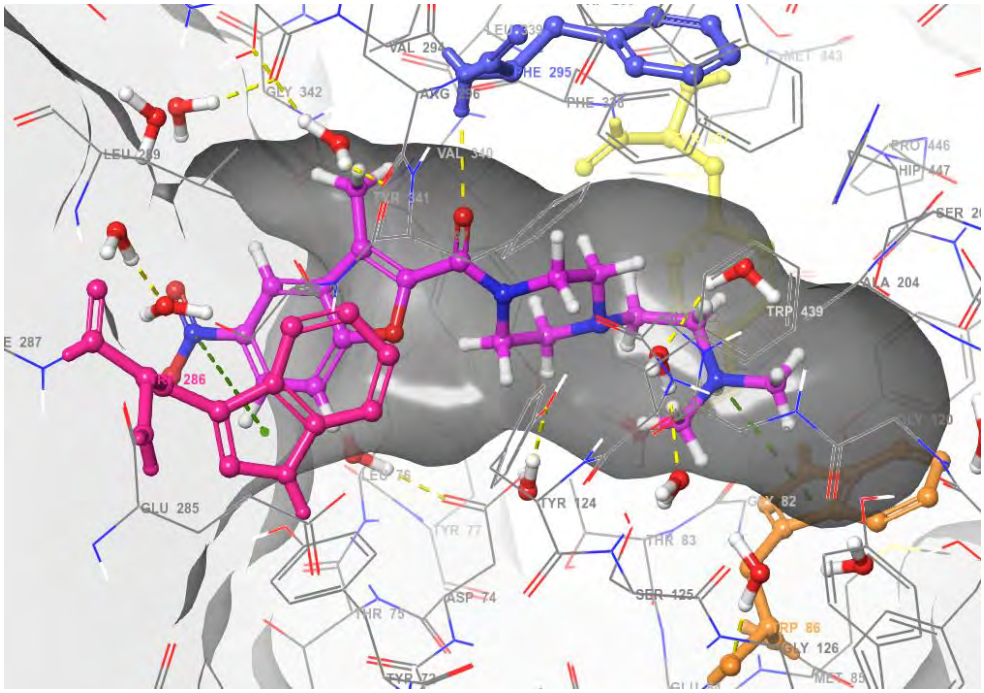


**Figure 5.235.** *Interactions of compound **D25** (pink) with AChE binding site residues; trp-286 (purple), phe-295 (blue), trp-86 (orange), tyr-337 (yellow)*

The superimposition of compound **D30** over donepezil as illustrated in Figure 5.236 shows that the carbonyl group of **D30** was shifted toward the inside of the active site pocket away from the position of the carbonyl of indanone in donepezil. This displacement led to the formation of a big void between **D30** and phe-295 which caused the failure to form a hydrogen bond in between contrary to what occurred with **D25**. Despite the better fit predicted for **D30**, the activity was lower than that of **D25**. This might be due to the fewer interactions formed in the case of **D30**.

The docking results in Figure 5.237 and Figure 5.238 of compound **D30** showed that similar pi-cation stacking interactions to those of **D25** were formed by $NO_2$ and dimethylamino groups to trp-286 and trp-86, respectively. The stack between dimethylamino and trp-86 was observed to occur *via* the two fused rings of indole of tryptophan. The stack between $NO_2$ and trp-286 is also a double stacking. An extra pi-pi stacking was formed between trp-286 and the benzene ring of benzofuran. No other bonds were recognized in other poses of **D30**. In comparison to the results of **D25**, compound **D30** might be incapable of forming efficient bonds with phe-295 and tyr-337 which explains the difference in the activity between **D30** and **D25**. It is worth mentioning that molecular docking can show the results of interacting a flexible ligand with rigid protein.

Hence, other bonds might be formed by **D30** with the active site residues, but they are weaker surely than the predicted bonds formed by **D25**.

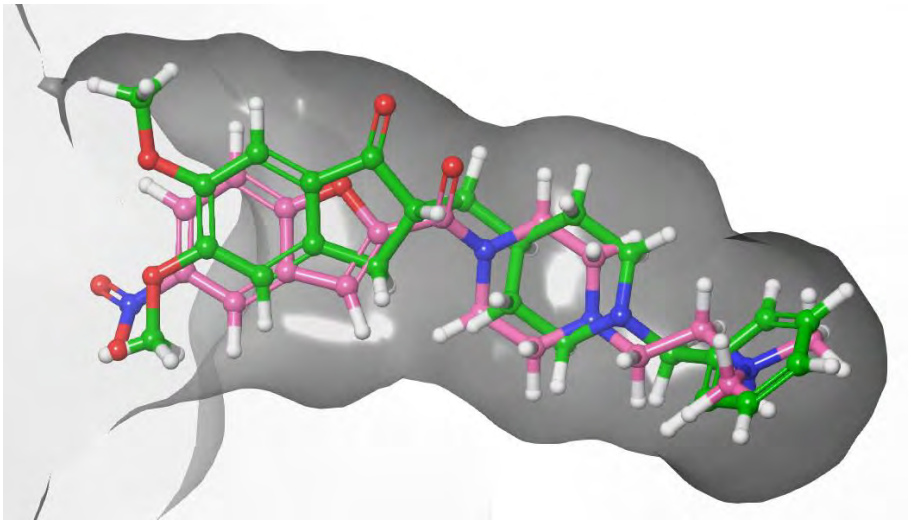

**Figure 5.236.** *Three-dimensional overlay of compound **D30** (pink) superimposed over donepezil (green)*

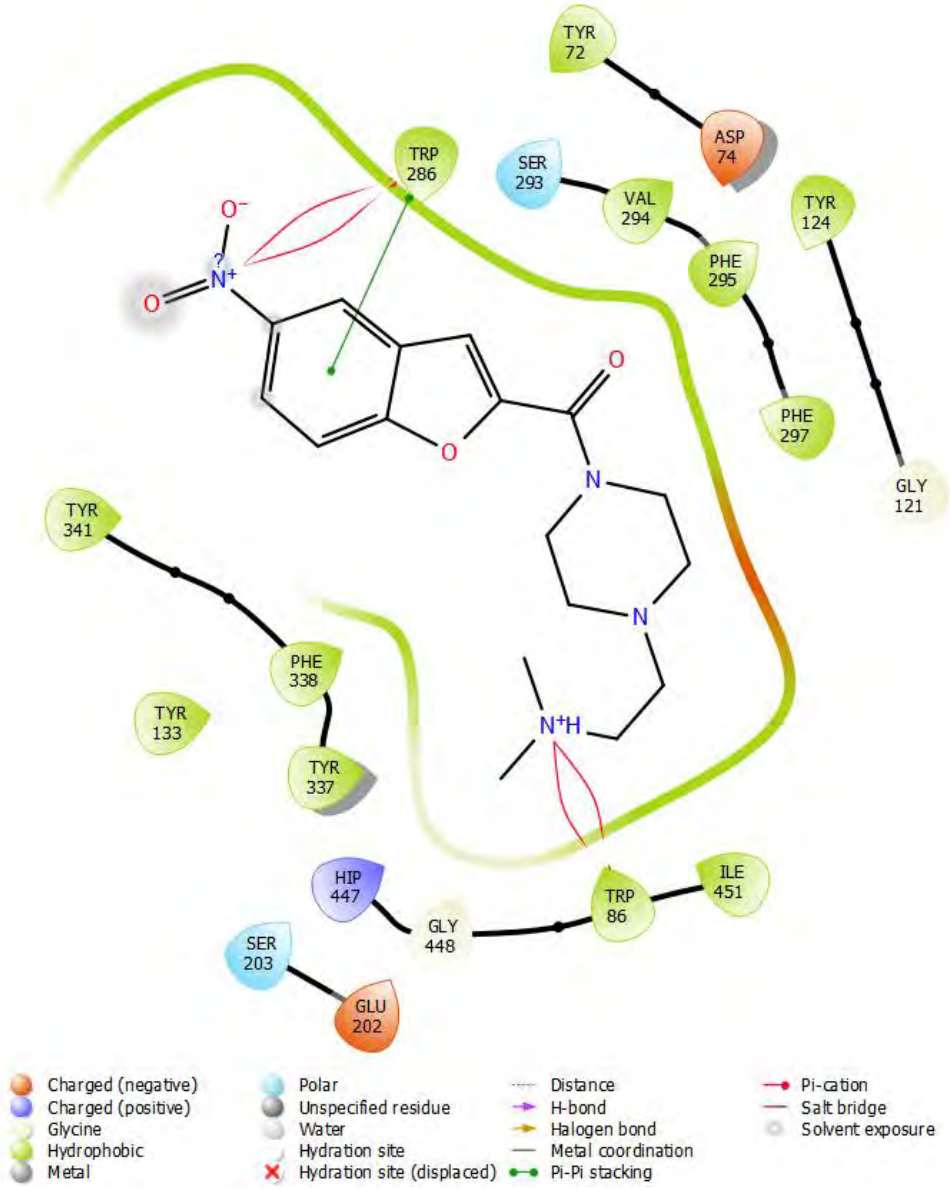


**Figure 5.237.** *Two-dimensional pose of compound **D30** and its interactions in AChE active site*

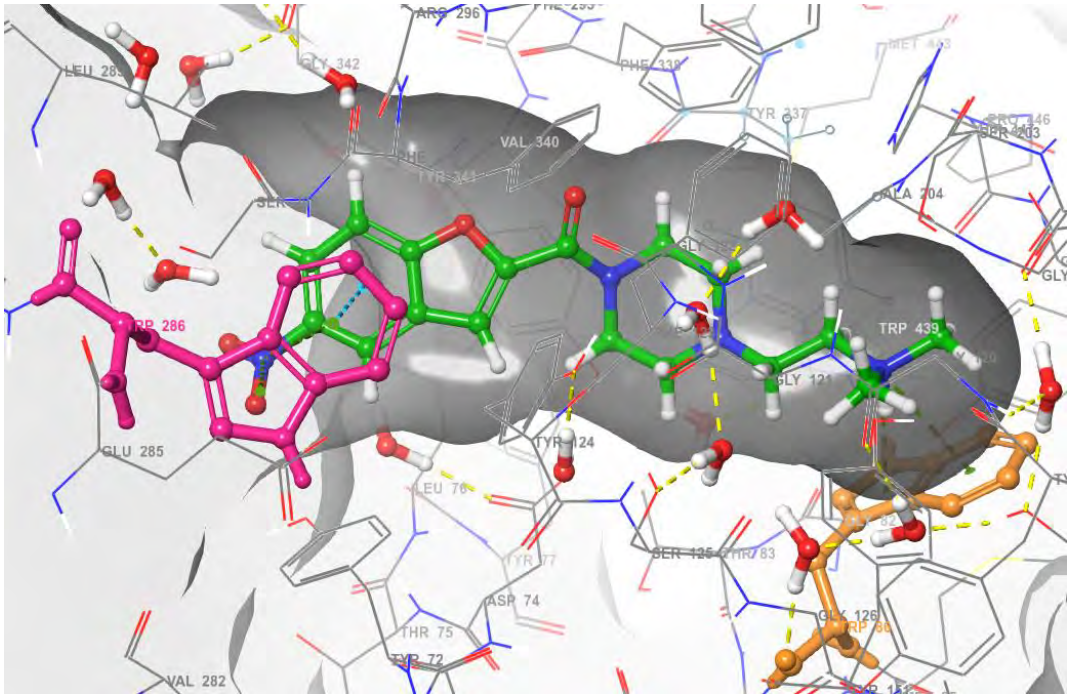


**Figure 5.238.** *Interactions of compound **D30** (green) with AChE binding site residues; trp-286 (purple), trp-86 (orange)*

Inspection of the overlay of compound **D40** over donepezil in Figure 5.239 shows good superimposition of benzofuran and piperazine parts of **D40** over indanone and piperidine parts of donepezil. As a result of this superimposition, the carbonyl group of **D40** is placed away from that of donepezil toward the inside of the active site pocket. The 5-methoxy group of benzofuran in **D40** is almost perfectly superimposing one methoxy of donepezil. As a result, compound **D40** is fitted very well in the active site of AChE.

The interactions of compound **D40** with the active site residues are illustrated in Figure 5.240 and Figure 5.241. The expected interactions with trp-286 and trp-86 were formed as pi-pi and pi-cation stacking, respectively. In addition, two pi-cation stacking was formed between the ionized nitrogen of piperazine and tyr-337 and phe-338. A hydrogen bond between the 5-methoxy group of benzofuran and a water molecule but no bridging with any amino acid residue was formed. The possibility of forming a water-mediated bridge is considerable. It is thought that if the benzofuran ring had an additional 6-methoxy, a water-mediated hydrogen bond with the surrounding amino acids would be formed.

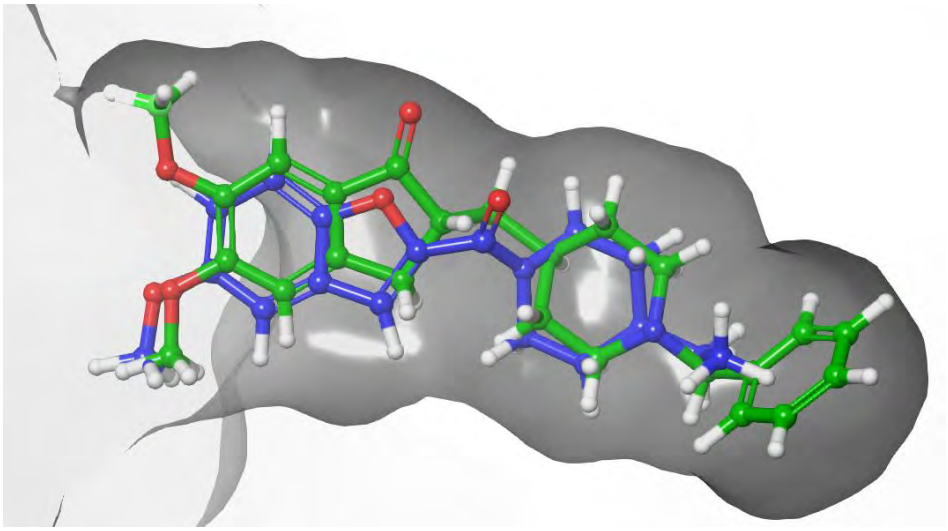

**Figure 5.239.** *Three-dimensional overlay of compound **D40** (blue) superimposed over donepezil (green)*

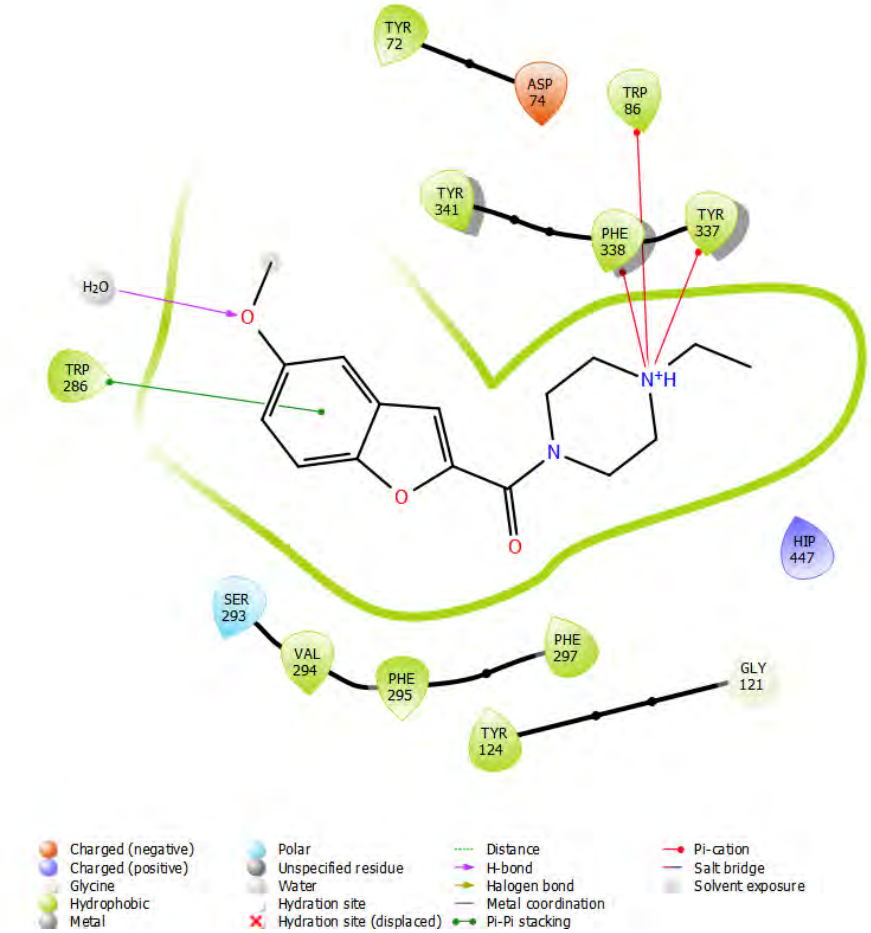


**Figure 5.240.** *Two-dimensional pose of compound **D40** and its interactions in AChE active site*

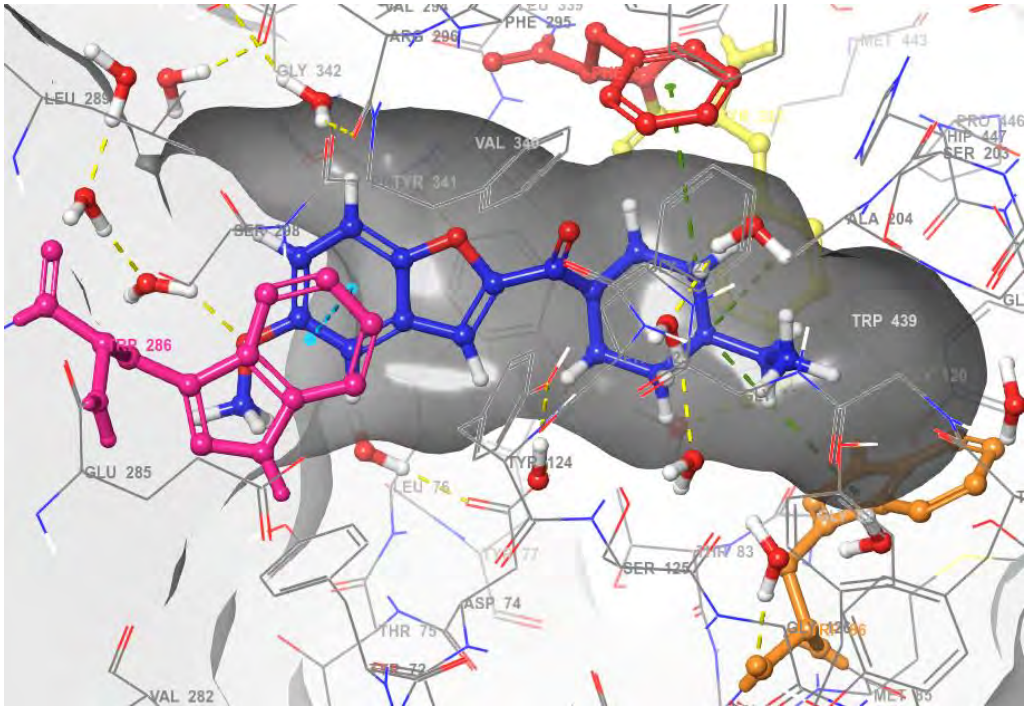


**Figure 5.241.** *Interactions of compound **D40** (blue) with AChE binding site residues; trp-286 (purple), phe-295 (blue), trp-86 (orange), tyr-337 (yellow), phe-338 (red)*

The superimposition of compound **D41** illustrated in Figure 5.242 shows that the compound was inserted further to the inner part of the active site pocket. The terminal dimethylamino group of **D41** is superimposing the terminal phenyl of donepezil. On the other hand, the insertion of **D41** is farther than that of **D40** despite the longer terminal chain of **D41**. The positioning and the additional dimethylamino group of compound **D41** lead to slight differences in the binding modes. The binding mode of **D41** led to a better inhibitory activity of the compound against AChE.

The interactions of compound **D41** with the active site residues of AChE are illustrated in Figure 5.243 and Figure 5.244. Pi-pi stack between trp-286 and benzofuran and pi-cation stack between trp-86 and the ionized dimethylamino group were formed. A double stack between the benzofuran ring and tyr-341 was also formed. Additionally, an important salt bridge was formed between the carboxylic oxygen of glu-202 and the nitrogen of the ionized dimethylamino group of compound **D41**. The interaction of **D41** with trp-86 and glu-202 is further stabilized by water-mediated hydrogen bonding *via* several water molecules between trp-86 and glu-202. As a result of the illustrated binding mode, compound **D41** gained the most potent inhibitory activity among the active compounds.

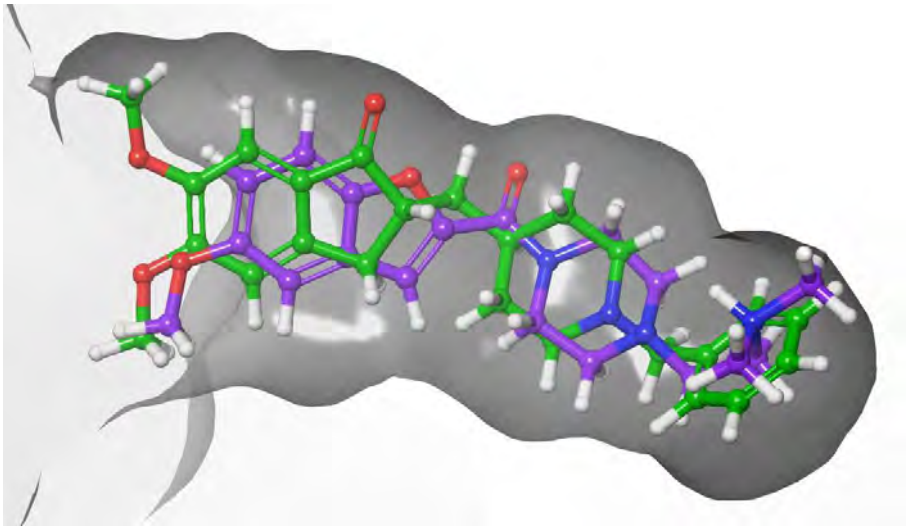

**Figure 5.242.** *Three-dimensional overlay of compound **D41** (violet) superimposed over donepezil (green)*

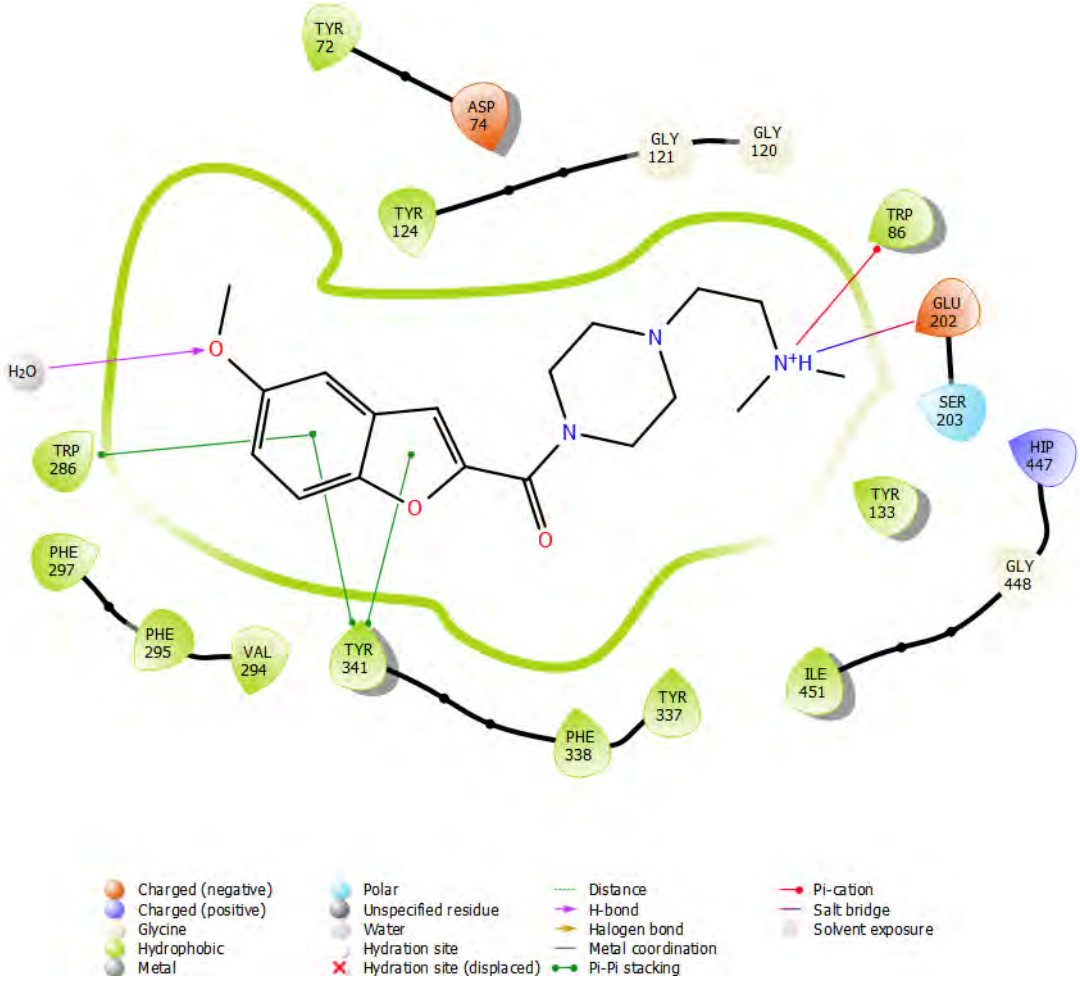


**Figure 5.243.** *Two-dimensional pose of compound **D41** and its interactions in AChE active site*

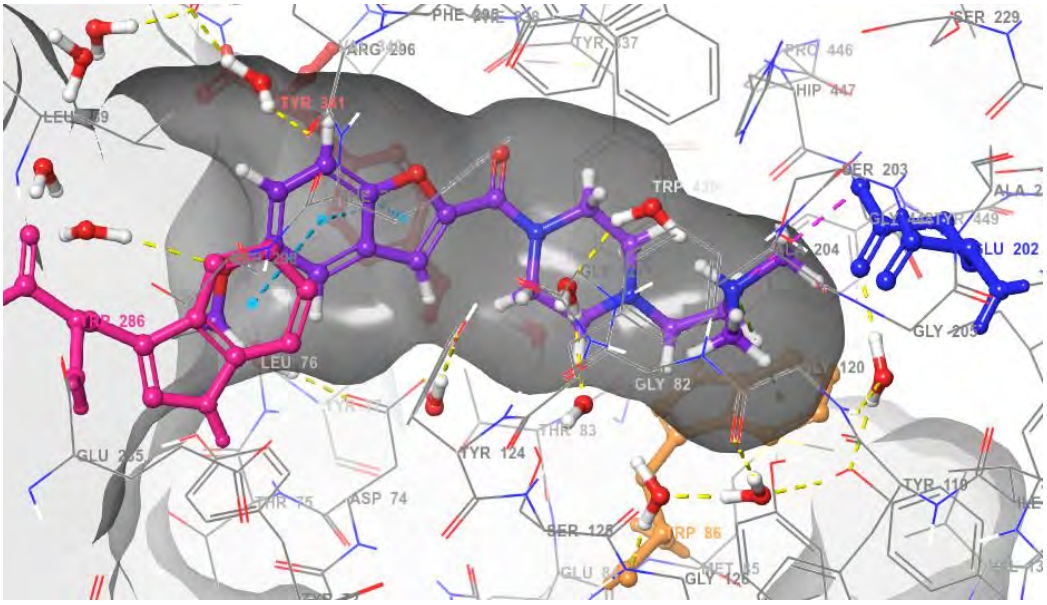


**Figure 5.244.** *Interactions of compound **D41** (violet) with AChE binding site residues; trp-286 (purple), trp-86 (orange), glu-202 (blue), tyr-341 (red)*

## 6. CONCLUSION AND RECOMMENDATIONS

Targeted 42 benzofuran-piperazine derivatives were synthesized as AChE inhibitors designed as therapeutic agents for AD. The first step of the synthesis involved the cyclization of benzofuran *via* Rap-Stoermer reaction. Two solvents acetonitrile and DMF were tried and DMF gave purer products in less time than that of acetonitrile. During the benzofuran synthesis, it is recommended to adjust the reaction temperature between 80-120ºC. Higher temperature led to the production of impurities that were recognizable by TLC. Lower temperatures made the reaction less efficient and could not complete.

The second step of the synthesis involved the hydrolysis of the ethyl ester of benzofuran-2-yl carboxylate. The hydrolysis seemed to be time-dependent rather than hydrolyzing agent concentration-dependent. The more the mixture has waited under reflux, the purer hydrolyzed product is formed.

The third step was the chlorination of the acid using thionyl chloride rather than phosphoryl chloride. The chosen thionyl chloride has two advantages which are it is the solvent at the same time it is the chlorinating agent, and it can be evaporated at RT in a short period without the need for any evaporation instruments. Hence, it made the reaction faster and easier than phosphoryl chloride which involves the use of solvent mixtures like DMF and water and the work-up step needs some care to obtain a good yield of the product.

The final step of the synthesis was the reaction of the piperazine derivatives with the acid chloride derivatives of benzofuran. It is recommended as concluded from the reaction rate that the piperazine is first treated with $K_2CO_3$ in acetone and the mixture is to be stirred for a while before the addition of the acid chloride. A better reaction was noted when this protocol was applied rather than the addition of all the reactants together at the same time.

The work-up of the products involved the extraction using chloroform. The NMR analysis of some products showed that chloroform was not evaporated and was still found. Various methods were attempted to get rid of the chloroform, but they were not effective. Such methods included heating the product with and without vacuum. It was believed that the use of a low boiling point solvent such as diethyl ether to form an azeotropic mixture with chloroform can lead to the evaporation of the chloroform. This method was effective enough and the chloroform-containing products were eventually cleaned. The

efficiency of this method is illustrated in Figure 6.1 for compound **D2** as an example where the NMR analysis showed that the compound was cleaned.

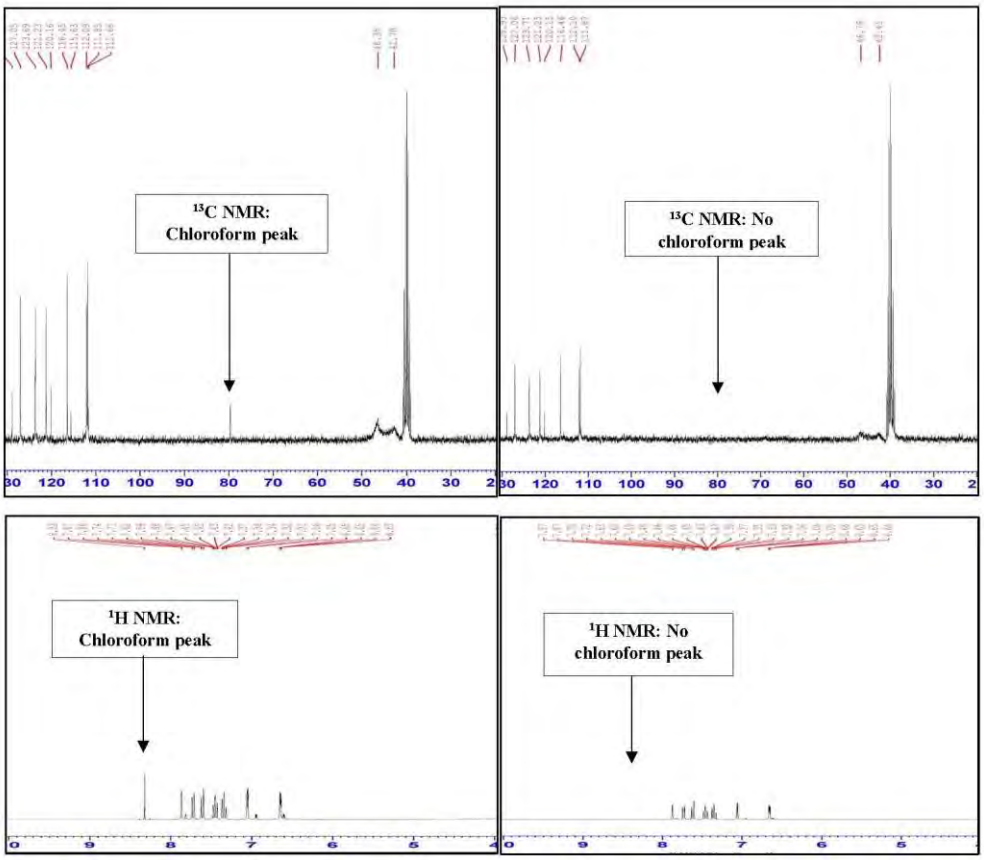


**Figure 6.1.** *NMR analysis of compound **D2** before and after the removal of chloroform*

The analysis of all the compounds confirmed the identity of each compound. **2D** NMR analysis was also achieved for four representative compounds to assign the unknown carbons and to affirm the relationship between the hydrogen and neighbor carbons. According to the final analysis, the compounds were determined to be suitable for the tests of therapeutic activity. Four compounds were concluded to be active in inhibiting AChE by comparing the results to the reference drug donepezil. On the other hand, no activity was observed against BChE. The advantage of specific inhibition of AChE without inhibiting BChE is the smaller adverse effect profile of the active compounds, whereas the disadvantage is that these compounds do not target BChE which is thought to be involved in the pathology of AD [176, 177]. Thus, it is concluded that the active compounds can still be useful in the treatment of AD but either in combination

with other cholinergic inhibitors or in strategies where selective inhibition of AChE is needed.

Compounds **D41** and **D25** were the most active to inhibit AChE *via in vitro* assay. The activity of **D41** was comparable to that of the reference donepezil, while compound **D25**'s activity was close to the activity of donepezil. Compounds **D40** and **D30** showed approximately half the activity of the reference. Generally, all four compounds are considerable for further studies and are thought to be promising AChE inhibitors.

Compounds **D36** and **D42** were not active inhibitors of AChE as shown *via* the *in vitro* assay. It is thought that the cause of such failure is the position of the carbonyl group found in these benzofuran derivatives. The carbonyl group of these molecules enters the active site of the enzyme to the same level of carbonyl of donepezil. And it is concluded that the interactions of the carbonyl group with certain amino acids in that location retracted the molecule backward and prevented the nitrogen-4 of piperazine and the benzyl group to form the required bonds with the surrounding amino acid residues. The idea of this conclusion is depicted in Figure 6.2. Another contributing factor to the inability of compounds **D36** and **D42** to display activity is believed to be that they do not have flexibility between the piperazine and benzofuran parts as compared to donepezil which has a methylene bridge that gives the molecule the ability to form various conformers suitable for the required interactions in the active site.

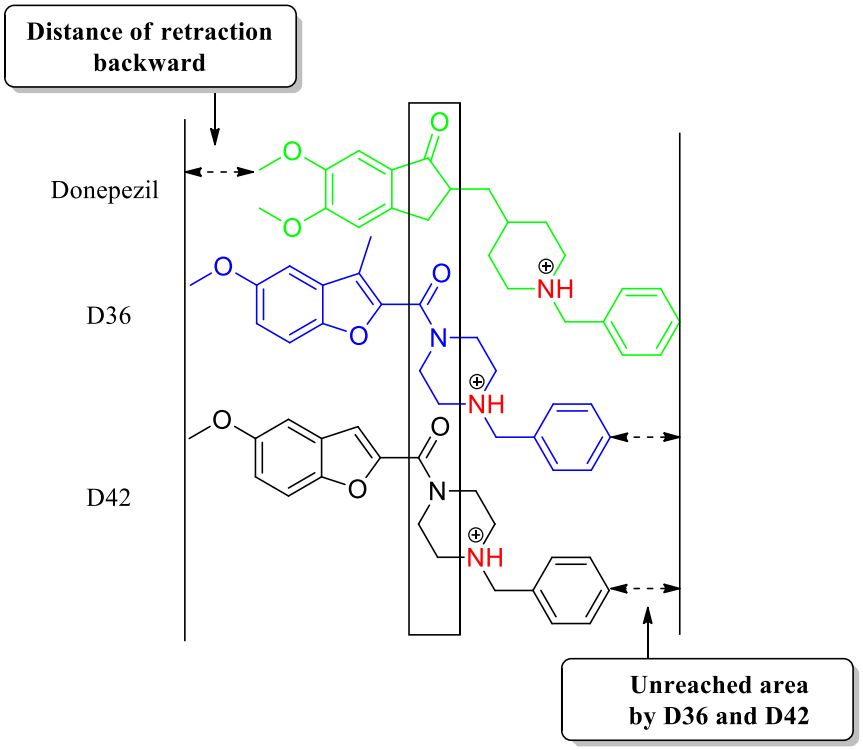


**Figure 6.2.** *Depicted analysis of the reasons for the failure of compounds **D36** and **D42** to inhibit AChE*

For future works, some modifications are recommended to make compounds **D36** and **D42** and also other derivatives effective inhibitors of AChE. The first modification is to introduce a methylene bridge between the piperazine and the carbonyl. This methylene can solve the issue of conformational flexibility and will also compensate for the retracted distance by the molecules and hence make the interactions between the benzyl group and nitrogen-4 of piperazine with the key amino acid residues possible. The second modification is to introduce a methoxy group at position 6 of benzofuran. This group together with the methoxy group on position 5 are thought to form water-mediated hydrogen bonding with certain amino acids that can enhance the activity of the compounds. The final shape of the suggested modifications on the structures is illustrated in Figure 6.3.

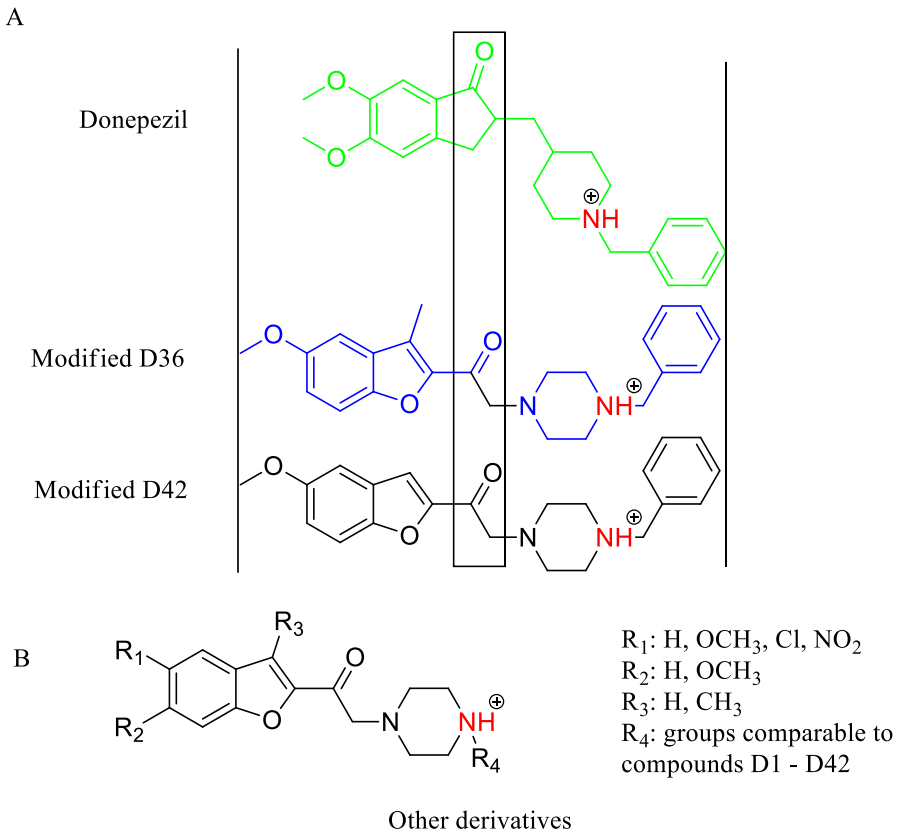


**Figure 6.3.** *Recommended modifications, A: modifications to improve the activity of compounds* ***D36*** *and* ***D42****, B: suggested other derivatives*

## REFERENCES


[1] Pujols, J., Peña-Díaz, S., Pallarès, I., Ventura, S. (2020). Chemical Chaperones as Novel Drugs for Parkinson's Disease. *Trends Mol. Med.*, 26 (4), 408–421.

[2] Chuanxin, Z., Shengzheng, W., Lei, D., Duoli, X., Jin, L., Fuzeng, R., Aiping, L., Ge, Z. (2020). Progress in 11β-HSD1 inhibitors for the treatment of metabolic diseases: A comprehensive guide to their chemical structure diversity in drug development. *Eur. J. Med. Chem.*, 191 (2020), 112–134.

[3] Roquero, I., Cantizani, J., Cotillo, I., Manzano, M.P., Kessler, A., Martín, J.J., McNamara, C.W. (2019). Novel chemical starting points for drug discovery in leishmaniasis and Chagas disease. *Int. J. Parasitol. Drugs Drug Resist.*, 10 (5), 58–68.

[4] Sun, H.Y., Hou, T.J., Zhang, H.Y. (2014). Finding chemical drugs for genetic diseases. *Drug Discov. Today*, 19 (12), 1836–1840.

[5] Sarkar, S. (2013). Chemical screening platforms for autophagy drug discovery to identify therapeutic candidates for Huntington's disease and other neurodegenerative disorders. *Drug Discov. Today Technol.*, 10 (1), e137–e144.

[6] Arosio, P., Vendruscolo, M., Dobson, C.M., Knowles, T.P.J. (2014). Chemical kinetics for drug discovery to combat protein aggregation diseases. *Trends Pharmacol. Sci.*, 35 (3), 127–135.

[7] Seale, J.P. (1990). Chemical targeting of drug therapy in asthma and airways disease. *Adv. Drug Deliv. Rev.*, 5 (1–2), 73–92.

[8] Hughes, J.P., Rees, S.S., Kalindjian, S.B., Philpott, K.L. (2011). Principles of early drug discovery. *Br. J. Pharmacol.*, 162 (6), 1239–1249.

[9] DeSimone, R., Currie, K., Mitchell, S., Darrow, J., Pippin, D. (2012). Privileged Structures: Applications in Drug Discovery. *Comb. Chem. High Throughput Screen.*, 7 (5), 473–493.

[10] Ahmed Mehanna. (2013). Cardiac Agents: Cardiac Glycosides, Antianginal, and Antiarrhythmic Drugs. W.O. Foye, T.L. Lemke, D.A. Williamms, V.F. Roche, and S.W. Zito (editors), *Principles of Medicinal Chemistry* (p. 700–727). Baltimore: Lippincott Williams & Wilkins.

[11] Cutler, S.J. (2011). Cardiovascular Agents. J.M. Beale, and J.H. Block (editors), *Textbook of Organic Medicinal and Pharmaceutical Chemistry* (p. 617–665).

Lippincott Williams & Wilkins.

[12] Beale, J.M. (2011). Anti-infective Agents. J.M. Beale, and J.H. Block (editors), *Textbook of Organic Medicinal and Pharmaceutical Chemistry* (p. 179–241). Lippincott Williams & Wilkins.

[13] Kamal, M., Shakya, A., Jawaid, T. (2011). Benzofurans: a new profile of biological activities. *Int. J. Med. Pharm. Sci.*, 1 (3), 1–15.

[14] David, A.W. (2013). Antidepressants. W.O. Foye, T.L. Lemke, D.A. Williamms, V.F. Roche, and S.W. Zito (editors), *Principles of Medicinal Chemistry* (p. 570–631). Baltimore: Lippincott Williams & Wilkins.

[15] Cutler, S.J. (2011). Cholinergic Drugs and Related Agents. J.M. Beale, and J.H. Block (editors), *Textbook of Organic Medicinal and Pharmaceutical Chemistry* (p. 558–606). Lippincott Williams & Wilkins.

[16] Fifer, E.K. (2013). Drugs Affecting Cholinergic Neurotransmission. W.O. Foye, T.L. Lemke, D.A. Williamms, V.F. Roche, and S.W. Zito (editors), *Foye's Principles of Medicinal Chemistry* (p. 309–339). Baltimore: Lippincott Williams & Wilkins.

[17] Waldemar, G., Gauthier, S., Jones, R., Wilkinson, D., Cummings, J., Lopez, O., Zhang, R., Xu, Y., Sun, Y., Knox, S., Richardson, S., Mackell, J. (2011). Effect of donepezil on emergence of apathy in mild to moderate Alzheimer's disease. *Int. J. Geriatr. Psychiatry*, 26 (2), 150–157.

[18] Zavod, R.M., Knittel, J.J. (2013). Drug Design and Relationship of Functional Groups to Pharmacologic Activity. W.O. Foye, T.L. Lemke, D.A. Williamms, V.F. Roche, and S.W. Zito (editors), *Principles of Medicinal Chemistry* (p. 29–60). Baltimore: Lippincott Williams & Wilkins.

[19] Klebe, G. (2013). Introduction. G. Klebe (editor), *Drug Design Methodology, Concepts, and Mode-of-Action* (p. ix–xv). Berlin: Springer Heidelberg.

[20] Imming, P. (2015). Medicinal Chemistry: Definitions and Objectives, Drug Activity Phases, Drug Classification Systems. C.G. Wermuth, D. Aldous, P. Raboisson, and D. Rognan (editors), *The Practice of Medicinal Chemistry* (p. 3–13). London: Academic Press.

[21] Klebe, G. (2013). Optimization of Lead Structure. G. Klebe (editor), *Drug Design Methodology, Concepts, and Mode-of-Action* (p. 153–171). Berlin: Springer Heidelberg.

[22] Kinghorn, A.D. (2013). Drug Discovery from Natural Products. W.O. Foye, T.L. Lemke, D.A. Williamms, V.F. Roche, and S.W. Zito (editors), *Principles of Medicinal Chemistry* (p. 13–28). Baltimore: Lippincott Williams & Wilkins.

[23] Mason, J.S., Pickett, S.D. (2003). Combinatorial Library Design, Molecular Similarity, and Diversity Applications. D.J. Abraham (editor), *Medicinal Chemistry and Drug Discovery - Volume 1: Drug Discovery* (p. 187–242). Wiley-Interscience.

[24] Klebe, G. (2013). Screening Technologies for Lead Structure Discovery. G. Klebe (editor), *Drug Design Methodology, Concepts, and Mode-of-Action* (p. 129–152). Berlin: Springer Heidelberg.

[25] Klebe, G. (2013). Drug Research: Yesterday, Today, and Tomorrow. G. Klebe (editor), *Drug Design Methodology, Concepts, and Mode-of-Action* (p. 3–22). Berlin: Springer Heidelberg.

[26] (2021). Drugs., https://www.drugs.com/search.php?searchterm=donepezil (Accessed: 8 November 2021).

[27] Brayfield, A., Cadart, C.R., Crehan, E.E., Eager, K., Foan, E.S., Gibbons, A.C., Hatwal, C.S., Ho, S.W., Khan, S.Z., Luckhurst, R.E., MacKershan, J., McGuirk, D., Sutton, S. (2014). Antidementia Drugs. A. Brayfield, C.R. Cadart, E.E. Crehan, K. Eager, E.S. Foan, A.C. Gibbons, C.S. Hatwal, S.W. Ho, S.Z. Khan, R.E. Luckhurst, J. MacKershan, D. McGuirk, and S. Sutton (editors), *Martindale: The Complete Drug Reference* (p. 388–389). London: Pharmaceutical Press.

[28] PubChem Compound Summary for CID 3152, Donepezil. *National Center for Biotechnology Information*, https://pubchem.ncbi.nlm.nih.gov/compound/Donepezil (Accessed: 11 August 2021).

[29] Cheung, J., Rudolph, M.J., Burshteyn, F., Cassidy, M.S., Gary, E.N., Love, J., Franklin, M.C., Height, J.J. (2012). Structures of human acetylcholinesterase in complex with pharmacologically important ligands. *J. Med. Chem.*, 55 (22), 10282–10286.

[30] Eicher, T., Hauptmann, S., Speicher, A. (2003). Five-Membered Heterocycles. T. Eicher, and S. Hauptmann (editors), *The Chemistry of Heterocycles: Structures, Reactions, Synthesis, and Applications* (p. 52–221). Grünstadt: John Wiley & Sons.

[31] Joule, J.A., Mills, K. (2010). Typical Reactivity of Indoles, Benzo[b] thiophenes, Benzo[b]furans, Isoindoles, Benzo[c]thiophenes and Isobenzofurans. J.A. Joule, and K. Mills (editors), *Heterocyclic Chemistry* (p. 369–372). West Sussex: Wiley.

[32] Katritzky, A.R., Ramsden, C.A., Joule, J.A., Zhdankin, V. V. (2011). Structure of Five-Membered Rings with One Heteroatom. A.R. Katritzky, C.A. Ramsden, J.A. Joule, and V. V. Zhdankin (editors), *Handbook of Heterocyclic Chemistry* (p. 87–138). Amsterdam: Elsevier.

[33] Sainsbury, M. (2001). Benzo[b]pyrrole, Benzo[b]furan and Benzo[b]thiophene. M. Sainsbury (editor), *Heterocyclic Chemistry* (p. 77–114). Cambridge: Royal Society of Chemistry.

[34] Black, P.J., Heffernan, M.L. (1965). The analysis of the proton magnetic resonance spectra o f heteroaromatic systems. *Aust. J. Chem.*, 18 (3), 353–361.

[35] Okuyama, T., Fueno, T. (1974). Substituent Effects in the Benzofuran System. I. Proton and Carbon-13 Chemical Shifts. *Bull. Chem. Soc. Jpn.*, 47 (5), 1263–1266.

[36] Hore, P.J. (2000). Chemical Shifts. P.J. Hore (editor), *Nuclear Magnetic Resonance*. New York: Oxford University Press.

[37] Skoog, D.A., West, D.M., Holler, F.J., Crouch, S.R. (2014). Introduction to Spectrochemical Methods. D.A. Skoog, D.M. West, F.J. Holler, and S.R. Crouch (editors), *Fundamentals of Analytical Chemistry* (p. 650–682). Belmont: Cengage learning.

[38] Smith, A.L. (1982). *The Coblentz Society Desk Book of Infrared Spectra*. 2nd ed. Kirkwood Missouri: The Coblentz Society.

[39] National Institute of Standards and Technology. Benzofuran IR Spectrum. *Coblentz Society*, https://webbook.nist.gov/cgi/cbook.cgi?ID=C271896&Type=IR-SPEC&Index=1 (Accessed: 20 August 2021).

[40] Hassner, A., Stumer, C. (2013). *Organic Syntheses Based on Name Reactions and Unnamed Reactions*. Amsterdam: Elsevier.

[41] Demirayak, Ş., Uçucu, Ü., Benkli, K., Gündoğdu-Karaburun, N., Karaburun, A. çarğrı, Akar, D., Karabacak, M., Kiraz, N. (2002). Synthesis and antifungal activities of some aryl(benzofuran-2-yl)ketoximes. *Farmaco*, 57 (7), 609–612.

[42] Gündoğdu-Karaburun, N., Benkli, K., Tunali, Y., Uçucu, Ü., Demirayak, Ş. (2006). Synthesis and antifungal activities of some aryl [3-(imidazol-1-yl/triazol-

1-ylmethyl) benzofuran-2-yl] ketoximes. *Eur. J. Med. Chem.*, 41 (5), 651–656.

[43] Alperen, B. (2019). *Bazı Ditiyokarbamat Sübstitüe Benzofuran Türevlerinin Sentezleri ve Antimikrobiyal Aktivitelerinin Araştırılması*. Master Thesis. Eskişehir: Anadolu University, Graduate School of Health Sciences.

[44] Zhao, S., Wang, X., Zhang, L. (2013). Polyethylene glycol (PEG-400) as an efficient and recyclable reaction medium for the synthesis of 2-aroylbenzofurans. *Org. Prep. Proced. Int.*, 45 (5), 421–428.

[45] El-Wahab, A.H.F.A., Al-Fifi, Z.I.A., Bedair, A.H., Ali, F.M., Halawa, A.H.A., El-Agrody, A.M. (2011). Synthesis, reactions and biological evaluation of some new naphtho[2,1-b]furan derivatives bearing a pyrazole nucleus. *Molecules*, 16 (1), 307–318.

[46] Abu-Hashem, A.A., Al-Hussain, S.A., Zaki, M.E.A. (2020). Synthesis of Novel Benzodifuranyl; 1,3,5-Triazines; 1,3,5-Oxadiazepines; and Thiazolopyrimidines Derived from Visnaginone and Khellinone as Anti-Inflammatory and Analgesic Agents. *Molecules*, 25 (220), 1–25.

[47] Yang, L., Lei, H., Mi, C.G., Liu, H., Zhou, T., Zhao, Y.L., Lai, X.Y., Li, Z.C., Song, H., Huang, W.C. (2011). Synthesis, antiproliferative activities and in vitro biological evaluation of novel benzofuransulfonamide derivatives. *Bioorganic Med. Chem. Lett.*, 21 (18), 5389–5392.

[48] Kumaraswamy, G., Ramakrishna, G., Raju, R., Padmaja, M. (2010). An expedient synthesis of enantioenriched substituted (2-benzofuryl) arylcarbinols via tandem Rap-Stoermer and asymmetric transfer hydrogenation reactions. *Tetrahedron*, 66 (52), 9814–9818.

[49] Wu, X.F., Li, Y. (2017). *Transition Metal-Catalyzed Benzofuran Synthesis: Transition Metal-Catalyzed Heterocycle Synthesis Series*. Amsterdam: Elsevier.

[50] Arcadi, A., Cacchi, S., Del Rosario, M., Fabrizi, G., Marinelli, F. (1996). Palladium-catalyzed reaction of o-ethynylphenols, o-((trimethylsilyl)ethynyl)phenyl acetates, and o-alkynylphenols with unsaturated triflates or halides: A route to 2-substituted-, 2,3-disubstituted-, and 2-substituted-3-acylbenzo[b]furans. *J. Org. Chem.*, 61 (26), 9280–9288.

[51] Kundu, N.G., Pal, M., Mahanty, J.S., Dasgupta, S.K. (1992). Palladium-catalysed Heteroannulation of Acetylenic Compounds: a Facile Method for the Synthesis of Benzofurans. *J. Chem. Soc. Chem. Commun.*, 16 (1992), 41–42.

[52] Wu, X.F., Li, Y. (2017). Pd-Catalyzed Benzofuran Synthesis. X.F. Wu, and Y. Li (editors), *Transition Metal-Catalyzed Benzofuran Synthesis: Transition Metal-Catalyzed Heterocycle Synthesis Series* (p. 3–27). Amsterdam: Elsevier.

[53] Willis, M.C., Taylor, D., Gillmore, A.T. (2004). Palladium-Catalyzed Intramolecular O-Arylation of Enolates : Application to Benzo[b]furan Synthesis. *Org. Lett.*, 6 (25), 4755–4757.

[54] Li, J., Li, C., Yang, S., An, Y., Wu, W., Jiang, H. (2016). Assembly of 3-Sulfenylbenzofurans and 3-Sulfenylindoles by Palladium-Catalyzed Cascade Annulation/Arylthiolation Reaction Reaction. *J. Org. Chem.*, 81 (7), 2875–2887.

[55] Yang, D., Zhu, Y., Yang, N., Jiang, Q., Liu, R. (2016). One-Step Synthesis of Substituted Benzofurans from ortho- Alkenylphenols via Palladium-Catalyzed C-H Functionalization. *Adv. Synth. Catal.*, 358 (11), 1731–1735.

[56] Wu, X.F., Li, Y. (2017). Cu-Catalyzed Benzofuran Synthesis. X.F. Wu, and Y. Li (editors), *Transition Metal-Catalyzed Benzofuran Synthesis: Transition Metal-Catalyzed Heterocycle Synthesis Series* (p. 29–41). Amsterdam: Elsevier.

[57] Chen, C., Dormer, P.G. (2005). Synthesis of Benzo[b]furans via CuI-Catalyzed Ring Closure. *J. Org. Chem.*, 70 (17), 6964–6967.

[58] Nagamochi, M., Fang, Y., Lautens, M. (2007). A General and Practical Method of Alkynyl Indole and Benzofuran Synthesis via Tandem Cu- and Pd-Catalyzed Cross-Couplings. *Org. Lett.*, 9 (15), 2955–2958.

[59] Tsai, T., Wang, E.-C., Li, S.-R., Chen, Y., Lin, Y., Wang, Y., Guang, K.-S. (2004). A New Synthesis of Benzofurans from Phenols via Claisen Rearrangement and Ring-Closing Metathesis. *J. Chinese Chem. Soc.*, 51 (6), 1307–1318.

[60] Hashmi, A.S.K., Wolfle, M. (2009). Gold catalysis : benzanellation versus alkylidenecyclopentenone synthesis. *Tetrahedron*, 65 (44), 9021–9029.

[61] Mezailles, N., Ricard, L., Gagosz, F. (2005). Phosphine Gold ( I ) Bis- ( trifluoromethanesulfonyl ) imidate Complexes as New Highly Efficient and Air-Stable Catalysts for the Cycloisomerization of Enynes. *Org. Lett.*, 7 (19), 4133–4136.

[62] Várela-Fernández, A., González-Rodríguez, C., Varela, J.A., Castedo, L., Saá, C. (2009). Cycloisomerization of aromatic homo and bis-homopropargylic alcohols via catalytic ru vinylidenes: Formation of benzofurans and isochromenes. *Org. Lett.*, 11 (22), 5350–5353.

[63] Kumar, M.P., Liu, R.S. (2006). Zn(OTf)2-catalyzed cyclization of proparyl alcohols with anilines, phenols, and amides for synthesis of indoles, benzofurans, and oxazoles through different annulation mechanisms. *J. Org. Chem.*, 71 (13), 4951–4955.

[64] Anxionnat, B., Gomez Pardo, D., Ricci, G., Rossen, K., Cossy, J. (2013). Iridium-catalyzed hydrogen transfer: Synthesis of substituted benzofurans, benzothiophenes, and indoles from benzyl alcohols. *Org. Lett.*, 15 (15), 3876–3879.

[65] Wongsa, N., Sommart, U., Ritthiwigrom, T., Yazici, A., Kanokmedhakul, S., Kanokmedhakul, K., Willis, A.C., Pyne, S.G. (2013). Concise synthesis of α-substituted 2-benzofuranmethamines and other 2-subsituted benzofurans via α-substituted 2-benzofuranmethyl carbocation intermediates. *J. Org. Chem.*, 78 (3), 1138–1148.

[66] Liu, J., Liu, Z., Liao, P., Bi, X. (2014). Modular synthesis of sulfonyl benzoheteroles by silver-catalyzed heteroaromatization of propargylic alcohols with p -toluenesulfonylmethyl isocyanide (TosMIC): Dual roles of TosMIC. *Org. Lett.*, 16 (23), 6204–6207.

[67] Ye, Y., Fan, R. (2011). Silver-catalyzed synthesis of 4-substituted benzofurans via a cascade oxidative coupling-annulation protocol. *Chem. Commun.*, 47 (19), 5626–5628.

[68] Radadiya, A., Shah, A. (2015). Bioactive benzofuran derivatives : An insight on lead developments , radioligands and advances of the last decade. *Eur. J. Med. Chem.*, 97 (2015), 356–376.

[69] Miao, Y.H., Hu, Y.H., Yang, J., Liu, T., Sun, J., Wang, X.J. (2019). Natural source, bioactivity and synthesis of benzofuran derivatives. *RSC Adv.*, 9 (47), 27510–27540.

[70] Khanam, H., Shamsuzzaman. (2015). Bioactive Benzofuran derivatives: A review. *Eur. J. Med. Chem.*, 97 (1), 483–504.

[71] Swahn, B., Sandell, J., Pyring, D., Bergh, M., Jeppsson, F., Juréus, A., Neelissen, J., Johnström, P., Schou, M., Svensson, S. (2012). Synthesis and evaluation of pyridylbenzofuran , pyridylbenzothiazole and pyridylbenzoxazole derivatives as 18 F-PET imaging agents for β-amyloid plaques. *Bioorg. Med. Chem. Lett.*, 22 (13), 4332–4337.

[72] Proksch, P., Rodriguez, E. (1983). Chromenes and benzofurans of the asteraceae, their chemistry and biological significance. *Phytochemistry*, 22 (11), 2335–2348.

[73] Kim, Y., Choi, H., Seo, P., Son, B. (2001). Synthesis of 2-Arylbenzofuran Derivatives Using w - ( Methylsulfinyl ) acetophenones. *J. Korean Chem. Soc.*, 45 (4), 391–394.

[74] Huang, H.-C., Chamberlain, T.S., Seibert, K., Koboldt, C.M., Isakson, P.C., Reitz, D.B. (1995). Diaryl Indenes and Benzofurans: Novel Classes of Potent and Selective Cyclooxygenase-2 Inhibitors. *Bioorganic Med. Chem. Lett.*, 5 (20), 2378–2380.

[75] Baumann, B., Bohnenstengel, F., Siegmund, D., Wajant, H., Weber, C., Herr, I., Debatin, K.M., Proksch, P., Wirth, T. (2002). Rocaglamide derivatives are potent inhibitors of NF-κB activation in T-cells. *J. Biol. Chem.*, 277 (47), 44791–44800.

[76] Xie, Y.S., Kumar, D., Bodduri, V.D.V., Tarani, P.S., Zhao, B.X., Miao, J.Y., Jang, K., Shin, D.S. (2014). Microwave-assisted parallel synthesis of benzofuran-2-carboxamide derivatives bearing anti-inflammatory, analgesic and antipyretic agents. *Tetrahedron Lett.*, 55 (17), 2796–2800.

[77] Salomé, C., Ribeiro, N., Chavagnan, T., Thuaud, F., Serova, M., Gramont, A. De, Faivre, S., Raymond, E., Désaubry, L. (2014). Benzofuran derivatives as anticancer inhibitors of mTOR signaling. *Eur. J. Med. Chem.*, 81 (2014), 181–191.

[78] Abdelhafez, O.M., Amin, K.M., Ali, H.I., Abdalla, M.M., Ahmed, E.Y. (2014). Design, synthesis and anticancer activity of benzofuran derivatives targeting VEGFR-2 tyrosine kinase. *RSC Adv.*, 4 (23), 11569–11579.

[79] Xie, F., Zhu, H., Zhang, H., Lang, Q., Tang, L. (2015). In vitro and in vivo characterization of a benzofuran derivative , a potential anticancer agent , as a novel Aurora B kinase inhibitor. *Eur. J. Med. Chem.*, 89 (2015), 310–319.

[80] Coskun, D., Erkisa, M., Ulukaya, E., Fatih, M., Ari, F. (2017). Chemistry Novel 1- ( 7-ethoxy-1-benzofuran-2-yl ) substituted chalcone derivatives : Synthesis , characterization and anticancer activity. *Eur. J. Med. Chem.*, 136 (2017), 212–222.

[81] Anbar, H.S., El-gamal, R., Ullah, S., Zaraei, S., Zaib, S., Pelletier, J., Jean, S., Iqbal, J., El-gamal, M.I. (2020). Evaluation of sulfonate and sulfamate derivatives possessing benzofuran or benzothiophene nucleus as inhibitors of nucleotide pyrophosphatases / phosphodiesterases and anticancer agents. *Bioorg. Chem.*, 104 (2020), 1–11.

[82] El-khouly, O.A., Henen, M.A., El-sayed, M.A., Shabaan, M.I., El-messery, S.M. (2021). Synthesis , anticancer and antimicrobial evaluation of new benzofuran based derivatives : PI3K inhibition , quorum sensing and molecular modeling study. *Bioorg. Med. Chem.*, 31 (2021), 1–18.

[83] Thévenin, M., Thoret, S., Grellier, P., Dubois, J. (2013). Synthesis of polysubstituted benzofuran derivatives as novel inhibitors of parasitic growth. *Bioorganic Med. Chem.*, 21 (17), 4885–4892.

[84] Pinto-Martinez, A., Hernández-Rodríguez, V., Rodríguez-Durán, J., Hejchman, E., Benaim, G. (2018). Anti-Trypanosoma cruzi action of a new benzofuran derivative based on amiodarone structure. *Exp. Parasitol.*, 189 (2018), 8–15.

[85] Martinez-Sotillo, N., Pinto-Martínez, A., Hejchman, E., Benaim, G. (2019). Antiproliferative effect of a benzofuran derivate based on the structure of amiodarone on Leishmania donovani affecting mitochondria, acidocalcisomes and intracellular Ca2+ homeostasis. *Parasitol. Int.*, 70 (2019), 112–117.

[86] Jiang, X., Liu, W., Zhang, W., Jiang, F., Gao, Z., Zhuang, H., Fu, L. (2011). Synthesis and antimicrobial evaluation of new benzofuran derivatives. *Eur. J. Med. Chem.*, 46 (8), 3526–3530.

[87] Khodarahmi, G., Asadi, P., Hassanzadeh, F., Khodarahmi, E. (2015). Benzofuran as a promising scaffold for the synthesis of antimicrobial and antibreast cancer agents: A review. *J. Res. Med. Sci.*, 20 (11), 1094–1104.

[88] Xu, Z., Zhao, S., Lv, Z., Feng, L., Wang, Y., Zhang, F., Bai, L., Deng, J. (2019). Benzofuran derivatives and their anti-tubercular, anti-bacterial activities. *Eur. J. Med. Chem.*, 162 (2019), 266–276.

[89] Zha, X., Lamba, D., Zhang, L., Lou, Y., Xu, C., Kang, D., Chen, L., Xu, Y., Zhang, L., DeSimone, A., Samez, S., Pesaresi, A., Stojan, J., Lopez, M.G., Egea, J., Andrisano, V., Bartolini, M. (2016). Novel Tacrine−Benzofuran Hybrids as Potent Multitarget-Directed Ligands for the Treatment of Alzheimer's Disease: Design, Synthesis, Biological Evaluation, and X-ray Crystallography. *J. Med. Chem.*, 59 (1), 114–131.

[90] Goyal, D., Kaur, A., Goyal, B. (2018). Benzofuran and Indole: Promising Scaffolds for Drug Development in Alzheimer's Disease. *ChemMedChem*, 13 (13), 1275–1299.

[91] Hiremathad, A., Chand, K., Keri, R.S. (2018). Development of coumarin–

benzofuran hybrids as versatile multitargeted compounds for the treatment of Alzheimer's Disease. *Chem. Biol. Drug Des.*, 92 (2), 1497–1503.

[92] Montanari, S., Mahmoud, A.M., Pruccoli, L., Rabbito, A., Naldi, M., Petralla, S., Moraleda, I., Bartolini, M., Monti, B., Iriepa, I., Belluti, F., Gobbi, S., Di Marzo, V., Bisi, A., Tarozzi, A., Ligresti, A., Rampa, A. (2019). Discovery of novel benzofuran-based compounds with neuroprotective and immunomodulatory properties for Alzheimer's disease treatment. *Eur. J. Med. Chem.*, 178 (2019), 243–258.

[93] Pfefferkorn, J.A., Guzman-Perez, A., Oates, P.J., Litchfield, J., Aspnes, G., Basak, A., Benbow, J., Berliner, M.A., Bian, J., Choi, C., Freeman-Cook, K., Corbett, J.W., Didiuk, M., Dunetz, J.R., Filipski, K.J., Hungerford, W.M., Jones, C.S., Karki, K., Ling, A., Li, J.C., Rolph, T.P., et al. (2011). Designing glucokinase activators with reduced hypoglycemia risk: Discovery of N,N-dimethyl-5-(2-methyl-6-((5-methylpyrazin-2-yl)-carbamoyl)benzofuran-4- yloxy)pyrimidine-2-carboxamide as a clinical candidate for the treatment of type 2 diabetes mellitus. *Medchemcomm*, 2 (9), 828–839.

[94] Lombardo, M., Bender, K., London, C., Kirkland, M., Mane, J., Pachanski, M., Geissler, W., Cummings, J., Habulihaz, B., Akiyama, T.E., Di Salvo, J., Madeira, M., Pols, J., Powles, M.A., Finley, M.F., Johnson, E., Roussel, T., Uebele, V.N., Crespo, A., Leung, D., Alleyne, C., Trusca, D., Lei, Y., Howard, A.D., Ujjainwalla, F., Tata, J.R., Sinz, C.J. (2016). Discovery of benzofuran propanoic acid GPR120 agonists: From uHTS hit to mechanism-based pharmacodynamic effects. *Bioorganic Med. Chem. Lett.*, 26 (23), 5724–5728.

[95] Wang, S., Xu, L., Lu, Y.T., Liu, Y.F., Han, B., Liu, T., Tang, J., Li, J., Wu, J., Li, J.Y., Yu, L.F., Yang, F. (2017). Discovery of benzofuran-3(2H)-one derivatives as novel DRAK2 inhibitors that protect islet β-cells from apoptosis. *Eur. J. Med. Chem.*, 130 (2017), 195–208.

[96] Spasov, A.A., Babkov, D.A., Prokhorova, T.Y., Sturova, E.A., Muleeva, D.R., Demidov, M.R., Osipov, D. V., Osyanin, V.A., Klimochkin, Y.N. (2017). Synthesis and biological evaluation of 2- acylbenzofuranes as novel α- glucosidase inhibitors with hypoglycemic activity. *Chem. Biol. Drug Des.*, 90 (6), 1184–1189.

[97] Prins, L.H.A., Petzer, J.P., Malan, S.F. (2010). Inhibition of monoamine oxidase by indole and benzofuran derivatives. *Eur. J. Med. Chem.*, 45 (10), 4458–4466.

[98] Pisani, L., Barletta, M., Soto-Otero, R., Nicolotti, O., Mendez-Alvarez, E., Catto, M., Introcaso, A., Stefanachi, A., Cellamare, S., Altomare, C., Carotti, A. (2013). Discovery, Biological Evaluation, and Structure−Activity and −Selectivity Relationships of 6′-Substituted (E)-2-(Benzofuran-3(2H)-ylidene)-N-methylacetamides, a Novel Class of Potent and Selective Monoamine Oxidase Inhibitors. *J. Med. Chem.*, 56 (6), 2651–2664.

[99] Nevagi, R.J., Dighe, S.N., Dighe, S.N. (2015). Biological and medicinal significance of benzofuran. *Eur. J. Med. Chem.*, 97 (1), 561–581.

[100] Takao, K., U, S., Kamauchi, H., Sugita, Y. (2019). Design, synthesis and evaluation of 2-(indolylmethylidene)-2,3-dihydro-1-benzofuran-3-one and 2-(indolyl)-4H-chromen-4-one derivatives as novel monoamine oxidases inhibitors. *Bioorg. Chem.*, 87 (March), 594–600.

[101] William, D.A., Roche, V.F., Roche, E.B. (2013). Central Analgesics. W.O. Foye, T.L. Lemke, D.A. Williamms, V.F. Roche, and S.W. Zito (editors), *Principles of Medicinal Chemistry* (p. 658–699). Baltimore: Lippincott Williams & Wilkins.

[102] Azevedo, V.F., Kos, I.A., Vargas-Santos, A.B., da Rocha Castelar Pinheiro, G., Dos Santos Paiva, E. (2019). Benzbromarone in the treatment of gout. *Adv. Rheumatol.*, 59 (15), 37–41.

[103] Balaram, G., Mandal, P., Chakraborty, S., Bera, R., Saha, C., Poddar, S., Barma, S., Khanam, J., Karmakar, S., Pal, T.K. (2021). Determination and quantitation of benzofuran, Indole and piperazine containing selective serotonin reuptake inhibitor vilazodone hydrochloride in human plasma by LC-ESI-MS/MS with an application to pharmacokinetic study under the frame work of bioequivale. *J. Anal. Pharm. Res.*, 110 (1), 1–12.

[104] Choi, E., Zmarlicka, M., Ehret, M.J. (2012). Vilazodone: A novel antidepressant. *Am. J. Heal. Pharm.*, 69 (18), 1551–1557.

[105] Cruz, M.P. (2012). Vilazodone HCL (Viibryd): A serotonin partial agonist and reuptake inhibitor for the treatment of major depressive disorder. *Pharm. Ther.*, 37 (1), 28–31.

[106] Stevenson, P.C., Veitch, N.C. (1998). A 2-Arylbenzofuran from Roots Of Cicer Bijugum Associated With Fusarium Wilt Resistance. *Phytochemistry*, 48 (6), 947–951.

[107] Dawood, K.M. (2013). Benzofuran derivatives : a patent review. *Expert Opin.*

*Ther. Pat.*, 23 (9), 1133–1156.

[108] Byun, J.H., Kim, H., Kim, Y., Mook-jung, I., Jin, D., Koo, W., Ho, K. (2008). Aminostyrylbenzofuran derivatives as potent inhibitors for A b fibril formation. *Bioorg. Med. Chem. Lett.*, 18 (20), 5591–5593.

[109] Nadri, H., Pirali-hamedani, M., Shekarchi, M., Abdollahi, M., Sheibani, V., Amanlou, M., Shafie, A., Foroumadi, A. (2010). Design , synthesis and anticholinesterase activity of a novel series pyridinium derivatives. *Bioorg. Med. Chem.*, 18 (17), 6360–6366.

[110] Rivière, C., Papastamoulis, Y., Fortin, P., Delchier, N., Andriamanarivo, S., Waffo-teguo, P., Kapche, G.D.W.F., Delaunay, J., Mérillon, J., Richard, T., Monti, J. (2010). New stilbene dimers against amyloid fibril formation. *Bioorg. Med. Chem. Lett.*, 20 (11), 3441–3443.

[111] Zhou, X., Li, M., Wang, X., Wang, T., Kong, L. (2010). Synthesis of Benzofuran Derivatives via Rearrangement and Their Inhibitory Activity on Acetylcholinesterase. *Molecules*, 15 (12), 8593–8601.

[112] Mitterreiter, S., Page, R.M., Kamp, F., Hopson, J., Winkler, E., Ha, H.R., Hamid, R., Herms, J., Mayer, T.U., Nelson, D.J., Steiner, H., Stahl, T., Zeitschel, U., Roßner, S., Haass, C., Lichtenthaler, S.F. (2010). Bepridil and amiodarone simultaneously target the Alzheimer's disease β- and γ-secretase via distinct mechanisms. *J. Neurosci.*, 30 (26), 8974–8983.

[113] Onishi, T., Iwashita, H., Uno, Y., Kunitomo, J., Saitoh, M., Kimura, E., Fujita, H., Uchiyama, N., Kori, M., Takizawa, M. (2011). A novel glycogen synthase kinase-3 inhibitor 2-methyl-5-(3-{4-[(S )-methylsulfinyl]phenyl}-1-benzofuran-5-yl)-1,3,4-oxadiazole decreases tau phosphorylation and ameliorates cognitive deficits in a transgenic model of Alzheimer's disease. *J. Neurochem.*, 119 (6), 1330–1340.

[114] Davidowitz, E.J., Moe, J.G., Reitz, A.B., Bian, H., Gluchowski, C., Hendrix, J., Yehaskel, A.S., McDonnell, M.E., Loughran, M.H. (2021). *Novel Benzofuran, Benzothiophene, and Indole Analogs That Inhibit the Formation of Tau Oligomers and Thier Method of Use*. US 2021/0130335 A1, USA.

[115] Crowe, A., Ballatore, C., Hyde, E., Trojanowski, J.Q., Lee, V.M. (2007). High throughput screening for small molecule inhibitors of heparin-induced tau fibril formation. *Biochem. Biophys. Res. Commun.*, 358 (1), 1–6.

[116] Baharloo, F., Hossein, M., Nadri, H., Asadipour, A. (2015). Chemistry

Benzofuran-derived benzylpyridinium bromides as potent acetylcholinesterase inhibitors. *Eur. J. Med. Med.*, 93 (2015), 196–201.

[117] Mostofi, M., Mohammadi Ziarani, G., Mahdavi, M., Moradi, A., Nadri, H., Emami, S., Alinezhad, H., Foroumadi, A., Shafiee, A. (2015). Synthesis and structure-activity relationship study of benzofuran-based chalconoids bearing benzylpyridinium moiety as potent acetylcholinesterase inhibitors. *Eur. J. Med. Chem.*, 103 (2015), 361–369.

[118] Delogu, G.L., Matos, M.J., Fanti, M., Era, B., Medda, R., Pieroni, E., Fais, A., Kumar, A., Pintus, F. (2016). 2-Phenylbenzofuran derivatives as butyrylcholinesterase inhibitors: Synthesis, biological activity and molecular modeling. *Bioorganic Med. Chem. Lett.*, 26 (9), 2308–2313.

[119] Pouramiri, B., Mahdavi, M., Moghimi, S., Firoozpour, L., Nadri, H., Moradi, A., Tavakolinejad-Kermani, E., Shafiee, A., Foroumadi, A. (2016). Synthesis and anti-acetylcholinesterase activity of scopoletin derivatives. *Lett. Drug Des. Discov.*, 13 (9), 897–902.

[120] Blain, J.F., Bursavich, M.G., Freeman, E.A., Hrdlicka, L.A., Hodgdon, H.E., Chen, T., Costa, D.E., Harrison, B.A., Kapadnis, S., Murphy, D.A., Nolan, S., Tu, Z., Tang, C., Burnett, D.A., Patzke, H., Koenig, G. (2016). Characterization of FRM-36143 as a new γ-secretase modulator for the potential treatment of familial Alzheimer's disease. *Alzheimer's Res. Ther.*, 8 (1), 1–14.

[121] Savonenko, A. V., Melnikova, T., Li, T., Price, D.L., Wong, P.C. (2015). Alzheimer Disease. M.J. Zigmond, L.P. Rowland, and J.T. Coyle (editors), *Neurobiology of Brain Disorders: Biological Basis of Neurological and Psychiatric Disorders* (p. 321–338). San Diego: Academic Press.

[122] Boughey, J.G.F., Graff-Radford, N.R. (2007). Alzheimer's Disease. A.H. V Schapira, E. Byrne, S. DiMauro, R.S.J. Frackowiak, R.T. Johnson, Y. Mizuno, M.A. Samuels, S.D. Silberstein, and Z.K. Wszolek (editors), *Neurology and Clinical Neuroscience* (p. 846–858). Philadelphia: Mosby.

[123] Doody, R.S. (2006). Alzheimer's Disease. R.T. Johnson, J.W. Griffin, and J.C. McArthur (editors), *Current Therapy in Neurologic Disease (Seventh Edition)* (p. 311–314). Philadelphia: Mosby.

[124] Calderon-Garcidueñas, A.L., Duyckaerts, C. (2018). Alzheimer disease. G.G. Kovacs, and I. Alafuzoff (editors), *Handbook of Clinical Neurology* (p. 325–337).

[125] Gaugler, J., James, B., Johnson, T., Marin, A., Weuve, J. (2019). *Alzheimer's Association Report: 2019 Alzheimer's disease facts and figures*. Elsevier, https://doi.org/10.1016/j.jalz.2019.01.010 (2019).

[126] Lopez, J.A.S., Gonzalez, H.M., Leger, G.C. (2019). Alzheimer's disease. S.T. Dekosky, and S. Asthana (editors), *Handbook of Clinical Neurology* (p. 231–255).

[127] Querfurth, H.W., Laferla, F.M. (2010). Mechanisms of Disease: Alzheimer's Disease. *N. Engl. J. Med.*, 362 (4), 329–344.

[128] Mclean, C.A., Cherny, R.A., Fraser, F.W., Fuller, S.J., Smith, M.J., Beyreuther, K., Bush, A.I., Masters, C.L. (1999). Soluble Pool of A-beta Amyloid as a Determinant of Severity of Neurodegeneration in Alzheimer's Disease. *Ann. Neurol.*, 46 (6), 860–866.

[129] Francis, P.T., Palmer, A.M., Snape, M., Wilcock, G.K. (1999). The cholinergic hypothesis of Alzheimer ' s disease : a review of progress. *J. Neurol. Neurosurg. Psychiatry*, 66 (2), 137–147.

[130] Prusiner, S.B. (2012). A Unifying Role for Prions in Neurodegenerative Diseases. *Science (80-. ).*, 1511 (June), 1–3.

[131] Mayeux, R. (2003). Apolipoprotein E, Alzheimer disease, and African Americans. *Arch. Neurol.*, 60 (2), 161–163.

[132] Green, R.C., Cupples, L.A., Go, R., Benke, K.S., Edeki, T., Griffith, P.A., Williams, M., Hipps, Y., Graff-Radford, N., Bachman, D., others. (2002). Risk of dementia among white and African American relatives of patients with Alzheimer disease. *JAMA*, 287 (3), 329–336.

[133] Andersen, K., Launer, L.J., Dewey, M.E., Letenneur, L., Ott, A., Copeland, J.R.M., Dartigues, J.-F., Kragh--Sorensen, P., Baldereschi, M., Brayne, C., others. (1999). Gender differences in the incidence of AD and vascular dementia: The EURODEM Studies. *Neurology*, 53 (9), 1992.

[134] Guo, Z., Cupples, L.A., Kurz, A., Auerbach, S.H., Volicer, L., Chui, H., Green, R.C., Sadovnick, A.D., Duara, R., DeCarli, C., others. (2000). Head injury and the risk of AD in the MIRAGE study. *Neurology*, 54 (6), 1316–1323.

[135] Plassman, B.L., Havlik, R.J., Steffens, D.C., Helms, M.J., Newman, T.N., Drosdick, D., Phillips, C., Gau, B.A., Welsh--Bohmer, K.A., Burke, J.R., others. (2000). Documented head injury in early adulthood and risk of Alzheimer's disease and other dementias. *Neurology*, 55 (8), 1158–1166.

[136] Casserly, I., Topol, E.J. (2004). Convergence of atherosclerosis and Alzheimer's disease: inflammation, cholesterol, and misfolded proteins. *Lancet*, 363 (9415), 1139–1146.

[137] George-Hyslop, P.S. (1994). Genetic Evidence for a Novel Familial Alzheimer's Disease Locus on Chromosome 14: Analysis of Candidate Genes.*Etiopathogenesis* (p. 3–18). Springer.

[138] Levy-Lahad, E., Wijsman, E.M., Nemens, E., Anderson, L., Goddard, K.A.B., Weber, J.L., Bird, T.D., Schellenberg, G.D. (1995). A familial Alzheimer's disease locus on chromosome I. *Science*, 269 (5226), 970–973.

[139] Kamboh, M.I. (2004). Molecular genetics of late-onset Alzheimer's disease. *Ann. Hum. Genet.*, 68 (4), 381–404.

[140] Szekely, C.A., Thorne, J.E., Zandi, P.P., Ek, M., Messias, E., Breitner, J.C.S., Goodman, S.N. (2004). Nonsteroidal anti-inflammatory drugs for the prevention of Alzheimer's disease: a systematic review. *Neuroepidemiology*, 23 (4), 159–169.

[141] Wyss-Coray, T., Rogers, J. (2012). Inflammation in Alzheimer disease-A brief review of the basic science and clinical literature. *Cold Spring Harb. Perspect. Med.*, 2 (1), 1–24.

[142] Wolozin, B., Kellman, W., Ruosseau, P., Celesia, G.G., Siegel, G. (2000). Decreased Prevalence of Alzheimer Disease Associated With 3-Hydroxy-3-Methyglutaryl Coenzyme A Reductase Inhibitors. *Arch. Neurol.*, 57 (10), 1439–1443.

[143] Morris, M.C., Evans, D.A., Bienias, J.L., Scherr, P.A., Tangney, C.C., Hebert, L.E., Bennett, D.A., Wilson, R.S., Aggarwal, N. (2004). Dietary niacin and the risk of incident Alzheimer's disease and of cognitive decline. *J. Neurol. Neurosurg. Psychiatry*, 75 (8), 1093–1099.

[144] Morris, M.C., Evans, D.A., Bienias, J.L., Tangney, C.C., Bennett, D.A., Aggarwal, N., Wilson, R.S., Scherr, P.A. (2002). Dietary intake of antioxidant nutrients and the risk of incident Alzheimer disease in a biracial community study. *J. Am. Med. Assoc.*, 287 (24), 3230–3237.

[145] Luchsinger, J.A., Tang, M.X., Shea, S., Mayeux, R. (2003). Antioxidant vitamin intake and risk of Alzheimer disease. *Arch. Neurol.*, 60 (2), 203–208.

[146] Pressman, P., Rabinovici, G.D. (2014). Alzheimer's Disease. *Encycl. Neurol. Sci.*, 1 (2014), 91–96.

[147] Schenk, D., Barbour, R., Dunn, W., Gordon, G., Grajeda, H., Guido, T., Hu, K., Huang, J., Johnson-Wood, K., Khan, K., others. (1999). Immunization with amyloid-B attenuates Alzheimer-disease-like pathology in the PDAPP mouse. *Nature*, 400 (6740), 173–177.

[148] Dodart, J.-C., Bales, K.R., Gannon, K.S., Greene, S.J., DeMattos, R.B., Mathis, C., DeLong, C.A., Wu, S., Wu, X., Holtzman, D.M., others. (2002). Immunization reverses memory deficits without reducing brain Aβ burden in Alzheimer's disease model. *Nat. Neurosci.*, 5 (5), 452–457.

[149] Begüm Nurpelin SAĞLIK. (2019). *Alzheimer Hastaliği Tedavisinde Kullanilacak Yeni Bileşiklerin Tasarimi, Sentezi Ve Biyolojik Aktivite Çalişmalari*. Doctorate Thesis. Eskişehir: Anadolu University, Graduate School of Health Sciences.

[150] Daina, A., Michielin, O., Zoete, V. (2017). SwissADME: A free web tool to evaluate pharmacokinetics, drug-likeness and medicinal chemistry friendliness of small molecules. *Sci. Rep.*, 7 (2016), 1–13.

[151] SwissADME Web Tool. *Swiss Institute of Bioinformatics*, http://www.swissadme.ch/index.php (Accessed: 6 October 2021).

[152] Lipinski, C.A., Lombardo, F., Dominy, B.W., Feeney, P.J. (1997). Experimental and computational approaches to estimate solubility and permeability in drug discovery and development settings. *Adv. Drug Deliv. Rev.*, 23 (1997), 3–25.

[153] Lipinski, C.A. (2004). Lead- and drug-like compounds: The rule-of-five revolution. *Drug Discov. Today Technol.*, 1 (4), 337–341.

[154] Schotten-Baumann reaction. *Organic Chemistry Portal*, https://www.organic-chemistry.org/namedreactions/schotten-baumann-reaction.shtm (Accessed: 30 October 2021).

[155] Clayden, J., Greeves, N., Warren, S. (2012). Nucleophilic substitution at the carbonyl group. J. Clayden, N. Greeves, and S. Warren (editors), *Organic chemistry* (p. 197–221). New York: Oxford University Press.

[156] Youssif, B.G.M., Mohamed, A.M., Eldin, E., Osman, A., Abou-ghadir, O.F., Elnaggar, D.H., Abdelrahman, M.H., Treamblu, L., Gomaa, H.A.M. (2019). 5-Chlorobenzofuran-2-carboxamides : From allosteric CB1 modulators to potential apoptotic antitumor agents. *Eur. J. Med. Chem.*, 177 (2019), 1–11.

[157] Engelhardt, H., Esch, I.J.P. De, Kuhn, D., Smits, R.A., Zuiderveld, O.P., Dobler, J., Mayer, M., Lips, S., Arnhof, H., Scharn, D., Haaksma, E.E.J., Leurs, R. (2012).

Detailed structure e activity relationship of indolecarboxamides as H 4 receptor ligands. *Eur. J. Med. Chem.*, 54 (2012), 660–668.

[158] Zou, G., Tu, Z.H., Lu, R.F., Jiang, X.J. (1981). [Neuropharmacological actions of some N-phenyl piperazine derivatives (author's transl)]. *Yao Xue Xue Bao*, 16 (5), 321–327.

[159] Alver, Ö., Parlak, C., Şenyel, M. (2007). FT-IR and NMR investigation of 1-phenylpiperazine: A combined experimental and theoretical study. *Spectrochim. Acta - Part A Mol. Biomol. Spectrosc.*, 67 (3–4), 793–801.

[160] 13C NMR Spectrum of 1-Methylpiperazine. *Chemical Book*, https://www.chemicalbook.com/SpectrumEN_109-01-3_13CNMR.htm (Accessed: 13 October 2021).

[161] 13C NMR Spectrum of 1-Ethylpiperazine. *Chemical Book*, https://www.chemicalbook.com/SpectrumEN_5308-25-8_13CNMR.htm (Accessed: 13 October 2021).

[162] 13C NMR Spectrum of 1(2-(dimethylamino)ethyl)piperazine. *Chemical Book*, https://www.chemicalbook.com/SpectrumEN_2759-28-6_13CNMR.htm (Accessed: 13 October 2021).

[163] Merck. IR Spectrum Table & Chart. *Merck Web Site*, https://www.sigmaaldrich.com/TR/en/technical-documents/technical-article/analytical-chemistry/photometry-and-reflectometry/ir-spectrum-table (Accessed: 30 October 2021).

[164] Castro, A., Martinez, A. (2005). Peripheral and Dual Binding Site Acetylcholinesterase Inhibitors: Implications in treatment of Alzheimers Disease. *Mini-Reviews Med. Chem.*, 1 (3), 267–272.

[165] Inestrosa, N.C., Dinamarca, M.C., Alvarez, A. (2008). Amyloid-cholinesterase interactions: Implications for Alzheimer's disease. *FEBS J.*, 275 (4), 625–632.

[166] García-Ayllón, M.S., Small, D.H., Avila, J., Sáez-Valero, J. (2011). Revisiting the role of acetylcholinesterase in Alzheimer-s disease: Cross-talk with β-tau and p-amyloid. *Front. Mol. Neurosci.*, 4 (2011), 1–9.

[167] Lushchekina, S. V., Kots, E.D., Novichkova, D.A., Petrov, K.A., Masson, P. (2017). Role of Acetylcholinesterase in β-Amyloid Aggregation Studied by Accelerated Molecular Dynamics. *Bionanoscience*, 7 (2017), 396–402.

[168] SoLo, C., Castafio, E.M., B, R.A.K., C, R.C.B., B, B.F. (1995). Fibrillogenesis of

synthetic amyloid-fl peptides is dependent on their initial secondary structure. *Neurosci. Lett.*, 200 (1995), 105–108.

[169] Harper, J.D., Lieber, C.M., Lansbury, P.T. (1997). Atomic force microscopic imaging of seeded fibril formation and fibril branching by the Alzheimer ' s disease amyloid-p protein. *Chem. Biol.*, 4 (1997), 951–959.

[170] Daina, A., Michielin, O., Zoete, V. (2017). SwissADME: A free web tool to evaluate pharmacokinetics, drug-likeness and medicinal chemistry friendliness of small molecules. *Sci. Rep.*, 7 (October 2016), 1–13.

[171] MMG, S. (2020). SwissADME. *Swiss Institute of Bioinformatics*, http://www.swissadme.ch/index.php.

[172] Wong, H.L., Wu, X.Y., Bendayan, R. (2012). Nanotechnological advances for the delivery of CNS therapeutics. *Adv. Drug Deliv. Rev.*, 64 (7), 686–700.

[173] Fromm, M.F. (2004). Importance of P-glycoprotein at blood – tissue barriers. *Trends Pharmacol. Sci.*, 25 (8), 423–429.

[174] Ashani, Y., Grunwald, J., Kronman, C., Velan, B., Shafferman, A. (1994). Role of tyrosine 337 in the binding of huperzine A to the active site of human acetylcholinesterase. *Mol. Pharmacol.*, 45 (3), 555–560.

[175] Sussman, J.L., Harel, M., Silman, I. (1993). Three-dimensional structure of acetylcholinesterase and of its complexes with anticholinesterase drugs. *Chem. Biol. Interact.*, 87 (1), 187–197.

[176] Greig, N.H., Lahiri, D.K., Sambamurti, K. (2002). Butyrylcholinesterase: An important new target in Alzheimer's disease therapy. *Int. Psychogeriatrics*, 14 (1), 77–91.

[177] Darvesh, S. (2016). Butyrylcholinesterase as a Diagnostic and Therapeutic Target for Alzheimer's Disease. *Curr. Alzheimer Res.*, 13 (10), 1173–1177.

## CURRICULUM VITAE

Name and Surname : Sam Ali Mohammed Mohammed Dawbaa

Date and Place of Birth : 1986, Dhamar, Yemen

Education:

Master of Science : Bursa University of Uludag, Graduate School of Applied Sciences, 24/04/2017

Bachelor : Pharmacy Department, Faculty of Medicine and Health Sciences, Dhamar University, Yemen, 30/06/2010

Secondary School : Uqbah High School, Dhamar, Yemen, 2003/2004

Languages : Arabic (mother tongue), English, Turkish

Experience:

Teaching assistant : Pharmacy department, Faculty of Medicine and Health Sciences, Thamar University, Dhamar, Yemen, since 2010.

Articles:

[1] Dawbaa, S., Evren, A.E., Cantürk, Z., Yurttaş, L. (2021). Synthesis of new thiazole derivatives and evaluation of their antimicrobial and cytotoxic activities. Phosphorus, Sulfur Silicon Relat. Elem.; 0 (0), 1–10.

[2] Evren, A.E., Dawbaa, S., Nuha, D., Yavuz, Ş.A., Gül, Ü.D., Yurttaş, L. (2021). Design and synthesis of new 4-methylthiazole derivatives: In vitro and in silico studies of antimicrobial activity. J. Mol. Struct.; 130692.

[3] Şahin, S., Aybastıer, Ö., Dawbaa, S., Karkar, B., Çakmak, T. (2020). Study of the Ability of Lutein and Neoxanthin as Standards and in the Extract of Chlamydomonas reinhardtii to Prevent Oxidatively Induced DNA Base Damage

Using Ultrasensitive GC–MS/MS Analysis. Chromatographia; 83 (2020), 919–926.

[4] Aybastıer, Ö., Dawbaa, S., Demir, C., Akgün, O., Ulukaya, E., Arı, F. (2018). Quantification of DNA damage products by gas chromatography tandem mass spectrometry in lung cell lines and prevention effect of thyme antioxidants on oxidative induced DNA damage. Mutat. Res. - Fundam. Mol. Mech. Mutagen.; 808. Epub ahead of print 2018. DOI: 10.1016/j.mrfmmm.2018.01.004.

[5] Aybastıer, Ö., Dawbaa, S., Demir, C. (2018). Investigation of antioxidant ability of grape seeds extract to prevent oxidatively induced DNA damage by gas chromatography-tandem mass spectrometry. J. Chromatogr. B Anal. Technol. Biomed. Life Sci.; 1072. Epub ahead of print 2018. DOI: 10.1016/j.jchromb.2017.11.044.

[6] Dawbaa, S., Aybastıer, Ö., Demir, C. (2017). Ultrasensitive determination of DNA oxidation products by gas chromatography–tandem mass spectrometry

and the role of antioxidants in the prevention of oxidative damage. J. Chromatogr. B; 1051 (2017), 84–91.

[7] Alakhali, K.M., Alzomar, A.K., Alavudeen, S.S., Khan, N.A., Dawbaa, S.A. (2013). Bacterial resistance of antibiotics used in urinary tract infection. Asian J. Pharm. Clin. Res.; 6.

Awards:

- PhD Scholarship by the Ministry of Higher Education and Scientific Research, 2018, Yemen.
- MSc Scholarship by the Turkish Government (YTB), 2013, Turkey.

Projects:

[1] Synthesis of thiazole derivatives bearing naphthalene ring and investigation of their biological activities. Anadolu University, General Purpose Projects.

[2] Synthesis and Investigation of Enzyme Activity of New 5-Methoxybenzofuran-2-Carboxylic Acid Derivatives. Anadolu University, Publication and Research Incentive Projects.

[3] Synthesis and Investigation of Anticancer Activities of Novel Pyridine-Hydrazinothiazole Derivatives. Anadolu University, Publication and Research Incentive Projects.

[4] Synthesis of new thiazole derivatives containing thiomorpholine and investigation of their anticancer activities. Anadolu University, Publication and Research Incentive Projects.